NUTRITIONAL PHYSIOLOGY AND GUT MICROBIOME, 2nd Edition

EDITED BY: Jia Yin, Konstantinos Papadimitriou, Tingtao Chen and Peng Huang

PUBLISHED IN: Frontiers in Microbiology

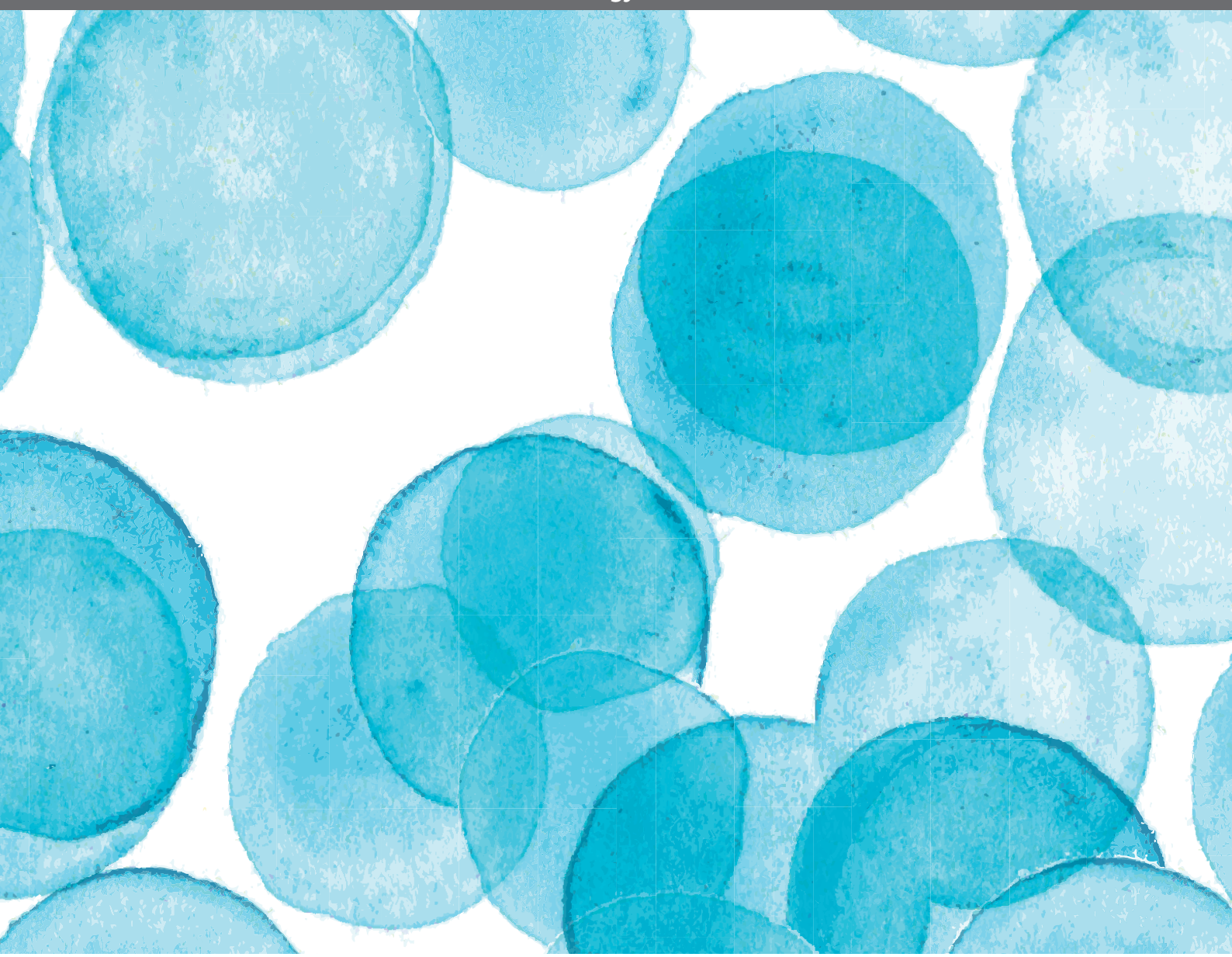

frontiers Research Topics

ISSN 1664-8714
ISBN 978-2-8325-2819-8
DOI 10.3389/978-2-8325-2819-8

About Frontiers

Frontiers is more than just an open-access publisher of scholarly articles: it is a pioneering approach to the world of academia, radically improving the way scholarly research is managed. The grand vision of Frontiers is a world where all people have an equal opportunity to seek, share and generate knowledge. Frontiers provides immediate and permanent online open access to all its publications, but this alone is not enough to realize our grand goals.

Frontiers Journal Series

The Frontiers Journal Series is a multi-tier and interdisciplinary set of open-access, online journals, promising a paradigm shift from the current review, selection and dissemination processes in academic publishing. All Frontiers journals are driven by researchers for researchers; therefore, they constitute a service to the scholarly community. At the same time, the Frontiers Journal Series operates on a revolutionary invention, the tiered publishing system, initially addressing specific communities of scholars, and gradually climbing up to broader public understanding, thus serving the interests of the lay society, too.

Dedication to Quality

Each Frontiers article is a landmark of the highest quality, thanks to genuinely collaborative interactions between authors and review editors, who include some of the world's best academicians. Research must be certified by peers before entering a stream of knowledge that may eventually reach the public - and shape society; therefore, Frontiers only applies the most rigorous and unbiased reviews.
Frontiers revolutionizes research publishing by freely delivering the most outstanding research, evaluated with no bias from both the academic and social point of view. By applying the most advanced information technologies, Frontiers is catapulting scholarly publishing into a new generation.

What are Frontiers Research Topics?

Frontiers Research Topics are very popular trademarks of the Frontiers Journals Series: they are collections of at least ten articles, all centered on a particular subject. With their unique mix of varied contributions from Original Research to Review Articles, Frontiers Research Topics unify the most influential researchers, the latest key findings and historical advances in a hot research area! Find out more on how to host your own Frontiers Research Topic or contribute to one as an author by contacting the Frontiers Editorial Office: frontiersin.org/about/contact

NUTRITIONAL PHYSIOLOGY AND GUT MICROBIOME, 2nd Edition

Topic Editors:
Jia Yin, Hunan Normal University, China
Konstantinos Papadimitriou, University of Peloponnese, Greece
Tingtao Chen, Nanchang University, China
Peng Huang, Hunan Agricultural University, China

Publisher's note: In this 2nd edition, the following article has been added: Papadimitriou K, Chen T, Huang P and Yin J (2023) Editorial: Nutritional physiology and gut microbiome. *Front. Microbiol*. 14:1227522. doi: 10.3389/fmicb.2023.1227522

Citation: Yin, J., Papadimitriou, K., Chen, T., Huang, P., eds. (2023). Nutritional Physiology and Gut Microbiome, 2nd Edition. Lausanne: Frontiers Media SA. doi: 10.3389/978-2-8325-2819-8

Table of Contents

frontiers | Frontiers in Microbiology

TYPE Editorial
PUBLISHED 13 June 2023
DOI 10.3389/fmicb.2023.1227522

OPEN ACCESS

EDITED AND REVIEWED BY
Takema Fukatsu,
National Institute of Advanced Industrial Science and Technology (AIST), Japan

*CORRESPONDENCE
Konstantinos Papadimitriou
✉ kpapadimitriou@aua.gr
Jia Yin
✉ jiayin@hunnu.edu.cn

RECEIVED 23 May 2023
ACCEPTED 30 May 2023
PUBLISHED 13 June 2023

CITATION
Papadimitriou K, Chen T, Huang P and Yin J (2023) Editorial: Nutritional physiology and gut microbiome. *Front. Microbiol.* 14:1227522. doi: 10.3389/fmicb.2023.1227522

Editorial: Nutritional physiology and gut microbiome

Konstantinos Papadimitriou[1]*, Tingtao Chen[2], Peng Huang[3,4] and Jia Yin[5,6]*

[1]Laboratory of Food Quality Control and Hygiene, Department of Food Science and Human Nutrition, Agricultural University of Athens, Athens, Greece, [2]Institute of Translational Medicine, Nanchang University, Nanchang, China, [3]College of Animal Science and Technology, Hunan Agricultural University, Changsha, China, [4]Hunan Key Laboratory of Traditional Chinese Veterinary Medicine, Hunan Agricultural University, Changsha, China, [5]Hunan Provincial Key Laboratory of Animal Intestinal Function and Regulation, College of Life Sciences, Hunan Normal University, Changsha, China, [6]Hunan International Joint Laboratory of Animal Intestinal Ecology and Health, College of Life Science, Hunan Normal University, Changsha, China

KEYWORDS

gut microbiome, animal nutrition, host metabolism, multi-omics analysis, host health

Editorial on the Research Topic
Nutritional physiology and gut microbiome

The gut microbiota is the largest symbiotic ecosystem in the host and has been demonstrated to play an important role in maintaining intestinal homeostasis. The symbiotic relationship between the microbiota and the host is mutually beneficial. The host provides important habitat and nutrients for the microbiome. The gut microbiota supports the development of the metabolic system and the intestinal immune system's maturation. Intestinal microbes ingest dietary components such as carbohydrates, proteins, and lipids, and the metabolites are reported to directly or indirectly affect human health. Therefore, there is an inseparable relationship between the gut microbiota and the nutrition of the host.

Gut microbiota not only participates in the digestion, absorption, and synthesis of some nutrients but also regulates host metabolism. A detailed understanding of this relationship between gut microbiota and animal nutrition physiology is necessary to rationalize dietary interventions targeted at the gut microbiota in the future. The emergence of omics methods and research on the animal microbiome has completely changed our understanding of gut microbiota and nutritional physiology. This Research Topic (RT) focuses on all aspects of the research on digestive tract microorganisms and nutritional physiology.

Various research articles submitted on this RT focus on the impact of specific dietary interventions on the microbiome and the physiology of certain farming animals, including pigs and piglets, lambs and goats, ducks, chickens, bullfrogs, and shrimps. Yang, Wang, et al. explored the impact of different dietary ratios of amylose and amylopectin on the gut health and microbiome of weaned pigs during feed transitions or after exposure to the lipopolysaccharide toxin of *Escherichia coli*. Wang M. et al. investigated the effects of an herbal extract mixture on the gut microbiota and intestinal antioxidant capacity of weaning piglets. Zhou H. et al. researched the effects of administering all-trans retinoic acid (ATRA) to pregnant sows on the gut bacterial community of neonatal piglets with different genetic backgrounds. Zheng et al. looked into the mechanisms underlying the effects of beta-hydroxy-beta-methylbutyrate (HMB) on lipid metabolism in Bama Xiang mini-pigs. Li et al. compared the effects of compound enzymes and antibiotics on growth performance, nutrient digestibility, blood biochemical index, and intestinal health in weaned pigs. All

these studies demonstrated that the dietary interventions could lead to alterations in the gut microbiome of pigs and piglets, suggesting improved gut health and physiological functions like resistance to bacterial toxins, enhanced anti-oxidative capacity, growth performance, etc.

Furthermore, Wang Q. et al. assessed the impact of different dietary energy levels in male Hu lambs during the fattening period, and Yang, Zhang, et al. assessed the effects of dietary supplementation with mannan oligosaccharide (MOS) on the passive transfer of immunoglobulin G (IgG), anti-oxidative capacity, immunity, and intestinal microbiota in neonatal goats. The first study suggested that the medium rather than the high dietary energy levels could be more appropriate during the lamb fattening period based on the changes observed in rumen fermentation, gastrointestinal tract histology, and microbiome diversity. The second study concluded that MOS could improve all parameters tested and thus its addition as a feed supplement for neonatal goats is suggested.

An additional three studies focused on dietary improvements in poultry. In ducks, Liu et al. and Peng et al. explored the effects on gut microbiota, growth performance, and intestinal morphology among other physiological parameters of dietary ferulic acid or *Bacillus* and non-starch polysaccharase, respectively. He et al. studied the effects of incorporating black soldier fly larvae meal (BSFLM) into the diets of Xuefeng Black-Bone chickens on their gut microbiota and intestinal morphology. The studies mentioned above indicated that the dietary interventions tested had positive effects on the gut health and productivity of poultry.

The final two studies on farming animals were on organisms related to aquaculture. Wang Z. et al. analyzed the effects of supplementing autochthonous gut bacteria in plant-based diets on the growth, nutrient digestibility, and gut health of bullfrogs (*Lithobates catesbeianus*). Wang W. et al. looked at the effects of dietary supplementation with *Phaffia rhodozyma* astaxanthin on growth performance, carotenoid analysis, biochemical and immune-physiological parameters, gut microbiota, and disease resistance in the giant tiger prawn *Penaeus monodon*. Again, a positive influence was recorded for each of the interventions in the two organisms which could be related to the gut microbiome, gut physiology, and growth performance.

The next five studies were performed in mice or rats as the model organisms. Wen et al. investigated the effects of heat stress on the gut microbiota and metabolomic profiles in mice. Heat stress was found to have a negative effect on the gut microbiome composition and caused metabolic alterations which could be related to inflammation and oxidative stress. Zhuang et al. studied the effects of resveratrol on growth performance, intestinal morphology, gut microbiota composition, and metabolism in mice. Zhai et al. unraveled the mechanisms underlying the effects of *Eucommia ulmoides* leaf extract (EULE) on colonic epithelium integrity in rats. Zhou D. et al. tested the application of phytic acid-degrading bacteria on mineral element content in mice. Wan et al. checked the effects of caffeic acid supplementation on colonic inflammation, oxidative stress, and gut microbiota in mice. Resveratrol had a positive impact on all physiological and morphological parameters tested. EULE supplementation led to improvements in colonic epithelium integrity, accompanied by a reduction in inflammation and oxidative stress. EULE action was found to be mediated through the gut microbiota-bile acids-TGR5 axis. Degradation of the anti-nutrient phytic acid, which binds to minerals and inhibits their absorption in the gut, led to their increased absorption and utilization. This effect was accompanied by positive alterations in the composition of the gut microbiome. Moreover, caffeic acid supplementation led to reductions in colonic inflammation and oxidative stress along with positive changes in the gut microbiota composition. The antioxidant and anti-inflammatory effects of caffeic acid were associated with changes in the level of gene expression.

Finally, three review articles were published in the RT. The first concentrated on the potential use of *Lonicera japonica* extracts (LJE) in animal production, with a focus on their effects on intestinal health. In this review, Tang et al. discussed the mechanisms underlying the positive effects of LJE on the gut microbiota, gut barrier function, and immune function. Overall, the review suggested that LJE has potential applications in animal production for promoting gut health, enhancing animal performance, and reducing the need for antibiotics. In the second review, Yang Y. et al. presented recent research on the relationship between cow's milk protein allergy (CMPA) and the gut microbiota in infants. The authors suggested a relation between CMPA and gut dysbiosis, as well as the potential use of probiotics, prebiotics, and synbiotics in the prevention and management of CMPA. In the third and final review, Hu et al. discussed the potential applications and functions of prophage activation in the intestine. The study highlighted that prophage activation could play a role in the modulation of gut microbiota composition and function, in the treatment of disease (e.g., inflammatory bowel disease) and infection (e.g., *Clostridioides difficile*), as well as in engineering the microbiome (e.g., production of therapeutic compounds).

The studies featured in this RT encompass significant contributions from diverse authors, highlighting the multifaceted aspects between nutritional physiology and the gut microbiome in animal and human health.

Author contributions

All authors listed have made a substantial, direct, and intellectual contribution to the work and approved it for publication.

Acknowledgments

We would like to thank all authors who published their work in this Research Topic. We would also like to thank the editorial staff at Frontiers in Microbiology for their initial invitation and support throughout the process.

Conflict of interest

The authors declare that the research was conducted in the absence of any commercial or financial relationships that could be construed as a potential conflict of interest.

Publisher's note

frontiers in Microbiology

ORIGINAL RESEARCH
published: 13 July 2021
doi: 10.3389/fmicb.2021.698213

Effects of Dietary Ferulic Acid on the Intestinal Microbiota and the Associated Changes on the Growth Performance, Serum Cytokine Profile, and Intestinal Morphology in Ducks

Yang Liu[1,2†], Qian Lin[3†], Xuan Huang[2], Guitao Jiang[2], Chuang Li[2], Xu Zhang[2], Shengli Liu[4], Lingyun He[5], Yali Liu[6], Qiuzhong Dai[2] and Xingguo Huang[1]**

[1] College of Animal Science and Technology, Hunan Agriculture University, Changsha, China, [2] Hunan Institute of Animal and Veterinary Science, Changsha, China, [3] Institute of Bast Fiber Crops, Chinese Academy of Agricultural Sciences, Changsha, China, [4] Shandong Lonct Enzymes Co., Ltd., Linyi, China, [5] Animal Husbandry and Fisheries Affairs Center, Huaihua, China, [6] Hunan Perfly Biotech Co., Ltd., Changsha, China

The present study investigated the effects of ferulic acid (FA) on the growth performance, serum cytokine profile, intestinal morphology, and intestinal microbiota in ducks at the growing stage. 300 female *Linwu* ducks at 28 days of age with similar body weights were randomly divided into five groups. Each group contained six replicates of 10 birds. The dietary treatments were corn-soybean-based diet supplemented with FA at the concentrations of 0 (control), 100, 200, 400, and 800 mg/kg diet. The results demonstrated that dietary FA at the levels of 200, 400, and 800 mg/kg increased the average daily gain (P = 0.01), 400 and 800 mg/kg FA increased the final body weight (P = 0.02), 100, 200, and 800 mg/kg FA increased the serum glutathione (P = 0.01), and 100, 400, and 800 mg/kg FA increased the glutathione peroxidase activities in birds ($P < 0.01$). Additionally, 200, 400, and 800 mg/kg dietary FA lowered the serum levels of interleukin-2 (P = 0.02) and interleukin-6 (P = 0.04). Moreover, the morphometric study of the intestines indicated that 400 mg/kg FA decreased the crypt depth in jejunum (P = 0.01) and caecum (P = 0.04), and increased the ratio of villus height to crypt depth in jejunum (P = 0.02). Significant linear and/or quadratic relationships were found between FA concentration and the measured parameters. 16S rRNA sequencing revealed that dietary FA increased the populations of genera *Faecalibacterium*, *Paludicola*, RF39, and *Faecalicoccus* in the cecum ($P < 0.05$), whereas decreased the populations of *Anaerofilum* and UCG-002 ($P < 0.05$). The Spearman correlation analysis indicated that phylum *Proteobacteria* were negatively, but order *Oscillospirales*, and family *Ruminococcaceae* were positively related to the

OPEN ACCESS

Edited by:
Jia Yin,
Hunan Normal University, China

Reviewed by:
Xin Wu,
Chinese Academy of Sciences (CAS), China
Guang-Hai Qi,
Feed Research Institute, Chinese Academy of Agricultural Sciences, China
Xuemei Ding,
Sichuan Agricultural University, China

***Correspondence:**
Qiuzhong Dai
daiqiuzhong@163.com
Xingguo Huang
hxg68989@hunau.edu.cn

† These authors have contributed equally to this work and share first authorship

Specialty section:
This article was submitted to Microbial Symbioses, a section of the journal Frontiers in Microbiology

Received: *21 April 2021*
Accepted: *09 June 2021*
Published: *13 July 2021*

Citation:
Liu Y, Lin Q, Huang X, Jiang G, Li C, Zhang X, Liu S, He L, Liu Y, Dai Q and Huang X (2021) Effects of Dietary Ferulic Acid on the Intestinal Microbiota and the Associated Changes on the Growth Performance, Serum Cytokine Profile, and Intestinal Morphology in Ducks. Front. Microbiol. 12:698213. doi: 10.3389/fmicb.2021.698213

parameters of the growth performance. Phylum *Bacteroidetes*, class *Negativicutes* and family *Rikenellaceae* were negatively associated with the parameters of the antioxidative capability. And phylum *Cyanobacteria*, *Elusimicrobia*, and *Bacteroidetes*, class *Bacilli*, family *Rikenellaceae*, and genus *Prevotella* were positively associated with the parameters of the immunological capability. Thus, it was concluded that the supplementations of 400 mg/kg FA in diet was able to improve the growth performance, antioxidative and immunological capabilities, intestinal morphology, and modulated the gut microbial construction of *Linwu* ducks at the growing stage.

Keywords: gut microbiota, ferulic acid, growth performance, serum cytokine, intestinal morphology, duck

INTRODUCTION

The intensive rearing system for poultry was widespread throughout the world. Better quantity and quality of poultry products were expected by breeding birds in indoor system with advanced technologies and management skills (Robins and Phillips, 2011). The intensive rearing system satisfied the increasing demands for the poultry product, but also brought many problems to the welfare of the birds, including the physiological and physical stresses (Lolli et al., 2010; Averós and Estevez, 2018), pathogenic infections (Zhu, 2011), and disturbance in the intestinal microbial construction (Wang S. et al., 2018). These problems might break the redox homeostasis and provoked immune response (Rehman et al., 2017; Lauridsen, 2018), leading to high mortality and lower productive efficiency (Averós and Estevez, 2018). In the past, antibiotic additives in poultry feed were commonly used in the intensive rearing system because they could effectively attenuate the negative influence of stress, and enhance the growth performance of birds (Castanon, 2007). However, the abuse of antibiotics led to the development of bacterial antibiotic-resistance and created huge pressure on the medication of bacterial infections in human and animal (Hayes et al., 2004). Starting from 2006, legislative bans on antibiotics in animal feed were issued worldwide gradually.

On this background, phytochemicals with characteristics of safety, multiple bioactivities and enhancement to animal growth became ideal alternations to the antibiotic additives in animal feed (Valenzuela-Grijalva et al., 2017). Ferulic acid (FA) is an active phenolic acid widely existing in the cell walls of plants, and it is the main active substance of Chinese herbs Chuangxiong (*Ligusticum chuanxiong*) and Danggui (*Angelica sinensis*) (Ou and Kwok, 2004). Previous researchers stated that FA possessed multiple bioactivities, such as anti-bacteria (Daglia, 2012), antioxidant (Mahmoud et al., 2020), anti-inflammatory (Lampiasi and Montana, 2016), anti-obesity (Wang et al., 2015), anti-tumor (Jinhua et al., 2018), and regulation of blood circulation (Zhou et al., 2017). Currently, FA was widely used in industries such as food preservation (Ou et al., 2005), cosmetics production (Gupta et al., 2020), and medication (Wang W. M. et al., 2018). A few studies demonstrated the antioxidative and growth promotional functions of FA and its derivatives in livestock, as supplement in the feed (Li et al., 2015; González-Ríos et al., 2016; Wang et al., 2019), but none referred to ducks. In the present study, we attempted to understand the effects of FA on the growth performance, serum cytokine profiles, intestine morphology, and intestinal microbiota composition in ducks.

MATERIALS AND METHODS

The experimental procedures of this study were approved by Hunan Agricultural University Institutional Animal Care and Use Committee.

Experimental Design and Diets

Linwu duck is an important indigenous breed in South China, with the characteristics of fast growth, high feed efficiency, and unique meat flavor and texture. The market age for *Linwu* duck is 70 days and the average body weight at that time is about 1,750 g per duck. From the age of 28–54 days was the maximum growing stage for *Linwu* ducks, when they suffered the most by the immune and oxidative stresses. Therefore, *Linwu* ducks at 28 days of age were chosen for this study. A total of 300 female ducks were obtained from Hunan Shunhua Duck Industrial Development Company (Linwu, China) and housed in plastic plain netting cages with the dimension of 1.8 m × 1.2 m × 2 m (10 ducks/cage). Ducks were accessed to the water and feed freely. Birds were randomly divided into five groups with six replicates per group. And each replicate had 10 birds. The whole experiment period was 29 days.

Birds in group 1 were fed the basal diets, and in group 2–5 were fed basal diets supplemented with 100, 200, 400, and 800 mg/kg FA, respectively. The basal diet, which meets the nutritional requirements for growing ducks (National Research Council, 1994), was given in **Table 1**. FA (≥99%) was purchased from Shanghai Rhawn Chemical Technology Co., Ltd. (Shanghai, China).

Growth Performance

The birds were fasted for 12 h before weighting and sampling. On 29th day of the experiment, birds were weighted, and the total feed consumptions were summed up by cages (replicates). Average daily weight gain (ADG), average daily feed intake (ADFI) and ratio of feed to gain (F/G) were calculated for the whole experimental period.

TABLE 1 | Ingredients and nutrient composition of the basal diet (dry matter basis, %).

Ingredients		Nutrient levels[1]	
Corn	50.68	Metabolic energy, MJ/kg	11.30
Soybean meal	24.50	Dry matter (DM)	87.3
Flour	10.00	Crude protein (CP)	17
Wheat middlings	7.00	Calcium (Ca)	0.90
$CaHPO_4$	1.30	Total phosphorus (TP)	0.56
Salt	0.30	Available phosphorus (AP)	0.35
L-Lysine H_2SO_4	0.27	Salt	0.33
DL-Methionine	0.12	Lysine	0.9
Limestone	1.20	Methionine	0.4
Bentonite	3.63	Methionine and cystine	0.789
Premix[2]	1.00	Isoleucinese	0.732
		Threonine	0.6
		Tryptophane	0.264

[1]The nutrient levels were calculated values. [2]The premix provided the following nutrients per kg diet: vitamin A 12,000 IU; vitamin D_3 2,500 IU; vitamin E 20 mg; vitamin K_3 3 mg; vitamin B_1 3 mg; vitamin B2 8 mg; vitamin B6 7 mg; vitamin B12 0.03 mg; D-pantothenic acid 20 mg, nicotinic acid 50 mg, biotin 0.1 mg, folic acid 1.5 mg, Cu (as copper sulfate) 9 mg, Zn (as zinc sulfate) 110 mg, Fe (as ferrous sulfate) 100 mg, Mn (as manganese sulfate) 100 mg, Se (as sodium selenite) 0.16 mg, and I (as potassium iodide) 0.6 mg.

Sample Collections

After weighting, one bird from each cage (6 birds per group) was randomly selected for sampling. Bloods were collected from the wing vein with vacuum blood collection tubes, and centrifuged at 3,000 × *g* for 10 min to obtain the serums. The birds were then sacrificed by bleeding in jugular vein and dissected for the duodenum, jejunal, ileal, and cecal tissue samples. Chyme in the cecum of each sampled duck were collected separately into 2 mL EP tubes, froze immediately in liquid nitrogen and stored at −80°C until analysis.

Serum Antioxidant and Inflammatory Biomarkers

The serum levels of antioxidant biomarkers including reduced glutathione (GSH), malonaldehyde (MDA), activities of superoxide dismutase (SOD) and glutathione peroxidase (GSH-Px), as well as the inflammatory biomarkers, such as immunoglobulin G (IgG), interlukin-1β (IL-1β), interlukin-6 (IL-6), and interleukin-2 (IL-2) were determined by the commercial assay kits (Nanjing Jiancheng Bioengineering Institute, Nanjing, China) with an automated fluorescence instrument (Multiskan^{TM} SkyHigh, Thermo Fisher Scientific, Waltham, MA, United States).

Intestinal Morphology

The intestinal sections, including duodenum, jejunum, ileum, and cecum, were removed and emptied. 2 cm sections of intestinal tissues were collected and embedded in paraffin. A microtome (RM-2235, Leica microsystems AG, Hessen, Germany) was used to make 5 μm slices of the tissue samples, which were subsequently stained with hematoxylin and eosin. The slides were observed under a microscope (Olympus Van-Ox S, Opelco, Washington, DC, United States) and the proper microscopic fields were selected for the following diagnoses. Five readings of the villus height, crypt depth, intestinal wall thickness and mucosal thickness from each slide were determined by an image analysis system (Image-Pro, Media Cybernetics, Inc., Silver Springs, MD, United States). The ratios of villus height to crypt depth (VCR) were calculated as well.

Gut Microbiota Composition by 16S rRNA Gene Sequencing

Microbial community genomic DNA was extracted from cecum digesta samples using the E.Z.N.A. soil DNA kits (Omega Bio-tech, Norcross, GA, United States) according to the manufacturer's instructions. The V3-V4 regions of the bacterial 16S rRNA gene were amplified using primer pairs 338F (5′-ACTCCTACGGGAGGCAGCAG-3′) and 806R (5′-GGACTACHVGGGTWTCTAAT-3′), and later purified using AxyPrep DNA Gel Extraction Kits (Axygen Bioscience, Union City, CA, United States). The purified amplicons were paired-end sequenced on an Illumina MiSeq PE300 platform (Illumina, San Diego, CA, United States). The raw reads in this study were uploaded to the National Center of Biotechnology Information (NCBI) Sequence Read Archive (SRA) database under accession number PRJNA723283.

Reads with length over 300 bp were kept for the following analysis. QIIME (version 1.17) software was used to filter the obtained sequences from the samples and the high-quality sequences were clustered into operational taxonomic units (OTUs) with a cut off of 97% similarity using UPARSE (version 7.1). Each OTU represented sequence was analyzed by Ramer–Douglas–Peucker (RDP) Classifier version 2.2 against the 16S rRND database.

The alpha and beta diversities of the cecal microbiota were estimated at genera level. Principal coordinate analysis (PCA) with analysis of similarities (ANOSIM) was carried out to determine the beta diversity of the bacteria. Statistical comparison of the relative abundance of the cecal microbiota was performed using one-way ANOVA to identify the differences in bacterial taxa among all groups, or using student's *t* test between two groups. The spearman correlation analysis was applied to evaluate the relationship of microbial species with the measured parameters. Correlations were considered significantly different at $P \leq 0.05$. The analysis procedures of cecal microbiota were processed on the free online platform of Majorbio Cloud Platform (Majorbio Bio-pharm Technology Co., Ltd., Shanghai, China).

Statistical Analysis

Cage was taken as experimental unit, and the homogeneity of variances of the data were tested before further analysis. One-way ANOVA followed by Duncan's multiple range test were used to test the significant mean differences among groups. Polynomial orthogonal contrasts were applied to determine linearly and quadratically responses of measured parameters to the dietary FA concentration. All data analysis was performed in SPSS statistical

TABLE 2 | Effect of different dietary FA supplementation on growth performance of experimental ducks[1].

Item	Treatments[2]					SEM	*P* value		
	Group 1	Group 2	Group 3	Group 4	Group 5		ANOVA	Linear	Quadratic
Initial BW, g	892.67	891.00	892.67	894.33	893.00	8.13	0.98	0.76	0.91
Final BW, g	1,553.33^{bc}	1,542.33^{c}	1,599.33^{ab}	1,615.00^{a}	1,609.67^{a}	49.65	0.02	0.01	<0.01
ADG, g	22.78^{c}	22.46^{bc}	24.37^{ab}	24.85^{a}	24.71^{a}	1.65	0.01	<0.01	<0.01
ADFI, g	149.00	150.98	150.97	152.15	151.72	6.98	0.96	0.56	0.74
F/G	6.57^{ab}	6.73^{a}	6.21^{b}	6.13^{b}	6.15^{b}	0.45	0.05	0.03	0.04

BW, body weight; ADG, average daily weight gain; ADFI, average daily feed intake; F/G, feed to gain ratio. [a to c]Within a row, mean values bearing different superscripts differ significantly ($P < 0.05$). [1]Data is the mean of six replicates per treatment. [2]Group 1 (control), Group 2 (dietary FA supplementation at 100 mg/kg feed), Group 3 (dietary FA supplementation at 200 mg/kg feed), Group 4 (dietary FA supplementation at 400 mg/kg feed), and Group 5 (dietary FA supplementation at 800 mg/kg feed).

TABLE 3 | Effect of different dietary FA supplementation on antioxidative parameters of experimental ducks[1].

Item	Treatments[2]					SEM	*P* value		
	Group 1	Group 2	Group 3	Group 4	Group 5		ANOVA	Linear	Quadratic
MDA, nmol/mL	3.19	2.55	2.49	2.81	2.43	0.83	0.52	0.32	0.55
GSH, μmol/L	76.64^{c}	118.89^{ab}	140.64^{a}	93.14^{bc}	137.48^{a}	36.14	0.01	0.14	0.34
SOD, U/mL	154.85	151.26	137.25	151.55	152.65	14.36	0.22	0.78	0.49
GSH-Px, U/mL	580.74^{c}	692.30^{ab}	644.77^{bc}	719.54^{ab}	776.92^{a}	99.97	<0.01	<0.01	<0.01

[a to c]Within a row, mean values bearing different superscripts differ significantly ($P < 0.05$). MDA, malonaldehyde; GSH, glutathione; SOD, superoxide dismutase; GSH-Px, glutathione peroxidase. [1]Data is the mean of six birds per treatment. [2]Group 1 (control), Group 2 (dietary FA supplementation at 100 mg/kg feed), Group 3 (dietary FA supplementation at 200 mg/kg feed), Group 4 (dietary FA supplementation at 400 mg/kg feed), and Group 5 (dietary FA supplementation at 800 mg/kg feed).

TABLE 4 | Effect of different dietary FA supplementation on immunological parameters of experimental ducks[1].

Item	Treatments[2]					SEM	*P* value		
	Group 1	Group 2	Group 3	Group 4	Group 5		ANOVA	Linear	Quadratic
IgG, mg/mL	20.26	28.52	20.71	21.87	19.75	7.81	0.28	0.38	0.65
IL-1β, ng/mL	214.11	195.49	200.81	219.54	202.87	26.24	0.51	1.00	0.93
IL-6, ng/L	104.30^{a}	94.31^{ab}	78.20^{b}	74.35^{b}	78.98^{b}	20.69	0.04	0.03	0.01
IL-2, ng/L	362.74^{a}	242.06^{ab}	223.16^{b}	197.01^{b}	139.50^{b}	112.94	0.02	<0.01	<0.01

[a to b] Within a row, mean values bearing different superscripts differ significantly ($P < 0.05$). IgG, immunoglobulin G; IL-1β, interlukin-1β; IL-6, interlukin-6; IL-2, interleukin-2. [1]Data is the mean of six birds per treatment. [2]Group 1 (control), Group 2 (dietary FA supplementation at 100 mg/kg feed), Group 3 (dietary FA supplementation at 200 mg/kg feed), Group 4 (dietary FA supplementation at 400 mg/kg feed), and Group 5 (dietary FA supplementation at 800 mg/kg feed).

program (SPSS25, IM Corp., Armonk, NY, United States). A probability of $P < 0.05$ was considered significant.

RESULTS

Growth Performance

The initial BW, final BW, ADG, ADFI, and F/G of experimental ducks were shown in **Table 2**. The birds in Group 4 and 5 exhibited significantly higher final BW ($P = 0.02$) and ADG ($P = 0.01$) than the birds in Group 1. Group 3 showed the same trend, but the differences with Group 1 were not statistically significant. The F/G ratios in Group 3, 4, and 5 were decreased compared to Group 1 without statistical significance ($P = 0.05$). Significant linear ($P < 0.05$) and quadratic relationships ($P < 0.05$) were observed between final BW, ADG and F/G, and dietary FA level.

Serum Cytokines Profile: Oxidant and Antioxidant Status

The serum oxidant and antioxidant statuses were listed in **Table 3**. Serum levels of MDA ($P = 0.52$) and SOD activities ($P = 0.22$) among groups were similar, but significant differences were noticed in GSH levels ($P = 0.01$) and GSH-Px ($P < 0.01$) activities among groups. Serum levels of GSH in all groups except Group 4, and GSH-Px activities in all groups except Group 3 were significantly higher, compared to those in Group 1. Moreover, as the diet FA increased, the activities of GSH-Px increased linearly ($P < 0.01$) and quadratically ($P < 0.01$).

Serum Cytokine Profile: Immune Status

As demonstrated in **Table 4**, there were no significant differences in serum levels of IgG ($P = 0.28$) and IL-1β ($P = 0.51$) among groups. However, Group 3, 4, and 5 showed significant lower

TABLE 5 | Effect of different dietary FA supplementation on intestinal morphology of experimental ducks[1].

Item	Treatments[2]					SEM	*P* value		
	Group 1	Group 2	Group 3	Group 4	Group 5		ANOVA	Linear	Quadratic
Duodenum									
VH, μm	429.59	417.97	328.82	404.75	413.75	77.62	0.16	0.59	0.71
CD, μm	100.15	111.71	90.10	103.49	107.56	15.53	0.14	0.30	0.49
VCR	4.39	3.76	3.65	3.96	3.88	0.79	0.56	0.43	0.33
IWT, μm	193.89	212.70	195.87	227.04	205.50	42.56	0.69	0.31	0.58
MT, μm	601.66	632.23	531.90	595.67	626.65	84.25	0.15	0.91	0.40
Jejunum									
VH, μm	343.11	363.83	357.62	350.50	350.54	54.25	0.98	0.66	0.91
CD, μm	101.44^{a}	102.36^{a}	89.10^{ab}	86.91^{b}	81.69^{b}	13.38	0.01	<0.01	<0.01
VCR	3.36^{c}	3.58^{bc}	4.00^{ab}	4.06^{ab}	4.35^{a}	0.59	0.02	<0.01	<0.01
IWT, μm	198.48	199.71	182.19	216.91	197.60	47.26	0.83	0.97	0.91
MT, μm	494.59	517.67	486.43	492.01	499.14	73.48	0.97	0.45	0.64
Ileum									
VH, μm	310.43	366.56	380.75	306.50	326.86	65.81	0.16	0.61	0.61
CD, μm	82.33	90.13	97.94	87.00	89.42	11.00	0.17	0.45	0.16
VCR	3.80	4.03	3.91	3.51	4.10	0.60	0.50	0.93	0.90
IWT, μm	183.44	227.78	224.17	196.97	195.51	38.29	0.19	0.90	0.14
MT, μm	444.07	536.80	524.59	454.07	497.22	91.48	0.31	0.85	0.54
Caecum									
VH, μm	191.94	189.09	197.99	182.21	173.82	28.93	0.68	0.26	0.38
CD, μm	53.77^{a}	50.38^{ab}	50.34^{ab}	47.16^{b}	56.48^{a}	5.77	0.04	0.77	0.03
VCR	3.59	3.75	3.94	3.94	3.08	0.66	0.12	0.34	0.04
IWT, μm	165.01	151.48	165.03	154.10	146.35	25.72	0.67	0.30	0.57
MT, μm	237.08	251.93	272.55	243.90	237.15	34.03	0.36	0.86	0.21

VH, villus height; CD, crypt depth; VCR, ratio of villus height to crypt depth; IWT, intestinal wall thickness; MT, mucosa thickness. $^{a\ to\ c}$*Within a row, mean values bearing different superscripts differ significantly (P < 0.05).* [1]*Data is the mean of six birds per treatment.* [2]*Group 1 (control), Group 2 (dietary FA supplementation at 100 mg/kg feed), Group 3 (dietary FA supplementation at 200 mg/kg feed), Group 4 (dietary FA supplementation at 400 mg/kg feed), and Group 5 (dietary FA supplementation at 800 mg/kg feed).*

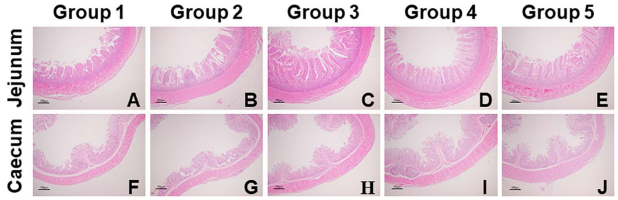

FIGURE 1 | Representative images of jejunal **(A–E)** and cecal **(F–J)** morphology of experimental ducks in different groups (40 × magnification). Intestinal issue samples were processed with hematoxylin and eosin stain.

levels of IL-6 ($P = 0.04$) and IL-2 ($P = 0.02$) comparing to Group 1. Negative linear ($P < 0.05$) and quadratic ($P < 0.05$) relationships were found between dietary FA concentration and the IL-6, as well as the IL-2 levels.

Intestinal Morphology

As shown in **Table 5**, compared to Group 1, Group 4 and 5 showed significantly decreased crypt depth in the jejunum ($P = 0.01$); Group 3, 4, and 5 showed significantly increased VCR in the jejunum ($P = 0.02$); and Group 4 showed significantly decreased crypt depth in the caecum ($P = 0.04$). Significant linear ($P < 0.01$) and quadratic ($P < 0.01$) relationships were noticed between dietary FA and the crypt depth (negative) and VCR (positive) in the jejunum; and significant quadratic but no linear relationship were found between the dietary FA and the crypt depth in the cecum ($P < 0.05$). In the representative images of jejunum and cecum tissues, it was noticeable that the intestinal mucosae in FA treated groups were more intact than those in Group 1 (**Figure 1**).

Modulation of Gut Microbiota

The compositions of cecal microbiota in all groups were analyzed by 16S rRNA sequencing. According to the α diversity result (**Table 6**), the cecal microbial abundances or diversities at the genera level were similar among groups ($P > 0.05$). PCA and ANOSIM further revealed no clear clustering patterns for cecal microbiota at genera level among groups ($P = 0.40$), as showed in **Figure 2**.

The eight most predominant microbial phyla among groups were *Firmicutes* (43.3–48.7%), *Bacteroidetes* (40.5–47.8%), *Spirochaetes* (1.0–6.5%), *Actinobacteriota* (1.9–3.2%), *Desulfobacterota* (1.0–3.0%), *Fusobacteriota* (0.4–5.6%), *Deferribacterota* (0.1–3.7%), and *Proteobacteria* (0.9–1.7%)

TABLE 6 | The parameters of α diversity of cecal microbiota in different groups[1].

Parameter	Treatments[2]					SEM	*P* value
	Group 1	Group 2	Group 3	Group 4	Group 5		
Shannon	3.28	3.27	3.22	3.18	3.31	0.28	0.95
Simpson	0.085	0.090	0.087	0.098	0.081	0.032	0.94
ACE	142.49	146.99	143.85	143.44	144.66	13.74	0.99
Chao	140.03	149.85	149.57	147.77	145.21	18.81	0.91

[1]Data is the mean of six birds per treatment. [2]Group 1 (control), Group 2 (dietary FA supplementation at 100 mg/kg feed), Group 3 (dietary FA supplementation at 200 mg/kg feed), Group 4 (dietary FA supplementation at 400 mg/kg feed), and Group 5 (dietary FA supplementation at 800 mg/kg feed).

(**Figure 3A**). No significant differences in mean proportion were found in microbial communities at the phyla level among groups ($P > 0.05$). But at genera level, a total of eight microbial genera were found significantly different among ($P < 0.05$) groups (**Figure 3B**). Pair-wise comparisons with Student's *T* test for the differences in microbial composition at genus level were further conducted between Group 1 and FA treated groups. Significant differences were found in proportions of *Faecalibacterium*, *Paludicola*, *Anaerofilum*, RF39, and *Faecalicoccus* between Group 1 and 2 ($P < 0.05$) (**Figures 4A–E**), *Paludicola* between Group 1 and 3 ($P < 0.05$) (**Figure 4B**), *Faecalibacterium*, RF39, and UCG-002 between Group 1 and 4 ($P < 0.05$) (**Figures 4A,D,F**), and *Faecalicoccus* and UCG-002 between Group 1 and 5 ($P < 0.05$) (**Figures 4E,F**).

The relationships between the cecal microbiota and the parameters relating to the growth performance, levels of cytokines representing the oxidative and inflammatory statuses were examined *via* Spearman's correlation analysis. Data were showed in **Figure 5**. ADG was positively associated with the phylum *Proteobacteria* ($P = 0.035$), order *Oscillospirales* ($P = 0.018$), and family *Ruminococcaceae* ($P = 0.006$); and F/G was negatively associated with the phylum *Proteobacteria* ($P = 0.002$). Additionally, GSH level was negatively associated with the class *Negativicutes* ($P = 0.036$); and GSH-Px activity was negatively associated with the phylum *Bacteroidetes* ($P = 0.013$) and family *Rikenellaceae* ($P = 0.003$). Finally, IgG level was positively associated with the class *Bacilli* ($P = 0.049$); IL-1β level was positively associated with the phylum *Cyanobacteria* ($P = 0.050$); IL-2 level was positively associated with the phylum *Elusimicrobia* ($P = 0.032$); and IL-6 level was positively associated with phylum *Bacteroidetes* ($P = 0.012$), family *Rikenellaceae* ($P = 0.013$), and genus *Prevotella* ($P = 0.017$).

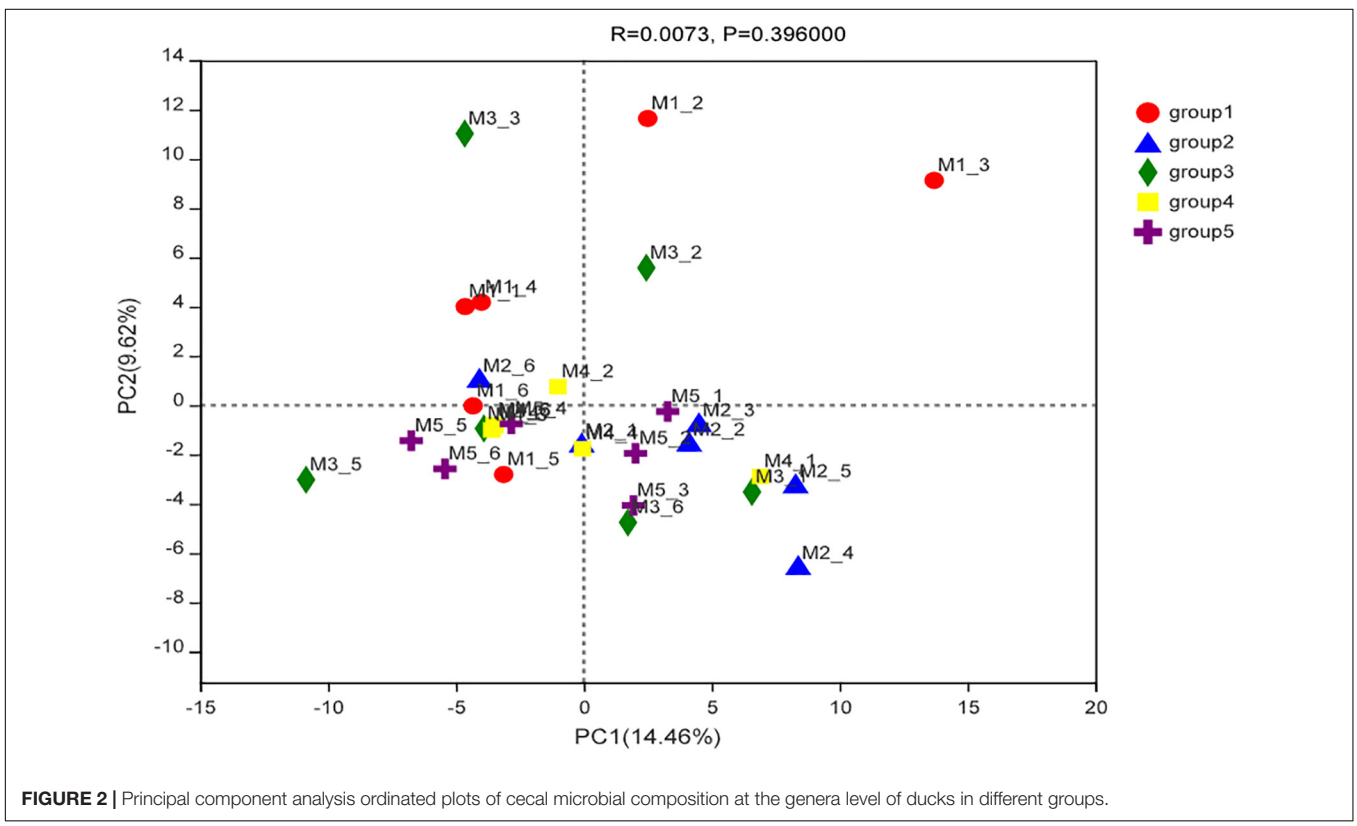

FIGURE 2 | Principal component analysis ordinated plots of cecal microbial composition at the genera level of ducks in different groups.

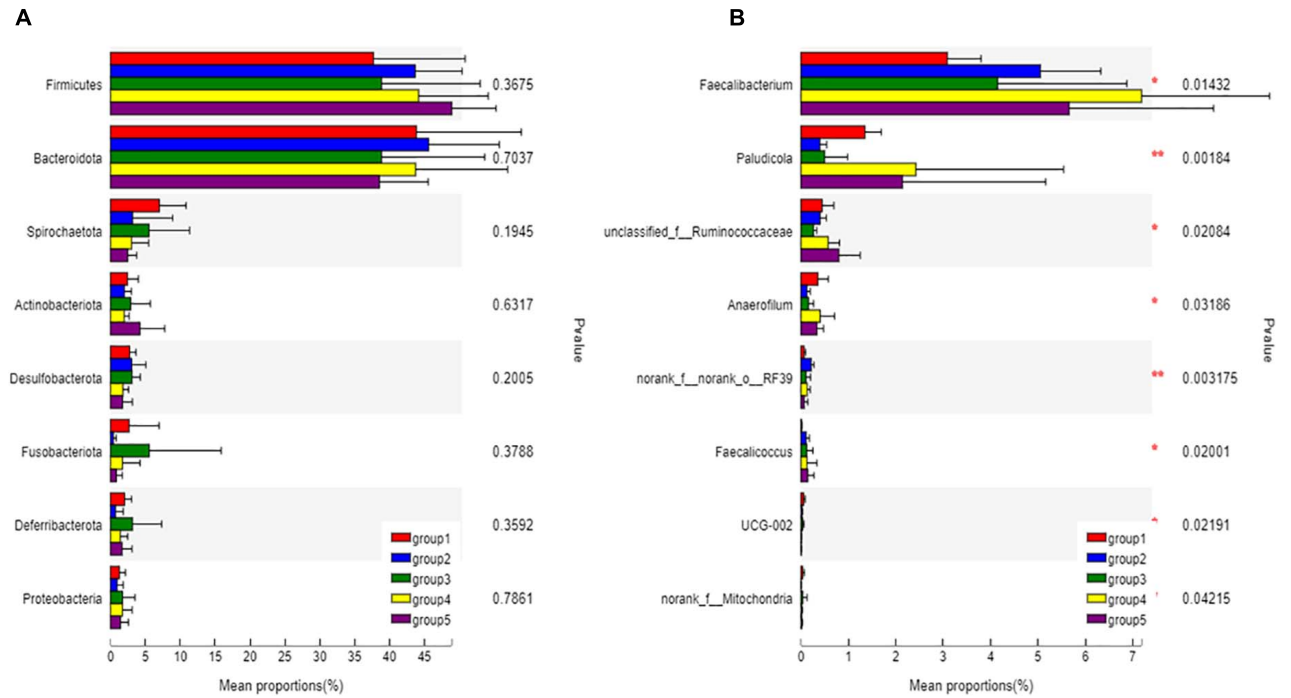

FIGURE 3 | Classification and differences in cecal microbial composition of ducks in different groups. The eight most abundant bacteria at the phyla level **(A)** and bacteria with significant difference at genus level **(B)** among five groups were showed. Relative abundance of altered cecal microbiota levels were tested under ANOVA and Tukey *post hoc* analysis. Significant correlations were marked by *$0.01 < P < 0.05$, **$0.001 < P \leq 0.01$.

DISCUSSION

Stresses were the main factors that deteriorated the profits in poultry industry as the intensive system developing (Vizzier Thaxton et al., 2016). FA was reported to be able to ameliorate the oxidative stress by capturing reactive oxygen species (ROS) with its structure characteristics (Maurya and Devasagayam, 2010), and triggering the productions of the antioxidant enzymes through Nrf2-Keap1-ARE signaling pathway (Krajka-Kuźniak et al., 2015). Additionally, it was reported that FA could mediated the inflammation through IKK/NF-κB signaling pathway (Lampiasi and Montana, 2016). Some researchers utilized FA as feed additive in livestock farming and proved its beneficial effects. Wang et al. (2020) found that 0.05 and 0.45% FA supplemented in the diet improved the lipid profile and antioxidant capacity of the weaning piglets. González-Ríos et al. (2016) reported that steers fed diet with 6 mg/kg FA supplementation in the last 30 days of the finishing phase acquired better meat quality, and delayed lipid oxidation during storage. However, few papers were published relating to the effects of FA on poultry. In the present study, significant increase in ADG, and decrease in F/G ratio in ducks that fed diets supplemented with 200–800 mg/kg FA were detected during the growing stage (28–56 days of age). And the trends of changes were linear and quadratic related to the FA supplement rate. These results suggested promotional effects of FA on the growth performance of the ducks. As the writer's knowledge, this study is the first time using pure FA as feed additive in poultry experiment. Previous researchers tried diets supplemented with propolis, sorghum or other materials, of which FA was considered as the main substances, with birds. Positive results were found with propolis that they improved the feed efficiency and ameliorated the effects of stresses on the weight gain (Seven, 2008; Hassan and Abdulla, 2011; Abdel-Rahman, 2013), which corroborated with our finding. However, birds offered sorghum-based diets showed decreased body weight gains (Truong et al., 2016). The variations in the effects of FA enriched materials on bird's growth performance could partly be explained by the condensed tannins, other than the FA in the sorghum, negatively influenced energy utilization of starch, so that the weight gain of the birds decreased. It was also reported that FA in conjugated forms in plants might form complexes with debranched starch which caused the resistance to digestion (Hung et al., 2012).

In the present study, serum parameters related to the avian antioxidative status were investigated. Oxidative stress was mainly caused by the excessive accumulations of the ROS. In the organism, redox balance was modulated by the antioxidant defense system, consisting of enzymatic components such as SOD and GSH-Px, and non-enzymatic components such as GSH (Surai et al., 2019). Once the accumulation of ROS overpassed the scavenging capability of antioxidant defense system, the redox balance would break and the oxidative stress occurred (Nisar et al., 2013). MDA was formed by ROS degrading the polyunsaturated lipids in the organism, and was considered as a common biomarker for oxidative stress (Fu et al., 2013). The present study revealed the antioxidant effects of dietary

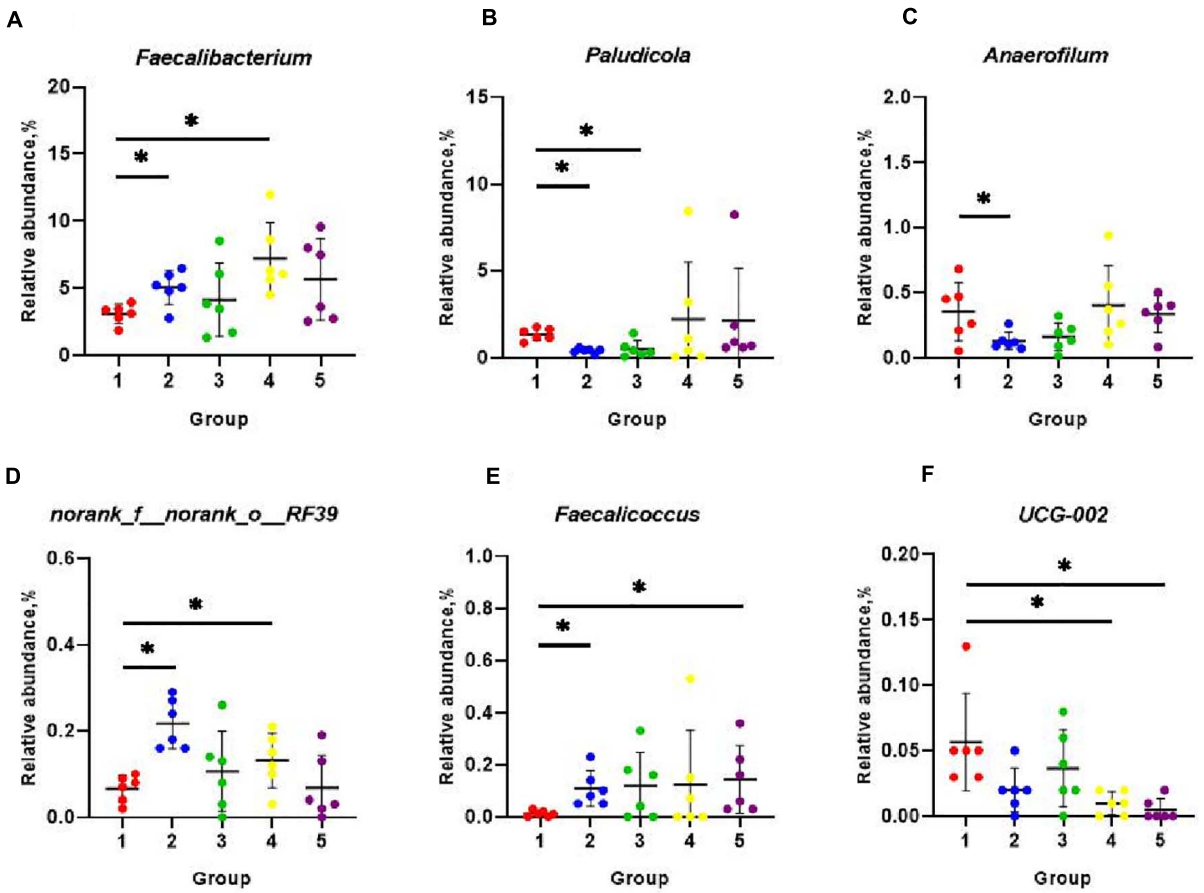

FIGURE 4 | Classification and differences in cecal microbial composition at the genera level among five groups. The relative abundance of microbial genera that significantly altered included *Faecalibacterium* **(A)**, *Paludicola* **(B)**, *Anaerofilum* **(C)**, norank_f_norank_o_RF39 **(D)**, *Faecalicoccus* **(E)**, and UCG-002 **(F)**. Data were shown as means ± SD ($n = 6$), $^*P < 0.05$ compared with Group 1.

FA, as it significantly improved the serum GSH levels and GSH-Px activities. Significant linear and quadratic relationships were noticed between the activities of GSH-Px and the rate of dietary FA. Similar results were found in multiple studies. The hepatic GSH contents and activities of SOD, catalase (CAT) and GSH-Px in methotrexate (MTX) induced rats were significantly alleviated after 15 days of oral supplements of 25 or 50 mg/kg FA (Mahmoud et al., 2020). It was also published that diets with 0.45% FA supplementation decreased the MDA contents, and increased the activities of CAT, total SOD and GSH-Px in the serums and the livers of the weaning pigs (Wang et al., 2020). Moreover, Wang et al. (2019) reported that 3-m-old lambs fed diet supplemented with 80 mg/kg FA showed higher plasma levels of GSH-Px, CAT and lower levels of MDA compared to the lambs fed basal diet.

Immunological stress was another notorious factor that deteriorated the animal performance (Lochmiller and Deerenberg, 2000). It usually occurred when animals were challenged by infectious agents, such as pathogenic organisms or environmental insults (Song et al., 2014). When immunological stress happened, both innate and adaptive systems in birds were triggered. Avian heterophils with strong phagocytic activities were firstly activated (Genovese et al., 2013). Later the basophils (Maxwell and Robertson, 1995), eosinophils (Maxwell, 1987), and dendritic cells (Ma S. et al., 2019) were involved as early modulators of inflammation and/or antigen presenters who initiated the adaptive immune responses. Lymphocyte cells in avian adaptive immune system were able to produce a diversity of antibodies, such as immunoglobulin M (IgM), IgG, and IgA, which served as the first line to fight against the intruders (Berghof et al., 2018). Simultaneously, the production of cytokines, such as IL-1β, IL-6, IL-2, were increased as chemical messengers that affected the proliferation, differentiation and activity of immune cells (Kaiser et al., 2005). In the present study, the addition of FA in diets significantly decreased the serum levels of IL-6 and IL-2, which outlined that the immunological status in the organism was ameliorated. Additionally, significant linear and quadratic relationships were noticed between the concentrations of dietary FA and the levels of the two cytokines. These results were partially consistent with previous findings in rats (Sadar et al., 2016; Mahmoud et al., 2020) and *in vitro* cell model (Cao et al., 2015), as FA

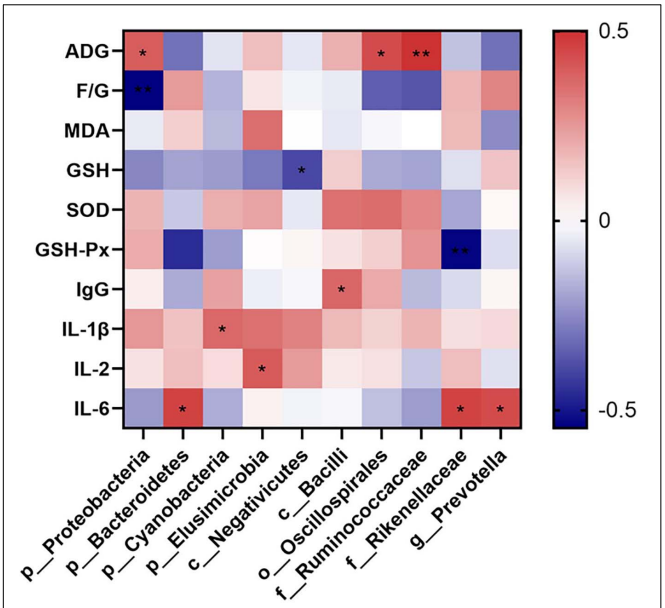

FIGURE 5 | Spearman correlation heatmap of cecal microbiota and the measured parameters. The intensity of the colors demonstrated the degree of association (blue, negative correlation; red, positive correlation). Significant correlations marked by *$0.01 < P \leq 0.05$, **$0.001 < P \leq 0.01$. ADG, average daily weight gain; F/G, ratio of feed intake to weight gain; MDA, malonaldehyde; GSH, glutathione; SOD, superoxide dismutase; GSH-Px, glutathione peroxidase; IgG, immunoglobulin G; IL-1β, interlukin-1β; IL-6, interlukin-6; IL-2, interleukin-2.

attenuated not only the level of IL-6 but also IL-1β in the pathogenic circumstances.

Gastrointestinal tract (GIT) was essential for the growth of animals, and its integrity was a key factor for preventing pathogenic microorganism invasion and utilizing the nutrients (Choct, 2009). Villus height reflected the intestinal absorptive capacities of the nutrients and the crypt depth represented the colonization rate and the maturities of the crypt cells (Feng et al., 2017). The ratio of these two parameters was regarded as a general indicator for the intestinal function. Additionally, intestinal wall and mucosa were the foundations to GIT's barrier function, of which the thickness was extremely critical. In our study, 200–800 mg/kg dietary FA supplementation linearly and quadratically decreased the crypt depth and increased the VCR of the jejunum, and 100–400 mg/kg dietary FA quadratically decreased the crypt depth of the caecum, demonstrating enhancing effects of dietary FA on the intestinal morphology in the ducks. This result was supported by previous research that 50 mg FA/kg body weight attenuated the effects of heat stress on rats' intestinal permeability and microvilli structure (He et al., 2016). It was further reported that the beneficial effects of FA on the intestinal morphology and barrier function were possibly contributed to the activation of Nrf2/HO-1 signaling pathway, which was associated to the process of ROS elimination as well (He et al., 2018).

Microorganism inhabiting in the GIT were involved in the digestion of food, breakdown of toxins, stimulation of immune system, exclusion of pathogens and endocrine activities. The interaction between the microorganism and GIT influenced the stability of microbial communities, the animal's health and the feed efficiency (Apajalahti et al., 2004). Cecum was the main location for the fermentation and digestion of complex substrates, so that it possesses the longest feed retention time and most diverse microorganism (Borda-Molina et al., 2018). In order to understand the effects of FA on the gut microbial environment, the chyme in the cecum were chosen in the present study for microbial community analysis. FA was reported to modulate gut microbiota composition in transverse aortic construction mice (Liu et al., 2019) and diabetic mice model (Ma y. et al., 2019; Huang et al., 2020). In present study, the differences of richness and diversity of cecal microbial community among groups were not statistically significant. The possible explanation to the inconsistencies might be the constructional and functional differences of the GIT between birds and mammals, as well as the sensitivities of the microbiome to FA in the diverse animal species. Previous papers illustrated that cecal bacterial microbiome of birds were usually dominated by members of the phyla *Bacteroidetes* and *Firmicutes*, followed by lower abundance of *Proteobacteria*, *Actinobacteria* and others (Costa et al., 2017; She et al., 2018; Xia et al., 2019). It was consistence with the cecal microbial construction in the present study. All groups in our study showed similar patterns of cecal microbial compositions at phyla level, but the changes in relative abundance of some bacteria at genera level were detected. Pair-wise comparison between the FA treated and untreated groups further suggested that different rates of dietary FA could alter the microbial compositions in the cecum. It was well documented that the intestinal microbiome closely interacted with the host through the exchange of nutrients, modulation of gut morphology and physiology, and maintenance of immune and redox homeostasis (Oakley et al., 2014; Pan and Yu, 2014; He et al., 2019)014). In the present study, the relative abundances of *Faecalibacterium* and *Faecalicoccus* were significantly increased with 400 and 800 mg/kg FA supplement, respectively. And the UCG-002 level was decreased in these two groups. Correspondingly, the ADGs were significantly higher in Group 4 (400 mg/kg FA) and 5 (800 mg/kg FA) compared to Group 1. Literatures indicated that species in *Faecalibacterium* were beneficial that improved the epithelial health and promoted the metabolite productions, especially butyrate and other SCFAs (Gangadoo et al., 2018), and *Faecalicoccus* belonged to family *Erysipelotrichaceae*, which was reported to be a major butyrate producer and considered more important in poultry cecum than those in human colon (Zhou et al., 2021). UCG-002 belongs to the family *Oscillospiraceae*, which was reported to be negatively related to the body weight gain of geese fed fermented feed (Yan et al., 2019). These studies were consistent with what we found, showing that the trends of changes in abundance of bacteria taxa mentioned above were correlative to the improvement in growth performance. *Anaerofilum* were published to be positively associated with the body weight gain in broilers fed dietary vitamins (Luo et al., 2013). But in the present study, we found inconsistent data regarding to the level of *Anaerofilum* and the body weight gains of the birds. *Paludicola* were a novel genus in the family

Ruminococcaceae, whose function in the gut was unknown yet (Li et al., 2017).

The Spearman correlation analysis disclosed that phylum *Proteobacteria*, order *Oscillospirales*, and family *Ruminococcaceae* were associated with the ADG, and phylum *Proteobacteria* were associated with the F/G ratio, which demonstrated the strong influences of such bacteria on the growth performance in ducks. Similar results were reported previously regarding to those bacteria. Though phylum *Proteobacteria* included several pathogens, they could degrade the nutrients in the diet and provide suitable environmental support for symbiotic bacteria, and eventually promoted the growth of layers (Li et al., 2020). Shi et al. (2019) stated that species in order *Oscillospirales*, such as *Oscillospira*, were butyrate producers and negatively related to the F/G ratio in broilers under heat stress. Additionally, major members in family *Ruminococcaceae* were short-chain fatty acids producing bacteria, and they were outstanding for improving feed efficiency and enhancing health for the host (Wong et al., 2006). In the present study, class *Negativicutes* was found negatively associated with the GSH levels, and phylum *Bacteroidetes* and family *Rikenellaceae* were negatively associated with the GSH-Px activities. These species might be possible positive symbols to the levels of oxidative stress of the host. It was consistent with previous studies that the relative abundances of class *Negativicutes* were reduced in ducks with oxidative stress caused by heat (He et al., 2019), phylum *Bacteroidetes* were positively related to oxidative stress in rats fed high-fat diets (Ortega-Hernández et al., 2020), and relative abundance of family *Rikenellaceae* decreased after polysaccharides from pollen of Chinese wolfberry, which attenuated the oxidative stress in cyclophosphamide-treated mice (Zhao et al., 2020). Moreover, we found that phylum *Bacteroidetes*, family *Rikenllaceae* and genus *Prevotella* were positively associated with IL-6 levels; and class *Bacilli*, phylum *Cyanobacteria*, and phylum *Elusimicrobia* were positively associated with IgG, IL-1β, and IL-2 levels respectively. These findings potentially indicated the positive relationships of the relative abundances of these markers to the levels of immune stress of the host. Besides the roles of representative to the oxidative stress, phylum *Bacteroidetes* were reported to be implicated in immune regulations including activations of inflammation and autoimmune diseases (Gibiino et al., 2018), and family *Rikenellaceae* were proved to be positive associated with the arise of immune response induced by *Pleurotus eryngii* polysaccharide in mice (Ma et al., 2017). *In vitro* study using human monocyte-derived dendritic cells proved that genus *Prevotella* exhibited capacities to induce inflammatory mediators like IL-6 (Horewicz et al., 2013). Additionally, members of family *bacilli*, including the Gram-negative *bacilli* were among the most common causative agents of infectious diseases, and triggers of the inflammation (Dandachi et al., 2019). Phylum *Cyanobacteria* were reported to be immune suppressing (Gemma et al., 2016), but some members in *Cyanobacteria*, for example *Microcystis aeruginosa*, whose lipopolysaccharide could trigger human immune response (Moosová et al., 2019). Moreover, phylum *Elusimicrobia* were proved to be positively correlated to multiple proinflammatory cytokines and promoted the occurrences of immunological stress in colitis rats (Tao et al., 2017), which was in line with our finding.

Even so, massive works were still required to clarify the mechanism of the influences of FA on ducks. The obtained alternations of microbial species associated with the dietary FA should be carefully validated. The molecular pathway associated with the amelioration of oxidative and immunological stress by FA was needed to be explored. And the participation of microbiota in the stress modulation still required to be discussed.

CONCLUSION

In conclusion, dietary supplementation of FA altered the intestinal microbiota at the genera level, which associated with the beneficial effects on the growth performance, anti-oxidant and anti-inflammatory capabilities, intestinal morphology, and epithelia barrier functions in *Linwu* ducks at the growing stage. Quantity effects were obvious as the significant linear and quadratic relationships were noticed between diet FA levels and the measured parameters. Considering the cost and the efficacy of dietary FA as feed additives, we concluded that 400 mg/kg was the suggested supplementation rate of FA in diets for *Linwu* ducks during growing stage for the future use as feed additive.

DATA AVAILABILITY STATEMENT

The datasets presented in this study can be found in online repositories. The names of the repository/repositories and accession number(s) can be found below: https://www.ncbi.nlm.nih.gov/, PRJNA723283.

ETHICS STATEMENT

The animal study was reviewed and approved by Hunan Agricultural University Institutional Animal Care and Use Committee.

AUTHOR CONTRIBUTIONS

QD and XGH conceived of and designed the experiments. YL, XH, CL, and GJ performed the sampling. XH performed the serum index measurement. XZ conducted the tissue section. QL performed the 16S rRNA sequencing experiment. YLL, QL, SL, and LH analyzed the data. YL wrote the manuscript. QL contributed to refining the text. All authors contributed to the article and approved the submitted version.

FUNDING

This study was funded by the National Waterfowl Industrial Technology System of China (CARS-42-21), Innovation and Entrepreneurship Technology Investment Project of Hunan Province (2018Gk5009), and Major and Special Science and Technology Project of Changsha City (kq1902034).

REFERENCES

Abdel-Rahman, M. A. (2013). Effect of propolis as additive on some behavioural patterns, performance and blood parameters in muscovy broiler ducks. *J. Adv. Vet. Res.* 3, 64–68.

Apajalahti, J., Kettunen, A., and Graham, H. (2004). Characteristics of the gastrointestinal microbial communities, with special reference to the chicken. *Worlds Poult. Sci. J.* 60, 223–232. doi: 10.1079/WPS200415

Averós, X., and Estevez, I. (2018). Meta-analysis of the effects of intensive rearing environments on the performance and welfare of broiler chickens. *Poult. Sci.* 97, 3767–3785. doi: 10.3382/ps/pey243

Berghof, T. V. L., Arts, J. A. J., Bovenhuis, H., Lammers, A., Van der Poel, J. J., and Parmentier, H. K. (2018). Antigen-dependent effects of divergent selective breeding based on natural antibodies on specific humoral immune responses in chickens. *Vaccine* 36, 1444–1452. doi: 10.1016/j.vaccine.2018.01.063

Borda-Molina, D., Seifert, J., and Camarinha-Silva, A. (2018). Current perspectives of the chicken gastrointestinal tract and its microbiome. *Comput. Struct. Biotechnol. J.* 16, 131–139. doi: 10.1016/j.csbj.2018.03.002

Cao, Y., Zhang, Y., Qi, J., Liu, R., Zhang, H., and He, L. (2015). Ferulic acid inhibits h2o2-induced oxidative stress and inflammation in rat vascular smooth muscle cells via inhibition of the nadph oxidase and nf-κb pathway. *Int. Immunopharmacol.* 28, 1018–1025. doi: 10.1016/j.intimp.2015.07.037

Castanon, J. I. R. (2007). History of the use of antibiotic as growth promoters in european poultry feeds. *Poult. Sci.* 86, 2466–2471. doi: 10.3382/ps.2007-00249

Choct, M. (2009). Managing gut health through nutrition. *Br. Poult. Sci.* 50, 9–15. doi: 10.1080/00071660802538632

Costa, M. C., Bessegatto, J. A., Alfieri, A. A., Weese, J. S., and Oba, A. (2017). Different antibiotic growth promoters induce specific changes in the cecal microbiota membership of broiler chicken. *PLoS One* 12:e0171642. doi: 10.1371/journal.pone.0171642

Daglia, M. (2012). Polyphenols as antimicrobial agents. *Curr. Opin. Biotechnol.* 23, 174–181. doi: 10.1016/j.copbio.2011.08.007

Dandachi, I., Chaddad, A., Hanna, J., Matta, J., and Daoud, Z. (2019). Understanding the epidemiology of multi-drug resistant gram-negative bacilli in the middle east using a one health approach. *Front. Microbiol.* 10:1941. doi: 10.3389/fmicb.2019.01941

Feng, G. D., He, J., Ao, X., and Chen, D. W. (2017). Effects of maize naturally contaminated with aflatoxin b1on growth performance, intestinal morphology, and digestive physiology in ducks. *Poult. Sci.* 96, 1948–1955. doi: 10.3382/ps/pew420

Fu, J., Liu, C. P., Zhang, Z. W., Xing, M. W., and Xu, S. W. (2013). Influence of inflammatory pathway markers on oxidative stress induced by cold stress in intestine of quails. *Res. Vet. Sci.* 95, 495–501. doi: 10.1016/j.rvsc.2013.05.006

Gangadoo, S., Dinev, I., Chapman, J., Hughes, R. J., Van, T. T. H., Moore, R. J., et al. (2018). Selenium nanoparticles in poultry feed modify gut microbiota and increase abundance of faecalibacterium prausnitzii. *Appl. Microbiol. Biotechnol.* 102, 1455–1466. doi: 10.1007/s00253-017-8688-4

Gemma, S., Molteni, M., and Rossetti, C. (2016). Lipopolysaccharides in cyanobacteria: a brief overview. *Adv. Microbiol.* 06, 391–397. doi: 10.4236/aim.2016.65038

Genovese, K. J., He, H., Swaggerty, C. L., and Kogut, M. H. (2013). The avian heterophil. *Dev. Comp. Immunol.* 41, 334–340. doi: 10.1016/j.dci.2013.03.021

Gibiino, G., Lopetuso, L., Scaldaferri, F., Rizzatti, G., Binda, C., and Gasbarrini, A. (2018). Exploring bacteroidetes: metabolic key points and immunological tricks of our gut commensals. *Digest. Liver Dis.* 50, 635–639. doi: 10.1016/j.dld.2018.03.016

González-Ríos, H., Dávila-Ramírez, J. L., Peña-Ramos, E. A., Valenzuela-Melendres, M., Zamorano-García, L., Islava-Lagarda, T. Y., et al. (2016). Dietary supplementation of ferulic acid to steers under commercial feedlot feeding conditions improves meat quality and shelf life. *Anim. Feed. Technol.* 222, 111–121. doi: 10.1016/j.anifeedsci.2016.10.011

Gupta, K. M., Das, S., Chow, P. S., and Macbeath, C. (2020). Encapsulation of ferulic acid in lipid nanoparticles as antioxidant for skin: mechanistic understanding through experiment and molecular simulation. *ACS Appl. Nano Mater.* 3, 5351–5361. doi: 10.1021/acsanm.0c00717

Hassan, M. G., and Abdulla, T. A. (2011). The effect of propolis feed supplementation on hygiene and performance. *Iraqi J. Vet. Sci.* 25, 77–82. doi: 10.33899/ijvs.2011.5647

Hayes, J., English, L., Carr, L., Wagner, D., and Joseph, S. (2004). Multiple-antibiotic resistance of enterococcus spp. Isolated from commercial poultry production environments. *Appl. Environ. Microbiol.* 70, 6005–6011. doi: 10.1128/aem.70.10.6005-6011.2004

He, S., Guo, Y., Zhao, J., Xu, X., Song, J., Wang, N., et al. (2018). Ferulic acid protects against heat stress-induced intestinal epithelial barrier dysfunction in iec-6 cells via the pi3k/akt-mediated nrf2/ho-1 signaling pathway. *Int. J. Hypertherm.* 35, 112–121. doi: 10.1080/02656736.2018.1483534

He, S., Liu, F., Xu, L., Yin, P., Li, D., Mei, C., et al. (2016). Protective effects of ferulic acid against heat stress-induced intestinal epithelial barrier dysfunction in vitro and in vivo. *PLoS One* 11:e0145236. doi: 10.1371/journal.pone.0145236

Horewicz, V. V., Barbuto, J. A., Cury, P. R., and Carmo, J. P. (2013). Altered phenotype and function of dendritic cells in individuals with chronic periodontitis. *Arch. Oral Biol.* 58, 1208–1216. doi: 10.1016/j.archoralbio.2013.03.013

Huang, J. Q., Wu, M. S., Tao, G., Lu, M. W., and Song, Y. (2020). Feruloylated oligosaccharides and ferulic acid alter gut microbiome to alleviate diabetic syndrome. *Food Res. Int.* 137:109410. doi: 10.1016/j.foodres.2020.109410

Hung, P. V., Phat, N. H., and Phi, N. T. L. (2012). Physicochemical properties and antioxidant capacity of debranched starch-ferulic acid complexes. *Starch Stärke* 65, 382–389. doi: 10.1002/star.201200168

Jinhua, G., Hui, Y., Weikang, G., Ying, K., Lina, G., Qi, L., et al. (2018). The anticancer effects of ferulic acid is associated with induction of cell cycle arrest and autophagy in cervical cancer cells. *Cancer Cell Int.* 18:102. doi: 10.1186/s12935-018-0595-y

He, J., He, Y., Pan, D., Cao, J., Sun, Y., and Zeng, X. (2019). Associations of gut microbiota with heat stress-induced changes of growth, fat deposition, intestinal morphology, and antioxidant capacity in ducks. *Front. Microbiol.* 10:903. doi: 10.3389/fmicb.2019.00903

Kaiser, P., Poh, T. Y., Rothwell, L., Avery, S., and Young, J. R. (2005). A genomic analysis of chicken cytokines and chemokines. *J. Interferon Cytokine Res.* 25, 467–484. doi: 10.1089/jir.2005.25.467

Krajka-Kuźniak, V., Paluszczak, J., Szaefer, H., and Baer-Dubowska, W. (2015). The activation of the nrf2/are pathway in hepg2 hepatoma cells by phytochemicals and subsequent modulation of phase ii and antioxidant enzyme expression. *J. Physiol. Biochem.* 71, 227–238. doi: 10.1007/s13105-015-0401-4

Lampiasi, N., and Montana, G. (2016). The molecular events behind ferulic acid mediated modulation of il-6 expression in lps-activated raw 264.7 cells. *Immunobiology* 221, 486–493. doi: 10.1016/j.imbio.2015.11.001

Lauridsen, C. (2018). From oxidative stress to inflammation: redox balance and immune system. *Poult. Sci.* 98, 4240–4246. doi: 10.3382/ps/pey407

Li, S., Yan, C., Liu, T., Xu, C., Wen, K., Liu, L., et al. (2020). Research note: increase of bad bacteria and decrease of good bacteria in the gut of layers with vs. Without hepatic steatosis. *Poult. Sci.* 99, 5074–5078. doi: 10.1016/j.psj.2020.07.007

Li, Y., Zhang, L., Liu, L., Tian, Y., Liu, X., Li, W., et al. (2017). Paludicola psychrotolerans gen. Nov., sp. Nov., a novel psychrotolerant chitinolytic anaerobe of the family ruminococcaceae. *Int. J. Syst. Evol. Microbiol.* 67, 4100–4103. doi: 10.1099/ijsem.0.002260

Li, Y. J., Li, L., Li, J. L., Zhang, L., and Zhou, G. H. (2015). Effects of dietary supplementation with ferulic acid or vitamin e individually or in combination on meat quality and antioxidant capacity of finishing pigs. *Asian Austrl. J. Anim. Sci.* 28, 374–381. doi: 10.5713/ajas.14.0432

Liu, Z., Ma, Z., Zhang, H., Summah, B. S., Liu, H., An, D., et al. (2019). Ferulic acid increases intestinal lactobacillus and improves cardiac function in tac mice. *Biomed. Pharmacother.* 120:109482. doi: 10.1016/j.biopha.2019.109482

Lolli, S., Meluzzi, A., Barbieri, S., Vezzoli, G., and Ferrante, V. (2010). Rearing conditions on broiler welfare. Effect of rearing conditions and litter type on

reactivity, plumage conditions and foot-pad lesions of broiler chickens. *Zootec. Int.* 4, 32–37.

Luo, Y. H., Peng, H. W., Wright, G. A. D., Bai, S. P., Ding, X. M., Zeng, Q. F., et al. (2013). Broilers fed dietary vitamins harbor higher diversity of cecal bacteria and higher ratio of clostridium, faecalibacterium, and lactobacillus than broilers with no dietary vitamins revealed by 16s RRNA gene clone libraries. *Poult. Sci.* 92, 2358–2366. doi: 10.3382/ps.2012-02935

Ma, G., Muinde, B., Zhao, L., Yang, W., and Hu, Q. (2017). In vivo fermentation of pleurotus eryngii polysaccharide and its effects on fecal microbiota composition and immune response. *Food Funct.* 8, 1810–1821. doi: 10.1039/C7FO00341B

Ma, S., Qiao, X., Xu, Y., Wang, L., and Li, Y. (2019). Screening and identification of a chicken dendritic cell binding peptide by using a phage display library. *Front. Immunol.* 10:1853. doi: 10.3389/fimmu.2019.01853

Ma, Y., Chen, K., Lv, L., Wu, S., and Guo, Z. (2019). Ferulic acid ameliorates nonalcoholic fatty liver disease and modulates the gut microbiota composition in high-fat diet fed apoe/ mice. *Biomed. Pharmacother.* 113:108753. doi: 10.1016/j.biopha.2019.108753

Mahmoud, A. M., Hussein, O. E., Hozayen, W. G., Bin-Jumah, M. N., and El-Tawab, S. A. (2020). Ferulic acid prevents oxidative stress, inflammation, and liver injury via upregulation of nrf2/ho-1 signaling in methotrexate-induced rats. *Environ. Sci. Pollut. Res.* 27, 7910–7921. doi: 10.1007/s11356-019-07532-6

Maurya, D. K., and Devasagayam, T. P. A. (2010). Antioxidant and prooxidant nature of hydroxycinnamic acid derivatives ferulic and caffeic acids. *Food Chem. Toxicol.* 48, 3369–3373. doi: 10.1016/j.fct.2010.09.006

Maxwell, M. H. (1987). The avian eosinophil—a review. *Worlds Poult. Sci. J.* 43, 190–207. doi: 10.1079/WPS19870013

Maxwell, M. H., and Robertson, G. W. (1995). The avian basophilic leukocyte: a review. *Worlds Poult. Sci. J.* 51, 307–325. doi: 10.1079/WPS19950021

Moosová, Z., Šindlerová, L., Ambrùzová, B., Ambrožová, G., Vašíèek, O., Velki, M., et al. (2019). Lipopolysaccharides from microcystis cyanobacteria-dominated water bloom and from laboratory cultures trigger human immune innate response. *Toxins (Basel)* 11:218. doi: 10.3390/toxins11040218

National Research Council. (1994). *Nutrient Requirements of Poultry*, 9th ed. Washington, DC: The National Academies Press.

Nisar, N. A., Sultana, M., Waiz, H. A., Para, P. A., and Dar, S. A. (2013). Oxidative stress - threat to animal health and production. *Int. J. Livestock Res.* 3, 76–83.

Oakley, B. B., Lillehoj, H. S., Kogut, M. H., Kim, W. K., Maurer, J. J., Pedroso, A., et al. (2014). The chicken gastrointestinal microbiome. *FEMS Microbiol. Lett.* 360, 100–112. doi: 10.1111/1574-6968.12608

Ortega-Hernández, A., Martínez-Martínez, E., Gómez-Gordo, R., López-Andrés, N., and Cachofeiro, V. (2020). The interaction between mitochondrial oxidative stress and gut microbiota in the cardiometabolic consequences in diet-induced obese rats. *Antioxidants* 9:640. doi: 10.3390/antiox9070640

Ou, S., and Kwok, K. C. (2004). Ferulic acid: pharmaceutical functions, preparation and applications in foods. *J.Sci. Food Agric.* 84, 1261–1269. doi: 10.1002/jsfa.1873

Ou, S., Yong, W., Tang, S., Huang, C., and Jackson, M. G. (2005). Role of ferulic acid in preparing edible films from soy protein isolate. *J. Food Eng.* 70, 205–210. doi: 10.1016/j.jfoodeng.2004.09.025

Pan, D., and Yu, Z. (2014). Intestinal microbiome of poultry and its interaction with host and diet. *Gut Microbes* 5, 108–119. doi: 10.4161/gmic.26945

Rehman, M. S., Mahmud, A., Mehmood, S., Pasha, T. N., Hussain, J., and Khan, M. T. (2017). Blood biochemistry and immune response in aseel chicken under free range, semi-intensive, and confinement rearing systems. *Poult. Sci.* 96, 226–233. doi: 10.3382/ps/pew278

Lochmiller, R. L., and Deerenberg, C. (2000). Trade-offs in evolutionary immunology: Just what is the cost of immunity? *Oikos* 88, 87–98. doi: 10.1034/j.1600-0706.2000.880110.x

Robins, A., and Phillips, C. J. C. (2011). International approaches to the welfare of meat chickens. *Worlds Poult. Sci. J.* 67, 351–369. doi: 10.1017/S0043933911000341

Sadar, S. S., Vyawahare, N. S., and Bodhankar, S. L. (2016). Ferulic acid ameliorates tnbs-induced ulcerative colitis through modulation of cytokines, oxidative stress, inos, cox-2, and apoptosis in laboratory rats. *Excli. J.* 15, 482–499. doi: 10.17179/excli2016-393

Seven, P. T. (2008). The effects of dietary turkish propolis and vitamin c on performance, digestibility, egg production and egg quality in laying hens under different environmental temperatures. *Asian Austrl. J. Anim. Sci.* 21, 1164–1170. doi: 10.1016/j.applanim.2007.10.001

She, Y., Cai, H., and Liu, G. (2018). Effects of antibiotic on microflora in ileum and cecum for broilers by 16s rrna sequence analysis. *Anim. Sci. J.* 89, 1680–1691. doi: 10.1111/asj.13113

Shi, D., Bai, L., Qu, Q., Zhou, S., Yang, M., Guo, S., et al. (2019). Impact of gut microbiota structure in heat-stressed broilers. *Poult. Sci.* 98, 2405–2413. doi: 10.3382/ps/pez026

Song, C., Jiang, J., Han, X., Yu, G., and Pang, Y. (2014). Effect of immunological stress to neuroendocrine and gene expression in different swine breeds. *Mol. Biol. Rep.* 41, 3569–3576. doi: 10.1007/s11033-014-3219-1

Surai, P., Kochish, I., Fisinin, V., and Kidd, M. (2019). Antioxidant defence systems and oxidative stress in poultry biology: an update. *Antioxidants* 8:235. doi: 10.3390/antiox8070235

Tao, J. H., Duan, J. A., Jiang, S., Feng, N. N., and Ling, Y. (2017). Polysaccharides from chrysanthemum morifolium ramat ameliorate colitis rats by modulating the intestinal microbiota community. *Oncotarget* 8, 80790–80803. doi: 10.18632/oncotarget.20477

Truong, H. H., Neilson, K. A., Mcinerney, B. V., Khoddami, A., Roberts, T. H., Cadogan, D. J., et al. (2016). Comparative performance of broiler chickens offered nutritionally equivalent diets based on six diverse, 'tannin-free' sorghum varieties with quantified concentrations of phenolic compounds, kafirin, and phytate. *Anim. Product. Sci.* 57, 828–838. doi: 10.1071/AN16073

Valenzuela-Grijalva, N. V., Pinelli-Saavedra, A., Muhlia-Almazan, A., Domínguez-Díaz, D., and González-Ríos, H. (2017). Dietary inclusion effects of phytochemicals as growth promoters in animal production. *J. Anim. Sci. Technol.* 59:8. doi: 10.1186/s40781-017-0133-9

Vizzier Thaxton, Y., Christensen, K. D., Mench, J. A., Rumley, E. R., Daugherty, C., Feinberg, B., et al. (2016). Symposium: animal welfare challenges for today and tomorrow. *Poult. Sci.* 95:2198. doi: 10.3382/ps/pew099

Wang, O., Liu, J., Cheng, Q., Guo, X., and Wang, Y. (2015). Effects of ferulic acid and γ-oryzanol on high-fat and high-fructose diet-induced metabolic syndrome in rats. *PLoS One* 10:e0118135. doi: 10.1371/journal.pone.0118135

Wang, S., Chen, L., He, M., Shen, J., Li, G., Tao, Z., et al. (2018). Different rearing conditions alter gut microbiota composition and host physiology in shaoxing ducks. *Sci. Rep.* 8:7387. doi: 10.1038/s41598-018-25760-7

Wang, W. M., Peng, H., and Zhang, G. J. (2018). Specificity of ferulic acid in the chinese pharmacopoeia as a quality evaluation index for various chinese medicinal materials. *China J. Tradition. Chin. Med. Pharm.* 12, 407–409.

Wang, Y., Chen, X., Huang, Z., Chen, D., Yu, B., Yu, J., et al. (2020). Dietary ferulic acid supplementation improves antioxidant capacity and lipid metabolism in weaned piglets. *Nutrients* 12:3811. doi: 10.3390/nu12123811

Wang, Y., Wang, W., Wang, R., Meng, Z., Duan, Y., An, X., et al. (2019). Dietary supplementation of ferulic acid improves performance and alleviates oxidative stress of lambs in a cold envrionment. *Can. J. Anim. Sci.* 99, 705–712. doi: 10.1139/cjas-2018-0200

Wong, J. M. W., De Souza, R., Kendall, C. W. C., Emam, A., and Jenkins, D. J. A. (2006). Colonic health: fermentation and short chain fatty acids. *J. Clin. Gastroenterol.* 40, 235–243. doi: 10.1097/00004836-200603000-00015

Xia, Y., Kong, J., Zhang, G., Zhang, X., and Kong, Y. (2019). Effects of dietary supplementation with lysozyme on the structure and function of the cecal microbiota in broiler chickens. *PLoS One* 14:e0216748. doi: 10.1371/journal.pone.0216748

Yan, J., Zhou, B., Xi, Y., Huan, H., and Li, M. (2019). Fermented feed regulates growth performance and the cecal microbiota community in geese. *Poult. Sci.* 98, 4673–4684. doi: 10.3382/ps/pez169

Zhao, Y., Yan, Y., Zhou, W., Chen, D., and Cao, Y. (2020). Effects of polysaccharides from bee collected pollen of chinese wolfberry on immune response and gut

microbiota composition in cyclophosphamide-treated mice. *J. Funct. Foods* 72:104057. doi: 10.1016/j.jff.2020.104057

Zhou, J., Wu, S., Qi, G., Fu, Y., Wang, W., Zhang, H., et al. (2021). Dietary supplemental xylooligosaccharide modulates nutrient digestibility, intestinal morphology, and gut microbiota in laying hens. *Anim. Nutr.* 7, 152–162. doi: 10.1016/j.aninu.2020.05.010

Zhou, Z., Xu, J., Zhao, W., Chen, X., Jin, Y., Tang, N., et al. (2017). Ferulic acid relaxed rat aortic, small mesenteric and coronary arteries by blocking voltage-gated calcium channel and calcium desensitization via dephosphorylation of erk1/2 and mypt1. *Eur. J. Pharmacol.* 815, 26–32. doi: 10.1016/j.ejphar.2017.10.008

Zhu, Z. (2011). Poultry rearing environment and poultry diseases prevention and control. *Bjing Agric.* 12, 102–103.

Conflict of Interest: SL was employed by the company Shandong Lonct Enzymes Co., Ltd. YLL was employed by the company Hunan Perfly Biotech Co., Ltd.

The remaining authors declare that the research was conducted in the absence of any commercial or financial relationships that could be construed as a potential conflict of interest.

frontiers in Microbiology

ORIGINAL RESEARCH
published: 20 July 2021
doi: 10.3389/fmicb.2021.693839

Effect of Dietary Amylose/Amylopectin Ratio on Intestinal Health and Cecal Microbes' Profiles of Weaned Pigs Undergoing Feed Transition or Challenged With *Escherichia coli* Lipopolysaccharide

Can Yang[1,2,3†], Min Wang[1†], XiaoWu Tang[4], HuanSheng Yang[1], FengNa Li[3], YanCan Wang[1], Jianzhong Li[1] and YuLong Yin[1,3*]*

[1] Hunan International Joint Laboratory of Animal Intestinal Ecology and Health, Laboratory of Animal Nutrition and Hunan Health, College of Life Science, Hunan Normal University, Changsha, China, [2] Hunan Provincial Key Laboratory of Biological Resources Protection and Utilization in Nanyue Mountain Area, College of Life Sciences and Environment, Hengyang Normal University, Hengyang, China, [3] Key Laboratory of Agro-ecological Processes in Subtropical Region, Hunan Provincial Engineering Research Center of Health Livestock, Institute of Subtropical Agriculture, Chinese Academy of Sciences, Changsha, China, [4] College of Bioengineering, Hunan Vocational Technical College of Environment and Biology, Hengyang, China

OPEN ACCESS

Edited by:
Peng Huang,
Hunan Agricultural University, China

Reviewed by:
Kai Qiu,
Chinese Academy of Agricultural Sciences (CAAS), China
Jaime Parra-Suescún,
National University of Colombia, Medellin, Colombia
Xiao Xu,
Wuhan Polytechnic University, China

***Correspondence:**
HuanSheng Yang
yhs@hunnu.edu.cn
YuLong Yin
yinyulong@isa.ac.cn

[†] These authors have contributed equally to this work

Specialty section:
This article was submitted to Microbial Symbioses, a section of the journal Frontiers in Microbiology

Received: 12 April 2021
Accepted: 09 June 2021
Published: 20 July 2021

Citation:
Yang C, Wang M, Tang XW, Yang HS, Li FN, Wang YC, Li JZ and Yin YL (2021) Effect of Dietary Amylose/Amylopectin Ratio on Intestinal Health and Cecal Microbes' Profiles of Weaned Pigs Undergoing Feed Transition or Challenged With Escherichia coli Lipopolysaccharide. Front. Microbiol. 12:693839. doi: 10.3389/fmicb.2021.693839

Background: Dietary amylose/amylopectin ratio (DAR) plays an important role in piglets' intestinal health. It is controversial whether diarrhea could be relieved by changing DAR in weaning piglets.

Methods: Sixty (Landrace × Yorkshire) castrated male pigs (initial body weight (BW) 6.51 ± 0.64 kg) were randomly allocated to five groups (one pig per cage and 12 replicates per group) according to their BW. Piglets received diets with different DARs (0.00, 0.20, 0.40, 0.60, and 0.80) for 29 days. Feed transition occurs at day 15. The piglets were challenged with lipopolysaccharides (*Escherichia coli* LPS, 100 μg/kg BW) on day 29 by intraperitoneal injection at 12 h before slaughter. Chyme was collected for pH value, short-chain fatty acid (SCFA), and cecal microbe analysis using 16S rRNA gene sequencing; mucosa was sampled for detecting gene expression.

Results: Rate and degree of diarrhea were higher when DAR was 0.40 than when it was 0.20 and 0.80 during the third week ($P < 0.05$). The chyme pH value in the cecum was higher ($P < 0.05$) in 0.20 DAR than in 0.00 and 0.80 DARs, but with no significant difference compared with 0.40 and 0.60 DARs ($P > 0.05$). Cecal isobutyric acid and isovaleric acid concentrations were higher in 0.20 than in other groups ($P < 0.01$). Cecal SCFAs such as acetic acid, propionic acid, and total SCFA, concentrations were higher in 0.40 DAR than in 0.00, 0.60, and 0.80 DARs ($P < 0.05$), but with no significant difference when compared with 0.20 ($P > 0.05$). Cecal crypt depth was lower ($P < 0.05$) in 0.80 than in other groups, but not 0.40. Claudin mRNA expression in the mucosa of the ileum was higher in 0.20 than in

other groups ($P < 0.01$). The alpha diversity of cecal microbe representative by goods coverage was higher in group 0.40 when compared with group 0.20 ($P < 0.05$). At the genus level, the abundances of the *Ruminococcaceae_NK4A214_group* and *Anaerotruncus* were higher but that of *Cetobacterium* was lower in the cecal chyme of group 0.20 than that of group 0.60 ($P < 0.05$), with no significant difference compared with other groups ($P > 0.05$). The diarrhea rate during the third week was negatively correlated with the abundances of *Rikenellaceae_RC9_gut_group* and *X.Eubacterium_coprostanoligenes_group* ($P < 0.05$).

Conclusion: Compared with diet high in amylose or amylopectin, diet with DAR 0.40 showed a worse degree of diarrhea in weaned piglets during feed transition. But the intestinal health will be improved the week after the microbes and metabolites are regulated by DAR.

Keywords: dietary amylose/amylopectin ratio, diarrhea, microorganism, metabolites, weaned piglet

IMPLICATIONS

Starch is composed of amylose and amylopectin. Our study confirmed that diarrhea was even worse in weaned piglets during the feed transition period when they received diet whose dietary amylose/amylopectin ratio was 0.40. Supplementation of amylose or amylopectin would be beneficial for weaned piglets undergoing feed transition and under lipopolysaccharide stress.

BACKGROUND

Weaning is a crucial stage as piglets have to face pathogenic challenges because pathways referring to innate system response were changed during this stage (Bomba et al., 2014). During weaning, piglets are exposed to a number of stressors: abrupt change in diet from milk to solid feed, radical change in the environment, and an immature digestive and immune system. Diarrhea is a consequence of this situation, which accounts for 17% death of piglets born in Europe (Lallès et al., 2007).

Gut microbiota such as segmented filamentous bacteria and *Candidatus Arthromitus* protect against pathogens by regulating the mammalian immune system (Schnupf et al., 2017). Gut microbial composition could be a cause or result of diarrhea; compared with that in healthy piglets, the abundances of Prevotellaceae, Lachnospiraceae, Ruminococcaceae, and Lactobacillaceae were lower in diarrheic piglets (Dou et al., 2017). The gut microbes exert a primordial role in promoting fermentation of fermentable fiber for production of short-chain fatty acid (SCFA). Production of SCFA is dependent on microbial composition and fermentable substrate. Rats with chronic kidney disease received a diet rich in fermentable fiber, promoting the integrity of the intestinal epithelial barrier and then attenuating both local and systemic inflammation (Vaziri et al., 2014). Resistant starch (RS), which cannot be digested in the small intestine but can act as a substrate for microbial fermentation in the large bowel, has been considered to reduce inflammation (Moraes et al., 2016). Dietary amylose/amylopectin ratio (DAR) was positively correlated with RS content, digestibility of starch, and gross energy, which was greater in low-DAR than in high-DAR samples (Li et al., 2015). Numbers of *Bacillus* in the intestine increased after piglets received pea starch diet with a DAR of 0.52 (Han et al., 2012). But the number of total bacteria in the colonic digesta decreased and proinflammatory cytokine interleukin (IL)-1β gene expression increased in growing–finishing pigs which received raw potato starch diet (133.5 g RS/kg diet) (Sun et al., 2015).

Escherichia coli lipopolysaccharide (LPS) is commonly used to activate the immune system; the effective dose of LPS was 25–150 mg/kg body weight (BW) of treated pigs (Wang et al., 2011). Gut injury was induced by 100 μg/kg dosage of *E. coli* LPS in pigs (Liu et al., 2008); ileal tumor necrosis factor-α (TNFα) and IL-1β were upregulated 96 h post challenge, which indicated the immune activation of pigs under LPS challenge (Yin et al., 2017). Therefore, the aim of this study was to determine the DAR on intestinal health reflected by inflammation gene expression and intestinal morphological structure of weaned piglets undergoing feed transition or challenged with *E. coli* LPS, and then the gut microbes and its metabolites (SCFA) were analyzed to find out how DAR affects the intestinal health of weaned piglets.

MATERIALS AND METHODS

The experimental procedure was reviewed and approved by the Animal Care and Use Committee of the Hunan International Joint Laboratory of Animal Intestinal Ecology and Health, Hunan Normal University.

Animals and Diets

Sixty 21-day-old castrated male pigs (Landrace × Yorkshire) with an initial average BW of 6.51 ± 0.64 kg were selected, blocked by BW and allotted to five dietary treatments with 12 cages per treatment and one pig per metabolic cage. The experimental diet was formulated according to the nutrient requirements of the National Research Council (National Research Council, 2012) for 7–11 kg pigs. The A, B, C, D, and E diets differed only in DAR, 0.00, 0.20, 0.40, 0.60, and 0.80, respectively (**Table 1**).

TABLE 1 | Composition of experimental diets (as-fed basis).

Ingredients[a],%	Pre-care period					Late-care period				
	0.00	0.20	0.40	0.60	0.80	0.00	0.20	0.40	0.60	0.80
Waxy corn starch	54.80	45.21	38.36	33.43	29.32	53.54	44.17	37.48	32.66	28.64
Hi-maize 1,043	–	9.59	16.44	21.37	25.48	–	9.37	16.06	20.88	24.90
Soybean meal	9.00	9.00	9.00	9.00	9.00	12.00	12.00	12.00	12.00	12.00
Full-fat extruded soybean	9.00	9.00	9.00	9.00	9.00	10.00	10.00	10.00	10.00	10.00
Fermented soybean meal	8.00	8.00	8.00	8.00	8.00	10.00	10.00	10.00	10.00	10.00
Fish meal	5.00	5.00	5.00	5.00	5.00	5.80	5.80	5.80	5.80	5.80
Whey, dried	5.00	5.00	5.00	5.00	5.00	5.00	5.00	5.00	5.00	5.00
Plasma protein powder	4.84	4.84	4.84	4.84	4.84	–	–	–	–	–
Monocalcium phosphate	1.17	1.17	1.17	1.17	1.17	1.33	1.33	1.33	1.33	1.33
Soybean oil	1.00	1.00	1.00	1.00	1.00	–	–	–	–	–
Premix[b]	0.92	0.92	0.92	0.92	0.92	0.92	0.92	0.92	0.92	0.92
Choline chloride	0.08	0.08	0.08	0.08	0.08	0.08	0.08	0.08	0.08	0.08
Limestone	0.74	0.74	0.74	0.74	0.74	0.72	0.72	0.72	0.72	0.72
DL-Lysine	0.23	0.23	0.23	0.23	0.23	0.21	0.21	0.21	0.21	0.21
DL-Methionine	0.22	0.22	0.22	0.22	0.22	0.21	0.21	0.21	0.21	0.21
Salt	–	–	–	–	–	0.19	0.19	0.19	0.19	0.19
Total	100	100	100	100	100	100	100	100	100	100
Calculated nutrient content[c]										
Amylose/amylopectin ratio[d]	0.00	0.20	0.40	0.60	0.80	0.00	0.20	0.40	0.60	0.80
Digestive energy, kcal/kg	3,500	3,500	3,500	3,500	3,500	3,408	3,408	3,408	3,408	3,408
Crude protein,%	18.50	18.50	18.50	18.50	18.50	18.00	18.00	18.00	18.00	18.00
Ca,%	0.85	0.85	0.85	0.85	0.85	0.92	0.92	0.92	0.92	0.92
Av.P,%	0.42	0.42	0.42	0.42	0.42	0.48	0.48	0.48	0.48	0.48
Salt,%	0.50	0.50	0.50	0.50	0.50	0.50	0.50	0.50	0.50	0.50
Amino acids,%SID[e]										
Lys	1.45	1.45	1.45	1.45	1.45	1.31	1.31	1.31	1.31	1.31
TSAA	0.79	0.79	0.79	0.79	0.79	0.71	0.71	0.71	0.71	0.71
Thr	0.83	0.83	0.83	0.83	0.83	0.74	0.74	0.74	0.74	0.74
Trp	0.25	0.25	0.25	0.25	0.25	0.23	0.23	0.23	0.23	0.23

[a]*DAR of waxy corn starch and Hi-maize 1,043 were 0.00 and 1.00, respectively.*
[b]*Vitamin–mineral premix supplied per kilogram of feed: 10,000 IU of vitamin A, 1,000 IU of vitamin D3, 80 IU of vitamin E, 2.0 mg of vitamin K3, 0.03 mg of vitamin B12, 12 mg of riboflavin, 40 mg of niacin, 25 mg of* D*-pantothenic acid, 0.25 mg of biotin, 1.6 mg of folic acid, 3.0 mg of thiamine, 2.25 mg of pyridoxine, 300 mg of choline chloride, 150 mg of Fe ($FeSO_4$), 100 mg of Zn ($ZnSO_4$), 30 mg of Mn ($MnSO_4$), 25 mg of Cu ($CuSO_4$), 0.5 mg of I (KIO_3), 0.3 mg of Co ($CoSO_4$), 0.3 mg of Se (Na_2SeO_3), and 4.0 mg of ethoxyquin.*
[c]*Nutrient content of diets based on estimated nutrient contents of ingredients according to NRC (2012).*
[d]*Analyzed data. Amylose and amylopectin contents were determined by using their assay kits (I-AMYL, Megazyme International Ireland Ltd., Wicklow, Ireland).*
[e]*SID, standardized ileal digestible.*

DAR was formulated by using different ratios of waxy corn starch (Fuyang Biological Starch Co. Ltd, Dezhou, Shandong, China) and High-Maize 1043 (National Starch and Chemical Company, Shanghai, China). Nursing diets were provided from days 1 to 14; weaned diets were provided from days 15 to 29. Feed and water were provided *ad libitum*. Six pigs from each treatment group were challenged with 100 μg/kg BW LPS (L2880, from *E. coli* O55:B5, Sigma Chemical Inc., St Louis, MO, United States) on day 29 of the experiment by intraperitoneal injection at 12 h before slaughter; sterile saline was administered to six other pigs.

Slaughter Surveys and Sampling

Diarrhea of piglets was recorded every day during the experimental period. On day 29, 12 h post challenge, pigs were slaughtered via electrical stunning followed by exsanguination. Digesta were collected from the stomach, proximal duodenum, distal jejunum, end of ileum, cecum, and colon. Mucosa from the jejunum and ileum was sampled by scraping the intestinal wall using a glass slide. Mucosa and digesta samples were stored at −80°C for further analysis. Intestinal segments such as the cecum and colon were fixed by immersion in 10% buffer neutral formalin.

ANALYSIS

Diarrhea Incidence

Fecal consistency was scored as follows: 0 = normal to 5 = liquid. The diarrhea degree was the sum of the fecal scores for every piglet each week. The diarrhea rate was calculated using following formula: diarrhea rate = total number of pigs with diarrhea/(total

number of pigs × experimental days) × 100. The total number of pigs with diarrhea referred to the number of pigs with diarrhea observed on each day.

pH Value Test

The pH value of digesta was measured using a pH meter (Testo 206, pH meter, Testo AG, Lenzkirch, Germany).

Intestinal Morphology

Fixed intestinal tissue samples were dehydrated, embedded, sectioned, and stained with hematoxylin and eosin. Mean crypt depth was measured using × 40 combined magnification and an image processing and anastem software (Leica Imaging Systems Ltd., Cambridge, United Kingdom). A minimum of 20 crypts was randomly chosen and measured per subject. Crypt depth was measured using the IPP software (Media Cybernetics Corporation, United States).

Volatile Fatty Acid (VFA) Analysis

SCFA of metaphosphoric acid-derived samples was tested according to the method described by Mathew et al. (1996). Gas chromatography (Agilent Technologies 7890B GC System; Agilent) and a DB-FFAP column (30 m × 250 μm × 0.25 μm) were used to determine propionate, acetate, butyrate, valerate, isobutyric, and isovaleric acid concentrations.

Gene Expression Analysis by RT-qPCR

Total RNA was isolated from mucosa using RNAiso Plus (Takara, Dalian, China); reverse-transcription reactions were conducted using an RT reagent kit (Takara, Dalian, China). Quantity and quality of RNA were determined with the NanoDrop ND-2000 spectrophotometer system (Thermo Fisher Scientific Inc., Wilmington, DE, United States). Real-time (RT)-PCR primers related to tight junction proteins (claudin, ZO-1, or occludin), inflammation cytokines (TNFα and IL-1β), and 18S gene were designed (**Table 2**). RT-PCRs were performed on a MyIQ instrument (Bio-Rad, Hercules, California, United States) using a SYBR Green quantitative PCR mix (Takara, Dalian, China).

16S Ribosomal RNA Sequencing

Total genome DNA from cecal digesta was extracted by using a DNA Isolation Kit (MoBio Laboratories, Carlsbad, CA, United States). 16S rRNA sequencing was conducted in a testing institution (Novogene, Beijing, China). Pyrosequencing was done on the V3–V4 variable region of the bacterial 16S rRNA genes. PCR amplification was conducted using the barcoded universal bacterial primers. Samples in triplicate were pooled for sequencing on the HiSeq 2500 platform (Illumina, United States) (Yin et al., 2018). Paired-end sequences were generated and analyzed using QIIME software (version 1.9.1). Sequences were quality checked, with a threshold of 97% set to assign reads to operational taxonomic units (OTUs). The Greengenes database was used as a reference for taxonomy assignment. Bacterial analysis was conducted using R software (version 2.15.3) with the "vegan" package.

Statistical Analysis

Gene expression data were analyzed using the method of Livak and Schmittgen (2001). Data of diarrhea occurrence were examined by a single-factor design. The cecal microbial community was examined by a single-factor design, and the false discovery rate (*Q*-value) method (Benjamini and Hochberg, 1995) was used to correct *P*-values. Other data were analyzed considering DAR and LPS stress as main effects as well as the interaction between DAR and LPS stress. Analysis of variance was conducted on SAS 8.0 (SAS Institute Inc., Cary, NC, United States) using the general linear model (GLM) procedure. Differences between groups were analyzed using Student's *t*-test. Results were presented as least squares means ± standard error. Means were considered statistically different at $P < 0.05$ and highly significant at $P < 0.01$.

RESULTS

Diarrhea Occurrence

The diarrhea rate and diarrhea degree were higher in 0.40 DAR than in 0.20 and 0.80 DARs during the third week ($P < 0.05$). No statistical difference of diarrhea rate and degree could be observed between different experimental treatments during the first, second, and fourth weeks and at the total of 4 weeks ($P > 0.05$) (**Table 3**).

pH Value and VFA of Digesta

No significant difference of pH was observed between five groups in digesta of the stomach, jejunum, and ileum ($P > 0.05$) (**Table 4**). Cecal pH was affected by DAR and LPS stress, and pH value was higher in 0.20 DAR than in 0.80 and 0.00 DARs ($P < 0.05$), but with no significant difference when compared with 0.40 and 0.60 DARs ($P > 0.05$). Cecal (not 0.80 DAR) and colonic (not 0.00 DAR) pH values increased after LPS stress ($P < 0.05$). No effect of interaction between DAR and LPS stress was found on pH value ($P > 0.05$).

The DAR had no significant effect on SCFA such as acetic acid, propionic acid, isobutyric acid, butyric acid, isovaleric acid, and total amount of SCFA concentration in the jejunum ($P > 0.05$) (**Table 5**). Jejunal butyric acid tended to increase after LPS stress ($P = 0.06$) but not in 0.60 DAR. Valeric acid concentration in the jejunum increased after LPS stress in groups with 0.00, 0.20, and 0.80 DARs but decreased in groups with 0.40 and 0.60 DARs ($P < 0.05$).

Ileal acetic acid, propionic acid, butyric acid, isobutyric acid, valeric acid, and total amount of SCFA were not affected by DAR or LPS stress, except that isovaleric acid of the ileum decreased after LPS stress ($P < 0.05$).

Cecal SCFAs, except butyric acid, were affected by DAR ($P < 0.05$). Acetic acid, propionic acid, and total SCFA concentrations were higher in the group with 0.40 DAR that in groups with 0.00, 0.60, and 0.80 DARs ($P < 0.05$). Isobutyric acid and isovaleric acid concentrations increased after LPS stress ($P < 0.05$) and were higher in the 0.20 DAR group than in the other groups ($P < 0.05$). Valeric acid concentration was higher in

TABLE 2 | RT-PCR primers related to tight junction and inflammation.

Name[1]	F/R	Primer	GenBank accession number	Productive size (bp)
Claudin-1	F	TTTCCTCAATACAGGAGGGAAGC	NM_001244539.1	196
	R	CCCTCTCCCCACATTCGAG		
Occludin-1	F	CAGGTGCACCCTCCAGATTG	NM_001163647.2	176
	R	GGACTTTCAAGAGGCCTGGAT		
ZO-1	F	CTGAGGGAATTGGGCAGGAA	XM_003353439.2	169
	R	TCACCAAAGGACTCAGCAGG		
IL-1β	F	ACCTGGACCTTGGTTCTC	NM_214055.1	85
	R	GGATTCTTCATCGGCTTC		
TNFα	F	ACGCTCTTCTGCCTACTGC	EU682384.1	128
	R	TCCCTCGGCTTTGACATT		
18S	F	GAGCGAAAGCATTTGCCAAG	NM_001206359.1	140
	R	GGCATCGTTTATGGTCGGAAC		

[1]*ZO-1, tight junction protein zonula occluden-1; IL-1 β, interleukin 1β; TNFα, tumor necrosis factor alpha.*

TABLE 3 | Effect of DAR on diarrhea occurrence of weaned piglets challenged with *E. coli* LPS.

Items	0.00	0.20	0.40	0.60	0.80	SEM	*P*-value
Diarrhea rate, head days							
First week	19.64	17.86	9.52	11.90	13.69	2.08	0.52
Second week	13.89	24.31	29.86	21.53	20.14	2.76	0.46
Third week	23.21^{AB}	11.31^{BC}	29.17^{A}	18.45^{ABC}	7.74^{C}	2.25	0.02
Fourth week[1]	19.64	8.33	24.40	19.05	9.52	2.79	0.29
Total 4 weeks[1]	19.29	15.12	22.99	17.59	12.50	1.51	0.24
Diarrhea degree, score							
First week	7.42	6.75	4.00	5.67	5.75	0.90	0.79
Second week	5.83	10.42	13.25	10.50	8.33	1.31	0.47
Third week	10.42^{AB}	4.67^{B}	14.25^{A}	9.17^{AB}	3.08^{B}	1.19	0.03
Fourth week[1]	8.92	3.67	11.92	10.17	4.42	1.45	0.30
Total 4 weeks[1]	32.58	25.50	43.42	35.50	21.58	3.19	0.22

[1]*Statistical analysis ended on day 27. Means within each row without the same superscript letter significantly differ ($P < 0.05$).*

TABLE 4 | Effect of DAR on the pH value of the digesta of weaned piglets challenged with *E. coli* LPS.

Items[1]	0.00		0.20		0.40		0.60		0.80		SEM	*P*-value		
	LPS	SAL	LPS	SAL	LPS	SAL	LPS	SAL	LPS	SAL		DAR	STRESS	D*S
Stomach	2.77	3.15	3.40	3.46	3.54	3.22	3.79	2.62	3.39	2.79	0.11	0.91	0.35	0.69
Jejunum	5.85	5.57	5.76	6.35	6.14	5.79	5.54	6.16	5.28	6.13	0.08	0.92	0.33	0.57
Ileum	6.84	6.50	6.21	7.17	6.49	7.20	6.92	6.66	6.84	7.10	0.05	0.83	0.15	0.11
Cecum	6.14^{B}	6.13	6.71^{A}	6.34	6.43^{AB}	6.15	6.55^{AB}	6.06	6.03^{B}	6.10	0.04	0.02	0.02	0.22
Colon	6.55	6.76	6.80	6.56	6.92	6.32	6.93	6.37	6.91	6.40	0.05	1.00	0.003	0.14

[1]*LPS, lipopolysaccharide; SAL, saline; DAR, dietary amylose/amylopectin ratio.*
Means within each row without the same superscript letter significantly differ ($P < 0.05$).

the group with 0.20 DAR that in groups with 0.00, 0.60, and 0.80 DARs ($P < 0.05$).

Colonic SCFAs, except valeric acid, were affected by LPS stress but not DAR; the SCFA including acetic acid, propionic acid (not in 0.00), and butyric acid decreased after LPS stress ($P < 0.05$).

Crypt Depth of the Large Intestine

The crypt depth of the cecum was lower in the 0.80 DAR group than in other groups, except 0.40 DAR ($P < 0.05$). The crypt depth of the colon was not affected by DAR and LPS stress ($P > 0.05$) (**Table 6**).

Expression of Genes Related to Gut Health

Expressions of genes related to tight junction and inflammation in mucosa are shown in **Table 7**. DAR did not alter the mRNA expression of ZO-1, IL-1β, and TNFα in the mucosa of the

TABLE 5 | Effect of DAR on concentrations of VFAs in the digesta of weaned piglets challenged with *E. coli* LPS.

Items[1], μg/g wet sample	0.00		0.20		0.40		0.60		0.80		SEM	*P*-value		
	LPS	SAL	LPS	SAL	LPS	SAL	LPS	SAL	LPS	SAL		DAR	STRESS	D*S
Jejunum														
Acetic acid	41.84	30.39	300.98	56.52	58.57	17.84	69.97	99.37	49.07	27.86	10.63	0.24	0.28	0.33
Propionic acid	11.14	7.23	77.46	28.46	22.61	7.96	13.32	20.08	24.19	10.67	2.95	0.28	0.33	0.70
Isobutyric acid	0.00	0.00	12.42	0.00	0.00	0.00	0.00	3.88	0.00	0.00	0.45	0.55	0.59	0.83
Butyric acid	11.14	7.23	21.90	6.24	22.61	7.96	13.32	20.08	24.19	10.69	1.97	0.78	0.06	0.40
Isovaleric acid	6.68	7.69	20.16	0.00	0.00	4.64	9.11	25.37	15.59	13.49	1.84	0.38	0.81	0.28
Valeric acid	27.52	9.05	46.52	0.00	27.48	33.69	7.90	18.08	37.25	23.59	1.88	0.23	0.04	0.004
Total amount of SCFA	97.53	54.37	520.04	84.98	108.66	64.13	100.30	173.35	163.97	162.40	13.92	0.25	0.26	0.13
Ileum														
Acetic acid	594.22	927.69	786.89	631.66	541.72	928.44	634.98	544.22	942.19	848.87	37.54	0.18	0.33	0.08
Propionic acid	44.18	58.87	91.71	41.11	81.28	73.66	48.28	60.25	77.71	104.72	11.91	0.83	0.97	0.88
Isobutyric acid	0.00	0.00	0.00	0.00	0.00	4.25	0.00	0.00	0.00	0.00	0.47	0.55	0.39	0.55
Butyric acid	48.89	52.47	51.66	28.96	44.53	62.24	27.83	30.76	78.89	68.53	5.35	0.14	0.87	0.82
Isovaleric acid	0.00	0.00	0.00	10.03	0.00	17.68	0.00	0.00	0.00	3.04	1.25	0.15	0.02	0.15
Valeric acid	1.32	0.00	0.00	0.00	0.00	0.00	0.00	0.00	0.00	0.00	0.15	0.60	0.39	0.60
Total amount of SCFA	688.62	1,039.03	930.26	711.75	667.53	1,086.28	711.09	635.23	1,098.79	1,025.16	39.02	0.06	0.33	0.06
Cecal														
Acetic acid	$2,746.25^{B}$	3,610.85	$3,433.77^{AB}$	4,426.02	$4,198.72^{A}$	4,643.30	$3,093.49^{B}$	3,187.17	$2,901.98^{B}$	3,329.84	148.66	0.03	0.08	0.90
Propionic acid	$1,242.81^{B}$	1,476.83	$1,631.64^{AB}$	1,805.10	$2,204.71^{A}$	1,844.70	$1,391.95^{B}$	1,414.73	$1,473.23^{B}$	1,279.86	69.77	0.02	0.87	0.67
Isobutyric acid	86.89^{BCb}	89.75	211.57^{Aa}	135.97	124.75^{Bb}	117.36	132.88^{BCb}	63.96	82.11^{Cb}	70.14	5.42	< 0.0001	0.01	0.10
Butyric acid	585.71	965.03	637.10	712.82	820.75	966.94	802.65	778.01	668.31	758.83	45.61	0.65	0.17	0.75
Isovaleric acid	113.68^{Bb}	110.53	309.97^{Aa}	184.45	201.58^{Bab}	122.02	255.10^{Bab}	80.98	117.09^{Bb}	83.84	10.09	0.001	0.0003	0.10
Valeric acid	192.85^{B}	200.68	379.11^{A}	292.34	295.05^{AB}	232.47	245.74^{B}	142.09	211.27^{B}	159.77	14.57	0.02	0.06	0.82
Total amount of SCFA	$4,968.18^{B}$	6,453.67	$6,603.15^{AB}$	7,556.70	$7,845.56^{A}$	7,926.79	$5,921.81^{B}$	5,666.94	$5,453.97^{B}$	5,682.28	260.26	0.03	0.37	0.86
Colon														
Acetic acid	2,862.32	3,032.80	2,292.78	3,213.04	2,378.01	3,367.35	2,104.43	3,360.75	1,701.21	3,347.96	65.92	0.40	< 0.0001	0.04
Propionic acid	1,225.44	1,169.05	1,080.91	1,280.66	1,030.95	1,375.93	940.75	1,397.74	772.60	1,348.47	33.87	0.71	0.0001	0.09
Isobutyric acid	126.31	132.60	185.56	144.87	161.69	110.50	134.54	128.63	161.95	125.40	5.36	0.26	0.03	0.45
Butyric acid	607.55	750.58	561.84	758.93	685.08	923.08	475.83	861.94	488.16	918.83	31.77	0.60	0.0001	0.62
Isovaleric acid	201.67	200.77	343.89	216.31	273.89	148.26	220.49	186.95	298.49	173.75	11.99	0.24	0.002	0.36
Valeric acid	229.56	225.36	355.00	240.91	259.62	241.07	190.01	236.07	235.32	241.87	9.30	0.08	0.39	0.12
Total amount of SCFA	5,252.84	5,511.16	4,819.99	5,854.72	4,789.24	6,166.18	4,066.05	6,172.07	3,657.73	6,156.28	124.10	0.64	< 0.0001	0.09

[1]*LPS, lipopolysaccharide; SAL, saline; DAR, dietary amylose/amylopectin ratio.*
Means within each row without the same superscript letter (A, B, and C) significantly differ ($P < 0.05$) and (a–c) highly significantly differ ($P < 0.01$).

TABLE 6 | Effect of DAR on crypt depth of the intestine of weaned piglets challenged with *E. coli* LPS.

Items[1], μm	0.00		0.20		0.40		0.60		0.80		SEM	*P*-value		
	LPS	SAL	LPS	SAL	LPS	SAL	LPS	SAL	LPS	SAL		DAR	STRESS	D*S
Cecal	429.98^{Aa}	424.59	401.36^{Aa}	429.59	396.38^{ABab}	385.18	396.34^{Aab}	414.19	372.74^{Bb}	362.18	5.26	0.01	0.73	0.69
Colon	436.03	475.67	470.36	461.69	450.36	474.08	446.81	477.60	464.20	434.81	7.12	0.96	0.45	0.55

[1]*LPS, lipopolysaccharide; SAL, saline; DAR, dietary amylose/amylopectin ratio.*
Means within each row without the same superscript letter (A, B, and C) significantly differ ($P < 0.05$) and (a, b, and c) highly significantly differ ($P < 0.01$).

jejunum and did not affect mRNA expression of occludin-1, ZO-1, and IL-1β in mucosa of the ileum ($P > 0.05$). LPS stress caused lower mRNA expression of claudin in jejunal mucosa ($P < 0.05$). Claudin-1 mRNA expression was higher in the 0.60 DAR group than in the other groups ($P = 0.045$) in the jejunum, and it was higher in the 0.20 DAR group than in other groups in the mucosa of the ileum ($P < 0.01$). Ingestion of diet with 0.00 DAR resulted in lower TNFα mRNA levels in

TABLE 7 | Effect of DAR on gene expression of intestinal mucosa of weaned piglets challenged with *E. coli* LPS.

Items[1]	0.00		0.20		0.40		0.60		0.80		SEM	*P*-value		
	LPS	SAL	LPS	SAL	LPS	SAL	LPS	SAL	LPS	SAL		DAR	STRESS	D*S
Jejunal mucosa														
Claudin-1	0.75^{B}	1.04	0.98^{B}	1.03	1.01^{B}	1.02	1.11^{A}	1.51	0.79^{B}	1.16	0.04	0.045	0.01	0.49
ZO-1	0.92	1.03	0.96	1.04	0.96	1.00	0.82	0.71	0.61	0.96	0.04	0.15	0.22	0.46
IL-1β	0.84	1.11	0.60	0.91	0.39	0.73	0.65	0.77	0.37	0.87	0.08	0.53	0.06	0.97
TNFα	1.25	1.06	0.75	1.63	0.61	0.83	0.65	0.73	0.47	0.79	0.13	0.50	0.32	0.78
Ileal mucosa											0.00			
Occludin-1	1.49	1.06	1.27	1.93	1.08	1.44	0.98	1.05	1.08	1.62	0.10	0.55	0.26	0.51
Claudin-1	1.15^{Bb}	1.04	2.37^{Aa}	2.20	1.25^{Bb}	1.53	1.13^{Bb}	1.24	1.22^{Bb}	1.38	0.05	< 0.0001	0.60	0.60
ZO-1	1.07	1.06	1.07	1.25	1.21	1.02	0.82	0.92	0.90	1.11	0.06	0.63	0.65	0.84
IL-1β	0.80	1.14	1.12	1.60	0.79	1.16	0.62	2.45	1.00	1.16	0.18	0.82	0.09	0.60
TNFα	0.76^{Cb}	1.02	0.97^{BCab}	1.02	1.96^{Aa}	1.25	1.30^{Aa}	1.84	1.46^{ABab}	1.42	0.07	0.01	0.87	0.10

[1]*LPS, lipopolysaccharide; SAL, saline; DAR, dietary amylose/amylopectin ratio.*
Means within each row without the same superscript letter (A, B, and C) significantly differ ($P < 0.05$) and (a, b, and c) highly significantly differ ($P < 0.01$).
ZO-1, tight junction protein zonula occluden-1; IL-1β, interleukin 1β; TNFα, tumor necrosis factor alpha.

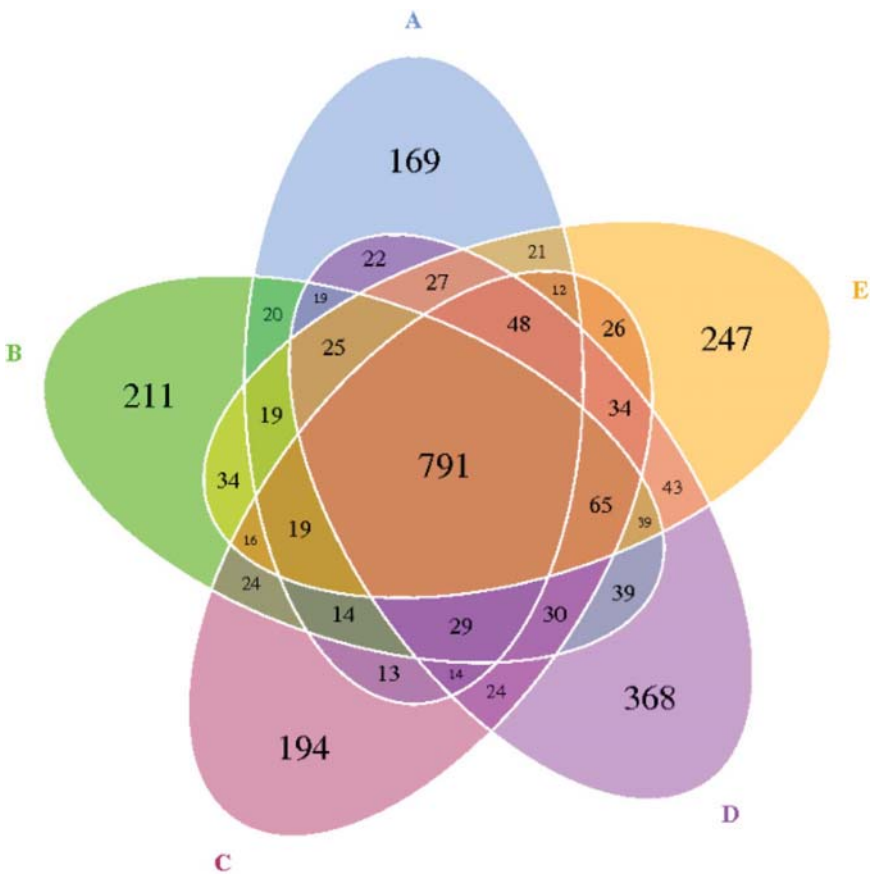

FIGURE 1 | The Venn diagram of the shared and unique OTUs between different DAR groups. DARs of **(A–E)** were 0.00, 0.20, 0.40,0.60, and 0.80 respectively.

ileal mucosa compared with diet with 0.40, 0.60, and 0.80 DARs ($P < 0.05$).

The Bacterial Community Composition in the Cecum

The reads for each sample are in the range of 70,049–96,176. After quality trimming and chimera checking, each sample has 77,296 ± 7,459 tags with a minimum length of 410 nucleotides and a maximum length of 426 nucleotides. Seven hundred and ninety-one OTUs were shared by the five groups, and 169, 211, 194, 368, and 247 OTUs were found only in the ceca of 0.00, 0.20, 0.40, 0.60, and 0.80 DAR groups, respectively (**Figure 1**). No significant differences were found on Shannon, Simpson, ACE, and PD_whole tree indexes of bacteria between different DAR groups (**Figures 2A,B**). The alpha diversity of cecal microbes in the 0.40 DAR group represented by chao1 tended to be lower than that in the 0.60 DAR group ($P = 0.076$), with no significant difference compared with other groups ($P > 0.05$). The alpha diversity of cecal microbes in 0.20 and 0.40 DAR groups represented by goods coverage was lower than in the 0.60 DAR group ($P < 0.05$), with no significant difference compared with the other groups ($P > 0.05$).

At the phylum level, Firmicutes, Bacteroidetes, Proteobacteria, and Spirochaetes were predominantly found in the cecal samples from different DAR groups. No significant difference was found in the phylum between different DAR groups ($P > 0.05$) (**Figure 3A**). At the genus level, the abundances of the *Ruminococcaceae_NK4A214_group* ($P < 0.05$) and *Anaerotruncus* ($P < 0.01$) in the cecal chyme of the 0.20 DAR

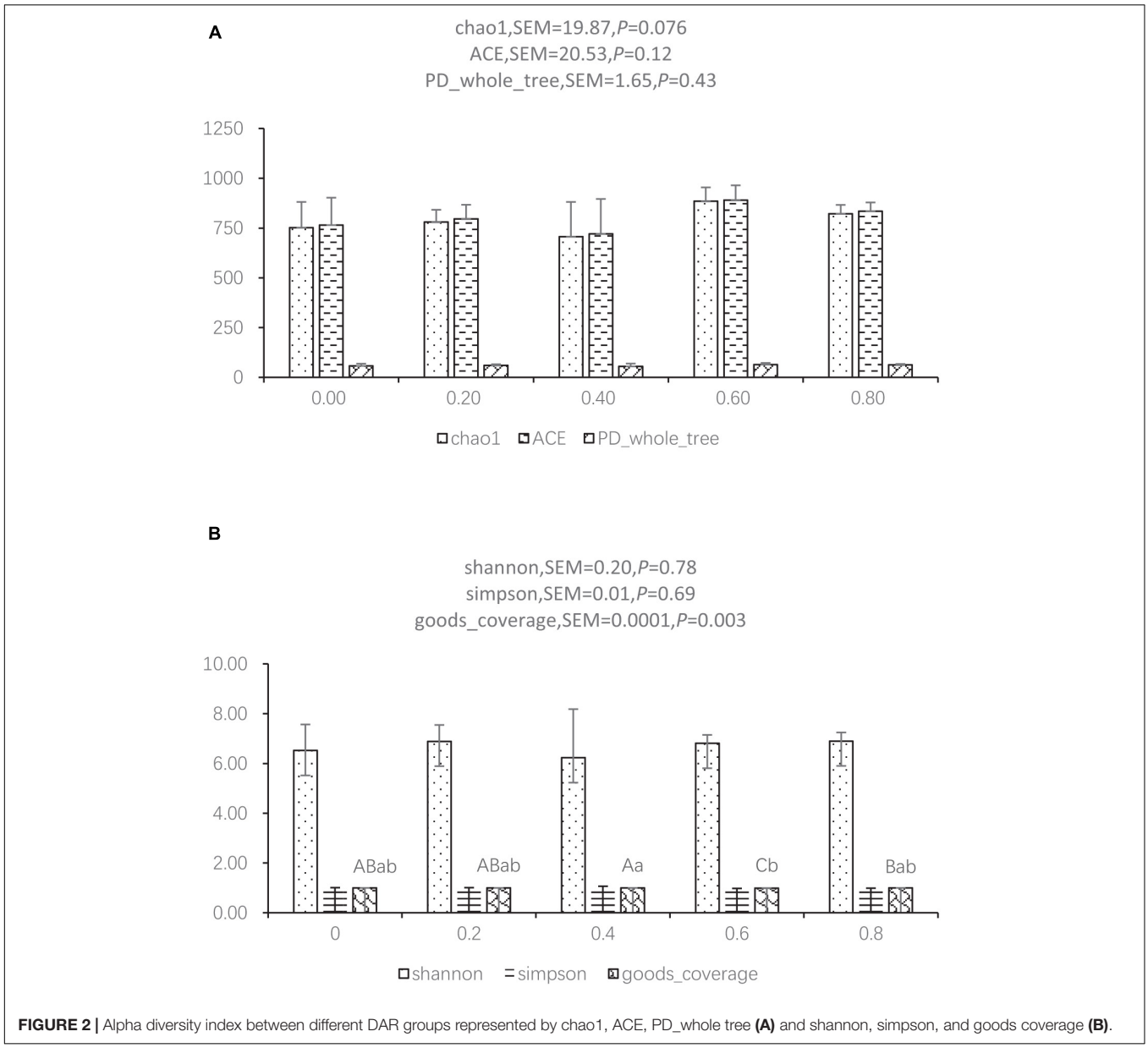

FIGURE 2 | Alpha diversity index between different DAR groups represented by chao1, ACE, PD_whole tree **(A)** and shannon, simpson, and goods coverage **(B)**.

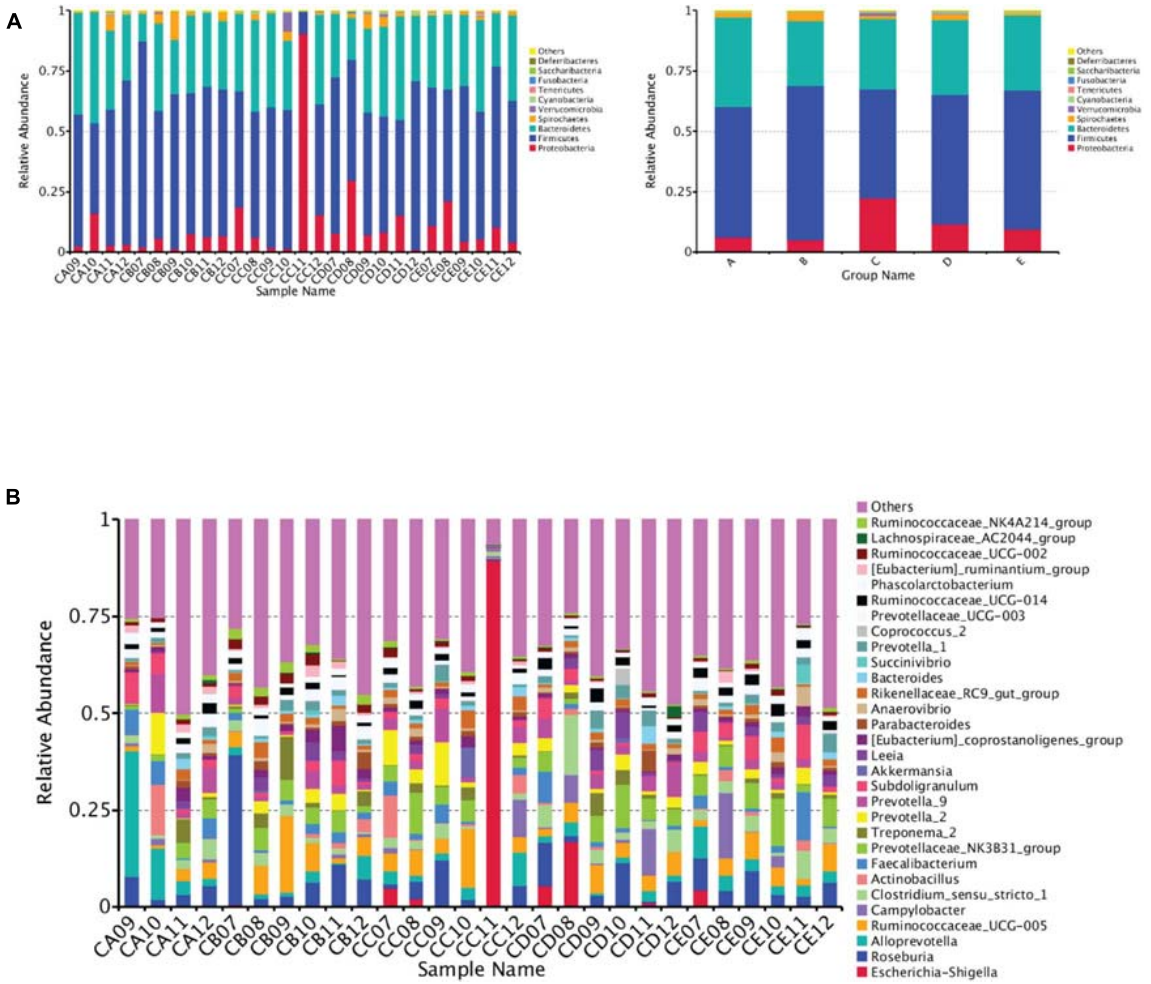

FIGURE 3 | Bar graph showing the top 10 **(A)** or top 30 **(B)** phylum level compositions of bacteria. Color-coded bar plot showing the relative abundance of bacterial phyla across the different samples (**A**, left) or different groups (**A**, right). One representative sequence from a set of related sequences belonging to the same OUT was selected for continuous species annotation with an RDP classifier, and the bacterial composition at the phylum level of each sample was stated and visualized with a histogram. The first C representing it comes from the cecal chyme. The second character represented DAR. DARs of A, B, C, D, and E were 0.00, 0.20, 0.40,0.60, and 0.80, respectively.

group were significantly higher than that in the 0.60 DAR group, with no significant difference compared with other groups ($P > 0.05$) (**Figure 3B**). The abundance of *Cetobacterium* in the cecal chyme was significantly lower in the 0.20 DAR group than in the 0.60 DAR group ($P < 0.01$), with no significant difference compared with other groups ($P > 0.05$).

Relationship Between Bacterial Abundance and Apparent Indicators

According to **Figure 4**, the diarrhea rate during the third week was negatively correlated with the abundances of the *Rikenellaceae_RC9_gut_group* and *X.Eubacterium_coprostanoligenes_group* ($P < 0.05$). The abundances of *Ruminococcaceae_UCG.002* and *Ruminococcaceae_NK4A214_group* were positively correlated with cecal total SCFA, acetic acid, propionic acid, isobutyric acid, isovaleric acid, and valeric acid concentrations ($P < 0.05$). The abundance of *Anaerotruncus* was positively correlated with cecal isovaleric acid concentrations ($P < 0.05$). The abundances of *Ruminococcaceae_UCG.005*, *Prevotellaceae_NK3B31_group*, *Leeia*, and *Ruminiclostridium_6* were positively correlated with serum cholesterol concentrations ($P < 0.05$).

DISCUSSION

An inappropriate imbalance between pro-inflammatory cytokines and the anti-inflammatory cytokines would lead to inflammation in the bowel. Elevation of TNFα and IL-6 is the hallmark of acute bowel inflammation (Kim et al., 2010). Therefore, mucosal cytokine profiling results suggest that there was acute bowel inflammation in the 0.40 and 0.60 DAR groups but not in 0.00 and 0.20 DAR groups under

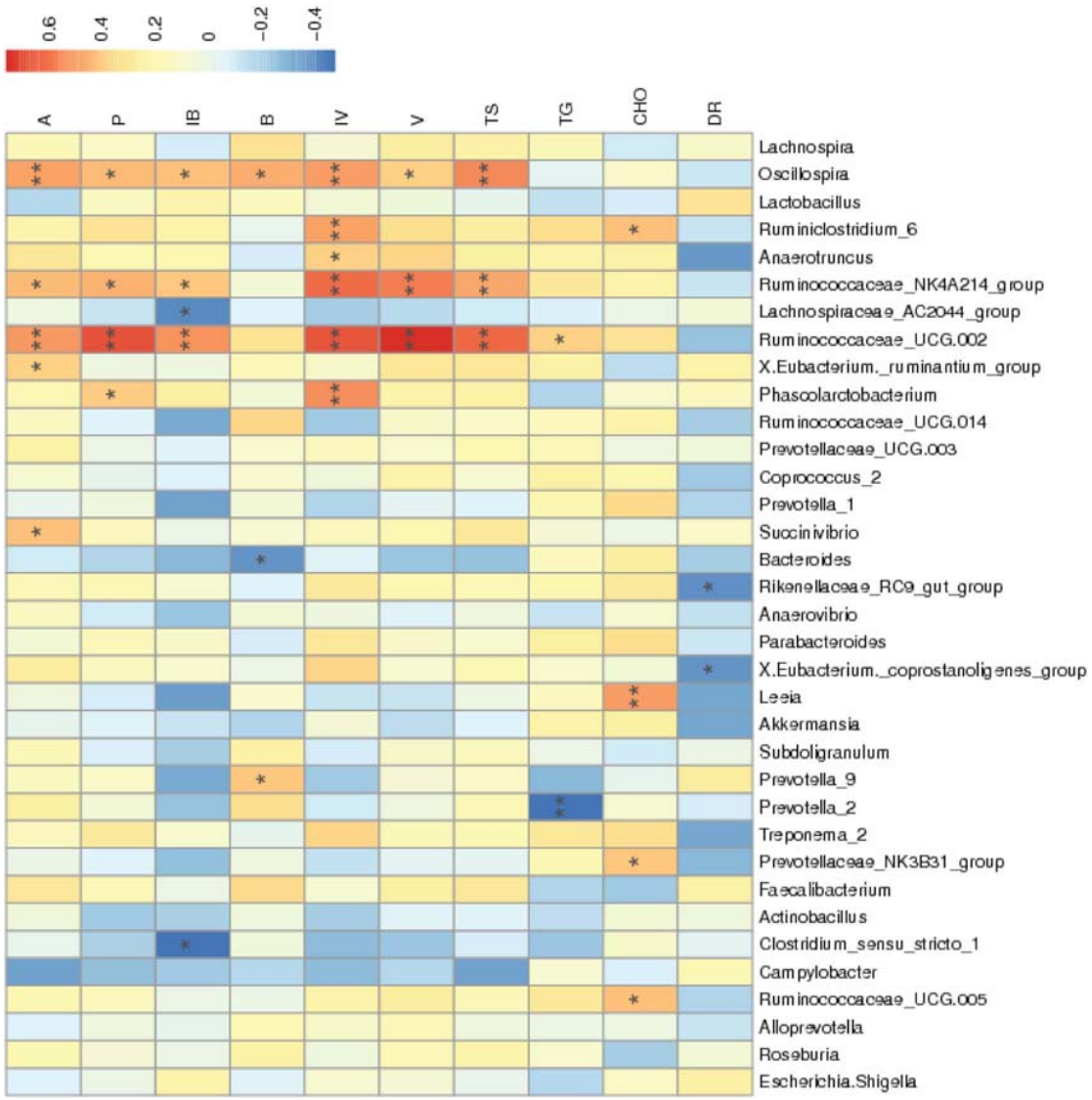

FIGURE 4 | Correlation of the environment and abundance of bacteria at the genus level. Species information is arranged in rows, and environment factors are arranged vertically and are on the horizontal axis (*x*-axis). Different colors indicate the relative abundance between species and environment factors; $r < 0$ represented a negative correlation, and $r > 0$ represented a positive correlation. *Means $P < 0.05$. **Means $P < 0.01$. A, acetic acid; P, propionic acid; IB, isobutyric acid; B, butyric acid; IV, isovaleric acid; V, valeric acid; TS, total amount of SCFA; TG, triglyceride; CHO, cholesterol; DR, diarrhea rate during the third week.

100 μg/kg of LPS stress in weaned pigs. This is inconsistent with other reports which showed that rats with chronic kidney disease supplemented with amylopectin exhibited inflammation, activation of NFκB, upregulation of pro-inflammatory cytokines, and disruption of colonic epithelial tight junction, but diet containing high RS could significantly attenuate these abnormalities (Vaziri et al., 2014). RS has proven to be effective in reducing inflammation in the state of the disease (Aliasgharzadeh et al., 2015). A study found a reduction of TNFα concentration in prediabetes patients supplemented with 45 g/day high-amylose maize for 12 weeks (Peterson et al., 2018). Supplementation of HAM-RS2 led to a decrease in serum IL-6 and TNFα in end-stage renal disease patients (Laffin et al., 2019). Moreover, consumption of retrograded high-amylose corn RS at 15% may protect the colon by enhancing anti-inflammatory cytokine IL-10 abundance in pigs, without affecting TNFα and IL-6 abundances in the colon (Fan et al., 2012). Though gut injury occurred in piglets that received 60 μg/kg (Waititu et al., 2016) or 100 μg/kg (Hou et al., 2010) of *E. coli* LPS and injection of LPS stimulated the production of IL-1, TNFα, and interferon (IFN)-γ (Kluger, 1991), but 12 h post challenge, LPS showed no effect on TNFα and IL-1β mRNA expressions in jejunal and ileal mucosa of weaning pigs in our result. The acute bowel inflammation in the 0.40 DAR group was due to severe diarrhea occurring during the third week before LPS stress.

Homeostasis of gut microbiota in the 0.40 DAR group might be disrupted because of the diarrhea. Phylum Proteobacteria abundance was higher in the 0.40 DAR group. A previous study indicated that the abnormal increase of Prevotellaceae abundance could exacerbate the occurrence of inflammation (Elinav et al., 2011). Genus *Sutterella* belongs to the Prevotellaceae phylum, and it has been found elevated in feces of dogs with acute hemorrhagic diarrhea (Suchodolski et al., 2012). The *Rikenellaceae_RC9_gut_group* increased in mice fed with high-fat diet with high-dose genistein (Zhou et al., 2018) and in an isoproterenol-induced acute myocardial ischemia group (Sun et al., 2019). We observed a significant negative correlation between abundance of the *Rikenellaceae_RC9_gut_group* and diarrhea rate during the third week in the present study. Thus, the increase of the *Rikenellaceae_RC9_gut_group* might be associated with gut inflammation. Although piglets from the 0.40 DAR group suffered severe diarrhea, they got the same average daily gain and feed intake as other groups during the whole four experimental weeks (data not shown). This result, in part, might be due to SCFAs' inflammation-modulating response. Piglets fed a diet with 0.40 DAR showed a significant increase in cecal SCFA compared with those fed a diet with 0.00, 0.60, and 0.80 DARs. SCFAs possess anti-inflammatory characteristics by increasing colonic regulatory T cells (Arpaia et al., 2013) and production of pro-inflammatory cytokines (Freeland and Wolever, 2010). Formation of pro-inflammatory and pro-oxidant uremic toxins from colonic bacteria decreased because of SCFA production increase and intestinal pH reduction (Vaziri et al., 2014).

Piglets fed a 0.20 DAR diet exhibited less microbial diversity than piglets fed a 0.6 DAR diet. More microbial diversity had a relation with a healthier phenotype generally (Human Microbiome Project Consortium, 2012). Intestinal microbiota can maintain the intestinal barrier by affecting intestinal permeability, enhancing the transfer of harmful substances into the blood, and stimulating inflammatory response (Kelly et al., 2016). The increase of gut microbiota such as *Ruminococcaceae_NK4A214_group* and *Anaerotruncus* in 0.20 DAR could result in an increase in cecal SCFA such as isobutyric acid, isovaleric acid, and valeric acid concentrations. Higher levels of iso-branched-chain fatty acids (BCFAs) may be associated with alteration in the metabolism of branched-chain amino acids (BCAAs) such as valine, leucine, and isoleucine, which can serve as precursors of BCFAs (Wallace et al., 2018). Thus, the increased production of isobutyric acid and isovaleric acid should indicate increased protein degradation during LPS stress in the 0.20 DAR group. Both Ile and Leu in the liver were increased after LPS stress in other groups but decreased after LPS in the 0.20 DAR group (data not shown). Plasma urea nitrogen levels increased after LPS challenge because of muscle proteolysis (Webel et al., 1997). There was an inverse correlation between serum iso-BCFAs and inflammatory marker C-reactive proteins in patients suffering from morbid obesity (Mika et al., 2016). Released amino acids resulting from inflammation seem to be channeled to the liver to synthesize proteins and to serve as an energy source (Owusu-Asiedu et al., 2003). LPS challenge caused lower claudin mRNA expression in the jejunal mucosa. As a result, the intestinal barrier function was improved as claudin mRNA expression increased in the 0.20 DAR group compared with other groups.

CONCLUSION

In conclusion, intestinal health was affected by DAR, which was characterized as both rate and degree of diarrhea being high in 0.40 DAR when weaned piglets undergo feed transition. Supplementing the diet with amylose can improve intestinal health through modulating gut microbes, increasing cecal acetic acid and propionic acid contents, and decreasing cecal crypt depth when weaned piglets undergo feed transition. Intestinal health was improved as claudin mRNA expression in the mucosa of the ileum increased, and cecal isobutyric acid and isovaleric acid concentrations increased when weaned piglets experiencing LPS stress received amylopectin.

DATA AVAILABILITY STATEMENT

The data presented in the study are deposited in the SRN, accession number is PRJNA733844.

ETHICS STATEMENT

Experimental procedure in this study was reviewed and approved by the Animal Care and Use Committee of the Hunan International joint laboratory of animal intestinal ecology and health, Hunan Normal University.

AUTHOR CONTRIBUTIONS

YLY and HSY organized the experiment and gave some advice on experiment idea. CY conducted the experiment and was a major contributor in writing the manuscript. CY, MW, XWT, and YCW conducted the experimental analysis. JZL and FNL reviewed the manuscript and gave some advice on the experiment idea. All authors read and approved the final manuscript.

FUNDING

This research was supported by the Research Foundation of the Education of Hunan Province (no. 18B374), China Postdoctoral Science Foundation-funded project (no. 2016M600630), and Applied Basic Research Programs of Science and Technology Foundation of Hunan Province (no. 2016JC2034).

SUPPLEMENTARY MATERIAL

The Supplementary Material for this article can be found online at: https://www.frontiersin.org/articles/10.3389/fmicb.2021.693839/full#supplementary-material

REFERENCES

Aliasgharzadeh, A., Dehghan, P., Gargari, B., and AsghariJafarabadi, M. (2015). Resistant dextrin, as a prebiotic, improves insulin resistance and inflammation in women with type 2 diabetes: a randomised controlled clinical trial. *Br. J. Nutr.* 113, 321–330.

Arpaia, N., Campbell, C., Fan, X., Dikiy, S., van der Veeken, J., deRoos, P., et al. (2013). Metabolites produced by commensal bacteria promote peripheral regulatory T-cell generation. *Nature* 504, 451–455. doi: 10.1038/nature12726

Benjamini, Y., and Hochberg, Y. (1995). Controlling the false discovery rate: a practical and powerful approach to multiple testing. *J. R. Stat. Soc. Ser. B (Methodological)* 57, 289–300.

Bomba, L., Minuti, A., Moisá Sonia, J., Trevisi, E., Eufemi, E., and Lizier, M. (2014). Gut response induced by weaning in piglet features marked changes in immune and inflammatory response. *Funct. Integr. Genomics* 14, 657–671. doi: 10.1007/s10142-014-0396-x

Dou, S., Gadonna-Widehem, P., Rome, V., Hamoudi, D., Rhazi, L., Lakhal, L., et al. (2017). Characterisation of early-life fecal microbiota in susceptible and healthy pigs to post-weaning diarrhoea. *PLoS One* 12:e0169851. doi: 10.1371/journal.pone.0169851

Elinav, E., Strowig, T., Kau, A., Henaomejia, J., Thaiss, C., and Booth, C. (2011). NLRP6 inflammasome regulates colonic microbialecology and risk for colitis. *Cell* 145, 745–757. doi: 10.1016/j.cell.2011.04.022

Fan, M. Z., Archbold, T., Lackeyram, D., Liu, Q., Mine, Y., and Paliyath, G. (2012). Consumption of guar gum and retrograded high-amylose corn resistant starch increases il-10 abundance without affecting pro-inflammatory cytokines in the colon of pigs fed a high-fat diet. *J. Anim. Sci.* 90(suppl_4), 278–280. doi: 10.2527/jas.54006

Freeland, K., and Wolever, T. (2010). Acute effects of intravenous and rectal acetate on glucagon-like peptide-1, peptide YY, ghrelin, adiponectin and tumour necrosis factor-alpha. *Br. J. Nutr.* 103, 460–466.

Han, G. Q., Xiang, Z. T., Yu, B., Chen, D. W., Qi, H. W., Mao, X. B., et al. (2012). Effects of different starch sources on Bacillus spp. in intestinal tract and expression of intestinal development related genes of weanling piglets. *Mol. Biol. Rep.* 39, 1869–1876. doi: 10.1007/s11033-011-0932-x

Hou, Y., Wang, L., Ding, B., Liu, Y., Zhu, H., and Liu, J. (2010). Dietary α-ketoglutarate supplementation ameliorates intestinal injury in lipopolysaccharide challenged piglets. *Amino Acids* 39, 555–564. doi: 10.1007/s00726-010-0473-y

Human Microbiome Project Consortium (2012). Structure, function and diversity of the healthy human microbiome. *Nature* 486, 207–214.

Kelly, T., Bazzano, L., Ajami, N., Hua, H., Zhao, J., and Petrosino, J. (2016). Gut microbiome associates with lifetime cardiovascular disease risk profile among bogalusa heart study participants. *Circ. Res.* 119, 956–964. doi: 10.1161/CIRCRESAHA.116.309219

Kim, C., Kovacs-Nolan, J., Yang, C., Archbold, T., Fan, M., and Mine, Y. (2010). L-Tryptophan exhibits therapeutic function in a porcine model of dextran sodium sulfate (DSS)-induced colitis. *J. Nutr. Biochem.* 21, 468–475. doi: 10.1016/j.jnutbio.2009.01.019

Kluger, M. (1991). Fever: role of pyrogens and cryogens. *Physiol. Rev.* 71, 93–127. doi: 10.1152/physrev.1991.71.1.93

Laffin, M., Khosroshahi, H., Park, H., Laffin, L., Madsen, K., Kafil, H., et al. (2019). Amylose resistant starch (HAM-RS2) supplementation increases the proportion of Faecalibacterium bacteria in end-stage renal disease patients: microbial analysis from a randomized placebo-controlled trial. *Hemodial. Int.* 23, 343–347. doi: 10.1111/hdi.12753

Lallès, J. P., Bosi, P., Smidt, H., and Stokes, C. R. (2007). Nutritional management of gut health in pigs around weaning. *Proc. Nutr. Soc.* 66, 260–268. doi: 10.1017/s0029665107005484

Li, Y., Zhang, A. R., Luo, H. F., Wei, H., Zhou, Z., Peng, J., et al. (2015). In vitro and in vivo digestibility of corn starch for weaned pigs: Effects of amylose:amylopectin ratio, extrusion, storage duration, and enzyme supplementation. *J. Anim. Sci.* 93, 3512–3520. doi: 10.2527/jas2014-8790

Liu, Y., Huang, J., Hou, Y., Zhu, H., Zhao, S., Ding, B., et al. (2008). Dietary arginine supplementation alleviates intestinal mucosal disruption induced by *Escherichia coli* lipopolysaccharide in weaned pigs. *Br. J. Nutr.* 100, 552–560.

Livak, K. J., and Schmittgen, T. D. (2001). Analysis of relative gene expression data using real-time quantitative PCR and the $2-\Delta\Delta$CT method. *Methods (San Diego, Calif.)* 25, 402–408. doi: 10.1006/meth.2001.1262

Mathew, A., Franklin, M., Upchurch, W., and Chattin, S. (1996). Effect of weaning on ileal short-chain fatty acid concentrations in pigs. *Nutr. Res.* 16, 1689–1698.

Mika, A., Stepnowski, P., Kaska, L., Proczko, M., Wisniewski, P., Sledzinski, M., et al. (2016). A comprehensive study of serum odd- and branched-chain fatty acids in patients with excess weight. *Obesity* 24, 1669–1676. doi: 10.1002/oby.21560

Moraes, C., Borges, N. A., and Mafra, D. (2016). Resistant starch for modulation of gut microbiota: Promising adjuvant therapy for chronic kidney disease patients? *Eur. J. Nutr.* 55, 1813–1821. doi: 10.1007/s00394-015-1138-0

National Research Council (2012). *Nutrient Requirements of Swine*. Washington, DC: National Academy Press.

Owusu-Asiedu, A., Nyachoti, C., and Marquardt, R. (2003). Response of early-weaned pigs to an enterotoxigenic (K88) challenge when fed diets containing spray-dried porcine plasma or pea protein isolate plus egg yolk antibody, zinc oxide, fumaric acid, or antibiotic. *J. Anim. Sci.* 81, 1790–1798. doi: 10.2527/2003.8171790x

Peterson, C., Beyl, R., Marlatt, K., Martin, C., Aryana, K., and Marco, M. (2018). Effect of 12 wk of resistant starch supplementation on cardiometabolic risk factors in adults with prediabetes: a randomized controlled trial. *Am. J. Clin. Nutr.* 108, 492–501. doi: 10.1093/ajcn/nqy121

Schnupf, P., Gaboriau-Routhiau, V., Sansonetti, P. J., and Cerf-Bensussan, N. (2017). Segmented filamentous bacteria, Th17 inducers and helpers in a hostile world. *Curr. Opin. Microbiol.* 35, 100–109. doi: 10.1016/j.mib.2017.03.004

Suchodolski, J., Markel, M., Garcia-Mazcorro, J., Unterer, S., Heilmann, R., Dowd, S., et al. (2012). The fecal microbiome in dogs with acute diarrhea and idiopathic inflammatory bowel disease. *PLoS One* 7:e51907. doi: 10.1371/journal.pone.0051907

Sun, L., Jia, H., Li, J., Yu, M., and Zou, Z. (2019). Cecal gut microbiota and metabolites might contribute to the severity of acute myocardial ischemia by impacting the intestinal permeability, oxidative stress, and energy metabolism. *Front. Microbiol.* 10:1745. doi: 10.3389/fmicb.2019.01745

Sun, Y., Zhou, L., Fang, L., Su, Y., and Zhu, W. (2015). Responses in colonic microbial community and gene expression of pigs to a long-term high resistant starch diet. *Front. Microbiol.* 6:877. doi: 10.3389/fmicb.2015.00877

Vaziri, N., Liu, S., Lau, W., Khazaeli, M., Nazertehrani, S., Farzaneh, S., et al. (2014). High amylose resistant starch diet ameliorates oxidative stress, inflammation, and progression of chronic kidney disease. *PLoS One* 9:e114881. doi: 10.1371/journal.pone.0114881

Waititu, S. M., Yin, F., Patterson, R., Rodriguez-Lecompte, J. C., and Nyachoti, C. M. (2016). Short-term effect of supplemental yeast extract without or with feed enzymes on growth performance, immune status and gut structure of weaned pigs challenged with *Escherichia coli* lipopolysaccharide. *J. Anim. Sci. Biotechnol.* 7, 378–390. doi: 10.1186/s40104-016-0125-5

Wallace, M., Green, C., Roberts, L., Lee, Y., McCarville, J., Sanchez-Gurmaches, J., et al. (2018). Enzyme promiscuity drives branched-chain fatty acid synthesis in adipose tissues. *Nat. Chem. Biol.* 14, 1021–1031. doi: 10.1038/s41589-018-0132-2

Wang, J. P., Yoo, J. S., Jang, H. D., Lee, J. H., Cho, J. H., and Kim, I. H. (2011). Effect of dietary fermented garlic by Weissella koreensis powder on growth performance, blood characteristics, and immune response of growing pigs challenged with *Escherichia coli* lipopolysaccharide. *J. Anim. Sci.* 89, 2123–2131. doi: 10.2527/jas.2010-3186

Webel, D., Finck, B., Baker, D., and Johnson, R. (1997). Time course of increased plasma cytokines, cortisol, and urea nitrogen in pigs following intraperitoneal injection of lipopolysaccharide. *J. Anim. Sci.* 75, 1514–1520. doi: 10.1111/j.1439-0388.1997.tb00509.x

Yin, C., Liu, W., Liu, Z., Huang, Y., Ci, L., Zhao, R., et al. (2017). Identification of potential serum biomarkers in pigs at early stage after Lipopolysaccharide

injection. *Res. Vet. Sci.* 111, 140–146. doi: 10.1016/j.rvsc.2017.02.016

Yin, J., Li, Y., Han, H., Chen, S., Gao, J., Liu, G., et al. (2018). Melatonin reprogramming of gut microbiota improves lipid dysmetabolism in high-fat diet-fed mice. *J. Pineal Res.* 65, e12524. doi: 10.1111/jpi.12524

Zhou, L., Xiao, X., Zhang, Q., Zheng, J., Li, M., and Yu, M. (2018). Improved glucose and lipid metabolism in the early life of female offspring by maternal dietary genistein is associated with alterations in the gut microbiota. *Front. Endocrinol.* 9:516. doi: 10.3389/fendo.2018.00516

Conflict of Interest: The authors declare that the research was conducted in the absence of any commercial or financial relationships that could be construed as a potential conflict of interest.

frontiers in Microbiology

ORIGINAL RESEARCH
published: 26 July 2021
doi: 10.3389/fmicb.2021.712212

Administration of All-Trans Retinoic Acid to Pregnant Sows Alters Gut Bacterial Community of Neonatal Piglets With Different Hoxa1 Genotypes

Haimei Zhou[1,2†], Huadong Wu[3†], Yixin Chen[1], Wanjie Zou[1], Wei Lu[1] and Yuyong He[1]**

[1] Jiangxi Province Key Laboratory of Animal Nutrition/Engineering Research Center of Feed Development, Jiangxi Agricultural University, Nanchang, China, [2] Department of Animal Science, Jiangxi Agricultural Engineering College, Zhangshu, China, [3] College of Animal Science and Technology, Jiangxi Agricultural University, Nanchang, China

OPEN ACCESS

Edited by:
Peng Huang,
Hunan Agricultural University, China

Reviewed by:
Xiangfeng Kong,
Institute of Subtropical Agriculture, Chinese Academy of Sciences, China
Miao Yu,
Guangdong Academy of Agricultural Sciences, China

***Correspondence:**
Yuyong He
wlkh1012@163.com
Wei Lu
lw20030508@163.com

† These authors have contributed equally to this work

Specialty section:
This article was submitted to Microbial Symbioses, a section of the journal Frontiers in Microbiology

Received: *20 May 2021*
Accepted: *29 June 2021*
Published: *26 July 2021*

Citation:
Zhou H, Wu H, Chen Y, Zou W, Lu W and He Y (2021) Administration of All-Trans Retinoic Acid to Pregnant Sows Alters Gut Bacterial Community of Neonatal Piglets With Different Hoxa1 Genotypes. Front. Microbiol. 12:712212. doi: 10.3389/fmicb.2021.712212

Administration of all-trans retinoic acid (ATRA) to pregnant sows improves developmental defects of Hoxa1$^{-/-}$ fetal pigs, and this study aimed to explore the influence of maternal ATRA administration during pregnancy on gut microbiota of neonatal piglets. Samples of jejunal and ileal meconium of neonatal piglets before suckling were collected including 5 Hoxa1$^{-/-}$ and 20 non-Hoxa1$^{-/-}$ (Hoxa1$^{+/+}$ and Hoxa1$^{+/-}$) neonatal piglets from the control group and 5 Hoxa1$^{-/-}$ and 7 non-Hoxa1$^{-/-}$ neonatal piglets from the experimental group. Results indicated that Hoxa1 mutation shaped the bacterial composition of the jejunum and ileum of neonatal piglets and Hoxa1$^{-/-}$ neonatal piglets had significantly higher diversity and species richness, higher relative abundance of phylum Bacteroidetes, lower relative abundances of phylum Firmicutes and genus *Lactobacillus*, and lower ratio of Firmicutes to Bacteroidetes than non-Hoxa1$^{-/-}$ neonatal piglets. After maternal ATRA administration, Hoxa1$^{-/-}$ neonatal piglets had significantly higher diversity and species richness, higher relative abundances of two bacterial phyla (Bacteroidetes and Proteobacteria), and lower relative abundances of phylum Firmicutes and genus *Lactobacillus* in the jejunum than non-Hoxa1$^{-/-}$ neonatal piglets. Hoxa1$^{-/-}$ neonatal piglets delivered by sows with maternal ATRA administration had lower diversity and species richness and higher relative abundance of phylum Firmicutes in the jejunum than Hoxa1$^{-/-}$ neonatal piglets born by sows with no maternal ATRA administration. Non-Hoxa1$^{-/-}$ neonatal piglets delivered by sows with maternal ATRA administration had higher diversity and species richness and significantly lower relative abundances of phyla Firmicutes and Actinobacteria and genus *Lactobacillus* in the ileum than non-Hoxa1$^{-/-}$ neonatal piglets born by sows with no maternal ATRA administration. Hoxa1 mutation decreased the expression of bacterial genes involved in ABC transporters, purine metabolism, and aminoacyl-tRNA biosynthesis and increased the expression of bacterial genes involved in two-component system, starch and sucrose metabolism, and arginine and proline metabolism. Maternal ATRA administration decreased the expression of bacterial genes

involved in arginine and proline metabolism, peptidoglycan biosynthesis, and fatty acid biosynthesis. Hoxa1 mutation resulted in bacterial dysbiosis of the small intestine of Hoaxa1$^{-/-}$ neonatal piglets, and maternal ATRA administration restored the bacterial dysbiosis of Hoxa1$^{-/-}$ neonatal piglets and altered the bacterial composition of the small intestine of non-Hoxa1$^{-/-}$ neonatal piglets.

Keywords: Hoxa1 mutation, all-trans retinoic acid, pregnant sows, gut bacterial community, neonatal piglets

INTRODUCTION

Gut microbiota is integral to feed digestion, nutrient absorption and metabolism, immune response, and gastrointestinal development (Morgavi et al., 2015), and the colonization of intestinal microbiota during early life could further influence the subsequent microbiota of adult host (Ben Salem et al., 2005). Many studies demonstrated that the intestine of prenatal animals really has microorganism (Alipour et al., 2018; Stinson et al., 2019; Hummel et al., 2020; Bi et al., 2021; Husso et al., 2021), and at present, no literature on the differences in intestinal microbiota composition between mutant and wild-type fetuses is found, but for postnatal individuals, there are differences in gut microbiota between mutant and wild-type host, for example, nucleotide-binding oligomerization domain-containing protein 2 (NOD2) mutation caused Crohn's disease (CD) (Hampe et al., 2001; Ogura et al., 2001) and Crohn's disease individuals had lower bacterial diversity than healthy controls (Joossens et al., 2011). Cystic fibrosis transmembrane conductance regulator (CFTR) mutation resulted in multiorgan defects, and CFTR$^{-/-}$ mice had significantly lower alpha diversity of intestinal bacterial community ($p < 0.05$) and had reduced relative abundance of protective species such as *Acinetobacter lwoffii* and Lactobacilliales members compared with wild-type mice (Lynch et al., 2013). Methyl-CpG-binding protein 2 (MeCP2) mutation developed into the Rett syndrome (RTT), and RTT patients had significantly less diversity in gut bacteria community compared with healthy controls ($p < 0.01$). Meanwhile, RTT individuals had the most abundant phylum of Actinobacteria, but healthy controls had the most abundant phylum of Firmicutes, and a significant decrease of Bacteroidetes was observed in RTT subjects (Strati et al., 2016).

Gene mutation not only can alter intestinal microbiota composition of postnatal animals but also can cause abnormal phenotypes of fetuses: cytochrome C oxidase subunit IV isoform 1 (COX4I1) mutation caused short stature and poor weight gain (Abu-Libdeh et al., 2017); mutations of Huntington (HTT) exhibited fetal ear defects (Murthy et al., 2019); K^+ channels Kir4.1 (KCNJ10) gene mutation resulted in seizures and ataxia (Ai Dhaibani et al., 2018); gamma-1 adaptin gene (*Ap1g1*) mutation developed abnormalities of the inner ear and testes (Johnson et al., 2016); WD repeat domain phosphoinositide-interacting protein 2 (WIPI2) mutation led to skeletal and cardiac abnormalities (Jelani et al., 2019); fibroblast growth factor receptor 2 (FGFR2) mutation induced midfacial hypoplasia and bilateral syndactyly of the hands and feet (Giancotti et al., 2014); solute carrier family 26a member 4 (SLC26A4) mutation developed deafness (Nonose et al., 2018); a Q186K mutation in Hoxa2 resulted in external ear malformation (Alasti et al., 2008); and the Hoxa1 mutation of g.50111251 G > TC developed abnormal auricle and external auditory canal, dyspnea, and even death in newborn piglets (Qiao et al., 2015). Some defects of phenotypes can be rescued by feeding special chemicals to pregnant animals during pregnancy at a specific time: administration of exogenous RA to pregnant mice at a dose of 2.5 mg/kg on day embryonic 7.5 or embryonic 8.5 effectively repaired the Hoxa1 mutant mice from inner ear defects (Pasqualetti et al., 2001), and all-trans retinoic acid (ATRA) administration to pregnant sows at the level of 4 mg/kg body weight on 14 days postcoitum (dpc) was also effective for the repair of ear defects of Hoxa1$^{-/-}$ fetal pigs (Zhou et al., 2021). As mentioned above, the abnormal phenotypes of fetus caused by gene mutation can be rescued *via* chemical administration during gestation, but there is no information if maternal administration of chemicals can also change the intestinal bacterial composition of mutant and wild-type individuals. Understanding the influence of maternal administration with special chemicals during pregnancy on the community composition and function of the neonatal gut bacteria may help to develop strategies to prevent young animals from suffering from some diseases and to guide the healthy development of the offspring. Our previous studies demonstrated that maternal administration with ATRA at the level of 4 mg/kg body weight on 14 dpc had the best effects in repairing ear defects of Hoxa1$^{-/-}$ fetal pigs, and the aims of this study are (1) to find out if maternal administration with ATRA can alter the intestinal bacterial compositions of Hoxa1$^{-/-}$ and non-Hoxa1$^{-/-}$ fetal piglets and (2) to compare the differences in intestinal bacterial compositions of neonate piglets between Hoxa1$^{-/-}$ and non-Hoxa1$^{-/-}$ genotypes.

MATERIALS AND METHODS

Animals and Sample Collection

Eight Hoxa1$^{+/-}$ sows derived from one Chinese Erhualian founder boar and one Shaziling founder sow were mated to one healthy Hoxa1$^{+/-}$ boar and randomly assigned to a control group (six sows) and an experimental group (two sows). Pregnant sows in the control group were orally administered with ATRA at a level of 0 mg/kg body weight, and pregnant sows in the experimental group were orally administered with ATRA at a level of 4 mg/kg body weight (Zhou et al., 2021).

After birth, all samples were collected before suckling. Samples of ears of all neonatal piglets were collected and stored in EP tubes containing 75% alcohol for Hoxa1 genotyping. Hoxa1$^{-/-}$

piglets delivered by sows from the control group had ear defects, and the ear defects of Hoxa1$^{-/-}$ piglets born by sows from the experimental group were effectively repaired; all non-Hoxa1$^{-/-}$ (Hoxa1$^{+/+}$, Hoxa1$^{+/-}$) either from the control group or the experimental group had normal ears (Zhou et al., 2021). Samples of meconium of all neonatal piglets were collected from jejunal and ileal sections by exsanguination after anesthetization with pentobarbital sodium (100 mg/kg body weight) according to the protocol approved by the Animal Ethics Committee of Jiangxi Agricultural University and immediately stored at −80°C for microbiome analysis. A total of 37 neonatal piglets were sampled, namely, 25 piglets (5 Hoxa1$^{-/-}$ and 20 non-Hoxa1$^{-/-}$) from the control group and 12 piglets (5 Hoxa1$^{-/-}$ and 7 non-Hoxa1$^{-/-}$) from the experimental group.

DNA Extraction, Amplification, and Sequencing

Genomic DNA of intestinal meconium was extracted with the QIAamp DNA Stool Mini Kit (Qiagen, Hilden, Germany) according to the instructions of the manufacturer, and the quantity and quality of DNA were measured with NanoDrop^{TM} 2000/2000c Spectrophotometer (Thermo Fisher Scientific, Waltham, MA, United States). The V3–V4 region of bacterial 16S rRNA genes was amplified using primers 341F (5′-CCTACGGGNGGCWGCAG-3′) and 806R (5′-GGACTACHVGGGTATCTAAT-3′). PCR reactions were performed in triplicate 50 μl mixture containing 5 μl of 10 × KOD buffer, 5 μl of 2 mM dNTPs, 3 μl of 25 mM $MgSO_4$, 1.5 μl of each primer (10 μM), 1 μl of KOD polymerase, and 100 ng of template DNA. The PCR conditions consisted of initial denaturation at 94°C for 2 min, followed by 30 cycles of denaturation at 98°C for 10 s, annealing at 65°C for 30 s, elongation at 768°C for 30 s, and finally 68°C for 5 min. The PCR products were subsequently subjected to electrophoresis on 2% agarose gel and stained with ethidium bromide, and the targeted fragment size was purified using the AMPure XP Beads (Beckman Agencourt, Brea, CA, United States) according to the manufacturer's instructions and quantified using ABI StepOnePlus Real-Time PCR System (Life Technologies, Foster City, CA, United States). Purified amplicons were pooled in equimolar and paired-end sequenced (PE250) on an Illumina HiSeq 2500 platform (Illumina, San Diego, CA, United States) according to standard protocols. The raw reads were deposited into the NCBI Sequence Read Archive (SRA) database (accession number: SRP239498).

Sequence Processing and Data Statistical Analysis

Raw reads were further filtered using FASTP (version 0.18.0) (Chen et al., 2018), and paired end clean reads were merged as raw tags using FLASH (version 1.2.11) (Magoč and Salzberg, 2011) with a minimum overlap of 10 bp and mismatch error rates of 20%. The clean tags were clustered into operational taxonomic units (OTUs) at 97% sequence similarity using UPARSE (version 9.2.64) pipeline (Edgar, 2013). According to the algorithm principle, the sequences with the highest occurrence frequency were selected as the representative sequence of OTUs. The representative OTU sequences were classified into organisms by a naive Bayesian model using RDP classifier (version 2.2) (Wang et al., 2007) based on the SILVA database (version 132) (Pruesse et al., 2007) with a confidence threshold value of 0.8 to obtain taxonomic information and the community composition of each sample at various classification levels; the abundance statistics of each taxonomy was visualized using Krona (version 2.6) (Ondov et al., 2011).

Chao1 and Shannon index were calculated in QIIME (version 1.9.1) (Caporaso et al., 2010) and alpha index comparison between groups was calculated by Welch's *t*-test in R project Vegan package (version 2.5.3) (Oksanen et al., 2010). Bacterial community structure and composition were compared using non-metric multidimensional scaling (NMDS) analysis by means of weighed UniFrac distances in R using the metaMDS function (Caporaso et al., 2012). Permutational multivariate analyses of variance (PERMANOVA; "adonis and anosim" in vegan R package) with 999 random permutations were performed to assess the influence of substrate on the community variances. The functional potentials of intestinal bacteria were predicted using Tax4Fun package in R software based on the Kyoto Encyclopedia of Genes and Genomes (KEGG) Orthology (KO) terms at level 3 with the observed 16S rRNA gene sequences (Aßhauer et al., 2015; Kanehisa et al., 2015). Analysis of function difference between groups was calculated by Welch's *t*-test in R project Vegan package (version 2.5.3) (Oksanen et al., 2010).

RESULTS

Bacterial Richness and Alpha Diversity

Table 1 shows the alteration of richness and diversity of small intestinal bacterial community between Hoxa1$^{-/-}$ and non-Hoxa1$^{-/-}$ neonatal piglets within the same treatment group. Hoxa1$^{-/-}$ neonatal piglets either from the control group or the experimental group had significantly higher OTU ($p < 0.01$), Chao1 ($p < 0.01$), and Shannon ($p < 0.05$) of jejunal bacterial community than non-Hoxa1$^{-/-}$ neonatal piglets, respectively. In the control group, Hoxa1$^{-/-}$ neonatal piglets had significantly higher OTU ($p < 0.05$), Chao1 ($p < 0.05$), and Shannon ($p < 0.01$) of ileal bacterial community than non-Hoxa1$^{-/-}$ neonatal piglets. However, in the experimental group, Hoxa1$^{-/-}$ neonatal piglets had no significantly higher OTU, Chao1, and Shannon of ileal bacterial community than non-Hoxa1$^{-/-}$ neonatal piglets, respectively ($p > 0.05$).

Table 2 indicates the change of richness and diversity of intestinal bacterial community of neonatal piglets with the same genotype between the control group and the experimental group. Hoxa1$^{-/-}$ neonatal piglets from the control group had no significantly higher OTU, Chao1, and Shannon of jejunal and ileal bacterial community than Hoxa1$^{-/-}$ neonatal piglets from the experimental group, respectively ($p > 0.05$). Non-Hoxa1$^{-/-}$ neonatal piglets from the control group had significantly lower OTU ($p < 0.01$) and Chao1 ($p < 0.01$) but had no significantly higher Shannon ($p > 0.05$) of jejunal bacterial community than non-Hoxa1$^{-/-}$ neonatal piglets from the experimental group,

TABLE 1 | Diversity comparison between Hoxa1$^{-/-}$ and Non-Hoxa1$^{-/-}$ newly born piglets in the same treatment group.

	Control group			Experimental group		
	Hoxa1$^{-/-}$ piglets	**Non-Hoxa1$^{-/-}$ piglets**	***p*-value**	**Hoxa1$^{-/-}$ piglets**	**Non-Hoxa1$^{-/-}$ piglets**	***p*-value**
Diversity of jejunal bacteria	KD-1	KD-2		KC-1	KC-2	
OTU	538.83 ± 75.02	180.67 ± 12.02	0.005	449.67 ± 24.59	309.67 ± 18.97	0.001
Chao1	806.80 ± 82.12	257.78 ± 14.97	0.001	721.33 ± 17.53	526.87 ± 40.38	0.003
Shannon	5.37 ± 0.68	3.43 ± 0.34	0.036	4.65 ± 0.27	3.07 ± 0.24	0.011
Diversity of ileal bacteria	HD-1	HD-2		HC-1	HC-2	
OTU	622.00 ± 67.02	203.33 ± 14.39	0.024	358.50 ± 44.77	351.00 ± 87.78	0.456
Chao1	659.05 ± 99.12	287.37 ± 23.32	0.030	573.82 ± 60.88	479.58 ± 78.72	0.604
Shannon	6.51 ± 0.82	3.20 ± 0.12	0.009	4.35 ± 0.35	3.67 ± 0.46	0.842

TABLE 2 | Diversity comparison of newly born piglets with the same genotype between the control group and the experimental group.

	Hoxa1$^{-/-}$ piglets			Non-Hoxa1$^{-/-}$ piglets		
	Control group	**Experimental group**	***p*-value**	**Control group**	**Experimental group**	***p*-value**
Diversity of jejunal bacteria	KD-1	KC-1		KD-2	KC-2	
OTU	538.83 ± 75.02	449.67 ± 24.59	0.301	180.67 ± 12.02	309.67 ± 18.97	0.000
Chao1	806.80 ± 82.12	721.33 ± 17.53	0.352	257.78 ± 14.97	526.87 ± 40.38	0.001
Shannon	5.37 ± 0.68	4.65 ± 0.27	0.357	3.43 ± 0.34	3.07 ± 0.24	0.407
Diversity of ileal bacteria	HD-1	HC-1		HD-2	HC-2	
OTU	622.00 ± 67.02	358.50 ± 44.77	0.064	203.33 ± 14.39	351.00 ± 87.78	0.123
Chao1	659.05 ± 99.12	573.82 ± 60.88	0.124	287.37 ± 23.32	479.58 ± 111.32	0.140
Shannon	6.51 ± 0.82	4.35 ± 0.35	0.056	3.20 ± 0.12	3.67 ± 0.46	0.362

respectively. Non-Hoxa1$^{-/-}$ neonatal piglets from the control group had no significant lower OTU, Chao1, and Shannon of ileal bacterial community than that of non-Hoxa1$^{-/-}$ neonatal piglets from the experimental group ($p > 0.05$).

These results demonstrate that the g.50111251 G > TC mutation in Hoxa1 significantly increased the OTU, Chao1, and Shannon of jejunal and ileal bacterial community, respectively, when comparing Hoxa1$^{-/-}$ neonatal piglets with non-Hoxa1$^{-/-}$ neonatal piglets. Maternal ATRA administration decreased the OTU, Chao1, and Shannon of jejunal and ileal bacterial community of Hoxa1$^{-/-}$ neonatal piglets but increased the OTU, Chao1, and Shannon of jejunal and ileal bacterial community of non-Hoxa1$^{-/-}$ neonatal piglets with an exception of Shannon in ileal bacteria.

Bacterial Community Composition

The compositions of bacteria in the jejunal and ileal meconium are presented in **Figures 1**, **2**. The phyla Firmicutes and Proteobacteria were the dominant bacteria in both meconium, and Hoxa1 mutation altered the relative abundances of intestinal bacteria at the phylum level (**Figures 1A**, **2A**). In the control group, Hoxa1$^{-/-}$ neonatal piglets had lower abundance of Firmicutes and higher abundances of Proteobacteria, Bacteroidetes, and Verrucomicrobia than non-Hoxa1$^{-/-}$ neonatal piglets in jejunal (KD-1:KD-2) and ileal meconium (HD-1:HD-2), respectively. In the experimental group, Hoxa1$^{-/-}$ neonatal piglets still had lower abundance of Firmicutes and higher abundances of Proteobacteria and Bacteroidetes than non-Hoxa1$^{-/-}$ neonatal piglets in jejunal (KC-1:KC-2) and ileal (HC-1:HC-2) meconium, respectively, but Hoxa1$^{-/-}$ neonatal piglets from the experimental group had higher abundance of Firmicutes and lower abundances of Bacteroidetes and Verrucomicrobia than Hoxa1$^{-/-}$ neonatal piglets from the control group in jejunal (KC-1:KD-1) and ileal meconium (HC-1:HD-1), respectively. Maternal administration with ATRA also had an influence on the phyla bacteria abundance of non-Hoxa1$^{-/-}$ neonatal piglets, and the data in **Figures 1A**, **2A** indicated that non-Hoxa1$^{-/-}$ neonatal piglets from the experimental group had higher abundance of Firmicutes and lower abundances of Proteobacteria and Bacteroidetes than non-Hoxa1$^{-/-}$ neonatal piglets from the control group in the jejunal meconium (KC-2:KD-2), but had lower abundance of Firmicutes and higher abundances of Proteobacteria, Bacteroidetes, and Verrucomicrobia than non-Hoxa1$^{-/-}$ neonatal piglets from the control group in the ileal meconium (HC-2:HD-2).

At the genus level, data in **Figure 1B** showed that in the control group, Hoxa1$^{-/-}$ neonatal piglets had lower abundances of *Lactobacillus*, *Actinobacillus*, and *Streptococcus* and higher abundances of *Escherichia–Shigella*, *Akkermansia*, and *Lachnospiraceae_NK4A136_group* than non-Hoxa1$^{-/-}$ neonatal piglets, respectively, in the jenunal meconium (KD-1:KD-2), but in the experimental group, Hoxa1$^{-/-}$ neonatal piglets had lower abundances of *Lactobacillus*, *Clostridium_sensu_stricto_1*, and *Veillonella* and higher abundances of *Escherichia–Shigella*, *Bacteroides*, and

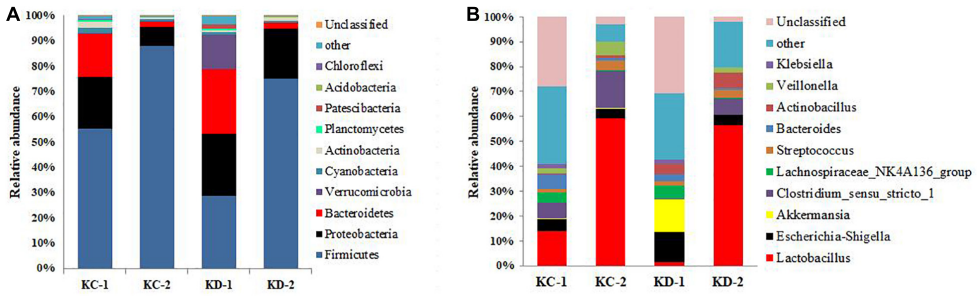

FIGURE 1 | Bacterial community composition of jejunal digesta. **(A)** Phylum level; **(B)** genus level. KC-1: bacterial composition of jejunal digesta sampled from Hoxa1$^{-/-}$ neonatal piglets delivered by sows administered with ATRA, KC-2: bacterial composition of jejunal digesta sampled from non-Hoxa1$^{-/-}$ neonatal piglets delivered by sows administered with ATRA, KD-1: bacterial composition of jejunal digesta sampled from Hoxa1$^{-/-}$ neonatal piglets delivered by sows administered without ATRA, KD-2: bacterial composition of jejunal digesta sampled from non-Hoxa1$^{-/-}$ neonatal piglets delivered by sows administered without ATRA.

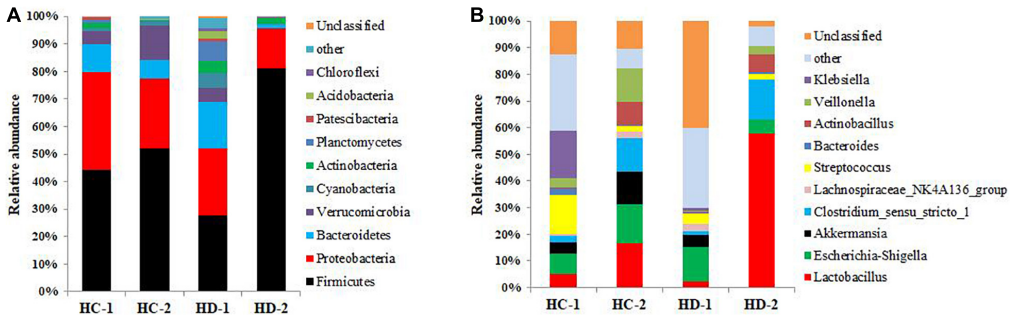

FIGURE 2 | Bacterial community composition of ileal digesta. **(A)** Phylum level; **(B)** genus level. HC-1: bacterial composition of ileal digesta sampled from Hoxa1$^{-/-}$ neonatal piglets delivered by sows administered with ATRA, HC-2: bacterial composition of ileal digesta sampled from non-Hoxa1$^{-/-}$ neonatal piglets delivered by sows administered with ATRA, HD-1: bacterial composition of ileal digesta sampled from Hoxa1$^{-/-}$ neonatal piglets delivered by sows administered without ATRA, HD-2: bacterial composition of ileal digesta sampled from non-Hoxa1$^{-/-}$ neonatal piglets delivered by sows administered without ATRA.

Lachnospiraceae_NK4A136_group than non-Hoxa1$^{-/-}$ neonatal piglets, respectively, in the jejunal meconium (KC-1:KC-2). Hoxa1$^{-/-}$ neonatal piglets from the experimental group had higher abundances of *Lactobacillus*, *Clostridium_sensu_stricto_1*, and *Bacteroides* and lower abundances of *Escherichia–Shigella*, *Lachnospiraceae_NK4A136_group*, and *Akkermansia* than Hoxa1$^{-/-}$ neonatal piglets from the control group, respectively, in the jejunal meconium (KC-1:KD-1). Results in **Figure 2B** indicated that in the control group, Hoxa1$^{-/-}$ neonatal piglets had lower abundances of *Lactobacillus*, *Clostridium_sensu_stricto_1*, *Bacteroides*, *Actinobacillus*, and *Veillonella* and higher abundances of *Escherichia–Shigella*, *Akkermansia*, *Streptococcus*, and *Lachnospiraceae_NK4A136_group* than non-Hoxa1$^{-/-}$ neonatal piglets, respectively, in the ileal meconium (HD-1:HD-2), but in the experimental group, Hoxa1$^{-/-}$ neonatal piglets had lower abundances of *Lactobacillus*, *Escherichia–Shigella*, *Akkermansia*, and *Clostridium_sensu_stricto_1* and higher abundances of *Streptococcus* and *Klebsiella* than non-Hoxa1$^{-/-}$ neonatal piglets, respectively, in the ileal meconium (HC-1:HC-2). Hoxa1$^{-/-}$ neonatal piglets from the experimental group had higher abundances of *Lactobacillus*, *Clostridium_sensu_stricto_1*, *Streptococcus*, *Bacteroides*, *Veillonella*, and *Klebsiella* and lower abundances of *Escherichia–Shigella* and *Akkermansia* than Hoxa1$^{-/-}$ neonatal piglets from the control group, respectively, in the ileal digesta (HC-1:HD-1).

Relative Abundance of Differentially Jejunal Bacterial Community

The relative abundances of differential bacterial taxa in the jejunal meconium (at least one of the relative abundances is greater than 0.01%) are presented as percentage in **Tables 3**, **4**. The results in **Table 3** indicate that four bacterial taxa with differential abundances at the phylum level and 10 bacterial taxa with differential abundances at the genus level were identified in the samples of jejunal meconium between Hoxa1$^{-/-}$ and non-Hoxa1$^{-/-}$ piglets from the control group, and Hoxa1$^{-/-}$ neonatal piglets had significantly lower relative abundances of Firmicutes ($p < 0.01$) at the phylum level and of *Lactobacillus* ($p < 0.01$), *Staphylococcus* ($p < 0.01$), and *Veillonella* ($p < 0.01$) at the genus level, respectively, in the jejunal digesta than non-Hoxa1$^{-/-}$ neonatal piglets. After maternal ATRA administration, Hoxa1$^{-/-}$ neonatal piglets from the experimental group still had significantly lower relative abundances of Firmicutes ($p < 0.01$) at the phylum level and of *Lactobacillus* ($p < 0.01$) at the genus level, respectively, in the jejunal digesta than non-Hoxa1$^{-/-}$ neonatal piglets.

TABLE 3 | The differential jejunal bacterial community of newborn piglets between different genotypes within the same treatment group (%).

	Control group				Experimental group		
	Hoxa1$^{-/-}$ piglets (KD-1)	Non-Hoxa1$^{-/-}$ piglets (KD-2)	*p*-value		Hoxa1$^{-/-}$ piglets (KC-1)	Non-Hoxa1$^{-/-}$ piglets (KC-2)	*p*-value
Phylum level				**Phylum level**			
Firmicutes	28.78 ± 7.11	75.09 ± 9.32	0.003	Firmicutes	55.36 ± 8.11	88.09 ± 4.68	0.008
Bacteroidetes	25.47 ± 5.54	2.54 ± 1.11	0.008	Proteobacteria	20.18 ± 3.06	7.28 ± 3.01	0.013
Patescibacteria	1.63 ± 0.62	0.01 ± 0.00	0.046	Bacteroidetes	17.05 ± 5.09	2.16 ± 0.19	0.032
Planctomycetes	0.56 ± 0.20	0.00 ± 0.00	0.039				
Genus level				**Genus level**			
Lactobacillus	1.39 ± 0.47	56.63 ± 10.10	0.003	*Lactobacillus*	14.02 ± 8.01	59.32 ± 7.68	0.002
Alloprevotella	1.18 ± 0.45	0.00 ± 0.00	0.046	*Acinetobacter*	0.71 ± 0.18	0.04 ± 0.01	0.036
Oscillibacter	0.60 ± 0.22	0.00 ± 0.00	0.044				
Eubacterium_fissicatena_group	0.34 ± 0.03	0.00 ± 0.00	0.044				
Lachnoclostridium	0.32 ± 0.07	0.05 ± 0.03	0.044				
Clostridium_sensu_stricto_1	0.22 ± 0.14	6.69 ± 2.21	0.033				
Staphylococcus	0.21 ± 0.05	2.72 ± 0.32	0.000				
Rothia	0.18 ± 0.03	0.89 ± 0.20	0.015				
Veillonella	0.03 ± 0.01	2.25 ± 0.44	0.004				
Moraxella	0.01 ± 0.00	0.81 ± 0.26	0.026				

TABLE 4 | The differential jejunal bacterial community of newborn piglets between the control and experimental groups within the same genotype (%).

	Hoxa1$^{-/-}$ piglets				Non-Hoxa1$^{-/-}$ piglets		
	Control group (KD-1)	Experimental group (KC-1)	*p*-value		Control group (KD-2)	Experimental group (KC-2)	*p*-value
	Phylum level				**Genus level**		
Firmicutes	28.78 ± 7.11	55.36 ± 8.11	0.034	*Rothia*	0.89 ± 0.02	0.14 ± 0.03	0.019
Patescibacteria	1.63 ± 0.62	0.04 ± 0.00	0.049	*Moraxella*	0.81 ± 0.26	0.03 ± 0.00	0.028
Genus level							
Eubacterium_fissicatena_group	0.34 ± 0.03	0.00 ± 0.00	0.046				

Data in **Table 4** show that Hoxa1$^{-/-}$ neonatal piglets from the experimental group had significantly higher relative abundance of Firmicutes ($p < 0.05$) and lower relative abundance of Patescibacteria ($p < 0.05$) at the phylum level and lower relative abundance of *Eubacterium_fissicatena_group* ($p < 0.05$) at the genus level, respectively, in the jejunal meconium than Hoxa1$^{-/-}$ neonatal piglets from the control group, and this means that maternal ATRA administration increased the relative abundance of phylum Firmicutes and decreased the relative abundances of phylum Patescibacteria and genus *Eubacterium_fissicatena_group* of Hoxa1$^{-/-}$ neonatal piglets, respectively. Non-Hoxa1$^{-/-}$ neonatal piglets from the experimental group only had significantly lower relative abundances of *Rothia* ($p < 0.05$) and *Moraxella* ($p < 0.05$) at the genus level in the jejunal meconium than non-Hoxa1$^{-/-}$ neonatal piglets from the control group.

Differential Abundance Analysis of Ileal Bacterial Community

The differential relative abundances of bacterial taxa of ileal meconium of neonatal piglets between different genotypes within the same treatment group are presented as percentages in **Table 5**. Three bacterial taxa with differential abundances at the phylum level and 12 bacterial taxa with differential abundances at the genus level were identified in the ileal meconium between Hoxa1$^{-/-}$ and non-Hoxa1$^{-/-}$ neonatal piglets from the control group (**Table 5**), and Hoxa1$^{-/-}$ neonatal piglets had significantly lower relative abundances of Firmicutes ($p < 0.01$) at the phylum level and of *Lactobacillus* ($p < 0.01$) and *Moraxella* ($p < 0.01$) at the genus level in the ileal meconium, respectively, than non-Hoxa1$^{-/-}$ neonatal piglets, but Hoxa1$^{-/-}$ neonatal piglets had significantly higher relative abundances of Bacteroidetes ($p < 0.05$) and Deferribacteres ($p < 0.05$) at the phylum level and of *Prevotellaceae_UCG-001* ($p < 0.05$), *Ruminococcaceae_UCG-014* ($p < 0.05$), *Eubacterium_xylanophilum_group* ($p < 0.05$), *Ruminiclostridium* ($p < 0.05$), *Acinetobacter* ($p < 0.05$), *Ruminococcus_1* ($p < 0.05$), *Mucispirillum* ($p < 0.05$), *Ruminococcaceae_UCG-005* ($p < 0.05$), and *Eubacterium_coprostanoligenes_group* ($p < 0.05$) at the genus level in the ileal meconium, respectively, than non-Hoxa1$^{-/-}$ neonatal piglets. After maternal ATRA administration, Hoxa1$^{-/-}$ neonatal piglets only had significantly lower relative abundance of Spirochaetes at the phylum level

TABLE 5 | The differential ileal bacterial community of newborn piglets between different genotypes within the same treatment group (%).

	Control group			Experimental group			
	Hoxa1$^{-/-}$ piglets (HD-1)	Non-Hoxa1$^{-/-}$ piglets (HD-2)	*p*-value		Hoxa1$^{-/-}$ piglets (HC-1)	Non-Hoxa1$^{-/-}$ piglets (HC-2)	*p*-value
Phylum level				**Phylum level**			
Firmicutes	27.60 ± 9.22	81.17 ± 3.79	0.001	Spirochaetes	0.00 ± 0.00	0.02 ± 0.00	0.027
Bacteroidetes	17.05 ± 4.99	1.32 ± 0.76	0.025				
Deferribacteres	0.11 ± 0.04	0.00 ± 0.00	0.037				
Genus level							
Lactobacillus	2.19 ± 0.39	57.75 ± 5.67	0.000				
Prevotellaceae_UCG-001	0.34 ± 0.12	0.01 ± 0.00	0.037				
Ruminococcaceae_UCG-014	0.33 ± 0.09	0.00 ± 0.00	0.017				
Eubacterium_xylanophilum_group	0.25 ± 0.09	0.00 ± 0.00	0.042				
Ruminiclostridium	0.23 ± 0.08	0.00 ± 0.00	0.039				
Acinetobacter	0.21 ± 0.06	0.04 ± 0.01	0.031				
Veillonella	0.17 ± 0.08	3.18 ± 1.08	0.038				
Ruminococcus_1	0.12 ± 0.04	0.00 ± 0.00	0.034				
Mucispirillum	0.11 ± 0.04	0.00 ± 0.00	0.037				
Ruminococcaceae_UCG-005	0.09 ± 0.03	0.00 ± 0.00	0.034				
Eubacterium_coprostanoligenes_group	0.09 ± 0.03	0.00 ± 0.00	0.040				
Moraxella	0.00 ± 0.00	0.70 ± 0.05	0.002				

in the ileal meconium than non-Hoxa1$^{-/-}$ neonatal piglets ($p < 0.05$).

The differential relative abundances of bacterial taxa of ileal meconium of neonatal piglets with the same genotype between different treatment groups are presented as percentages in **Table 6**. Data indicated that Hoxa1$^{-/-}$ piglets from the experimental group had significantly lower relative abundances of Deferribacteres ($p < 0.05$) at the phylum level and of *Mucispirillum* ($p < 0.05$) and *Ruminococcaceae_UCG-005* ($p < 0.05$) at the genus level in the ileal meconium, respectively, than Hoxa1$^{-/-}$ neonatal piglets from the control group, and non-Hoxa1$^{-/-}$ neonatal piglets from the experimental group had significantly lower relative abundances of Firmicutes ($p < 0.05$) and Actinobacteria ($p < 0.05$) at the phylum level and of *Lactobacillus* ($p < 0.01$), *Staphylococcus* ($p < 0.05$), *Moraxella* ($p < 0.01$), *Rothia* ($p < 0.01$), and *Pedobacter* ($p < 0.05$) at the genus level in the ileal meconium, respectively, than non-Hoxa1$^{-/-}$ neonatal piglets from the control group.

Predicted Gene Functions of Bacteria

The Tax4Fun package in R software was used to predict the functional potentials of intestinal bacteria based on the KEGG KO terms at level 3 with the observed 16S rRNA gene sequences, and the Welch's *t*-test results indicated that there were significant differences in 64 microbial metabolic pathways between jejunal bacteria of non-Hoxa1$^{-/-}$ (KD-2) and Hoxa1$^{-/-}$ (KD-1) neonatal piglets from the control group. The abundances of 22 functions were significantly higher and the abundances of 42 functions were significantly lower in KD-1 compared with KD-2 (**Figure 3A**). After maternal ATRA administration, a total of 22 microbial metabolic pathways were significantly different between jejunal bacteria of non-Hoxa1$^{-/-}$ (KC-2) and Hoxa1$^{-/-}$ (KC-1) neonatal piglets from the experimental group, and KC-1 had significantly higher expression of genes involved in starch and sucrose metabolism, oxidative phosphorylation, chloroalkane and chloroalkene degradation, meiosis, GABAergic synapse, glutamatergic synapse, retinol metabolism, non-homologous end-joining, and basal transcription factors compared with KC-2 (**Figure 3B**). KC-1 had significantly higher expression of genes involved in chloroalkane and chloroalkene degradation, retinol metabolism, proximal tubule bicarbonate reclamation, bile secretion, steroid biosynthesis, and hypertrophic cardiomyopathy than KD-1 (**Figure 4A**), and KC-2 had significantly lower expression of genes involved in nicotinate and nicotinamide metabolism, fatty acid biosynthesis, ribosome biogenesis in eukaryotes, phosphatidylinositol signaling system, mineral absorption, non-homologous end-joining, and betalain biosynthesis than KD-2 (**Figure 4B**).

A total of 36 microbial metabolic pathways were significantly different between ileal bacteria of non-Hoxa1$^{-/-}$ (HD-2) and Hoxa1$^{-/-}$ (HD-1) neonatal piglets from the control group, and 10 pathways were significantly upregulated and 26 pathways were significantly downregulated in HD-1 compared with HD-2 (**Figure 5A**). After maternal ATRA administration, 40 microbial metabolic pathways were significantly different between ileal bacteria of non-Hoxa1$^{-/-}$ (HC-2) and Hoxa1$^{-/-}$ (HC-1) neonatal piglets from the experimental group, and 36 pathways were significantly upregulated and 4 pathways were significantly downregulated in HC-1 compared with HC-2 (**Figure 5B**). HC-1 had significantly lower expression of genes involved in arginine and proline metabolism and significantly higher expression of genes involved in RNA degradation, pyruvate metabolism, renal cell carcinoma, and type II diabetes mellitus than HD-1 (**Figure 6A**), and HC-2

TABLE 6 | The differential ileal bacterial community of newborn piglets with the same genotype between the control and experimental groups (%).

	Hoxa1$^{-/-}$ piglets				Non-Hoxa1$^{-/-}$ piglets		
	Control group (HD-1)	**Experimental group (HC-1)**	***p*-value**		**Control group (HD-2)**	**Experimental group (HC-2)**	***p*-value**
Phylum level				**Phylum level**			
Deferribacteres	0.11 ± 0.04	0.00 ± 0.00	0.038	Firmicutes	81.17 ± 3.79	52.16 ± 6.18	0.035
				Actinobacteria	1.76 ± 0.62	0.53 ± 0.19	0.039
Genus level				**Genus level**			
Mucispirillum	0.11 ± 0.04	0.00 ± 0.00	0.038	*Lactobacillus*	57.75 ± 5.67	16.78 ± 7.48	0.002
Ruminococcaceae_UCG-005	0.09 ± 0.03	0.00 ± 0.00	0.036	*Staphylococcus*	1.35 ± 0.25	0.20 ± 0.07	0.022
				Moraxella	0.70 ± 0.05	0.06 ± 0.01	0.001
				Rothia	0.66 ± 0.09	0.05 ± 0.02	0.001
				Pedobacter	0.06 ± 0.01	0.01 ± 0.00	0.036

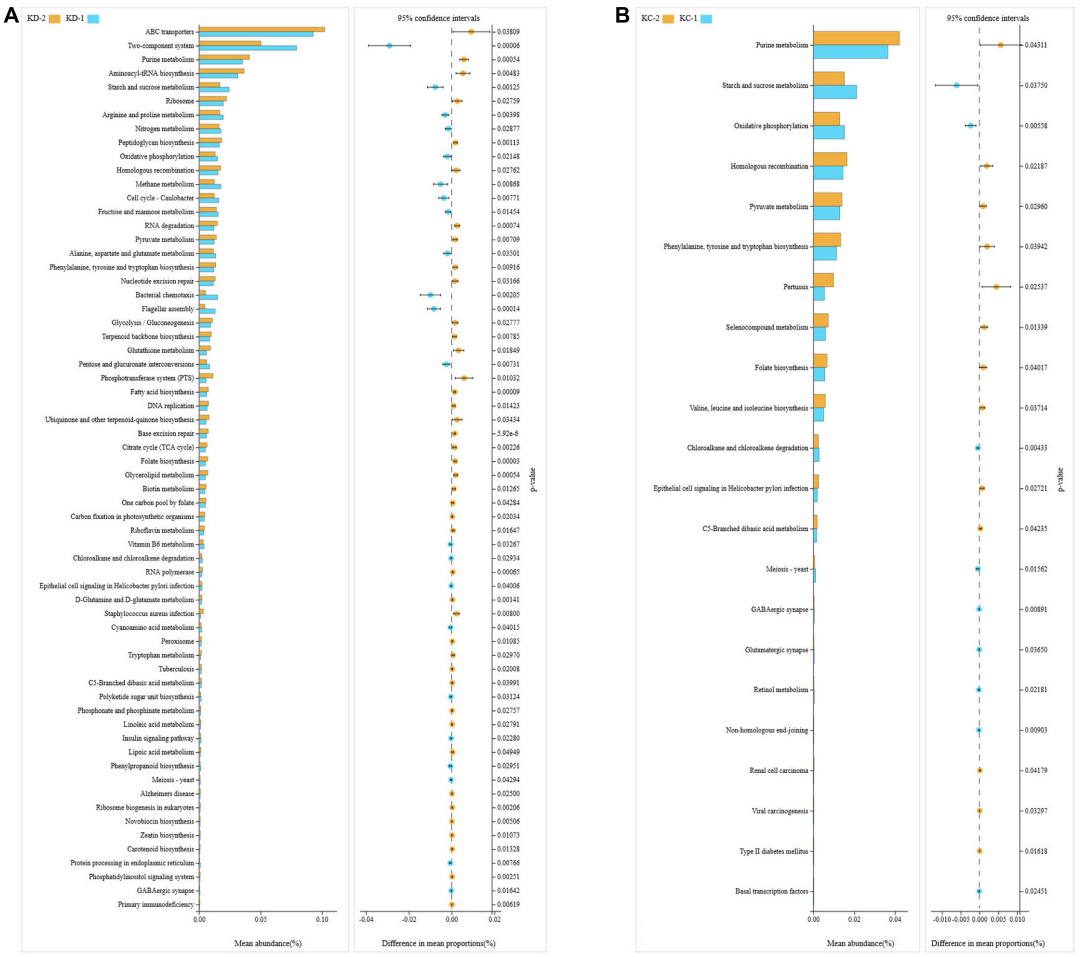

FIGURE 3 | KEGG pathways for bacteria in jejunal meconium of neonatal piglets before suckling. KD-1: bacteria of jejunal meconium of Hoxa1$^{-/-}$ neonatal piglets from the control group. KD-2: bacteria of jejunal meconium of non-Hoxa1$^{-/-}$ neonatal piglets from the control group. KC-1: bacteria of jejunal meconium of Hoxa1$^{-/-}$ neonatal piglets from the experimental group. KC-2: bacteria of jejunal meconium of non-Hoxa1$^{-/-}$ neonatal piglets from the experimental group. **(A)** Control group. **(B)** Experimental group.

had significantly higher expression of genes involved in flagellar assembly and *Salmonella* infection and significantly lower expression of genes involved in peptidoglycan biosynthesis, fatty acid biosynthesis, base excision repair, D-glutamine and D-glutamate metabolism, peroxisome, tuberculosis, peroxisome proliferator-activated receptors (PPAR) signaling pathway, ribosome biogenesis in eukaryotes, adipocytokine signaling pathway, phosphatidylinositol signaling system, steroid

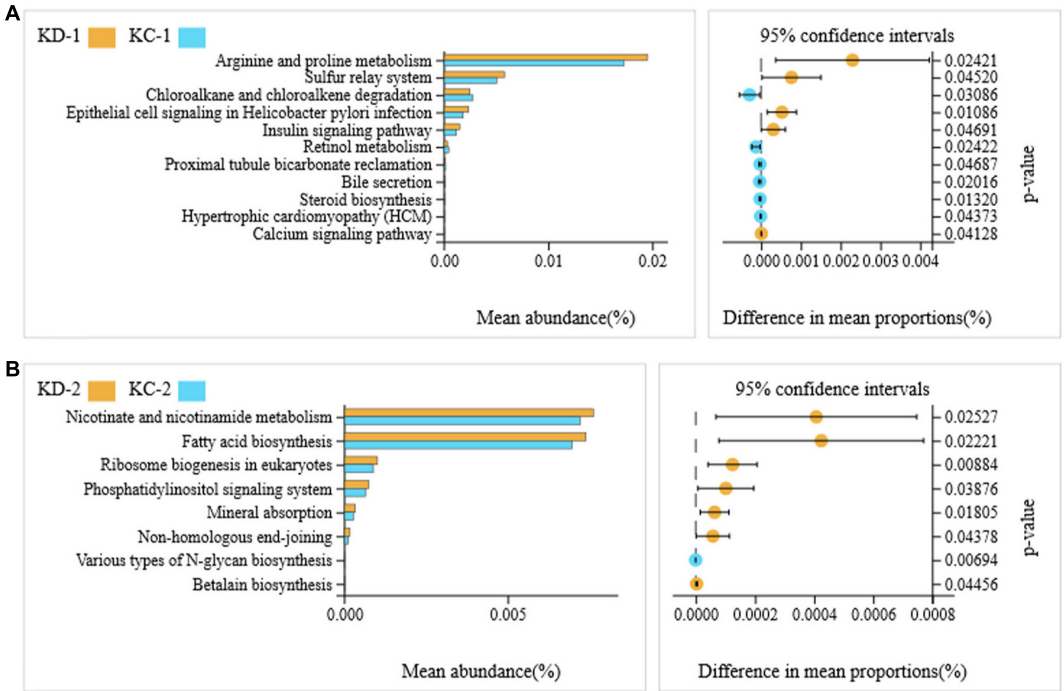

FIGURE 4 | KEGG pathways for bacteria in jejunal meconium of neonatal piglets before suckling. KD-1: bacteria of jejunal meconium of Hoxa1$^{-/-}$ neonatal piglets from the control group. KC-1: bacteria of jejunal meconium of Hoxa1$^{-/-}$ neonatal piglets from the experimental group. KD-2: bacteria of jejunal meconium of non-Hoxa1$^{-/-}$ neonatal piglets from the control group. KC-2: bacteria of jejunal meconium of non-Hoxa1$^{-/-}$ neonatal piglets from the experimental group. **(A)** Hoxa1$^{-/-}$ piglets. **(B)** Non-Hoxa1$^{-/-}$piglets.

degradation, mineral absorption, non-homologous end-joining, renin–angiotensin system, proteasome, sesquiterpenoid and triterpenoid biosynthesis, and biosynthesis of type II polyketide products than HD-2 (**Figure 6B**).

DISCUSSION

The normal colonization and development of intestinal microbiota is crucial for the normal function of the physiology and immunity of the host (Chung et al., 2012; Furusawa et al., 2013). The highly diverse intestine microbiota is generally considered beneficial for host health and is also regarded as a sign of mature intestine microbiota (Turnbaugh et al., 2007; Le Chatelier et al., 2013), but some studies found that premature development and diversification of the gut microbiota may negatively impact immune function and the highly diverse and rich bacterial community is probably not beneficial for the immature intestinal tract of young animals (Nylund et al., 2013; Wood et al., 2015). The data in our study also indicated that decreasing the number and alpha diversity of small intestinal bacterial community is beneficial to the neonatal piglets, because Hoxa1$^{-/-}$ neonatal piglets delivered by sows with ATRA administration during pregnancy had lower number and alpha diversity of small intestinal bacterial community, heavier birth live weight, and less symptom with dyspnea than Hoxa1$^{-/-}$ neonatal piglets born by sows with no ATRA administration.

Maternal genetics (Goodrich et al., 2014), gene mutation (Strati et al., 2016), delivery methods (Bi et al., 2021; Husso et al., 2021), age (Yatsunenko et al., 2012), disease (Alkanani et al., 2015), diet (David et al., 2014; Angoa-Pérez et al., 2020), and medication (Forslund et al., 2013) are the dominant factors in shaping the composition and abundance of intestinal microbiota. It is reported that the composition of intestinal bacterial communities in human and other mammals after suckling is mainly dominated by the phyla Firmicutes and Bacteroidetes, followed by the phyla Proteobacteria, Actinobacteria, and Verrucomicrobia (Gill et al., 2006; Duncan et al., 2008; Ley et al., 2008); however, the compositions of bacteria in the meconium of fetal bovine and lamb delivered by cesarean section were primarily composed of the phyla Proteobacteria and Firmicutes instead of Firmicutes and Bacteroidetes (Bi et al., 2021; Husso et al., 2021), and data in our study also indicated that Firmicutes and Proteobacteria were the most abundant phyla in the meconium of vaginal-delivered neonatal piglets before suckling.

Gene mutation can cause dysbiosis of gut microbiota by altering the relative abundance of gut microbiota and often develop a wide variety of diseases (Johansson et al., 2011; Alkanani et al., 2015; Strati et al., 2016). Microbial dysbiosis of the gut can destroy body immunity and intestinal mucosal barrier and increase gut permeability *via* the outgrowth of pathogens or the imbalance production of chemical substances in the gut (Earley et al., 2015). Mutations in the *MECP2* gene decreased the relative abundances of Firmicutes

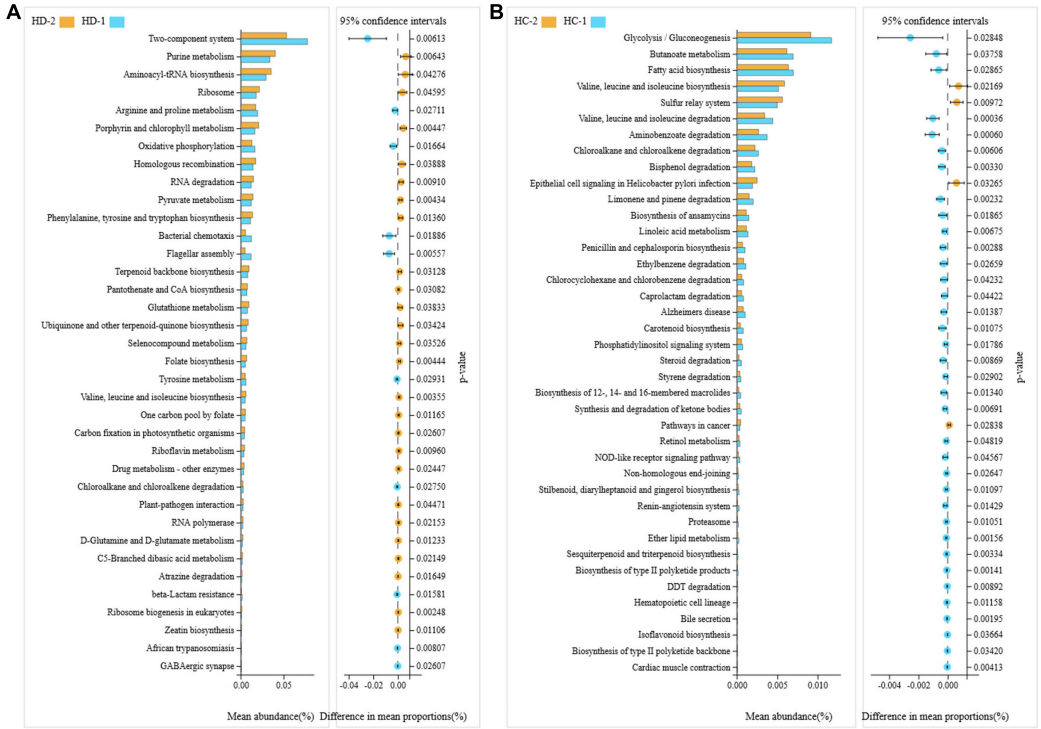

FIGURE 5 | KEGG pathways for bacteria in ileal meconium of neonatal piglets before suckling. HD-1: bacteria of ileal meconium of Hoxa1$^{-/-}$ neonatal piglets from the control group. HD-2: bacteria of ileal meconium of non-Hoxa1$^{-/-}$ neonatal piglets from the control group. HC−1: bacteria of ileal meconium of Hoxa1$^{-/-}$ neonatal piglets from the experimental group. HC-2: bacteria of ileal meconium of non-Hoxa1$^{-/-}$ neonatal piglets from the experimental group. **(A)** Control group. **(B)** Experimental group.

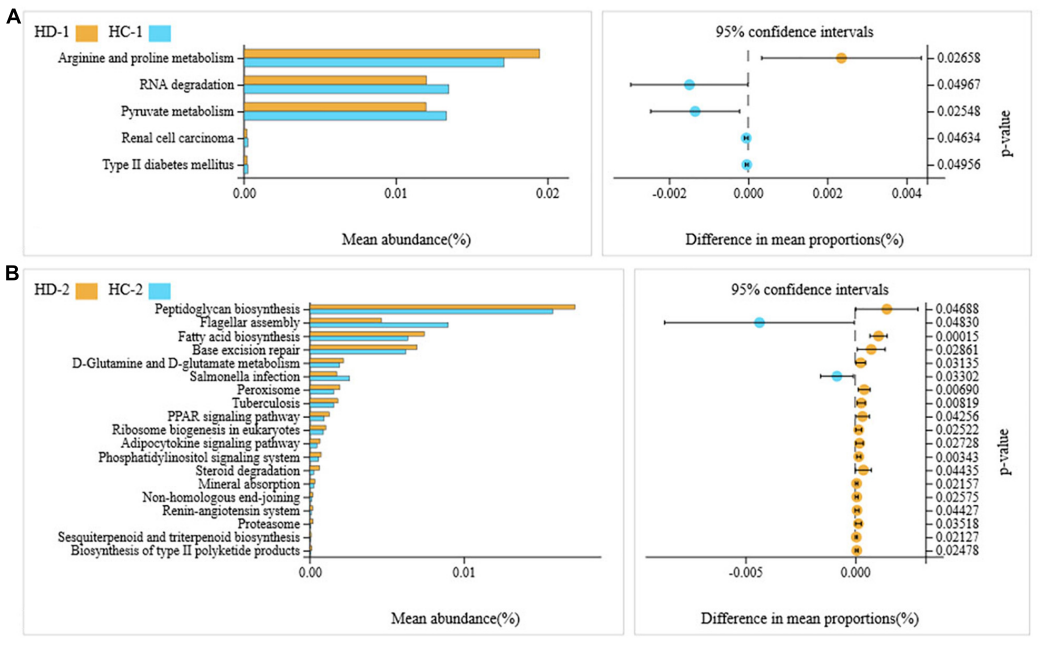

FIGURE 6 | KEGG pathways for bacteria in ileal meconium of neonatal piglets before suckling. HD-1: bacteria of ileal meconium of Hoxa1$^{-/-}$ neonatal piglets from the control group. HC-1: bacteria of ileal meconium of Hoxa1$^{-/-}$ neonatal piglets from the experimental group. HD-2: bacteria of ileal meconium of non-Hoxa1$^{-/-}$ neonatal piglets from the control group. HC-2: bacteria of ileal meconium of non-Hoxa1$^{-/-}$ neonatal piglets from the experimental group. **(A)** Hoxa1$^{-/-}$ piglets. **(B)** Non-Hoxa1$^{-/-}$piglets.

and Bacteroidetes and increased the relative abundance of Actinobacteria at the phyla level of patients compared with healthy controls (Strati et al., 2016). Our study showed that Hoxa1 mutation changed the relative abundances of small intestinal microbiota, Hoxa1$^{-/-}$ neonatal piglets had lower relative abundances of phylum Firmicutes and genera *Lactobacillus*, *Clostridium_sensu_stricto_1*, *Rothia*, and *Veillonella* and higher relative abundances of phyla Proteobacteria, Bacteroidetes, and Verrucomicrobia and genera *Escherichia–Shigella* and *Akkermansia* than non-Hoxa1$^{-/-}$ neonate piglets.

The normal ratio of Firmicutes to Bacteroidetes and the relative abundance of microbiota are essential for host health, and gene mutation often changes the Firmicutes to Bacteroidetes ratio and the microbial relative abundance. Tougaard et al. (2015) reported that tumor necrosis factor-like ligand 1A gene knockout mice had lower Firmicutes/Bacteroidetes ratio in the cecum content compared with wild-type mice (Tougaard et al., 2015), and the results of this study also indicated that Hoxa1 mutation resulted in a significantly lower ratio of Firmicutes to Bacteroidetes in the small intestine of Hoxa1$^{-/-}$ neonatal piglets than that of non-Hoxa1$^{-/-}$ neonatal piglets. Alteration in the ratio of Firmicutes to Bacteroidetes and the relative abundances of microbiota often develop into different kinds of diseases in the host. The increased ratio of Firmicutes to Bacteroidetes was reported in obese animals (Bäckhed et al., 2004), and the decreased ratio between Firmicutes and Bacteroidetes was associated with a higher risk of developing type 1 diabetes or celiac disease (Murri et al., 2013; Calderón de la Barca et al., 2020) or autism (Finegold et al., 2010) in children. The combination of significantly decreased ratio of Firmicutes to Bacteroidetes; the lower relative abundances of Firmicutes, *Lactobacillus*, *Clostridium_sensu_stricto_1*, *Staphylococcus*, *Rothia*, and *Veillonella*; and the higher relative abundances of Bacteroidetes and Patescibacteria might be some of the important factors to develop in Hoxa1$^{-/-}$ neonatal piglets undesirable symptoms of bad birth live weight, dyspnea, and death. Previous studies reported that the significantly decreased relative abundances of phylum Firmicutes and of genus *Lactobacillus* were correlated with prenatal stress (Zijlmans et al., 2015), multiple sclerosis (Chen et al., 2016), type 1 diabetes (Murri et al., 2013; Alkanani et al., 2015), and diarrheal disease (Zhuang et al., 2017). The decreased levels of *Veillonella*, *Lachnospira*, *Rothia*, *Roseburia*, and *Faecalibacterium* were also associated with asthma in children (Hilty et al., 2010; Hufnagl et al., 2020). Decreasing the numbers of Firmicutes, *Lactobacillus*, *Veillonella*, *Rothia*, and *Clostridium_sensu_stricto_1* will increase the growth and colonization of bacterial pathogens (Kim et al., 2017; Vitetta et al., 2017) and weaken gastrointestinal digestion, development, and immune functions (Edwards et al., 2017; Granja-Salcedo et al., 2017). The increased relative abundance of Bacteroidetes can generate more propionate, and the surplus of propionate can lower food intake, increase energy expenditures (Chambers et al., 2015, 2018), and facilitate the absorption of iron (Sfera et al., 2020); chronic iron overload increases the risk of reactive oxygen species and DNA damage (Sfera et al., 2020) and decreases weight gain (Calarge et al., 2016).

Preventing microbial dysbiosis in early life can reduce the risk of diseases such as intrauterine growth retardation (IUGR), allergic asthma, type 1 diabetes, and diarrhea. Studies showed that increased *Lactobacillus* can modulate gut microbiota dysbiosis (Wu et al., 2019), and early colonization with *Lactobacillus* during the infant period can reduce the risk of allergic asthma (Johansson et al., 2011). The data of our studies demonstrated that maternal ATRA administration increased the birth live weight of Hoxa1$^{-/-}$ neonatal piglets (Zhou et al., 2021). The increased ratio of Firmicutes to Bacteroidetes; the higher relative abundances of Firmicutes, Proteobacteria, and *Lactobacillus*; and the lower relative abundance of Bacteroidetes were observed in the meconium of the small intestine of Hoxa1$^{-/-}$ neonatal piglets, and the symptom of respiratory distress was not observed in Hoxa1$^{-/-}$ neonatal piglets delivered by sows with ATRA administration.

Gut microbiota may play important roles in the health and nutrient metabolism of the host, and prenatal colonization of a metabolically active microbiome is clinically vital for the health development of the fetus (Bi et al., 2021). A previous study found that microbiota in the gut of fetal lambs had high enrichment of KEGG pathways related to carbohydrate metabolism, energy metabolism, signal transduction, and amino acid metabolism (Bi et al., 2021). Our study indicated that meconium bacteria of the small intestine of neonatal piglets have functional enrichments mainly in membrane transport (ABC transporters), signal transduction (two-component system), nucleotide metabolism (purine metabolism), translation (aminoacyl-tRNA biosynthesis, ribosome), carbohydrate metabolism (starch and sucrose metabolism, fructose and mannose metabolism, pyruvate metabolism), amino acid metabolism (arginine and proline metabolism; alanine, aspartate, and glutamate metabolism; phenylalanine, tyrosine, and tryptophan biosynthesis), energy metabolism (nitrogen metabolism, oxidative phosphorylation, methane metabolism), and cell motility (bacterial chemotaxis). Hoxa1$^{-/-}$ neonatal piglets had lower functional enrichments of small intestinal bacteria in ABC transporters, purine metabolism, aminoacyl-tRNA biosynthesis, and ribosome and pyruvate metabolism and higher functional enrichments of small intestinal bacteria in two-component system; starch and sucrose metabolism; fructose and mannose metabolism; arginine and proline metabolism; alanine, aspartate, and glutamate metabolism; nitrogen metabolism; and bacterial chemotaxis than non-Hoxa1$^{-/-}$ neonatal piglets. In addition, maternal ATRA administration during pregnancy not only can shape the functional enrichments of small intestinal bacteria of Hoxa1$^{-/-}$ neonatal piglets but also can alter the functional enrichments of small intestinal bacteria of non-Hoxa1$^{-/-}$ neonatal piglets. Data showed that non-Hoxa1$^{-/-}$ neonatal piglets delivered by sows with ATRA administration had significantly lower functional enrichments of small intestinal bacteria in nicotinate and nicotinamide metabolism, fatty acid biosynthesis, ribosome biogenesis in eukaryotes, phosphatidylinositol signaling system, mineral absorption, peptidoglycan biosynthesis, base excision repair, D-glutamine and D-glutamate metabolism, tuberculosis, and PPAR signaling pathway and significantly higher functional enrichments of small intestinal bacteria in flagellar assembly and

Salmonella infection than non-Hoxa1$^{-/-}$ neonatal piglets born by sows with no ATRA administration.

CONCLUSION

Hoxa1 mutation altered the diversity of the bacterial community and the relative abundances of several dominant taxa; Hoxa1$^{-/-}$ neonatal piglets had significantly higher alpha diversity of bacterial community, lower phylum Firmicutes and genus *Lactobacillus*, and higher phylum Bacteroidetes than non-Hoxa1$^{-/-}$ neonatal piglets in the meconium of the jejunum and ileum. Maternal ATRA administration altered the bacterial diversity and the relative abundances of dominant taxa of Hoxa1$^{-/-}$ and non-Hoxa1$^{-/-}$ neonatal piglets; Hoxa1$^{-/-}$ neonatal piglets delivered by sows with ATRA administration had lower alpha diversity of bacterial community and significantly higher relative abundance of phylum Firmicutes than Hoxa1$^{-/-}$ neonatal piglets born by sows with no ATRA administration, but had higher alpha diversity of bacterial community, higher relative abundances of phyla Proteobacteria and Bacteroidetes, and lower relative abundances of phylum Firmicutes and genus *Lactobacillus* than non-Hoxa1$^{-/-}$ neonatal piglets delivered by sows with ATRA administration. Compared with non-Honx1$^{-/-}$ neonatal piglets delivered by sows with no ATRA administration, non-Hoxa1$^{-/-}$ neonatal piglets born by sows with ATRA administration had higher alpha diversity of bacterial community and lower relative abundances of the genera *Rothia* and *Moraxella*.

DATA AVAILABILITY STATEMENT

The datasets presented in this study can be found in online repositories. The names of the repository/repositories and accession number(s) can be found in the article/supplementary material.

ETHICS STATEMENT

The animal study was reviewed and approved by the Ethics Committee for Animal Experimentation of Jiangxi Agricultural University. Written informed consent was obtained from the owners for the participation of their animals in this study.

AUTHOR CONTRIBUTIONS

YH conceived the study. YH and WL designed the study. HZ, HW, YC, and WZ performed the experiments. HZ performed the data analysis. YH and HZ writing the manuscript. All authors read and approved the final manuscript.

FUNDING

This study was supported by the National Natural Science Foundation of China (31560303).

REFERENCES

Abu-Libdeh, B., Douiev, L., Amro, S., Shahrour, M., Ta-Shma, A., Miller, C., et al. (2017). Mutation in the COX4I1 gene is associated with short stature, poor weight gain and increased chromosomal breaks, simulating Fanconi anemia. *Eur. J. Hum. Genet.* 25, 1142–1146. doi: 10.1038/ejhg.2017.112

Ai Dhaibani, M. A., El-Hattab, A. W., Holroyd, K. B., Orthmann-Murphy, J., Larson, V. A., Siddiqui, K. A., et al. (2018). Novel mutation in the KCNJ10 gene in three siblings with seizures, ataxia and no electrolyte abnormalities. *J. Neurogenet.* 32, 1–5. doi: 10.1080/01677063.2017.1404057

Alasti, F., Sadeghi, A., Sanati, M. H., Farhadi, M., Stollar, E., Somers, T., et al. (2008). A mutation in Hoxa2 is responsible for autosomal-recessive microtia in an Iranian family. *Am. J. Hum. Genet.* 82, 982–991. doi: 10.1016/j.ajhg.2008.02.015

Alipour, M. J., Jalanka, J., Pessa-Morikawa, T., Kokkonen, T., Satokari, R., Hynönen, U., et al. (2018). The composition of the perinatal intestinal microbiota in cattle. *Sci. Rep.* 8:10437. doi: 10.1038/s41598-018-31494-3

Alkanani, A. K., Hara, N., Gottlieb, P. A., Ir, D., Robertson, C. E., Wagner, B. D., et al. (2015). Alterations in intestinal microbiota correlate with susceptibility to type 1 diabetes. *Diabetes* 64, 3510–3520. doi: 10.2337/db14-1847

Angoa-Pérez, M., Zagorac, B., Francescutti, D. M., Winters, A. D., Greenberg, J., Ahmad, M. M., et al. (2020). Effects of a high fat diet on gut microbiome dysbiosis in a mouse model of gulf war illness. *Sci. Rep.* 10:9529. doi: 10.1038/s41598-020-66833-w

Aßhauer, K. P., Wemheuer, B., Daniel, R., and Meinicke, P. (2015). Tax4Fun: predicting functional profiles from metagenomic 16S rRNA data. *Bioinformatics* 31, 2882–2884. doi: 10.1093/bioinformatics/btv287

Bäckhed, F., Ding, H., Wang, T., Hooper, L. V., Koh, G. Y., Nagy, A., et al. (2004). The gut microbiota as an environmental factor that regulates fat storage. *Proc. Natl. Acad. Sci. U. S. A.* 101, 15718–15723. doi: 10.1073/pnas.0407076101

Ben Salem, H., Nefzaoui, A., Makkar, H. P. S., Hochlef, H., Ben Salem, I., and Ben Salem, L. (2005). Effect of early experience and adaptation period on voluntary intake, digestion, and growth in Barbarine lambs given tannin-containing (Acacia cyanophylla Lindl. foliage) or tannin-free (oaten hay) diets. *Anim. Feed Sci. Technol.* 122, 59–77. doi: 10.1016/j.anifeedsci.2005.04.014

Bi, Y. L., Tu, Y., Zhang, N. F., Wang, S. Q., Zhang, F., Suen, G., et al. (2021). Multiomics analysis reveals the presence of a microbiome in the gut of fetal lambs. *Gut* 70, 853–864. doi: 10.1136/gutjnl-2020-320951

Calarge, C. A., Murry, D. J., Ziegler, E. E., and Arnold, L. E. (2016). Serum ferritin, weight gain, disruptive behavior, and extrapyramidal symptoms in risperidone-treated youth. *J. Child Adolesc. Psychopharmacol.* 26, 471–477. doi: 10.1089/cap.2015.0194

Calderón de la Barca, A. M., Castillo-Fimbres, R. S., Mejía-León, M. E., Quihui-Cota, L., Ochoa-Leyva, A., and Aguayo-Patrón, S. V. (2020). Enteric parasitic infection disturbs bacterial structure in Mexican children with autoantibodies for type 1 diabetes and/or celiac disease. *Gut Pathog.* 12:37. doi: 10.1186/s13099-020-00376-3

Caporaso, J. G., Kuczynski, J., Stombaugh, J., Bittinger, K., Bushman, F. D., Costello, E. K., et al. (2010). QIIME allows analysis of high-throughput community sequencing data. *Nat. Methods* 7, 335–336. doi: 10.1038/nmeth.f.303

Caporaso, J. G., Lauber, C. L., Walters, W. A., Berg-Lyons, D., Huntley, J., Fierer, N., et al. (2012). Ultra-high-throughput microbial community analysis on the Illumina HiSeq and MiSeq platforms. *ISME J.* 6, 1621–1624. doi: 10.1038/ismej.2012.8

Chambers, E. S., Byrne, C. S., Aspey, K., Chen, Y. J., Khan, S., Morrison, D. J., et al. (2018). Acute oral sodium propionate supplementation raises resting energy expenditure and lipid oxidation in fasted humans. *Diabetes Obes. Metab.* 20, 1034–1039. doi: 10.1111/dom.13159

Chambers, E. S., Viardot, A., Psichas, A., Morrison, D. J., Murphy, K. G., Zac-Varghese, S. E. K., et al. (2015). Effects of targeted delivery of propionate to the human colon on appetite regulation, body weight maintenance and adiposity in overweight adults. *Gut* 64, 1744–1754. doi: 10.1136/gutjnl-2014-307913

Chen, J., Chia, N., Kalari, K. R., Yao, J. Z., Novotna, M., Soldan, M. M. P., et al. (2016). Multiple sclerosis patients have a distinct gut microbiota compared to healthy controls. *Sci. Rep.* 6:28484. doi: 10.1038/srep28484

Chen, S. F., Zhou, Y. Q., Chen, Y. R., and Gu, J. (2018). fastp: an ultra-fast all-in-one FASTQ preprocessor. *Bioinformatics* 34, i884–i890. doi: 10.1093/bioinformatics/bty560

Chung, H., Pamp, S. J., Hill, J. A., Surana, N. K., Edelman, S. M., Troy, E. B., et al. (2012). Gut immune maturation depends on colonization with a host-specific microbiota. *Cell* 149, 1578–1593. doi: 10.1016/j.cell.2012.04.037

David, L. A., Maurice, C. F., Carmody, R. N., Gootenberg, D. B., Button, J. E., Wolfe, B. E., et al. (2014). Diet rapidly and reproducibly alters the human gut microbiome. *Nature* 505, 559–563. doi: 10.1038/nature12820

Duncan, S. H., Lobley, G. E., Holtrop, G., Ince, J., Johnstone, A. M., Louis, P., et al. (2008). Human colonic microbiota associated with diet, obesity and weight loss. *Int. J. Obes.* 32, 1720–1724. doi: 10.1038/ijo.2008.155

Earley, Z. M., Akhtar, S., Green, S. J., Naqib, A., Khan, O., Cannon, A. R., et al. (2015). Burn injury alters the intestinal microbiome and increases gut permeability and bacterial translocation. *PLoS One* 10:e0129996. doi: 10.1371/journal.pone.0129996

Edgar, R. C. (2013). UPARSE: highly accurate OTU sequences from microbial amplicon reads. *Nat. Methods* 10, 996–998. doi: 10.1038/nmeth.2604

Edwards, J. E., Forster, R. J., Callaghan, T. M., Dollhofer, V., Dagar, S. S., Cheng, Y. F., et al. (2017). PCR and omics based techniques to study the diversity, ecology and biology of anaerobic fungi: insights, challenges and opportunities. *Front. Microbiol.* 8:1657. doi: 10.3389/fmicb.2017.01657

Finegold, S. M., Dowd, S. E., Gontcharova, V., Liu, C. X., Henley, K. E., Wolcott, R. D., et al. (2010). Pyrosequencing study of fecal microflora of autistic and control children. *Anaerobe* 16, 444–453. doi: 10.1016/j.anaerobe.2010.06.008

Forslund, K., Sunagawa, S., Kultima, J. R., Mende, D. R., Arumugam, M., Typas, A., et al. (2013). Country-specific antibiotic use practices impact the human gut resistome. *Genome Res.* 23, 1163–1169. doi: 10.1101/gr.155465.113

Furusawa, Y., Obata, Y., Fukuda, S., Endo, T. A., Nakato, G., Takahashi, D., et al. (2013). Commensal microbe-derived butyrate induces the differentiation of colonic regulatory T cells. *Nature* 504, 446–450. doi: 10.1038/nature12721

Giancotti, A., Ambrosio, V. D., De Filippis, A., Aliberti, C., Pasquali, G., Bernardo, S., et al. (2014). Comparison of ultrasound and magnetic resonance imaging in the prenatal diagnosis of Apert syndrome: report of a case. *Childs Nerv. Syst.* 30, 1445–1448. doi: 10.1007/s00381-014-2377-8

Gill, S. R., Pop, M., Deboy, R. T., Eckburg, P. B., Turnbaugh, P. J., Samuel, B. S., et al. (2006). Metagenomic analysis of the human distal gut microbiome. *Science* 312, 1355–1359. doi: 10.1126/science.1124234

Goodrich, J. K., Waters, J. L., Poole, A. C., Sutter, J. L., Koren, O., Blekhman, R., et al. (2014). Human genetics shape the gut microbiome. *Cell* 159, 789–799. doi: 10.1016/j.cell.2014.09.053

Granja-Salcedo, Y. T., Messana, J. D., de Souza, V. C., Dias, A. V. L., Kishi, L. T., Rebelo, L. R., et al. (2017). Effects of partial replacement of maize in the diet with crude glycerin and/or soyabean oil on ruminal fermentation and microbial population in Nellore steers. *Br. J. Nutr.* 118, 651–660. doi: 10.1017/s0007114517002689

Hampe, J., Cuthbert, A., Croucher, P. J., Mirza, M. M., Mascheretti, S., Fisher, S., et al. (2001). Association between insertion mutation in NOD2 gene and Crohn's disease in German and British populations. *Lancet* 357, 1925–1928. doi: 10.1016/S0140-6736(00)05063-7

Hilty, M., Burke, C., Pedro, H., Cardenas, P., Bush, A., Bossley, C., et al. (2010). Disordered microbial communities in asthmatic airways. *PLoS One* 5:e8578. doi: 10.1371/journal.pone.0008578

Hufnagl, K., Pali-Schöll, I., Roth-Walter, F., and Jensen-Jarolim, E. (2020). Dysbiosis of the gut and lung microbiome has a role in asthma. *Semin. Immunopathol.* 42, 75–93. doi: 10.1007/s00281-019-00775-y

Hummel, G. L., Woodruff, K. L., Austin, K. J., Smith, T. L., and Cunningham-Hollinger, H. C. (2020). Evidence for the amnion-fetal gut-microbial axis in late gestation beef calves. *Transl. Anim. Sci.* 4, S174–S177. doi: 10.1093/tas/txaa138

Husso, A., Lietaer, L., Pessa-Morikawa, T., Grönthal, T., Govaere, J., Soom, A. V., et al. (2021). The composition of the microbiota in the full-term fetal gut and amniotic fluid: a bovine caesarean section study. *Front. Microbiol.* 12:626421. doi: 10.3389/fmicb.2021.626421

Jelani, M., Dooley, H. C., Gubas, A., Sheikh, H., Mohamoud, H. S. A., Masood, T., et al. (2019). A mutation in the major autophagy gene, WIPI2, associated with global developmental abnormalities. *Brain* 142, 1242–1254. doi: 10.1093/brain/awz075

Johansson, M. A., Sjögren, Y. M., Persson, J. O., Nilsson, C., and Sverremark-Ekström, E. (2011). Early colonization with a group of Lactobacilli decreases the risk for allergy at five years of age despite allergic heredity. *PLoS One* 6:e23031. doi: 10.1371/journal.pone.0023031

Johnson, K. R., Gagnon, L. H., and Chang, B. (2016). A hypomorphic mutation of the gamma-1 adaptin gene (Ap1g1) causes inner ear, retina, thyroid, and testes abnormalities in mice. *Mamm. Genome* 27, 200–212. doi: 10.1007/s00335-016-9632-0

Joossens, M., Huys, G., Cnockaert, M., Cnockaert, M., De Preter, V., Verbeke, K., et al. (2011). Dysbiosis of the faecal microbiota in patients with Crohn's disease and their unaffected relatives. *Gut* 60, 631–637. doi: 10.1136/gut.2010.223263

Kanehisa, M., Sato, Y., Kawashima, M., Furumichi, M., and Tanabe, M. (2015). KEGG as a reference resource for gene and protein annotation. *Nucleic Acids Res.* 44, D457–D462. doi: 10.1093/nar/gkv1070

Kim, Y. G., Sakamoto, K., Seo, S. U., Pickard, J. M., Gillilland, M. G., Pudlo, N. A., et al. (2017). Neonatal acquisition of Clostridia species protects against colonization by bacterial pathogens. *Science* 356, 315–319. doi: 10.1126/science.aag2029

Le Chatelier, E., Nielsen, T., Qin, J., Prifti, E., Hildebrand, F., Falony, G., et al. (2013). Richness of human gut microbiome correlates with metabolic markers. *Nature* 500, 541–546. doi: 10.1038/nature12506

Ley, R. E., Hamady, M., Lozupone, C., Turnbaugh, P. J., Ramey, R. R., Bircher, J. S., et al. (2008). Evolution of mammals and their gut microbes. *Science* 320, 1647–1651. doi: 10.1126/science.1155725

Lynch, S. V., Goldfarb, K. C., Wild, Y. K., Kong, W. D., De Lisle, R. C., and Brodie, E. L. (2013). Cystic fibrosis transmembrane conductance regulator knockout mice exhibit aberrant gastrointestinal microbiota. *Gut Microbes* 4, 41–47. doi: 10.4161/gmic.22430

Magoč, T., and Salzberg, S. L. (2011). FLASH: fast length adjustment of short reads to improve genome assemblies. *Bioinformatics* 27, 2957–2963. doi: 10.1093/bioinformatics/btr507

Morgavi, D. P., Rathahao-Paris, E., Popova, M., Boccard, J., Nielsen, K. F., and Boudra, H. (2015). Rumen microbial communities influence metabolic phenotypes in lambs. *Front. Microbiol.* 6:1060. doi: 10.3389/fmicb.2015.01060

Murri, M., Leiva, I., Gomez-Zumaquero, J. M., Tinahones, F. J., Cardona, F., Soriguer, F., et al. (2013). Gut microbiota in children with type 1 diabetes differs from that in healthy children: a case-control study. *BMC Med.* 11:46. doi: 10.1186/1741-7015-11-46

Murthy, V., Tebaldi, T., Yoshida, T., Erdin, S., Calzonetti, T., Vijayvargia, R., et al. (2019). Hypomorphic mutation of the mouse Huntington's disease gene orthologue. *PLoS Genet.* 15:e1007765. doi: 10.1371/journal.pgen.1007765

Nonose, R. W., Lezirovitz, K., de Mello Auricchio, M. T. B., Batissoco, A. C., Yamamoto, G. L., and Mingroni-Netto, R. C. (2018). Mutation analysis of SLC26A4 (Pendrin) gene in a Brazilian sample of hearing-impaired subjects. *BMC Med. Genet.* 19:73. doi: 10.1186/s12881-018-0585-x

Nylund, L., Satokari, R., Nikkila, J., Rajilić-Stojanović, M., Kalliomäki, M., Isolauri, E., et al. (2013). Microarray analysis reveals marked intestinal microbiota aberrancy in infants having eczema compared to healthy children in at-risk for atopic disease. *BMC Microbiol.* 13:12. doi: 10.1186/1471-2180-13-12

Ogura, Y., Bonen, D. K., Inohara, N., Nicolae, D. L., Chen, F. F., Ramos, R., et al. (2001). A frameshift mutation in NOD2 associated with susceptibility to Crohn's disease. *Nature* 411, 603–606. doi: 10.1038/35079114

Oksanen, J., Blanchet, F. G., Kindt, R., Legendre, P., and Minchin, P. R. (2010). *Vegan: Community Ecology Package. R Package Version 1.17-4*.

Ondov, B. D., Bergman, N. H., and Phillippy, A. M. (2011). Interactive metagenomic visualization in a Web browser. *BMC Bioinformatics* 12:385. doi: 10.1186/1471-2105-12-385

Pasqualetti, M., Neun, R., Davenne, M., and Rijli, F. M. (2001). Retinoic acid rescues inner ear defects in Hoxa1 deficient mice. *Nat. Genet.* 29, 34–39. doi: 10.1038/ng702

Pruesse, E., Quast, C., Knittel, K., Fuchs, B. M., Ludwig, W., Peplies, J. X., et al. (2007). SILVA: a comprehensive online resource for quality checked and aligned ribosomal RNA sequence data compatible with ARB. *Nucleic Acids Res.* 35, 7188–7196. doi: 10.1093/nar/gkm864

Qiao, R. M., He, Y. Y., Pan, B., Xiao, S. J., Zhang, X. F., Li, J., et al. (2015). Understanding the molecular mechanisms of human microtia via a pig model of HOXA1 syndrome. *Dis. Model Mech.* 8, 611–622. doi: 10.1242/dmm.018291

Sfera, A., Osorio, C., Diaz, E. L., Maguire, G., and Cummings, M. (2020). The other obesity epidemic-of drugs and bugs. *Front. Endocrinol.* 11:488. doi: 10.3389/fendo.2020.00488

Stinson, L. F., Boyce, M. C., Payne, M. S., and Keelan, J. A. (2019). The not-so-sterile womb: evidence that the human fetus is exposed to bacteria prior to birth. *Front. Microbiol.* 10:1124. doi: 10.3389/fmicb.2019.01124

Strati, F., Cavalieri, D., Albanese, D., De Felice, C., Donati, C., Hayek, J., et al. (2016). Altered gut microbiota in Rett syndrome. *Microbiome* 4:41. doi: 10.1186/s40168-016-0185-y

Tougaard, P., Skov, S., Pedersen, A. E., Krych, L., Nielsen, D. S., Bahl, M. I., et al. (2015). TL1A regulates TCRγδ+ intraepithelial lymphocytes and gut microbial composition. *Eur. J. Immunol.* 45, 865–875. doi: 10.1002/eji.201444528

Turnbaugh, P. J., Ley, R. E., Hamady, M., Fraser-Liggett, C. M., Knight, R., and Gordon, J. I. (2007). The human microbiome project. *Nature* 449, 804–810. doi: 10.1038/nature06244

Vitetta, L., Coulson, S., Thomsen, M., Nguyen, T., and Hall, S. (2017). Probiotics, D-Lactic acidosis, oxidative stress and strain specificity. *Gut Microbes* 8, 311–322. doi: 10.1080/19490976.2017.1279379

Wang, Q., Garrity, G. M., Tiedje, J. M., and Cole, J. R. (2007). Naive Bayesian classifier for rapid assignment of rRNA sequences into the new bacterial taxonomy. *Appl. Environ. Microb.* 73, 5261–5267. doi: 10.1128/AEM.00062-07

Wood, K. M., Palmer, S. I., Steele, M. A., Metcalf, J. A., and Penner, G. B. (2015). The influence of age and weaning on permeability of the gastrointestinal tract in Holstein bull calves. *J. Dairy Sci.* 98, 7226–7237. doi: 10.3168/jds.2015-9393

Wu, C. H., Ko, J. L., Liao, J. M., Huang, S. S., Lin, M. Y., Lee, L. H., et al. (2019). D-methionine alleviates cisplatin-induced mucositis by restoring the gut microbiota structure and improving intestinal inflammation. *Ther. Adv. Med. Oncol.* 11, 1–18. doi: 10.1177/1758835918821021

Yatsunenko, T., Rey, F. E., Manary, M. J., Trehan, I., Dominguez-Bello, M. G., Contreras, M., et al. (2012). Human gut microbiome viewed across age and geography. *Nature* 486, 222–227. doi: 10.1038/nature11053

Zhou, H. M., Chen, Y. X., Hu, Y. Q., Gao, S., Lu, W., and He, Y. Y. (2021). Administration of all-Trans retinoic acid to pregnant sows improves the developmental defects of Hoxa1$^{-/-}$ fetal pigs. *Front. Vet. Sci.* 7:618660. doi: 10.3389/fvets.2020.618660

Zhuang, X., Xiong, L., Li, L., Li, M. Y., and Chen, M. H. (2017). Alterations of gut microbiota in patients with irritable bowel syndrome: a systematic review and meta-analysis. *J.Gastroenterol. Hepatol.* 32, 28–38. doi: 10.1111/jgh.13471

Zijlmans, M. A. C., Korpela, K., Riksen-Walraven, J. M., de Vos, W. M., and de Weerth, C. (2015). Maternal prenatal stress is associated with the infant intestinal microbiota. *Psychoneuroendocrino* 53, 233–245. doi: 10.1016/j.psyneuen.2015.01.006

Conflict of Interest: The authors declare that the research was conducted in the absence of any commercial or financial relationships that could be construed as a potential conflict of interest.

Publisher's Note: All claims expressed in this article are solely those of the authors and do not necessarily represent those of their affiliated organizations, or those of the publisher, the editors and the reviewers. Any product that may be evaluated in this article, or claim that may be made by its manufacturer, is not guaranteed or endorsed by the publisher.

frontiers in Microbiology

ORIGINAL RESEARCH
published: 28 July 2021
doi: 10.3389/fmicb.2021.706758

Herbal Extract Mixture Modulates Intestinal Antioxidative Capacity and Microbiota in Weaning Piglets

*Meiwei Wang[1], Huijun Huang[1], Lei Wang[1], Huansheng Yang[1], Shengwen He[2], Feng Liu[3], Qiang Tu[3] and Shanping He[1]**

[1] State Key Laboratory of Developmental Biology of Freshwater Fish, Hunan Provincial Key Laboratory of Animal Intestinal Function and Regulation, Hunan Normal University, Changsha, China, [2] Anhui Tianan Biotechnology Company Limited, Luan, China, [3] Yucheng Baolikang Biological Feed Company Limited, Dezhou, China

Recently, herbal extracts have been applied in multiple aspects, such as medicine and animal feed. Different compositions of herbal extract mixture (HEM) have various components and diverse functions. This study aimed to evaluate the effects of HEM (*Lonicera japonica, Astragalus membranaceus*, *Eucommia folium*, and *Codonopsis pilosula*) on intestinal antioxidant capacity and colonic microbiota in weaned pigs. A total of 18 piglets [Duroc × (Landrace × Yorkshire)] with the initial body weight of 5.99 ± 0.13 kg (weaned at 21 days) were randomly divided into two groups (n = 9): the control group (CON, basal diet) and the HEM treatment group (HEM, 1,000 mg/kg HEM + basal diet). The experiment period lasted for 14 days. Our results showed that dietary supplementation with HEM modulated the antioxidant capacity through decreasing the activity of superoxide dismutase (SOD) in the ileum and glutathione peroxidase (GSH-PX) in the serum, and decreasing the mRNA expression of Kelch like-ECH-associated protein 1 (Keap1) in the jejunum and the protein level of Keap1 in the ileum. Moreover, the HEM group modified the composition of colonic microbiota with affecting relative abundances of the Firmicutes and Bacteroidetes at the phylum level. Taken together, supplementation of HEM can regulate the antioxidant capacity and modify the composition of colonic bacteria in weaning piglets. This study provides new insights into the combination effects of herbal extracts on weaning piglets.

Keywords: colonic microbiota, herbal extract mixture, intestinal antioxidant capacity, weaning piglets, Nrf2 pathway

OPEN ACCESS

Edited by:
Peng Huang,
Hunan Agricultural University, China

Reviewed by:
Marko Samardžija,
University of Zagreb, Croatia
Md. Abul Kalam Azad,
Institute of Subtropical Agriculture, Chinese Academy of Sciences, China

****Correspondence:***
Shanping He
hesp@hunnu.edu.cn

Specialty section:
This article was submitted to Microbial Symbioses, a section of the journal Frontiers in Microbiology

Received: *08 May 2021*
Accepted: *14 June 2021*
Published: *28 July 2021*

Citation:
Wang M, Huang H, Wang L, Yang H, He S, Liu F, Tu Q and He S (2021) Herbal Extract Mixture Modulates Intestinal Antioxidative Capacity and Microbiota in Weaning Piglets. Front. Microbiol. 12:706758. doi: 10.3389/fmicb.2021.706758

INTRODUCTION

Early weaning is a beneficial practice for improving sow reproductive performance in pig industry (Robert et al., 1999). However, early weaning reduces the growth performance of weaning piglets. Moreover, early weaning damages the intestinal function and gives rise to poor immunity status, thereby leading to weaning stress on early weaning piglets (Blecha et al., 1983). Disruption of

Abbreviations: HEM, herbal extract mixture; CON, the control group; SOD, superoxide dismutase; GSH-PX, glutathione peroxidase; Keap1, Kelch like-ECH-associated protein 1; MDA, malondialdehyde; CAT, catalase; SCFA, short chain fatty acid; PCoA, principal co-ordinates analysis; PCA, principal component analysis; LEfSe, linear discriminant analysis coupled with effect size measurements analysis.

intestinal function after weaning is correlated with shorter intestinal villus, hyperplasia of the intestinal crypt, disrupted intestinal barrier, and decreased digestive capacity (Smith et al., 2010; Yang et al., 2013). Moreover, because of the insufficient immune function of weaning piglets, they are easy to suffer weaning stress incurred by pathogens in feed (McLamb et al., 2013). Early weaning also destroys the antioxidant system and leads to excessive reactive oxygen species, thus resulting in intestinal oxidative stress in weaning piglets (Lauridsen, 2019). Weaning stress increases harmful bacteria to colonize in the intestine and disrupts intestinal homeostasis (Gresse et al., 2017). At present, functional amino acids, plant extracts, and organic acids are commonly used to alleviate weaning stress in swine farms (Jayaraman and Nyachoti, 2017; Modina et al., 2019).

In livestock production, plant extracts have been recommended as feed additives to substitute antibiotics because they are natural products and have various beneficial activities, including antiviral, antibacterial, and antioxidant activities (Liu et al., 2018). Liu et al. (2016) have reported that the dietary supplementation of *Scutellaria baicalensis* and *Lonicera japonica* extract mixture (0.025 and 0.05%) for 12 weeks improves the growth performance through increasing the overall average daily growth (ADG) and the ratio of gain to feed, elevates the nutrient digestibility of nitrogen, energy, and dry matter, decreases the serum cortisol concentration, and improves meat quality through increasing the pH of meat and decreasing the concentration of 2-thiobarbituric acid in finishing pigs. Manzanilla et al. (2004) reported that plant extract mixture (containing 5% *carvacrol* extracted from oregano, 3% *cinnamaldehyde* extracted from cinnamon, and 2% *capsicum oleoresin* extracted from Mexican pepper) and formic acid in the diet modify the gastrointestinal ecosystem through increasing the ratio of lactobacilli to enterobacteria, increase stomach contents, and decrease the stomach emptying rate through extending the gastric retention time of weaning piglets. Dietary supplementation of herbal extract (0.75% inclusion, including *cinnamon*, *thyme*, and *oregano* extract) affects the composition of gut microbiota through inhibiting the proliferation of coliform bacteria and increases the pH of colon in weaning piglets (Namkung et al., 2004). These studies suggested that herbal extract mixtures have different effects on the physiology of piglets.

Golden-and-silver honeysuckle (*Lonicera japonica*), huangqi (*Astragalus membranaceus*), duzhong leaves (*Eucommia folium*), and dangshen (*Codonopsis pilosula*) contain various active ingredients, including organic acids, isoflavonoids, flavones, iridoids, polysaccharides, and sand saponins. In addition, the active ingredients of the four plant extracts have antioxidant and anti-inflammatory activities (Yen and Hsieh, 1998; He et al., 2015). However, different combinations of herbal extract mixture have different functions to weaning pigs, and the combination of several herbal extracts has more biological activity than each of the herbal extract alone. The combination of these plant extracts (*Lonicera japonica, Astragalus membranaceus*, *Eucommia folium*, and *Codonopsis pilosula*) has not been fully investigated in weaning piglets. Moreover, our previous study has shown that dietary supplementation of the herbal extract mixture (HEM), which contains golden-and-silver honeysuckle (*Lonicera japonica*), huangqi (*Astragalus membranaceus*), duzhong leaves (*Eucommia folium*), and dangshen (*Codonopsis pilosula*), improves intestinal morphology through increasing the ratio of villus height to crypt depth in the duodenum, and elevates the mRNA expression of nutrient transporters in the ileum of weaning piglets (Wang et al., 2020). Thus, in the present study, we aimed to further investigate the effects of HEM on the antioxidant capacity and colonic microbiota of weaning piglets.

MATERIALS AND METHODS

Animals and Treatment

A total of 18 weaning piglets (Duroc × [Landrace × Yorkshire], weaned at 21 days, initial body weight = 5.99 ± 0.13 kg) were randomly allotted to two treatments: a control group with the basal diet and the HEM group with 1,000 mg/kg HEM directly added into the basal diet. The basal diet did not have any antibiotics. All piglets were raised in the same environment in the 14 days. All the pigs had *ad libitum* access to feed and water. The feeding environment was supplied, as described in the previous study (Chen S. et al., 2019). Briefly, piglets were raised in an indoor environment, which had the space of 0.5 × 1 m for movement and cleanly plastic slatted flooring (temperature: 25 ± 2°C, humidity: 65 ± 5%). The diet composition of this experiment (**Supplementary Table 1**) met the 2012 version NRC standard. HEM was provided by the Anhui Tianan Biotechnology Company Limited, in Luan City, China. HEM was composed of golden-and-silver honeysuckle (*Lonicera japonica*), huangqi (*Astragalus membranaceus*), duzhong leaves (*Eucommia folium*), and dangshen (*Codonopsis pilosula*).

Sample Collection

At the end of the experiment, the piglets were anesthetized after fasting overnight as described previously (Zong et al., 2018). Briefly, all the pigs were anesthetized with the injection of a 4% sodium pentobarbital solution (40 mg/kg BW). Blood samples were collected from the precaval vein of the piglets and poured into sterile tubes. Serum samples were extracted of supernatant fluid after the centrifugation of blood (845 g, 10 min). The mesenterium was peeled off, and then the intestinal mucosal layer of the jejunum and the ileum was collected as described previously (Zong et al., 2018). Segments (10 cm) of the jejunum (5 m before the ileal–cecal junction) and the ileum (30 cm before the ileal–cecal junction) were rinsed three times with physiological saline, then the clear segments were sheared and scraped off by sterile microslides for collecting the intestinal mucosa layer, and the samples were packaged by a silver paper and rapidly frozen in liquid nitrogen. The colonic content was separately collected into two sterile tubes. All the samples were stored at an ultralow temperature freezer (−80°C), the serum and intestinal mucosal layer were analyzed for antioxidant enzyme activity and malondialdehyde (MDA) concentration, the sample of the intestinal mucosal layer was measured via the gene expression and protein expression, and the colonic content was

used to analyze the intestinal bacterial and short-chain fatty acid (SCFA) concentrations.

Determination of MDA Concentration and Antioxidant Activity

The intestinal mucosal layers of the jejunum, the ileum, and the serum were treated as described previously (Zong et al., 2018). The MDA (the thiobarbituric acid method) concentrations and enzymatic activities of superoxide dismutase (SOD, the hydroxylamine method), catalase (CAT, the ammonium molybdate method), and glutathione peroxidase (GSH-PX) were determined using commercially available kits according to the instructions of the manufacturer (Nanjing Jiancheng Bioengineering Institute, Nanjing, China).

Quantitative Real-Time PCR (qPCR)

Quantitative real-time PCR was performed as described in our previous study (Chen S. et al., 2019). Total RNA was extracted using the Trizol reagent (Takara, Tokyo, Japan) and dissolved in diethyl pyrocarbonate (DEPC)-treated water (Sangon Biotech, shanghai, China). The quality of RNA was checked using agarose gel electrophoresis, and the concentration of RNA was measured with an Eppendorf Biophotometer (Eppendorf AG, Hamburg, Germany). cDNA was synthesized using a commercial reverse transcription kit (Takara, Tokyo, Japan) according to the instructions of the manufacturer. Briefly, first-strand cDNA was synthesized through incubating 1.0 μg total RNA with DNase I for 2 min at 42°C and reverse-transcribed using Oligo (dT) primers for 15 min at 37°C, 5 s at 85°C in a 20-μl reaction volume. Primers were designed on the National Center of Biotechnology Information (NCBI) online website based on the mRNA sequences of *Sus scrofa*. The sequences of primers used in this study were shown in **Supplementary Table 2**. SYBR Green mix in the quantitative real-time PCR was purchased from Thermo Scientific company (Waltham, United States). Each sample was determined with qPCR three times. The qPCR reaction mixture (10 μl) was composed of 0.3 μl forward primers (10 μM), 0.3 μl reverse primers (10 μM), 0.25 μl sample buffer, 5 μl SYBR Green (2 ×), 5 μl cDNA template (diluted fivefolds with RNase-free water), and 3.15 μl sterile water. The qPCR procedure included a 10-min pre-denaturation at 95°C and 40 cycles of amplification (denaturation at 95°C for 15 s and annealing and extension at 60°C for 20 s), followed with the melting curve program that was conducted at 60–99°C with a heating rate of 0.1°C/s. The melting curve and the amplification curve were checked to ensure the specificity of both primers and PCR products. The relative mRNA expression levels of target genes were calculated by the formula of $2^{-\Delta\ \Delta\ Ct}$ using β-actin as the internal control. The mRNA expression of the target gene was presented as the fold change to the CON group.

Western Blotting

Western blotting was performed as described in our previous study (Wang et al., 2019). Tween-20, RIPA buffer, protease inhibitor cocktail, bicinchoninic acid assay, 5 × loading buffer, SDS-PAGE (sodium dodecyl sulfate polyacrylamide gel electrophoresis) gels kit, and horseradish peroxidase-linked secondary antibodies were purchased from Beyotime Biotechnology (Shanghai, China). β-Actin was used as the loading control, and the protein bands of each sample were determined by the Alpha Imager 2200 software (Alpha Innotech Corporation, CA, United States). The antibody against β-actin was obtained from Bimake (Shanghai, China), and the antibodies against nuclear factor erythroid 2-related factor 2 (Nrf2) and Kelch like-ECH-associated protein 1 (Keap1) were purchased from Proteintech (Wuhan, China).

Measurement of SCFAs Concentrations

The SCFAs in the colon were analyzed according to a previous study (Zhou et al., 2019). One gram of colon digesta was diluted with distilled water, then vortexed and centrifuged at 12,000 g for 15 min. The supernatant was mixed with 25% metaphosphoric acid solution overnight, and then the fluid was centrifuged and filtered through a 0.22-μm membrane filter. The concentrations of SCFAs, including acetate, propionate, butyrate, isobutyrate, valerate, and isovalerate, were analyzed by gas chromatography (Agilent Technologies 7890B GC System; AGILENT) on a DB-FFAP column (30 m × 250 μm × 0.25 μm).

Bacteria 16S rRNA Sequencing and Bioinformatics Analysis

The bacteria 16S rRNA sequencing of the colonic content was performed according to our previous study (Chen S. et al., 2019). The DNA of the colonic contents was extracted with the DNA Stool Mini Kit (Qiagen, Dusseldorf, Germany). The DNA sample from the colonic content and the amplification products were detected by 1% agarose gel electrophoresis. The V3–V4 region of the 16S rRNA gene was amplified by PCR using primers (forward primer, 5′-CCTACGGGNGGCWGCAG-3′; reverse primer, 5′-GACTACHVGGGTATCTAATCC-3′). The PCR mixture (20 μl) was composed of 1 μl DNA template, 2 μl deoxyribonucleotide triphosphate (TransGen Biotech, China), 0.4 μl forward primer (10 μM), 0.4 μl reverse primer (10 μM), 0.4 μl of fastpfu polymerase (TransGen Biotech, China), 4 μl of 5 × fastpfu buffer (TransGen Biotech, China), and 11.8 μl of sterile water. The PCR procedure includes pre-denaturation for 3 min at 95°C, 30 cycles of denaturation for 30 s at 95°C, annealing for 30 s at 55°C, and extension for 30 s at 72°C, followed by final extension for 6 min at 72°C. The PCR products were purified with a GeneJET Gel Extraction kit (Thermo Fisher Scientific, Waltham, United States). Purified DNA was subjected to paired-end sequencing on the Illumina MiSeq platform (Illumina, Sand Diego, CA, United States) according to the instructions of the manufacturer. Illumina MiSeq sequencing, processing of sequencing data, and bioinformatics analysis were performed by Novogene Bioinformatics Technology Co., Ltd. (Beijing, China). High-quality clean reads were obtained through filtering the adapters and low-quality reads (such as trailing quality score < 20, reads with primer mismatches > 2) according to the quality-controlled process. Raw tags, clean tags, effective

tags, and good coverage were provided by the commercial service company. Operational taxonomic unit (OTU, sequence similarity of 97%) clustering and species taxonomy were analyzed by the Uparse software. Based on OTU clustering results, the alpha diversity of Shannon and Chao1 was analyzed. The beta diversity of principal coordinates analysis (PCOA) and principal component analysis (PCA) was generated through calculating the distance of unweighted Unifrac. Based on OTU clustering results, the information of relevant species and the species abundance on the top 10 in the phylum and genus level was obtained. The statistical data of the linear discriminant analysis effect size (LEfSe) was analyzed using the linear discriminant analysis to assess species with significant difference among treatments. The environmental factor correlation analysis was performed using the R software (psych and heatmap package) on the online platform of Novogene Bioinformatics Technology Co., Ltd. (Beijing, China).

Statistical Analysis

All the data in the present study were expressed as means ± SEM and analyzed using the SPSS software (SPSS Inc., Chicago, IL, United States) through Student's *t*-test. All the statistical data of the colonic bacterial community in the phylum and genus were analyzed by the Mann–Whitney *U*-test. Spearman correlations analysis was used to determine the association between environmental factors and colonic microbiota. Tables and figures in the current study were prepared by Word 2016 software (Microsoft, Redmond, United States) and GraphPad Prism 6.0 (GraphPad Software Inc., La Jolla, CA), respectively. A value of $p < 0.05$ means a statistical significance between treatments exists, while a value of $p < 0.10$ means there is a trend toward significance between treatments.

RESULTS

Effect of HEM on Antioxidant Capacity

The effect of HEM on the antioxidant capacity (GSH-PX, SOD, and CAT) of weaned piglets is shown in **Table 1**. Compared with the CON group, the HEM group decreased the GSH-PX activity ($p < 0.05$) in the serum and the SOD activity ($p < 0.05$) in the ileum of the weaned piglets. The activity of other antioxidant enzymes and the content of MDA in both the serum and the intestine of the weaned piglets had no difference between these two groups.

Effect of HEM on the Nrf2-Keap1 Pathway

As shown in **Figure 1**, HEM significantly decreased the protein level of Keap1 ($p < 0.05$) in the ileum, while it increased the mRNA expression of Keap1 ($p < 0.05$) in the ileum of the weaned piglets compared with the CON group. In addition, HEM treatment significantly decreased the mRNA expression of Keap1 ($p < 0.05$) in the jejunum of the weaned piglets. The mRNA and protein levels of Nrf2 in both the ileum and the jejunum were similar between the CON and HEM groups.

Effect of HEM on Colonic SCFA Concentrations

The results of colonic SCFA concentrations are shown in **Table 2**. The concentrations of propionate ($p < 0.10$) had a tendency to decrease in the HEM group. The concentrations of other SCFAs had no difference between the CON and HEM groups.

Effect of HEM on Colonic Microbiota

The results of colonic microbiota, including raw tags, clean tags, effective tags, and good coverage, were presented in **Supplementary Table 3**. These results showed that the data

TABLE 1 | Effects of dietary supplementation with herbal extract mixture (HEM) on antioxidant indexes of weaned piglets[1].

	Dietary treatment		
Item	**CON**	**HEM**	***p*-value**
CAT, μg/mg of protein			
Serum	46.03 ± 11.86	48.86 ± 10.87	0.862
Jejunum	5.88 ± 0.70	6.28 ± 0.46	0.390
Ileum	3.49 ± 0.58	3.94 ± 0.59	0.428
GSH-PX, μmol/μg of protein			
Serum	443.06 ± 4.76[a]	427.33 ± 3.00[b]	0.020
Jejunum	16.43 ± 2.72	19.30 ± 3.64	0.305
Ileum	35.37 ± 3.45	40.19 ± 4.60	0.164
MDA, nmol/mg of protein			
Serum	4.76 ± 0.51	4.30 ± 0.61	0.567
Jejunum	1.47 ± 0.17	1.58 ± 0.12	0.380
Ileum	1.26 ± 0.05	1.50 ± 0.12	0.174
SOD, μg/mg of protein			
Serum	19.14 ± 0.63	17.43 ± 1.28	0.248
Jejunum	53.95 ± 3.75	59.06 ± 1.98	0.373
Ileum	50.71 ± 3.74[a]	37.03 ± 2.28[b]	0.007

[1]*Values are expressed as mean ± SEM; n = 9. CON, basal diet; HEM, basal diet supplemented with 1,000 mg/kg herbal extract mixture.*
[a,b]*Values in the same row not sharing a common superscript differ significantly.*

TABLE 2 | Effects of dietary supplementation with herbal extract mixture (HEM) on the concentrations of short-chain fatty acid (SCFA) in the colon of weaned piglets[a].

	Dietary treatment		
Item	**CON**	**HEM**	***p*-value**
SCFAs concentrations in colon digesta, μmol/g			
Acetate	3.33 ± 0.13	3.06 ± 0.10	0.133
Propionate	1.72 ± 0.11	1.46 ± 0.08	0.068
Butyrate	0.88 ± 0.11	0.79 ± 0.07	0.624
Isobutyrate	0.19 ± 0.01	0.20 ± 0.01	0.516
Valerate	0.22 ± 0.03	0.20 ± 0.02	0.512
Isovalerate	0.24 ± 0.03	0.26 ± 0.02	0.687
Total SCFAs	6.58 ± 0.34	5.98 ± 0.26	0.181

[a]*Values are expressed as mean ± SEM; n = 9. CON, basal diet; HEM, basal diet supplemented with 1,000 mg/kg herbal extract mixture.*

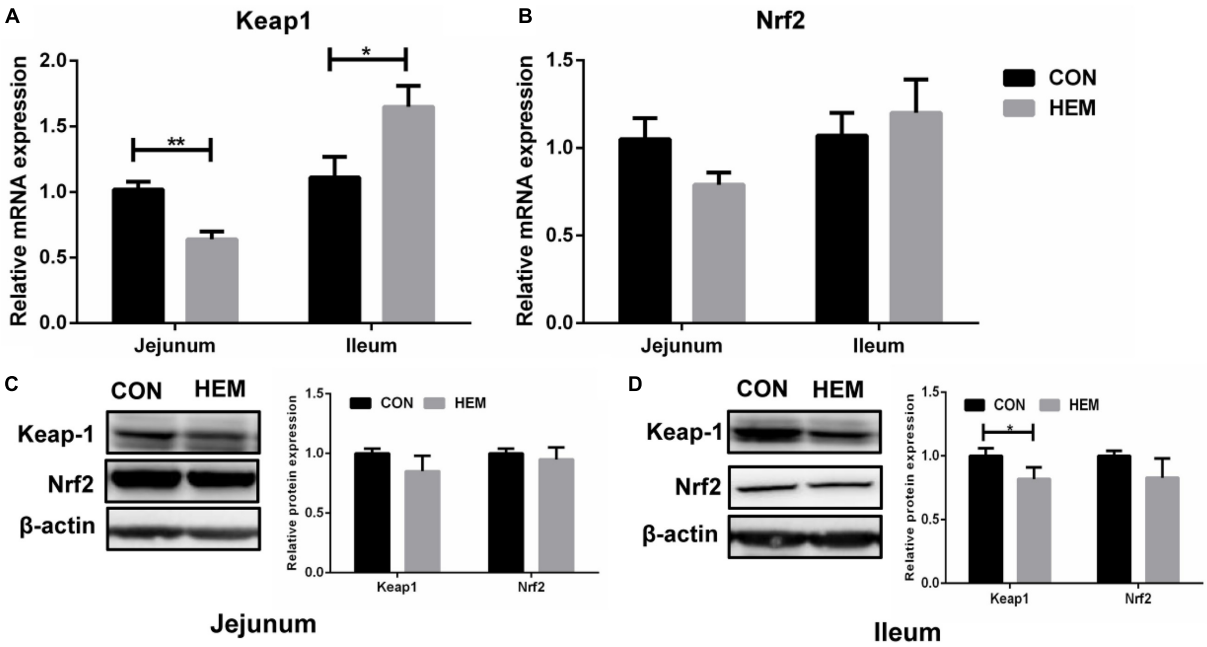

FIGURE 1 | Effects of dietary supplementation with herbal extract mixture (HEM) on the Nrf2–Keap1 pathway in weaning pigs. Relative mRNA expression of Keap1 **(A)** and Nrf2 **(B)** in the jejunum and the ileum was measured by quantitative real-time PCR. Relative protein expression and quantitative analysis of Keap1 **(C)** and Nrf2 **(D)** in the jejunum and the ileum was measured by Western blotting. CON, basal diet; HEM, basal diet supplemented with 1,000 mg/kg herbal extract mixture. Data are presented as mean ± SEM, $n = 9$. $^{*}p < 0.05$. $0.01 < {}^{**}p < 0.05$.

met the demands for further analysis. The index of observed species, the alpha diversity of Shannon, and Chao1 had the same intendency of colonic microbiota in the experiment (**Figures 2A–C**). In addition, the beta diversity of PCoA and PCA is shown in **Figures 2D,E**. These results showed that the distance between the HEM and CON groups was far because of some different species. As shown in **Figure 3A**, the most dominant phyla in the colon bacterium were Firmicutes, Bacteroidetes, Spirochaetes, Tenericutes, and Actinobacteria. Compared with the CON group, both the abundance of Firmicutes and the ratio of Firmicutes to Bacteroidetes were lower in the HEM groups, while the abundance of Bacteroidetes was higher in the HEM groups at the phylum level (**Figures 4A–C**). The distribution of the abundance at the genus level is shown in **Figure 3B**. The significantly different species at the genus level are shown in **Figures 4D,E**. Dietary supplementation with HEM significantly reduced the abundance of *unidentified Clostridiales* and increased the abundance of others species at the genus level. The bacterial biomarkers were shown with LEfSe. There were 10 specific microbes in the CON group and 17 specific microbes in the HEM group (**Figure 5A**). We further explored the correlation between the SCFAs and the colonic microbiota at the phylum level (**Figure 5B**). The abundances of Firmicutes and Chlamydiae were positively related to acetate, while the abundances of Actinobacteria were negatively related to acetate. The abundances of Verrucomicrobia were negatively associated with butyrate and valerate, while the abundances of Bacteroidetes were positively associated with valerate. In addition, the abundances of Tenericutes were negatively correlated with isovalerate.

DISCUSSION

Weaning stress is the main factor to cause oxidative stress in the intestine and blood of the piglets (Zhu et al., 2012). To protect against oxidative stress, the antioxidant system, including the antioxidant enzymes of SOD, CAT, and GSH-PX, reduces the production of free radicals (Bauché et al., 1994; Urso and Clarkson, 2003). The content of MDA reflects the degree of lipid peroxidation in animals (Urso and Clarkson, 2003). In this study, we found that the dietary supplementation of HEM decreased the enzyme activities of GSH-PX and SOD in the serum and the ileum, respectively. However, the content of MDA had no difference between the HEM and CON groups. Plant extracts with antioxidant capacity have been widely used in both medicine and livestock production (Jiang et al., 2014; Chen J. S. et al., 2019). For example, Jiang et al. (2014) reported that dietary supplementation with plant polyphenols (apples, grape seeds, green teas, and olive leaves) has the tendency to enhance the activities of plasma GSH-PX (day 25) and T-AOC (day 27) in the weaning piglets challenged with *Escherichia coli*. A study showed that dietary supplementation with *Lycium barbarum* polysaccharides increases the activities of SOD, CAT, and GSH-PX and decreases the content of MDA in the serum and liver of weaning piglets (Chen J. S. et al., 2019). Furthermore, dietary supplementation with *Astragalus membranaceus* root powder and *Astragalus* polysaccharides increases the total antioxidant capacity of lamb plasma but regulates the antioxidant capacity of broilers in an age-dependent manner (Zhong et al., 2012; Zhang et al., 2013). However, our results are different from previous

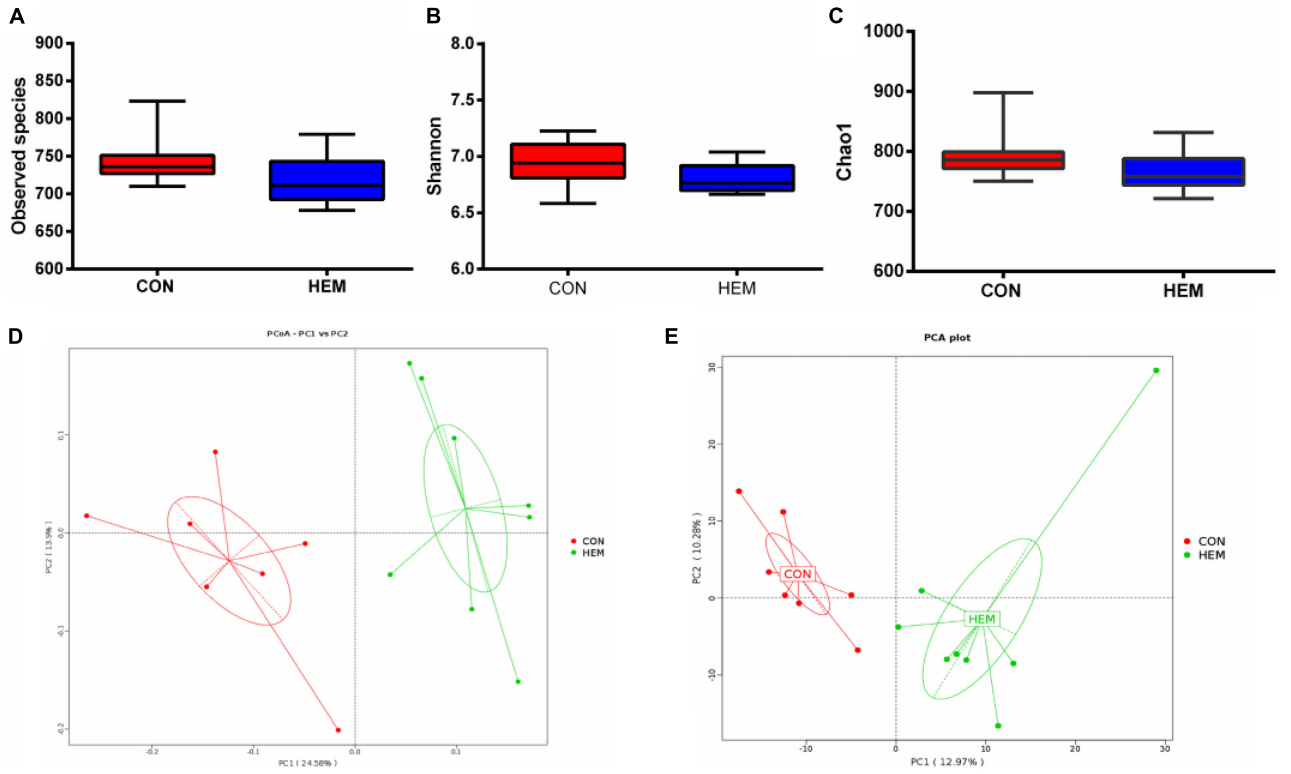

FIGURE 2 | Effects of dietary supplementation with herbal extract mixture (HEM) on alpha diversity and beta diversity in weaning pigs. Alpha diversity in colonic microbiota includes observed species **(A)**, Shannon **(B)**, and Chao1 **(C)**. Beta diversity in colonic microbiota includes principal coordinates analysis **(D)** and principal component analysis **(E)**. CON (n = 9), basal diet; HEM (n = 9), basal diet supplemented with 1,000 mg/kg herbal extract mixture.

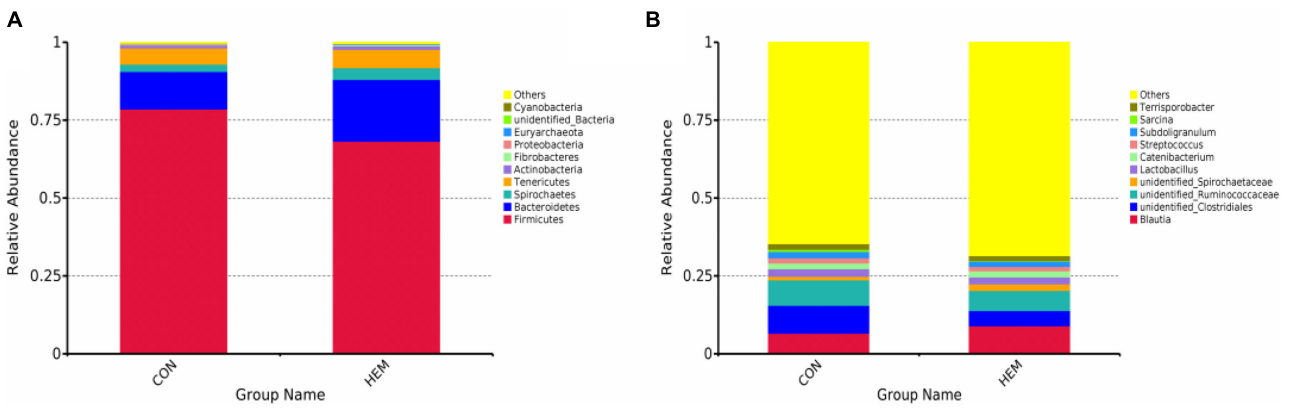

FIGURE 3 | Effects of dietary supplementation with herbal extract mixture (HEM) on the colonic bacterial community structure in weaning pigs. Distribution colonic microbiota of the phylum level **(A)** and the genus level **(B)**. CON (n = 9), basal diet; HEM (n = 9), basal diet supplemented with 1,000 mg/kg herbal extract mixture.

studies. We speculate that dietary HEM alleviates weaning stress in piglets; therefore, it is not necessary for the antioxidant system to produce more antioxidant enzymes to alleviate oxidative stress. In addition, one of the most significant body defense mechanisms against oxidative stress is mediated by the Nrf2-Keap1 pathway, which stimulates the expression of genes encoding antioxidant proteins (Kobayashi and Yamamoto, 2005). Thus, we examined whether the Nrf2-Keap1 pathway is involved in mitigating oxidative stress in weaning piglets. Nrf2 is bound by the negative regulator Keap1 in the normal condition. When cells are attacked by environmental factors, such as oxidative stress, electrophiles, and chemopreventive agents, Keap1 is degraded by the ubiquitin–proteasome system, and then Nrf2 is released from Keap1, thereby stimulating the expression of antioxidant enzymes to maintain redox homeostasis (Zhang, 2006). Previous studies have shown that the plant extract containing *Magnolia*

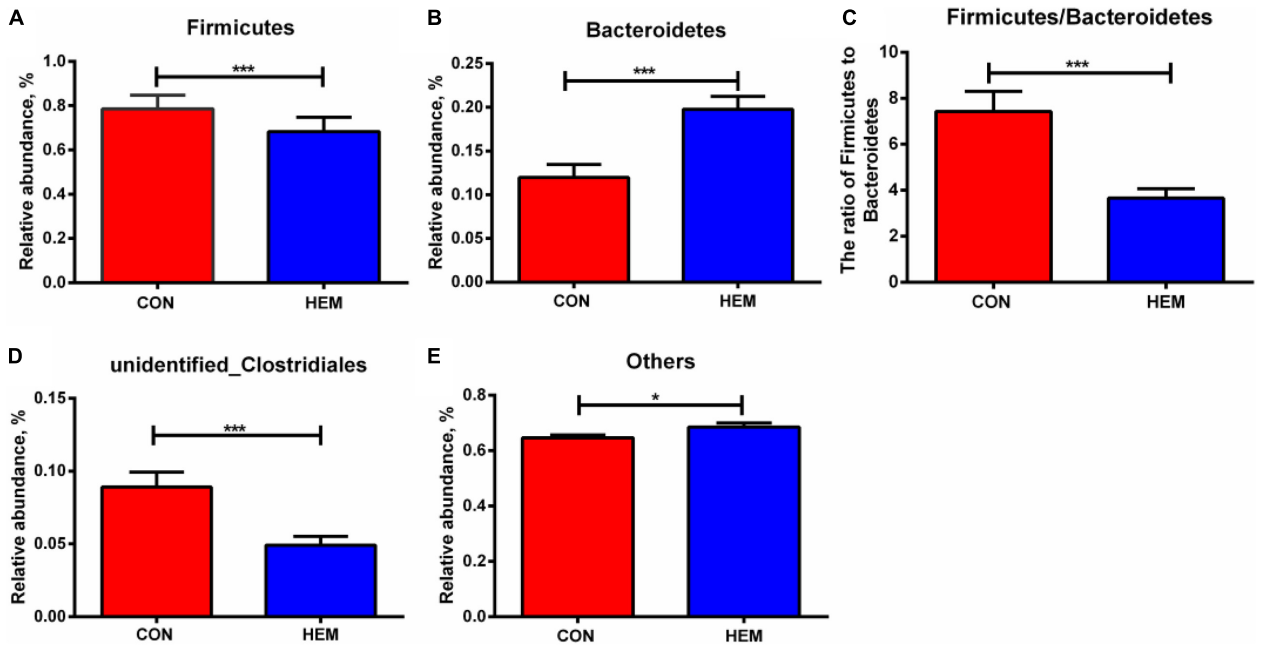

FIGURE 4 | Effects of dietary supplementation with herbal extract mixture (HEM) on taxonomic differences in weaning pigs. The significantly different bacteria in the phylum of Firmicutes **(A)**, Bacteroidetes **(B)**, and the ratio of Firmicutes to Bacteroidetes **(C)** were compared between the CON and HEM groups. The significantly different bacteria in the genus of unidentified *Clostridiales* **(D)** and others **(E)** were compared between the CON and HEM groups. Data are presented as mean ± SEM. CON (n = 9), basal diet; HEM (n = 9), basal diet supplemented with 1,000 mg/kg herbal extract mixture. $^{*}p < 0.05$, $^{***}p < 0.01$.

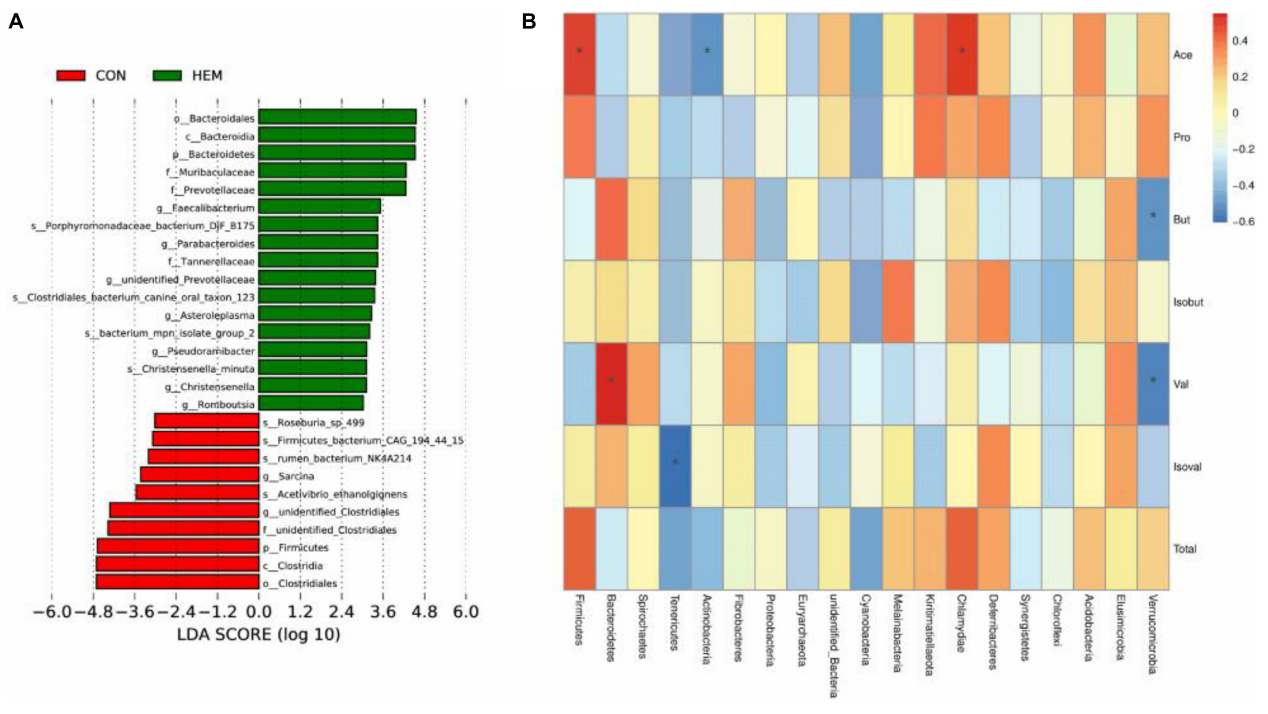

FIGURE 5 | Linear discriminant analysis coupled with effect size measurements (LEfSe) analysis for the enriched microbiota **(A)** and correlations between the bacteria in the phylum and the concentrations of SCFAs in the colon **(B)**. CON (n = 9), basal diet; HEM (n = 9), basal diet supplemented with 1,000 mg/kg herbal extract mixture. $^{*}p < 0.05$.

officinalis, bark extract, and *Astragalus membranaceus* activate the Nrf2 pathway to protect against oxidative stress in cells (Rajgopal et al., 2016; Adesso et al., 2018). We found that dietary HEM regulated the Nrf2–Keap1 pathway through decreasing the mRNA expression of Keap1 in the jejunum and the protein level of Keap1 in the ileum. However, our results showed that dietary HEM decreased the mRNA expression of Keap1 in the jejunum and the protein expression of Keap1 in the ileum, but increased the mRNA expression of Keap1 in the ileum. We speculated that this situation (inconsistent mRNA and protein expression of Keap1 in the ileum) might be associated with transcription and translation process, in which mRNA levels do not precisely predict protein levels in eukaryotic cells (Rojas-Duran and Gilbert, 2012).

Active compounds in the diet show a tight connection to gut microbial composition, which further influence host health (Yin et al., 2018). Previous studies have shown that dietary supplementation with herbal extracts reduces the abundances of harmful bacteria and increases the abundances of beneficial bacteria in livestock production (Namkung et al., 2004; Rahimi et al., 2011). In this study, we reported that HEM decreased the ratio of Firmicutes to Bacteroidetes through decreasing the abundance of Firmicutes and increasing the abundance of Bacteroidetes in the phylum. It is well known that gram-positive Firmicutes and gram-negative Bacteroidetes are the main bacteria in the microbial composition of host intestines (Eckburg et al., 2005). Furthermore, the ratio of Firmicutes to Bacteroidetes is associated with the overall health status (Mariat et al., 2009; Koliada et al., 2017). Koliada et al. (2017) observed that the obese people of the Ukrainian adult population have a higher ratio of Firmicutes to Bacteroidetes. Likewise, total parenteral nutrition also decreases the ratio of Firmicutes to Bacteroidetes, which is associated with intestinal Paneth cell activation in rats (Hodin et al., 2012). Our results are consistent with these findings. Our results indicated that HEM may alter the microbial composition, which could further have beneficial effects on host health. However, our results showed that HEM did not further change the bacteria of Bacteroides and Firmicutes in the genus level but changed the other bacteria in the genus level. One possible explanation for these results is that HEM supplementation modified the other bacteria that belong to Bacteroides and Firmicutes at the phylum level. A previous study indicates that intestinal SCFAs, which are produced by the gut microbiota, are involved in regulating the intestinal homeostasis (Ríos-Covián et al., 2016). Thus, we further determined the colonic concentrations of SCFAs to explore the relationship between intestinal bacteria and SCFAs. Polysaccharide from *Ganoderma atrum* increases the concentrations of SCFAs in the liver, serum, and feces of type 2 diabetic rats (Zhu et al., 2016). Dietary *Astragalus membranaceus* fiber does not modify the concentrations of SCFAs in the cecum of weaned pigs (Che et al., 2019). Similarly, our results indicated that dietary HEM did not change the concentrations of SCFAs in the colon of weaned piglets. Our results also showed that colonic bacteria had a negative or positive correlation with SCFAs.

CONCLUSION

In conclusion, the dietary supplementation of the herbal extract mixture (*Lonicera japonica, Astragalus membranaceus, Eucommia folium,* and *Codonopsis pilosula*) modulates intestinal antioxidant capacity with decreasing the enzyme activity of SOD in the ileum and that of GSH-PX in the serum, and activates the Nrf2-keap1 pathway through decreasing the mRNA expression of Keap1 in the jejunum and the protein expression of Keap1 in the ileum of weaned piglets. Additionally, HEM modifies the composition of colonic microbiota with decreasing the ratio of Firmicutes to Bacteroidetes at the phylum level in weaned piglets. These findings could help to further understand the beneficial effects of HEM on the intestinal health of weaning piglets.

DATA AVAILABILITY STATEMENT

The datasets presented in this study can be found in online repositories. The names of the repository/repositories and accession number(s) can be found below: https://www.ncbi.nlm.nih.gov/, PRJNA727453.

ETHICS STATEMENT

The animal study was reviewed and approved by the Animal Care and Use Committee of Hunan Normal University. Written informed consent was obtained from the owners for the participation of their animals in this study.

AUTHOR CONTRIBUTIONS

MW: methodology, investigation, data curation, writing—original draft, and funding acquisition. HH and LW: investigation and data curation. HY: validation and data curation. SWH, QT, and FL: investigation and resources. SPH: methodology, supervision, writing—review and editing, and funding acquisition. All authors contributed to the article and approved the submitted version.

FUNDING

This study was supported by the Key R&D Program of Hunan Province (2019NK2161), the Hunan Science and Technology Project (2017XK2020), the Special Funds for Construction of Innovative Provinces in Hunan Province (2019RS302), and the Hunan Provincial Innovation Foundation for Postgraduate (CX20200527).

SUPPLEMENTARY MATERIAL

The Supplementary Material for this article can be found online at: https://www.frontiersin.org/articles/10.3389/fmicb.2021.706758/full#supplementary-material

REFERENCES

Adesso, S., Russo, R., Quaroni, A., and Marzocco, S. (2018). *Astragalus membranaceus* extract attenuates inflammation and oxidative stress in intestinal epithelial cells via NF-κB activation and Nrf2 response. *Int. J. Mol. Sci.* 19:800. doi: 10.3390/ijms19030800

Bauché, F., Fouchard, M., and Jégou, B. (1994). Antioxidant system in rat testicular cells. *FEBS Lett.* 349, 392–396. doi: 10.1016/0014-5793(94)00709-8

Blecha, F., Pollman, D. S., and Nichols, D. A. (1983). Weaning pigs at an early age decreases cellular immunity. *J. Anim. Sci.* 2, 396–400. doi: 10.2527/jas1983.562396x

Che, D., Adams, S., Wei, C., Gui, Q., Atiba, E., and Hailong, J. (2019). Effects of *Astragalus membranaceus* fiber on growth performance, nutrient digestibility, microbial composition, VFA production, gut pH, and immunity of weaned pigs. *Microbiol. Open* 8:e00712. doi: 10.1002/mbo3.712

Chen, J. S., Long, L. N., Jiang, Q., Kang, B. J., Li, Y. H., and Yin, J. (2019). Effects of dietary supplementation of *Lycium barbarum* polysaccharides on growth performance, immune status, antioxidant capacity and selected microbial populations of weaned piglets. *J. Anim. Physiol. Anim. Nutr.* 104, 1106–1115. doi: 10.1111/jpn.13247

Chen, S., Tan, B. E., Xia, Y. Y., Liao, S. M., Wang, M. W., Yin, J., et al. (2019). Effects of dietary gamma-aminobutyric acid supplementation on the intestinal functions in weaning piglets. *Food Funct.* 10, 366–378. doi: 10.1039/C8FO02161A

Eckburg, P., Bik, E., Bernstein, C., Purdom, E., Dethlefsen, L., Sargent, M., et al. (2005). Diversity of the human intestinal microbial flora. *Science* 308, 1635–1638. doi: 10.1126/science.1110591

Gresse, R., Chaucheyras-Durand, F., Fleury, M., Van de Wiele, T., Forano, E., and Blanquet-Diot, S. (2017). Gut microbiota dysbiosis in postweaning piglets: understanding the keys to health. *Trends Microbiol.* 25, 851–873. doi: 10.1016/j.tim.2017.05.004

He, J., Ma, N., Zhu, S., Komatsu, K., Li, Z., and Fu, W. (2015). The genus *Codonopsis* (Campanulaceae): a review of phytochemistry, bioactivity and quality control. *J. Nat. Med.* 69, 1–21. doi: 10.1007/s11418-014-0861-9

Hodin, C., Visschers, R., Rensen, S., Boonen, B., Damink, S., Lenaerts, K., et al. (2012). Total parenteral nutrition induces a shift in the Firmicutes to Bacteroidetes ratio in association with Paneth cell activation in rats. *J. Nutr.* 142, 2141–2147. doi: 10.3945/jn.112.162388

Jayaraman, B., and Nyachoti, C. (2017). Husbandry practices and gut health outcomes in weaned piglets: a review. *Anim. Nutr.* 3, 205–211. doi: 10.1016/j.aninu.2017.06.002

Jiang, X., Zhang, H.J., Mantovani, G., Alborali, G., Caputo, J., Savoini, G., et al. (2014). The effect of plant polyphenols on the antioxidant defense system of weaned piglets subjected to an *Escherichia coli* challenge. *J. Anim. Feed Sci.* 663:127.

Kobayashi, M., and Yamamoto, M. (2005). Molecular mechanisms activating the Nrf2-Keap1 pathway of antioxidant gene regulation. *Antioxid. Redox Signal.* 7, 385–394. doi: 10.1089/ars.2005.7.385

Koliada, A., Syzenko, G., Moseiko, V., Budovska, L., Puchkov, K., Perederiy, V., et al. (2017). Association between body mass index and Firmicutes/Bacteroidetes ratio in an adult Ukrainian population. *BMC Microbiol.* 17:120. doi: 10.1186/s12866-017-1027-1

Lauridsen, C. (2019). From oxidative stress to inflammation: redox balance and immune system. *Poult. Sci.* 98, 4240–4246. doi: 10.3382/ps/pey407

Liu, W., Pi, S., and Kim, I. (2016). Effects of *Scutellaria baicalensis* and *Lonicera japonica* extract mixture supplementation on growth performance, nutrient digestibility, blood profiles and meat quality in finishing pigs. *Ital. J. Anim. Sci.* 15, 446–452. doi: 10.1080/1828051x.2016.1202736

Liu, Y., Espinosa, C., Abelilla, J., Casas, G., Lagos, L., Lee, S., et al. (2018). Non-antibiotic feed additives in diets for pigs: a review. *Anim. Nutr.* 4, 113–125. doi: 10.1016/j.aninu.2018.01.007

Manzanilla, E., Perez, J., Martin, M., Kamel, C., Baucells, F., and Gasa, J. (2004). Effect of plant extracts and formic acid on the intestinal equilibrium of early-weaned pigs. *J. Anim. Sci.* 82, 3210–3218. doi: 10.2527/2004.82113210x

Mariat, D., Firmesse, O., Levenez, F., Guimarães, V., Sokol, H., Doré, J., et al. (2009). The Firmicutes/Bacteroidetes ratio of the human microbiota changes with age. *BMC Microbiol.* 9:123. doi: 10.1186/1471-2180-9-123

McLamb, B., Gibson, A., Overman, E., Stahl, C., Moeser, A., and Collete, L. (2013). Early weaning stress in pigs impairs innate mucosal immune responses to enterotoxigenic E. coli challenge and exacerbates intestinal injury and clinical disease. *PLoS One* 8:e59838. doi: 10.1371/journal.pone.0059838

Modina, S., Polito, U., Rossi, R., Corino, C., and Di Giancamillo, A. (2019). Nutritional regulation of gut barrier integrity in weaning piglets. *Animals* 9:1045. doi: 10.3390/ani9121045

Namkung, H., Li, J., Gong, M., Yu, H., Cottrill, M., and De Lange, C. (2004). Impact of feeding blends of organic acids and herbal extracts on growth performance, gut microbiota and digestive function in newly weaned pigs. *Can. J. Anim. Sci.* 84, 697–704. doi: 10.1073/pnas.0704665104

Rahimi, S., Teymouri, Z., Karimi, T., Omidbaigi, R., and Rokni, H. (2011). Effect of the three herbal extracts on growth performance, immune system, blood factors and intestinal selected bacterial population in broiler chickens. *J. Agric. Sci. Tech.* 13, 527–539. doi: 10.1002/jsfa.4492

Rajgopal, A., Missler, S., and Scholten, J. (2016). *Magnolia officinalis* (Hou Po) bark extract stimulates the Nrf2 pathway in hepatocytes and protects against oxidative stress. *J. Ethnopharmacol.* 193, 657–662. doi: 10.1016/j.jep.2016.10.016

Ríos-Covián, D., Ruas-Madiedo, P., Margolles, A., Gueimonde, M., de los Reyes-Gavilán, C., and Salazar, N. (2016). Intestinal short chain fatty acids and their link with diet and human health. *Front. Microbiol.* 7:185. doi: 10.3389/fmicb.2016.00185

Robert, S., Weary, D. M., and Gonyou, H. (1999). Segregated early weaning and welfare of piglets. *J. Appl. Anim Welf. Sci.* 2, 31–40. doi: 10.1207/s15327604jaws0201_3

Rojas-Duran, M. F., and Gilbert, W. V. (2012). Alternative transcription start site selection leads to large differences in translation activity in yeast. *RNA* 18, 2299–2305. doi: 10.1261/rna.035865.112

Smith, F., Clark, J. B., Overman, B. L., Tozel, C. C., Huang, J. H., Rivier, J. E., et al. (2010). Early weaning stress impairs development of mucosal barrier function in the porcine intestine. *Am. J. Physiol Gastrointest. Liver. Physiol.* 298, G352–G363. doi: 10.1097/01.ta.0000245981.22931.43

Urso, M., and Clarkson, M. (2003). Oxidative stress, exercise, and antioxidant supplementation. *Toxicology* 189, 41–54. doi: 10.1016/s0300-483x(03)00151-3

Wang, M. W., Huang, H. J., Hu, Y. P., Liu, Y. T., Zeng, X., Zhuang, Y., et al. (2020). Effects of dietary supplementation with herbal extract mixture on growth performance, organ weight and intestinal morphology in weaning piglets. *J. Anim. Physiol. Anim. Nutr. (Berl.)* 104, 1462–1470. doi: 10.1111/jpn.13422

Wang, M. W., Huang, H. J., Liu, S., Zhuang, Y., Yang, H. S., Li, L. Y., et al. (2019). Tannic acid modulates intestinal barrier functions associated with intestinal morphology, antioxidative activity, and intestinal tight junction in a diquat-induced mouse model. *RSC Adv.* 9, 31988–31998. doi: 10.1039/C9RA04943F

Yang, H. S., Xiong, X., and Yin, Y. L. (2013). "Development and renewal of intestinal villi in pigs," in *Nutritional and Physiological Functions of Amino Acids in Pigs*, eds F. Blachier, G. Wu, and Y. Yin (Vienna: Springer), 29–47. doi: 10.1007/978-3-7091-1328-83

Yen, G., and Hsieh, C. (1998). Antioxidant activity of extracts from Du-zhong (*Eucommia ulmoides*) toward various lipid peroxidation models in vitro. *J. Agric. Food Chem.* 46, 3952–3957. doi: 10.1021/jf9800458

Yin, J., Ren, W. K., Chen, S., Li, Y. Y., Han, H., Li, T. J., et al. (2018). Metabolic regulation of methionine restriction in diabetes. *Mol. Nutr. Food Res.* 62:1700951. doi: 10.1002/mnfr.201700951

Zhang, D. D. (2006). Mechanistic studies of the Nrf2-Keap1 signaling pathway. *Drug Metab. Rev.* 38, 769–789. doi: 10.1080/03602530600971974

Zhang, G. G., Yang, Z. B., Wang, Y., and Wang, W. R. (2013). Effects of *Astragalus membranaceus* root processed to different particle sizes on growth performance, antioxidant status, and serum metabolites of broiler chickens. *Poult. Sci.* 92, 178–183. doi: 10.3382/ps.2012-02432

Zhong, R. Z., Yu, M., Liu, H. W., Sun, H. X., Cao, Y., and Zhou, D. W. (2012). Effects of dietary *Astragalus polysaccharide* and *Astragalus membranaceus* root supplementation on growth performance, rumen fermentation, immune responses, and antioxidant status of lambs. *Anim. Feed Sci Tech.* 174, 60–67. doi: 10.1016/j.anifeedsci.2012.02.013

Zhou, Z., Zhang, J., Zhang, X., Mo, S., Tan, X., Wang, X. L., et al. (2019). The production of short chain fatty acid and colonic development in weaning

piglets. *J. Anim. Physiol. Anim. Nutr.* 103, 1530–1537. doi: 10.1111/jpn.13164

Zhu, K., Nie, S., Tan, L., Li, C., Gong, D., and Xie, M. (2016). A polysaccharide from *Ganoderma atrum* improves liver function in type 2 diabetic rats via antioxidant action and short-chain fatty acids excretion. *J. Agric. Food. Chem.* 64, 1938–1944. doi: 10.1021/acs.jafc.5b06103

Zhu, L. H., Zhao, K. L., Chen, X. L., and Xu, J. X. (2012). Impact of weaning and an antioxidant blend on intestinal barrier function and antioxidant status in pigs. *J. Anim. Sci.* 90, 2581–2589. doi: 10.2527/jas.2012-4444

Zong, E. Y., Huang, P. F., Zhang, W., Li, J. Z., Li, Y. L., Ding, X. Q., et al. (2018). The effects of dietary sulfur amino acids on growth performance, intestinal morphology, enzyme activity, and nutrient transporters in weaning piglets. *J. Anim. Sci.* 96, 1130–1139.

Conflict of Interest: SH was employed by the company Anhui Tianan Biotechnology Company Limited. FL and QT were employed by the company Yucheng Baolikang Biological Feed Company Limited.

The remaining authors declare that the research was conducted in the absence of any commercial or financial relationships that could be construed as a potential conflict of interest.

Publisher's Note: All claims expressed in this article are solely those of the authors and do not necessarily represent those of their affiliated organizations, or those of the publisher, the editors and the reviewers. Any product that may be evaluated in this article, or claim that may be made by its manufacturer, is not guaranteed or endorsed by the publisher.

frontiers in Microbiology

REVIEW
published: 09 August 2021
doi: 10.3389/fmicb.2021.719877

Potential Application of *Lonicera japonica* Extracts in Animal Production: From the Perspective of Intestinal Health

Xiaopeng Tang[1], Xuguang Liu[1], Jinfeng Zhong[2] and Rejun Fang[3]**

[1]State Engineering Technology Institute for Karst Desertfication Control, School of Karst Science, Guizhou Normal University, Guiyang, China, [2]Hunan Polytechnic of Environment and Biology, College of Biotechnology, Hengyang, China, [3]College of Animal Science and Technology, Hunan Agricultural University, Changsha, China

Lonicera japonica (*L. japonica*) extract is rich in active substances, such as phenolic acids, essential oils, flavones, saponins, and iridoids, which have a broad spectrum of antioxidant, anti-inflammatory, and anti-microbial effect. Previous studies have demonstrated that *L. japonica* has a good regulatory effect on animal intestinal health, which can be used as a potential antibiotic substitute product. However, previous studies about intestinal health regulation mainly focus on experimental animals or cells, like mice, rats, HMC-1 Cells, and RAW 264.7 cells. In this review, the intestinal health benefits including antioxidant, anti-inflammatory, and antimicrobial activity, and its potential application in animal production were summarized. Through this review, we can see that the effects and mechanism of *L. japonica* extract on intestinal health regulation of farm and aquatic animals are still rare and unclear. Further studies could focus on the regulatory mechanism of *L. japonica* extract on intestinal health especially the protective effects of *L. japonica* extract on oxidative injury, inflammation, and regulation of intestinal flora in farm animals and aquatic animals, thereby providing references for the rational utilization and application of *L. japonica* and its extracts in animal production.

Keywords: ***Lonicera japonica*** **extract, intestinal microorganisms, intestinal immunity, intestinal health, animal production**

OPEN ACCESS

Edited by:
Jia Yin,
Hunan Normal University, China

Reviewed by:
Xiao Bin Zeng,
Jinan University, China
Karthik Loganathan,
Salem Microbes Pvt. Ltd., India

****Correspondence:***
Xiaopeng Tang
tangxiaopeng110@126.com
Rejun Fang
fangrj63@126.com

Specialty section:
This article was submitted to Microbial Symbioses, a section of the journal Frontiers in Microbiology

Received: *03 June 2021*
Accepted: *16 July 2021*
Published: *09 August 2021*

Citation:
Tang X, Liu X, Zhong J and Fang R (2021) Potential Application of Lonicera japonica Extracts in Animal Production: From the Perspective of Intestinal Health. Front. Microbiol. 12:719877. doi: 10.3389/fmicb.2021.719877

INTRODUCTION

The animal intestinal tract is the direct place for the communication between the internal environment and the external environment, and is an important defense line for animals to maintain the homeostasis of the internal environment (Tang et al., 2016). A healthy gut is essential for the growth and development of animals. However, the intestinal epithelium homeostasis of animals is affected by numerous factors, such as bacterial infection, endotoxin challenge, weaning stress, and oxidative stress, leading to intestinal damage and intestinal barrier function dysfunction (Campbell et al., 2013; Yin et al., 2014; Zhu H. et al., 2018). Traditionally, antibiotics are generally used as growth and health promoters, which have achieved certain achievements and promoted the development of animal husbandry (Barton, 2014). However, the abuse of antibiotics in livestock and poultry feeds will destroy the intestinal

microecological balance, and lead to the resistance of bacteria (Hashemi and Davoodi, 2011; Looft et al., 2014), which would bring serious negative effects on human health and environmental safety. Therefore, the use of antibiotics as intestinal microecological regulator is no longer popular. Exploring new antibiotic substitutes to regulate intestinal microflora and to maintain the intestinal health of animals is an urgent task in the field of animal nutrition in the post-antibiotic era.

Plant extract is a complex mixture of compounds. It has been reported to possess multiple bioactivities such as antioxidant (Liu et al., 2018), anti-inflammatory (Wu et al., 2017), anti-microbial (Kavoosi et al., 2013), and immune regulation (Boskabady et al., 2013). Plant extracts have been used for centuries in traditional medicine and as food preservatives, and more recently have been studied as possible feed additives used in animal nutrition due to their multiple biological functions (Kim et al., 2012; Yejun et al., 2019). *Lonicera japonica* (*L. japonica*) extract is extracted from *L. japonica* Thunberg, a medicine food homologous herb rich in organic acids, volatile oils, flavonoids, iridoids, and saponins (Shang et al., 2011; Fan et al., 2019; Li R. et al., 2020), which have high value of health benefits. *Lonicera japonica* extract is widely used in pharmacological preparations, cosmetics, food, and animal husbandry because of its diverse pharmacological effects such as antioxidant, anti-microbial, antiviral, antitoxic, antiseptic, and anti-inflammatory properties (Kang et al., 2010; Park et al., 2012; Yejun et al., 2019). The application of *L. japonica* extract in animal production mainly focuses on pigs (Liu W. et al., 2016), beef cattle (Yejun et al., 2019), dairy cows (Ma et al., 2020b; Zhao et al., 2020), broiler (Müştak et al., 2015), laying hens (Long et al., 2018), *Penaeus monodon* (Chen et al., 2013), grass carp (Meng et al., 2019), and olive flounder (Dharaneedharan et al., 2016). From the results of these studies, *L. japonica* extract can function as a potential alternative antibiotic in animal feeds. However, the studies of the impacts of *L. japonica* extract on the intestinal health of animals are scattered in different pieces of literature, and little research could aggregate these findings into a single review. Therefore, the objective of this study was to review the effects of *L. japonica* extract on intestinal health and summarize its application in animal production.

BIOACTIVE COMPOUNDS OF *L. JAPONICA* EXTRACT

Lonicera japonica, also known as Japanese honeysuckle, Jin YinHua or Ren Dong, belongs to the member of the *Caprifoliaceae* family, is a perennial deciduous shrub native to East Asia and spread throughout Argentina, Brazil, Mexico, Australia, New Zealand, and American (Kim et al., 2015). Traditionally, the flower bud of *L. japonica*, which has been listed in the Chinese Pharmacopeia as *L. japonica* Flos, is a traditional Chinese medicine that reportedly has antioxidant, anti-inflammatory, antibacterial, antiviral, antitumor, and antidiabetic properties (Liu Z. et al., 2016; Shi et al., 2016; Wang et al., 2017), which has been widely used for preventing and treating influenza, cold, fever, and infections (Kashiwada et al., 2013; Ge et al., 2018; Fang et al., 2020). *Lonicera japonica extract* is extracted from *L. japonica*, has complicated chemical composition. So far, more than 300 chemical compounds have been isolated from and identified from *L. japonica*, and the major compositions are phenolic acids, essential oils, flavones, saponins, and iridoids (Shang et al., 2011; Li et al., 2017, 2019; Li R. et al., 2020).

Phenolic Acids

There are more than 49 kinds of phenolic acids in *L. japonica*, which is mainly composed of chlorogenic acid (CGA) derivatives and cinnamic acid derivatives (Duan et al., 2018; Li et al., 2019; Li and Han, 2020; Qiu et al., 2021). A total of 27 CGA have been isolated and identified from *L. japonica*, such as CGA, neochlorogenic acid (NGC), isochlorogenic acid A, isochlorogenic acid B, isochlorogenic acid C, etc. (Iwahashi et al., 1986; Chang and Hsu, 1992; Peng et al., 2000; Lee et al., 2010; Seo et al., 2012; Yu et al., 2015; Duan et al., 2018; Li et al., 2019; Liu et al., 2020; Wang H. et al., 2020). About 16 cinnamic acid derivatives, like caffeic acid (CA), 1-*O*-caffeoylquinic acid, trans-cinnamic acid, trans-ferulic acid, caffeic acid methyl ester, and so on, have been isolated and identified from *L. japonica* (Iwahashi et al., 1986; Chang and Hsu, 1992; Choi et al., 2007; Jeong et al., 2015; Yu et al., 2015; Duan et al., 2018; Li et al., 2019). Other phenolic acids including 2,5-dihydroxybenzoic acid-5-O-β-D-glucopyranoside, vanillic acid, vanillic acid 4-O-β-D-(6-O-benzoyl glucopyranoside), vanillic acid-4-O-β-D-(6-O-benzoyl pyranoside), and protocatechuic acid (Choi et al., 2007; Lee et al., 2010; Li et al., 2019) were also identified from *L. japonica*. Among them, CGA and CA are the two most studied compounds in *L. japonica*, which have confirmed to possess potent activities of anti-inflammation, antioxidant, and antibacterial (Hsu et al., 2016; Hou et al., 2017; Li et al., 2019; Li R. et al., 2020). In particular, CGA is the most abundant phenolic acid in *L. japonica*, and it has been used as a marker to characterize the chemical qualities of *L. japonica* (Tzeng et al., 2014; Chen et al., 2017a; Li et al., 2019).

Essential Oils

Essential oils are one of the bioactivity components of *L. japonica*, which mainly composed of acids, aldehydes, alcohols, ketones, and their esters (Li et al., 2019). They exist in the aerial parts of *L. japonica*, flower (fresh and dry), leaves, and vines with a different content and composition (Shang et al., 2011). Vukovic et al. (2012) showed that the main constituents in the flowers fraction were (Z,Z)-farnesole (16.2%) and linalool (11.0%), the main constituents in the leaves fraction were hexadecanoic acid (16.0%) and linalool (8.7%), and the main constituents in the stems were hexadecanoic acid (31.4%). Essential oils in *L. japonica* are also affected by different habitats. Du et al. (2015) identified 35 volatile constituents in *L. japonica* from Guangxi Zhuang Autonomous Region (China), mainly including methyl linolenate, n-hexadecanoic acid, and ε-muurolene, and 18 volatile constituents in LJF from Hunan province (China), mainly including n-hexadecanoic acid, linoleic acid, and α-curcumene. Essential oils, the most kinds of bioactivity

component in *L. japonica*, have important pharmacological effects, and have been used in cosmetics, spices, and other industries widely (Wang L. et al., 2016). It also suggests that the characterization of the volatile compounds could be used as an indicator of the identity and the quality of *L. japonica* (Cai et al., 2013).

Flavonoids

Flavonoids are secondary metabolites and widely exist in natural plants including *L. japonica* (Han et al., 2016; Li R. et al., 2020; Liu et al., 2020), a group of natural or synthetic compounds containing parent cyclic structures and their O- and C-glycosylated derivatives with structural diversity (Rauter et al., 2018). Up to now, about 52 flavonoids have been isolated from *L. japonica*, which is mainly composed of flavonols (12 kinds) and flavones (36 kinds), and most of them are glycosides (Li et al., 2019). The flavonols mainly include rutin, quercetin, isoquercitrin, astragalin, Quercetin 3-O-hexoside, and so on (Chang and Hsu, 1992; Choi et al., 2007; Lee et al., 2010; Seo et al., 2012; Ge et al., 2019). The main flavones including cynaroside, luteolin, chrysoeriol 7-O-neohesperidoside, chrysoeriol 7-O-glucoside, lonicerin, tricin, etc. (Choi et al., 2007; Lee et al., 2010; Ge et al., 2019; Fang et al., 2020). Other flavonoids including one flavonolignan (hydnocarpin), one flavanone (eriodictyol) and three biflavonoids [3'-O-methyl loniflavone (5,5",7,7"-tetrahydroxy 3'-methoxy4',4"'-biflavonyl ether), loniflavone (5,5",7,7",30-pentahydroxy 4',4"'-biflavonyl ether) and (5,7,8,4'-tetrahydroxyflavone)-3'-4-(5,7-dihydroxyflavone)] were also have been isolated and identified from *L. japonica* (Kumar et al., 2005; Ge et al., 2018; Li et al., 2019). According to modern pharmacological research, flavonoids extracted from *L. japonica* has health benefits for the prevention of cancer, diabetes, cardiovascular disease, liver injury, and cerebrovascular disease (Han et al., 2016; Ge et al., 2018; Wan H. et al., 2019).

Saponins

Most of saponins from *L. japonica* belong to the oleanane type and hederagenin type (Shang et al., 2011). Saponins in *L. japonica* were first studied by Kawai et al. (1988), and 15 chemical compounds were found. So far, about 30 saponins, such as α-Hederin, Loniceroside A–E have been isolated and identified from *L. japonica* (Kawai et al., 1988; Son et al., 1994; Choi et al., 2007; Lin et al., 2008; Qi et al., 2009; Shang et al., 2011; Kuroda et al., 2014; Yu et al., 2015; Wang L. et al., 2016; Li et al., 2019). Studies showed that saponins from *L. japonica* have anti-inflammatory activities *in vitro* and *in vivo* (Lee et al., 1995; Kwak et al., 2003; Li et al., 2017; Ge et al., 2019).

Iridoids

Iridoids are the most abundant compounds in *L. japonica*, which mostly presenting as glycosides (Wang L. et al., 2016; Li et al., 2019). So far, more than 92 iridoids, like loganin, sweroside, secologanoside, ethyl secologanoside, centauroside etc., have been isolated from *L. japonica* (Kakuda et al., 2000; Yu et al., 2011, 2013; Zheng et al., 2012; Kashiwada et al., 2013; Liu et al., 2015, 2020; Ge et al., 2019; Yang R. et al., 2020; Qiu et al., 2021). Studies showed that these iridoids have anti-inflammatory (Song et al., 2008; Yu et al., 2011; Qiu et al., 2021) and antiviral activities (Kashiwada et al., 2013; Yu et al., 2013) *in vitro* and *in vivo*.

Others

Other chemical components except for phenolic acids, essential oils, flavonoids, saponins, and iridoids have also been isolated from *L. japonica*. Zhao et al. (2018) had identified 13 trace elements (Mg, Cr, Mn, Fe, Ni, Cu, Zn, As, Se, Mo, Cd, Hg, and Pb) with inductively coupled plasma mass-spectrometry (ICP-MS) and high-performance liquid chromatography-photodiode array (HPLC-PDA) method. Cai et al. (2019, 2021) had identified 13 amino acids (Alanine, Serine, Proline, Valine, Threonine, Isoleucine, Leucine, Aspartic acid, Glutamate, Lysine, Histidine, Phenylalanine, and Arginine) and four nucleosides (Cytidine, Uridine, Adenosine, and Inosine) in *L. japonica*.

LONICERA JAPONICA (EXTRACTS) AND INTESTINAL ANTIOXIDANT

In addition to its medicinal uses, *L. japonica* is also widely used in healthy foods and cosmetics in the world because of its health benefits (Seo et al., 2012; Fang et al., 2020; Zhang T. et al., 2020). Modern pharmacological researches have demonstrated that *L. japonica* extract has a variety of biological activities, which the antioxidant activity is an important biological property of great interest (Hsu et al., 2016; Wan H. et al., 2019; Zhang T. et al., 2020). Antioxidant activity of *L. japonica* was mainly related to its abundant polyphenols (Lee et al., 2019) and polysaccharides (Zhou et al., 2020).

Antioxidant Activity of Polyphenols

The antioxidative property of *L. japonica* is mainly attributed to the specific chemical structure of polyphenols, a widespread group of secondary metabolites that include various phenolic acids and flavonoids, which have a common character of having at least one aromatic ring substituted with one or more hydroxyl groups (Kong et al., 2017; Fan et al., 2019). Lee et al. (2019) who reported that the antioxidant activities of *L. japonica* were positively correlated with total phenolic, total flavonoid, CGA, CA, and quercetin contents, and Kong et al. (2017) who reported that antioxidative activity of *L. japonica* presented a significant positive correlation with the content of CGA, cynaroside, rutin, and hyperoside can demonstrate this conclusion. **Figure 1** presented the main phenolic acids (GCA, CA, and NGA) and flavonoids (luteolin 7-galactoside, quercetin, and luteolin) in *L. japonica*. It showed that all these compounds contain an aromatic nucleus and hydroxyl group, which is related to their strong antioxidant capacity (Choi et al., 2007; Guo et al., 2014; Hsu et al., 2016).

The ability to scavenge free radicals may play an important role in preventing some diseases caused by free radicals (Gheisar and Kim, 2018). Normally, 1,1-diphenyl-2-picrylhydrazyl (DPPH) scavenging activity assay, 2,2'-azino-bis (3-ethylbenzothiazoline-6-sulfonic) acid (ABTS) scavenging activity assay, superoxide

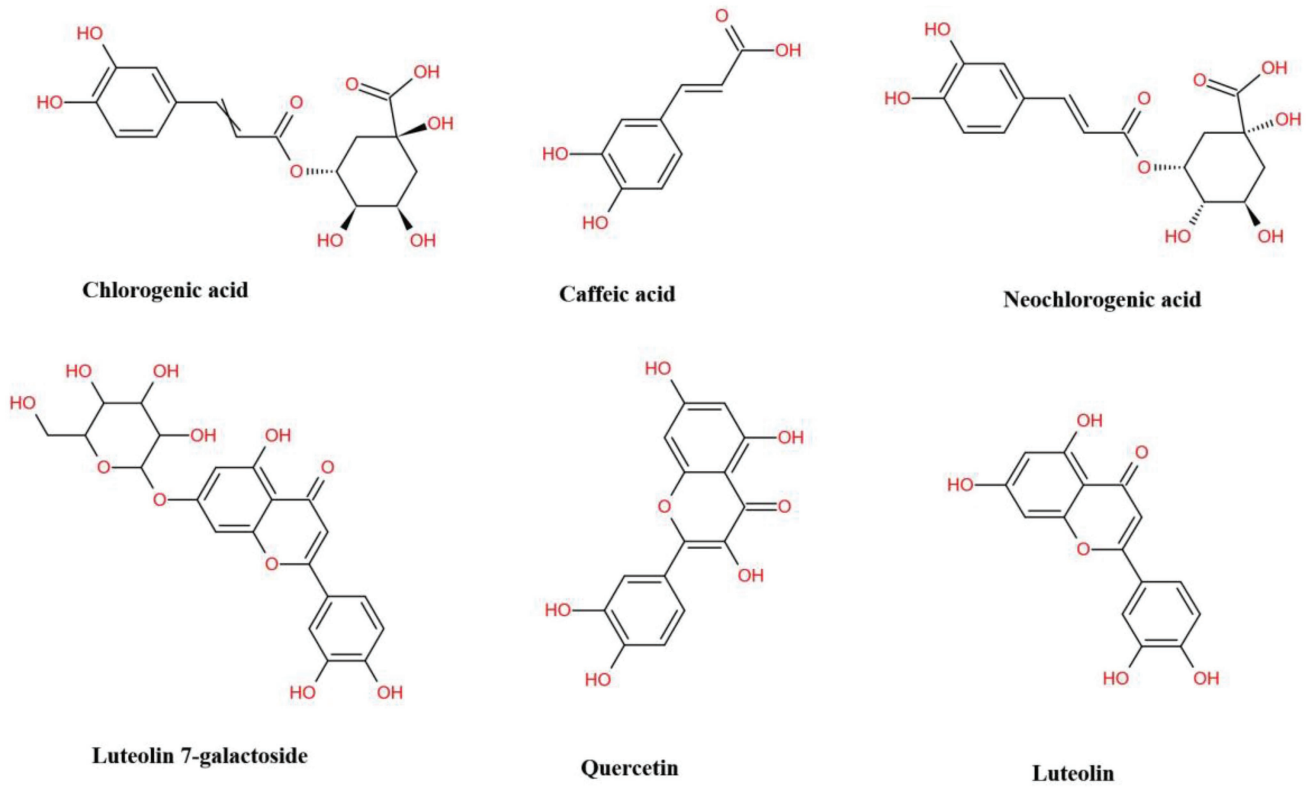

FIGURE 1 | The structural formula of major phenolic acids and flavonoids presenting in *Lonicera japonica*.

radical scavenging activity assay, ferric-reducing antioxidant power (FRAP) assay, and reducing power (RP) assay are the most frequently used to evaluate the antioxidant activity of plant extracts (Lee et al., 2011, 2019; Kong et al., 2017; Zhang T. et al., 2020). DPPH radical scavenging activity and ABTS radical scavenging activity reflect the ability of hydrogen-donating antioxidants and electron transfer to scavenge DPPH and $ABTS^{+}$ radicals (Lee et al., 2019). Superoxide radical scavenging activity denotes the ability to remove free radicals, such as peroxyl, alkoxyl, hydroxyl, and nitric oxide, which formed from superoxide anions through the Fenton reaction, lipid oxidation, or nitric oxidation (Hsu et al., 2016). FRAP and RP assays represent their ability to reduce the of ferric (Fe^{3+}) form to the ferrous (Fe^{2+}) form (Seo et al., 2012; Lee et al., 2019). Chaowuttikul et al. (2017) reported that the ethanolic extract of *L. japonica* showed DPPH and nitric oxide scavenging activities as well as RP property. Lee et al. (2019) showed that DPPH and ABTS radical scavenging activity of *L. japonica* were significantly increased during 60 min of heating and were retained for 90 min.

Antioxidant Activity of Polysaccharides

Polysaccharides are a kind of natural polymer linked by aldose or ketose through glycosidic bonds (Zhou et al., 2018a, 2021). Previous studies have found that polysaccharides extracted from plants can relieve oxidative stress through exerting their antioxidation potentials (Surin et al., 2018; Zhou et al., 2020). Polysaccharide is one of the main active ingredients of *L. japonica*, which have been isolated and identified in previous studies (Zhou et al., 2018a, 2020; Liu et al., 2019; Zhang T. et al., 2020). *In vitro* study showed that polysaccharide extracts from *L. japonica* exhibited obvious DPPH-scavenging activity, $ABTS^{+}$-scavenging activity, hydroxyl radical-scavenging activity, superoxide radical-scavenging activity, and excellent inhibitory activity on erythrocyte hemolysis induced by H_2O_2 (Zhang T. et al., 2020). Polysaccharide extracts from *L. japonica* could protect cardiomyocytes of mice injured by hydrogen peroxide *via* increasing the activities of catalase (CAT), glutathione peroxidase (GSH-Px), and superoxide dismutase (SOD), and decreasing ROS production (Zhou et al., 2020). *In vivo* study showed that crude polysaccharides extracted from *L. japonica* could alleviate the oxidative damage of liver in streptozotocin (STZ)-induced diabetic rats by decreasing alanine aminotransferase (ALT), aspartate aminotransferase (AST), and gamma-glutamyl transpeptidase (GGT) in serum, and improving levels of CAT, SOD, and GSH in liver (Wang et al., 2017). It reveals that the polysaccharides play an important role in the antioxidant function of *L. japonica*.

Potential Intestinal Antioxidant Effects of *L. japonica* (Extract)

Reactive oxygen species (ROS) are generated along with the process of cell respiration and normal metabolism continuously, and mitochondrion is the primary source of the majority of ROS in organisms (Wang Y. et al., 2020; Yan Z. et al., 2020).

ROS includes free radical ROS and non-radical ROS. Free radical ROS mainly include superoxide anion free radicals (O_2^-), hydroxyl radical ($\cdot OH^-$), peroxyl radical (ROO), and alkoxyl radical (RO), and non-radical ROS mainly consist of hydrogen peroxide (H_2O_2), oxygen (O_2), ozone (O_3), hypochlorous acid (HOCL), hypobromous acid (HOBr), chloramines (RNHCL), and organic hydroperoxides (ROOH; Wang Y. et al., 2020). Under normal physiological conditions, ROS can act as signaling molecules involved in cell growth and cellular adaptive responses (Lum and Roebuck, 2001). However, in commercial animal production, animals often suffer from bacterial infection (Zhang X. et al., 2020), endotoxin challenge (Chen et al., 2021), mycotoxin challenge (Xu et al., 2020), and weaning stress (Zhou et al., 2018b), which may induce a large number of ROS. When the body cannot remove these ROS in time, oxidative stress injury occurs (Campbell et al., 2013; Yin et al., 2014; Zhu H. et al., 2018; Saracila et al., 2021). Numerous studies have demonstrated that oxidative stress is associated with many pathological conditions, including intestinal barrier dysfunction and various digestive tract diseases (Almenier et al., 2012; Navarro-Yepes et al., 2014; Cao et al., 2018; Tang et al., 2018b; Chen et al., 2020, 2021). Thus, alleviating the negative effects of oxidative stress damage is crucial for the development of the animal husbandry.

The latest research progress of antioxidant activity of *L. japonica* has been summarized in **Table 1**. These studies suggested that *L. japonica* might be potential natural antioxidants and beneficial chemopreventive agent, which can be inferred that the extract of *L. japonica* may have a protective effect on intestinal oxidative damage of animals. However, the direct evidence of the protective effects *L. japonica* on intestinal oxidative damage is still lack. Therefore, further studies are needed to confirm whether *L. japonica* have a regulating effect on the intestinal oxidative damage of animals including farm animals and aquatic animals.

LONICERA JAPONICA (EXTRACTS) AND INTESTINAL INFLAMMATION

The intestine is different from the other organs of animal because it is not only the main part of animal nutrition

TABLE 1 | Antioxidant activity of *Lonicera japonica in vitro* and *in vivo*.

Animal/Cell models	Active compounds	Main results	References
LPS-induced RAW264.7 cells	Ethanolic extract	Significantly decreased the ROS level in the stimulated macrophage cells	Yoo et al., 2008
6-OHDA-induced SH-SY5Y cells	Ethyl acetate extract	Significantly decrease ROS and increase the GSH level, SOD activity, and CAT activity in 6-OHDA-induced SH-SY5Y cells	Kwon et al., 2012
H_2O_2-induced rat cardiomyocytes	Caffeoylquinic acids	Significantly attenuated hypoxia-induced ROS generation and reduced the ratio of GSSG/GS total	Wang C. et al., 2016
High-fat-induced hyperlipidemia rats	Water extracts	Could suppress the oxidative stress by increasing serum SOD, GSH-Px, and reducing MDA concentration in hyperlipidemia rats	Wang F. et al., 2016
Streptozotocin (STZ)-inducd diabetic rats	Polysaccharide	The oxidant stress in liver was restored by increasing the levels of CAT, SOD, and GSH in liver	Wang et al., 2017
H_2O_2-induced HepG 2 cells	Flavonoids	Dose-dependent increased CAT and SOD activity	Tzeng et al., 2014
H_2O_2-induced RAW264.7 cells	Flavonoids	Dose-dependent reduced MDA content in cells and culture supernatant, improve SOD activity and GSH content, and increase intracellular lactate dehydrogenase activity.	Luo et al., 2018
Carbon tetrachloride-induced liver fibrosis mice	Water extract	Alleviated liver oxidative stress injury and enhanced the activation of Nrf2 anti-oxidant signaling pathway	Miao et al., 2019
H_2O_2-induced hepatoma cells	Japoflavone D	Treatment of Japoflavone D suppressed the activation of ERK and mTOR and activated the KEAP1/NRF2/ARE signaling axis	Wan H. et al., 2019
Gastritis and peptic ulcer rats	BST-104	BST-104 treatment increased antioxidant activities (higher levels of CAT, SOD, and GSH/GSSG, and lower MDA levels)	Bang et al., 2019
H_2O_2-induced HepG2 cells	4,5-CQME	Reduced ROS and MDA levels and rescued GSH depletion; 4,5-CQME regulated the Keap1/Nrf2 signaling pathway and enhanced both the mRNA and protein expressions of HO-1 and NQO1	Xiao et al., 2020
H_2O_2-induced mice cardiomyocytes	Polysaccharide	Significantly increased the activities CAT, GSH-Px, and SOD, and decrease ROS production	Zhou et al., 2020
Beef cattle under heat stress	Not mentioned	Serum SOD, GSH-Px, and T-AOC was increased, and serum MDA was decreased	Fu et al., 2016
Dairy cows	Not mentioned	Quadratically increased the activity of GSH-Px and T-AOC in serum but decreased concentration of MDA	Ma et al., 2020a
Dairy cows	Not mentioned	*Lonicera japonica* supplementation decreased the concentrations of reactive ROM, meanwhile increased the T-AOC and SOD concentrations in blood	Zhao et al., 2020

BST-104, a water extract of L. japonica; LPS, lipopolysaccharide; CAT, catalase; GSH-Px, glutathion peroxidase; SOD, superoxide dismutase; T-AOC, total antioxidant capacity; MDA, malonaldehyde; ROM, reactive oxygen metabolites; 6-OHDA, 6-hydroxydopamine; rCMEC, rat cardiac microvascular endothelial cells; ROS, reactive oxygen species; 4,5-CQME, 4,5-di-O-caffeoylquinic acid methyl ester; Keap1, kelch-like ECH-associated protein 1; Nrf2, nuclear factor erythroid 2-related factor 2; ARE, antioxidant response elements; HO-1, heme oxygenase; NQO1, quinone oxidoreductase; ERK, extracellular signal-related kinases; and mTOR, mammalian target of rapamycin protein.

digestion and absorption, but also consists of a physical and immunological protective barrier against foreign antigens and pathogens from the external environment into the circulation system (Tang et al., 2016, 2018b, 2021; Curciarello et al., 2019). Optimum intestinal health is of prime importance to animal growth as well as animal health. Disruption of the intestinal epithelial homeostasis has been reported to increase intestinal permeability, which can cause numerous gastrointestinal diseases (Miner-Williams and Moughan, 2016; Tang et al., 2019; Peng et al., 2020; Tang and Xiong, 2021). *Lonicera japonica* extract has a significant effect on the intestinal health regulation of animals due to its various biological activities including anti-inflammatory activity (Kang et al., 2010; Han et al., 2016; Zhou et al., 2021).

Anti-inflammatory Activity of *L. japonica* (Extracts)

Inflammation is a normal protective response induced by tissue injury or infection. It has been proved that *L. japonica* presents significant anti-inflammatory effects *in vitro* and *in vivo* (Jiang et al., 2014; Li R. et al., 2020; Zhou et al., 2021). As we know, proinflammatory cytokines, such as tumor necrosis factor α (TNF-α), interleukin 1β (IL-1β), and IL-6 contribute to inflammatory injury and triggers an inflammatory cascade (Bang et al., 2019; Li R. et al., 2020). Kang et al. (2010) showed that *L. japonica* extract could suppress inflammatory mediators, such as IL6, IL-8, and TNF-α release by blocking nuclear factor-κB (NF-κB) and mitogen-activated protein kinase (MAPKs) activation pathways in HMC-1 Cells. Su et al. (2021) showed that ethanol extract of *L. japonica* caulis significantly inhibit the expression of pro-inflammatory factors such as TNF-α, IL-1β, IL-6, and interferon γ (IFN-γ) in mice. The study Li R. et al. (2020) suggested that the flower buds, leaves, and stems of *L. japonica* extracts showed a cytoprotective effect on lipopolysaccharide (LPS) stimulated RAW 264.7 macrophages by suppressing proinflammatory cytokines including TNF-α, IL-1β, and IL-6 production. Bang et al. (2019) showed that the anti-inflammatory effects of BST-104 (a water extract of *L. japonica*) were attributed to reduced levels of proinflammatory cytokines, such as TNF-α, IL-1β, and IL-6 in gastric mucosal tissues. All of these researches suggest that *L. japonica* is a good anti-inflammatory agent for treating inflammatory disorders.

Lonicera japonica (Extracts) Inhibits Intestinal Inflammation

The intestinal tract is the largest immune organ in the body and acts as the first line of defense against infection and a barrier that prevents commensal bacteria from penetrating the intestinal epithelium (Tang et al., 2016; Clavijo and Flórez, 2018; Qamar et al., 2021). The gut immune system comprises mucosal layer, epithelial cells, antibacterial peptides, immunoglobulins, and cytokines (Yitbarek et al., 2019; Qamar et al., 2021). Previous studies had demonstrated that *L. japonica* can promote intestinal immune function and has a preventive effect on intestinal inflammation (Park et al., 2012; Yang X. et al., 2020). Yang X. et al. (2020) showed that the treatment of the alcohol extract of *L. japonica* to mice significantly increased intestinal sIgA content. Zhou et al. (2021) showed that with the supplementation of *L. japonica* polysaccharides, the content of immunoglobulin A (sIgA) secreted from the intestine was significantly higher than that of dextran sulfate sodium (DSS)-induced ulcerative colitis mice. sIgA, an immunoglobulin secreted by plasma cells of the intestinal mucosa, is a major effector of the intestinal mucosal immunity, which acts as the first line of defense in the intestinal mucosa that neutralizes pathogens in the intestinal mucosa and plays an important role in local anti-infection of the body (Salerno-Goncalves et al., 2016; Zhou et al., 2021). These studies indicated that prompting the secretion of sIgA is one of the ways to enhance the immune ability of the intestine by *L. japonica* (Yang X. et al., 2020; Zhou et al., 2021). In addition to promoting the secretion of sIgA, *L. japonica* can also play the role of intestinal immune function by regulating the secretion of intestinal mucosal cytokines (Park et al., 2012; Zhou et al., 2018a). Lee et al. (2011) showed that buthanol (BuOH) extracts of *L. japonica* inhibited the synthesis of IL-6 in a LPS-stimulated colonic epithelial cell line (HT-29 cell) *in vitro* and a DSS-induced ulcerative colitis mouse *in vivo*. Park et al. (2012) showed that *L. japonica* inhibited the cytokines including TNF-α, IL-1β, IL-6, IFN-γ, IL-12, and IL-17 in DSS-induced ulcerative colitis mice. In an immunosuppressed mice model, the researchers found that polysaccharide extracts from *L. japonica* could restore the levels of serum cytokines IL-2, TNF-α, and IFN-γ level in cyclophosphamide-induced mice, which indicated that *L. japonica* can be used as a potential immunomodulatory agent (Zhou et al., 2018a). Through these studies, we can speculate that *L. japonica* extract may also had regulation on intestinal immune function and intestinal inflammation of farm and aquatic animals, which of course needs further researches to demonstrate it.

LONICERA JAPONICA (EXTRACTS) AND GUT MICROBIOTA

Gut Microbiota and Intestinal Health

The gastrointestinal tract, the largest organ in the animal body, provides a broad colonization surface for the flora. Thousands of bacteria colonize the entire gut, which directly interrelates with the host and contributes to the regulation of the host intestinal barrier function and homeostasis (Chen et al., 2017b; Wan M. et al., 2019; Hayashi et al., 2021; Qamar et al., 2021). The gut barrier is central to the maintenance of gut homeostasis and breakdown of the barrier is involved in a wide variety of clinical conditions (Alam and Neish, 2018). Gut microbiota plays a vital role in host health, which is thought to tightly associate with the intestinal barrier function including physical barrier, chemical barrier, immune barrier, and microbial barrier (**Figure 2**; Guevarra et al., 2018; Makki et al., 2018). First of all, the intestinal microbial barrier is composed of many normal intestinal floras, which play an important role in intestinal microecological balance regulation,

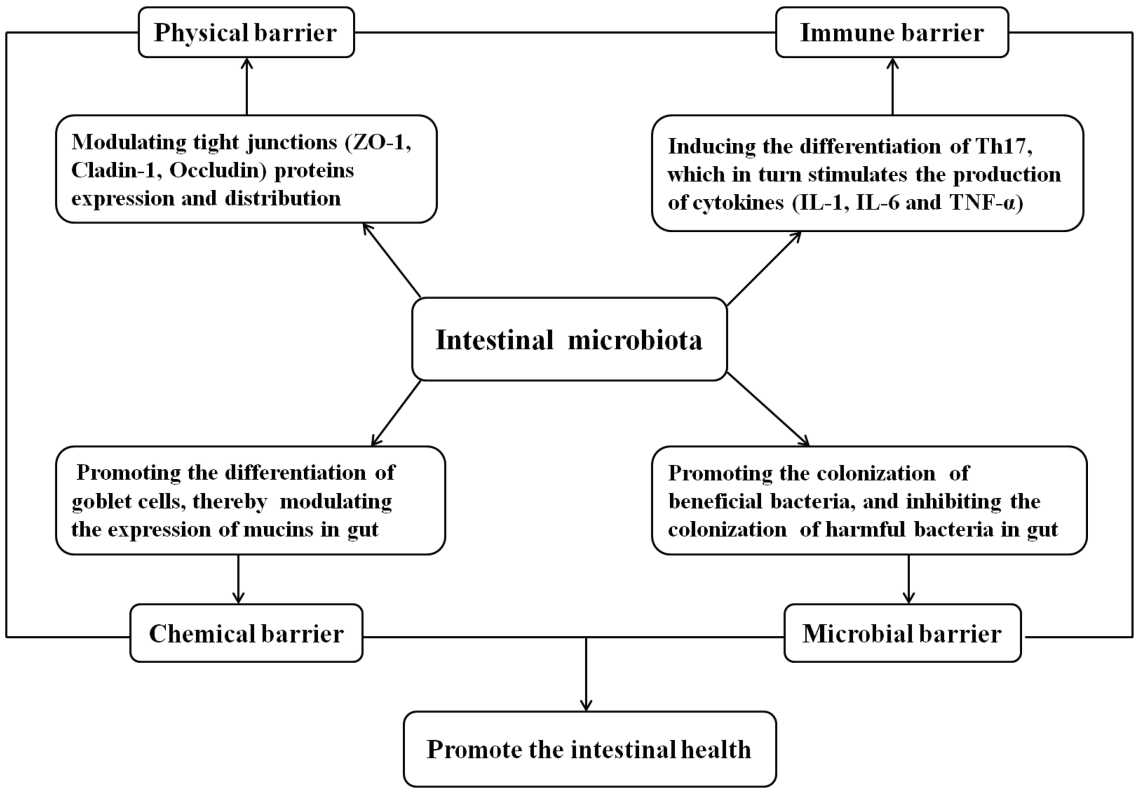

FIGURE 2 | Relationship between gut microbiota and intestinal health.

and the imbalance of intestinal floras may result in intestinal dysfunction (Tan et al., 2015; Li X. et al., 2020). Second, intestinal commensal segmented filamentous bacteria can induce the differentiation of T helper 17 (Th17) in the lamina prima, which in turn stimulates the production of cytokines, IL-1, IL-6, and TNF-α by a variety of cells (Goto et al., 2014; Villena et al., 2014). Metabolites such as short-chain fatty acids (SCFA) produced by the gut bacteria are considered as key molecular intermediates between the microbiota and its host (Beaumont et al., 2020). SCFA can induce the proliferation and differentiation of Treg, thus activating the intestinal immune system and playing the function of immune barrier (Horai et al., 2017). Third, the intestinal floras can influence the intestinal physical barrier by modulating tight junction (TJ) proteins expression and distribution (Zhu L. et al., 2018; Li X. et al., 2020). For example, Hu et al. (2020) reported that piglets receiving protocatechuic acid promoted the expression of ZO-1 and Claudin-1 in the intestinal mucosa by increasing the abundance of the beneficial bacteria *Roseburia* in the intestinal tract thus maintaining the function of the intestinal barrier. Finally, the intestinal floras can also influence the intestinal chemical barrier by promoting the differentiation of goblet cells, thereby modulating the expression of mucins (MUCs), a family of highly glycosylated protein that are secreted by specialize cells in the gut, which is the main component of intestinal mucus (Sicard et al., 2017). In a word, intestinal flora is closely related to intestinal health.

Lonicera japonica (Extracts) Modulates Intestinal Micobiota

Modern pharmacological research has confirmed the strong antimicrobial activity of *L. japonica in vivo* and *in vitro* (Rhee and Lee, 2011; Xiong et al., 2013; Yang et al., 2016; Minami and Makino, 2020; Yan L. et al., 2020). *In vitro* study showed that *L. japonica* has antimicrobial effects such as *Bacteroides fragilis*, *Bacteroides ovatus*, *Clostridium difficile*, *Clostridium perfringenes*, *Propionebacterium acnes*, *Staphylococcus aureus*, *Shigella*, *Salmonella*, and *Escherichia coli* (*E. coli*; Rhee and Lee, 2011; Xiong et al., 2013; Yang et al., 2016, 2018; Yan L. et al., 2020). *In vivo* study showed that *L. japonica* could significantly promote the colonization of beneficial bacteria and inhibit the reproduction of harmful bacteria (Minami and Makino, 2020; Yang X. et al., 2020). Wang et al. (2014) showed that unfermented or fermented *L. japonica* both can significant alteration of the distribution of intestinal flora, especially affecting the population of *Akkermansia* spp. and Bacteroidetes/Firmicutes ratio in obesity rats, which play an essential role in high fat diet or LPS induced enhancement in gut permeability, development of endotoximia, and inflammation. Minami and Makino (2020) showed that *L. japonica* significantly increased the survival rate and decreased *Citrobacter rodentium* (*C. rodentium*) colonization in the large intestine of mice. *Citrobacter rodentium* is a mucosal pathogen of murine, which has long used as a model to elucidate the molecular and cellular pathogenesis of infection with enteropathogenic *E. coli* and

enterohaemorrhagic *E. coli*, two clinically important human gastrointestinal pathogens (Collins et al., 2014; Bouladoux et al., 2017; Mullineaux-Sanders et al., 2019). Yang X. et al. (2020) showed that the water extract of *L. japonica* and alcohol extract of *L. japonica* did not damage the intestinal structure, and both of them could promote the growth of beneficial bacteria *Lactobacillus* and inhibit the growth of potential pathogenic bacteria *E. coli*. *Lactobacillus* is a predominant indigenous bacterial genus found in the human and animal gastrointestinal tract, and species of this genus like *Lactobacillus plantarum* (*L. plantarum*; Wang et al., 2018), *Lactobacillus casei* (Eun et al., 2011), *Lactobacillus rhamnosus* (Villena et al., 2014), and *Lactobacillus reuteri* (Yang et al., 2015) etc., are commonly used as probiotics, which can affect transepithelial electrical resistance (TER) and epithelial permeability, modulate TJ proteins distribution, and enhance the immune function. *Escherichia coli* strains are important pathogens that cause diverse diseases in humans and animals, which is a major challenge for intestinal health (Dautzenberg et al., 2016; Stromberg et al., 2017; Desvaux et al., 2020). Therefore, it reveals that *L. japonica* has a good regulatory effect on animal intestinal microbiota, thus promoting the intestinal health of animals. However, the studies of *L. japonica* extract on intestinal microbiota of farm and aquatic animals are still lack, which perhaps is a good research direction in the future.

APPLICATION OF *L. JAPONICA* IN ANIMAL PRODUCTION

Various herbs and their extracts have been used as feed additives due to their anti-oxidative effect, anti-inflammatory activity, anti-microbial effect, and growth-promoting effect (Windisch et al., 2008; Hanczakowska et al., 2015; Lei et al., 2018; Lin et al., 2020). Among them, *L. japonica* (extract) was widely investigated in animal husbandry because of its diverse pharmacological effects such as antioxidant, anti-microbial, antiviral, antitoxic, antiseptic, and anti-inflammatory properties (Kang et al., 2010; Park et al., 2012; Wang et al., 2014; Li R. et al., 2020). **Table 2** summarized the application of *L. japonica* (extract) in animal production in recently years. It showed that these studies mainly focus on pigs (Liu W. et al., 2016), beef cattle (Fu et al., 2016; Yejun et al., 2019), dairy cows (Ma et al., 2020a,b; Zhao et al., 2020), broiler (Müştak et al., 2015), laying hens (Long et al., 2018), *Penaeus monodon* (Chen et al., 2013), grass carp (Meng et al., 2019), and olive flounder (Dharaneedharan et al., 2016).

Studies on beef cattle showed that *L. japonica* extract can effectively alleviate heat stress, improve antioxidant function, and have a good repair effect on skeletal muscle fiber structure damage of beef cattle (Song et al., 2015; Fu et al., 2016). Moreover, *in vitro* studies showed that *L. japonica* extract could regulate rumen fermentation and reduce methane production by inhibiting the growth of methanogenic bacteria (Huang et al., 2019; Yejun et al., 2019). Studies on dairy cows showed that dietary supplementation of *L. japonica* extract could relieve heat stress of dairy cows by improving immune and antioxidant capacity (Ma et al., 2020a,b; Gao et al., 2021), enhancing anti-inflammatory activity (Zhao et al., 2020). Meanwhile, *L. japonica* extract can improve rumen microbial diversity and improve rumen fermentation capacity (Tang et al., 2018a). In pig production, herbal extract mixture (HEM) may have a better application effect (Liu W. et al., 2016; Wang M. et al., 2020). For instance, Liu W. et al. (2016) indicated that dietary supplementation with a mixture of 55% *Scutellaria baicalensis* extract and 25% *L. japonica* extract administration could improve growth performance and nutrient digestibility, decrease serum cortisol levels, as well as benefit the meat quality in finishing pigs, and Wang Y. et al. (2020) showed that dietary supplementation with 1,000 mg/kg a mixture extract of golden-and-silver honeysuckle (*L. japonica* Thunb.), huangqi (*Astragalus menbranaceus*), duzhong leaves (*Eucommia folium*), and dangshen (*Codonopsis pilosula*) had beneficial effects on intestinal morphology modulation and the mRNA expression of nutrients transporters of pigs. For broilers, dietary supplementation with *L. japonica* extract could increase weight gain, blood cells, antioxidant activity, and meat quality of broilers (Park et al., 2014), while did not affect the proximate composition of the breast meat, but could increase the antioxidative potential and overall preference of breast meat during cold storage (Jang et al., 2008). Drinking water containing GCA extracted from *L. japonica* can effectively increase the body weight of broilers and reduce Mycoplasma gallisepticum infection of broilers (Müştak et al., 2015). Studies on laying hens showed that dietary supplementation with *L. japonica* extract (Long et al., 2018) or HEM containing *L. japonica* extract (Liu and Kim, 2017) could improve laying performance, eggshell strength, egg quality, and shelf life in laying hens. For aquatic animals, dietary supplementation with *L. japonica* could improve the growth performance, health condition and survival rate of *Penaeus monodon* (Chen et al., 2013), and could effectively improve the lipid metabolism and ameliorate the lipid deposition of grass carp (Meng et al., 2019). Flounder fish fed with 0.025, 0.05, 0.1, 0.2, and 0.4% *L. japonica* leaf powder for 4 weeks showed significantly increased respiratory burst, lysozyme, phagocytic activity, immune function, and antioxidant activity (Dharaneedharan et al., 2016).

CONCLUSION

Intestinal health determines the health status of animals. To regulate intestinal health is always been an important issue in the post-antibiotic era of animal husbandry. As a kind of natural plant extract, *L. japonica* extract is rich in phenolic acids, essential oils, flavonoids, iridoids, and saponins, which has a good regulating effect on the intestinal health of animals, and is an ideal product of antibiotics substitution. According to the published literature, although the application of *L. japonica* extract in animal production has been reported, it mainly focuses on the regulation of animal production performance, meat quality, egg quality, rumen fermentation capacity, and anti-heat stress, etc. In animal production, the effects of *L. japonica* extract on intestinal health may be related to its

TABLE 2 | Application of *L. japonica* in animal production.

Animals	*In vivo*/*In vitro*	Optimal added amount	Significant effects	References
Beef cattle	*In vivo*	0.2% in concentrate	Dietary supplementation of *L. japonica* extract improved the antioxidant and restored the morphosis of damaged muscle	Song et al., 2015
Beef cattle	*In vivo*	0.2% in concentrate	Dietary supplementation of *L. japonica* extracts improve antioxidant capability, and relieve stress reaction of beef cattle, while had no significant effects on weight gain	Fu et al., 2016
Beef cattle	*In vitro*	3, 5, 7, and 9%	*Lonicera japonica* extract supplementation could significantly reduce rumen methane (CH4) production as well as inhibit fiber-decomposition bacteria and methanogens	Huang et al., 2019
Beef cattle	*In vitro*	3, 5, 7, and 9%	*Lonicera japonica* extract supplementation linear decreased gas production and dry matter degradability, decreased CH4 production, and fibrolytic bacteria and ciliate associated methanogen abundance	Yejun et al., 2019
Dairy cow	*In vivo*	28 g/d	Dietary supplemented with *L. japonica* extract could relieve heat stress of dairy cows without affect the performance of lactating cows as well as cause changes of hepatic gene expression, such as immune, antioxidant capacity, and liver glucose metabolism related genes	Gao et al., 2021
Dairy cow	*In vivo*	28 g/d	Dietary *L. japonica* extract supplementation had no significant effect on the performance of cows under heat stress, but can improve the immune response and alleviate the heat stress of cows	Ma et al., 2020b
Dairy cow	*In vivo*	28 g/d	Dietary *L. japonica* extract supplementation had no negative effects on lactation performance but helped to alleviate heat stress by improving antioxidant status and promoting endocrine and immune functions	Ma et al., 2020a
Dairy cow	*In vivo*	1 and 2 g/kg dry matter	Supplementation with 1 and 2 g/kg dry matter *L. japonica* extract could improve lactation performance, increase milk production, and enhance anti-inflammatory and antioxidant capacities of dairy cows during perinatal period	Zhao et al., 2020
Dairy cow	*In vitro*	1 mg/g	Supplementation with *L. japonica* extract can effectively regulate the fermentative state of rumen microorganism under the *in vitro* condition	Tang et al., 2018a
Pig	*In vivo*	0.025 and 0.05% herbal extract mixture (HEM)[1]	Administration of HEM (0.025 and 0.05%) could improve growth performance and nutrient digestibility, decrease serum cortisol levels, as well as benefit the meat quality in finishing pigs	Liu W. et al., 2016
Pig	*In vivo*	1,000 mg/kg HEM[2]	Supplementation with *L. japonica* extract had benefit effects on intestinal morphology modulation and the mRNA expression of nutrients transporters	Wang Y. et al., 2020
Broiler	*In vivo*	0.3 and 1% HEM[3]	Supplementation with *L. japonica* extract did not affect proximate composition of the breast meat, but could increase total phenols content of the breast meats; could increase the antioxidative potential and overall preference of breast meat during cold storage	Jang et al., 2008
Broiler	*In vivo*	0.2%	Supplementation with *L. japonica* extract increased weight gain, blood cells, antioxidant activity, and meat quality of broilers	Park et al., 2014
Broiler	*In vivo*	190 μg/d	Supplementation with *L. japonica* extract could improve the live body weight as well as decrease *Mycoplasma gallisepticum* colonization of broilers	Müştak et al., 2015
Laying hens	*In vivo*	0.025 and 0.05% HEM[4]	Supplementation with HEM could improve eggshell strength and shelf life in laying hens when reared under hot climatic conditions.	Liu and Kim, 2017
Laying hens	*In vivo*	300 mg/kg	Supplementation with *L. japonica* extract could increase the average egg weight, average daily feed intake, and egg Haugh unit, improve the lipid metabolism, and reduce cholesterol content of egg yolk	Long et al., 2018
Penaeus monodon	*In vivo*	0.2 and 0.4%	Supplementation with *L. japonica* extra could improve the growth performance, health condition, and survival rate of *Penaeus monodon*	Chen et al., 2013
Grass carp	*In vivo*	20 and 40 g/kg	Supplementation with *L. japonica* extract could effectively improve the lipid metabolism and ameliorate the lipid deposition of grass carp	Meng et al., 2019
Olive flounder	*In vivo*	0.025, 0.05, 0.1, 0.2, and 0.4%	Fish fed with *L. japonica* leaf powder showed decreased cumulative mortality and enhanced immunity response and resistance to *Vibrio anguillarum* infection	Dharaneedharan et al., 2016

[1]*A mixture of 55% Scutellaria baicalensis powder extract, 25% L. japonica powder extract, and 20% carrier (wheat bran).*
[2]*A mixture extract of golden-and-silver honeysuckle (L. japonica Thunb.), huangqi (Astragalus menbranaceus), duzhong leaves (Eucommia folium), and dangshen (Codonopsis pilosula).*
[3]*A mixture of mulberry leaf, Japanese honeysuckle, and goldthread at a ratio of 48.5:48.5:3.0.*
[4]*A mixture of 55% S. baicalensis powder extract, 25% L. japonica powder extract, and 20% carrier (wheat bran).*

antioxidant, anti-inflammatory, and antimicrobial activities. Although previous studies had demonstrated that about *L. japonica* has a good regulatory effect on animal intestinal health, but mainly focus on experimental animals or cells, like mice, rats, HMC-1 Cells, and RAW 264.7 cells, the studies of *L. japonica* extract on intestinal health regulation of farm and

aquatic animals are still rare and unclear. Therefore, it is necessary to increase the research on the regulatory mechanism of *L. japonica* extract on intestinal health especially the protective effects of *L. japonica* extract on oxidative injury, inflammation, and regulation of intestinal flora in farm and aquatic animals in the future, so as to provide a theoretical basis for the application of *L. japonica* extract in animal production.

AUTHOR CONTRIBUTIONS

XT and RF advocated to writing this review, and reviewed, edited, and approved its final version. XT collected literature and wrote the manuscript. XL and JZ helped to collect and review literatures. All authors contributed to the article and approved the submitted version.

FUNDING

This research was funded by grants from the World Top Discipline Program of Guizhou Province (No. 125 2019 Qianjiao Keyan Fa), the China Overseas Expertise Introduction Program for Discipline Innovation (No. D17016), the Natural Science Research Project of Education Department of Guizhou Province [Qianjiaohe KY Zi (2021) 294], and the Doctoral Launched Scientifc Research Program of Guizhou Normal University [GZNUD (2018) 26].

ACKNOWLEDGMENTS

We thank Kangning Xiong from the State Engineering Technology Institute for Karst Desertfication Control (Guiyang, China) for his financial support and paper revision.

REFERENCES

Alam, A., and Neish, A. (2018). Role of gut microbiota in intestinal wound healing and barrier function. *Tissue Barriers* 6:e1539595. doi: 10.1080/21688370.2018.1539595

Almenier, H. A., Menshawy, H. H. A., Maher, M. M., and Gamal, S. A. (2012). Oxidative stress and inflammatory bowel disease. *Front. Biosci.* 4, 1335–1344. doi: 10.2741/463

Bang, B. W., Park, D., Kwon, K. S., Lee, D. H., Jang, M. J., Park, S. K., et al. (2019). BST-104, a water extract of *Lonicera japonica*, has a gastroprotective effect via antioxidant and anti-inflammatory activities. *J. Med. Food* 22, 140–151. doi: 10.1089/jmf.2018.4231

Barton, M. D. (2014). Impact of antibiotic use in the swine industry. *Curr. Opin. Microbiol.* 19, 9–15. doi: 10.1016/j.mib.2014.05.017

Beaumont, M., Paës, C., Mussard, E., Knudsen, C., Cauquil, L., Aymard, P., et al. (2020). Gut microbiota derived metabolites contribute to intestinal barrier maturation at the suckling-to-weaning transition. *Gut Microbes* 11, 1268–1286. doi: 10.1080/19490976.2020.1747335

Boskabady, M. H., Mehrjardi, S. S., Rezaee, A., Rafatpanah, H., and Jalali, S. (2013). The impact of Zataria multiflora Boiss extract on in vitro and in vivo Th1/Th2 cytokine (IFN-γ/IL4) balance. *J. Ethnopharmacol.* 15, 1024–1031. doi: 10.1016/j.jep.2013.10.003

Bouladoux, N., Harrison, O. J., and Belkaid, Y. (2017). The mouse model of infection with *Citrobacter rodentium*. *Curr. Protoc. Immunol.* 119, 19.15.1–19.15.25. doi: 10.1002/cpim.34

Cai, H., Cao, G., Li, L., Liu, X., Ma, X. Q., Tu, S. C., et al. (2013). Profiling and characterization of volatile components from non-fumigated and sulfur-fumigated Flos *Lonicerae Japonica* using comprehensive two-dimensional gas chromatography time-of-flight mass spectrometry coupled with chemical group separation. *Molecules* 18, 1368–1382. doi: 10.3390/molecules18021368

Cai, Z., Wang, C., Chen, C., Zou, L., Chai, C., Chen, J., et al. (2021). Quality evaluation of *Lonicerae Japonica* Flos and *Lonicerae Flos* based on simultaneous determination of multiple bioactive constituents combined with multivariate statistical analysis. *Phytochem. Anal.* 32, 129–140. doi: 10.1002/pca.2882

Cai, Z., Wang, C., Zou, L., Liu, X., Chen, J., Tan, M., et al. (2019). Comparison of multiple bioactive constituents in the flower and the caulis of *Lonicera japonica* based on UFLC-QTRAP-MS/MS combined with multivariate statistical analysis. *Molecules* 24:1936. doi: 10.3390/molecules24101936

Campbell, J. M., Crenshaw, J. D., and Polo, J. (2013). The biological stress of early weaned piglets. *Anim. Sci. Biotechnol.* 4:19. doi: 10.1186/2049-1891-4-19

Cao, S., Wu, H., Wang, C., Zhang, Q., Jiao, L., Lin, F., et al. (2018). Diquat-induced oxidative stress increases intestinal permeability, impairs mitochondrial function, and triggers mitophagy in piglets. *J. Anim. Sci.* 96, 1795–1805. doi: 10.1093/jas/sky104

Chang, W. C., and Hsu, F. L. (1992). Inhibition of platelet activation and endothelial cell injury by polyphenolic compounds isolated from *Lonicera japonica* Thunb. *Prostaglandins Leukot. Essent. Fat. Acids* 45, 307–312. doi: 10.1016/0952-3278(92)90088-Z

Chaowuttikul, C., Palanuvej, C., and Ruangrungsi, N. (2017). Pharmacognostic specification, chlorogenic acid content, and in vitro antioxidant activities of *Lonicera japonica* flowering bud. *Pharm. Res.* 9, 128–132. doi: 10.4103/pr.pr_117_16

Chen, F., Chen, J., Chen, Q., Yang, L., Yin, J., Li, Y., et al. (2021). *Lactobacillus delbrueckii* protected intestinal integrity, alleviated intestinal oxidative damage, and activated toll-like receptor-bruton's tyrosine kinase-nuclear factor erythroid 2-related factor 2 pathway in weaned piglets challenged with lipopolysaccharide. *Antioxidants* 10:468. doi: 10.3390/antiox10030468

Chen, X., Lin, H. Z., Jiang, S. G., Wu, K. C., Liu, Y. J., Tian, L. X., et al. (2013). Dietary supplementation of honeysuckle improves the growth, survival and immunity of *Penaeus monodon*. *Fish Shellfish Immunol.* 35, 161–169. doi: 10.1016/j.fsi.2013.04.020

Chen, L., Liu, C. S., Chen, Q. Z., Wang, S., Xiong, Y. A., Jing, J., et al. (2017a). Characterization, pharmacokinetics and tissue distribution of chlorogenic acid-loaded self-microemulsifying drug delivery system. *Eur. J. Pharm. Sci.* 100, 102–108. doi: 10.1016/j.ejps.2017.01.011

Chen, F., Wang, H., Chen, J., Liu, Y., Wen, W., Li, Y., et al. (2020). *Lactobacillus delbrueckii* ameliorates intestinal integrity and antioxidant ability in weaned piglets after a lipopolysaccharide challenge. *Oxidative Med. Cell. Longev.* 2020:6028606. doi: 10.1155/2020/6028606

Chen, L., Xu, Y., Chen, X., Fang, C., Zhao, L., and Chen, F. (2017b). The maturing development of gut microbiota in commercial piglets during the weaning transition. *Front. Microbiol.* 8:1688. doi: 10.3389/fmicb.2017.01688

Choi, C. W., Jung, H. A., Kang, S. S., and Choi, J. (2007). Antioxidant constituents and a new triterpenoid glycoside from *Flos Lonicerae*. *Arch. Pharm. Res.* 30, 1–7. doi: 10.1007/BF02977770

Clavijo, V., and Flórez, M. J. V. (2018). The gastrointestinal microbiome and its association with the control of pathogens in broiler chicken production: a review. *Poult. Sci.* 97, 1006–1021. doi: 10.3382/ps/pex359

Collins, J. W., Keeney, K. M., Crepin, V. F., Rathinam, V. A. K., Fitzgerald, K. A., Finlay, B. B., et al. (2014). Citrobacter rodentium: infection, inflammation and the microbiota. *Nat. Rev. Microbiol.* 12, 612–623. doi: 10.1038/nrmicro3315

Curciarello, R., Canziani, K. E., Docena, G. H., and Muglia, C. I. (2019). Contribution of non-immune cells to activation and modulation of the intestinal inflammation. *Front. Immunol.* 10:647. doi: 10.3389/fimmu.2019.00647

Dautzenberg, M. J., Haverkate, M. R., Bonten, M. J., and Bootsma, M. C. (2016). Epidemic potential of *Escherichia coli* ST131 and *Klebsiella pneumoniae* ST258: a systematic review and meta-analysis. *BMJ Open* 6:e009971. doi: 10.1136/bmjopen-2015-009971

Desvaux, M., Dalmasso, G., Beyrouthy, R., Barnich, N., Delmas, J., and Bonnet, R. (2020). Pathogenicity factors of genomic islands in intestinal and extraintestinal *Escherichia coli*. *Front. Microbiol.* 11:2065. doi: 10.3389/fmicb.2020.02065

Dharaneedharan, S., Kim, D. H., Park, O., Jang, Y. H., Balasundaram, C., and Heo, M. S. (2016). Dietary effect of *Lonicera japonica* on immune expression

in olive flounder *Paralichthys olivaceus*, challenged with vibrio anguillarum. *Isr. J. Aquacult. Bamidgeh* 68:20812. doi: 10.46989/001c.20812

Du, C. Z., Feng, X., and Wang, H. (2015). Analysis of volatile constituents in *Lonicera japonica* Thunb. from different originals by GC-MS. *Agric. Sci. Technol.* 5, 1081–1083.

Duan, M. H., Fang, T., Ma, J. F., Shi, Q. L., Peng, Y., Ge, F. H., et al. (2018). Homogenate-assisted high-pressure disruption extraction for determination of phenolic acids in *Lonicerae Japonica* Flos. *J. Chromatogr. B Anal. Technol. Biomed. Life Sci.* 1097–1098, 119–127. doi: 10.1016/j.jchromb.2018.07.032

Eun, C. S., Kim, Y. S., Han, D. S., Choi, J. H., Lee, A. R., and Park, Y. K. (2011). *Lactobacillus casei* prevents impaired barrier function in intestinal epithelial cells. *APMIS* 119, 49–56. doi: 10.1111/j.1600-0463.2010.02691.x

Fan, Z., Li, L., Bai, X., Zhang, H., Liu, Q., Zhang, H., et al. (2019). Extraction optimization, antioxidant activity, and tyrosinase inhibitory capacity of polyphenols from *Lonicera japonica*. *Food Sci. Nutr.* 7, 1786–1794. doi: 10.1002/fsn3.1021

Fang, H., Qi, X., Li, Y., Yu, X., Xu, D., Liang, C., et al. (2020). De novo transcriptomic analysis of light-induced flavonoid pathway, transcription factors in the flower buds of *Lonicera japonica*. *Trees* 34, 267–283. doi: 10.1007/s00468-019-01916-4

Fu, Y., Huang, T., Qu, M., Song, X., Chen, Y., Yang, S., et al. (2016). Effects of honeysuckle extracts on serum hormones and antioxidant indexes of beef cattle under heat stress. *Chinese J. Anim. Nutr.* 28, 926–931. doi: 10.3969/j.issn.1006-267x.2016.03.035

Gao, Z., Ma, F., Dan, Q., Jin, H., Li, H., Chang, M., et al. (2021). Hepatic transcriptome analyses revealed molecular mechanism of *Lonicera japonica* extract in relieving heat stress of dairy cows. *Chinese J. Anim. Nutr.* [Epub ahead of print]

Ge, W., Li, H. B., Fang, H., Yang, B., Huang, W. Z., Xiao, W., et al. (2019). A new dimeric secoiridoids derivative, japonicaside E, from the flower buds of *Lonicera japonica*. *Nat. Prod. Res.* 33, 53–58. doi: 10.1080/14786419.2018.1431641

Ge, L. L., Li, J. M., Wan, H. Q., Zhang, K. D., Wu, W. G., Zou, X. T., et al. (2018). Novel flavonoids from *Lonicera japonica* flower buds and validation of their anti-hepatoma and hepatoprotective activity in vitro studies. *Ind. Crop. Prod.* 125, 114–122. doi: 10.1016/j.indcrop.2018.08.073

Gheisar, M. M., and Kim, I. H. (2018). Phytobiotics in poultry and swine nutrition-a review. *Ital. J. Anim. Sci.* 17, 92–99. doi: 10.1080/1828051X.2017.1350120

Goto, Y., Panea, C., Nakato, G., Cebula, A., Lee, C., Diez, M. G., et al. (2014). Segmented flamentous bacteria antigens presented by intestinal dendritic cells drive mucosal Th17 cell differentiation. *Immunity* 40, 594–607. doi: 10.1016/j.immuni.2014.03.005

Guevarra, R. B., Hong, S. H., Cho, J. H., Kim, B. R., Shin, J., Lee, J. H., et al. (2018). The dynamics of the piglet gut microbiome during the weaning transition in association with health and nutrition. *J. Anim. Sci. Biotechnol.* 9:54. doi: 10.1186/s40104-018-0269-6

Guo, A. L., Chen, L. M., Wang, Y. M., Liu, X. Q., Zhang, Q. W., Gao, H. M., et al. (2014). Influence of sulfur fumigation on the chemical constituents and antioxidant activity of buds of *Lonicera japonica*. *Molecules* 2014, 16640–16655. doi: 10.3390/molecules191016640

Han, M. H., Lee, W. S., Nagappan, A., Hong, S. H., Jung, J. H., Park, C., et al. (2016). Flavonoids isolated from flowers of *Lonicera japonica* Thunb. inhibit inflammatory responses in BV2 microglial cells by suppressing TNF-α and IL-β through PI3K/Akt/NF-kb signaling pathways. *Phytother. Res.* 30, 1824–1832. doi: 10.1002/ptr.5688

Hanczakowska, E., Świątkiewicz, M., and Grela, E. R. (2015). Effect of dietary inclusion of a herbal extract mixture and different oils on pig performance and meat quality. *Meat Sci.* 108, 61–66. doi: 10.1016/j.meatsci.2015.05.020

Hashemi, S. R., and Davoodi, H. (2011). Herbal plants and their derivatives as growth and health promoters in animal nutrition. *Vet. Res. Commun.* 35, 169–180. doi: 10.1007/s11259-010-9458-2

Hayashi, A., Nagao-Kitamoto, H., Kitamoto, S., Kim, C. H., and Kamada, N. (2021). The butyrate-producing bacterium *Clostridium butyricum* suppresses *Clostridioides difficile* infection via neutrophil- and antimicrobial cytokine–dependent but GPR43/109a-independent mechanisms. *J. Immunol.* 206, 1576–1585. doi: 10.4049/jimmunol.2000353

Horai, R., Sen, H. N., and Caspi, R. R. (2017). Commensal microbiota as a potential trigger of autoimmune uveitis. *Expert Review Clin. Immu.* 13, 291–293. doi: 10.1080/1744666X.2017.1288098

Hou, N., Liu, N., Han, J., Yan, Y., and Li, J. (2017). Chlorogenic acid induces reactive oxygen species generation and inhibits the viability of human colon cancer cells. *Anti-Cancer Drugs* 28, 59–65. doi: 10.1097/CAD.0000000000000430

Hsu, H. F., Hsiao, P. C., Kuo, T. C., Chiang, S. T., Chen, S. L., Chiou, S. J., et al. (2016). Antioxidant and anti-inflammatory activities of *Lonicera japonica* Thunb. Var. sempervillosa Hayata flower bud extracts prepared by water, ethanol and supercritical fluid extraction techniques. *Ind. Crop. Prod.* 89, 543–549. doi: 10.1016/j.indcrop.2016.05.010

Hu, R., He, Z., Liu, M., Tan, J., Zhang, H., Hou, D. X., et al. (2020). Dietary protocatechuic acid ameliorates inflammation and up-regulates intestinal tight junction proteins by modulating gut microbiota in LPS-challenged piglets. *J. Anim. Sci. Biotechnol.* 11:92. doi: 10.1186/s40104-020-00492-9

Huang, X., Tang, W., and Long, B. (2019). Effects of honeysuckle extract on rumen fermentation, volatile fatty acid composition and gas production in beef cattle. *Feed* 24, 55–58. doi: 10.15906/j.cnki.cn11-2975/s.20192413

Iwahashi, H., Negoro, Y., Ikeda, A., Morishita, H., and Kido, R. (1986). Inhibition by chlorogenic acid of haematin-catalysed retinoic acid 5,6-epoxidation. *Biochem. J.* 239, 641–646. doi: 10.1042/bj2390641

Jang, A., Liu, X. D., Shin, M. H., Lee, B. D., Lee, S. K., Lee, J. H., et al. (2008). Antioxidative potential of raw breast meat from broiler chicks fed a dietary medicinal herb extract mix. *Poult. Sci.* 87, 2382–2389. doi: 10.3382/ps.2007-00506

Jeong, Y. T., Jeong, S. C., Hwang, J. S., and Kim, J. H. (2015). Modulation effects of sweroside isolated from the *Lonicera japonica* on melanin synthesis. *Chem. Biol. Interact.* 238, 33–39. doi: 10.1016/j.cbi.2015.05.022

Jiang, M., Han, Y. Q., Zhou, M. G., Zhao, H. Z., Xiao, X., Hou, Y. Y., et al. (2014). The screening research of anti-inflammatory bioactive markers from different flowering phases of Flos *Lonicerae japonica*. *PLoS One* 9:e96214. doi: 10.1371/journal.pone.0096214

Kakuda, R., Imai, M., Yaoita, Y., Machida, K., and Kikuchi, M. (2000). Secoiridoid glycosides fromthe flower buds of *Lonicera japonica*. *Phytochemistry* 55, 879–881. doi: 10.1016/s0031-9422(00)00279-x

Kang, O. H., Choi, J. G., Lee, J. H., and Kwon, D. Y. (2010). Luteolin isolated from the flowers of *Lonicera japonica* suppresses inflammatory mediator release by blocking NF-κB and MAPKs activation pathways in HMC-1 cells. *Molecules* 15, 385–398. doi: 10.3390/molecules15010385

Kashiwada, Y., Omichi, Y., Kurimoto, S., Shibata, H., Miyake, Y., Kirimoto, T., et al. (2013). Conjugates of a secoiridoid glucoside with a phenolic glucoside from the flower buds of *Lonicera japonica* Thunb. *Phytochemistry* 96, 423–429. doi: 10.1016/j.phytochem.2013.09.021

Kavoosi, G., Tafsiry, A., Ebdam, A. A., and Rowshan, V. (2013). Evaluation of antioxidant and antimicrobial activities of essential oils from *Carum copticum* seed and Ferula assafoetida latex. *J. Food Sci.* 78, T356–T361. doi: 10.1111/1750-3841.12020

Kawai, H., Kuroyanagi, M., Umehara, K., Ueno, A., and Satake, M. (1988). Studies on the saponins of *Lonicera japonica* Thunb. *Chem. Pharm. Bull.* 36:4769. doi: 10.1248/CPB.36.4769

Kim, S. J., Kim, J. S., Choi, H. S., Kim, Y. M., Hong, S. W., Yeon, S. H., et al. (2015). HS-23, a *Lonicera japonica* extract, reverses sepsis-induced immunosuppression by inhibiting lymphocyte apoptosis. *J. Ethnopharmacol.* 171, 231–239. doi: 10.1016/j.jep.2015.05.049

Kim, E. T., Kim, C. H., Min, K. S., and Lee, S. S. (2012). Effects of plant extracts on microbial population, methane emission and ruminal fermentation characteristics in in vitro. *Asian-Australs. J. Anim. Sci.* 25, 806–811. doi: 10.5713/ajas.2011.11447

Kong, D., Li, Y., Bai, M., Deng, N. Y., Liang, G., and Wu, H. (2017). A comparative study of the dynamic accumulation of polyphenol components and the changes in their antioxidant activities in diploid and tetraploid *Lonicera japonica*. *Plant Physiol. Biochem.* 112, 87–96. doi: 10.1016/j.plaphy.2016.12.027

Kumar, N., Singh, B., Bhandari, P., Gupta, A. P., Uniyal, S. K., and Kaul, V. K. (2005). Biflavonoids from *Lonicera japonica*. *Phytochemistry* 66, 2740–2744. doi: 10.1016/j.phytochem.2005.10.002

Kuroda, M., Shizume, T., and Mimaki, Y. (2014). Triterpene glycosides from the stems and leaves of *Lonicera japonica*. *Chem. Pharm. Bull.* 62, 92–96. doi: 10.1248/cpb.c13-00592

Kwak, W. J., Han, C. K., and Chang, H. W. (2003). Loniceroside C, an anti-inflammatory saponin from *Lonicera japonica*. *Chem. Pharm. Bull.* 51, 333–433. doi: 10.1248/cpb.51.333

Kwon, S. H., Hong, S. I., Jung, Y. H., Kim, M. J., Kim, S. Y., Kim, H. C., et al. (2012). *Lonicera japonica* THUNB. protects 6-hydroxydopamine-induced neurotoxicity by inhibiting activation of MAPKs, PI3K/Akt, and NF-κB in SH-SY5Y cells. *Food Chem. Toxicol.* 50, 797–807. doi: 10.1016/j.fct.2011.12.026

Lee, E. J., Kim, J. S., Kim, H. P., Lee, J. H., and Kang, S. S. (2010). Phenolic constituents from the flower buds of *Lonicera japonica* and their 5-lipoxygenase inhibitory activities. *Food Chem.* 120, 134–139. doi: 10.1016/j.foodchem.2009.09.088

Lee, J., Park, G., and Chang, Y. H. (2019). Nutraceuticals and antioxidant properties of *Lonicera japonica* Thunb. as affected by heating time. *Int. J. Food Prop.* 22, 630–645. doi: 10.1080/10942912.2019.1599389

Lee, S. J., Shin, E. J., Son, K. H., Chang, H. W., Kang, S. S., and Kim, H. P. (1995). Anti-inflammatory activity of the major constituents of *Lonicera japonica*. *Arch. Pharm. Res.* 18, 133–135. doi: 10.1007/BF02979147

Lee, K. H., Whang, K. S., and Rhee, K. H. (2011). Effects of *Lonicera japonica* Thunb. on dextran sulfate sodium-induced experimental colitis in mice. *J. Med. Plant Res.* 5, 5437–5443. doi: 10.1002/cbic.201100354

Lei, X. J., Yun, H. M., and Kim, I. H. (2018). Effects of dietary supplementation of natural and fermented herbs on growth performance, nutrient digestibility, blood parameters, meat quality and fatty acid composition in growing-finishing pigs. *Ital. J. Anim. Sci.* 17, 984–993. doi: 10.1080/1828051X.2018.1429955

Li, J., and Han, Y. Y. (2020). Research advances on non-flower bud parts of *Lonicera japonica* Thunb. *Chin. Arch. Tradit. Chin. Med.* 38, 43–50.

Li, X. Y., He, C., Zhu, Y., and Lu, N. H. (2020). Role of gut microbiota on intestinal barrier function in acute pancreatitis. *World J. Gastroenterol.* 26, 2187–2193. doi: 10.3748/wjg.v26.i18.2187

Li, R., Kuang, X., Wang, W., Wan, C., and Li, W. (2020). Comparison of chemical constitution and bioactivity among different parts of *Lonicera japonica* Thunb. *J. Sci. Food Agric.* 100, 614–622. doi: 10.1002/jsfa.10056

Li, Y., Li, W., Fu, C., Song, Y., and Fu, Q. (2019). *Lonicerae japonica* flos and Lonicerae flos: a systematic review of ethnopharmacology, phytochemistry and pharmacology. *Phytochem. Rev.* 22, 1–61. doi: 10.1007/s11101-019-09655-7

Li, H. B., Yu, Y., Mei, Y. D., Meng, Z. Q., Wang, Z. Z., Huang, W. Z., et al. (2017). A new hetero dimeric terpenoid derivative, japonicaside C, from the flower buds of *Lonicera japonica*. *Nat. Prod. Res.* 31, 143–148. doi: 10.1080/14786419.2016.1219859

Lin, Z. N., Ye, L., Li, Z. W., Huang, X. S., Lu, Z., Yang, Y. Q., et al. (2020). Chinese herb feed additives improved the growth performance, meat quality, and nutrient digestibility parameters of pigs. *Animal Model Exp. Med.* 3, 47–54. doi: 10.1002/ame2.12104

Lin, L. M., Zhang, X. G., Zhu, J. J., Gao, H. M., Wang, Z. M., and Wang, W. H. (2008). Two new triterpenoid saponins from the flowers and buds of *Lonicera japonica*. *J. Asian Nat. Prod. Res.* 10, 925–929. doi: 10.1080/10286020802217366

Liu, P., Bai, X., Zhang, T., Zhou, L., Li, J., and Zhang, L. (2019). The protective effect of *Lonicera japonica* polysaccharide on mice with depression by inhibiting NLRP3 inflammasome. *Ann. Transl. Med.* 7:811. doi: 10.21037/atm.2019.12.64

Liu, Z. X., Cheng, Z. Y., He, Q. J., Lin, B., Gao, P. Y., Li, L. Z., et al. (2016). Secondary metabolites from the flower buds of *Lonicera japonica* and their in vitro anti-diabetic activities. *Fitoterapia* 110, 44–51. doi: 10.1016/j.fitote.2016.02.011

Liu, W., and Kim, I. H. (2017). Influence of extract mixture from *Scutellaria baicalensis* and *Lonicera japonica* on egg production, nutrient digestibility, blood profiles and egg quality in laying hens reared in hot humid season. *Anim. Nutr. Feed. Technol.* 17, 137–146. doi: 10.5958/0974-181X.2017.00014.2

Liu, Z. X., Liu, C. T., Liu, Q. B., Ren, J., and Song, S. J. (2015). Iridoid glycosides from the flower buds of *Lonicera japonica* and their nitric oxide production and α-glucosidase inhibitory activities. *J. Funct. Foods* 18, 512–519. doi: 10.1016/j.jff.2015.08.017

Liu, W., Pi, S. H., and Kim, I. H. (2016). Effects of *Scutellaria baicalensis* and *Lonicera japonica* extract mixture supplementation on growth performance, nutrient digestibility, blood profiles and meat quality in finishing pigs. *Ital. J. Anim. Sci.* 15, 446–452. doi: 10.1080/1828051x.2016.1202736

Liu, T., Yang, J., Liu, S., Zhao, Y., Zhou, J., Jin, Y., et al. (2020). Regulation of chlorogenic acid, flavonoid, and iridoid biosynthesis by histone H3K4 and H3K9 methylation in *Lonicera japonica*. *Mol. Biol. Rep.* 47, 9301–9311. doi: 10.1007/s11033-020-05990-7

Liu, S., You, L., Zhao, Y., and Chang, X. (2018). Wild *Lonicera caerulea* berry polyphenol extract reduces cholesterol accumulation and enhances antioxidant capacity in vitro and in vivo. *Food Res. Int.* 107, 73–83. doi: 10.1016/j.foodres.2018.02.016

Long, B., Li, Z., Dong, G., Wang, Q., and Yu, Z. (2018). Effects of honeysuckle extract on performance, egg quality, lipid metabolism and yolk cholesterol content of laying hens. *Chinese J. Anim. Nutr.* 30, 212–218. doi: 10.3969/j.issn.1006-267x.2018.01.026

Looft, T., Allen, H. K., Cantarel, B. L., Levine, U. Y., Bayles, D. O., Alt, D. P., et al. (2014). Bacteria, phages and pigs: the effects of in-feed antibiotics on the microbiome at different gut locations. *ISME J.* 8:1566. doi: 10.1038/ismej.2014.12

Lum, H., and Roebuck, K. A. (2001). Oxidant stress and endothelial cell dysfunction. *Am. J. Phys. Cell Physiol.* 280, C719–C741. doi: 10.1152/ajpcell.2001.280.4.C719

Luo, L., Zhang, B., Ma, L., Fan, J., Zhu, W., Guan, N., et al. (2018). Antioxidant activity in vitro and protective effect of flavonoids from *Lonicera japonica* Thunb. leaves on H_2O_2-induced toxicity in RAW264.7 cells. *Food Sci.* 39, 139–145. doi: 10.7506/spkx1002-6630-201811022

Ma, F. T., Shan, Q., Jin, Y. H., Gao, D., Li, H. Y., Chang, M. N., et al. (2020a). Effect of *Lonicera japonica* extract on lactation performance, antioxidant status, and endocrine and immune function in heat-stressed mid-lactation dairy cows. *J. Dairy Sci.* 103, 10074–10082. doi: 10.3168/jds.2020-18504

Ma, F. T., Shan, Q., Jin, Y. H., Li, H. Y., Gao, D., and Sun, P. (2020b). Effects of *Lonicera japonica* extract on performance, serum biochemical indexes and immune function of heat-stressed dairy cows. *Chinese J. Anim. Nutr.* 32, 2209–2217. doi: 10.3969/j.issn.1006-267x.2020.05.030

Makki, K., Deehan, E. C., Walter, J., and Bäckhed, F. (2018). The impact of dietary fiber on gut microbiota in host health and disease. *Cell Host Microbe* 23, 705–715. doi: 10.1016/j.chom.2018.05.012

Meng, X. L., Zhu, Z. X., Lu, R. H., Li, S., Hu, W. P., Qin, C. B., et al. (2019). Regulation of growth performance and lipid metabolism in juvenile grass carp (*Ctenopharyngodon idella*) with honeysuckle (*Lonicera japonica*) extract. *Fish Physiol. Biochem.* 45, 1563–1573. doi: 10.1007/s10695-019-00644-3

Miao, H., Zhang, Y., Huang, Z., Lu, B., and Ji, L. (2019). *Lonicera japonica* attenuates carbon tetrachloride-induced liver fibrosis in mice: molecular mechanisms of action. *Am. J. Chin. Med.* 47, 351–367. doi: 10.1142/S0192415X19500174

Minami, M., and Makino, T. (2020). Effects of *Lonicera japonica* flower bud extract on citrobacter rodentium-induced digestive tract infection. *Medicine* 7:52. doi: 10.3390/medicines7090052

Miner-Williams, W. M., and Moughan, P. J. (2016). Intestinal barrier dysfunction: implications for chronic inflammatory conditions of the bowel. *Nutr. Res. Rev.* 29, 40–59. doi: 10.1017/S0954422416000019

Mullineaux-Sanders, C., Sanchez-Garrido, J., Hopkins, E. G. D., Shenoy, A. R., Barry, R., and Frankel, G. (2019). Citrobacter rodentium–host–microbiota interactions: immunity, bioenergetics and metabolism. *Nat. Rev. Microbiol.* 17, 701–705. doi: 10.1038/s41579-019-0252-z

Müştak, H. K., Torun, E., Özen, D., Yücel, G., Akan, M., and Diker, K. S. (2015). Effect of *Lonicera japonica* extract on *mycoplasma gallisepticum* in naturally infected broiler flocks. *Br. Poult. Sci.* 56, 299–303. doi: 10.1080/00071668.2015.1022711

Navarro-Yepes, J., Burns, M., Anandhan, A., Khalimonchuk, O., del Razo, L. M., Quintanilla-Vega, B., et al. (2014). Oxidative stress, redox signaling, and autophagy: cell death versus survival. *Antioxid. Redox Signal.* 21, 66–85. doi: 10.1089/ars.2014.5837

Park, J. H., Kang, S. N., Chu, G. M., and Jin, S. K. (2014). Growth performance, blood cell profiles, and meat quality properties of broilers fed with *Saposhnikovia divaricata*, *Lonicera japonica*, and *Chelidonium majus extracts*. *Livest. Sci.* 165, 87–94. doi: 10.1016/j.livsci.2014.04.014

Park, K. I., Kang, S. R., Park, H. S., Lee, D. H., Nagappan, A., Kim, J. A., et al. (2012). Regulation of proinflammatory mediators via NF-κB and p38 MAPK-dependent mechanisms in RAW 264.7 macrophages by polyphenol components isolated from Korea *Lonicera japonica* THUNB. *Evid. Based Complement. Alternat. Med.* 2012:828521. doi: 10.1155/2012/828521

Peng, P., Deng, D., Chen, S. J., Li, C. L., Luo, J., Romeo, A., et al. (2020). The effects of dietary porous zinc oxide supplementation on growth performance, inflammatory cytokines and tight junction's gene expression

in early-weaned piglets. *J. Nutr. Sci. Vitaminol.* 66, 311–318. doi: 10.3177/jnsv.66.311

Peng, L. Y., Mei, S. X., Jiang, B., Zhou, H., and Sun, H. D. (2000). Constituents from *Lonicera japonica*. *Fitoterapia* 71, 713–715. doi: 10.1016/S0367-326X(00)00212-4

Qamar, A., Waheed, J., Hamza, A., Mohyuddin, S. G., Lu, Z., Namula, Z., et al. (2021). The role of intestinal microbiota in chicken health, intestinal physiology and immunity. *J. Anim. Plant Sci.* 31, 342–351. doi: 10.36899/JAPS.2021.2.0221

Qi, L. W., Chen, C. Y., and Li, P. (2009). Structural characterization and identification of iridoid glycosides, saponins, phenolic acids and flavonoids in *Flos Lonicerae Japonica* by a fast liquid chromatography method with diode-array detection and time-of-flight mass spectrometry. *Rapid Commun. Mass Spectrom.* 23, 3227–3242. doi: 10.1002/rcm.4245

Qiu, S., Bai, M., Zhao, P., Liu, Z. X., Huang, X. X., and Song, S. J. (2021). Phytochemical and network-based chemotaxonomic study of *Lonicera japonica* thunb. *Biochem. Syst. Ecol.* 94:104210. doi: 10.1016/j.bse.2020.104210

Rauter, A. P., Ennis, M., Hellwich, K. H., Herold, B. J., Horton, D., Moss, G. P., et al. (2018). Nomenclature of flavonoids (IUPAC recommendations 2017). *Pure Appl. Chem.* 90, 1429–1486. doi: 10.1515/pac-2013-0919

Rhee, K. H., and Lee, K. H. (2011). Antimicrobial effects of *Lonicera japonica* against gram positive and gram negative anaerobic bacteria. *Nat. Prod. Sci.* 17, 23–25.

Salerno-Goncalves, R., Safavie, F., Fasano, A., and Sztein, M. B. (2016). Free and complexed-secretory immunoglobulin A triggers distinct intestinal epithelial cell responses. *Clin. Exp. Immunol.* 185, 338–347. doi: 10.1111/cei.12801

Saracila, M., Panaite, T. D., Papuc, C. P., and Criste, R. D. (2021). Heat stress in broiler chickens and the effect of dietary polyphenols, with special reference to willow (*Salix* spp.) bark supplements-a review. *Antioxidants* 10:686. doi: 10.3390/antiox10050686

Seo, O. N., Kim, G. S., Park, S., Lee, J. H., Kim, Y. H., Lee, W. S., et al. (2012). Determination of polyphenol components of *Lonicera japonica* thunb. Using liquid chromatography–tandem mass spectrometry: contribution to the overall antioxidant activity. *Food Chem.* 134, 572–577. doi: 10.1016/j.foodchem.2012.02.124

Shang, X., Pan, H., Li, M., Miao, X., and Ding, H. (2011). *Lonicera japonica* Thunb. ethnopharmacology, phytochemistry and pharmacology of an important traditional Chinese medicine. *J. Ethnopharmacol.* 138, 1–21. doi: 10.1016/j.jep.2011.08.016

Shi, Z., Liu, Z., Liu, C., Wu, M., Su, H., Ma, X., et al. (2016). Spectrum-effect relationships between chemical fingerprints and antibacterial effects of *Lonicerae Japonica* Flos and *Lonicerae* Flos base on UPLC and microcalorimetry. *Front. Pharmacol.* 7:12. doi: 10.3389/fphar.2016.00012

Sicard, J. F., Le Bihan, G., Vogeleer, P., Jacques, M., and Harel, J. (2017). Interactions of intestinal bacteria with components of the intestinal mucus. *Front. Cell. Infect. Microbiol.* 7:387. doi: 10.3389/fcimb.2017.00387

Son, K. H., Jung, K. Y., Chang, H. W., Kim, H. P., and Kang, S. S. (1994). Triterpenoid saponins from the aerial parts of *Lonicera japonica*. *Phytochemistry* 35, 1005–1008. doi: 10.1016/S0031-9422(00)90656-3

Song, X., Fu, Y., Huang, T., Qu, M., Chen, Y., Yang, S., et al. (2015). Effects of honeysuckle extract on antioxidant function and skeletal muscle morphology of beef cattle under hot environment. *Chinese J. Anim. Nutr.* 27, 3534–3540. doi: 10.3969/j.issn.1006-267x.2015.11.026

Song, W., Li, S., Wang, S., Wu, Y., Zi, J., Gan, M., et al. (2008). Pyridinium alkaloid-coupled secoiridoids from the flower buds of *Lonicera japonica*. *J. Nat. Prod.* 71, 922–925. doi: 10.1021/np800040k

Stromberg, Z. R., Johnson, J. R., Fairbrother, J. M., Kilbourne, J., Van Goor, A., Curtiss Rd, R., et al. (2017). Evaluation of *Escherichia coli* isolates from healthy chickens to determine their potential risk to poultry and human health. *PLoS One* 12:e0180599. doi: 10.1371/journal.pone.0180599

Su, X., Zhu, Z. H., Zhang, L., Wang, Q., Xu, M. M., Lu, C., et al. (2021). Anti-inflammatory property and functional substances of *Lonicerae Japonica* caulis. *J. Ethnopharmacol.* 267:113502. doi: 10.1016/j.jep.2020.113502

Surin, S., Surayot, U., Seesuriyachan, P., You, S. G., and Phimolsiripol, Y. (2018). Antioxidant and immunomodulatory activities of sulphated polysaccharides from purple glutinous rice bran (*Oryza sativa* L.). *Int. J. Food Sci. Technol.* 53, 994–1004. doi: 10.1111/ijfs.13674

Tan, C., Ling, Z., Huang, Y., Cao, Y., Liu, Q., Cai, T., et al. (2015). Dysbiosis of intestinal microbiota associated with inflammation involved in the progression of acute pancreatitis. *Pancreas* 44, 868–875. doi: 10.1097/MPA.0000000000000355

Tang, X. P., Fang, R. J., Pan, G. C., and Xiong, K. N. (2019). Acute effect of epidermal growth factor on phosphate diffusion across intestinal mucosa of hens using the ussing chamber system. *Pak. J. Zool.* 51, 2209–2216. doi: 10.17582/journal.pjz/2019.51.6.2209.2216

Tang, Z., Jiang, L., Yang, L., Sun, F., and Xiong, B. (2018a). Effects of honeysuckle extract on rumen in vitro fermentation parameters and gas production. *Chinese J. Anim. Nutr.* 30, 790–796. doi: 10.3969/j/issn.1006-267x.2018.02.045

Tang, X. P., Liu, X. G., and Liu, H. (2021). Mechanisms of epidermal growth factor effect on animal intestinal phosphate absorption: a review. *Front. Vet. Sci.* 8:670140. doi: 10.3389/fvets.2021.670140

Tang, X. P., Liu, B., Wang, X. R., Yu, Q. F., and Fang, R. J. (2018b). Epidermal growth factor, through alleviating oxidative stress, protect IPEC-J2 cells from lipopolysaccharides-induced apoptosis. *Int. J. Mol. Sci.* 19:848. doi: 10.3390/ijms19030848

Tang, X. P., Liu, H., Yang, S. F., Li, Z. H., Zhong, J. F., and Fang, R. J. (2016). Epidermal growth factor and intestinal barrier function. *Mediat. Inflamm.* 2016:1927348. doi: 10.1155/2016/1927348

Tang, X. P., and Xiong, K. N. (2021). Effects of epidermal growth factor on glutamine and glucose absorption by IPEC-J2 cells challenged by lipopolysaccharide using the Ussing chamber system. *Pak. J. Zool.* 53, 417–422. doi: 10.17582/journal.pjz/20200117080156

Tzeng, T. F., Liou, S. S., Chang, C. J., and Liu, I. M. (2014). The ethanol extract of *Lonicera japonica* (Japanese honeysuckle) attenuates diabetic nephropathy by inhibiting p-38 MAPK activity in streptozotocin-induced diabetic rats. *Planta Med.* 80, 121–129. doi: 10.1055/s-0033-1360196

Villena, J., Chiba, E., Vizoso-Pinto, M. G., Tomosada, Y., Takahashi, T., Ishizuka, T., et al. (2014). Immunobiotic *lactobacillus rhamnosus* strains differentially modulate antiviral immune response in porcine intestinal epithelial and antigen presenting cells. *BMC Microbiol.* 14:126. doi: 10.1186/1471-2180-14-126

Vukovic, N., Kacaniova, M., Hleba, L., and Sukdolak, S. (2012). Chemical composition of the essential oils from the flower, leaf and stem of *Lonicera japonica*. *Nat. Prod. Commun.* 7, 641–644.

Wan, H., Ge, L., Li, J., Zhang, K., Wu, W., Peng, S., et al. (2019). Effects of a novel biflavonoid of *Lonicera japonica* flower buds on modulating apoptosis under different oxidative conditions in hepatoma cells. *Phytomedicine* 57, 282–291. doi: 10.1016/j.phymed.2018.12.044

Wan, M. L. Y., Ling, K. H., El-Nezami, H., and Wang, M. F. (2019). Influence of functional food components on gut health. *Crit. Rev. Food Sci. Nutr.* 59, 1927–1936. doi: 10.1080/10408398.2018.1433629

Wang, J. H., Bose, S., Kim, G. C., Hong, S. U., Kim, J. H., Kim, J. E., et al. (2014). *Flos Lonicera* ameliorates obesity and associated endotoxemia in rats through modulation of gut permeability and intestinal microbiota. *PLoS One* 9:e86117. doi: 10.3389/fmicb.2018.01953

Wang, Y., Chen, Y., Zhang, X., Lu, Y., and Chen, H. (2020). New insights in intestinal oxidative stress damage and the health intervention effects of nutrients: a review. *J. Funct. Foods* 75:104248. doi: 10.1016/j.jff.2020.104248

Wang, M., Huang, H., Hu, Y., Liu, Y., Zeng, X., Zhuang, Y., et al. (2020). Effects of dietary supplementation with herbal extract mixture on growth performance, organ weight and intestinal morphology in weaning piglets. *J. Anim. Physiol. Anim. Nutr.* 104, 1462–1470. doi: 10.1111/jpn.13422

Wang, J., Ji, H., Wang, S., Liu, H., Zhang, W., Zhang, D., et al. (2018). Probiotic *lactobacillus plantarum* promotes intestinal barrier function by strengthening the epithelium and modulating gut microbiota. *Front. Microbiol.* 9:1953. doi: 10.3389/fmicb.2018.01953

Wang, L., Jiang, Q., Hu, J., Zhang, Y., and Li, J. (2016). Research progress on chemical constituents of *Lonicerae japonica* flos. *Biomed. Res. Int.* 2016:8968940. doi: 10.1155/2016/8968940

Wang, H., Li, Y., Wang, S., Kong, D., Sahu, S. K., Bai, M., et al. (2020). Comparative transcriptomic analyses of chlorogenic acid and luteolosides biosynthesis pathways at different flowering stages of diploid and tetraploid *Lonicera japonica*. *Peer J.* 8:e8690. doi: 10.7717/peerj.8690

Wang, F., Miao, M., Xia, H., Yang, L. G., Wang, S. K., and Sun, G. J. (2016). Antioxidant activities of aqueous extracts from 12 Chinese edible flowers in vitro and in vivo. *Food Nutr. Res.* 61:1265324. doi: 10.1080/16546628.2017.1265324

Wang, C., Wang, G., Liu, H., and Hou, Y. L. (2016). Protective effect of bioactive compounds from *Lonicera japonica* Thunb. against H_2O_2-induced cytotoxicity using neonatal rat cardiomyocytes. *Iran. J. Basic Med. Sci.* 19, 97–105.

Wang, D. Y., Zhao, X. M., and Liu, Y. L. (2017). Hypoglycemic and hypolipidemic effects of a polysaccharide from flower buds of *Lonicera japonica* in streptozotocin-induced diabetic rats. *Int. J. Biol. Macromol.* 102, 396–404. doi: 10.1016/j.ijbiomac.2017.04.056

Windisch, W., Schedle, K., Plitzner, C., and Kroismayr, A. (2008). Use of phytogenic products as feed additives for swine and poultry. *J. Anim. Sci.* 86, E140–E148. doi: 10.2527/jas.2007-0459

Wu, S., Yano, S., Chen, J., Hisanaga, A., Sakao, K., He, X., et al. (2017). Polyphenols from *Lonicera caerulea* L. berry inhibit LPS-induced inflammation through dual modulation of inflammatory and antioxidant mediators. *J. Agric. Food Chem.* 65, 5133–5141. doi: 10.1021/acs.jafc.7b01599

Xiao, L., Liang, S., Ge, L., Wan, H., Wu, W., Fei, J., et al. (2020). 4,5-di-O-caffeoylquinic acid methyl ester isolated from *Lonicera japonica* Thunb. targets the Keap1/Nrf2 pathway to attenuate H2O2-induced liver oxidative damage in HepG2 cells. *Phytomedicine* 70:153219. doi: 10.1016/j.phymed.2020.153219

Xiong, J., Li, S., Wang, W., Hong, Y., Tang, K., and Luo, Q. (2013). Screening and identification of the antibacterial bioactive compounds from *Lonicera japonica* Thunb. leaves. *Food Chem.* 138, 327–333. doi: 10.1016/j.foodchem.2012.10.127

Xu, X., Yan, G., Chang, J., Wang, P., Yin, Q., Liu, C., et al. (2020). Astilbin ameliorates deoxynivalenol-induced oxidative stress and apoptosis in intestinal porcine epithelial cells (IPEC-J2). *J. Appl. Toxicol.* 40, 1362–1372. doi: 10.1002/jat.3989

Yan, L., Xie, Y., Wang, Y., Zhu, J., Li, M., Liu, X., et al. (2020). Variation in contents of active components and antibacterial activity in different parts of *Lonicera japonica* thunb. *Asian Biomed.* 14, 19–26. doi: 10.1515/abm-2020-0004

Yan, Z., Zhong, Y., Duan, Y., Chen, Q., and Li, F. (2020). Antioxidant mechanism of tea polyphenols and its impact on health benefits. *Anim. Nutr.* 6, 115–123. doi: 10.1016/j.aninu.2020.01.001

Yang, L., Aguilar, Z. P., Qu, F., Xu, H., Xu, H., and Wei, H. (2016). Enhanced antimicrobial activity of silver nanoparticles-*Lonicera japonica* Thunb combo. *IET Nanobiotechnol.* 10, 28–32. doi: 10.1049/iet-nbt.2015.0027

Yang, R., Hao, H., Li, J., Xuan, J., Xia, M. F., and Zhang, Y. Q. (2020). Three new secoiridoid glycosides from the flower buds of *Lonicera japonica*. *Chin. J. Nat. Med.* 18, 70–74. doi: 10.1016/S1875-5364(20)30006-6

Yang, J., Li, Y. C., Zhou, X. R., Xu, X. J., Fu, Q. Y., and Liu, C. Z. (2018). Two thymol derivatives from the flower buds of *Lonicera japonica* and their antibacterial activity. *Nat. Prod. Res.* 32, 2238–2243. doi: 10.1080/14786419.2017.1371153

Yang, F., Wang, A., Zeng, X., Hou, C., Liu, H., and Qiao, S. (2015). *Lactobacillus reuteri* I5007 modulates tight junction protein expression in IPEC-J2 cells with LPS stimulation and in newborn piglets under normal conditions. *BMC Microbiol.* 15:32. doi: 10.1186/s12866-015-0372-1

Yang, X., Zhang, F., Xiang, F., Dai, Z., Yu, C., and Li, S. (2020). Honeysuckle extract promotes host health by improving intestinal microbes and enhancing intestinal mucosal immunity. *Genom. Appl. Biol.* 39, 1257–1263. doi: 10.13417/j.gab.039.001257

Yejun, L., Su Kyoung, L., Shin Ja, L., Jong-Su, E., and Sung Sill, L. (2019). Effects of *Lonicera japonica* extract supplementation on in vitro ruminal fermentation, methane emission, and microbial population. *Anim. Sci. J.* 90, 1170–1176. doi: 10.1111/asj.13259

Yin, J., Wu, M. M., Xiao, H., Ren, W. K., Duan, J. L., Yang, G., et al. (2014). Development of an antioxidant system after early weaning in piglets. *J. Anim. Sci.* 92, 612–619. doi: 10.2527/jas.2013-6986

Yitbarek, A., Astill, J., Hodgins, D. C., Parkinson, J., Nagy, É., and Sharif, S. (2019). Commensal gut microbiota can modulate adaptive immune responses in chickens vaccinated with whole inactivated avian influenza virus subtype H9N2. *Vaccine* 37, 6640–6647. doi: 10.1016/j.vaccine.2019.09.046

Yoo, H. J., Kang, H. J., Song, Y. S., Park, E. H., and Lim, C. J. (2008). Anti-angiogenic, antinociceptive and anti-inflammatory activities of *Lonicera japonica* extract. *J. Pharm. Pharmacol.* 60, 779–786. doi: 10.1211/jpp.60.6.0014

Yu, Y., Jiang, Z., Song, W., Yang, Y., Li, Y., Jiang, J., et al. (2015). Glucosylated caffeoylquinic acid derivatives from the flower buds of *Lonicera japonica*. *Acta Pharm. Sin. B* 5, 210–214. doi: 10.1016/j.apsb.2015.01.012

Yu, Y., Song, W., Zhu, C., Lin, S., Zhao, F., Wu, X., et al. (2011). Homosecoiridoids from the flower buds of *Lonicera japonica*. *J. Nat. Prod.* 74, 2151–2160. doi: 10.1021/np2004566

Yu, Y., Zhu, C., Wang, S., Song, W., Yang, Y., and Shi, J. (2013). Homosecoiridoid alkaloids with amino acid units from the flower buds of *Lonicera japonica*. *J. Nat. Prod.* 76, 2226–2233. doi: 10.1021/np4005773

Zhang, T., Liu, H., Bai, X., Liu, P., Yang, Y., Huang, J., et al. (2020). Fractionation and antioxidant activities of the water-soluble polysaccharides from *Lonicera japonica* Thunb. *Int. J. Biol. Macromol.* 151, 1058–1066. doi: 10.1016/j.ijbiomac.2019.10.147

Zhang, X., Zhao, Q., Ci, X., Chen, S., Xie, Z., Li, H., et al. (2020). Evaluation of the efficacy of chlorogenic acid in reducing small intestine injury, oxidative stress, and inflammation in chickens challenged with *Clostridium perfringens* type A. *Poult. Sci.* 99, 6606–6618. doi: 10.1016/j.psj.2020.09.082

Zhao, Y., Dou, D., Guo, Y., Qi, Y., Li, J., and Jia, D. (2018). Comparison of the trace elements and active components of *Lonicera japonica* flos and *Lonicera flos* using ICP-MS and HPLC-PDA. *Biol. Trace Elem. Res.* 183, 379–388. doi: 10.1007/s12011-017-1138-4

Zhao, Y., Tang, Z., Nan, X., Sun, F., Jiang, L., and Xiong, B. (2020). Effects of *Lonicera japonica* extract on performance, blood biomarkers of inflammation and oxidative stress during perinatal period in dairy cows. *Asian-Australas. J. Anim. Sci.* 33, 1096–1102. doi: 10.5713/ajas.19.0388

Zheng, Z. F., Zhang, Q. J., Chen, R. Y., and Yu, D. Q. (2012). Four new N-contained iridoid glycosides from flower buds of *Lonicera japonica*. *J. Asian Nat. Prod. Res.* 14, 729–737. doi: 10.1080/10286020.2012.688038

Zhou, X., Dong, Q., Kan, X., Peng, L., Xu, X., Fang, Y., et al. (2018a). Immunomodulatory activity of a novel polysaccharide from *Lonicera japonica* in immunosuppressed mice induced by cyclophosphamide. *PLoS One* 13:e0204152. doi: 10.1371/journal.pone.0204152

Zhou, X., He, G., Ma, J., Tang, M., Tian, G., Gong, X., et al. (2020). Protective effect of a novel polysaccharide from *Lonicera japonica* on cardiomyocytes of mice injured by hydrogen peroxide. *Biomed. Res. Int.* 2020:5279193. doi: 10.1155/2020/5279193

Zhou, X., Lu, Q., Kang, X., Tian, G., Ming, D., and Yang, J. (2021). Protective role of a new polysaccharide extracted from *Lonicera japonica* Thunb in mice with ulcerative colitis induced by dextran sulphate sodium. *Biomed. Res. Int.* 2021:8878633. doi: 10.1155/2021/8878633

Zhou, X., Zhang, Y., Wu, X., Wan, D., and Yin, Y. (2018b). Effects of dietary serine supplementation on intestinal integrity, inflammation and oxidative status in early-weaned piglets. *Cell. Physiol. Biochem.* 48, 993–1002. doi: 10.1159/000491967

Zhu, H., Wang, H., Wang, S., Tu, Z., Zhang, L., Wang, X., et al. (2018). Flaxeed oil attenuates intestinal damage and inflammation by regulating necroptosis and TLR4/NOD signaling pathways following lipopolysaccharide challenge in a piglet model. *Mol. Nutr. Food Res.* 62:e1700814. doi: 10.1002/mnfr.201700814

Zhu, L., Zhang, D., Zhu, H., Zhu, J., Weng, S., Dong, L., et al. (2018). Berberine treatment increases Akkermansia in the gut and improves high-fat diet-induced atherosclerosis in Apoe−/− mice. *Atherosclerosis* 268, 117–126. doi: 10.1016/j.atherosclerosis.2017.11.023

Conflict of Interest: The authors declare that the research was conducted in the absence of any commercial or financial relationships that could be construed as a potential conflict of interest.

Publisher's Note: All claims expressed in this article are solely those of the authors and do not necessarily represent those of their affiliated organizations, or those of the publisher, the editors and the reviewers. Any product that may be evaluated in this article, or claim that may be made by its manufacturer, is not guaranteed or endorsed by the publisher.

frontiers in Microbiology

ORIGINAL RESEARCH
published: 16 August 2021
doi: 10.3389/fmicb.2021.736997

HMB Improves Lipid Metabolism of Bama Xiang Mini-Pigs via Modulating the *Bacteroidetes*-Acetic Acid-AMPKα Axis

Jie Zheng[1,2†], Changbing Zheng[1†], Bo Song[1,2], Qiuping Guo[1], Yinzhao Zhong[1], Shiyu Zhang[1], Lingyu Zhang[1,2], Geyan Duan[1,2], Fengna Li[1] and Yehui Duan[1]*

[1] CAS Key Laboratory of Agro-Ecological Processes in Subtropical Region, Hunan Provincial Key Laboratory of Animal Nutritional Physiology and Metabolic Process, National Engineering Laboratory for Pollution Control and Waste Utilization in Livestock and Poultry Production, Institute of Subtropical Agriculture, Chinese Academy of Sciences, Changsha, China, [2] College of Advanced Agricultural Sciences, University of Chinese Academy of Sciences, Beijing, China

OPEN ACCESS

Edited by:
Jia Yin,
Hunan Normal University, China

Reviewed by:
Shuai Zhang,
China Agricultural University, China
Tarique Hussain,
Nuclear Institute for Agriculture and Biology, Pakistan
Miao Yu,
Institute of Animal Science, Guangdong Academy of Agricultural Sciences, China

***Correspondence:**
Yehui Duan
duanyehui@isa.ac.cn

[†] These authors have contributed equally to this work

Specialty section:
This article was submitted to Microbial Symbioses, a section of the journal Frontiers in Microbiology

Received: 06 July 2021
Accepted: 28 July 2021
Published: 16 August 2021

Citation:
Zheng J, Zheng C, Song B, Guo Q, Zhong Y, Zhang S, Zhang L, Duan G, Li F and Duan Y (2021) HMB Improves Lipid Metabolism of Bama Xiang Mini-Pigs via Modulating the Bacteroidetes-Acetic Acid-AMPKα Axis. Front. Microbiol. 12:736997. doi: 10.3389/fmicb.2021.736997

Here, we used Bama Xiang mini-pigs to explore the effects of different dietary β-hydroxy-β-methylbutyrate (HMB) levels (0, 0.13, 0.64 or 1.28%) on lipid metabolism of adipose tissue. Results showed that HMB decreased the fat percentage of pigs (linearly, $P < 0.05$), and the lowest value was observed in the 0.13% HMB group. Moreover, the colonic acetic acid concentration and the relative *Bacteroidetes* abundance were increased in response to HMB supplementation ($P < 0.05$). Correlation analysis identified a positive correlation between the relative *Bacteroidetes* abundance and acetic acid production, and a negative correlation between fat percentage and the relative *Bacteroidetes* abundance or acetic acid production. HMB also upregulated the phosphorylation (p) of AMPKα, Sirt1, and FoxO1, and downregulated the p-mTOR expression. Collectively, these findings indicate that reduced fat percentage in Bama Xiang mini-pigs could be induced by HMB supplementation and the mechanism might be associated with the *Bacteroidetes*-acetic acid-AMPKα axis.

Keywords: β-hydroxy-β-methylbutyrate, lipid metabolism, gut microbiota, acetic acid, AMPKα, Bama Xiang mini-pigs

INTRODUCTION

Obesity has increased at an alarming rate over the past years, subsequently resulting in diabetes and other metabolic diseases (Duan Y.H. et al., 2017; Duan Y. et al., 2017). There is a wealth of data indicating that an effective strategy to combat obesity is to reduce the weight of adipose tissue (Yao et al., 2016; Yin et al., 2018). Notably, there are regional differences in the sensitivity of adipose tissue depots in response to dietary manipulations and the most sensitive depot is the subcutaneous white adipose tissue (WAT) (Fickova et al., 1998; Gaiva et al., 2001; Rodríguez et al., 2002). Moreover, subcutaneous WAT accounts for ∼85% total fat mass, and a lower subcutaneous

Abbreviations: AMPKα, AMP-activated protein kinase α; ASA, abdominal subcutaneous adipose tissue; DSA, dorsal subcutaneous adipose tissue; FoxO1, forkhead box O 1; HMB, β-hydroxy-β-methylbutyrate; mTOR, mammalian target of rapamycin; MUFA, monounsaturated fatty acid; PUFA, polyunsaturated fatty acid; SCFA, short chain fatty acid; SFA, saturated fatty acid; Sirt1, silent information regulator 2 related enzyme 1.

WAT is more protective compared to visceral WAT (Booth et al., 2018). Therefore, subcutaneous WAT was a focus of this study, with the goal to understand dietary nutrients to combat obesity. Evidence in the literature has demonstrated that WAT has a variety of well-documented functions, including serving as an energy storage site, regulating glucose and lipid homeostasis, and producing adipokines (Cummins et al., 2014). The two primary metabolic activities of WAT (lipogenesis and lipolysis) cooperate to maintain the relative constancy of body fat under normal conditions (Proença et al., 2014). In humans, excessive body fat contributes to obesity and diabetes (Zheng J. et al., 2021). In the meat industry, the increased WAT mass has a deleterious effect on production efficiency and meat quality (Lebret and Mourot, 1998). Therefore, maintaining an appropriate WAT mass is an important objective pursuit of animal production and human health.

Leucine functions as a direct-acting nutrient signal in WAT to affect lipid metabolism, thus favoring adiposity reduction (Yao et al., 2016; Zhang et al., 2020). Despite these positive outcomes, multiple lines of evidence have pointed out that elevated levels of circulating leucine may precede or coincide with insulin resistance and cardiovascular dysfunction, thus seriously threatening human health (Felig et al., 1969; Yang et al., 2015). In explanation of these observations, previous studies have hypothesized that the ability of adipocytes to degrade or oxidize leucine is lost (Gannon et al., 2018). Interestingly, β-hydroxy-β-methylbutyrate (HMB), a metabolite of leucine, has been reported to share similar regulatory effects on lipid metabolism with leucine (Duan et al., 2018). More importantly, HMB cannot be reversibly converted to leucine (Nissen and Abumrad, 1997). Of note, a growing number of evidence has demonstrated convincingly that dietary HMB supplementation is an effective way to regulate lipid metabolism. For example, HMB treatment (0.62%, 45 days) gave rise to fat loss in growing pigs (Duan et al., 2018). Other experiments conducted in rodent models also confirmed that animals having access to HMB showed a decline in fat mass (Wilson et al., 2012; Park et al., 2013). Thus, we shifted the focus from leucine to HMB, which may provide an alternative for safe and efficacious regulation of lipid metabolism.

Alterations in the gut-microbiota community have been reported to be associated with the occurrence and development of obesity (Marchesi et al., 2016; Wang Z. et al., 2018). The metabolic activity of the gut microbiota can be linked to host body energy homoeostasis by short-chain fatty acids (SCFAs), which are produced by gut microbiota catabolizing dietary fibers (Topping and Clifton, 2001). There is compelling evidence that nutrients can attenuate obesity by reprogramming gut microbiota (Xu et al., 2017; Yin et al., 2018; Zhang et al., 2019; Wang et al., 2020; Zhong et al., 2020). Using a rodent model, we also found that HMB could mitigate lipid metabolism disorders by reprogramming gut microbiota, as manifested by the increased ratio of *Bacteroidetes* to *Firmicutes* and elevated *Bacteroidetes*-produced propionic acid (Duan et al., 2019). However, the literature on the possible relationship between HMB treatment and gut microbiota is dominated by studies in rodents, whether the beneficial effects of HMB in larger mammals including pigs are mediated by gut microbiota requires further interrogation.

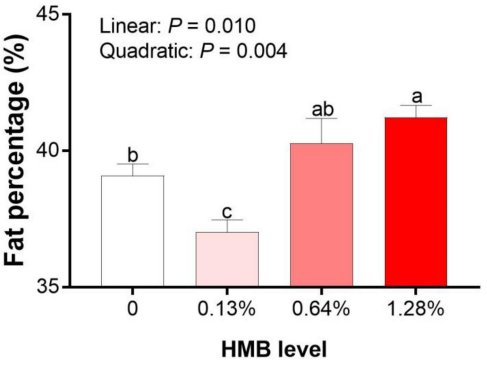

FIGURE 1 | Effects of dietary HMB supplementation on fat percentage of Bama Xiang mini-pigs. Data are presented as mean ± SEM (n = 8). ^{a,b,c} Values with different letters are significantly different among dietary HMB treatments ($P < 0.05$).

Bama Xiang mini-pig, a fat pig breed, is an optimal model to explore the regulation role of diets on obesity due to its anatomical and physiological similarities with humans (Chen et al., 2009; Jiang et al., 2015; Koopmans and Schuurman, 2015; Niu et al., 2017). Therefore, in this study, Bama Xiang mini-pigs were used to (1) investigate the effects of dietary HMB levels on lipid metabolism in the WAT, and (2) illustrate the potential mechanisms underlying the action of HMB on lipid metabolism. It was hypothesized that the optimal dietary HMB level could reduce fat accumulation in the WAT of Bama Xiang mini-pigs through regulating gut microbiota.

MATERIALS AND METHODS

Animals and Diets

The experiments in the present study were approved by the Animal Welfare Committee of the Institute of Subtropical Agriculture, Chinese Academy of Sciences. The ethic approval number is ISA-2017-023.

Thirty-two Bama Xiang mini-pigs (8.58 ± 0.40 kg, barrow) were selected and randomly allotted to four dietary treatments (8 piglets per treatment). The HMB-Ca level of the four dietary treatments were as follows: 0 (control), 0.13, 0.64, and 1.28%. The HMB-Ca (purity ≥ 99.0%) was obtained from Jiangyin TSI Pharmaceutical Co., Ltd. All diets were isoenergetic and isonitrogenous (Zheng C. et al., 2021), and met the nutritional needs for growing-mini pigs (Gao and Liu, 2009). The pigs raised individually in cages with *ad libitum* access to diets and water. This experiment lasted for 60 days.

Sample Collection and Fat Percentage Measurement

At the end of the experiment, pigs were fasted overnight (12 h) and then slaughtered by electrical stunning (250 V, 0.5 A, for 5–6 s) and exsanguinating. After slaughter, samples of WAT including DSA and ASA were rapidly excised from the right side of the carcass. The samples were then either stored at −20°C

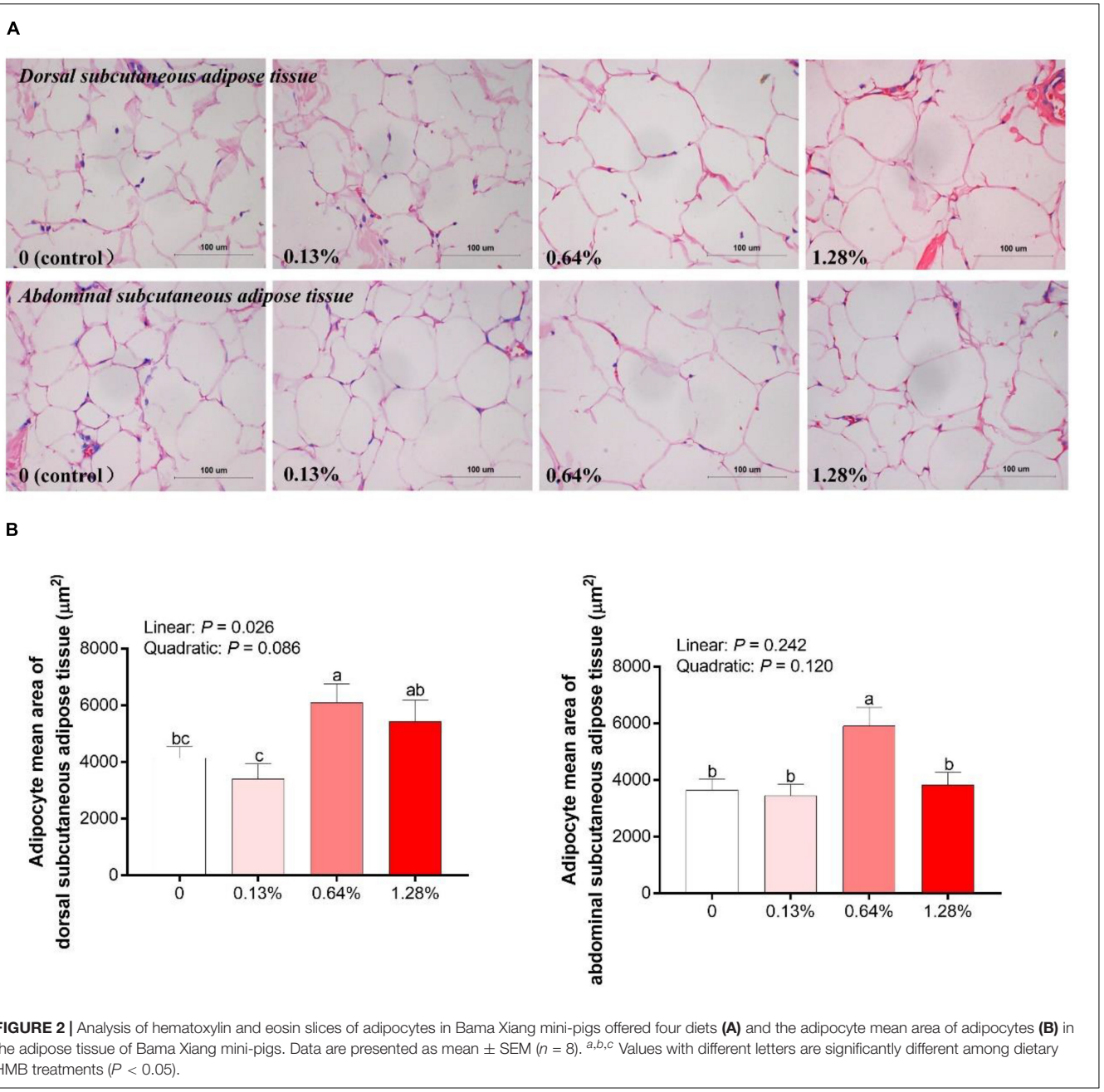

FIGURE 2 | Analysis of hematoxylin and eosin slices of adipocytes in Bama Xiang mini-pigs offered four diets **(A)** and the adipocyte mean area of adipocytes **(B)** in the adipose tissue of Bama Xiang mini-pigs. Data are presented as mean ± SEM (n = 8). ^{a,b,c} Values with different letters are significantly different among dietary HMB treatments ($P < 0.05$).

for the determination of fatty acid composition or quickly frozen in liquid nitrogen and then stored at −80°C for the analysis of Western blotting. Meanwhile, carcass weight and fat mass weight were recorded, and the fat percentage was calculated by dividing the fat mass weight by carcass weight. Subsequently, the colon was quickly separated and the colonic contents were collected from a region 10 cm posterior to the ileocecal valve into sterile tubes and stored at −80°C for further analysis.

Determination of Fatty Acid Composition

The fatty acid composition of DSA and ASA was analyzed via gas-liquid chromatography of methyl esters using an Agilent 7890A GC as previously described (Yin et al., 2000; Liu et al., 2015). The following indices were calculated based on fatty acid composition: the sum of saturated fatty acids (SFA), monounsaturated fatty acids (MUFA), and polyunsaturated fatty acids (PUFA), respectively. Then, the ratio of PUFA to SFA and the ratio of n-6 to n-3 PUFA were assessed.

Adipose Tissue Histologic Analysis

At the time of sacrifice, samples of DSA and ASA (1 cm^3) were collected and fixed in 4% paraformaldehyde in PBS (pH 7.3) for paraffin sections and hematoxylin and eosin staining as previously described (Zhang et al., 2021). Tissue sections

were imaged at 100 × magnification using a microscope (Eclise Ci-L, Nikon, Japan). The adipocyte size (10 fields/sample) was quantified using DIXI3000 (Leica Camera, Wetzlar, Germany).

Determination of Colonic SCFAs Concentrations

About 1 g of colonic contents were used to measure the concentrations of SCFAs (acetate, propionate, butyrate, isobutyrate, valerate, and isovalerate) by using an Agilent 6890A gas chromatography (Agilent Technologies, Santa Clara, CA, United States) according to our previous study (Yin et al., 2018).

Gut Microbiota Analysis

Gut microbiota in the colon of Bama Xiang mini-pigs were determined as previously described (Duan et al., 2019; Song et al., 2019). Alpha diversity indices, including Shannon, Simpson, Chao1, and ACE, were used to evaluate the diversity and richness of gut microbiota (Lemieux-Labonte et al., 2017).

Western Blotting Analysis

The relative protein expression of phosphorylated AMPKα (p-AMPKα), FoxO1 (p-FoxO1), mTOR (p-mTOR), and Sirt1 (p-Sirt1) in the DSA and ASA were determined as previously described (Duan et al., 2013). All the primary antibodies were purchased from Cell Signaling Technology (Danvers, MA) and the secondary antibodies were obtained from Thermo Scientific Inc. (Waltham, MA, United States). The protein bands were visualized by a chemiluminescent reagent (Pierce, Rockford, United States) with a ChemiDoc XRS system (Bio-Rad, Philadelphia, PA, United States). We quantified the resultant signals using Alpha Imager 2200 software (Alpha Innotech Corporation, CA, United States) and normalized the data with the value of the inner control GAPDH.

Statistical Analysis

Data were analyzed using one-way analysis of variance (ANOVA) using the SAS version 8.2 (SAS Institute Inc., Cary, NC, United States) software followed by Duncan's multiple comparison test. Orthogonal polynomial contrasts

TABLE 1 | Fatty acid composition of dorsal subcutaneous adipose tissue in Bama Xiang mini-pigs fed the diets with various levels of HMB (% of total fatty acids).

Items	Dietary levels of HMB, %				SEM	*P*-value[1]		
	0	0.13	0.64	1.28		ANOVA	Linear	Quadratic
C10:0	0.10^{ab}	0.09^{b}	0.11^{ab}	0.12^{a}	0.041	0.074	0.034	0.059
C12:0	0.13	0.11	0.13	0.13	0.052	0.517	0.960	0.641
C14:0	1.76	1.56	1.73	1.80	0.165	0.299	0.488	0.302
C16:0	27.13	26.98	27.25	27.82	0.319	0.322	0.121	0.167
C16:1	1.57	1.42	1.62	1.65	0.176	0.412	0.338	0.455
C17:0	0.28^{a}	0.25^{ab}	0.22^{b}	0.23^{b}	0.065	0.048	0.012	0.022
C18:0	18.01	18.91	18.06	17.63	0.389	0.336	0.391	0.291
C18:1 n9t	0.12	0.13	0.12	0.12	0.054	0.747	0.714	0.600
C18:1 n9c	35.55	35.91	36.61	35.86	0.388	0.495	0.463	0.413
C18:2 n6c	11.05^{a}	10.43^{ab}	10.16^{b}	10.82^{ab}	0.285	0.113	0.464	0.053
C20:0	0.35^{ab}	0.37^{a}	0.36^{ab}	0.31^{b}	0.071	0.096	0.122	0.039
C20:1	1.89	1.94	1.89	1.71	0.203	0.641	0.322	0.424
C18:3 n3	0.52^{ab}	0.56^{a}	0.46^{b}	0.46^{b}	0.087	0.023	0.022	0.061
C20:2	0.93	0.88	0.82	0.82	0.124	0.389	0.087	0.223
C20:3 n6	0.15	0.14	0.13	0.14	0.049	0.424	0.163	0.301
C22:1 n9	0.20	0.18	0.17	0.17	0.057	0.196	0.046	0.100
C20:4 n6	0.24^{a}	0.22^{b}	0.21^{b}	0.21^{b}	0.048	0.014	0.003	0.006
SFA[2]	47.75	48.29	47.86	48.04	0.408	0.906	0.855	0.932
MUFA[3]	39.32	39.57	40.42	39.50	0.400	0.472	0.564	0.464
PUFA[4]	12.89^{a}	12.23^{ab}	11.79^{b}	12.44^{ab}	0.295	0.081	0.205	0.040
ΣPUFA:SFA	0.27^{a}	0.25^{ab}	0.25^{b}	0.26^{ab}	0.047	0.175	0.250	0.085
Σn6 PUFA[5]	11.45^{a}	10.79^{ab}	10.51^{b}	11.17^{ab}	0.288	0.107	0.404	0.049
Σn3 PUFA[6]	0.52^{ab}	0.56^{a}	0.46^{b}	0.46^{b}	0.087	0.023	0.022	0.061
Σn6:n3 PUFA	22.36^{ab}	19.79^{b}	22.98^{ab}	24.47^{a}	0.562	0.032	0.073	0.039

[1] *Duncan, linear, and quadratic effects for HMB inclusion levels.*
[2] *SFA = C10:0 + C12:0 + C14:0 + C16:0 + C17:0 + C18:0 + C20:0.*
[3] *MUFA = C16:1 + C18:1n9t + C18:1n9c + C20:1 + C22:1n9.*
[4] *PUFA = C18:2n6c + C18:3n3 + C20:2 + C20:3n6 + C20:4n6.*
[5] *n3 PUFA = C18:3n3.*
[6] *n6 PUFA = C18:2n6c + C20:3n6 + C20:4n6.*
[a,b] *Values (n = 8) within a row with different superscripts differ significantly ($P < 0.05$).*

were performed to determine linear and quadratic effects of increasing dietary HMB on the measured indicators using SPSS 22.0 software (SPPS Inc., Chicago, IL, United States). Results are presented as means ± standard errors. Differences between significant means were considered statistically different at $P < 0.05$. Probability values between 0.05 and 0.10 were considered trends.

RESULTS

Fat Percentage and Adipocyte Size

As shown in **Figure 1**, linear effects of increased HMB levels on fat percentage was observed, with the highest value observed in the 1.28% HMB group and the lowest value observed in the 0.13% HMB group ($P < 0.05$).

As presented in **Figure 2**, HMB linearly increased the adipocyte mean area of DSA, and the highest/lowest value was obtained in the 0.64% HMB group/0.13% HMB group, respectively ($P < 0.05$). The adipocyte mean area of ASA in the 0.64% HMB group was higher than that in the other three groups ($P < 0.05$), and there was no significant difference among the three groups.

Fatty Acid Composition

As depicted in **Table 1**, dietary HMB supplementation significantly influenced the fatty acid composition in the DSA. HMB supplementation linearly increased the concentration of C18:3 n3, with the highest value observed in the 0.13% HMB group ($P < 0.05$). As dietary HMB levels increased, the concentration of C18:2 n6c showed a downward trend (quadratic, $P = 0.053$). The concentration of C20:4 n6 was decreased in the HMB groups compared with the control (linear and quadratic, $P < 0.05$). The n6:n3 PUFA ratio was the highest in the 1.28% HMB group and the lowest in the 0.13% HMB group, with intermediate values observed in the other two groups (quadratic, $P < 0.05$). HMB quadratically decreased the sum of PUFA ($P < 0.05$) and the ratio of PUFA:SFA ($P = 0.085$). Dietary treatments did not significantly affect the sum of SFA and MUFA ($P > 0.05$).

TABLE 2 | Fatty acid composition of abdominal subcutaneous adipose tissue in Bama Xiang mini-pigs fed the diets with various levels of HMB (% of total fatty acids).

Items	Dietary levels of HMB, %				SEM	*P*-value[1]		
	0	0.13	0.64	1.28		ANOVA	Linear	Quadratic
C10:0	0.13	0.11	0.12	0.14	0.057	0.310	0.591	0.057
C12:0	0.15	0.12	0.14	0.13	0.055	0.163	0.920	0.055
C14:0	1.88^{a}	1.53^{b}	1.73^{ab}	1.86^{a}	0.168	0.047	0.800	0.168
C16:0	27.92^{ab}	26.76^{b}	27.51^{ab}	28.53^{a}	0.352	0.038	0.222	0.352
C16:1	1.49	1.28	1.45	1.48	0.189	0.550	0.806	0.189
C17:0	0.24^{a}	0.23^{ab}	0.20^{b}	0.20^{b}	0.060	0.042	0.007	0.060
C18:0	19.81	20.77	20.77	19.97	0.462	0.661	0.874	0.462
C18:1 n9t	0.11	0.12	0.11	0.10	0.042	0.195	0.342	0.042
C18:1 n9c	34.80	36.00	35.61	35.30	0.427	0.550	0.679	0.427
C18:2 n6c	9.93	9.79	9.19	8.92	0.331	0.179	0.028	0.331
C20:0	0.31^{ab}	0.28^{b}	0.33^{a}	0.28^{b}	0.064	0.056	0.444	0.064
C20:1	1.61	1.44	1.57	1.54	0.219	0.895	0.888	0.219
C18:3 n3	0.49^{ab}	0.50^{a}	0.42^{b}	0.43^{ab}	0.086	0.062	0.022	0.086
C20:2	0.72	0.66	0.66	0.62	0.120	0.541	0.162	0.120
C20:3 n6	0.13	0.11	0.13	0.11	0.044	0.067	0.170	0.044
C22:1 n9	0.15	0.14	0.14	0.13	0.054	0.672	0.212	0.054
C20:4 n6	0.25	0.25	0.26	0.23	0.069	0.552	0.343	0.069
SFA[2]	50.44	49.79	50.80	51.11	0.479	0.643	0.369	0.479
MUFA[3]	38.15	38.98	38.88	38.55	0.453	0.815	0.716	0.453
PUFA[4]	11.52	11.30	10.65	10.31	0.350	0.149	0.020	0.350
ΣPUFA:SFA	0.23	0.23	0.21	0.20	0.056	0.189	0.034	0.056
Σn6 PUFA[5]	10.32	10.15	9.57	9.26	0.336	0.185	0.028	0.336
Σn3 PUFA[6]	0.49^{ab}	0.50^{a}	0.42^{b}	0.43^{ab}	0.086	0.062	0.022	0.086
Σn6:n3 PUFA	21.14	20.77	22.90	21.83	0.453	0.156	0.195	0.453

[1] *Duncan, linear, and quadratic effects for HMB inclusion levels.*
[2] *SFA = C10:0 + C12:0 + C14:0 + C16:0 + C17:0 + C18:0 + C20:0.*
[3] *MUFA = C16:1 + C18:1n9t + C18:1n9c + C20:1 + C22:1n9.*
[4] *PUFA = C18:2n6c + C18:3n3 + C20:2 + C20:3n6 + C20:4n6.*
[5] *n3 PUFA = C18:3n3.*
[6] *n6 PUFA = C18:2n6c + C20:3n6 + C20:4n6.*
[a,b] *Values (n = 8) within a row with different superscripts differ significantly ($P < 0.05$).*

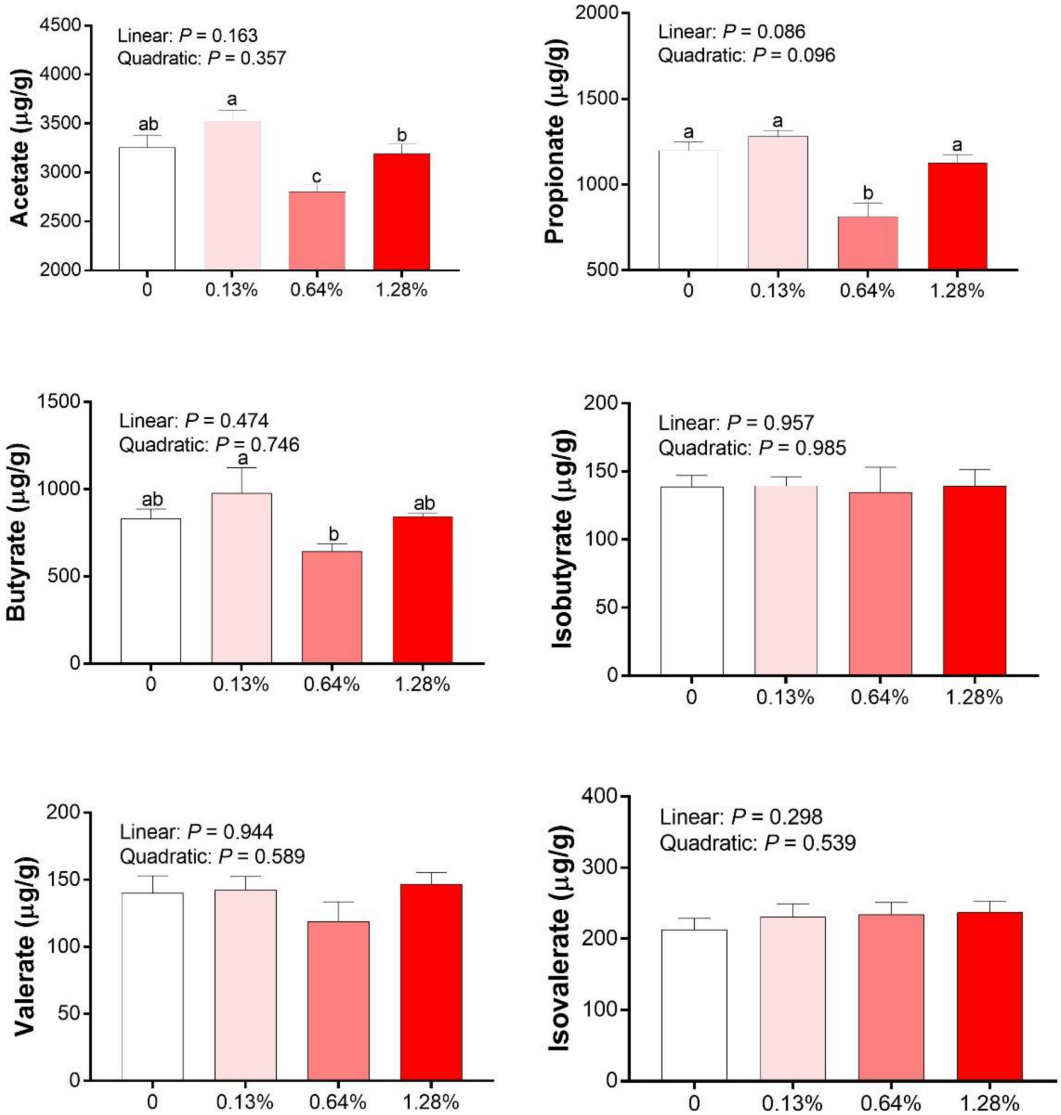

FIGURE 3 | The SCFAs concentrations in the colonic contents of Bama Xiang mini-pigs. Data are presented as mean ± SEM (n = 8). ^{a,b,c} Values with different letters are significantly different among dietary HMB treatments ($P < 0.05$).

The results concerning the fatty acid composition of ASA were presented in **Table 2**. No significant difference was observed in the contents of C18:2 n6c, C20:3 n6, and C20:4 n6, the sum of n6 PUFA, SFA, MUFA, and PUFA, the ratio of PUFA to SFA, and the ratio of n6 to n3 PUFA ($P > 0.05$). HMB linearly increased the concentration of C18:3 n3, with the highest value observed in the 0.13% HMB group and the lowest value in 0.64% HMB group ($P < 0.05$).

Colonic SCFA Concentrations

As shown in **Figure 3**, there were no linear or quadratic effects of increased HMB levels on colonic isobutyrate, valerate, and isovalerate concentrations ($P > 0.05$). The highest and the lowest concentrations of acetate, propionate and butyrate appeared in the 0.13% HMB group and 0.64% HMB group, respectively ($P < 0.05$). In addition, correlation analyses between the fat percentage and colonic acetate, propionate, butyrate, isobutyrate, valerate, and isovalerate concentrations were conducted by Pearson correlation analysis (**Figure 4**). The fat percentage negatively correlated with the colonic acetic acid and butyrate production ($P < 0.05$).

Gut Microbiota Composition of Bama Xiang Mini-Pigs

As shown in **Figure 5A**, there were no significant differences in indexes of Shannon and Simpson among the groups ($P > 0.05$). However, linear and quadratic effects of HMB supplementation on indexes of Chao1 and ACE (Chao1, linear, $P = 0.014$, quadratic, $P = 0.001$; ACE, linear, $P = 0.012$, quadratic,

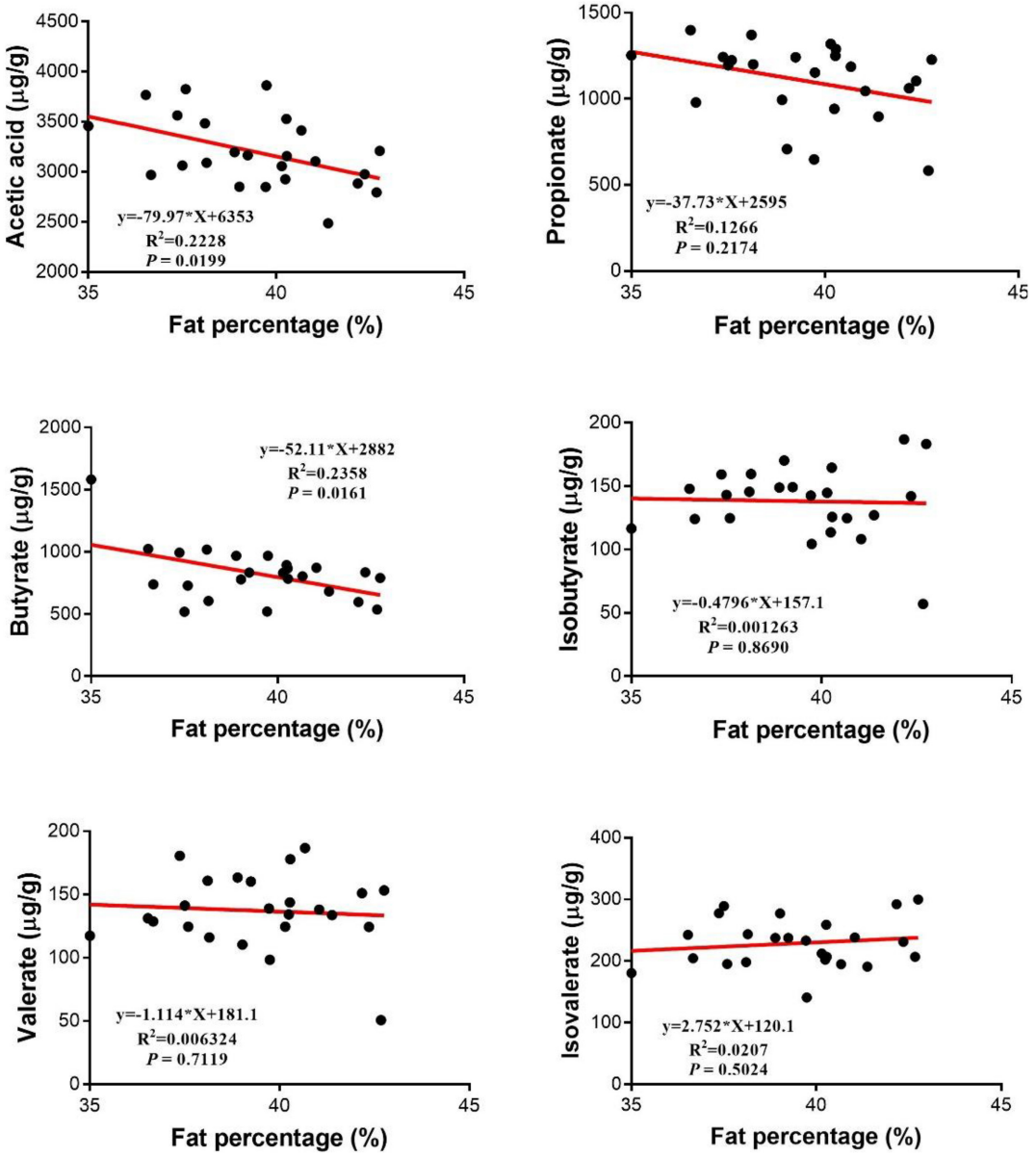

FIGURE 4 | Relationship between SCFAs and the fat percentage. Pearson correlations were used to determine the association between the fat percentage and colonic acetate, propionate, butyrate, valerate, isobutyrate, and isobutyrate concentrations.

P = 0.021) were observed, with the highest value observed in the 0.13% HMB group and the lowest value observed in the 1.28% HMB group. To further explore the overall microbial composition, we analyzed the relative abundance of dominant taxa at the phylum level. As shown in **Figure 5B**, the most dominant phyla in the bacterial communities were *Firmicutes*, *Bacteroidetes*, and *Proteobacteria*. HMB supplementation did not significantly affect the relative abundance of *Firmicutes* ($P > 0.05$). The relative abundance of *Bacteroidetes* reached its greatest value in the 0.13% HMB group and was higher than that in other three groups (quadratic, $P < 0.05$). The relative abundance of *Proteobacteria* was the highest in the 0.64% HMB group and the lowest in the 0.13% HMB group ($P < 0.05$). Furthermore, correlation analyses between the fat percentage and the relative abundances of *Bacteroidetes* and *Proteobacteria* were conducted by Pearson correlation analysis (**Figure 5C**). The acetic acid concentration was positively/negatively correlated with the abundance of *Bacteroidetes/Proteobacteria*, respectively ($P < 0.05$). Moreover, the abundance of *Bacteroidetes* was negatively correlated with the fat percentage ($P < 0.05$). No correlation was observed between the abundance of *Proteobacteria* and the fat percentage, and between the butyrate production and the relative abundance of *Bacteroidetes* or *Proteobacteria* ($P > 0.05$).

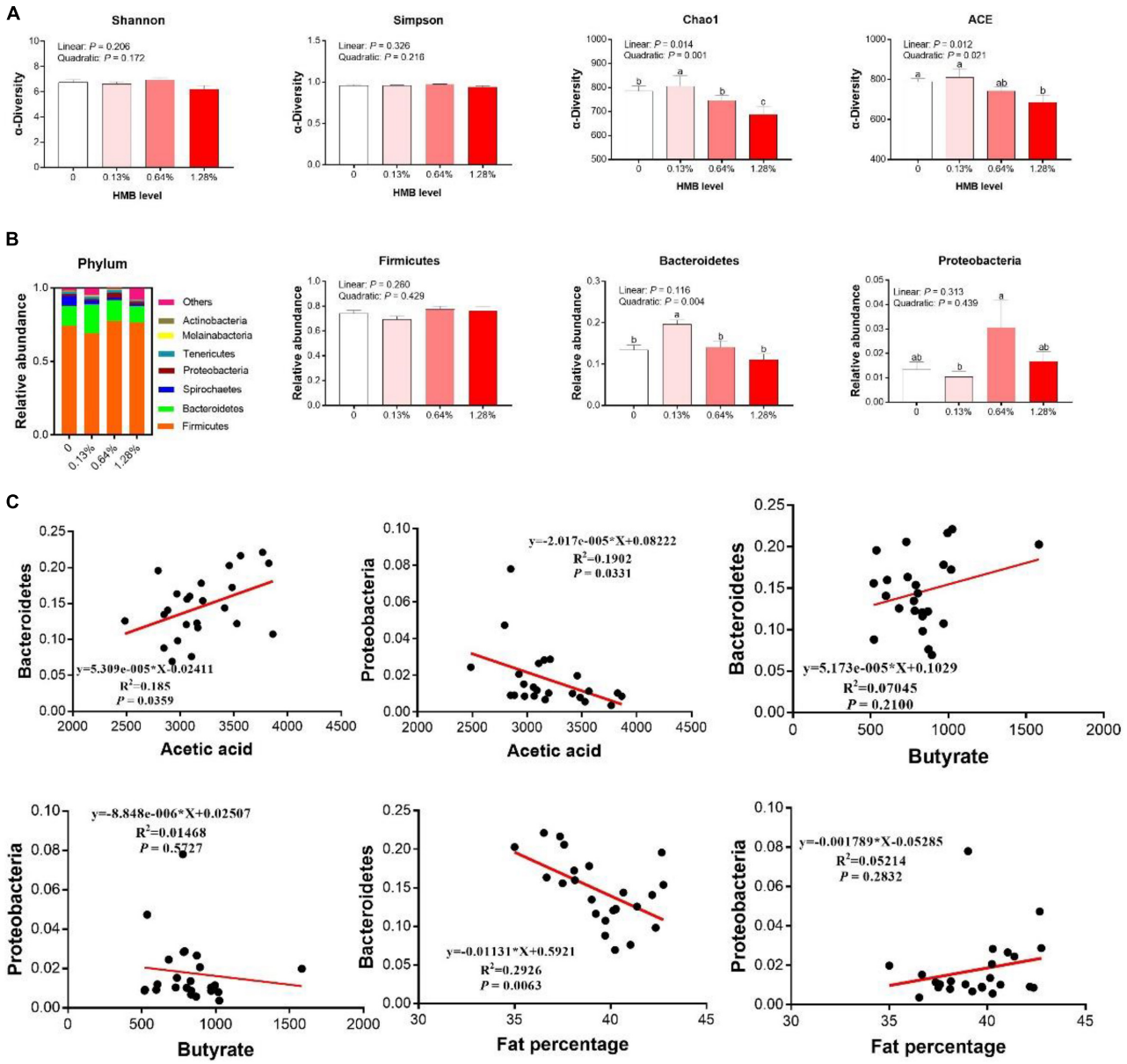

FIGURE 5 | Dietary HMB supplementation improved gut microbiota in Bama Xiang mini-pigs. The α-diversity analysis **(A)**, microbiota composition at the phylum level **(B)**, the correlation analyses between the relative abundance of *Bacteroidetes*/*Proteobacteria* and acetic acid/butyrate, the correlation analyses between the relative abundance of *Bacteroidetes*/*Proteobacteria* and fat percentage **(C)**. Data are presented as mean ± SEM (n = 8). ^{a,b,c} Values with different letters are significantly different among dietary HMB treatments ($P < 0.05$).

Protein Expression of p-AMPKα, p-FoxO1, p-mTOR, and p-Sirt1

The protein expression of p-AMPKα, p-FoxO1, p-mTOR, and p-Sirt1 in the control and 0.13% HMB groups were shown in **Figure 6**. In the DSA (**Figure 6A**), compared to the control group, the 0.13% HMB supplementation significantly upregulated the protein expression of p-AMPKα, p-FoxO1, and p-Sirt1 ($P < 0.05$), and downregulated the p-mTOR protein expression ($P < 0.05$). In the ASA (**Figure 6B**), compared to the control group, the 0.13% HMB supplementation significantly upregulated the protein expression of p-AMPKα and p-Sirt1 ($P < 0.05$), and downregulated the p-mTOR protein expression ($P < 0.05$). The protein expression of p-FoxO1 showed a trend to increase in response to HMB supplementation ($P = 0.0815$).

DISCUSSION

In the current study, we presented evidence that dietary supplementation of HMB with optimal level (0.13%) significantly inhibited fat deposition in Bama Xiang mini-pigs, as evidenced

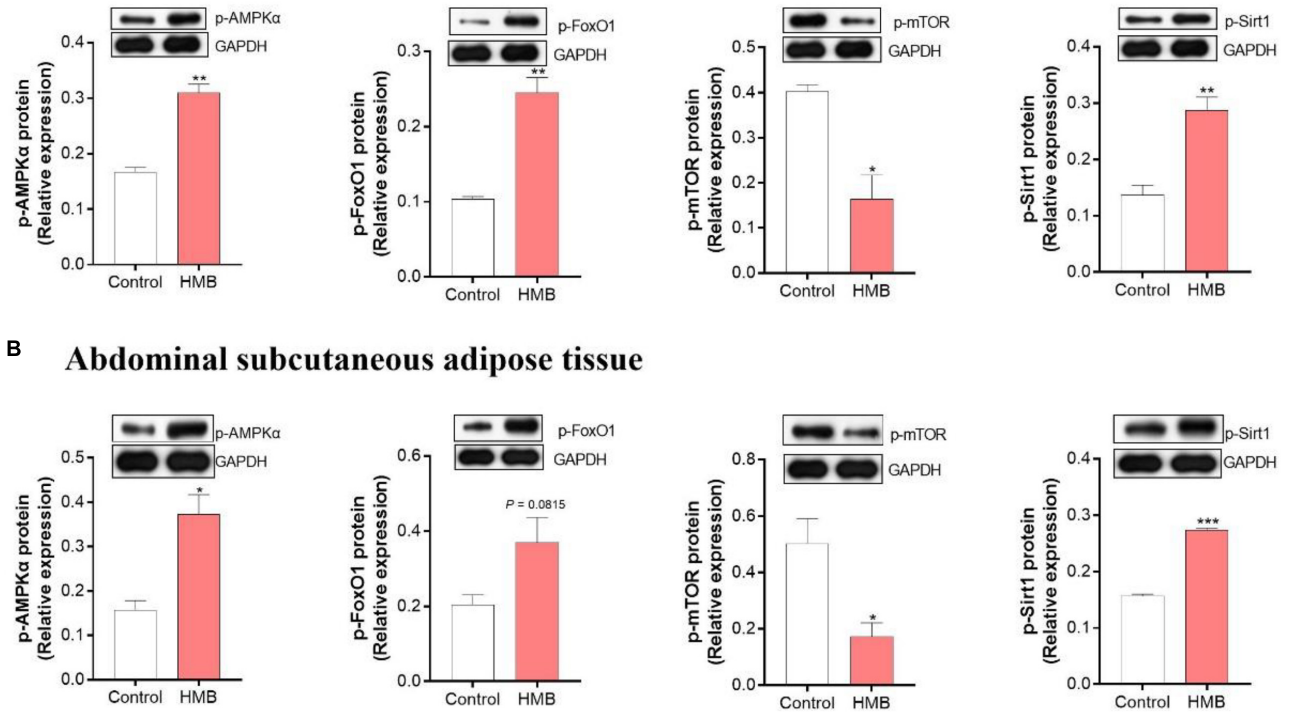

FIGURE 6 | The expression of phosphorylation (p)-AMPKα, FoxO1, mTOR and Sirt1 in DSA **(A)** and ASA **(B)** of Bama Xiang mini-pigs fed diets with 0.13% HMB-Ca. Data are presented as mean ± SEM ($n = 8$). $^{*}P < 0.05$, $^{**}P < 0.01$, $^{***}P < 0.001$. AMPK, AMP-activated protein kinase; FoxO1, forkhead box O1; mTOR, mammalian target of rapamycin; Sirt1, silent information regulator 2 related enzyme 1.

by the decreased fat percentage and adipocyte mean area of DSA. Notably, these observations did not occur at higher levels of HMB. In good agreement with our results, evidence from a rodent model has demonstrated that the maximum reduction of fat mass and mean size of WAT occurred at the HMB level of 1% (wt/vol), with higher concentrations of HMB being ineffective (Duan et al., 2019). Similar observations were also obtained in protein metabolism, with higher doses of HMB being ineffective (Wheatley et al., 2014). However, the reason why higher concentrations of HMB are unable to regulate lipid metabolism positively requires further interrogation. In addition, unlike DSA, HMB supplementation failed to reduce the adipocyte mean area of ASA. Therefore, these results suggest that the appropriate HMB dosage was 0.13% and that HMB mainly reduced the fat mass of DSA rather than of ASA.

Given the site differences in adipocyte size of subcutaneous fat depots following HMB supplementation, we speculated that there were differences in the fatty acid composition of subcutaneous fat depots in different regions. Moreover, there is compelling evidence that adipose tissue fatty acid composition is greatly associated with fat cell size (Raclot et al., 1997; Garaulet et al., 2006). It has been reported that n3 and n6 PUFAs are negatively correlated with the adipocyte size. In contrast, SFA is positively correlated with the adipocyte size (Garaulet et al., 2006). In the current study, although the SFA in DSA and ASA upon the HMB diets did not achieve the statistical significance, dietary HMB supplementation greatly elevated the n3 PUFA in selected WAT compared to the control group, and the maximum elevation of the n3 PUFA occurred at the HMB level of 0.13%. Unlike the n3 PUFA, HMB supplementation quadratically decreased n6 PUFA concentration in DSA, with the lowest value observed in the 0.64% HMB group, and did not significantly affect this parameter in ASA. These observations might underlie the mechanistic explanation for a beneficial role of HMB on the adipocyte mean area of DSA rather than ASA. Site differences in numerous metabolic activities in subcutaneous fat depots have been reported by studies in obese and non-obese humans (Lithell and Boberg, 1978; Malcom et al., 1989). Therefore, the differences in fatty acid composition between DSA and ASA indicate that HMB might differently affect metabolic activities (such as rate of deposition and mobilization) in the two subcutaneous sites.

It is well-known that the occurrence and development of obesity is closely associated with alterations in composition, diversity, and function of the gut microbiota (Shen et al., 2013; Gérard, 2015; 'Graham et al., 2015). To explore whether dietary HMB supplementation reduced the fat deposition via gut microbiota, we analyzed the composition of gut microbiota in the colon of Bama Xiang mini-pigs. Our data showed that HMB supplementation (0.13%) increased the relative abundance of *Bacteroidetes*, and the increased *Bacteroidetes* was positively

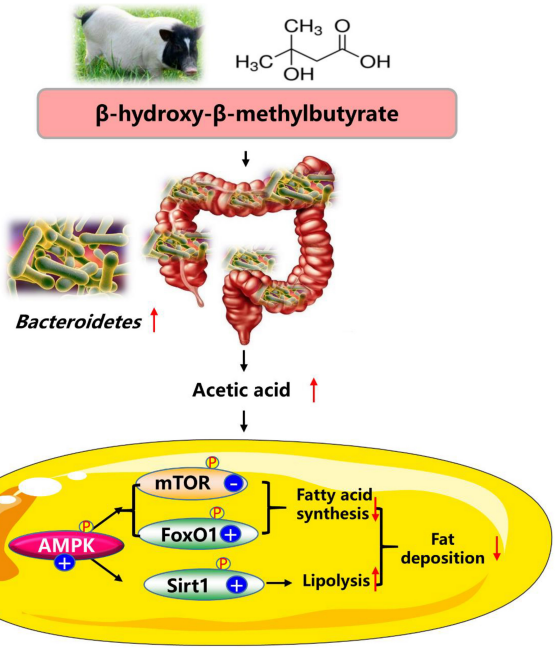

FIGURE 7 | Proposed mechanisms of dietary HMB supplementation for modulating the lipid metabolism in adipose tissue of Bama Xiang mini-pigs. AMPK, AMP-activated protein kinase; FoxO1, forkhead box O1; mTOR, mammalian target of rapamycin; Sirt1, silent information regulator 2 related enzyme 1.

associated with the reduction of fat percentage. These results are well-matched with works in a rodent model (Duan et al., 2019). Moreover, our data showed that the relative abundance of *Proteobacteria* was the highest in the 0.64% HMB group and the lowest in the 0.13% HMB group. It has been reported that *Proteobacteria* is related to intestinal inflammation and gastrointestinal diseases (Kang et al., 2019; Bakhti et al., 2020; Zeng et al., 2020). Therefore, evidence from the current study shows that HMB supplementation at the level of 0.13% leads to the elevation of the beneficial bacteria *Bacteroidetes* and the reduction of the harmful bacteria *Proteobacteria*. Based on the results from our previous study (Duan et al., 2019) and the present study, we speculated that alterations in gut microbiota composition might contribute to the reduced fat deposition of Bama Xiang mini-pigs observed in the 0.13% HMB group. However, our knowledge of how HMB targets gut microbiota to reduce fat deposition is far from complete so that it needs to be further explored.

Several recent studies have demonstrated that the bacterial metabolites SCFAs exert a role in the action of gut microbiota (Yin et al., 2018; Duan et al., 2019; Hu et al., 2019), which motivated us to analyze the concentrations of SCFAS in the colon of Bama Xiang mini-pigs. Our data showed that HMB supplementation (0.13%) tended to reverse the decrease of acetic acid, and acetic acid production was negatively correlated with the fat percentage. These results are in accordance with other studies, which have demonstrated that diets-elevated colonic production of acetic acid contributes to the reduction of body weight in high fat diets-induced obese mice (Yin et al., 2018). Upon further investigation, we found that the colonic acetic acid production and the relative *Bacteroidetes* abundance showed a positive correlation. A major route to form acetic acid from dietary carbohydrates is driven by the abundant *Bacteroidetes* (Miller, 1978). Therefore, these results partially indicated that HMB supplementation affects gut microbiota compositions (especially for *Bacteroidetes*), which further generated acetic acid to reduce fat deposition. Strong evidence for the role of acetic acid on obesity comes from several rodent studies (Yamashita et al., 2007, 2009; Beh et al., 2017). In contrast to the results observed in Bama Xiang mini-pigs, data from rodent studies showed that the beneficial effects of HMB on obesity was mediated by gut microbiota-propionic acid axis (Duan et al., 2019). The inconsistency of the two reports might be due to the differences in experimental models, the experimental approaches, and the varied doses used in each experiment. This discrepancy suggests that results from rodent studies are not readily translated to human models of obesity.

Interestingly, there is evidence showing that the activation of AMPKα in adipose tissue could be one possible contributing mechanism for the beneficial effects of acetic acid (Fu et al., 2018; Liu et al., 2019). The enzyme AMPKα exerts key roles in regulating energy homeostasis (Shen et al., 2013; Yamashita, 2016). Evidence from *in vivo* and *in vitro* studies suggests that AMPKα activation in adipose tissue could suppressing lipogenesis by impairing the mTOR signaling (Gaidhu et al., 2009; Wang Q. et al., 2018) and promoting the phosphorylation of FoxO1 (Greer et al., 2007; Chen et al., 2010). On the other hand, the phosphorylation of AMPKα could promote lipolysis by activating Sirt1 directly (Canto et al., 2009). In the current study, Western blot analysis revealed that HMB markedly upregulated the phosphorylation of AMPK, FoxO1, and Sirt1, and downregulated the phosphorylation of mTOR in selected WAT. These results are perfectly in line with a recent study which reported that HMB might regulate lipid metabolism via the AMPKα-mTOR and AMPKα-Sirt1 signaling pathways in the perirenal adipose tissue of Large white × Landrace pigs (Duan et al., 2018).

CONCLUSION

In summary, our data showed that dietary HMB supplementation at the level of 0.13% increased n3 PUFA and reduced fat mass in adipose tissue of Bama Xiang mini-pigs, and the favorable effects were more pronounced in the DSA. The beneficial effects of HMB on reducing fat deposition were likely regulated by the *Bacteroidetes*-acetic acid-AMPKα axis (**Figure 7**). These findings may provide valuable information for understanding the mechanisms of action of HMB in combating obesity. Areas that need further exploration include the research of mechanisms whereby HMB elevated the relative *Bacteroidetes* abundance and the acetic acid production. Although our data were encouraging, these findings should be confirmed with clinical studies with long-term follow-up.

DATA AVAILABILITY STATEMENT

The raw data supporting the conclusions of this article will be made available by the authors, without undue reservation.

ETHICS STATEMENT

The animal study was reviewed and approved by Animal Welfare Committee of the Institute of Subtropical Agriculture, Chinese Academy of Sciences. Written informed consent was obtained from the owners for the participation of their animals in this study.

AUTHOR CONTRIBUTIONS

YD contributed to the conception of the study. JZ, CZ, BS, SZ, YZ, LZ, and GD performed the experiment. JZ and CZ contributed equally to data analysis and manuscript preparation. FL and QG revised the manuscript. All authors read and finalized the manuscript.

FUNDING

This study was jointly supported by the Natural Science Foundation of Guangxi Province (2020JJA130102 and 2018JJB130239), the National Natural Science Foundation of China (U19A2037 and 31802077), the Changsha Natural Science Funds for Distinguished Young Scholar (kq2009020), Young Elite Scientists Sponsorship Program by CAST (2019QNRC001), Special funds for the construction of innovative provinces in Hunan Project (2019NK2193 and 2019RS3022), China Agriculture Research System of MOF and MARA (CARS-35), the "Strategic Priority Research Program" of the Chinese Academy of Sciences (XDA24030204), Open Fund of Key Laboratory of Agro-ecological Processes in Subtropical Region, Chinese Academy of Sciences (ISA2020203), and Taishan industry leading talent project special funds.

REFERENCES

Bakhti, S. Z., Latifi-Navid, S., and Safaralizadeh, R. (2020). *Helicobacter pylori*-related risk predictors of gastric cancer: the latest models, challenges, and future prospects. *Cancer Med.* 9, 4808–4822. doi: 10.1002/cam4.3068

Beh, B. K., Mohamad, N. E., Yeap, S. K., Ky, H., Boo, S. Y., Chua, J. Y. H., et al. (2017). Anti-obesity and anti-inflammatory effects of synthetic acetic acid vinegar and Nipa vinegar on high-fat-diet-induced obese mice. *Sci. Rep.* 7:6664.

Booth, A. D., Magnuson, A. M., Fouts, J., Wei, Y., Wang, D., Pagliassotti, M. J., et al. (2018). Subcutaneous adipose tissue accumulation protects systemic glucose tolerance and muscle metabolism. *Adipocyte* 7, 261–272. doi: 10.1080/21623945.2018.1525252

Canto, C., Gerhart-Hines, Z., Feige, J. N., Lagouge, M., Noriega, L., Milne, J. C., et al. (2009). AMPK regulates energy expenditure by modulating NAD(+) metabolism and SIRT1 activity. *Nature* 458, 1056–U1140.

Chen, B. L., Ma, Y. D., Meng, R. S., Xiong, Z. J., Wang, H. N., Zeng, J. Y., et al. (2010). Activation of AMPK inhibits cardiomyocyte hypertrophy by modulating of the FOXO1/MuRF1 signaling pathway in vitro. *Acta Pharmacol. Sin.* 31, 798–804. doi: 10.1038/aps.2010.73

Chen, H., Liu, Y. Q., Li, C. H., Guo, X. M., and Huang, L. J. (2009). The susceptibility of three strains of Chinese minipigs to diet-induced type 2 diabetes mellitus. *Lab. Anim. (NY)* 38, 355–363. doi: 10.1038/laban1109-355

Cummins, T. D., Holden, C. R., Sansbury, B. E., Gibb, A. A., Shah, J., Zafar, N., et al. (2014). Metabolic remodeling of white adipose tissue in obesity. *Am. J. Physiol. Endocrinol. Metab.* 307, E262–E277.

Duan, Y., Li, F., Li, L., Fan, J., Sun, X., and Yin, Y. (2013). n-6:n-3 PUFA ratio is involved in regulating lipid metabolism and inflammation in pigs. *Br. J. Nutr.* 111, 445–451. doi: 10.1017/s0007114513002584

Duan, Y., Li, F., Wang, W., Guo, Q., Wen, C., Li, Y., et al. (2017). Interleukin-15 in obesity and metabolic dysfunction: current understanding and future perspectives. *Obes. Rev.* 18, 1147–1158. doi: 10.1111/obr.12567

Duan, Y., Zhang, L., Li, F., Guo, Q., Long, C., Yin, Y., et al. (2018). beta-Hydroxy-beta-methylbutyrate modulates lipid metabolism in adipose tissues of growing pigs. *Food Funct.* 9, 4836–4846. doi: 10.1039/c8fo00898a

Duan, Y., Zhong, Y., Xiao, H., Zheng, C., Song, B., Wang, W., et al. (2019). Gut microbiota mediates the protective effects of dietary beta-hydroxy-beta-methylbutyrate (HMB) against obesity induced by high-fat diets. *FASEB J.* 33, 10019–10033. doi: 10.1096/fj.201900665rr

Duan, Y. H., Li, F. N., Tan, B., Yao, K., and Yin, Y. L. (2017). Metabolic control of myofibers: promising therapeutic target for obesity and type 2 diabetes. *Obes. Rev.* 18, 647–659. doi: 10.1111/obr.12530

Felig, P., Marliss, E., and Cahill, G. F. Jr. (1969). Plasma amino acid levels and insulin secretion in obesity. *N. Engl. J. Med.* 281, 811–816. doi: 10.1056/nejm196910092811503

Fickova, M., Hubert, P., Cremel, G., and Leray, C. (1998). Dietary (n-3) and (n-6) polyunsaturated fatty acids rapidly modify fatty acid composition and insulin effects in rat adipocytes. *J. Nutr.* 128, 512–519. doi: 10.1093/jn/128.3.512

Fu, C., Liu, L., and Li, F. (2018). Acetate alters the process of lipid metabolism in rabbits. *Animal* 12, 1895–1902. doi: 10.1017/s1751731117003275

Gaidhu, M. P., Fediuc, S., Anthony, N. M., So, M., Mirpourian, M., Perry, R. L. S., et al. (2009). Prolonged AICAR-induced AMP-kinase activation promotes energy dissipation in white adipocytes: novel mechanisms integrating HSL and ATGL. *J. Lipid Res.* 50, 704–715. doi: 10.1194/jlr.m800480-jlr200

Gaiva, M. H., Couto, R. C., Oyama, L. M., Couto, G. E., Silveira, V. L., Riberio, E. B., et al. (2001). Polyunsaturated fatty acid-rich diets: effect on adipose tissue metabolism in rats. *Br. J. Nutr.* 86, 371–377. doi: 10.1079/bjn2001392

Gannon, N. P., Schnuck, J. K., and Vaughan, R. A. (2018). BCAA metabolism and insulin sensitivity–dysregulated by metabolic status? *Mol. Nutr. Food. Res.* 62:e1700756.

Gao, Q., and Liu, Y. (2009). Research advances on nutrient requirements of laboratory minipigs. *Chin. J. Comp. Med.* 19, 74–78.

Garaulet, M., Hernandez-Morante, J. J., Lujan, J., Tebar, F. J., and Zamora, S. (2006). Relationship between fat cell size and number and fatty acid composition in adipose tissue from different fat depots in overweight/obese humans. *Int. J. Obes. (Lond)* 30, 899–905. doi: 10.1038/sj.ijo.0803219

Gérard, P. (2015). Gut microbiota and obesity. *Cell. Mol. Life. Sci.* 73, 147–162.

Graham, C., Mullen, A., and Whelan, K. (2015). Obesity and the gastrointestinal microbiota: a review of associations and mechanisms. *Nutr. Rev.* 73, 376–385. doi: 10.1093/nutrit/nuv004

Greer, E. L., Dowlatshahi, D., Banko, M. R., Villen, J., Hoang, K., Blanchard, D., et al. (2007). An AMPK-FOXO pathway mediates longevity induced by a novel method of dietary restriction in C. elegans. *Curr. Biol.* 17, 1646–1656. doi: 10.1016/j.cub.2007.08.047

Hu, C., Li, F., Duan, Y., Yin, Y., and Kong, X. (2019). Dietary supplementation with leucine or in combination with arginine decreases body fat weight and

alters gut microbiota composition in finishing pigs. *Front. Microbiol.* 10:1767. doi: 10.3389/fmicb.2019.01767

Jiang, G., Li, L., Fan, J., Zhang, B., Oso, A. O., Xiao, C., et al. (2015). Dietary soy isoflavones differentially regulate expression of the lipid-metabolic genes in different white adipose tissues of the female Bama mini-pigs. *Biochem. Biophys. Res. Commun.* 461, 159–164. doi: 10.1016/j.bbrc.2015.04.006

Kang, Z., Lu, M., Jiang, M., Zhou, D., and Huang, H. (2019). Proteobacteria acts as a pathogenic risk-factor for chronic abdominal pain and diarrhea in post-cholecystectomy syndrome patients: a gut microbiome metabolomics study. *Med. Sci. Monit.* 25, 7312–7320. doi: 10.12659/msm.915984

Koopmans, S. J., and Schuurman, T. (2015). Considerations on pig models for appetite, metabolic syndrome and obese type 2 diabetes: from food intake to metabolic disease. *Eur. J. Pharmacol.* 759, 231–239. doi: 10.1016/j.ejphar.2015.03.044

Lebret, B., and Mourot, J. (1998). Characteristics and quality of pig adipose tissues. Influence of rearing factors. *Prod. Anim.* 11, 131–143.

Lemieux-Labonte, V., Simard, A., Willis, C. K. R., and Lapointe, F. J. (2017). Enrichment of beneficial bacteria in the skin microbiota of bats persisting with white-nose syndrome. *Microbiome* 5:115.

Lithell, H., and Boberg, J. (1978). The lipoprotein lipase activity of adipose tissue from different sites in obese women and the relationships to the cell size. *Int. J. Obes.* 2, 47–52.

Liu, L., Fu, C., and Li, F. (2019). Acetate affects the process of lipid metabolism in rabbit liver, skeletal muscle and adipose tissue. *Animals (Basel)* 9:799. doi: 10.3390/ani9100799

Liu, Y., Li, F., He, L., Tan, B., Deng, J., Kong, X., et al. (2015). Dietary protein intake affects expression of genes for lipid metabolism in porcine skeletal muscle in a genotype-dependent manner. *Br. J. Nutr.* 113, 1069–1077. doi: 10.1017/s0007114514004310

Malcom, G. T., Bhattacharyya, A. K., Velez-Duran, M., Guzman, M. A., Oalmann, M. C., and Strong, J. P. (1989). Fatty acid composition of adipose tissue in humans: differences between subcutaneous sites. *Am. J. Clin. Nutr.* 50, 288–291. doi: 10.1093/ajcn/50.2.288

Marchesi, J. R., Adams, D. H., Fava, F., Hermes, G. D., Hirschfield, G. M., Hold, G., et al. (2016). The gut microbiota and host health: a new clinical frontier. *Gut* 65, 330–339. doi: 10.1136/gutjnl-2015-309990

Miller, T. L. (1978). The pathway of formation of acetate and succinate from pyruvate by *Bacteroides succinogenes*. *Arch. Microbiol.* 117, 145–152. doi: 10.1007/bf00402302

Nissen, S. L., and Abumrad, N. N. (1997). Nutritional role of the leucine metabolite β-hydroxy β-methylbutyrate (HMB). *J. Nutr. Biochem.* 8, 300–311. doi: 10.1016/s0955-2863(97)00048-x

Niu, M., Xiang, L., Liu, Y., Zhao, Y., Yuan, J., Dai, X., et al. (2017). Adiponectin induced AMP-activated protein kinase impairment mediates insulin resistance in Bama mini-pig fed high-fat and high-sucrose diet. *Asian Australas. J. Anim. Sci.* 30, 1190–1197. doi: 10.5713/ajas.17.0006

Park, B. S., Henning, P. C., Grant, S. C., Lee, W. J., Lee, S. R., Arjmandi, B. H., et al. (2013). HMB attenuates muscle loss during sustained energy deficit induced by calorie restriction and endurance exercise. *Metabolism* 62, 1718–1729. doi: 10.1016/j.metabol.2013.06.005

Proença, A. R. G., Sertié, R. A. L., Oliveira, A. C., Campaãa, A. B., Caminhotto, R. O., Chimin, P., et al. (2014). New concepts in white adipose tissue physiology. *Braz. J. Med. Biol. Res.* 47, 192–205.

Raclot, T., Groscolas, R., Langin, D., and Ferré, P. (1997). Site-specific regulation of gene expression by n-3 polyunsaturated fatty acids in rat white adipose tissues. *J. Lipid Res.* 38, 1963–1972. doi: 10.1016/s0022-2275(20)37127-3

Rodríguez, V. M., Picó, C., Portillo, M. P., Teresa Macarulla, M., and Palou, A. (2002). Dietary fat source regulates ob gene expression in white adipose tissue of rats under hyperphagic feeding. *Br. J. Nutr.* 87, 427–434. doi: 10.1079/bjnbjn2002570

Shen, J., Obin, M. S., and Zhao, L. (2013). The gut microbiota, obesity and insulin resistance. *Mol. Aspects Med.* 34, 39–58. doi: 10.1016/j.mam.2012.11.001

Song, B., Zhong, Y. Z., Zheng, C. B., Li, F. N., Duan, Y. H., and Deng, J. P. (2019). Propionate alleviates high-fat diet-induced lipid dysmetabolism by modulating gut microbiota in mice. *J. Appl. Microbiol.* 127, 1546–1555. doi: 10.1111/jam.14389

Topping, D. L., and Clifton, P. M. (2001). Short-chain fatty acids and human colonic function: roles of resistant starch and nonstarch polysaccharides. *Physiol. Rev.* 81, 1031–1064. doi: 10.1152/physrev.2001.81.3.1031

Wang, Q., Liu, S., Zhai, A., Zhang, B., and Tian, G. (2018). AMPK-mediated regulation of lipid metabolism by phosphorylation. *Biol. Pharm. Bull.* 41, 985–993. doi: 10.1248/bpb.b17-00724

Wang, Y., Yao, W., Li, B., Qian, S., Wei, B., Gong, S., et al. (2020). Nuciferine modulates the gut microbiota and prevents obesity in high-fat diet-fed rats. *Exp. Mol. Med.* 52, 1959–1975. doi: 10.1038/s12276-020-00534-2

Wang, Z., Yuan, D., Duan, Y., Li, S., and Hou, S. (2018). Key factors involved in obesity development. *Eat. Weight Disord.* 23, 267–274. doi: 10.1007/s40519-017-0428-3

Wheatley, S. M., El-Kadi, S. W., Suryawan, A., Boutry, C., Orellana, R. A., Nguyen, H. V., et al. (2014). Protein synthesis in skeletal muscle of neonatal pigs is enhanced by administration of beta-hydroxy-beta-methylbutyrate. *Am. J. Physiol. Endocrinol. Metab.* 306, E91–E99.

Wilson, J. M., Grant, S. C., Lee, S. R., Masad, I. S., Park, Y. M., Henning, P. C., et al. (2012). Beta-hydroxy-beta-methyl-butyrate blunts negative age-related changes in body composition, functionality and myofiber dimensions in rats. *J. Int. Soc. Sports Nutr.* 9:18. doi: 10.1186/1550-2783-9-18

Xu, P., Wang, J., Hong, F., Wang, S., Jin, X., Xue, T., et al. (2017). Melatonin prevents obesity through modulation of gut microbiota in mice. *J. Pineal. Res.* 62:e12399. doi: 10.1111/jpi.12399

Yamashita, H. (2016). Biological function of acetic acid-improvement in obesity and glucose tolerance by acetic acid in type 2 diabetic rats. *Crit. Rev. Food. Sci. Nutr.* 56 (Suppl. 1), S171–S175.

Yamashita, H., Fujisawa, K., Ito, E., Idei, S., Kawaguchi, N., Kimoto, M., et al. (2007). Improvement of obesity and glucose tolerance by acetate in type 2 diabetic Otsuka Long-Evans Tokushima Fatty (OLETF) rats. *Biosci. Biotechnol. Biochem.* 71, 1236–1243. doi: 10.1271/bbb.60668

Yamashita, H., Maruta, H., Jozuka, M., Kimura, R., Iwabuchi, H., Yamato, M., et al. (2009). Effects of acetate on lipid metabolism in muscles and adipose tissues of type 2 diabetic Otsuka Long-Evans Tokushima Fatty (OLETF) rats. *Biosci. Biotechnol. Biochem.* 73, 570–576. doi: 10.1271/bbb.80634

Yang, Y., Wu, Z., Meininger, C. J., and Wu, G. (2015). L-Leucine and NO-mediated cardiovascular function. *Amino Acids* 47, 435–447. doi: 10.1007/s00726-014-1904-y

Yao, K., Duan, Y., Li, F., Tan, B., Hou, Y., Wu, G., et al. (2016). Leucine in obesity: therapeutic prospects. *Trends Pharmacol. Sci.* 37, 714–727. doi: 10.1016/j.tips.2016.05.004

Yin, J., Li, Y., Han, H., Chen, S., Gao, J., Liu, G., et al. (2018). Melatonin reprogramming of gut microbiota improves lipid dysmetabolism in high-fat diet-fed mice. *J. Pineal. Res.* 65:e12524. doi: 10.1111/jpi.12524

Yin, Y. L., McEvoy, J., Schulze, H., Hennig, U., Souffrant, W.-B., and McCracken, K. (2000). Apparent digestibility (ileal and overall) of nutrients and endogenous nitrogen losses in growing pigs fed wheat (var. Soissons) or its by-products without or with xylanase supplementation. *Live. Prod. Sci.* 62, 119–132. doi: 10.1016/s0301-6226(99)00129-3

Zeng, H., Larson, K. J., Cheng, W. H., Bukowski, M. R., Safratowich, B. D., Liu, Z., et al. (2020). Advanced liver steatosis accompanies an increase in hepatic inflammation, colonic, secondary bile acids and Lactobacillaceae/Lachnospiraceae bacteria in C57BL/6 mice fed a high-fat diet. *J. Nutr. Biochem.* 78:108336. doi: 10.1016/j.jnutbio.2019.108336

Zhang, L., Li, F., Guo, Q., Duan, Y., Wang, W., Yang, Y., et al. (2021). Different proportions of branched-chain amino acids modulate lipid metabolism in a finishing pig model. *J. Agric. Food. Chem.* 69, 7037–7048. doi: 10.1021/acs.jafc.1c02001

Zhang, L., Li, F., Guo, Q., Duan, Y., Wang, W., Zhong, Y., et al. (2020). Leucine supplementation: a novel strategy for modulating lipid

metabolism and energy homeostasis. *Nutrients* 12:1299. doi: 10.3390/nu12051299

Zhang, L., Shi, M., Ji, J., Hu, X., and Chen, F. (2019). Gut microbiota determines the prevention effects of *Luffa cylindrica* (L.) roem supplementation against obesity and associated metabolic disorders induced by high-fat diet. *FASEB J.* 33, 10339–10352. doi: 10.1096/fj.201900488r

Zheng, C., Song, B., Guo, Q., Zheng, J., Li, F., Duan, Y., et al. (2021). Alterations of the muscular fatty acid composition and serum metabolome in bama xiang mini-pigs exposed to dietary beta-hydroxy beta-methyl butyrate. *Animals* 11:1190. doi: 10.3390/ani11051190

Zheng, J., Xiao, H., Duan, Y., Song, B., Zheng, C., Guo, Q., et al. (2021). Roles of amino acid derivatives in the regulation of obesity. *Food Funct.* 12, 6214–6225. doi: 10.1039/d1fo00780g

Zhong, Y., Song, B., Zheng, C., Zhang, S., Yan, Z., Tang, Z., et al. (2020). Flavonoids from mulberry leaves alleviate lipid dysmetabolism in high fat diet-fed mice: involvement of gut microbiota. *Microorganisms* 8:860. doi: 10.3390/microorganisms8060860

Conflict of Interest: The authors declare that the research was conducted in the absence of any commercial or financial relationships that could be construed as a potential conflict of interest.

Publisher's Note: All claims expressed in this article are solely those of the authors and do not necessarily represent those of their affiliated organizations, or those of the publisher, the editors and the reviewers. Any product that may be evaluated in this article, or claim that may be made by its manufacturer, is not guaranteed or endorsed by the publisher.

frontiers in Microbiology

MINI REVIEW
published: 16 August 2021
doi: 10.3389/fmicb.2021.716667

Advances in the Relationships Between Cow's Milk Protein Allergy and Gut Microbiota in Infants

Yudie Yang[1], Xiaoqi Li[1], Ying Yang[2], Saeed Shoaie[3,4], Cheng Zhang[1,3], Boyang Ji[5] and Yongjun Wei[1,6]**

[1] Key Laboratory of Advanced Drug Preparation Technologies, Ministry of Education, School of Pharmaceutical Sciences, Henan Children's Hospital, Zhengzhou Children's Hospital, Children's Hospital Affiliated to Zhengzhou University, Zhengzhou University, Zhengzhou, China, [2] Jing'an District Central Hospital of Shanghai, Jing'an Branch, Huashan Hospital, Fudan University, Shanghai, China, [3] Science for Life Laboratory, KTH Royal Institute of Technology, Stockholm, Sweden, [4] Faculty of Dentistry, Oral and Craniofacial Sciences, Centre for Host-Microbiome Interactions, King's College London, London, United Kingdom, [5] Department of Biology and Biological Engineering, Chalmers University of Technology, Gothenburg, Sweden, [6] Laboratory of Synthetic Biology, Zhengzhou University, Zhengzhou, China

Cow's milk protein allergy (CMPA) is an immune response to cow's milk proteins, which is one of the most common food allergies in infants and young children. It is estimated that 2–3% of infants and young children have CMPA. The diet, gut microbiota, and their interactions are believed to be involved in the alterations of mucosal immune tolerance, which might lead to the development of CMPA and other food allergies. In this review, the potential molecular mechanisms of CMPA, including omics technologies used for analyzing microbiota, impacts of early microbial exposures on CMPA development, and microbiota–host interactions, are summarized. The probiotics, prebiotics, synbiotics, fecal microbiota transplantation, and other modulation strategies for gut microbiota and the potential application of microbiota-based design of diets for the CMPA treatment are also discussed. This review not only summarizes the current studies about the interactions of CMPA with gut microbiota but also gives insights into the possible CMPA treatment strategies by modulating gut microbiota, which might help in improving the life quality of CMPA patients in the future.

Keywords: cow's milk allergy, gut microbiota, probiotics, prebiotics, synthetic microbiota, fecal microbiota transplantation

OPEN ACCESS

Edited by:
Jia Yin,
Hunan Normal University, China

Reviewed by:
Dominika Lendvai-Emmert,
University of Pécs, Hungary
Flavio Tidona,
Council for Agricultural and Economics Research (CREA), Italy

****Correspondence:***
Yongjun Wei
yongjunwei@zzu.edu.cn
Boyang Ji
boyang.ji@chalmers.se

Specialty section:
This article was submitted to Microbial Symbioses, a section of the journal Frontiers in Microbiology

Received: *29 May 2021*
Accepted: *22 July 2021*
Published: *16 August 2021*

Citation:
Yang Y, Li X, Yang Y, Shoaie S, Zhang C, Ji B and Wei Y (2021) Advances in the Relationships Between Cow's Milk Protein Allergy and Gut Microbiota in Infants. Front. Microbiol. 12:716667. doi: 10.3389/fmicb.2021.716667

INTRODUCTION

Food allergy has become a major public health issue worldwide. The prevalence of food allergies has been growing steadily, affecting 3–6% of the United States population (Sicherer and Sampson, 2014). Cow's milk protein allergy (CMPA) is one of the most common food allergies in early childhood, affecting 2–3% of the children under 3 years of age (Sicherer, 2011; Savage and Johns, 2015). Besides, 1% of adults show severe allergic reactions related to milk consumption (Nwaru et al., 2014; Schocker et al., 2019). CMPA is an immune response to cow's milk proteins derived from the infant formula. The infants suffering from CMPA cannot consume cow's milk and need amino acid-based formula (AAF) or extensively hydrolyzed casein formula (EHCF). However, some infants are intolerant to AAF and EHCF. Therefore, CMPA decreases the life quality of infants, affects their health, and causes financial burdens to their families (Vanderhoof and Kleinman, 2015).

Altogether, the exploration of the molecular mechanisms of CMPA might be a crucial step to developing cost-effective treatment strategies for CMPA.

Based on the immune responses, CMPA can be classified into three types, including the non-immunoglobulin E (IgE)-mediated CMPA, IgE-mediated CMPA, and mixed CMPA. The IgE-mediated CMPA is the most common form of CMPA (Wiley et al., 2015), which often occurs at the first-time exposure of infants to cow' milk (infant formula or other foods, containing cow's milk or cereal). It could be diagnosed when the infants have a history of immediate, acute, and objective symptoms within 2 h after the ingestion of dairy products (D'Auria and Venter, 2020; Munblit et al., 2020). Within 2 h of the exposure, the infants with IgE-mediated CMPA experience erythema, angioedema, urticaria, vomiting, lethargy, or respiratory symptoms, which can vanish soon and happen again upon exposure to cow's milk. In contrast, the non-IgE-mediated CMPA occurs without stable symptoms and no efficient diagnostic methods are available (Flom and Sicherer, 2019). The non-IgE-mediated CMPA appears at least 2 h after exposure to cow's milk, which is usually accompanied by the food protein-induced enterocolitis syndrome, allergic proctocolitis, chronic cutaneous, or gastrointestinal symptoms. Since the symptoms are similar to the other infant diseases, the delayed diagnosis and misdiagnosis of non-IgE-mediated CMPA are common in clinical practices (Munblit et al., 2020). The mixed CMPA is a combination of the IgE- and non-IgE-mediated CMPA and is sophisticated in diagnosis and treatment. Therefore, the investigation of its molecular mechanisms is necessary for effective treatment.

GUT MICROBIOTA IN EARLY CHILDHOOD

Human bodies are colonized by various microorganisms, the most influential of which is gut microbiota (Sprockett et al., 2018). The wide applications of next-generation sequencing (NGS) technologies have potentiated the investigation of the structure and function of gut microbiota in a cost-effective way (Berni Canani et al., 2019; Liu et al., 2021). The 16S rRNA gene sequencing technology is used to identify the composition of gut microbiota at the genus and phylum levels, while the shotgun metagenomic analysis and other strategies are used to explore the taxonomic and functional compositions of gut microbiota at species or strain level (**Supplementary Figure 1**; Bunyavanich and Berin, 2019). The differences at the strain-level diversity of microbiota have shown distinct effects on the host phenotypes (Chen et al., 2018). Therefore, the understanding of interspecies diversity is important for the development of microbiome-based biomarkers linked to human health and disease (Bunyavanich and Berin, 2019). The integration of multi-omics technologies, including genomics, epigenomics, transcriptomics, proteomics, metabolomics, and microbiome, can help in the investigation, characterization, and quantification of microorganisms in human gut microbiota, giving insights into the interactions between host and its gut microbiota (Dhondalay et al., 2018; Shi et al., 2020). Based on the functional properties and microbial associations, the potential microbial biomarkers can be identified and the personalized medicine protocols, including drugs, live probiotics, and microbial metabolites, can be designed for treatment purposes (Sicherer and Sampson, 2018; Berni Canani et al., 2019).

The microbiota has close interactions with the homeostasis of immune response and various interconnections with the host metabolic pathways (Conway and Boddy, 2013; Gensollen et al., 2016). The microbial colonization in early life strongly affects humans' health and diseases for their whole lifetime (Turnbaugh et al., 2009; Benson et al., 2010; Gensollen et al., 2016). The gut microbiota changes dramatically during the first year of life and is relatively stable and mature after 3 years of age (Yatsunenko et al., 2012; Stewart et al., 2018). The maturation of gut microbiome can be divided into the developmental phase (months 3–14), transitional phase (months 15–30), and stable phase (months 31–46) (Stewart et al., 2018). Understanding the colonization process of gut microbiota in early life is critical for further understanding CMPA and other food allergies. The total amounts of gut microbes (especially anaerobic microbes) in children with CMPA are relatively higher as compared to those of healthy children (Bunyavanich and Schadt, 2015). The composition of gut microbiota at the age of 3–6 months was found to be associated with milk allergy by the age of 8 years with the enrichment of class Clostridia and phylum Firmicutes in the infant's gut microbiota (Bunyavanich et al., 2016). Moreover, a recent study has shown that the newborns, who developed IgE-mediated allergic sensitization by 1 year of their age, exhibited less diverse gut metabolic activities at their birth, and the specific metabolic clusters were associated with the abundance of key taxa, driving the maturation of gut microbiota (Petersen et al., 2021).

The progression of microbiota is associated with various perinatal characteristics, such as mode of delivery, type of feeding, lifestyle, antibiotic usage, and geographic distribution (Adak and Khan, 2019). The mode of delivery affects the initial infant's gut microbiota (Biasucci et al., 2010; Wampach et al., 2018) and maturation (Chu et al., 2017). The vaginally delivered newborns mainly obtain their gut microbiota from the mother's vaginal microbiota, and the gut microbiota is mainly composed of the genera *Lactobacillus* and *Prevotella*; on the other hand, the gut microbiota of cesarean section-delivered newborns is similar to the skin microbiota, which is mainly composed of the genera *Staphylococcus*, *Corynebacterium*, and *Propionibacterium* (Dominguez-Bello et al., 2010; Tamburini et al., 2016). After birth, the microorganisms from the mother and the surrounding environments colonize rapidly (Vandenplas et al., 2020) and some opportunistic pathogens might also colonize the infants' gut, causing infections (Shao et al., 2019). The initial gut microbiota subsequently affects child health, and the cesarean section-delivered newborns might have a higher risk of food allergies and other diseases (Arrieta et al., 2015; Rachid and Chatila, 2016). Moreover, the metabolic maturation of infants' gut microbiota can be predicted by the feeding types and maternal gestational weight gain (Bäckhed et al., 2015; Baumann-Dudenhoeffer et al., 2018). Further insights into the development of an infant's gut microbiota suggested that it was affected by diverse environmental factors, including diet, breastfeeding,

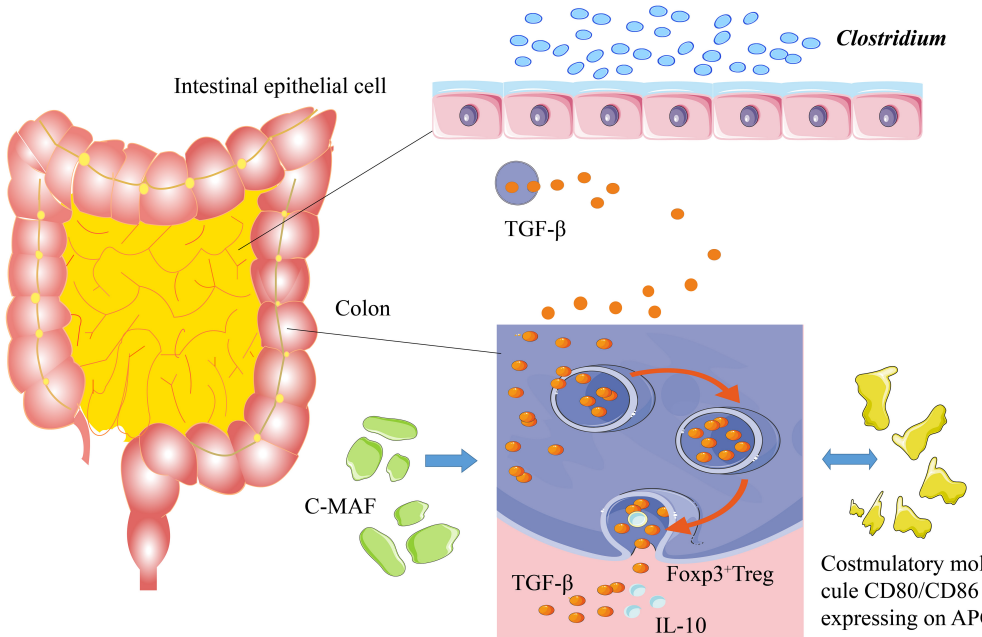

FIGURE 1 | Mechanism of immune tolerance. Some *Clostridium* species stimulate the intestines to secrete TGF-β. TGF-β can induce Foxp3$^+$ Treg cells in the colon to secrete IL-10, thereby promoting immune tolerance. c-MAF, a T cell transcription factor, is the key factor to sustain the stability of gut microbiota. The costimulatory molecules of CD80/CD86, which are expressed on the antigen-presenting cells, stimulate the secretion of TGF-β and IL-10.

and antibiotics (Bokulich et al., 2016; Yassour et al., 2016; Bazanella et al., 2017), and the gut microbiota was not mature even at the age of 5 (Roswall et al., 2021).

MICROBIOTA–HOST INTERACTIONS AND CMPA

A healthy immune system is tolerant to self-antigens and only shows allergic reactions to the foreign antigens, such as pathogens (Stephen-Victor and Chatila, 2019). The food-allergic infants are sensitive to the specific food antigens with the assistance of a pathogenic T-helper 2 (Th2) response (Johnston et al., 2014). Dendritic cells (DCs) and specific antigen-presenting cells (APCs) are widely distributed in the human body, playing essential roles in immune responses. Usually, the DCs can identify and process foreign antigens, as well as the injured host cells, thereby inducing juvenile T cells to activate the adaptive immune responses. On the other hand, the DC can limit the response of effector cells by developing central and peripheral tolerance (Qian and Cao, 2018). The gut-draining lymph nodes (gLNs) show distinct immune functions in the different areas of the gut. The gene expression of DC in gLNs is diverse, resulting in different immune responses against the same antigen. The gLNs can determine the host's adaptive immune responses *via* the compartmentalization of the gut into segments for different antigens (Esterhazy et al., 2019). The DC promotes immune tolerance by inducing and inhibiting T cell response, accelerating apoptosis, and producing regulatory T (Treg) cells (Kushwah and Hu, 2011). Unlike the Treg cells in other organs, the intestinal Treg antigen receptor (TCR) can inhibit the immune responses to harmless antigens and symbiotic microbiota in diet (Tanoue et al., 2016). The regulation of Treg cells in intestinal immunity at a steady state is essential for sustaining tolerogenic response by adaptive immunity. Some species in the *Clostridium* genus or other species can induce the generation of colonic Foxp3$^+$ Treg cells by transforming growth factor-beta (TGF-β). Meanwhile, the CD80/86 proteins expressed by the Treg cells can inhibit CD28 of effector T cells by releasing TGF-β and interleukin-10 (IL-10) to mediate the immune tolerance (**Figure 1**; Russler-Germain et al., 2017).

Intestinal Treg cells, especially the Foxp3$^+$ Treg cells, are critical for maintaining the balance of gut microbiota and the physiological stability of the intestinal tract (Fujimura et al., 2016). The interaction of gut microbiota with intestinal Treg cells requires the regulation of c-MAF (T cell transcription factor), and a deficiency in c-MAF would lead to severe diseases related to the disorder of gut microbiota (Campbell et al., 2018; Xu et al., 2018; Neumann et al., 2019). In addition, the short-chain fatty acids (SCFAs), generated by the gut microbiota, can increase the number of Treg cells in the colon and enhance their ability to secrete IL-10 (Smith et al., 2013; Russler-Germain et al., 2017). IL-22 protects the integrity of the intestinal epithelial barrier and reduces the intestinal permeability of dietary antigens (Brandl et al., 2021). The germ-free mice, colonized with genus *Clostridium*, produced a great amount of IL-22 and reduced the number of allergens entering the bloodstream; the introduction of some *Clostridium* species into gut microbiota alleviated the host allergen sensitization (**Figure 1**; Stefka et al., 2014). The gut microbiota maintains tolerance to dietary antigens by mediating

a protective response to the intestinal epithelial barrier. For example, as a local Ig, IgA protects intestinal mucosa through interacting with gut microbiota and antigenic rejection, thereby participating in immune tolerance (Stefka et al., 2014; Donaldson et al., 2018).

MICROBIAL INTERACTIONS AND CMPA

The early-life gut microbiota of infants is associated with the development of the immune system. Several pieces of evidence showed that the development of gut microbiota was associated with the level of IgE, thereby increasing the occurrence of allergy (Sarkar et al., 2021). Therefore, the development of gut microbiota is essential for stimulating the immune system (Cahenzli et al., 2013). The transmission of gut microbiota from mother to infant could help in the development of proper gut microbiota, and the strain-level microbial profiling revealed that the infant's gut microbiota shifted from maternal vaginal microbiota to distinct maternal sources with selections after birth (Ferretti et al., 2018). The diets have a major impact on the establishment of early-life gut microbiota. The breast-feeding bacteria, such as *Streptococcus* spp. and *Veillonella dispar*, transferred from breast milk to infant gut microbiota, which influenced its development (Di Luccia et al., 2020). Although the gut microbiota of infants is dynamic and variable, it has similar trajectories and different maturation paces (Bäckhed et al., 2015; Weström et al., 2020; Roswall et al., 2021). Moreover, the under-nutrition states affected the response of oral cholera vaccination, suggesting that the diets have global effects on the immune system and might interact with allergy, including CMPA (Di Luccia et al., 2020).

The gut microbiota protects the intestinal barrier and mediates immune tolerance by secreting active metabolites, such as inosine and SCFAs (Mager et al., 2020; Yang et al., 2020), while food provides nutrients and habitat for the microbes (Ma et al., 2017). The gut microbiota of the infants with CMPA was introduced into the germ-free mice, which showed lower sensitivity to the allergic materials of cow's milk (Feehley et al., 2019), suggesting the potential microbial involvement in the development of CMPA. As compared to that of healthy children, the gut microbiota of the children with CMPA showed enrichment in the relative abundance of families Trichocomaceae and Ruminococcaceae as well as genera *Bacteroides* and *Alistipes* while a decrease in that of genus *Bifidobacterium*, suggesting that the gut microbiota of children with CMPA might be under imbalanced state (Berni Canani et al., 2018; Mauras et al., 2019). A long-term investigation of gut microbiota of children with CMPA showed that the children that recovered from CMPA had enriched Clostridia and Firmicutes, and further metagenomic analyses predicted that their gut microbiota had decreased ability of fatty acid metabolism (Bunyavanich et al., 2016).

PROBIOTICS, PREBIOTICS, AND CMPA

A low amount of whey was absorbed by the epithelium, most of which was transferred to the Peyer's patches, suggesting that the physicochemical features of proteins could affect allergic responses (Graversen et al., 2020). In order to alleviate or avoid CMPA, the AAF and deep hydrolyzed milk powder were used as the main food for infants and children with CMPA. Moreover, cow's milk after heat treatment or being processed by other ways was used for the feeding of infants with CMPA; however, these strategies could not cure CMPA directly (Geiselhart et al., 2021). Avoiding the allergens in food or other materials is difficult in daily life. Therefore, the transfer from food avoidance to active treatment is essential. Omalizumab and oral immunotherapy have been used for treating IgE-mediated food allergy, which has shown the potential to be used for CMPA treatment (Inuo et al., 2018; Costa et al., 2020). Nowadays, a few other active treatment strategies, such as probiotics and prebiotics (Qamer et al., 2019), transplantation of fecal microbiota (Feehley et al., 2019), and precise personalized designed diets, have been developed for the treatment of infants with CMPA (**Figure 2**).

Probiotics are defined as live microorganisms, which are beneficial for the host's health. They modulate the structure and function of gut microbiota and interact with the enterocytes through decreasing gut permeability, enhancing mucus thickness, stimulating secretory immunoglobulin A, and producing defensin (Maldonado Galdeano et al., 2019). Moreover, probiotics can modulate the cytokine's response by immune cells and help in preventing allergies (Berni Canani et al., 2012, 2016; Hardy et al., 2013; Hill et al., 2014; Muraro et al., 2014). Therefore, probiotics and prebiotics have been used for the prevention and treatment of food allergy *via* the modulation of gut microbiota and immune system (**Figure 2A**; D'Auria et al., 2019). The supplementation of *Lactobacillus* and *Bifidobacterium* species has been used in a practical treatment for CMPA, which accelerated the immune tolerance to cow's milk in infants with CMPA (Hol et al., 2008; Berni Canani et al., 2012). A randomized, double-blind, and placebo-controlled trial indicated that the probiotics *Lactobacillus rhamnosus* and *Lactobacillus casei* strains could improve the symptoms of infants with CMPA (Cukrowska et al., 2021). A meta-analysis suggested that probiotics could improve the symptoms of CMPA, but there was no evidence of improving tolerance to cow's milk (Berni Canani et al., 2017; Tan-Lim and Esteban-Ipac, 2018). The tolerance to cow's milk can be developed if the infants with CMPA can use extensively hydrolyzed formula containing *L. rhamnosus* GG (LGG) (Berni Canani et al., 2012). The LGG is a butyrate producer, which might modulate the expression of genes involved in the allergic pathway, to improve the tolerance to cow's milk proteins (Berni Canani et al., 2012, 2013; Elce et al., 2017; Nocerino et al., 2019). Moreover, the supplementation of *L. rhamnosus* LA305, *Lactobacillus salivarius* LA307, or *Bifidobacterium longum* subsp. to CMPA-mouse models altered the gut microbiota at the species level and immune responses, which led to the acquisition of tolerance to some food allergies (Esber et al., 2020). However, further assessment of the probiotics supplementation effect on the development of immune tolerance is necessary before the clinical application.

Prebiotics are beneficial substances, which promote the performance of the indigenous microorganisms and host immune system (Hardy et al., 2013; Hill et al., 2014).

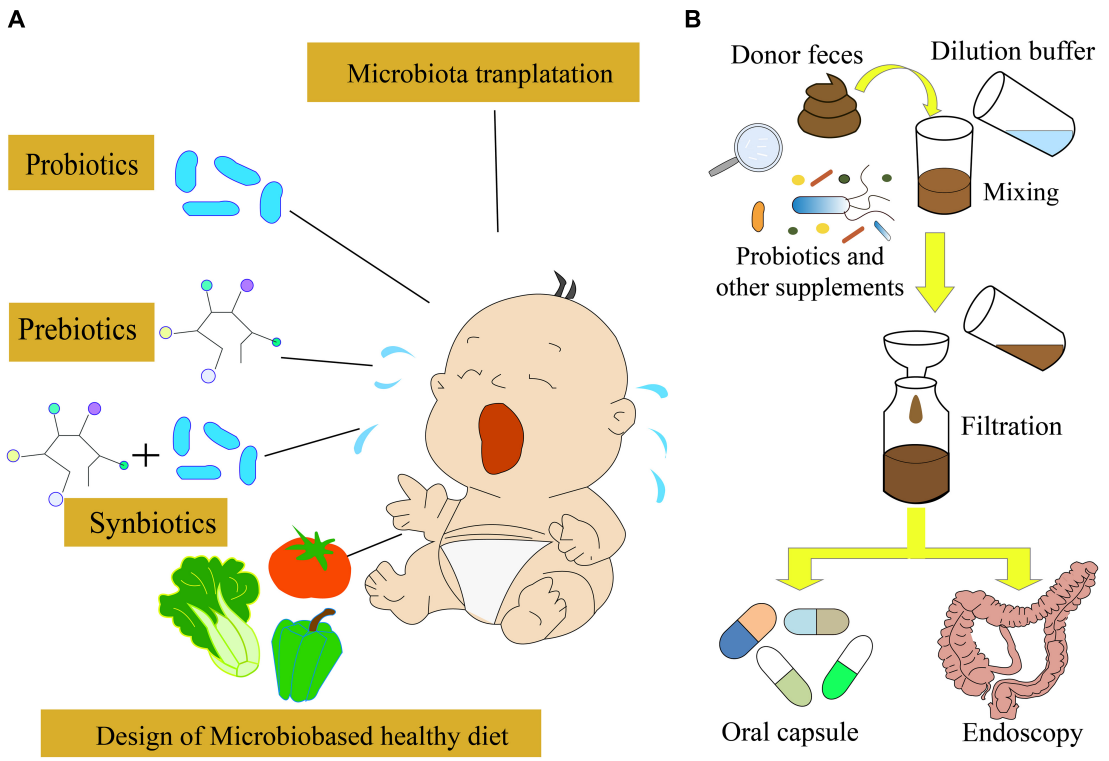

FIGURE 2 | Different strategies for CMPA treatment. **(A)** Probiotics, prebiotics, and synbiotics are often used for CMPA treatment. In the future, the microbiota-targeted design of a healthy diet might be possible to treat CMPA infants. **(B)** Fecal microbiota transplantation strategy used for CMPA treatment.

They are abundant in human breast milk and include galactooligosaccharides (GOS), fructooligosaccharides (FOS), 2′-fucosyllactose, and lacto-*N*-neo-tetraose. They have direct effects on the host by interacting with the host epithelial barrier and indirect effects via the metabolites (Miqdady et al., 2020). They also act as the energy and nutrient sources for selective fermentation by resident health-promoting microorganisms in the gastrointestinal tract, which can protect against pathogens, improve intestinal barrier function, and orchestrate immune pathways (Parnell and Reimer, 2012; Wasilewski et al., 2015).

A mixture of prebiotics could reduce the incidence of allergic responses before 2 years of life and had long-term immune-modulating effects (Arslanoglu et al., 2008). Prebiotics also showed preventive effects in allergy and promoted a tolerogenic environment (Brosseau et al., 2019). The supplementation of prebiotics has been suggested as an effective intervention strategy to treat allergic disorders (Sestito et al., 2020). Although the use of prebiotics has positive effects on the improvement of allergic responses, available evidence is insufficient. Therefore, further global and rigorous studies with randomized, double-blind, and placebo-controlled designs are necessary before the recommendation of any prebiotic as a routine supplementation for the prevention of allergy in formula-fed food. Synbiotics are combinations of useful probiotics and prebiotics, which provide a synergistic effect on human health (Markowiak and Śliżewska, 2017). Compared to probiotics and prebiotics, the design of proper synbiotics would enrich specific taxa in gut microbiota and provide long-term benefits for CMPA infants (Phavichitr et al., 2021).

MICROBIOTA-TARGETED PREVENTION AND TREATMENT OF CMPA

As previously described, the gut microbiota is associated with the occurrence of allergic reactions (Shu et al., 2019). A recent study showed that the gut microbiota of cesarean section-delivered newborns was restored to the normal state similar to the vaginally delivered newborns by maternal fecal microbiota transplantation (FMT) (Korpela et al., 2020), suggesting that FMT can modulate infants' gut microbiota and might be a possible treatment strategy for CMPA (Albuhairi and Rachid, 2020). FMT is the transfer of normal gut microbiota from healthy people to patients, rebuilding the gut microbiota ecosystem (**Figure 2B**). It has been applied to treat several diseases, including inflammatory bowel disease (IBD), and *Clostridioides difficile* infection (CDI) (Mohajeri et al., 2018; Galan-Ros et al., 2020; Glassner et al., 2020; Zhang et al., 2020). The survival rate of IBD caused by CDI using the FMT strategy could reach 90% (Basson et al., 2020). The animal trials demonstrated that FMT could improve CMPA symptoms. However, the use of FMT for the CMPA treatment is still under development. As the gut microbiota of infants is immature (Stokholm et al., 2018; Moore and Townsend, 2019),

the curative effects of FMT on CMPA treatment need comprehensive evaluation.

Nowadays, the incidences of food allergy have been increased due to the alterations in genome–environment interaction and modern lifestyles (Loh and Tang, 2018). Diets play vital roles in food allergy and the development of CMPA, and the early dietary interventions have been proved to be an effective strategy to prevent food allergy (Du Toit et al., 2016). The introduction of solid food at the early life might reduce the incidence of food allergy (Caffarelli et al., 2018; Mastrorilli et al., 2020). High-fiber foods lead to the high level of SCFAs' release, which might enhance oral tolerance and protect the host from food allergy (Tan et al., 2016; Makki et al., 2018). In contrast, high-fat diet induces post-diet alteration in gut microbiota, which might increase the incidence of food allergy (Hussain et al., 2019). Moreover, the extensive casein formula, supplemented with LGG and EHCF which designed for the treatment of infants with CMPA, significantly increased the fecal butyrate levels, which increased the infants' tolerance to CMPA (Berni Canani et al., 2016) via the alteration of gut microbiota (Berni Canani et al., 2016).

A recent study showed that cranberries attenuated the impact of an animal-based diet to a less favorable profile (Rodríguez-Morató et al., 2018), suggesting that healthy food can induce changes in the composition and function of human gut microbiota. The baseline gut microbiota could affect the final diet intervention results based on a diet-induced weight-loss study, and the abundance of some microbial species, including *Ruminococcus gnavus*, *Akkermansia muciniphila*, *Blautia wexlerae*, and *Bacteroides dorei*, was found to be linked to the weight loss during diet interventions (Jie et al., 2021). Moreover, the changes in gut microbiota induced by the diet were temporary and the long-term dietary interventions are still unknown (Leeming et al., 2019). Therefore, the modulation of gut microbiota should consider the personal baseline microbiota and personalized responses to diets. The microbiota-based design of healthy food is crucial for the personalized nutrient supplementation strategy in the future (Fan and Pedersen, 2021). After understanding the keystone microbial taxa in infants with CMPA and diet–microbiota interactions, the design of personalized diets might contribute to the CMPA treatments (**Figure 2A**; Kolodziejczyk et al., 2019). With the development of synthetic biology and computational approaches, the intervention of engineered live microbiota that produces active molecules into infants with CMPA is a potential treatment strategy for CMPA via the integration of multi-omics data and clinical characteristics (Guan et al., 2020; Wang et al., 2020; Peng et al., 2021).

FUTURE PERSPECTIVES AND CONCLUSION

An insight into the gut microbiota of infants with CMPA and the identification of keystone taxa in its development are required for the diagnosis and treatment of CMPA. Moreover, current focus should be shifted from the descriptive CMPA gut microbiota to the cause-and-effect host–microbiota investigation, which will reveal the CMPA-related microbiota. The global profiling of long-term changes and the dietary intervention effects on gut microbiota are required for the dietary modulation of CMPA gut microbiota. Besides, the supplementation of probiotics, prebiotics, synbiotics, FMT, and microbiota-based design of a healthy diet is intrigued to implement for the treatment of CMPA in the future. Based on the relationship of gut microbiota and CMPA, the microorganism-based diagnosis and treatment strategies of CMPA might be developed soon, which may improve the health and life quality of CMPA infants.

AUTHOR CONTRIBUTIONS

YW and BJ conceived the study. YDY, XL, and YY drafted the manuscript. YDY prepared the figures. CZ and SS revised the manuscript. YW and BJ designed the whole study and revised the manuscript. All authors read, revised, and approved the manuscript.

FUNDING

This work was supported by Henan Provincial Key Laboratory of Children's Genetics and Metabolic Diseases Foundation (No. SS201909), the National Natural Science Foundation of China (Nos. 31800079 and 32111530179), and Clinical Laboratories, Shenyou Bio.

ACKNOWLEDGMENTS

We would like to thank TopEdit (www.topeditsci.com) for the English language editing of this manuscript.

SUPPLEMENTARY MATERIAL

The Supplementary Material for this article can be found online at: https://www.frontiersin.org/articles/10.3389/fmicb.2021.716667/full#supplementary-material

REFERENCES

Adak, A., and Khan, M. R. (2019). An insight into gut microbiota and its functionalities. *Cell. Mol. Life Sci.* 76, 473–493. doi: 10.1007/s00018-018-2943-4

Albuhairi, S., and Rachid, R. (2020). Novel therapies for treatment of food allergy. *Immunol. Allergy Clin. North Am.* 40, 175–186. doi: 10.1016/j.iac.2019.09.007

Arrieta, M. C., Stiemsma, L. T., Dimitriu, P. A., Thorson, L., Russell, S., Yurist-Doutsch, S., et al. (2015). Early infancy microbial and metabolic alterations affect risk of childhood asthma. *Sci. Transl. Med.* 7:307ra152. doi: 10.1126/scitranslmed.aab2271

Arslanoglu, S., Moro, G. E., Schmitt, J., Tandoi, L., Rizzardi, S., and Boehm, G. (2008). Early dietary intervention with a mixture of prebiotic oligosaccharides

reduces the incidence of allergic manifestations and infections during the first two years of life. *J. Nutr.* 138, 1091–1095. doi: 10.1093/jn/138.6.1091

Bäckhed, F., Roswall, J., Peng, Y., Feng, Q., Jia, H., Kovatcheva-Datchary, P., et al. (2015). Dynamics and Stabilization of the human gut microbiome during the first year of life. *Cell Host Microbe* 17, 690–703.

Basson, A. R., Zhou, Y., Seo, B., Rodriguez-Palacios, A., and Cominelli, F. (2020). Autologous fecal microbiota transplantation for the treatment of inflammatory bowel disease. *Transl. Res.* 226, 1–11. doi: 10.1016/j.trsl.2020.05.008

Baumann-Dudenhoeffer, A. M., D'souza, A. W., Tarr, P. I., Warner, B. B., and Dantas, G. (2018). Infant diet and maternal gestational weight gain predict early metabolic maturation of gut microbiomes. *Nat. Med.* 24, 1822–1829. doi: 10.1038/s41591-018-0216-2

Bazanella, M., Maier, T. V., Clavel, T., Lagkouvardos, I., Lucio, M., Maldonado-Gòmez, M. X., et al. (2017). Randomized controlled trial on the impact of early-life intervention with bifidobacteria on the healthy infant fecal microbiota and metabolome. *Am. J. Clin. Nutr.* 106, 1274–1286.

Benson, A. K., Kelly, S. A., Legge, R., Ma, F., Low, S. J., Kim, J., et al. (2010). Individuality in gut microbiota composition is a complex polygenic trait shaped by multiple environmental and host genetic factors. *Proc. Natl. Acad. Sci. U. S. A.* 107, 18933–18938. doi: 10.1073/pnas.1007028107

Berni Canani, R., De Filippis, F., Nocerino, R., Paparo, L., Di Scala, C., Cosenza, L., et al. (2018). Gut microbiota composition and butyrate production in children affected by non-IgE-mediated cow's milk allergy. *Sci. Rep.* 8:12500.

Berni Canani, R., Di Costanzo, M., Bedogni, G., Amoroso, A., Cosenza, L., Di Scala, C., et al. (2017). Extensively hydrolyzed casein formula containing *Lactobacillus rhamnosus* GG reduces the occurrence of other allergic manifestations in children with cow's milk allergy: 3-year randomized controlled trial. *J. Allergy Clin. Immunol.* 139, 1906–1913.e4.

Berni Canani, R., Nocerino, R., Terrin, G., Coruzzo, A., Cosenza, L., Leone, L., et al. (2012). Effect of Lactobacillus GG on tolerance acquisition in infants with cow's milk allergy: a randomized trial. *J. Allergy Clin. Immunol.* 129, 580–582.e5.

Berni Canani, R., Nocerino, R., Terrin, G., Frediani, T., Lucarelli, S., Cosenza, L., et al. (2013). Formula selection for management of children with cow's milk allergy influences the rate of acquisition of tolerance: a prospective multicenter study. *J. Pediatr.* 163, 771–777.e1.

Berni Canani, R., Paparo, L., Nocerino, R., Di Scala, C., Della Gatta, G., Maddalena, Y., et al. (2019). Gut microbiome as target for innovative strategies against food allergy. *Front. Immunol.* 10:191. doi: 10.3389/fimmu.2019.00191

Berni Canani, R., Sangwan, N., Stefka, A. T., Nocerino, R., Paparo, L., Aitoro, R., et al. (2016). *Lactobacillus rhamnosus* GG-supplemented formula expands butyrate-producing bacterial strains in food allergic infants. *ISME J.* 10, 742–750. doi: 10.1038/ismej.2015.151

Biasucci, G., Rubini, M., Riboni, S., Morelli, L., Bessi, E., and Retetangos, C. (2010). Mode of delivery affects the bacterial community in the newborn gut. *Early Hum. Dev.* 86(Suppl. 1), 13–15. doi: 10.1016/j.earlhumdev.2010.01.004

Bokulich, N. A., Chung, J., Battaglia, T., Henderson, N., Jay, M., Li, H., et al. (2016). Antibiotics, birth mode, and diet shape microbiome maturation during early life. *Sci. Transl. Med.* 8:343ra382.

Brandl, C., Bucci, L., Schett, G., and Zaiss, M. M. (2021). Crossing the barriers: revisiting the gut feeling in rheumatoid arthritis. *Eur. J. Immunol.* 51, 798–810. doi: 10.1002/eji.202048876

Brosseau, C., Selle, A., Palmer, D. J., Prescott, S. L., Barbarot, S., and Bodinier, M. (2019). Prebiotics: mechanisms and preventive effects in allergy. *Nutrients* 11:1841. doi: 10.3390/nu11081841

Bunyavanich, S., and Berin, M. C. (2019). Food allergy and the microbiome: current understandings and future directions. *J. Allergy Clin. Immunol.* 144, 1468–1477. doi: 10.1016/j.jaci.2019.10.019

Bunyavanich, S., and Schadt, E. E. (2015). Systems biology of asthma and allergic diseases: a multiscale approach. *J. Allergy Clin. Immunol.* 135, 31–42. doi: 10.1016/j.jaci.2014.10.015

Bunyavanich, S., Shen, N., Grishin, A., Wood, R., Burks, W., Dawson, P., et al. (2016). Early-life gut microbiome composition and milk allergy resolution. *J. Allergy Clin. Immunol.* 138, 1122–1130. doi: 10.1016/j.jaci.2016.03.041

Caffarelli, C., Di Mauro, D., Mastrorilli, C., Bottau, P., Cipriani, F., and Ricci, G. (2018). Solid food introduction and the development of food allergies. *Nutrients* 10:1790. doi: 10.3390/nu10111790

Cahenzli, J., Köller, Y., Wyss, M., Geuking, M. B., and Mccoy, K. D. (2013). Intestinal microbial diversity during early-life colonization shapes long-term IgE levels. *Cell Host Microbe* 14, 559–570. doi: 10.1016/j.chom.2013.10.004

Campbell, C., Dikiy, S., Bhattarai, S. K., Chinen, T., Matheis, F., Calafiore, M., et al. (2018). Extrathymically generated regulatory T cells establish a niche for intestinal border-dwelling bacteria and affect physiologic metabolite balance. *Immunity* 48, 1245–1257.e9.

Chen, Y. E., Fischbach, M. A., and Belkaid, Y. (2018). Skin microbiota-host interactions. *Nature* 553, 427–436. doi: 10.1038/nature25177

Chu, D. M., Ma, J., Prince, A. L., Antony, K. M., Seferovic, M. D., and Aagaard, K. M. (2017). Maturation of the infant microbiome community structure and function across multiple body sites and in relation to mode of delivery. *Nat. Med.* 23, 314–326. doi: 10.1038/nm.4272

Conway, K. R., and Boddy, C. N. (2013). ClusterMine360: a database of microbial PKS/NRPS biosynthesis. *Nucleic Acids Res.* 41, D402–D407.

Costa, C., Coimbra, A., Vitor, A., Aguiar, R., Ferreira, A. L., and Todo-Bom, A. (2020). Food allergy-from food avoidance to active treatment. *Scand. J. Immunol.* 91:e12824.

Cukrowska, B., Ceregra, A., Maciorkowska, E., Surowska, B., Zegadło-Mylik, M. A., Konopka, E., et al. (2021). The effectiveness of probiotic *Lactobacillus rhamnosus* and *Lactobacillus casei* strains in children with atopic dermatitis and cow's milk protein allergy: a multicenter, randomized, double blind, placebo controlled study. *Nutrients* 13:1169. doi: 10.3390/nu13041169

D'Auria, E., Salvatore, S., Pozzi, E., Mantegazza, C., Sartorio, M. U. A., Pensabene, L., et al. (2019). Cow's milk allergy: immunomodulation by dietary intervention. *Nutrients* 11:1399. doi: 10.3390/nu11061399

D'Auria, E., and Venter, C. (2020). Precision medicine in cow's milk allergy. *Curr. Opin. Allergy Clin. Immunol.* 20, 233–241. doi: 10.1080/00325481.1982.11716263

Dhondalay, G. K., Rael, E., Acharya, S., Zhang, W., Sampath, V., Galli, S. J., et al. (2018). Food allergy and omics. *J. Allergy Clin. Immunol.* 141, 20–29.

Di Luccia, B., Ahern, P. P., Griffin, N. W., Cheng, J., Guruge, J. L., Byrne, A. E., et al. (2020). Combined prebiotic and microbial intervention improves oral cholera vaccination responses in a mouse model of childhood undernutrition. *Cell Host Microbe* 27, 899–908.e5.

Dominguez-Bello, M. G., Costello, E. K., Contreras, M., Magris, M., Hidalgo, G., Fierer, N., et al. (2010). Delivery mode shapes the acquisition and structure of the initial microbiota across multiple body habitats in newborns. *Proc. Natl. Acad. Sci. U. S. A.* 107, 11971–11975. doi: 10.1073/pnas.1002601107

Donaldson, G. P., Ladinsky, M. S., Yu, K. B., Sanders, J. G., Yoo, B. B., Chou, W.-C., et al. (2018). Gut microbiota utilize immunoglobulin A for mucosal colonization. *Science* 360, 795–800. doi: 10.1126/science.aaq0926

Du Toit, G., Foong, R. X., and Lack, G. (2016). Prevention of food allergy – early dietary interventions. *Allergol. Int.* 65, 370–377. doi: 10.1016/j.alit.2016.08.001

Elce, A., Amato, F., Zarrilli, F., Calignano, A., Troncone, R., Castaldo, G., et al. (2017). Butyrate modulating effects on pro-inflammatory pathways in human intestinal epithelial cells. *Benef. Microbes* 8, 841–847. doi: 10.3920/bm2016.0197

Esber, N., Mauras, A., Delannoy, J., Labellie, C., Mayeur, C., Caillaud, M. A., et al. (2020). Three candidate probiotic strains impact gut microbiota and induce anergy in mice with cow's milk allergy. *Appl. Environ. Microbiol.* 86:e01203-20.

Esterhazy, D., Canesso, M. C. C., Mesin, L., Muller, P. A., De Castro, T. B. R., Lockhart, A., et al. (2019). Compartmentalized gut lymph node drainage dictates adaptive immune responses. *Nature* 569, 126–130. doi: 10.1038/s41586-019-1125-3

Fan, Y., and Pedersen, O. (2021). Gut microbiota in human metabolic health and disease. *Nat. Rev. Microbiol.* 19, 55–71. doi: 10.1038/s41579-020-0433-9

Feehley, T., Plunkett, C. H., Bao, R., Choi Hong, S. M., Culleen, E., Belda-Ferre, P., et al. (2019). Healthy infants harbor intestinal bacteria that protect against food allergy. *Nat. Med.* 25, 448–453. doi: 10.1038/s41591-018-0324-z

Ferretti, P., Pasolli, E., Tett, A., Asnicar, F., Gorfer, V., Fedi, S., et al. (2018). Mother-to-infant microbial transmission from different body sites shapes the developing infant gut microbiome. *Cell Host Microbe* 24, 133–145.e5.

Flom, J. D., and Sicherer, S. H. (2019). Epidemiology of cow's milk allergy. *Nutrients* 11:1051.

Fujimura, K. E., Sitarik, A. R., Havstad, S., Lin, D. L., Levan, S., Fadrosh, D., et al. (2016). Neonatal gut microbiota associates with childhood multisensitized atopy and T cell differentiation. *Nat. Med.* 22, 1187–1191. doi: 10.1038/nm.4176

Galan-Ros, J., Ramos-Arenas, V., and Conesa-Zamora, P. (2020). Predictive values of colon microbiota in the treatment response to colorectal cancer. *Pharmacogenomics* 21, 1045–1059. doi: 10.2217/pgs-2020-0044

Geiselhart, S., Podzhilkova, A., and Hoffmann-Sommergruber, K. (2021). Cow's milk processing—friend or foe in food allergy? *Foods* 10:572. doi: 10.3390/foods10030572

Gensollen, T., Iyer, S. S., Kasper, D. L., and Blumberg, R. S. (2016). How colonization by microbiota in early life shapes the immune system. *Science* 352, 539–544. doi: 10.1126/science.aad9378

Glassner, K. L., Abraham, B. P., and Quigley, E. M. M. (2020). The microbiome and inflammatory bowel disease. *J. Allergy Clin. Immunol.* 145, 16–27.

Graversen, K. B., Ballegaard, A. R., Kraemer, L. H., Hornslet, S. E., Sørensen, L. V., Christoffersen, H. F., et al. (2020). Cow's milk allergy prevention and treatment by heat-treated whey-A study in Brown Norway rats. *Clin. Exp. Allergy* 50, 708–721. doi: 10.1111/cea.13587

Guan, R., Wang, M., Guan, Z., Jin, C.-Y., Lin, W., Ji, X., et al. (2020). Metabolic engineering for glycyrrhetinic acid production in *Saccharomyces cerevisiae*. *Front. Bioeng. Biotechnol.* 8:588255. doi: 10.3389/fbioe.2020.588255

Hardy, H., Harris, J., Lyon, E., Beal, J., and Foey, A. D. (2013). Probiotics, prebiotics and immunomodulation of gut mucosal defences: homeostasis and immunopathology. *Nutrients* 5, 1869–1912. doi: 10.3390/nu5061869

Hill, C., Guarner, F., Reid, G., Gibson, G. R., Merenstein, D. J., Pot, B., et al. (2014). Expert consensus document. The international scientific association for probiotics and prebiotics consensus statement on the scope and appropriate use of the term probiotic. *Nat. Rev. Gastroenterol. Hepatol.* 11, 506–514. doi: 10.1038/nrgastro.2014.66

Hol, J., Van Leer, E. H., Elink Schuurman, B. E., De Ruiter, L. F., Samsom, J. N., Hop, W., et al. (2008). The acquisition of tolerance toward cow's milk through probiotic supplementation: a randomized, controlled trial. *J. Allergy Clin. Immunol.* 121, 1448–1454. doi: 10.1016/j.jaci.2008.03.018

Hussain, M., Bonilla-Rosso, G., Kwong Chung, C. K. C., Bäriswyl, L., Rodriguez, M. P., Kim, B. S., et al. (2019). High dietary fat intake induces a microbiota signature that promotes food allergy. *J. Allergy Clin. Immunol.* 144, 157–170.e8.

Inuo, C., Tanaka, K., Suzuki, S., Nakajima, Y., Yamawaki, K., Tsuge, I., et al. (2018). Oral immunotherapy using partially hydrolyzed formula for cow's milk protein allergy: a randomized, controlled trial. *Int. Arch. Allergy Immunol.* 177, 259–268. doi: 10.1159/000490804

Jie, Z., Yu, X., Liu, Y., Sun, L., Chen, P., Ding, Q., et al. (2021). The baseline gut microbiota directs dieting-induced weight loss trajectories. *Gastroenterology* 160, 2029–2042.e16.

Johnston, L. K., Chien, K. B., and Bryce, P. J. (2014). The immunology of food allergy. *J. Immunol.* 192, 2529–2534.

Kolodziejczyk, A. A., Zheng, D., and Elinav, E. (2019). Diet-microbiota interactions and personalized nutrition. *Nat. Rev. Microbiol.* 17, 742–753. doi: 10.1038/s41579-019-0256-8

Korpela, K., Helve, O., Kolho, K. L., Saisto, T., Skogberg, K., Dikareva, E., et al. (2020). Maternal fecal microbiota transplantation in cesarean-born infants rapidly restores normal gut microbial development: a proof-of-concept study. *Cell* 183, 324–334.e5.

Kushwah, R., and Hu, J. (2011). Role of dendritic cells in the induction of regulatory T cells. *Cell Biosci.* 1:20.

Leeming, E. R., Johnson, A. J., Spector, T. D., and Le Roy, C. I. (2019). Effect of diet on the gut microbiota: rethinking intervention duration. *Nutrients* 11:2862. doi: 10.3390/nu11122862

Liu, Y., Li, X., Yang, Y., Liu, Y., Wang, S., Ji, B., et al. (2021). Exploring potential gut microbiota in patients with colorectal disease based on 16S rRNA gene amplicon and metagenomics. *Front. Mol. Biosci.* 8:703638. doi: 10.3389/fmolb.2021.703638

Loh, W., and Tang, M. L. K. (2018). The epidemiology of food allergy in the global context. *Int. J. Environ. Res. Public Health* 15, 2043. doi: 10.3390/ijerph15092043

Ma, N., Tian, Y., Wu, Y., and Ma, X. (2017). Contributions of the interaction between dietary protein and gut microbiota to intestinal health. *Curr. Protein Pept. Sci.* 18, 795–808.

Mager, L. F., Burkhard, R., Pett, N., Cooke, N. C. A., Brown, K., Ramay, H., et al. (2020). Microbiome-derived inosine modulates response to checkpoint inhibitor immunotherapy. *Science* 369, 1481–1489. doi: 10.1126/science.abc3421

Makki, K., Deehan, E. C., Walter, J., and Bäckhed, F. (2018). The impact of dietary fiber on gut microbiota in host health and disease. *Cell Host Microbe* 23, 705–715. doi: 10.1016/j.chom.2018.05.012

Maldonado Galdeano, C., Cazorla, S. I., Lemme Dumit, J. M., Vélez, E., and Perdigón, G. (2019). Beneficial effects of probiotic consumption on the immune system. *Ann. Nutr. Metab.* 74, 115–124. doi: 10.1159/000496426

Markowiak, P., and Śliżewska, K. (2017). Effects of probiotics, prebiotics, and synbiotics on human health. *Nutrients* 9:1021. doi: 10.3390/nu9091021

Mastrorilli, C., Santoro, A., and Caffarelli, C. (2020). Primary prevention of allergic diseases: the role of early exposure to cow's milk formula. *Front. Pediatr.* 8:420. doi: 10.3389/fped.2020.00420

Mauras, A., Wopereis, H., Yeop, I., Esber, N., Delannoy, J., Labellie, C., et al. (2019). Gut microbiota from infant with cow's milk allergy promotes clinical and immune features of atopy in a murine model. *Allergy* 74, 1790–1793. doi: 10.1111/all.13787

Miqdady, M., Al Mistarihi, J., Azaz, A., and Rawat, D. (2020). Prebiotics in the infant microbiome: the past, present, and future. *Pediatr. Gastroenterol. Hepatol. Nutr.* 23, 1–14. doi: 10.5223/pghn.2020.23.1.1

Mohajeri, M. H., Brummer, R. J. M., Rastall, R. A., Weersma, R. K., Harmsen, H. J. M., Faas, M., et al. (2018). The role of the microbiome for human health: from basic science to clinical applications. *Eur. J. Nutr.* 57, 1–14. doi: 10.1007/s00394-018-1703-4

Moore, R. E., and Townsend, S. D. (2019). Temporal development of the infant gut microbiome. *Open Biol.* 9:190128. doi: 10.1098/rsob.190128

Munblit, D., Perkin, M. R., Palmer, D. J., Allen, K. J., and Boyle, R. J. (2020). Assessment of evidence about common infant symptoms and cow's milk allergy. *JAMA Pediatr.* 174, 599–608. doi: 10.1001/jamapediatrics.2020.0153

Muraro, A., Werfel, T., Hoffmann-Sommergruber, K., Roberts, G., Beyer, K., Bindslev-Jensen, C., et al. (2014). EAACI food allergy and anaphylaxis guidelines: diagnosis and management of food allergy. *Allergy* 69, 1008–1025.

Neumann, C., Blume, J., Roy, U., Teh, P. P., Vasanthakumar, A., Beller, A., et al. (2019). c-Maf-dependent Treg cell control of intestinal TH17 cells and IgA establishes host-microbiota homeostasis. *Nat. Immunol.* 20, 471–481. doi: 10.1038/s41590-019-0316-2

Nocerino, R., Di Costanzo, M., Bedogni, G., Cosenza, L., Maddalena, Y., Di Scala, C., et al. (2019). Dietary Treatment with extensively hydrolyzed casein formula containing the probiotic *Lactobacillus rhamnosus* GG prevents the occurrence of functional gastrointestinal disorders in children with cow's milk allergy. *J. Pediatr.* 213, e132.

Nwaru, B. I., Hickstein, L., Panesar, S. S., Muraro, A., Werfel, T., Cardona, V., et al. (2014). The epidemiology of food allergy in Europe: a systematic review and meta-analysis. *Allergy* 69, 62–75. doi: 10.1111/all.12305

Parnell, J. A., and Reimer, R. A. (2012). Prebiotic fibres dose-dependently increase satiety hormones and alter bacteroidetes and firmicutes in lean and obese JCR:LA-cp rats. *Br. J. Nutr.* 107, 601–613. doi: 10.1017/s0007114511003163

Peng, J., Wang, L., Wang, M., Du, R., Qin, S., Jin, C.-Y., et al. (2021). Yeast synthetic biology for the production of *Lycium barbarum* polysaccharides. *Molecules* 26:1641. doi: 10.3390/molecules26061641

Petersen, C., Dai, D. L. Y., Boutin, R. C. T., Sbihi, H., Sears, M. R., Moraes, T. J., et al. (2021). A rich meconium metabolome in human infants is associated with early-life gut microbiota composition and reduced allergic sensitization. *Cell Rep. Med.* 2:100260. doi: 10.1016/j.xcrm.2021.100260

Phavichitr, N., Wang, S., Chomto, S., Tantibhaedhyangkul, R., Kakourou, A., Intarakhao, S., et al. (2021). Impact of synbiotics on gut microbiota during early life: a randomized, double-blind study. *Sci. Rep.* 11:3534.

Qamer, S., Deshmukh, M., and Patole, S. (2019). Probiotics for cow's milk protein allergy: a systematic review of randomized controlled trials. *Eur. J. Pediatr.* 178, 1139–1149. doi: 10.1007/s00431-019-03397-6

Qian, C., and Cao, X. (2018). Dendritic cells in the regulation of immunity and inflammation. *Semin. Immunol.* 35, 3–11. doi: 10.1016/j.smim.2017.12.002

Rachid, R., and Chatila, T. A. (2016). The role of the gut microbiota in food allergy. *Curr. Opin. Pediatr.* 28, 748–753. doi: 10.1097/mop.0000000000000427

Rodríguez-Morató, J., Matthan, N. R., Liu, J., De La Torre, R., and Chen, C. O. (2018). Cranberries attenuate animal-based diet-induced changes in microbiota composition and functionality: a randomized crossover controlled feeding trial. *J. Nutr. Biochem.* 62, 76–86. doi: 10.1016/j.jnutbio.2018.08.019

Roswall, J., Olsson, L. M., Kovatcheva-Datchary, P., Nilsson, S., Tremaroli, V., Simon, M.-C., et al. (2021). Developmental trajectory of the healthy human gut microbiota during the first 5 years of life. *Cell Host Microbe* 29, 765–776.e3.

Russler-Germain, E. V., Rengarajan, S., and Hsieh, C. S. (2017). Antigen-specific regulatory T-cell responses to intestinal microbiota. *Mucosal Immunol.* 10, 1375–1386. doi: 10.1038/mi.2017.65

Sarkar, A., Yoo, J. Y., Valeria Ozorio Dutra, S., Morgan, K. H., and Groer, M. (2021). The association between early-life gut microbiota and long-term health and diseases. *J. Clin. Med.* 10:459. doi: 10.3390/jcm10030459

Savage, J., and Johns, C. B. (2015). Food allergy: epidemiology and natural history. *Immunol. Allergy Clin. North Am.* 35, 45–59.

Schocker, F., Kull, S., Schwager, C., Behrends, J., and Jappe, U. (2019). Individual sensitization pattern recognition to cow's milk and human milk differs for various clinical manifestations of milk allergy. *Nutrients* 11:1331. doi: 10.3390/nu11061331

Sestito, S., D'auria, E., Baldassarre, M. E., Salvatore, S., Tallarico, V., Stefanelli, E., et al. (2020). The role of prebiotics and probiotics in prevention of allergic diseases in infants. *Front. Pediatr.* 8:583946. doi: 10.3389/fped.2020.583946

Shao, Y., Forster, S. C., Tsaliki, E., Vervier, K., Strang, A., Simpson, N., et al. (2019). Stunted microbiota and opportunistic pathogen colonization in caesarean-section birth. *Nature* 574, 117–121. doi: 10.1038/s41586-019-1560-1

Shi, X., Wei, Y., and Ji, B. (2020). Systems biology of gastric cancer: perspectives on the omics-based diagnosis and treatment. *Front. Mol. Biosci.* 7:203. doi: 10.3389/fmolb.2020.00203

Shu, S. A., Yuen, A. W. T., Woo, E., Chu, K. H., Kwan, H. S., Yang, G. X., et al. (2019). Microbiota and food allergy. *Clin. Rev. Allergy Immunol.* 57, 83–97.

Sicherer, S. H. (2011). Epidemiology of food allergy. *J. Allergy Clin. Immunol.* 127, 594–602.

Sicherer, S. H., and Sampson, H. A. (2014). Food allergy: epidemiology, pathogenesis, diagnosis, and treatment. *J. Allergy Clin. Immunol.* 133, 291–307. quiz 308, doi: 10.1016/j.jaci.2013.11.020

Sicherer, S. H., and Sampson, H. A. (2018). Food allergy: a review and update on epidemiology, pathogenesis, diagnosis, prevention, and management. *J. Allergy Clin. Immunol.* 141, 41–58. doi: 10.1016/j.jaci.2017.11.003

Smith, P. M., Howitt, M. R., Panikov, N., Michaud, M., Gallini, C. A., Bohlooly, Y. M., et al. (2013). The microbial metabolites, short-chain fatty acids, regulate colonic Treg cell homeostasis. *Science* 341, 569–573. doi: 10.1126/science.1241165

Sprockett, D., Fukami, T., and Relman, D. A. (2018). Role of priority effects in the early-life assembly of the gut microbiota. *Nat. Rev. Gastroenterol. Hepatol.* 15, 197–205. doi: 10.1038/nrgastro.2017.173

Stefka, A. T., Feehley, T., Tripathi, P., Qiu, J., Mccoy, K., Mazmanian, S. K., et al. (2014). Commensal bacteria protect against food allergen sensitization. *Proc. Natl. Acad. Sci. U. S. A.* 111, 13145–13150. doi: 10.1073/pnas.1412008111

Stephen-Victor, E., and Chatila, T. A. (2019). Regulation of oral immune tolerance by the microbiome in food allergy. *Curr. Opin. Immunol.* 60, 141–147. doi: 10.1016/j.coi.2019.06.001

Stewart, C. J., Ajami, N. J., O'brien, J. L., Hutchinson, D. S., Smith, D. P., Wong, M. C., et al. (2018). Temporal development of the gut microbiome in early childhood from the TEDDY study. *Nature* 562, 583–588.

Stokholm, J., Blaser, M. J., Thorsen, J., Rasmussen, M. A., Waage, J., Vinding, R. K., et al. (2018). Maturation of the gut microbiome and risk of asthma in childhood. *Nat. Commun.* 9:141.

Tamburini, S., Shen, N., Wu, H. C., and Clemente, J. C. (2016). The microbiome in early life: implications for health outcomes. *Nat. Med.* 22, 713–722. doi: 10.1038/nm.4142

Tan, J., Mckenzie, C., Vuillermin, P. J., Goverse, G., Vinuesa, C. G., Mebius, R. E., et al. (2016). Dietary fiber and bacterial SCFA enhance oral tolerance and protect against food allergy through diverse cellular pathways. *Cell Rep.* 15, 2809–2824. doi: 10.1016/j.celrep.2016.05.047

Tan-Lim, C. S. C., and Esteban-Ipac, N. A. R. (2018). Probiotics as treatment for food allergies among pediatric patients: a meta-analysis. *World Allergy Organ. J.* 11:25. doi: 10.1186/s40413-018-0204-5

Tanoue, T., Atarashi, K., and Honda, K. (2016). Development and maintenance of intestinal regulatory T cells. *Nat. Rev. Immunol.* 16, 295–309. doi: 10.1038/nri.2016.36

Turnbaugh, P. J., Hamady, M., Yatsunenko, T., Cantarel, B. L., Duncan, A., Ley, R. E., et al. (2009). A core gut microbiome in obese and lean twins. *Nature* 457, 480–484. doi: 10.1038/nature07540

Vandenplas, Y., Carnielli, V. P., Ksiazyk, J., Luna, M. S., Migacheva, N., Mosselmans, J. M., et al. (2020). Factors affecting early-life intestinal microbiota development. *Nutrition* 78:110812. doi: 10.1016/j.nut.2020.110812

Vanderhoof, J. A., and Kleinman, R. E. (2015). Iron requirements for infants with cow milk protein allergy. *J. Pediatr.* 167, S36–S39.

Wampach, L., Heintz-Buschart, A., Fritz, J. V., Ramiro-Garcia, J., Habier, J., Herold, M., et al. (2018). Birth mode is associated with earliest strain-conferred gut microbiome functions and immunostimulatory potential. *Nat. Commun.* 9:5091.

Wang, M., Wei, Y., Ji, B., and Nielsen, J. (2020). Advances in Metabolic engineering of saccharomyces cerevisiae for cocoa butter equivalent production. *Front. Bioeng. Biotechnol.* 8:594081. doi: 10.3389/fbioe.2020.594081

Wasilewski, A., Zielinska, M., Storr, M., and Fichna, J. (2015). Beneficial effects of probiotics, prebiotics, synbiotics, and psychobiotics in inflammatory bowel disease. *Inflamm. Bowel Dis.* 21, 1674–1682. doi: 10.1097/mib.0000000000000364

Weström, B., Arévalo Sureda, E., Pierzynowska, K., Pierzynowski, S. G., and Pérez-Cano, F. J. (2020). The immature gut barrier and its importance in establishing immunity in newborn mammals. *Front. Immunol.* 11:1153. doi: 10.3389/fimmu.2020.01153

Wiley, A. S., Winberg, A., West, C. E., Strinnholm, Å, Nordström, L., Hedman, L., et al. (2015). Assessment of allergy to milk, egg, cod, and wheat in swedish schoolchildren: a population based cohort study. *Plos One* 10:e0131804. doi: 10.1371/journal.pone.0131804

Xu, M., Pokrovskii, M., Ding, Y., Yi, R., Au, C., Harrison, O. J., et al. (2018). c-MAF-dependent regulatory T cells mediate immunological tolerance to a gut pathobiont. *Nature* 554, 373–377. doi: 10.1038/nature25500

Yang, W., Yu, T., Huang, X., Bilotta, A. J., Xu, L., Lu, Y., et al. (2020). Intestinal microbiota-derived short-chain fatty acids regulation of immune cell IL-22 production and gut immunity. *Nat. Commun.* 11:4457.

Yassour, M., Vatanen, T., Siljander, H., Hämäläinen, A. M., Härkönen, T., Ryhänen, S. J., et al. (2016). Natural history of the infant gut microbiome and impact of antibiotic treatment on bacterial strain diversity and stability. *Sci. Transl. Med.* 8:343ra381.

Yatsunenko, T., Rey, F. E., Manary, M. J., Trehan, I., Dominguez-Bello, M. G., Contreras, M., et al. (2012). Human gut microbiome viewed across age and geography. *Nature* 486, 222–227. doi: 10.1038/nature11053

Zhang, L., Zhou, W., Zhan, L., Hou, S., Zhao, C., Bi, T., et al. (2020). Fecal microbiota transplantation alters the susceptibility of obese rats to type 2 diabetes mellitus. *Aging (Albany NY)* 12, 17480–17502. doi: 10.18632/aging.103756

Conflict of Interest: The authors declare that the research was conducted in the absence of any commercial or financial relationships that could be construed as a potential conflict of interest.

Publisher's Note: All claims expressed in this article are solely those of the authors and do not necessarily represent those of their affiliated organizations, or those of the publisher, the editors and the reviewers. Any product that may be evaluated in this article, or claim that may be made by its manufacturer, is not guaranteed or endorsed by the publisher.

frontiers in Microbiology

ORIGINAL RESEARCH
published: 18 August 2021
doi: 10.3389/fmicb.2021.727681

The Gut Microbiota-Bile Acids-TGR5 Axis Mediates *Eucommia ulmoides* Leaf Extract Alleviation of Injury to Colonic Epithelium Integrity

*Zhenya Zhai[1,2,3], Kai-Min Niu[1,2,3], Yichun Liu[1,4], Chong Lin[1,4] and Xin Wu[1,2,3,5]**

[1] *Jiangxi Functional Feed Additive Engineering Laboratory, Institute of Biological Resource, Jiangxi Academy of Sciences, Nanchang, China,* [2] *CAS Key Laboratory of Agro-ecological Processes in Subtropical Region, Institute of Subtropical Agriculture, Chinese Academy of Sciences, Changsha, China,* [3] *National Engineering Laboratory for Pollution Control and Waste Utilization in Livestock and Poultry Production, Changsha, China,* [4] *College of Animal Science and Technology, Jiangxi Agricultural University, Nanchang, China,* [5] *Tianjin Institute of Industrial Biotechnology, Chinese Academy of Sciences, Tianjin, China*

Eucommia ulmoides leaves (EL) are rich in phenolic acids and flavonoids, showing enhancing intestinal health effects. The intestinal microbiota-bile acid axis plays important roles in the occurrence and recovery of inflammatory bowel disease (IBD). However, whether EL extract (ELE) has regulatory effects on the intestinal microbiota, bile acid metabolism, and IBD is still unclear. To fill this gap, 2% dextran sulfate sodium (DSS)-induced mild IBD in a C57BL/6J mouse model that was treated with 200 or 400 mg/kg (intake dose/body weight) ELE was used. Oral ELE supplementation alleviated DSS-induced shortening of colon and colonic epithelial injury. Compared with the DSS group, ELE supplementation significantly decreased Toll-like receptor 4 (TLR4) and interlukin-6 (IL-6) and increased occludin and claudin-1 mRNA expression level in the colon ($p < 0.05$). Combined 16S rRNA gene sequencing and targeted metabolomic analyses demonstrated that ELE significantly improved the diversity and richness of the intestinal microbiota, decreased the abundance of *Bacteroidaceae*, and increased *Akkermansiaceae* and *Ruminococcaceae* abundance ($p < 0.05$) compared with DSS-induced IBD mice. Moreover, ELE significantly increased the serum contents of deoxycholic acid (DCA) and tauroursodeoxycholic acid (TUDCA), which were highly positively correlated with *Akkermansia* and unidentified_*Ruminococccaceae* relative to the DSS group. We then found that ELE increased Takeda G-protein coupled receptor 5 (TGR5), claudin-1, and occludin mRNA expression levels in the colon. In the Caco-2 cell model, we confirmed that activation of TGR5 improved the reduction in transepithelial electoral resistance (TEER) and decreased the permeability of FITC-dextran on monolayer cells induced by LPS ($p < 0.05$). siRNA interference assays showed that the decrease in TGR5 expression led to the decrease in TEER, an increase in FITC-dextran permeability, and a decrease in claudin-1 protein expression in Caco-2 cells. In summary, ELE alleviated IBD by influencing the intestinal microbiota structure

OPEN ACCESS

Edited by:
Jia Yin,
Hunan Normal University, China

Reviewed by:
Yu Pi,
China Agricultural University, China
Shad Mahfuz,
Sylhet Agricultural University, Bangladesh

***Correspondence:**
Xin Wu
wuxin@isa.ac.cn

Specialty section:
This article was submitted to Microbial Symbioses, a section of the journal Frontiers in Microbiology

Received: *19 June 2021*
Accepted: *09 July 2021*
Published: *18 August 2021*

Citation:
Zhai Z, Niu K-M, Liu Y, Lin C and Wu X (2021) The Gut Microbiota-Bile Acids-TGR5 Axis Mediates Eucommia ulmoides Leaf Extract Alleviation of Injury to Colonic Epithelium Integrity. Front. Microbiol. 12:727681. doi: 10.3389/fmicb.2021.727681

and composition of bile acids, which in turn activated the colonic *TGR5* gene expression in the colon and promoted the expression of tight junction proteins. These findings provide new insight for using ELE as a functional food with adjuvant therapeutic effects in IBD.

Keywords: *Eucommia ulmoides* leaves extracts, inflammatory bowel disease, gut microbiota, bile acids, epithelial barrier, Caco-2

INTRODUCTION

In Western countries, the incidence rate of inflammatory bowel disease (IBD) exceeds 0.3% (more than 2 million people), while in some Asian countries (such as China and Japan), the incidence of IBD also has begun to increase rapidly (Ng et al., 2017). IBD can aggravate inflammation, and then induce a lower level of tight junction protein expression between gut epithelial cells, resulting in structural damage to the gut epithelium, decrease of transepithelial electrical resistance (TEER), an increase in macromolecular permeability, and invasion of harmful pathogenic microorganisms (Citi, 2018; Mehandru and Colombel, 2021). The main factor that induces IBD is the disorder of intestinal microbiota and host metabolism caused by high-fat and high-protein "Western diet" (Tang et al., 2019; Sinha et al., 2020). Therefore, an effective way to prevent and improve IBD is adjusting the diet and increasing the intake of functional food, to improve the intestinal microbiota community and host metabolism.

Appropriate bacterial community structure and homeostasis are essential for gastrointestinal health. Studies have shown that increase in *Bacteroides*, *Proteobacteria*, and *Enterobacteriaceae* have been found in the intestinal contents and feces of IBD mice and human patients (Zhai Z. et al., 2019). Probiotics such as *Akkermansia* and *Lactobacillus* were enriched in mice at the convalescent stage of IBD. Additionally, probiotic intervention or fecal bacteria transplantation has been effective in relieving IBD symptoms (Lee and Chang, 2020).

Metagenomic and metabolomic studies have shown that metabolic changes in response to the intestinal microbiota may be the inducement or protective factor of IBD (Lee and Chang, 2020). Bile acids (BAs), short-chain fatty acids (SCFAs), and tryptophan metabolites play essential roles in gut epithelial repair, homeostasis, and immune regulation (Lee and Chang, 2020). Bile acids, a class of microbiota-host-related metabolites, play a role in regulating gut inflammation, barrier function, and cell proliferation (Connors et al., 2020; Sinha et al., 2020; Sorrentino et al., 2020). Secondary bile acids such as Lithocholic acid (LCA) and deoxycholic acid (DCA) can alleviate dextran sulfate sodium (DSS)-induced IBD by promoting intestinal stem cell proliferation and generation of regulatory T cells (Campbell et al., 2020; Sorrentino et al., 2020). In addition, partially hydrophilic bile acids such as tauroursodeoxycholic acid (TUDCA) and ursodeoxycholic acid (UDCA), showed beneficial effect on DSS-induced IBD in mice through reducing endoplasmic reticulum stress (Cao et al., 2013) and intestinal barrier disruption (Wang W. et al., 2018). The BA receptor TGR5-related pathway may play a key role in epithelium barrier function and formation (Xu et al., 2015; Merlen et al., 2020; Sinha et al., 2020). In biliary epithelium, activation of TGR5 enhanced the barrier function and decreased epithelium permeability (Merlen et al., 2020). In the intestinal crypt, TGR5 was only expressed in Lgr5-labeled intestinal stem cells and was necessary for DSS-induced recovery of IBD in mice (Sorrentino et al., 2020). However, whether TGR5 can regulate colon epithelium barrier function remains unclear.

Eucommia ulmoides tea, is a well-known Chinese functional food made from *Eucommia ulmoides* leaves. In recent years, EL extract (ELE) has been found to have beneficial effects on immune regulation, antioxidants, bone injury wound healing, and intestinal health enhancement (Zhu and Sun, 2018). EL extract, for example, has been reported to alleviate intestinal epithelium injury, which induced by obesity in mice (Murakami et al., 2018). Although the potential mechanism of ELE in alleviating IBD remains unclear, the protective effect may be attributed to bioactive components such as polyphenols, flavonoids, and polysaccharides in ELE. The flavonoids within ELE can relieve intestinal oxidative stress in piglets (Xiao et al., 2019). Polyphenols from blueberries have been shown to expand *Akkermansia* and *Bifidobacterium*, increase LCA and chenodeoxycholic acid (CDCA), and decrease hyodeoxycholic acid (HDCA) (Guo et al., 2019). Polysaccharides are the carbon source of gut microbiota and promote the proliferation of *Bifidobacterium* and *Lactobacillus*, reduce the colonization of pathogenic bacteria (Schroeder et al., 2018). Taken together, ELE exhibits antioxidant, anti-inflammatory, and immunomodulatory functions. However, whether ELE has a regulating effect on IBD alleviation, gut microbiota, and bile acid metabolism is still unclear.

To clarify this situation, with the purpose of evaluating the potential regulatory effects of compounds in ELE on IBD, microbiota, and bile acids, we employed a 2% DSS-induced IBD mouse model combined with ELE intervention. The gut microbiota and serum bile acid composition were also then investigated by integrated microbiome-metabolomic methods. Furthermore, using a Caco-2 cell model, we evaluated the repair effect of bile acids on lipopolysaccharide-induced monolayer epithelial barrier injury and its potential mechanism.

MATERIALS AND METHODS

Ethics Statement

In this study, the experimental design and procedures in this study were reviewed and approved by the Committee of the Institute of Subtropical Agriculture at the Chinese Academy of Sciences. All the experiment operations were

conducted following the guidelines of the institute of Subtropical Agriculture on Animal Care, Chinese Academy of Sciences (No. ISA-2020-18).

Preparation of Plant Extracts

Eucommia ulmoides leaves (EL) were grinded and filtered with 2 mm screener. The EL powder (500 g) was extracted by soaking twice in 5 L 95% alcohol for 7 days at room temperature, and the collected supernatant was filtered and concentrated using vacuum evaporator. Subsequently, the EL concentrate was decolorized with petroleum ether and then rotated again, then the extract of ELE was obtained by vacuum freeze-drying.

Determination of Total Flavonoids, Total Phenolic Acid, and Sugars in ELE

The content of total flavonoid and total phenolic acids in ELE was determined by using the plant flavonoids test kit (A142-1-1, Nanjing Jiancheng Bioengineering Institute, Nanjing, China) and plant total phenols test kit (A143-1-1, Nanjing Jiancheng Bioengineering Institute). The content of sugar was determined by using the plant total sugar and reducing sugar test kit (Shanghai Yuanye Bio-Technology Co., Ltd, Shanghai). All operations are in accordance with the relevant instructions. The content of total flavonoid, total phenolic acids, total soluble sugar, and reducing sugar in ELE was 44.59, 89.27, 104.23, and 25.81 mg/g, respectively.

Small Molecular Metabolites in ELE Detected by LC-MS/MS Analysis

The small molecule metabolites in ELE were detected by using liquid chromatography tandem secondary mass spectrometry (LC-MS/MS). The instrument parameters are as follows: LC was conducted by using UltiMate 3000 (Thermofisher, Waltham, MA, United States) and equipped with C18 chromatographic column (the column temperature is 18℃ during operation). Mobile phase was A: 100% acetonitrile + 0.1% formic acid, B: H_2O + 0.1% formic acid. Elution gradient: A: 0−7 min, 5−50%; 7−8 min, 50−75%; 8−9 min, 75−80%; 9−11 min, 80−90%; 11−15 min, 90−95%; 15−20 min, 95%. Velocity of flow: 0.2 ml/min. MS/MS was conducted by using Q-Exactive Focus (Thermofisher, Waltham, MA, United States). Ion source: ESI source, atomization temperature: 300℃, atomization gas (sheath gas) pressure: 40 ARB, auxiliary gas pressure: 10 ARB; transmission capillary temperature: 3p 20℃, scanning mode: (1) full scan, resolution 35,000, in source CID: 0 ev; ddms2, resolution 17,500, HCD-stepped NCE 10, 30, and 50. All the reagents for LC-MS were purchased from Sigma-Aldrich; the mass spectrum data were compared with the mzVault and MassList database. The relative content of metabolites was reflected by peak area. The relative content of metabolites was reflected by peak area. The relative abundance of the small molecular components is presented in peak area relative to the total peak area. Geniposide and chlorogenic acid accounted for 12% and 10%, respectively. The top 30 small molecular metabolites are shown in **Supplementary Table 1**.

Establishment of 2% DSS-Induced IBD Model in Mice and Treated With Different Dose of ELE

C57BL/6 mice (11 weeks of age) were purchased from STJ Laboratory Animal Co., LTD (Hunan, China). The mice were housed in four per cage under the same condition (temperature, 25 ± 1℃; lighting cycle, 12 h:12 h light/dark; 8:00−20:00 for light) and had free access to food and drinking water. Dextran sulfate sodium (36,000–5,000 MW) was purchased from MP Biomedicals (Santa Ana, CA, United States) and dissolved in drinking water to 2% (w/v) and given *ad libitum* to mice beginning on day 0 for 7 days (Tanaka et al., 2003). EL extract were dissolved in distilled water. The mice were then gavage with distilled water (CON and DSS group), 200 and 400 mg/kg (according to the body weight) ELE for 11 days (D5–D8). All the mice were evaluated in terms of body weight change and diarrhea index every day.

Sample Collection

At the end of this experiment, all the mice were fasted for 6 h, and anesthesia was induced by intraperitoneal injection of 2% pentobarbital sodium (45 mg/kg body weight). The blood samples were collected in 1.5 ml centrifuge tubes (germ-RNase- and DNase-free) after enucleation of the eyeball. The distal ileum (near the cecum to 2 cm) and colon were collected and stored in 4% neutral polyformaldehyde fixative or frozen in liquid nitrogen for real-time quantitative PCR (RT-qPCR) or western blotting. The cecum contents were collected in sterile enzyme free centrifuge tube and frozen in liquid nitrogen, and then stored at −80℃ until total genomic DNA extraction. The genomic DNA was used for subsequent 16S rRNA gene sequencing analysis.

Colon Tissue Histological Examination

The colonic tissue was embedded in paraffin, cut into 5 μm sections, and stained with hematoxylin and eosin (H&E). The colon crypt depth was observed by microscope (Olympus, Japan), and the depth of crypt was measured using VistarImage (Olympus, Japan) software, matching with the Olympus microscope (Zhai Z. et al., 2019).

RNA Extraction and Real-Time Quantitative PCR

To evaluate the inflammatory and colon epithelium integrity, we assessed the expression level of genes related to inflammation, tight junction, and bile acid receptor. RNA was extracted from colon tissue using column RNA extraction kit (R4121, Magen, Guangzhou, China). The total RNA concentration was measured using a NanoDrop 2000C spectrophotometer (Thermo Fisher Scientific, Waltham, MA, United States). The total RNA was reverse transcribed into cDNA by using cDNA synthesis kit (CW2582M, CWBIO, Jiangsu, China). The RT-qPCR primers were designed and synthesized by a commercial service of Sangon Biotech (Shanghai, China); the primer sequences are shown in **Supplementary Table 2**. The RT-qPCR was then performed according to the direction of FastSYBR Mixtrue (CW0955M, CWBIO) and run in the ABI 7500 FAST system

(Applied Biosystems Instruments, Thermo Fisher Scientific, United States). The values of the target genes were normalized by the housekeeping gene.

16S rRNA Gene Sequencing With Ion S5^{TM} XL

The process of genomic DNA extraction, quality detection and sequencing operation of intestinal microbiota were performed by the methods described in our previous study (Zhai Z. et al., 2019). Briefly, the sequencing raw data was obtained the Ion S5^{TM} XL platform. The raw data was measured by Cutadapt (version 1.9.1) to obtain the clean data. Operational taxonomy units (OTUs) were clustered with 97% identity by using Uparse (v7.0.1001). The non-metric multidimensional scaling (NMDS) were conducted based on OTU by the using R software. OTU is annotated and divided into phylum, class, order, family, genus, and species. The linear discriminant analysis (LDA) effect size (LEfSe) was used to elucidate the differences among bacterial taxa. An LDA score $\geq$4 was considered to be an important contributor to the model. The Spearman's analysis was used to measure the correlation between gut microbiota and bile acids.

Serum Bile Acid Analysis

The BA concentration in serum was measured by LC-MS. The standard curves of 25 BAs were established (**Supplementary Table 3**). Internal standards (**Supplementary Table 4**) were added into 50 μl serum samples and concentrated in a concentrator. After concentration, samples were redissolved with 100 μl 50% methanol-H_2O solution (v:v). LC was conducted by using LC30AD (Shimadzu, Japan) and equipped with C18 chromatographic column. Mobile phase was composed of solution A: acetonitrile (containing 0.01% acetic acid) and solution B: H_2O (0.01% acetic acid and 5 mmol/L ammonium acetate). Elution gradient is shown in **Supplementary Table 5**. MS was conducted by using QTRAP 6500 (ABSCIEX, MA, United States). Ion source: ESI source, scanning mode: negative ion scanning, Sperry voltage: 4,500 V (negative), capillary temperature: 550℃, curtain gas: 35 psi. The content of bile acid in blood was calculated by standard curve.

Preparation and Culture of Caco-2 Cell

Human colon cell line Caco-2 was kindly provided by Professor Baichuan Deng (College of Animal Science, South China agricultural University). The cell was cultured in DMEM/F12 (1:1) medium supplemented with 10% fetal bovine serum (FBS) (Gibco, Thermo Fisher, Waltham, MA, United States) and then incubated at 37°C in a humidified atmosphere containing 5% CO_2 in air. For transwell experiment, 1×10^6 cells were seeded in 0.32 cm^2 (0.4 μm) transwell plate and detect the TEER until differentiation is complete (Xiaojun et al., 2020). The cells were then treated with 40 μg/ml LPS (derived from *Escherichia coli*, O111: B4, Beyotime Biotechnology, Shanghai, China) for and treated with 12.5 μM TGR5 agonist INT-777 (I884046, $\geq$ 99%, MedChemExpress, Shanghai, China) at the same time, then the TEER was detected at 24h and 48h. For TGR5 RNA interference assay, the operation was carried out according to the kit instructions. In brief, negative control (NC) and TGR5-siRNA were mixed with serum-free DMEM/F12 medium and Lipo8000^{TM} (Beyotime Biotechnology) and incubated at room temperature for 20 min. The mix was then added to each well and treated for 24 and 48 h. The NC and TGR5-siRNA sequences were designed and synthesized by (Sangon Biotech) and the sequence were shown in **Supplementary Table 6**. The FITC-dextran (M.w.10000, MACKLIN, Shanghai, China) permeability of monolayer cell detection has been described in a previous study (Zhai et al., 2018). Briefly, 200 μl FITC-dextran solution (dissolved in HBSS, 5 mg/ml) was added to the apical compartment of transwell plate and 500 μl HBSS were added to basal compartment and cultured for 2 h. The absorbance in the basal compartment was measured using microplate reader (Spark10M, TECAN, Männedorf, Switzerland), and the content of FITC-dextran was calculated relative to a standard curve.

Cell Protein Sample Collection and Western Blot Analysis

For the experiment, 1×10^6 cells were seed in cell culture dish (6 cm diameter, JET, Guangzhou, China). After 24 h of being seeded, the cells were treated with LPS, LPS + INT-777, and INT-777 for 24 h. Caco-2 samples were lysed in Radio Immunoprecipitation Assay Lysis buffer (RIPA) lysate buffer (containing 1 mM PMSF) on ice for 15 min and then collected. RIPA buffer and PMSF are purchased from Beyotime Technology (Shanghai, China). The total protein concentration was detected by using BCA protein assay kit (Pierce BCA Protein Assay Kit, Beyotime technology) and mixed with loading buffer, and the protein was denatured in a metal bath (95℃, 5 min). In electrophoresis, 60 μg protein samples were loaded in each sampling well. After electrophoresis and membrane transfer, the primary and secondary antibodies were incubated, and electrochemiluminescence (ECL) was detected. The primary and secondary antibodies were shown as follows: claudin-1 (51-9000) was purchased from Thermo Fisher Scientific. TGR5 (NBP2-23669) were purchased from NOVUS (CO, United States). Goat antimouse (bs-40296G-HRP) and goat anti-rabbit (bs-0295G-HRP) antibodies were purchased from Bioss (Beijing, China). In order to detect proteins with similar molecular weight, we used striping buffer to remove antibodies, and then performed blocking, first antibody and second antibody incubation, and ECL chemiluminescence detection. The gray value of protein bands was measured by ImageJ (National Institutes of Health, Germany). The relative protein expression was expressed by the ratio of target protein to β -actin.

Statistical Analysis

Data are expressed as the mean ± SEM. One-way ANOVA and the least significance difference (LSD) method were used to determine the differences among the groups by using SPSS 20.0 (IBM, SPSS, United States) with significant criteria set to $^*p < 0.05$, $^{**}p < 0.01$, and $^{***}p < 0.001$. GraphPad Prism 7 (GraphPad Software Inc., San Diego, CA, United States) was used to generate statistical plots.

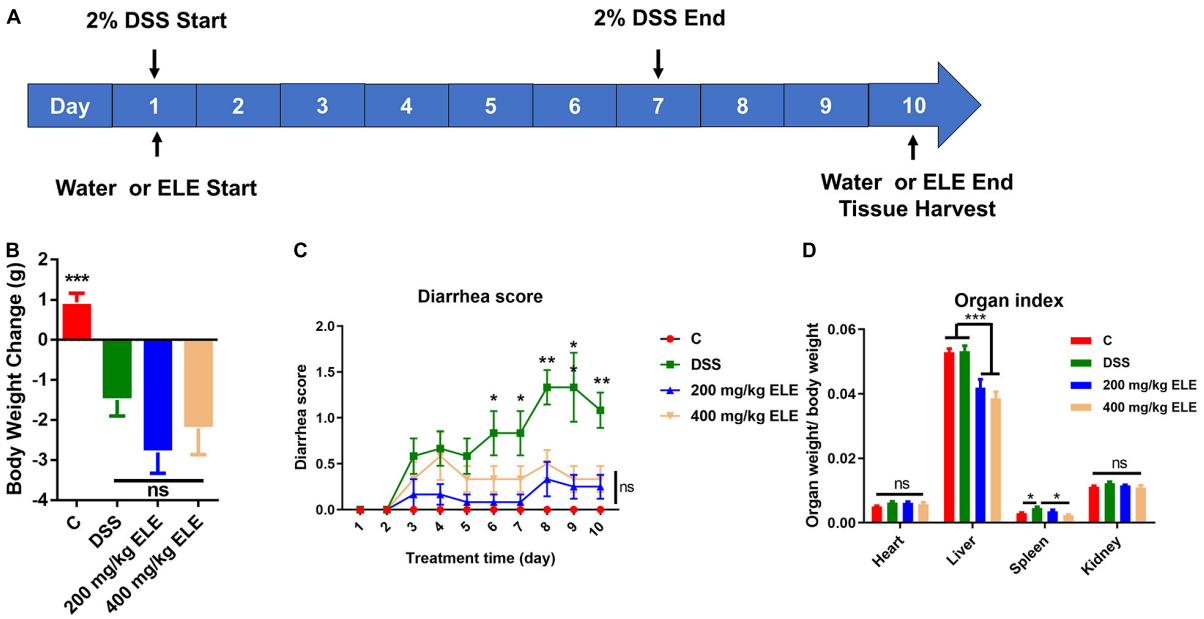

FIGURE 1 | Effects of ELE on body weight, diarrhea score, and organ index in mice. **(A)** The experimental process of this study. **(B)** Oral administration of ELE could not improve DSS-induced weight loss in mice. **(C)** Oral administration of ELE significantly improved DSS-induced diarrhea in mice. **(D)** Oral administration of ELE significantly decreased liver index and improved spleen index induced by DSS. Differences in data in mouse subjects were assessed by one-way ANOVA. n = 10–12 mice/group. $^{*}p < 0.05$; $^{**}p < 0.01$; $^{***}p < 0.001$. ELE, *Eucommia ulmoides* leaf extract; DSS, dextran sulfate sodium.

RESULTS

The Therapeutic Effect of ELE on DSS-Induced IBD in Mice

To evaluate the therapeutic effect of ELE on IBD, we constructed IBD mouse model using 2% DSS in drinking water for 1 week and administered different doses of ELE by gavage for 10 days, as shown in **Figure 1A**. Compared with the DSS group, ELE did not promote the recovery of body weight loss (**Figure 1B**) but remarkably attenuated the diarrhea status (**Figure 1C**, $p < 0.05$). In addition, oral administration alleviated DSS-induced splenic hypertrophy (**Figure 1D**).

The Effect of ELE on Colon Length, Epithelium Morphology, and the mRNA Expression of Inflammatory Factors

The effects of oral ELE administration on colon length and the epithelium morphology were evaluated. ELE supplementation alleviated the DSS-induced shortening of colon length ($p < 0.05$, **Figures 2A,B**) and crypt depth ($p < 0.05$, **Figures 2C,D**). Furthermore, ELE administration downregulated inflammation-related gene expression in the colon, including TLR4 and IL-6, which were more highly expressed in the DSS-treated group (**Figure 2E**).

The Effect of ELE on the Gut Microbiota in DSS-Treated IBD Mice

Oral administration of 200 and 400 mg/kg ELE showed similar effects in the preliminary results, thus 200 mg/kg was chosen for assessment in the following experiments. The supplementary effect of 200 mg/kg ELE on the gut microbiota in DSS-induced mice was further investigated. The rank abundance and rarefaction curve showed that the selected sequences were sufficient to determine most bacterial diversity (**Supplementary Figure 1**). The NMDS plot showed a clear separation of the gut microbiota among the control, ELE, and DSS groups (**Figure 3A**). The Venn plot showed that there were 1,862, 2,023, and 1,807 OTUs in control, ELE, and DSS groups, respectively (**Figure 3B**). The observed species (OS) and Shannon, Simpson, Chao1, and ACE indexes showed that ELE supplementation recovered the DSS-induced decline in OS and Chao1 index-dependent richness and Simpson and Shannon index-dependent diversity of the microbiota (**Figure 3C**). The phyla *Firmicutes*, *Proteobacteria*, *Bacteroidetes*, *Verrucomicrobia*, and *unidentified_Bacteria* were the microbiota with the top 5 relative abundances (**Figure 3D**). Compared with the DSS group, ELE increased the relative abundance of *Verrucomicrobia*. At the family level, DSS significantly reduced the relative abundance of *Lactobacillaceae* and increased the levels of *Bacteroides* and *Marinifilaceae* compared with the control group. After ELE treatment, the relative abundances of *Burkhoderiaceae*, *Akkermansiaceae*, and *Ruminococcaceae* were increased, while those of *Erysipelotrichaceae* and *Bacteroidaceae* were decreased compared with those in the DSS group (**Figure 3E**). LEfSe analysis demonstrated that *Bacteroidetes*, *Marinifilaceae*, and *Helicobacteraceae* were the main features in IBD mice. *Akkermansia* belonging to the *Verrucomicrobia* phylum was a feature in ELE-administrated mice. However, compared with the control group, the relative abundances

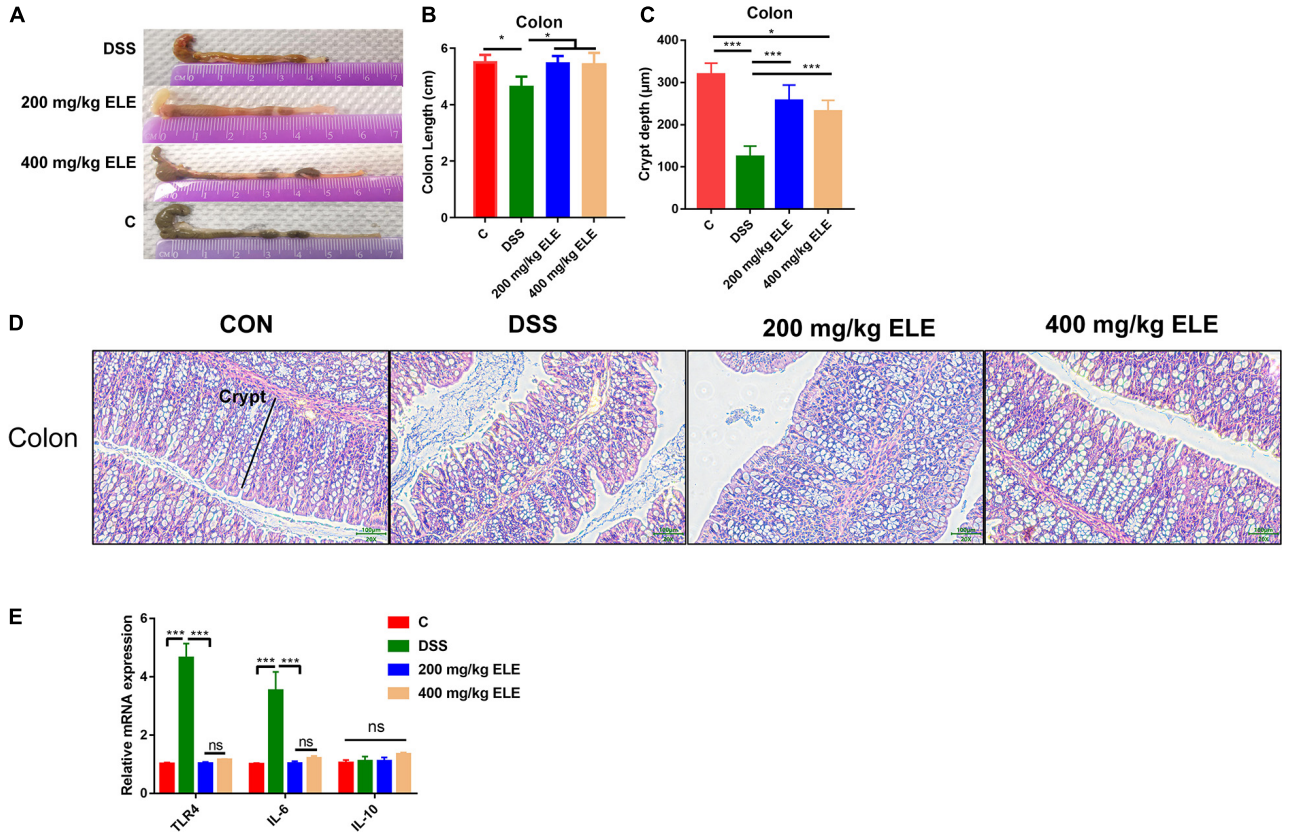

FIGURE 2 | Oral administration of ELE improved DSS induced colon length shortening and epithelial destruction. **(A)** Representative picture of colon length. **(B)** Colon length of mice in each group, n = 10–12 mice/per group. **(C)** The crypt depth of mice in colon, n = 6 mice/group. **(D)** Representative picture of colon epithelium, objective × 20, the scale indicates 100 μm. **(E)** The relative mRNA expression level of Toll-like receptor 4 (TLR4), IL-6, and IL-10 in colon, n = 9–12 mice/group. Differences in data in mouse subjects were assessed by one-way ANOVA. *$p < 0.05$; ***$p < 0.001$.

of *Lactobacillus*, *Dubosiella*, and *unidentified_Ruminococcaceae* belonging to *Firmicutes* were significantly decreased in IBD- and ELE-treated mice (**Figure 3F**).

Effect of ELE on Bile Acid Composition in Serum of Mice

The content of bile acids in the serum of mice was analyzed by LC-MS. ELE administration reduced the DSS-induced changes higher in total bile acids ($p < 0.05$) and tended to reduce the DSS-induced changes higher in total primary bile acids ($0.05 < p < 0.1$) in the serum (**Figures 4A,B**). Compared with the control group, ELE administration did not recover the DSS-induced changes of total secondary bile acids (**Figure 4C**) or the P/S ratio (**Figure 4D**).

Furthermore, we analyzed the composition of bile acids in the serum of mice in each group. Compared with the control group mice, DSS significantly increased the content of CA and β-MCA and decreased the DCA and ω-MCA content ($p < 0.05$, **Figures 4E,F**). EL extract treatment restored CA, β-MCA, and DCA to normal levels. Additionally, compared with the DSS and control groups, ELE significantly increased the contents of TCA and TUDCA ($p < 0.05$). The intestinal microbiota can regulate the process of bile acid synthesis, uncoupling, and secondary bile acid production in mice. We analyzed the correlation between bile acid content and the relative abundance of intestinal microbiota (**Figure 4G**). Consistent with the above results, in normal mice, *unidentified_Ruminococcaceae*, *Lactobacillus* showed a negative correlation with primary bile acids, such as β-MCA, Tβ-MCA TCDCA, CA ($-0.55 < R^2 < -0.40$). Bacteroides showed positive correlation with primary bile acids such as Tβ-MCA and CDCA ($0.4 < R^2 < 0.5$),while with negative correlation with DCA and TDCA ($0.4 < R^2 < 0.5$). In addition, *Dubosiella* showed strong positive correlation with α-MCA, UDCA and ω-MCA ($R^2 = 0.54$, 0.62, and 0.51). The feature taxon *Akkermansia* in ELE treated mice showed strong positive correlation with TUDCA ($R^2 = 0.53$).

Effects of ELE on the TGR5 and Tight Junction Protein Expression in Mice

Based on the change in bile acid content in serum, we further detected the mRNA expression levels of TGR5, a bile acid receptor and tight junction protein in the mouse colons. The data showed that, compared with DSS treatment, ELE

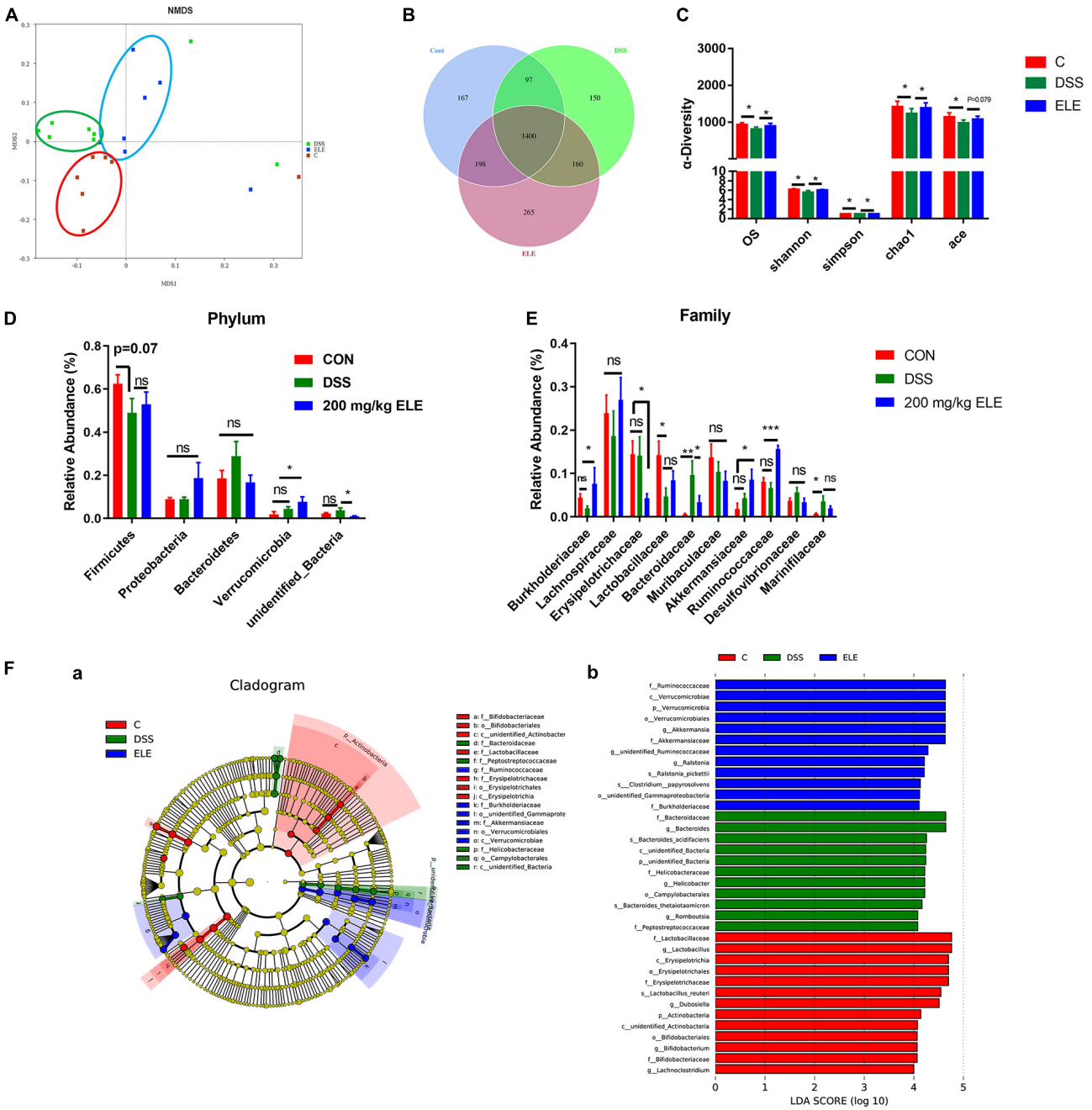

FIGURE 3 | Effects of ELE on the gut microbiota in mice. **(A)** The NMDS plot of gut microbiota. **(B)** The Venn plot based on OTUs of gut microbiota. **(C)** The OS, diversity, and abundance index of gut microbiota. **(D)** Oral administration of ELE regulates the microbiota of IBD mice in phylum level. **(E)** Oral administration of ELE regulates the microbiota of IBD mice in family level. **(F)** Identification of characteristic microbiota in cecal contents of mice with different treatments by LEfSe analysis, **(a)** LefSe taxonomic cladogram and **(b)** LDA score. n = 7–8 mice/group. Differences in data in mouse subjects were assessed by one-way ANOVA. $^{*}p < 0.05$; $^{**}p < 0.01$; $^{***}p < 0.001$. NMDS, non-metric multidimensional scaling. OTU, operational taxonomic unit; LEfse, LDA effect size; LDA, linear discriminant analysis.

treatment significantly increased the decreased mRNA levels of TGR5, claudin-1, and occludin ($p < 0.05$, **Figures 5A–C**) while had no significant effect on ZO-1 (**Figure 5D**). Immunofluorescence results showed that claudin-1 was expressed from the top to the bottom of the crypt in the control group. Dextran sulfate sodium administration decreased this expression due to the destruction of intestinal epithelial structure. After ELE treatment, the expression of claudin-1 gradually increased from the bottom to the top of the crypt, suggesting that the expression and distribution of claudin-1 are involved in the process of recovery (**Figure 5E**).

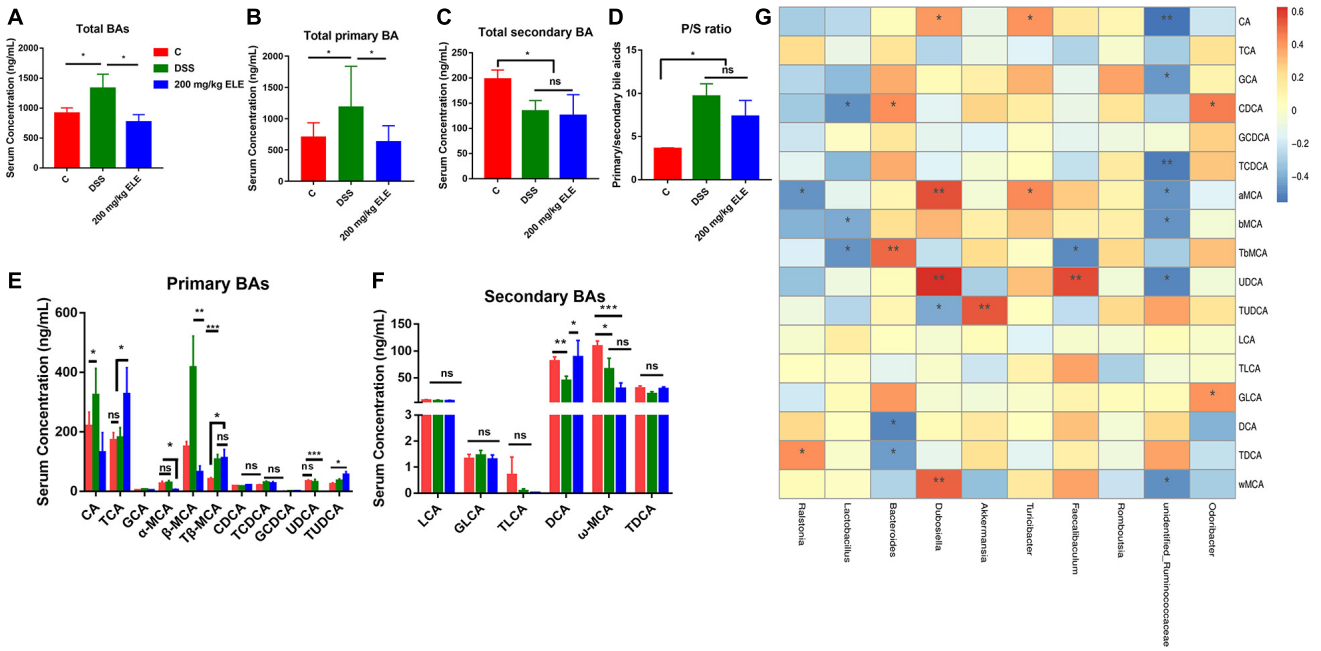

FIGURE 4 | Oral administration of ELE regulated the bile acids through gut microbiota regulatory effect in mice. **(A)** Content of total BA in serum. **(B)** The content of total primary BA in serum. **(C)** Content of total secondary BA in serum. **(D)** Ratio of primary bile acid to secondary bile acid content in serum. **(E)** Qualitative and quantitative analysis of primary bile acids. **(F)** Qualitative and quantitative analysis of secondary bile acids. **(G)** Correlation analysis of gut microbiota and bile acids. $^{*}p < 0.05$; $^{**}p < 0.01$; $^{***}p < 0.001$.

TGR5 Involved in the Enhancement of Monolayer Cell Barrier Function

In this study, we used Caco-2, a human colon epithelium cell line, to confirm the role of bile acid receptor TGR5 in alleviating the process of colon epithelium injury. To activate TGR5, a selective agonist INT-777 was used. The results showed that INT-777 prevented the LPS-induced decrease in the TEER value in the Caco-2 monolayer cell barrier and increase in FITC-dextran permeability (**Figures 6A,B**). Western blotting data showed that INT-777 significantly increased LPS-induced reductions in claudin-1 protein level (**Figures 6C,D**), suggesting that INT-777 can promote the barrier function of colon cells. TGR5-siRNA was then used for TGR5 mRNA interference and TEER and FITC-dextran permeability were also evaluated after treatment for 24 and 48 h. The results showed that interference with TGR5 expression could significantly decrease TEER and increase the permeability of FITC-dextran in monolayer cells ($p < 0.05$, **Figures 7A,B**). Western blotting results showed that, TGR5 interference significantly decreased claudin-1 expression ($p < 0.05$, **Figures 7C,D**).

DISCUSSION

To date, there is no ideal drug to treat IBD. Conventional treatment mainly includes oral intake antibacterial and anti-inflammatory drugs, or taking surgery, etc. In recent years, researchers have found that effective components in plant can be used to prevent or treat intestinal inflammation (Zhao et al., 2019; Long et al., 2021). *Eucommia ulmoides* is a traditional Chinese herbal medicine that has also been approved for use as a functional food. *Eucommia ulmoides* has anti-inflammatory and wound-healing promoting effects, but its protective effect on animals has not been fully elucidated. Here, based on our findings, we discuss the effect of ELE on mouse IBD and its potential mechanisms. To better elucidate the mechanisms by which ELE alleviates IBD, we first determined the main components in the extract. The results showed that the main components were phenolic acids, total flavonoids, and sugars. Furthermore, the LC-MS showed chlorogenic acid and geniposide as the most abundant ingredients in ELE. In this study, we constructed a mild enteritis model in mice treated with 2% DSS for 7 days. ELE significantly alleviated the DSS-induced diarrhea rate and colon shortening in mice. Furthermore, we found that ELE significantly improved DSS-induced colon epithelial injury and reduced the mRNA expression of TLR4 and IL-6, which might attribute to the enriched phenolic acids, flavonoid, and polysaccharide contents in ELE. Previously, studies have shown that the phenolic acid, total flavonoids, and polysaccharides alleviate IBD by relieving inflammation and oxidative stress (Zhao et al., 2019; Hussain et al., 2020; Sandoval-Ramirez et al., 2020). Chlorogenic acid, the main component of ELE, showed beneficial effect on ameliorating LPS-induced inflammation in different cell types (i.e., macrophages, hepatocytes, and intestinal cells) by suppressing the TLR4 signaling pathway (Shi et al., 2013; Ruan et al., 2014; Ruifeng et al., 2014). TLR4 is the receptor of lipopolysaccharide, the main component of the cell wall

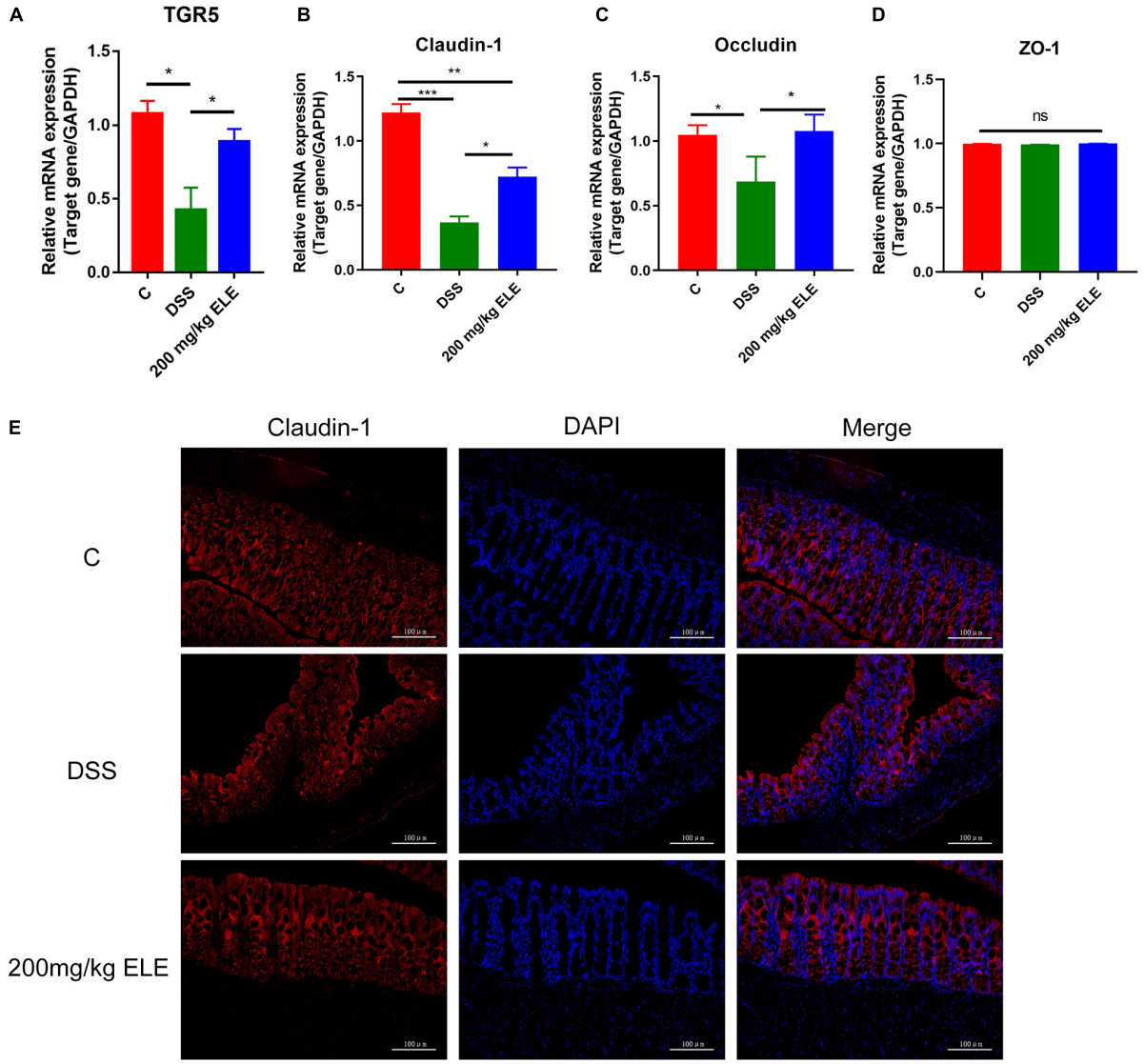

FIGURE 5 | Oral ELE improves DSS-induced decrease of TGR5 and tight junction expression in colon. **(A–D)** mRNA expression level of TGR5, claudin-1, occludin, and ZO-1, n = 7–8 mice/group. **(E)** Representative image of tissue immunofluorescence of claudin-1, n = 3 mice/group. Differences in data in mouse subjects were assessed by one-way ANOVA. $^{*}p < 0.05$; $^{**}p < 0.01$; $^{***}p < 0.001$.

of Gram-negative bacteria. TLR4 can resist the invasion of pathogens such as *Enterobacter* and *Bacteroides* by initiating the inflammatory response of the body (Lu et al., 2018). In this study, the change in TLR4 expression suggests that ELE may promote the recovery of IBD by inhibiting the binding of antigens from the intestinal microbiota. In addition to directly participating in the wound-healing process of the gut epithelium, in recent years, studies have also shown that the "gut microbiota-bile acid metabolism" axis is critical for flavonoids, phenolic acids, and polysaccharides to regulate intestinal health (Zhang et al., 2016; Guo et al., 2019; Huang et al., 2019).

Bacteroides have been reported to induce IBD and worsen the disease by producing enterotoxins, degrading mucin, activating TLRs, and inducing the secretion of proinflammatory cytokines (Chung et al., 2018; Elahi, 2018; Menghini et al., 2019). Numerous studies have shown that the abundance of *Bacteroides* is significantly increased in both DSS-induced mice and IBD patients (Rodriguez-Palacios et al., 2018; Wang K. et al., 2018; Ryan et al., 2020). In this study, the reduction in OS, richness, and diversity of gut microbiota were improved by ELE in IBD mice. Furthermore, ELE decreased *Bacteroidaceae* and *Erysipelotrichaceae* abundance and increased *Burkhoderiaceae*, *Akkermansiaceae*, and *Ruminococcaceae* abundance compared with the DSS group, which is in accordance with TLR4 mRNA upregulation. In addition, we found that *Akkermansia* was a feature taxon in ELE-treated mice by LEfSe analysis. Alternatively, *Akkermansiaceae* have been considered probiotics

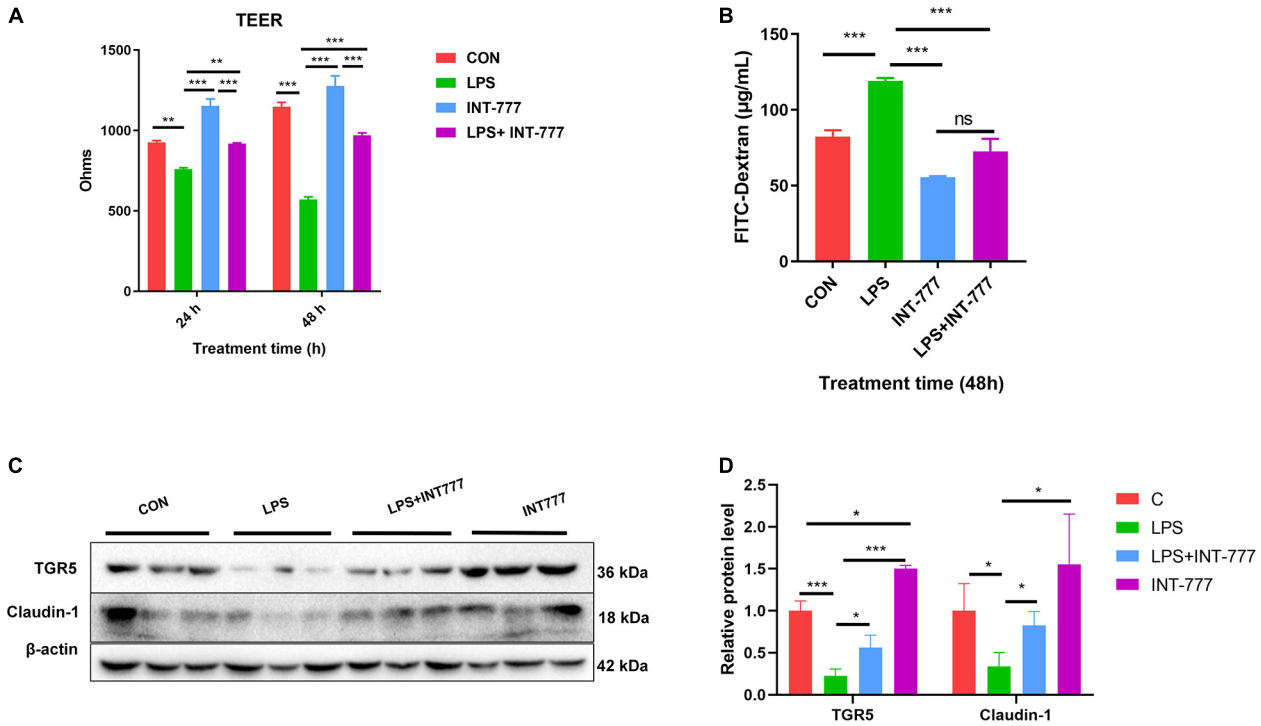

FIGURE 6 | Activation of TGR5 can alleviate LPS-induced epithelium barrier injury of Caco-2 cell. **(A)** The TEER of the cell monolayer of Caco-2, $n = 3$. **(B)** The FITC-dextran permeability of the cell monolayer of Caco-2, $n = 3$. **(C,D)** Protein expression of TGR5 and Claudin-1 relative to β-actin. The results were confirmed by three independent experiments. Differences in data in cell subjects were assessed by one-way ANOVA. $^{*}p < 0.05$; $^{**}p < 0.01$; $^{***}p < 0.001$.

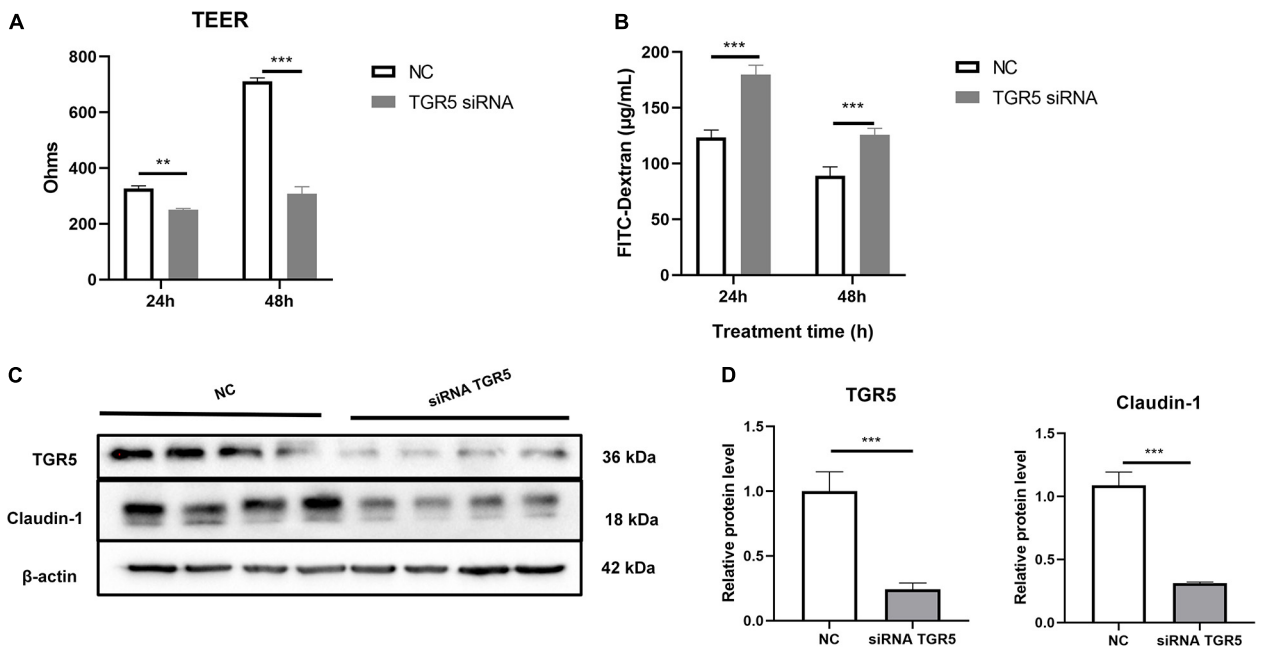

FIGURE 7 | Interference with TGR5 mRNA expression reduces Caco-2 monolayer epithelium barrier function. **(A)** The TEER of the cell monolayer of caco-2, $n = 3$. **(B)** The FITC-dextran permeability of the cell monolayer of Caco-2, $n = 3$. **(C,D)** Protein expression of TGR5 and Claudin-1 relative to β-actin. The results were confirmed by three independent experiments. Differences in data in cell subjects were assessed by one-way ANOVA. $^{*}p < 0.05$; $^{**}p < 0.01$; $^{***}p < 0.001$.

involved in reducing inflammation, promoting intestinal epithelial wound healing, and alleviating enteritis (Zhang et al., 2020). *Akkermansia muciniphila* can significantly alleviate DSS-induced chronic colitis by reducing the expression of TNF-α and IFN-γ, promoting the differentiation of Treg cells, and increasing the production of short-chain fatty acid (Zhai R. et al., 2019). Consistent with a previous study, caffeic acid, which is also a main components and metabolite of chlorogenic acid in ELE, can ameliorate DSS-induced colitis and increase the abundance of *Akkermansia* (Zhang et al., 2016).

Although homeostasis of the gut microbiota is crucial for intestinal health, the specific mechanism has not been fully elucidated. Studies have shown that the intestinal metabolites, which play important roles in host intestinal inflammatory response, cell proliferation, apoptosis and other processes, can be regulated by gut microbiota (Koh and Backhed, 2020).

Bile acid is a type of small molecule metabolite that is abundant in the intestine and is considered a biomarker involved in gut health and the pathogenesis of IBD. As early as in the 1980s, researchers found that there was a high correlation between blood bile acid content and IBD (Holzbach et al., 1980). The type and content of bile acids are highly correlated with the structure of intestinal flora. *Enterobacteriaceae* and *Bacteroides* are highly positively correlated with enteritis, and affected the metabolism of bile acids in the liver and gut. Differences in fecal bile acid and the microbial community were found in the children with remission and non-remission of Crohn's disease. Primary bile acids (CA, CDCA) were dominant in the non-remission fecal samples of children, and were a highly positively correlated with the higher abundance of *Bacteroidetes*. In contrast, secondary bile acids were dominant in the remission fecal samples of children and were positively correlated with *Rominococcus_torques* belonging to *Firmicutes* (Connors et al., 2020). Similarly, LCA and DCA, but not CDCA, were found to have alleviation effect of DSS- and TNBS-induced colitis (Sinha et al., 2020). Furthermore, 3β-hydroxydeoxycholic acid, a derivate of DCA can act on dendritic cells and promote the differentiation of regulatory T cells, thus alleviating inflammation (Campbell et al., 2020). Alternatively, some researchers found that increased levels of BAs, especially secondary bile acids (DCA and ω-MCA) showed negative correlations with intestinal permeability, and decreased the expression levels of tight junctions (Murakami et al., 2016). These hydrophobic bile acids may induce cytotoxicity, oxidative DNA damage, cell apoptosis, and mitochondrial perturbations in the colon (Barrasa et al., 2013). In this study, oral administration of ELE restored the diversity and abundance of intestinal microbiota in mice with IBD and reduced the abundance of *Bacteroides*. Consistent with the results in this study, we also found that in IBD mice, the level of primary bile acids such as CA, β-MCA, and Tβ-MCA are increased. The level of secondary bile acid (DCA, TDCA) was recovered to a similar level compared with normal mice after ELE treatment. We also found that the level of TUDCA was positively correlated with the abundance of *Akkermansia*. Tauroursodeoxycholic acid is an effective drug that is approved by the US Food and Drug Administration (FDA) for bile acid metabolism regulation, hepatocyte protection, and biliary cholangitis treatment. Tauroursodeoxycholic acid has anti-inflammatory effects in steatohepatitis and non-alcoholic fatty liver disease through alleviation of endoplasmic reticulum stress and downregulation of inflammatory responses (Wang W. et al., 2018). Studies have shown that the mechanism of TUDCA, LCA, and DCA in alleviating enteritis is to activate the bile acid receptor TGR5 in colon (Kusaczuk, 2019; Sorrentino et al., 2020). The bile acid receptor TGR5 plays important roles in the occurrence, development, and recovery of intestinal inflammation. Activation of TGR5 can significantly improve the proliferation of intestinal stem cells and promote intestinal epithelial reconstruction in DSS-induced enteritis mice, but TGR5 knockout can hinder the recovery of the intestinal tract (Sorrentino et al., 2020). Activation of TGR5 not only promotes cell proliferation but also enhances the barrier function of epithelial tissue in mice (Cipriani et al., 2011; Merlen et al., 2020). Consistent with a previous study, we found that compared with DSS treatment, ELE significantly increased the mRNA expression of TGR5 in the colon of IBD mice. To further clarify the role of TGR5 in the regulation of gut epithelial barrier function in the colon, in Caco-2 cell model, the expression of TGR5 was found to be significantly decreased by LPS and RNA interference treatment, while the permeability of TEER and macromolecules (FITC-dextran) permeability was increased. This phenomenon was reversed after the addition of INT-777, a TGR5 selective agonist, indicating that TGR5 is necessary to maintain the barrier function of intestinal epithelial cells. However, in the porcine jejunal epithelial cell line IPEC-J2, mRNA interference with TGR5 did not affect the function of intestinal barrier (Song et al., 2019), which may be a result from the different expression levels of TGR5 in different intestinal sections. TGR5 was found to be highly expressed in the colon and lowly expressed in the jejunum (Wahlstrom et al., 2016); this suggests that TGR5 plays different roles in the gastrointestinal tract. In addition, due to the difference of species and cell types, the function of TGR5 may be different. Therefore, the role of TGR5 on the function of epithelial barrier is worth further study.

In future studies on mice or human subjects, some aspects still need to be clarified, including the effects of long-term use of ELE on intestinal health and gut microbiota regulation and a single compound or multiple compounds within the ELE exert protective effects from IBD and gut barrier injury through the "intestinal microbiota-bile acid-TGR5" axis. In addition, and the potential mechanisms and pathways by which TGR5 regulates the intestinal barrier also need to be further studied.

CONCLUSION

In summary, our findings demonstrate that ELE alleviates DSS-induced IBD. Furthermore, we found that ELE treatment significantly increased serum bile acids such as TUDCA and DCA, which showed a high positive correlation with *Akkermansia* and *Rominococcus*. The change of bile acid composition upregulated the expression of TGR5 mRNA in colon tissues. In Caco-2 cells, the activation of TGR5 enhanced

cell barrier function and upregulated the expression of tight junction proteins, and this result was reversed by TGR5 mRNA interference. These findings suggest that ELE may be useful as a functional food in alleviating IBD through "gut microbiota-bile acid-TGR5" axis.

DATA AVAILABILITY STATEMENT

The data that support the findings of this study are openly available in National Center for Biotechnology Information (NCBI), BioProject accession number PRJNA730339.

ETHICS STATEMENT

All the experiment operations were conducted following the guidelines of the institute of Subtropical Agriculture on Animal Care, Chinese Academy of Sciences (No. ISA-2020-18).

AUTHOR CONTRIBUTIONS

ZZ, K-MN, and XW conceived and designed the experiments. ZZ, K-MN, YL, and CL performed the experiments and collected the samples. ZZ and K-MN analyzed the data. XW provided the funding. All authors read and approved the final manuscript.

FUNDING

This project was funded by the General Projects of Key Research and Development Plan in Jiangxi Province (20203BBFL63054), Jiangxi Provincial Innovation and Entrepreneurship Projects and the earmarked fund for China Agriculture Research System (CARS-35), Project funded by China Postdoctoral Science Foundation (2020M682108), Research and Development Project of Jiangxi Academy of Sciences – Doctoral Fund Project (2020-YYB-01), and Guangdong Province enterprise special person special plan project (GDKTP2020054600).

SUPPLEMENTARY MATERIAL

The Supplementary Material for this article can be found online at: https://www.frontiersin.org/articles/10.3389/fmicb.2021.727681/full#supplementary-material

REFERENCES

Barrasa, J. I., Olmo, N., Antonia Lizarbe, M., and Turnay, J. (2013). Bile acids in the colon, from healthy to cytotoxic molecules. *Toxicol. Vitro* 27, 964–977. doi: 10.1016/j.tiv.2012.12.020

Campbell, C., McKenney, P. T., Konstantinovsky, D., Isaeva, O. I., Schizas, M., et al. (2020). Bacterial metabolism of bile acids promotes generation of peripheral regulatory T cells. *Nature* 581, 475–479. doi: 10.1038/s41586-020-2193-0

Cao, S. S., Zimmermann, E. M., Chuang, B., Song, B., Nwokoye, A., et al. (2013). The unfolded protein response and chemical chaperones reduce protein misfolding and colitis in mice. *Gastroenterology* 144, 989. doi: 10.1053/j.gastro.2013.01.023

Chung, L., Thiele, O. E., Geis, A. L., Chan, J. L., Fu, K., et al. (2018). *Bacteroides* fragilis Toxin Coordinates a Pro-carcinogenic Inflammatory Cascade via Targeting of Colonic Epithelial Cells. *Cell Host Microbe* 23, 203–214. doi: 10.1016/j.chom.2018.01.007

Cipriani, S., Mencarelli, A., Chini, M. G., Distrutti, E., Renga, B., et al. (2011). The bile acid receptor GPBAR-1 (TGR5) modulates integrity of intestinal barrier and immune response to experimental colitis. *PLoS One* 6:e25637. doi: 10.1371/journal.pone.0025637

Citi, S. (2018). Intestinal barriers protect against disease. *Science* 359, 1097–1098. doi: 10.1126/science.aat0835

Connors, J., Dunn, K. A., Allott, J., Bandsma, R., Rashid, M., et al. (2020). The relationship between fecal bile acids and microbiome community structure in pediatric Crohn's disease. *ISME J.* 14, 702–713. doi: 10.1038/s41396-019-0560-3

Elahi, E. (2018). Altered gut microbiome and metabolome in patients with multiple system atrophy. *Mov. Disord.* 33, 174. doi: 10.1002/mds.27203

Guo, J., Han, X., Tan, H., Huang, W., You, Y., et al. (2019). Blueberry extract improves obesity through regulation of the gut microbiota and bile acids via pathways involving FXR and TGR5. *IScience* 19, 676–690. doi: 10.1016/j.isci.2019.08.020

Holzbach, R. T., Marsh, M. E., Freedman, M. R., et al. (1980). Portal vein bile acids in patients with severe inflammatory bowel disease. *Gut* 21, 428–435. doi: 10.1136/gut.21.5.428

Huang, F., Zheng, X., Ma, X., Jiang, R., Zhou, W., et al. (2019). Theabrownin from Pu-erh tea attenuates hypercholesterolemia via modulation of gut microbiota and bile acid metabolism. *Nat. Commun.* 10:4971. doi: 10.1038/s41467-019-12896-x

Hussain, T., Yuan, D., Tan, B., Murtaza, G., Rahu, N., et al. (2020). Eucommia ulmoides flavones (EUF) abrogated enterocyte damage induced by LPS involved in NF-kappaB signaling pathway. *Toxicol. Vitro* 62, 104674. doi: 10.1016/j.tiv.2019.104674

Koh, A., and Backhed, F. (2020). From association to causality: The role of the gut microbiota and its functional products on host metabolism. *Mol. Cell* 78, 584–596. doi: 10.1016/j.molcel.2020.03.005

Kusaczuk, M. (2019). Tauroursodeoxycholate-Bile acid with chaperoning activity: Molecular and cellular effects and therapeutic perspectives. *Cells* 8:cells8121471. doi: 10.3390/cells8121471

Lee, M., and Chang, E. B. (2020). Inflammatory bowel diseases (IBD) (Inflammatory bowel diseases and the microbiome: Searching the crime scene for clues). *Gastroenterology* 2020:056. doi: 10.1053/j.gastro.2020.09.056

Long, H., Xin, Z., Zhang, F., Zhai, Z., Ni, X., et al. (2021). The cytoprotective effects of dihydromyricetin and associated metabolic pathway changes on deoxynivalenol treated IPEC-J2 cells. *Food Chem.* 338:128116. doi: 10.1016/j.foodchem.2020.128116

Lu, P., Sodhi, C. P., Yamaguchi, Y., Jia, H., Prindle, T. J., et al. (2018). Intestinal epithelial Toll-like receptor 4 prevents metabolic syndrome by regulating interactions between microbes and intestinal epithelial cells in mice. *Mucosal Immunol.* 11, 727–740. doi: 10.1038/mi.2017.114

Mehandru, S., and Colombel, J. F. (2021). The intestinal barrier, an arbitrator turned provocateur in IBD. *Nat. Rev. Gastroenterol. Hepatol.* 18, 83–84. doi: 10.1038/s41575-020-00399-w

Menghini, P., Corridoni, D., Butto, L. F., Osme, A., Shivaswamy, S., et al. (2019). Neutralization of IL-1alpha ameliorates Crohn's disease-like ileitis by functional alterations of the gut microbiome. *Proc. Natl. Acad. Sci. U S A.* 2019:1915043116. doi: 10.1073/pnas.1915043116

Merlen, G., Kahale, N., Ursic-Bedoya, J., Bidault-Jourdainne, V., Simerabet, H., et al. (2020). TGR5-dependent hepatoprotection through the regulation of biliary epithelium barrier function. *Gut* 69, 146–157. doi: 10.1136/gutjnl-2018-316975

Murakami, S., Tasaka, Y., Takatori, S., Tanaka, A., Kawasaki, H., et al. (2018). Effect of Eucommia ulmoides Leaf Extract on Chronic Dextran Sodium Sulfate-Induced Colitis in Mice. *Biol. Pharm. Bull.* 41, 864–868. doi: 10.1248/bpb.b17-00878

Murakami, Y., Tanabe, S., and Suzuki, T. (2016). High-fat diet-induced intestinal hyperpermeability is associated with increased bile acids in the large intestine of mice. *J. Food Sci.* 81, H216–H222. doi: 10.1111/1750-3841.13166

Ng, S. C., Shi, H. Y., Hamidi, N., Underwood, F. E., Tang, W., et al. (2017). Worldwide incidence and prevalence of inflammatory bowel disease in the 21st century: A systematic review of population-based studies. *Lancet* 390, 2769–2778. doi: 10.1016/S0140-6736(17)32448-0

Rodriguez-Palacios, A., Harding, A., Menghini, P., Himmelman, C., Retuerto, M., et al. (2018). The artificial sweetener splenda promotes gut *proteobacteria*, dysbiosis, and myeloperoxidase reactivity in crohn's Disease-Like ileitis. *Inflamm. Bowel Dis.* 24, 1005–1020. doi: 10.1093/ibd/izy060

Ruan, Z., Liu, S., Zhou, Y., Mi, S., Liu, G., et al. (2014). Chlorogenic acid decreases intestinal permeability and increases expression of intestinal tight junction proteins in weaned rats challenged with LPS. *PLoS One* 9:e97815. doi: 10.1371/journal.pone.0097815

Ruifeng, G., Yunhe, F., Zhengkai, W., Ershun, Z., Yimeng, L., et al. (2014). Chlorogenic acid attenuates lipopolysaccharide-induced mice mastitis by suppressing TLR4-mediated NF-kappaB signaling pathway. *Eur. J. Pharmacol.* 729, 54–58. doi: 10.1016/j.ejphar.2014.01.015

Ryan, F. J., Ahern, A. M., Fitzgerald, R. S., Laserna-Mendieta, E. J., Power, E. M., et al. (2020). Colonic microbiota is associated with inflammation and host epigenomic alterations in inflammatory bowel disease. *Nat. Commun.* 11, 15342–15345. doi: 10.1038/s41467-020-15342-5

Sandoval-Ramirez, B. A., Catalan, U., Pedret, A., Valls, R. M., Motilva, M. J., et al. (2020). Exploring the effects of phenolic compounds to reduce intestinal damage and improve the intestinal barrier integrity: A systematic review of in vivo animal studies. *Clin. Nutr.* 2020:027. doi: 10.1016/j.clnu.2020.09.027

Schroeder, B. O., Birchenough, G., Stahlman, M., Arike, L., Johansson, M., et al. (2018). Bifidobacteria or Fiber Protects against Diet-Induced Microbiota-Mediated Colonic Mucus Deterioration. *Cell Host Microbe* 23, 27–40. doi: 10.1016/j.chom.2017.11.004

Shi, H., Dong, L., Dang, X., Liu, Y., Jiang, J., et al. (2013). Effect of chlorogenic acid on LPS-induced proinflammatory signaling in hepatic stellate cells. *Inflamm. Res.* 62, 581–587. doi: 10.1007/s00011-013-0610-7

Sinha, S. R., Haileselassie, Y., Nguyen, L. P., Tropini, C., Wang, M., et al. (2020). Dysbiosis-Induced secondary bile acid deficiency promotes intestinal inflammation. *Cell Host Microbe* 2020:021. doi: 10.1016/j.chom.2020.01.021

Song, M., Ye, J., Zhang, F., Su, H., Yang, X., et al. (2019). Chenodeoxycholic Acid (CDCA) Protects against the Lipopolysaccharide-Induced Impairment of the Intestinal Epithelial Barrier Function via the FXR-MLCK Pathway. *J. Agric. Food Chem.* 67, 8868–8874. doi: 10.1021/acs.jafc.9b03173

Sorrentino, G., Perino, A., Yildiz, E., El Alam, G., Sleiman, M. B., et al. (2020). Bile acids signal via TGR5 to activate intestinal stem cells and epithelial regeneration. *Gastroenterology* 159:956. doi: 10.1053/j.gastro.2020.05.067

Tanaka, T., Kohno, H., Suzuki, R., Yamada, Y., Sugie, S., et al. (2003). A novel inflammation-related mouse colon carcinogenesis model induced by azoxymethane and dextran sodium sulfate. *Cancer Sci.* 94, 965–973. doi: 10.1111/j.1349-7006.2003.tb01386.x

Tang, W., Li, D. Y., and Hazen, S. L. (2019). Dietary metabolism, the gut microbiome, and heart failure. *Nat. Rev. Cardiol.* 16, 137–154. doi: 10.1038/s41569-018-0108-7

Wahlstrom, A., Sayin, S. I., Marschall, H. U., and Backhed, F. (2016). Intestinal Crosstalk between Bile Acids and Microbiota and its Impact on Host Metabolism. *Cell Metab.* 24, 41–50. doi: 10.1016/j.cmet.2016.05.005

Wang, K., Jin, X., Li, Q., Sawaya, A. C. H. F., Le Leu, R. K., et al. (2018). Propolis from Different Geographic Origins Decreases Intestinal Inflammation and *Bacteroides* spp. Populations in a Model of DSS-Induced Colitis. *Mol. Nutr. Food Res.* 62:201800080. doi: 10.1002/mnfr.201800080

Wang, W., Zhao, J., Gui, W., Sun, D., Dai, H., et al. (2018). Tauroursodeoxycholic acid inhibits intestinal inflammation and barrier disruption in mice with non-alcoholic fatty liver disease. *Br. J. Pharmacol.* 175, 469–484. doi: 10.1111/bph.14095

Xiao, D., Yuan, D., Tan, B., Wang, J., Liu, Y., et al. (2019). The role of nrf2 signaling pathway in eucommia ulmoides flavones regulating oxidative stress in the intestine of piglets. *Oxid. Med. Cell Longev.* 2019:9719618. doi: 10.1155/2019/9719618

Xiaojun, N., Zhenya, Z., Zhongquan, X., Chengquan, T., Yiliang, C., et al. (2020). Antioxidant properties and transepithelial transportation of di-/tripeptides derived from simulated gastrointestinal digestion of pig blood cells hydrolysates. *EFood* 1:001.

Xu, J., Li, M., and Sun, R. (2015). Identifying the impact of ultrasound-assisted extraction on polysaccharides and natural antioxidants from Eucommia ulmoides Oliver. *Proc. Biochem.* 50, 473–481. doi: 10.1016/j.procbio.2014.12.021

Zhai, R., Xue, X., Zhang, L., Yang, X., Zhao, L., and Zhang, C. (2019). Strain-Specific Anti-inflammatory Properties of Two *Akkermansia muciniphila* Strains on Chronic Colitis in Mice. *Front. Cell Infect. Microbiol.* 9:00239. doi: 10.3389/fcimb.2019.00239

Zhai, Z., Ni, X., Jin, C., Ren, W., Li, J., et al. (2018). Cecropin a modulates tight Junction-Related protein expression and enhances the barrier function of porcine intestinal epithelial cells by suppressing the MEK/ERK pathway. *Int. J. Mol. Sci.* 19:ijms19071941. doi: 10.3390/ijms19071941

Zhai, Z., Zhang, F., Cao, R., Ni, X., Xin, Z., et al. (2019). Cecropin a alleviates inflammation through modulating the gut microbiota of C57BL/6 mice with DSS-Induced IBD. *Front. Microbiol.* 10:1595. doi: 10.3389/fmicb.2019.01595

Zhang, T., Li, P., Wu, X., Lu, G., Marcella, C., et al. (2020). Alterations of Akkermansia muciniphila in the inflammatory bowel disease patients with washed microbiota transplantation. *Appl. Microbiol. Biotechnol.* 104, 10203–10215. doi: 10.1007/s00253-020-10948-7

Zhang, Z., Wu, X., Cao, S., Wang, L., Wang, D., et al. (2016). Caffeic acid ameliorates colitis in association with increased Akkermansia population in the gut microbiota of mice. *Oncotarget* 7, 31790–31799. doi: 10.18632/oncotarget.9306

Zhao, Y., Guo, Q., Zhu, Q., Tan, R., Bai, D., et al. (2019). Flavonoid VI-16 protects against DSS-induced colitis by inhibiting Txnip-dependent NLRP3 inflammasome activation in macrophages via reducing oxidative stress. *Mucosal Immunol.* 12, 1150–1163. doi: 10.1038/s41385-019-0177-x

Zhu, M. Q., and Sun, R. C. (2018). Eucommia ulmoides Oliver: A Potential Feedstock for Bioactive Products. *J. Agric. Food Chem.* 66, 5433–5438. doi: 10.1021/acs.jafc.8b01312

Conflict of Interest: The authors declare that the research was conducted in the absence of any commercial or financial relationships that could be construed as a potential conflict of interest.

Publisher's Note: All claims expressed in this article are solely those of the authors and do not necessarily represent those of their affiliated organizations, or those of the publisher, the editors and the reviewers. Any product that may be evaluated in this article, or claim that may be made by its manufacturer, is not guaranteed or endorsed by the publisher.

frontiers in Microbiology

ORIGINAL RESEARCH
published: 20 August 2021
doi: 10.3389/fmicb.2021.706772

Heat Stress Alters the Intestinal Microbiota and Metabolomic Profiles in Mice

*Chaoyue Wen[1,2,3,4], Siyu Li[5], Jiaojiao Wang[5], Yimin Zhu[5], Xin Zong[1,2,3,4], Yizhen Wang[1,2,3,4] and Mingliang Jin[1,2,3,4,5]**

[1] Institute of Feed Science, College of Animal Sciences, Zhejiang University, Hangzhou, China, [2] Key Laboratory of Animal Feed and Nutrition of Zhejiang Province, College of Animal Sciences, Zhejiang University, Hangzhou, China, [3] Key Laboratory of Molecular Animal Nutrition, Ministry of Education, College of Animal Sciences, Zhejiang University, Hangzhou, China, [4] Key Laboratory of Animal Nutrition and Feed Science in Eastern China, Ministry of Agriculture, College of Animal Sciences, Zhejiang University, Hangzhou, China, [5] School of Life Sciences, Northwestern Polytechnical University, Xi'an, China

Background: Heat stress has negative effects on the intestinal health of humans and animals. However, the impact of heat stress on intestinal microbial and metabolic changes remains elusive. Here, we investigated the cecal microbial and metabolic profiles in mice in response to heat stress.

Methods: The mouse heat stress model was constructed by simulating a high-temperature environment. Twenty mice were randomly assigned to two groups, the control group (CON, 25°C) and the heat treatment group (HS, 40°C from 13:00 to 15:00 every day for 7 days). Serum and cecal contents were collected from the mice for serum biochemical analysis, 16S rRNA high-throughput sequencing, and non-targeted metabolomics.

Results: Both core body temperature and water intake were significantly increased in the HS group. Serum biochemical indicators were also affected, including significantly increased triglyceride and decreased low-density lipoprotein in the heat stress group. The composition and structure of intestinal microbiota were remarkably altered in the HS group. At the species level, the relative abundance of *Candidatus Arthromitus* sp. *SFB-mouse-Japan* and *Lactobacillus murinus* significantly reduced, while that of *Lachnospiraceae bacterium 3-1* obviously increased after HS. Metabolomic analysis of the cecal contents clearly distinguished metabolite changes between the groups. The significantly different metabolites identified were mainly involved in the fatty acid synthesis, purine metabolism, fatty acid metabolism, cyanoamino acid metabolism, glyceride metabolism, and plasmalogen synthesis.

Conclusion: In summary, high temperature disrupted the homeostatic balance of the intestinal microbiota in mice and also induced significant alterations in intestinal metabolites. This study provides a basis for treating intestinal disorders caused by elevated temperature in humans and animals and can further formulate nutritional countermeasures to reduce heat stress-induced damage.

Keywords: heat stress, gut microbiota, metabolomics, fatty acids, SFB

OPEN ACCESS

Edited by:
Jia Yin,
Hunan Normal University, China

Reviewed by:
Luiz Gustavo Gardinassi,
Universidade Federal de Goiás (IPTSP - UFG), Brazil
Fei Liu,
Northeast Agricultural University, China

***Correspondence:**
Mingliang Jin
mljin@zju.edu.cn

Specialty section:
This article was submitted to Microbial Symbioses, a section of the journal Frontiers in Microbiology

Received: *08 May 2021*
Accepted: *26 July 2021*
Published: *20 August 2021*

Citation:
Wen C, Li S, Wang J, Zhu Y, Zong X, Wang Y and Jin M (2021) Heat Stress Alters the Intestinal Microbiota and Metabolomic Profiles in Mice. Front. Microbiol. 12:706772. doi: 10.3389/fmicb.2021.706772

INTRODUCTION

High ambient temperature is the main factor threatening animal production in tropical and subtropical regions (Mueller et al., 2014; Slimen et al., 2015). Numerous studies have indicated that high temperatures impact not only the growth performance but also immune and intestinal mucosal barrier function in livestock (St-Pierre et al., 2003; Lrar and Rostagno, 2013; Faiz-ul et al., 2019) resulting in increased morbidity, mortality, and economic loss.

The stress response can trigger the organism's defense system, mitigating the damage caused by the stressor and maintaining physiological balance (Wen et al., 2019, 2020a). In the case of excessive stress or long-term stress on the organism, the stress response will gradually weaken and finally present as a pathological state (Wen et al., 2020b). Heat stress can seriously damage the intestinal tract, significantly increasing intestinal permeability (Cui and Gu, 2015; Zhang et al., 2017). Heat stress can also affect the immune function, potentially leading to intestinal mucosal damage (Gu et al., 2012; Tao et al., 2012). Through the study of the intestinal contents of heat-stressed broilers, it was found that the viable counts of *Lactobacillus* and *Bifidobacterium* were significantly reduced, resulting in an imbalance of intestinal microecology (Song et al., 2013, 2014; Al-Fataftah and Abdelqader, 2014).

The host metabolism is altered in response to environmental changes, specifically in terms of metabolic adaptations (Virtue et al., 2019). For example, a reduction in food intake can result in shortening of the jejunum (Lemme and Mitchell, 2008; Payne, 2019). The level of serum triglyceride (TG) was found to be significantly lower under chronic heat stress (He et al., 2019b). Water intake is an efficient way to alleviate heat stress, resulting in a lower rectal temperature and respiration rate (Marai et al., 2001). In broilers, both the total water intake and water intake per access were significantly increased at a high-temperature house (Bruno et al., 2011). Postabsorptive carbohydrate and lipid metabolism are also markedly altered (Baumgard and Rhoad, 2012). Together, these results suggested that heat stress exerts a negative effect on an organism's metabolism.

The microbiota appears to play an important role in the stress response (Sekirov et al., 2010; Zong et al., 2020) and the microbiota composition is related to heat tolerance (Ziegler et al., 2017). These intestinal microorganisms can assist in the maintenance of the intestinal barrier, thus effectively ensuring the host's health (Guarner and Malagelada, 2003). Disruption of the intestinal temperature may allow pathogen invasion and the consequent development of disease (Harvell et al., 2002). Although heat treatment has no great effect on the alpha diversity of the microbiome, alterations at the phylum and genus levels were observed (Zhong et al., 2019). Segmented filamentous bacteria (SFB) are host-specific gut symbionts that induce a multifaceted immune response, leading to host protection from gut pathogens (Pamp et al., 2012). It has been found that SFB can prevent the colonization of enteropathogenic *Escherichia coli* O103 (Heczko et al., 2000). Moreover, SFB is involved in lipid metabolism (Nguyen et al., 2007). Homeostatic disturbance of the gut microbiota may cause abnormal growth of microorganisms and inadequate absorption of host nutrients that be captured by microorganisms.

Heat stress has a deleterious effect on human and animal welfare and causes economic losses in livestock production. Therefore, in the present study, a mouse model was used to investigate the impact of heat stress on the diversity and metabolism of intestinal microbiota by next-generation sequencing and GC-TOF/MS. The aim was to explore the effects of heat stress on intestinal microbial diversity, metabolism, physiological and biochemical parameters in mice. Correlation analysis was used to determine the relationship between regulatory processes induced by heat stress and the intestinal microbiome community, thus providing a theoretical and experimental basis for our understanding of the effects of high temperature on humans and animals.

Abbreviations: AUC, area under the curve; LDL, low-density lipoprotein; OPLS-DA, Orthogonal partial least squares method-discriminant analysis; PCoA, principal coordinates analysis; SCFAs, short-chain fatty acids; SFB, segmented filamentous bacteria; TG, triglyceride.

MATERIALS AND METHODS

Animal Experiments

All animal experiments in the present study were approved by the Institutional Animal Care and Use Committee of Northwestern Polytechnical University, China, and performed following the institutional ethical guideline of experimental animals. Adult female ICR mice (30.2 ± 2.5 g) aged 7 weeks were purchased from the Animal Experimental Center of Xi'an Jiaotong University, China. The heat stress model was established according to previous study (Minho et al., 2017; Chen et al., 2020). The core temperature of mice is 37 ± 1°C. Under conditions when the increasing temperature is beyond the upper critical temperature of the range, the animals begin to suffer heat stress (Rojas-Downing et al., 2017). The hottest time of the day is between 1 and 3 PM. Taking these together, we chosen 40°C lasted 2 h as the heat stress condition. All animals had free access to food and drinking water and were housed in plastic cages in a controlled environment (temperature, 25°C; relative humidity, 60%; lighting cycle, 12 h/d). After 10 days of acclimatization under normal conditions, a total of 20 mice were randomly assigned to two groups (n = 10), including the control group (CON) and the heat stress group (HS). Starting from the 11th day, the temperature of the HS group was raised to 40°C from 13:00 to 15:00 during feeding every day and returned to 25°C for the remainder of the day. The experiment lasted for 7 days. At the end of the experiment, the animals were anesthetized and blood was withdrawn by orbital bleeding. Serum samples were separated after centrifugation at 4,000 × g for 15 min at 4°C. The cecum contents were also collected for 16S rRNA sequencing and GC-TOF/MS analysis.

Body Weight, Water Intake, and Core Body Temperature

After the HS treatment, the body weights were measured every 2 days. The daily water intake of the mice was also determined.

Serum Biochemical Parameters

The serum biochemical parameters included total cholesterol, TG, high-density lipoprotein, and low-density lipoprotein (LDL) were investigated using an automatic biochemical analyzer (Shenzhen Redbang Electronics Co., Ltd., China).

DNA Extraction, Library Construction, and Sequencing

Total DNA from the cecal contents was extracted using the E.Z.N.A.®Genomic DNA Isolation Kit (Omega Bio-Tek, United States) according to the manufacturer's instructions. To investigate the bacterial community structure, we used next-generation 16S rRNA sequencing to analyze the composition of the cecal microbiota. The V3-V4 hypervariable region of the bacterial 16S rRNA gene in each sample was amplified using the broadly conserved primers, 27F (5′-AGAGTTTGATCCTGGCTCAG-3′) and 533R (5′-TTACCGCGGCTGCTGGCAC-3′), and then sequenced using an Illumina MiSeq PE250 (Illumina, San Diego, CA, United States). The assembled MiSeq sequences were submitted to the NCBI'S Sequence Read Archive (SRA BioProject No. PRJNA730381) for open access. The resulting raw sequences were filtered and assembled according to previous research (Jin et al., 2019; Zhou et al., 2019) and using the QIIME (v1.9.1) and FLASH (v1.2.11) software packages. The filtered sequences were compared with SILVA (v132) small subunit ribosomal RNA database, and the similarity more than 80% of the species information was screened out. In the taxonomic analysis of each OTU, sequences with 97% similarity were selected first, and the consistency of these sequences was analyzed. Finally, the species information of each OTU was taken as the species information of its nearest ancestor. The analysis and production of rarefaction curves were performed by Mothur (v1.30.2) and R software, respectively. To investigate bacterial richness and diversity, Mothur was also used to analyze the alpha diversity, including the Chao, Ace, Shannon, and Simpson indices. The OTU coverage curves were expressed using the "vegan" R package.

Sample Preparation and GC-TOF/MS Analysis

Cecal samples (100 μL) were slowly thawed at 4°C. 200 μL acetonitrile was added, followed by sonication for 10 min, and centrifugation at 10,000 × *g* for 10 min at 4°C. The supernatant was removed and vacuum-dried at 40°C. For mass spectrometry, 50 μL 15 mg/mL methoxyamine pyridine solution was reconstituted, vortexed, and incubated at 70°C for 1 h. 50 μL silanization reagent (MSTFA: TMCS = 100:1) was added to the centrifuge tube for derivatization, mixed well, allowed to stand for 1 h, and then added to a concentration of 0.1 mg/mL n-heptane containing 150 μL docosane, before thorough mixing and centrifugation at 10,000 × *g* for 10 min at 4°C. The supernatant was retained and transferred to a sample bottle for GC-TOF/MS analysis (Agilent 7890A gas chromatograph equipped with an Agilent DB-5MS capillary column (30 m × 250 μm × 0.25 μm, J&W Scientific, Folsom, CA, United States).

The derivatized sample (1.0 μL) was injected by the splitless mode. The helium carrier gas flow rate was 1 mL/min. The oven temperature ramp program was set as follows: initial holding at 50°C for 1 min, increasing to 240°C at 10°C/min, and finally holding for 2 min. The temperatures of the front inlet, transfer line, and ion source were set at 280, 270, and 220°C, respectively. The ionization voltage was set to − 70 eV, the quality control ranged from 50 to 500 *m/z*, the scan rate was 20 spectra/s, and the solvent delay time was 6 min.

GC-TOF/MS Data Processing and Differential Metabolites Identification

After the raw data was collected, the LECO's ChromaTOF software was used for peak alignment, retention time correction, deconvolution analysis, peak identification, and area extraction. Principle component analysis (PCA) and orthogonal partial least squares method-discriminant analysis (OPLS-DA) were performed using SIMCA software. After the analyzed data was matched with the KEGG data ID, path enrichment and network construction were performed (Haug et al., 2019). Analysis of differential metabolites and metabolic pathways were performed based on MetaboAnalyst 4.0.[1] The RAW data of GC–TOF/MS has been submitted to Metabolights NO. MTBLS2874.[2]

Data Analysis

All statistical analyses were performed using SAS 8.2 software (SAS Institute, Inc.). The data relating to the microbiota community were analyzed on the free online platform of Majorbio Cloud Platform.[3] Metagenomes were predicted from the copy number-normalized 16S rRNA data according to the previous report (Zhou et al., 2018). The molecular functions were categorized into KEGG pathways on the web-based Galaxy according to the instructions described by developers.[4] [5] Correlation analysis was computed with spearman test in R using corrplot package (Wei and Simko, 2013). The codes used in the analysis could be found on the websites.[6] Details can be found in the legends of the corresponding figures and tables. The difference between CON and HS was compared using an unpaired *t*-test. *P*-values < 0.05 indicated statistical significance.

RESULTS

Body Weight, Water Intake, and Core Body Temperature

In the heat stress mouse model, no significant difference was found in body weight between the groups (**Figure 1A**). As expected, both the relative intake of water (**Figure 1B**) on the 7th day and the body temperature significantly increased in the

[1]http://www.metaboanalyst.ca

[2]www.ebi.ac.uk/metabolights/MTBLS2990

[3]www.majorbio.com

[4]http://huttenhower.sph.harvard.edu/galaxy/

[5]http://picrust.github.io/picrust

[6]https://github.com/zlabx/zlab-qiime2

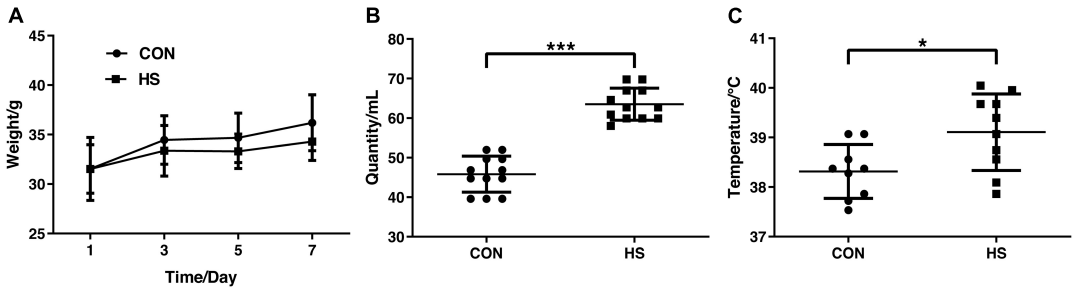

FIGURE 1 | Changes in body weight **(A)** water intake **(B)** and core body temperature **(C)** on day 7. CON, control group; HS, heat stress group. $^{*}P < 0.05$, $^{***}P < 0.001$.

HS group (**Figure 1C**) ($n = 10$ per treatment). This indicated the successful establishment of the heat stress model.

Serum Biochemical Indices

We further analyzed serum concentrations of lipids. The fasting serum lipids values are presented in **Figure 2**. There were no significant changes in the levels of total cholesterol and high-density lipoprotein (**Figures 2A, C**). Compared with the CON group, the level of serum TG increased significantly, and LDL decreased remarkably in the HS group (**Figures 2B, D**) ($n = 10$ per treatment).

Cecal Microbial Community

Across all 20 samples, 1451173 high-quality sequences were identified, with an average length of 411 bp. No remarkable differences were found in the richness estimators (Ace and Chao), diversity indices (Shannon and Simpson), and observed OTUs (**Supplementary Table 1**). The normalized microbiome data has been added in the supplementary material (**Supplementary Table 2**).

We further investigated the shifts in bacterial taxa that were responsible for heat stress adaptation. Principal coordinates analysis (PCoA) based on weighted_unifrac revealed distinct clustering of microbiota composition for the two groups (**Figure 3A**). Analysis of the similarities in the Bray-Curtis distance indicated that the heat-stressed and control mice tended to be different ($P = 0.052$) with an R-value of 0.1237, suggesting that the microbiota of the two groups were different. A non-metric multidimensional scaling (NMDS) ordination plot based on the Bray-Curtis distance metric showed that the cecal bacterial communities in the samples could be differentiated by heat treatment (**Figure 3B**).

The overall microbial composition of the two groups differed at the phylum, family, genus, and species levels. The five largest phyla represented in each group were Firmicutes, Proteobacteria, Bacteroidetes, Tenericutes, and Deferribacteres. The thermoneutral mice had a higher relative abundance of Proteobacteria (28.1%), Bacteroidetes (16.4%), and Tenericutes (3.1%), but a lower relative abundance of Firmicutes (48.7%) and Deferribacteres (0.5%) (**Figure 3C**). Heat-treated mice contained largely bacteria of the phyla Bacteroidetes 14.9%, Firmicutes 52.5%, Proteobacteria 26.7%, Tenericutes 1.3%, and Actinobacteria 1.0% (**Figure 3C**). No statistical differences were observed in the relative abundance of the five largest phyla. However, heat treatment tended to decrease the proportion of Tenericutes and Actinobacteria ($P = 0.071$ and 0.098, respectively) (**Figure 3C**). These results suggested that the gut microbiota composition of mice remained relatively stable under heat stress. At the family level, *Clostridiaceae_1* was significantly enriched in thermoneutral conditions (**Figure 3D** and **Supplementary Figure 1A**). The relative abundance at the levels of class and order were presented in supplementary materials (**Supplementary Figures 1D–F**). At the genus level, *Lachnospiraceae bacterium 3-1* and *unclassified g-Anaerotruncus* were significantly increased, while *Candidatus Arthromitus* sp. *SFB-mouse-Japan*, *Lachnoclostridium*, and *Lactobacillus murinus* were significantly decreased in the heat-treated mice (**Figure 3E** and **Supplementary Figure 1B**). At the OTU level, OTU1468, and OUT1733 were significantly increased in the HS group, while OTU1364 and OTU778 were significantly decreased in the CON group (**Supplementary Figure 1C**).

Predicted Molecular Functions of Cecal Microbiota

We found that multiple KEGG (level 3) categories were disturbed in the heat-treated group. The KEGG at level 2 category results were consistent with the findings of KEGG at level 3 (**Figure 3F**). Specifically, the enriched pathways were membrane transport, lipid metabolism, infectious disease: bacterial, infectious disease: parasitic, immune disease, excretory system, cellular community-prokaryotes, cell motility, glycan biosynthesis, and metabolism, and signaling molecules and interaction (**Supplementary Figure 2**). Moreover, carbohydrate digestion and absorption, DNA replication proteins, translation proteins, and pyrimidine metabolism were significantly upregulated in the CON group (**Figure 3F**).

Variations in Cecal Metabolite Profiles

To explore the effects of heat treatment on cecal metabolites in mice, GC-TOF/MS was applied to investigate the intestinal metabolite profiles. A total of 532 effective peaks were obtained, of which 235 compounds were relatively quantified, 120 were labeled "analyte," 173 were labeled "unknown" as compared against the LECO-Fiehn Rtx5 database. The differences of

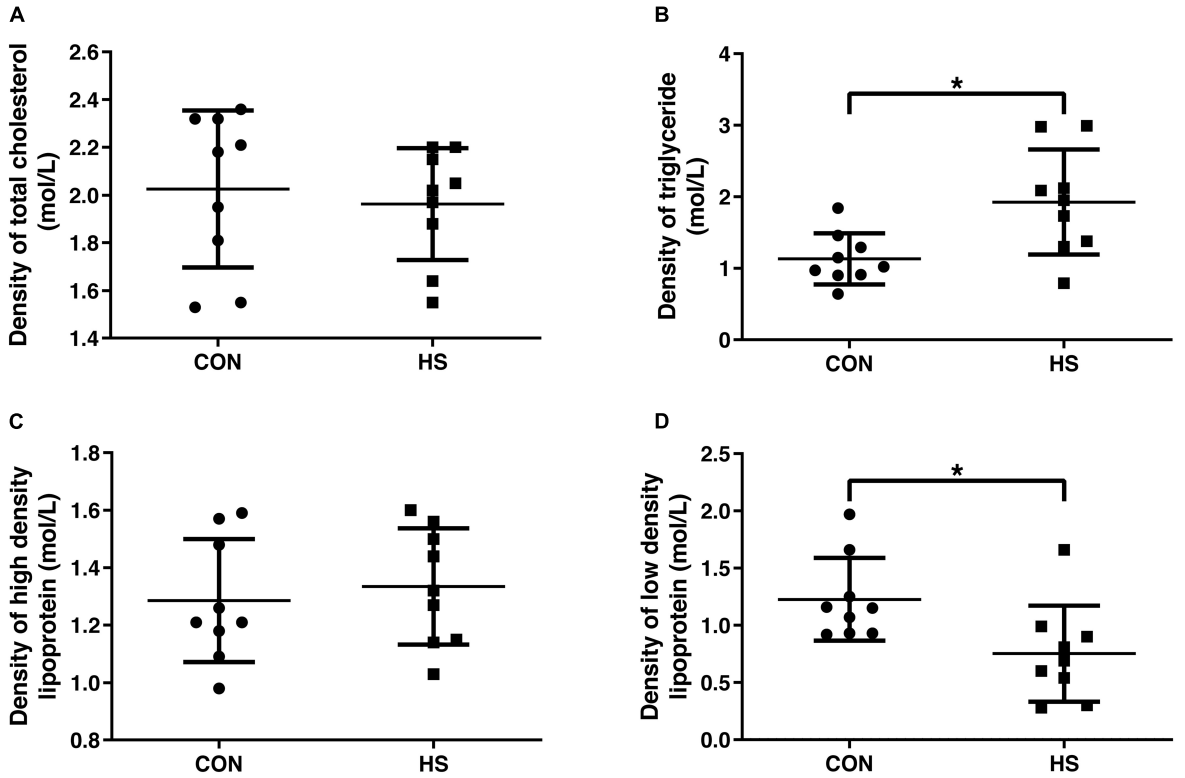

FIGURE 2 | Changes of blood lipid indicators. Density of total cholesterol **(A)**, triglyceride **(B)**, high density lipoprotein **(C)** and low density lipoprotein **(D)** in serum. CON, control group; HS, heat stress group. *$P < 0.05$.

metabolomics profiles between CON and HS groups by the multivariate analysis are shown in **Figures 4A, B**. Principal component analysis (PCA) of the metabolites showed no clear distinction between the groups (**Figure 4A**). To further verify the differences between the groups, we did an OPLS-DA which clearly distinguished the metabolites (**Figure 4B**). It indicated that the GC-TOF/MS-based metabolomics and PLS-DA model was suitable to be applied in identifying the differences between the two groups. Furthermore, the heatmap showed significant changes in the intestinal metabolites between the two groups (**Figure 4C**). Compared with the CON, the heat stress group showed significant up-and down-regulation of 7 metabolites and 10 metabolites, respectively (**Supplementary Table 3**). In these metabolites, xanthine, shikimic acid, salicin, purine riboside, diglycerol, 3,5-dihydroxyphenylglycine, and 2-deoxy-D-glucose were enriched in the HS group. Conversely, there was a increase of metabolites such as stearic acid, pipecolinic acid, palmitic acid, oleic acid, myristic acid, mannose, carbazole, behenic acid, 4-hydroxyphenylacetic acid, and 3-aminopropionitrile in the CON group (**Supplementary Table 3**). The normalized metabolomics data is provided in spreadsheets on the supplementary material (**Supplementary Table 4**).

Differential Metabolic Pathway Analysis

KEGG analysis of the 17 significantly different metabolites showed enrichment of the fatty acid biosynthesis, purine metabolism, fatty acid metabolism, cyanoamino acid metabolism, tyrosine metabolism, amino sugar and nucleotide sugar metabolism, and lysine degradation pathways (**Figure 4D**). Further analysis of the metabolic pathways by bubble diagram and metabolic pathway enrichment revealed that heat treatment significantly inhibited the fatty acid synthesis pathway.

Analysis and Verification of Biomarkers

Based on variable importance for projection (VIP) > 1.0 in the OPLS-DA and P-value < 0.05 between the two groups, carbazole, purine nucleoside, and stearic acid were selected as biomarkers in the intestine that responded to heat stress (**Figure 4E**). The AUCs of carbazole (AUC value = 0.85), purine nucleoside (AUC value = 0.87), and stearic acid (AUC value = 0.855), as well as the levels of these three compounds in the intestine, are shown in **Figure 4E**. Besides, cross-validation prediction of the samples with three metabolites indicated that CON and HS showed a significant separation trend (**Supplementary Figure 3**). The results of comprehensive prediction with these three biomarkers showed that the average AUC was 0.973, which was extremely close to 1 (**Supplementary Figure 3**), and that the two groups of samples were clear separated and discriminated.

Correlation Analysis Between Serum Index, Significantly Different Microbiota and Metabolites

To further study the correlation between gut microbiota, metabolites, and serum biochemical markers, Spearman analyses

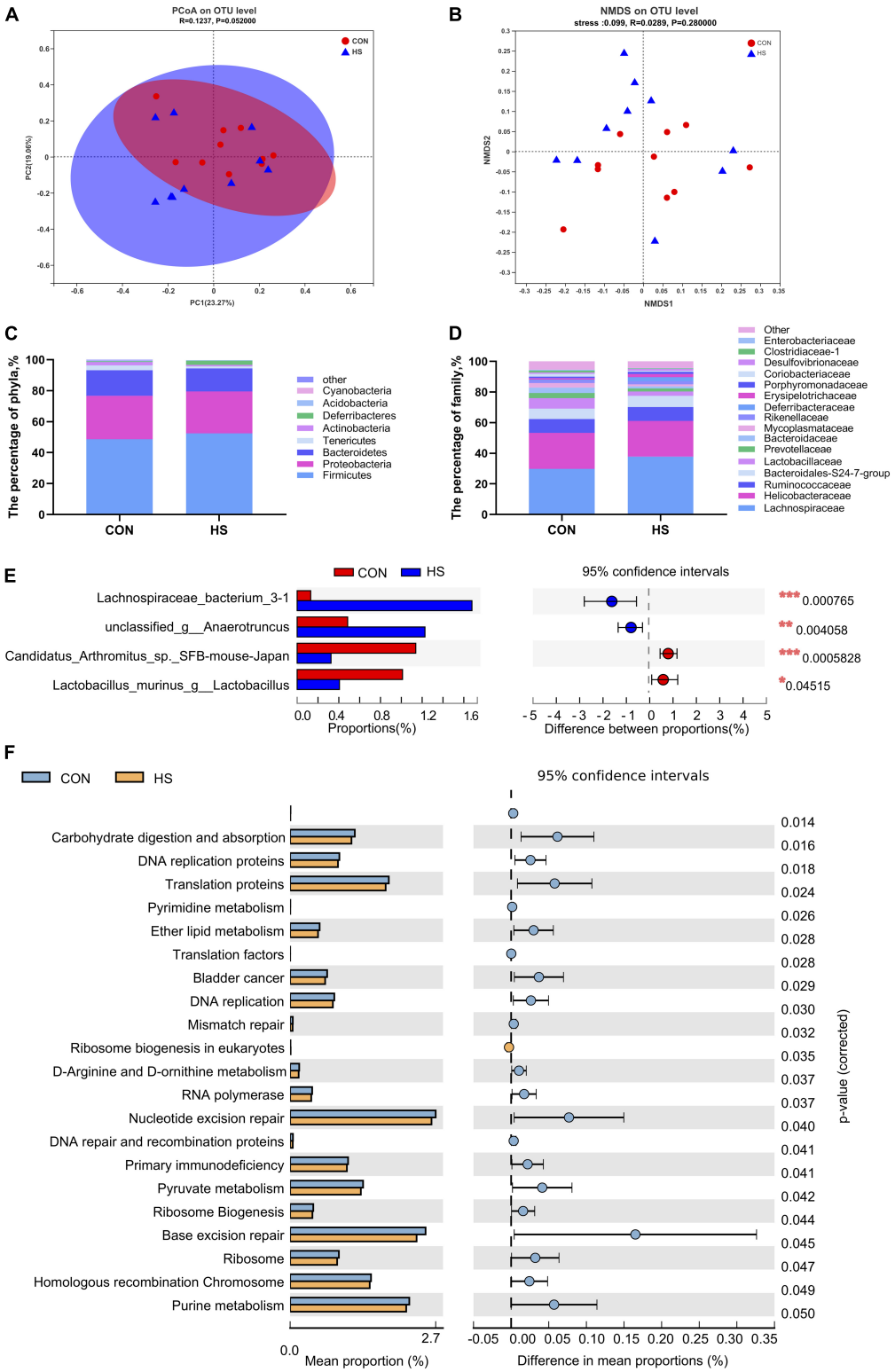

FIGURE 3 | Effects of heat stress on mouse gut microbiota. **(A)** Analysis of the PCoA plots based on a Bray-Curtis distance metric. **(B)** NMDS ordination plots of cecal bacterial communications in the HS and CON group based on the Bray-Curtis distance metric. **(C)** Differential microorganisms at the phylum level. **(D)** Differential microorganisms at the family level. **(E)** *T*-test bar plot of significantly different species between the groups (relative abundance > 1%). **(F)** *T*-test bar plot of significantly differed pathways enriched at KEGG level 3. CON, control group; HS, heat stress group; PCoA, principal coordinates analysis; NMDS, Non-metric multidimensional scaling.

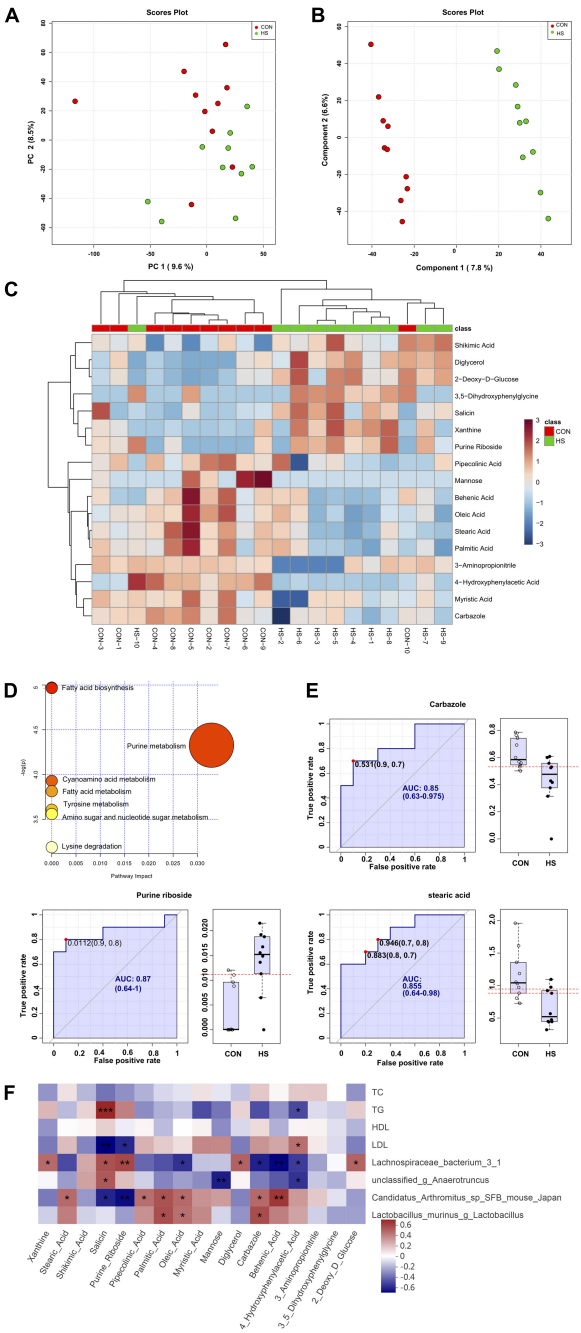

FIGURE 4 | Changes in cecal metabolite profile of mice shaped by heat stress. **(A)** PCA score plot. **(B)** OPLS-DA score plot. **(C)** heatmap tree show metabolites significantly different between groups and their phylogenic relationships. **(D)** Metabolic pathway enrichment analysis. **(E)** Biomarker analysis. **(F)** Correlations between serum indicators and gut microbiota, and cecum metabolic indicators mediated by heat stress. CON, control group; HS, heat stress group; OPLS-DA, Orthogonal partial least squares method-discriminant analysis. *$P < 0.05$, **$P < 0.01$, ***$P < 0.001$.

were performed (**Figure 4F**). It was observed that TG showed a significant negative correlation with 4-hydroxyphenylacetic acid ($\rho = -0.45$, $P = 0.049$) and a positive correlation with the salicin level ($\rho = 0.68$, $P < 0.001$). However, the correlation between LDL and 4-hydroxyphenylacetic acid ($\rho = 0.46$, $P = 0.043$) and salicin ($\rho = -0.63$, $P = 0.003$) level was exactly the opposite of TG.

There is a close relationship between gut microbiota and metabolites. For instance, *Candidatus Arthromitus* sp. *SFB-mouse-Japan* showed a negative correlation with salicin ($\rho = -0.55$, $P = 0.013$) and purine riboside ($\rho = -0.60$, $P = 0.005$) and a positive correlation with behenic acid ($\rho = 0.63$, $P = 0.003$). *Lactobacillus murinus* was positively correlated with carbazole ($\rho = 0.56$, $P = 0.010$) and palmitic acid ($\rho = 0.55$, $P = 0.011$). Moreover, *Lachnospiraceae bacterium 3-1* was positively associated with salicin ($\rho = 0.54$, $P = 0.013$), purine riboside ($\rho = 0.58$, $P = 0.008$), and diglycerol ($\rho = 0.50$, $P = 0.026$, but negatively associated with behenic acid ($\rho = -0.62$, $P = 0.004$), oleic acid ($\rho = -0.51$, $P = 0.022$), and carbazole ($\rho = -0.56$, $P = 0.011$). *Unclassified-g-Anaerotruncus* was positively associated with salicin ($\rho = 0.52$, $P = 0.018$) but negatively correlated with both mannose ($\rho = -0.57$, $P = 0.009$) and 4-hydroxyphenylacetic acid ($\rho = -0.50$, $P = 0.024$).

DISCUSSION

Temperature is a crucial environmental signal that controls the growth and development of bacteria. Continuous high temperature may cause functional disorders, including intestinal dysbiosis (Bouchama and Knochel, 2002; Kovats and Hajat, 2008; He et al., 2019a). The impact of heat stress on microbial composition and metabolites in mice is still limited. A better understanding of the physiological alterations of the microbial community and its metabolites under heat stress could help to develop targeted approaches to alleviate heat stress.

Heat stress induces weight loss was reported in ducks (He et al., 2019b), broiler (Luo et al., 2018). In our study, we also found a body weight loss in the HS group. Animals developed a phenotypic response to heat acclimation which results in decreased feed intake and increased water intake to accommodate increased evaporative heat loss requirements (Robert et al., 2018). The core temperature is significantly increased in the HS group, which indicated that our heat stress model was successfully established.

Blood biochemical indicators can be used to determine metabolic status. It was found that the TG content was significantly increased with the LDL level showing an opposite trend in HS mice. LDL is mainly responsible for transporting cholesterol from the liver to the tissues of the body, and then metabolizing cholesterol by the body (Cirulli and Ginsburg, 2017). When the body is subjected to heat stress, cholesterol metabolism is slowed down, resulting in a decrease in LDL levels. In broilers, heat stress was found to increase the TG concentration (Luo et al., 2018), consistent with our results. In general, there is an alteration in the metabolic response to heat stress characterized by an increase in the use of carbohydrates and a decrease in fat usage (Febbraio, 2001). It follows that the TG content in the blood is significantly increased.

The effect of heat stress on the intestinal microbiota and their microecological structure in mice was studied by 16S

rRNA high-throughput sequencing. Analysis of the rarefaction curves and alpha diversity showed that there were no significant differences in the alpha diversity indices, indicating that HS had no significant effect on intestinal microbiota diversity. According to the sequencing, the mouse intestinal microbiome consists mainly of five phyla, the Firmicutes, Proteobacteria, Bacteroidetes, Tenericutes, and Deferribacteres. Among these, the dominant microbial group was Firmicutes, accounting for more than 60% of the microbiome. Besides these, we also detected Verrucomicrobia, Acidobacteria, Actinomycetes, and Cyanobacteria in the mouse intestine, with low proportions of less than 0.2%. The Firmicutes/Bacteroidetes ratio, a parameter to evaluate the imbalance of microbial composition, has been used to indicate obesity in the host (Wen et al., 2008). In our study, the Firmicutes/Bacteroidetes ratio increased by 21.5% in the heat-treated group (**Supplementary Figure 1G**).

Accumulating evidence has revealed the dysbiosis of intestinal microbiota induced by heat stress in mammals and poultry (Song et al., 2013; Zhang et al., 2017; Zhu et al., 2018; He et al., 2019b). Stress-induced by extreme environments such as simulated weightlessness can also change the composition of the intestinal microbiota, decrease the diversity of intestinal microorganisms (Chen et al., 2016), lead to changes in the homeostasis of colonic epithelial cells and barrier function, and also cause pathological changes of the intestinal mechanical barrier, including intestinal villus damage and down-regulation of tight junction protein expression, thereby changing intestinal permeability (Shi et al., 2017; Jin et al., 2018). The present study indicated that heat stress significantly reduced the abundance of *Candidatus Arthromitus* sp. *SFB-mouse-Japan*, *Lactobacillus murinus* in the gut, and significantly increased the abundance of *Lachnospiraceae bacterium 3-1*. *Candidatus Arthromitus* plays an important role in host immune regulation, as it is in contact with epithelial cells and be transplanted into host epithelial cells, thereby triggering a series of physiological responses related to the host immune system (Pamp et al., 2012; Bolotin et al., 2014). SFB are host-specific intestinal symbionts that comprise a distinct clade within the *Clostridiaceae*, designated *Candidatus Arthromitus* (Pamp et al., 2012). SFB induces a multifaceted immune response, leading to host protection from intestinal pathogens (Pamp et al., 2012). *Candidatus Arthromitus* sp. *SFB-mouse-Japan* was one of the five SFB filaments isolated from a mouse (Pamp et al., 2012). SFB has a relatively high abundance of predicted proteins devoted to cell cycle control and to envelope biogenesis (Pamp et al., 2012). The dominance of *Lactobacillus* in the intestine is associated with protection against pathogens and infections (Reid and Burton, 2002). *Lactobacillus* plays an essential role in food fermentation and is used in probiotic applications (Heeney et al., 2018). The most abundant lactobacilli included *L. murinus*, *L. casei* and *L. ruminus*, and *L. murinus* is considered a gut-autochthonous microorganism. *Lactobacillus* has been reported to be remarkably enriched in the distal gut (Rossi et al., 2016). The depletion of intestinal *Lactobacillus* is frequently associated with the disease. *Oscillibacter*, a beneficial bacterium, is significantly reduced in patients (Fang et al., 2016), piglets with intrauterine growth retardation (Zhang et al., 2019), and obese mice (Gong et al., 2020), indicating that the intestinal microflora constitution was disturbed. *Ruminococcaceae* is significantly higher in the intestinal flora of a high-risk colorectal cancer population than in a low-risk population (Moore and Moore, 1995). It was speculated that a high-temperature environment may have specific effects on patients with colorectal cancer. *Lachnospiraceae* are the main producers of short-chain fatty acids (SCFAs) and have been associated with intestinal diseases (Vacca et al., 2020). They are also increased in obese subjects, which suggested that the metabolic syndrome may be related to a gut microbiota disorder (Zhao et al., 2019). The study of microbial excavation and interaction is useful to reveal the influence of heat stress on the intestinal mucosal barrier and can provide a theoretical basis and experimental ideas for the prevention and repair of body damage caused by heat stress. The gut flora plays a key role in host energy metabolism (Guarner and Malagelada, 2003; Dai et al., 2011; Pérez-Cobas et al., 2013). Indigestible carbohydrates are degraded by fermentation of colonic microflora to produce metabolic end products, such as SCFAs, these metabolites have been shown to affect host physiological activities (Topping and Clifton, 2001; Wong et al., 2006; Wang et al., 2019; Guo et al., 2020). Recent studies have confirmed that SCFAs can inhibit the production of anti-inflammatory factors and inhibit colonic inflammation (Tan et al., 2014; van der Beek et al., 2017; Kurata et al., 2019; Zeng et al., 2019).

To determine the effect of heat stress on the mice's cecal metabolites, GC-TOF/MS was used to explore the chemical constituents of the intestinal contents in both groups. The results showed that heat treatment produced significant changes in the cecal metabolites with most metabolites significantly reduced compared with the CON, including oleic acid, palmitic acid, stearic acid, mannose, myristic acid, and carbazole. These metabolites are involved in the physiological and biochemical processes of energy metabolism and lipid metabolism (Savage et al., 2007; Loscalzo, 2011; Li et al., 2017). Heat treatment inhibited fatty acid synthesis, shown by combining a bubble diagram and metabolic pathway enrichment. Meanwhile, three metabolites were screened as biomarkers, namely carbazole, purine nucleoside, and stearic acid, and these were used to cross-validate and predict the HS and CON samples. Salicin showed a potential therapeutic agent against LPS induced acute injury (Li et al., 2015). In our study, the salicin was significantly increased in the HS group (**Supplementary Table 3**). It suggested that the host triggered an adapted response to counter heat stress-induced inflammatory processes.

Intestinal metabolites are agents between the microbiota and energy metabolism (Karl et al., 2018). Previous study have found that heat stress could induce the increase of fatty acids (Cui et al., 2019). The correlation analysis in this study suggested that TG was significant negative correlation with 4-hydroxyphenylacetic acid and positive correlation with the salicin level Interestingly, the correlation between LDL and 4-hydroxyphenylacetic acid and salicin level was exactly the opposite of TG. *Candidatus Arthromitus* sp. *SFB-mouse-Japan* showed a negative correlation with salicin and purine riboside and a positive correlation with behenic acid. These results indicated that microbiota are involved in the regulation of energy metabolism.

In conclusion, this study revealed the important relationship between intestinal microbiota structure and metabolism under heat stress. We need not only to identify changes in the intestinal flora structure but also to understand the correlation between the microflora and disease under heat treatment. Our study screened some metabolites and microbiota in the cecum of heat-stressed mice might have potential beneficial properties. This study provides a theoretical and experimental basis for further research into high-temperature damage in humans and animals.

DATA AVAILABILITY STATEMENT

The assembled MiSeq sequences were submitted to the NCBI'S Sequence Read Archive (SRA BioProject No. PRJNA730381) for open access. The RAW data of GC–TOF/MS has been submitted to metabolights no. MTBLS2990 (www.ebi.ac.uk/metabolights/MTBLS2990).

ETHICS STATEMENT

The animal study was reviewed and approved by Institutional Animal Care and Use Committee of Northwestern Polytechnical University, China.

AUTHOR CONTRIBUTIONS

MJ designed the experiment. YZ conducted the experiment. CW and MJ collected and analyzed the data. MJ, SL, YW, and XZ helped with the discussion. CW, SL, JW, and MJ wrote and revised the manuscript. All authors contributed to the article and approved the submitted version.

FUNDING

This work was supported by the National Natural Science Foundation of China (Grant Nos. 32022079 and 31630075), Zhejiang Provincial Natural Science Foundation of China (Grant No. LZ20C170005), and Fundamental Research Founds for the Central Universities (Grant No.2020-KYY-517102-0001). This study was supported by Shanghai Biotree Biomedical Technology Co., Ltd.

SUPPLEMENTARY MATERIAL

The Supplementary Material for this article can be found online at: https://www.frontiersin.org/articles/10.3389/fmicb.2021.706772/full#supplementary-material

Supplementary Figure 1 | Effect of heat stress on cecal microbiota of mice. **(A)** Welch's *t*-test bar plot at the family level (relative abundance >1%). **(B)** Welch's *t*-test bar plot at the genus level (relative abundance >1%). **(C)** Welch's *t*-test bar plot at the OTU level (relative abundance >1%). **(D)** Relative abundance of microbiome at the class level. **(E)** Relative abundance of microbiome at the order level. **(F)** Relative abundance of microbiome at the genus level. **(G)** The ratio of Firmicutes/Bacteroidetes. CON=control group; HS=heat stress group.

Supplementary Figure 2 | The heatmap of KEGG pathway level 2. CON=control group; HS=heat stress group.

Supplementary Figure 3 | Biomarker analysis of metabolites based on the random forests algorithm. ROC view **(A)**, probability view **(B)**, and cross validation **(C)** of three selected metabolites, namely carbazole, purine nucleoside and stearic acid. CON=control group; HS=heat stress group.

Supplementary Table 1 | The influence of HS on α-diversity of gut microbiota.

Supplementary Table 2 | The normalized microbiome data.

Supplementary Table 3 | Significantly different metabolites in cecal contents between CON and HS groups.

Supplementary Table 4 | The normalized metabolomics data.

REFERENCES

Al-Fataftah, A.-R., and Abdelqader, A. (2014). Effects of dietary *Bacillus subtilis* on heat-stressed broilers performance, intestinal morphology and microflora composition. *Anim. Feed Sci. Tech.* 198, 279–285. doi: 10.1016/j.anifeedsci.2014.10.012

Baumgard, L. H., and Rhoad, P. R. (2012). Ruminant nutrition symposium: ruminant production and metabolic responses to heat stress. *J. Anim. Sci.* 90, 1855–1865. doi: 10.2527/jas.2011-4675

Bolotin, A., de Wouters, T., Schnupf, P., Bouchier, C., Loux, V., Rhimi, M., et al. (2014). Genome sequence of "*Candidatus arthromitus*" sp. strain SFB-mouse-nl, a commensal bacterium with a key role in postnatal maturation of gut immune functions. *Genome Announc.* 2, e705–e714. doi: 10.1128/genomeA.00705-14

Bouchama, A., and Knochel, J. P. (2002). Heat stroke. *New Engl. J. Med.* 346, 1978–1988. doi: 10.1056/NEJMra011089

Bruno, L. D. G., Maiorka, A., Macari, M., Furlan, R. L., and Givisiez, P. E. N. (2011). Water intake behavior of broiler chickens exposed to heat stress and drinking from bell or and nipple drinkers. *Braz. J. Poult. Sci.* 13, 147–152. doi: 10.1590/S1516-635X2011000200009

Chen, P., Yu, Y., Tan, C., Liu, H., Wu, F., Li, H., et al. (2016). Human metabolic responses to microgravity simulated in a 45-day 6° head-down tilt bed rest (HDBR) experiment. *Anal. Methods* 8, 4334–4344. doi: 10.1039/C6AY00644B

Chen, Y., Jiang, W., Liu, X., Du, Y., Liu, L., Ordovas, J. M., et al. (2020). Curcumin supplementation improves heat-stress-induced cardiac injury of mice: physiological and molecular mechanisms. *J. Nutr. Biochem.* 78:108331. doi: 10.1016/j.jnutbio.2019.108331

Cirulli, E. T., and Ginsburg, G. S. (2017). Studying genetic resilience to improve human health. *Oral Dis.* 23, 685–688. doi: 10.1111/odi.12567

Cui, Y., and Gu, X. (2015). Proteomic changes of the porcine small intestine in response to chronic heat stress. *J. Mol. Endocrinol.* 55, 277–293. doi: 10.1530/JME-15-0161

Cui, Y., Wang, Y., Hao, Y., Gu, X., and Wang, H. (2019). Chronic heat stress induces acute phase responses and serum metabolome changes in finishing pigs. *Animals* 9:395. doi: 10.3390/ani9070395

Dai, Z., Wu, G., and Zhu, W. (2011). Amino acid metabolism in intestinal bacteria: links between gut ecology and host health. *Front. Biosci.* 16, 1768–1786. doi: 10.2741/3820

Faiz-ul, H., Ayesha, N., Rehman, M. S., Muhammad, A. A., Dilshad, S. M. R., and Yang, C. (2019). Prospects of HSP70 as a genetic marker for thermo-tolerance and immuno-modulation in animals under climate change scenario. *Anim. Nutr.* 5, 340–350. doi: 10.1016/j.aninu.2019.06.005

Fang, X., Wang, X., Yang, S., Meng, F., Wang, X., Wei, H., et al. (2016). Evaluation of the microbial diversity in amyotrophic lateral sclerosis using high-throughput sequencing. *Front. Microbiol.* 7:1479. doi: 10.3389/fmicb.2016.01479

Febbraio, M. A. (2001). Alterations in energy metabolism during exercise and heat stress. *Sports Med.* 31, 47–59. doi: 10.2165/00007256-200131010-00004

Gong, S., Ye, T., Wang, M., Wang, M., Li, Y., Ma, L., et al. (2020). Traditional chinese medicine formula kang shuai lao pian improves obesity, gut dysbiosis, and fecal metabolic disorders in high-fat diet-fed mice. *Front. Pharmacol.* 11:297. doi: 10.3389/fphar.2020.00297

Gu, X. H., Hao, Y., and Wang, X. L. (2012). Overexpression of heat shock protein 70 and its relationship to intestine under acute heat stress in broilers: 2. *Intestinal Oxidat. Stress Poult. Sci.* 91, 790–799. doi: 10.3382/ps.2011-01628

Guarner, F., and Malagelada, J. R. (2003). Gut flora in health and disease. *Lancet* 361, 512–519.

Guo, Y., Bian, X., Liu, J., Zhu, M., Li, L., Yao, T., et al. (2020). Dietary components, microbial metabolites and human health: reading between the lines. *Foods* 9:1045. doi: 10.3390/foods908145

Harvell, C. D., Mitchell, C. E., Ward, J. R., Altizer, S., Dobson, A. P., Ostfeld, R. S., et al. (2002). Climate warming and disease risks for terrestrial and marine biota. *Science* 296, 2158–2162. doi: 10.1126/science.1063699

Haug, K., Cochrane, K., Nainala, V. C., Williams, M., Chang, J., Jayaseelan, K. V., et al. (2019). MetaboLights: a resource evolving in response to the needs of its scientific community. *Nucleic Acids Res.* 48, D440–D444. doi: 10.1093/nar/gkz1019

He, J., Guo, H., Zheng, W., Xue, Y., Zhao, R., and Yao, W. (2019a). Heat stress affects fecal microbial and metabolic alterations of primiparous sows during late gestation. *J. Anim. Sci. Biotech.* 10:84. doi: 10.1186/s40104-019-0391-0

He, J., He, Y., Pan, D., Cao, J., Sun, Y., and Zeng, X. (2019b). Associations of gut microbiota with heat stress-induced changes of growth, fat deposition, intestinal morphology and antioxidant capacity in ducks. *Front. Microbiol.* 10:903. doi: 10.3389/fmicb.2019.00903

Heczko, U., Abe, A., and Finlay, B. B. (2000). Segmented filamentous bacteria prevent colonization of Enteropathogenic *Escherichia coli* O103 in rabbits. *J. Infect. Dis.* 181, 1027–1033. doi: 10.1086/315348

Heeney, D. D., Gareau, M. G., and Marco, M. L. (2018). Intestinal Lactobacillus in health and disease, a driver or just along for the ride? *Curr. Opin. Biotech.* 49, 140–147. doi: 10.1016/j.copbio.2017.08.004

Jin, M., Zhang, H., Wang, J., Shao, D., Yang, H., Huang, Q., et al. (2019). Response of intestinal metabolome to polysaccharides from mycelia of Ganoderma lucidum. *Int. J. Biol. Macromol.* 122, 723–731. doi: 10.1016/j.ijbiomac.2018.10.224

Jin, M., Zhang, H., Zhao, K., Xu, C., Shao, D., Huang, Q., et al. (2018). Responses of intestinal mucosal barrier functions of rats to simulated weightlessness. *Front. Physiol.* 9:729. doi: 10.3389/fphys.2018.00729

Karl, J. P., Hatch, A. M., Arcidiacono, S. M., Pearce, S. C., Pantoja-Feliciano, I. G., Doherty, L. A., et al. (2018). Effects of psychological, environmental and physical stressors on the gut microbiota. *Front. Microbiol.* 9:2013. doi: 10.3389/fmicb.2018.02013

Kovats, R. S., and Hajat, S. (2008). Heat stress and public health: a critical review. *Annu. Rev. Publ. Health* 29, 41–55. doi: 10.1146/annurev.publhealth.29.020907.090843

Kurata, N., Tokashiki, N., Fukushima, K., Misao, T., Hasuoka, N., Kitagawa, K., et al. (2019). Short chain fatty acid butyrate uptake reduces expressions of prostanoid EP4 receptors and their mediation of cyclooxygenase-2 induction in HCA-7 human colon cancer cells. *Eur. J. Pharmacol.* 853, 308–315. doi: 10.1016/j.ejphar.2019.04.014

Lemme, A., and Mitchell, M. A. (2008). Examination of the composition of the luminal fluid in the small intestine of broilers and absorption of amino acids under various ambient temperatures measured in vivo. *Int. J. Poult. Sci.* 7, 223–233. doi: 10.3923/IJPS.2008.223.233

Li, X., Yu, X., Sun, D., Li, J., Wang, Y., Cao, P., et al. (2017). Effects of polar compounds generated from the deep -frying process of palm oil on lipid metabolism and glucose tolerance in kunming mice. *J. Agric. Food Chem.* 65, 208–215. doi: 10.1021/acs.jafc.6b04565

Li, Y., Wu, Q., Deng, Y., Lv, H., Qiu, J., Chi, G., et al. (2015). D(-)-Salicin inhibits the LPS-induced inflammation in RAW264.7 cells and mouse models. *Int. Immunopharmacol.* 26, 286–294. doi: 10.1016/j.intimp.2015.04.016

Loscalzo, J. (2011). Lipid metabolism by gut microbes and atherosclerosis. *Circ. Res.* 109, 127–129. doi: 10.1161/RES.0b013e3182290620

Lrar, L. J., and Rostagno, M. H. (2013). Impact of heat stress on poultry production. *Animals* 3, 356–369. doi: 10.3390/ani3020356

Luo, J., Song, J., Liu, L., Xue, B., Tian, G., and Yang, Y. (2018). Effect of epigallocatechin gallate on growth performance and serum biochemical metabolites in heat-stressed broilers. *Poult. Sci.* 97, 599–606. doi: 10.3382/ps/pex353

Marai, I. F., Ayyat, M. S., and Abd el-Monem, U. M. (2001). Growth performance and reproductive traits at first parity of New Zealand white female rabbits as affected by heat stress and its alleviation under Egyptian conditions. *Trop. Anim. Health Prod.* 33, 451–462. doi: 10.1023/A:1012772311177

Minho, M., Eugene, H., Wonil, L., Eun, J. S., Deok-Sang, H., Tae, H. L., et al. (2017). Coptidis rhizoma prevents heat stress-induced brain damage and cognitive impairment in mice. *Nutrients* 9:1057. doi: 10.3390/nu9101057

Moore, W. E. C., and Moore, L. H. (1995). Intestinal floras of populations that have a high-risk of colon-cancer. *Appl. Environ. Microb.* 61, 3202–3207. doi: 10.1128/AEM.61.9.3202-3207.1995

Mueller, V., Gray, C., and Kosec, K. (2014). Heat stress increases long-term human migration in rural Pakistan. *Nat. Clim. Change* 4, 182–185. doi: 10.1038/nclimate2103

Nguyen, T. D. T., Kang, M. S., and Lee, M. S. (2007). Characterization of Lactobacillus plantarum PH04, a potential probiotic bacterium with cholesterol-lowering effects. *Int. J. Food Microbiol.* 113, 358–361. doi: 10.1016/j.ijfoodmicro.2006.08.015

Pamp, S. J., Harrington, E. D., Quake, S. R., Relman, D. A., and Blainey, P. C. (2012). Single-cell sequencing provides clues about the host interactions of segmented filamentous bacteria (SFB). *Genome Res.* 22, 1107–1119. doi: 10.1101/gr.131482.111

Payne, C. G. (2019). Practical aspects of environmental temperature for laying hens. *World Poultry Sci. J.* 22, 126–139. doi: 10.1079/WPS19660020

Pérez-Cobas, A. E., Gosalbes, M. J., Friedrichs, A., Knecht, H., Artacho, A., Eismann, K., et al. (2013). Gut microbiota disturbance during antibiotic therapy: a multi-omic approach. *Gut* 62, 1591–1601. doi: 10.1136/gutjnl-2012-303184

Reid, G., and Burton, J. (2002). Use of Lactobacillus to prevent infection by pathogenic bacteria. *Microbes Infect.* 4, 319–324. doi: 10.1016/S1286-4579(02)01544-7

Robert, J. C., Lance, H. B., Rosemarie, B. Z., and Yao, X. (2018). Heat stress: physiology of acclimation and adaptation. *Anim. Front.* 9, 12–19. doi: 10.1093/af/vfy031

Rojas-Downing, M. M., Nejadhashemi, A. P., Harrigan, T., and Woznicki, S. A. (2017). Climate change and livestock: Impacts, adaptation, and mitigation. *Clim. Risk Manag.* 16, 145–163. doi: 10.1016/j.crm.2017.02.001

Rossi, M., Martínez, D., Amaretti, A., Ulrici, A., Raimondi, S., and Moya, A. (2016). Mining metagenomic whole genome sequences revealed subdominant but constant Lactobacillus population in the human gut microbiota. *Environ. Microbiol. Rep.* 8, 399–406. doi: 10.1111/1758-2229.12405

Savage, D. B., Petersen, K. F., and Shulman, G. I. (2007). Disordered lipid metabolism and the pathogenesis of insulin resistance. *Physiol. Rev.* 87, 507–520. doi: 10.1152/physrev.00024.2006

Sekirov, I., Russell, S. L., Antunes, L. C., and Finlay, B. B. (2010). Gut microbiota in health and disease. *Physiol. Rev.* 90, 859–904. doi: 10.1152/physrev.00045.2009

Shi, J., Wang, Y., He, J., Li, P., Jin, R., Wang, K., et al. (2017). Intestinal microbiota contributes to colonic epithelial changes in simulated microgravity mouse model. *FASEB J.* 31, 3695–3709. doi: 10.1096/fj.201700034R

Slimen, I. B., Najar, T., Ghram, A., and Abdrrabba, M. (2015). Heat stress effects on livestock: molecular, cellular and metabolic aspects, a review. *J. Anim. Physiol. Anim. Nutr.* 100, 401–412. doi: 10.1111/jpn.12379

Song, J., Jiao, L. F., Xiao, K., Luan, Z. S., Hu, C. H., Shi, B., et al. (2013). Cello-oligosaccharide ameliorates heat stress-induced impairment of intestinal microflora, morphology and barrier integrity in broilers. *Anim. Feed Sci. Tech.* 185, 175–181. doi: 10.1016/j.anifeedsci.2013.08.001

Song, J., Xiao, K., Ke, Y. L., Jiao, L. F., Hu, C. H., Diao, Q. Y., et al. (2014). Effect of a probiotic mixture on intestinal microflora, morphology, and barrier integrity of broilers subjected to heat stress. *Poult. Sci.* 93, 581–588. doi: 10.3382/ps.2013-03455

St-Pierre, N. R., Cobanov, B., and Schnitkey, G. (2003). Economic losses from heat stress by us livestock industries. *J. Dairy Sci.* 86, E52–E77. doi: 10.3168/jds.S0022-0302(03)74040-5

Tan, J., McKenzie, C., Potamitis, M., Thorburn, A. N., Mackay, C. R., and Macia, L. (2014). The role of short-chain fatty acids in health and disease. *Adv. Immunol.* 121, 91–119. doi: 10.1016/B978-0-12-800100-4.00003-9

Tao, S., Monteiro, A. P. A., Thompson, I. M., Hayen, M. J., and Dahl, G. E. (2012). Effect of late-gestation maternal heat stress on growth and immune function of dairy calves. *J. Dairy Sci.* 95, 7128–7136. doi: 10.3168/jds.2012-5697

Topping, D. L., and Clifton, P. M. (2001). Short-chain fatty acids and human colonic function: roles of resistant starch and nonstarch polysaccharides. *Physiol. Rev.* 81, 1031–1064. doi: 10.1152/physrev.2001.81.3.1031

Vacca, M., Celano, G., Calabrese, F. M., Portincasa, P., Gobbetti, M., and Angelis, D. M. (2020). The controversial role of human gut lachnospiraceae. *Microorganisms* 8:573. doi: 10.3390/microorganisms8040573

van der Beek, C. M., Dejong, C. H. C., Troost, F. J., Masclee, A. M., and Lenaerts, K. (2017). Role of short-chain fatty acids in colonic inflammation, carcinogenesis, and mucosal protection and healing. *Nutr. Rev.* 75, 286–305. doi: 10.1093/nutrit/nuw067

Virtue, A. T., McCright, S. J., Wright, J. M., Jimenez, M. T., Mowel, W. K., Kotzin, J. J., et al. (2019). The gut microbiota regulates white adipose tissue inflammation and obesity via a family of microRNAs. *Sci. Transl. Med.* 11:aav1892. doi: 10.1126/scitranslmed.aav1892

Wang, L., Ravichandran, V., Yin, Y., Yin, J., and Zhang, Y. (2019). Natural products from mammalian gut microbiota. *Trends Biotechnol.* 37, 492–504. doi: 10.1016/j.tibtech.2018.10.003

Wei, T., and Simko, V. (2013). *Corrplot: Visualization of a correlation matrix, R package, 11 version 0.73 230.231*.

Wen, C., Guo, Q., Wang, W., Duan, Y., Zhang, L., Li, J., et al. (2020a). Taurine alleviates intestinal injury by mediating tight junction barriers in diquat-challenged piglet models. *Front. Physiol.* 11:449. doi: 10.3389/fphys.2020.00449

Wen, C., Li, F., Guo, Q., Zhang, L., Duan, Y., Wang, W., et al. (2020b). Protective effects of taurine against muscle damage induced by diquat in 35 days weaned piglets. *J. Anim Sci. Biotechnol.* 11, 1–14.

Wen, C., Li, F., Duan, Y., Guo, Q., Wang, W., Zhang, L., et al. (2019). Dietary taurine regulates free amino acid profiles and taurine metabolism in piglets with diquat-induced oxidative stress. *J. Funct. Foods* 62:103569. doi: 10.1016/j.jff.2019.103569

Wen, L., Ley, R. E., Volchkov, P. Y., Stranges, P. B., Avanesyan, L., Stonebraker, A. C., et al. (2008). Innate immunity and intestinal microbiota in the development of Type 1 diabetes. *Nature* 455, 1109–1113. doi: 10.1038/nature07336

Wong, J. M. W., de Souza, R., Kendall, C. W. C., Emam, A., and Jenkins, D. J. A. (2006). Colonic health: fermentation and short chain fatty acids. *J. Clin. Gastroenterol.* 40, 235–243. doi: 10.1097/00004836-200603000-00015

Zeng, H., Umar, S., Rust, B., Lazarova, D., and Bordonaro, M. (2019). Secondary bile acids and short chain fatty acids in the colon: a focus on colonic microbiome, cell proliferation, inflammation, and cancer. *Int. J. Mol. Sci.* 20:1214. doi: 10.3390/ijms20051214

Zhang, C., Zhao, X. H., Yang, L., Chen, X. Y., Jiang, R. S., Jin, S. H., et al. (2017). Resveratrol alleviates heat stress-induced impairment of intestinal morphology, microflora, and barrier integrity in broilers. *Poultry Sci.* 96, 4325–4332. doi: 10.3382/ps/pex266

Zhang, W., Ma, C., Xie, P., Zhu, Q., Wang, X., Yin, Y., et al. (2019). Gut microbiota of newborn piglets with intrauterine growth restriction have lower diversity and different taxonomic abundances. *J. Appl. Microbiol.* 127, 354–369. doi: 10.1111/jam.14304

Zhao, Z., Shi, A., Wang, Q., and Zhou, J. (2019). High oleic acid peanut oil and extra virgin olive oil supplementation attenuate metabolic syndrome in rats by modulating the gut microbiota. *Nutrients* 11:3005. doi: 10.3390/nu11123005

Zhong, S., Ding, Y., Wang, Y., Zhou, G., Guo, H., Chen, Y., et al. (2019). Temperature and humidity index (THI)-induced rumen bacterial community changes in goats. *Appl. Microbiol. Biotechnol.* 103, 3193–3203. doi: 10.1007/s00253-019-09673-7

Zhou, J., Xiong, X., Wang, K., Zou, L., Ji, P., and Yin, Y. (2018). Ethanolamine enhances intestinal functions by altering gut microbiome and mucosal anti-stress capacity in weaned rats. *Br. J. Nutr.* 120, 241–249. doi: 10.1017/S0007114518001101

Zhou, J., Xiong, X., Yin, J., Zou, L., Wang, K., Shao, Y., et al. (2019). Dietary lysozyme alters sow's gut microbiota, serum immunity and milk metabolite profile. *Front. Microbiol.* 10:177. doi: 10.3389/fmicb.2019.00177

Zhu, L., Liao, R., Wu, N., Zhu, G., and Yang, C. (2018). Heat stress mediates changes in fecal microbiome and functional pathways of laying hens. *Appl. Microbiol. Biotechnol.* 103, 461–472. doi: 10.1007/s00253-018-9465-8

Ziegler, M., Seneca, F. O., Yum, L. K., Palumbi, S. R., and Voolstra, C. R. (2017). Bacterial community dynamics are linked to patterns of coral heat tolerance. *Nat. Commun.* 8:14213. doi: 10.1038/ncomms14213

Zong, X., Fu, J., Xu, B., Wang, Y., and Jin, M. (2020). Interplay between gut microbiota and antimicrobial peptides. *Anim. Nutr.* 6, 389–396. doi: 10.1016/j.aninu.2020.09.002

Conflict of Interest: This study received funding from Shanghai Biotree Biomedical Technology CO., LTD. The funder was involved in the collection of data. All authors declare no other competing interests.

frontiers in Microbiology

ORIGINAL RESEARCH
published: 03 September 2021
doi: 10.3389/fmicb.2021.726878

Resveratrol Improves Growth Performance, Intestinal Morphology, and Microbiota Composition and Metabolism in Mice

*Yu Zhuang[1,2], Huijun Huang[1], Shuang Liu[1], Feng Liu[3], Qiang Tu[3], Yulong Yin[1] and Shanping He[1]**

[1] State Key Laboratory of Developmental Biology of Freshwater Fish, Hunan Provincial Key Laboratory of Animal Intestinal Function and Regulation, Hunan Normal University, Changsha, China, [2] Jiangxi Provincial Key Laboratory for Animal Health, Institute of Animal Population Health, College of Animal Science and Technology, Jiangxi Agricultural University, Nanchang, China, [3] Yucheng Baolikang Biological Feed Co., Ltd., Dezhou, China

OPEN ACCESS

Edited by:
Tingtao Chen, Nanchang University, China

Reviewed by:
Limei Zhang, China Agricultural University, China
Ruiwen Fan, Shanxi Agricultural University, China
Jian Wang, St. Jude Children's Research Hospital, United States

***Correspondence:**
Shanping He
hesp@hunnu.edu.cn

Specialty section:
This article was submitted to Microbial Symbioses, a section of the journal Frontiers in Microbiology

Received: *17 June 2021*
Accepted: *12 July 2021*
Published: *03 September 2021*

Citation:
Zhuang Y, Huang H, Liu S, Liu F, Tu Q, Yin Y and He S (2021) Resveratrol Improves Growth Performance, Intestinal Morphology, and Microbiota Composition and Metabolism in Mice. Front. Microbiol. 12:726878. doi: 10.3389/fmicb.2021.726878

Background: Resveratrol (RSV) plays a vital role in alleviating various stresses and improving intestinal health. The current study was conducted to explore whether RSV alleviates weaning stress through improving gut health in a weaning mouse model. Forty 21-day-old weaned mice were randomly assigned to a control group without RSV treatment and three treatment groups with 10, 20, and 50 mg/kg RSV for 28 days.

Results: The results showed that RSV at a dose of 20 mg/kg improved total body weight, intestinal morphology (villus length and the ratio of villus length to crypt depth), and the levels of intestinal barrier proteins (claudin-1 and occludin), but had little effect on the food intake, crypt depth, and serum free amino acids of mice. Compared with the control group, mice supplemented with RSV had decreased mRNA expression of genes related to inflammatory cytokines (IL-6 and IL-1β), but increased mRNA expression of genes related to host defense peptides (Defa3, Defa5, Defa20, and Lyz) and short-chain fatty acids (SCFAs) production (propionic acid, isobutyric acid, butyric acid, and isovaleric acid). In addition, 16S rRNA sequencing results showed that RSV supplementation increased the richness indices of intestinal microbiota (Chao, ACE) and shaped the composition of intestinal microbiota (e.g., increased β-diversity of intestinal microbiota community). Meanwhile, RSV supplementation increased genes of *Butyricicoccus*, *Ruminococcus_1*, and *Roseburia*, which are producers of SCFAs. Furthermore, RSV supplementation significantly influenced the metabolism of intestinal microbiota, namely, amino acids metabolism, lipid metabolism, and defense mechanisms.

Conclusion: RSV can improve growth performance and intestinal morphology in weaning mice, possibly through improving gut immune response and microbiota function.

Keywords: resveratrol, growth performance, intestinal morphology, microbiota community, weaning stress

INTRODUCTION

Weaning is a critical period for newborn mammals and profoundly affects gut health and the immune system (Melo et al., 2016; Furbeyre et al., 2017). During this phase, newborns are exposed to various stresses, such as lactational immunity depletion, immature gut, and changes in gut microbiota. As a consequence, weaning results in decreased feed intake, serious diarrhea, and depressed immune systems. Additionally, a number of studies have revealed that juvenile stress, such as weaning stress, has a profound impact on social behavior and metabolism in adulthood (Shtoots et al., 2018; Heard-Garris et al., 2019). For example, early life adversity (weaning stress) in piglets induces chronic functional diarrhea, intestinal permeability, and lasting alterations in gastrointestinal (GI) function (Pohl et al., 2017).

Recently, numerous studies have suggested that the gut ecosystem is involved in the pathogenesis of multiple diseases (Zhang et al., 2019). A growing number of evidence has suggested that gut microbiota is closely associated with host health (Patil et al., 2019; Ross et al., 2019). Gut microbiota provides enzymes to digest nutrients and interacts with host signaling pathways, thus affecting host metabolism and immunity through itself or microbial-derived metabolites. Furthermore, gut microbiota is tightly associated with the incidence of many chronic diseases (Cruz-Lebron et al., 2019; Lv et al., 2019), namely, diabetes, metabolic syndrome, and colon cancer. However, during the period of weaning, the state of the gut ecosystem is weakened and highly malleable. Early life establishment of infant gut microbiota sets the stage for adult microbiome and has profound effects on host metabolism and health. Therefore, improving infant gut ecology to profoundly affect the metabolism in adulthood has been the focus of recent studies.

Resveratrol (RSV) is a plant-derived stilbene that has various biological activities (Rauf et al., 2017; Zhang et al., 2018; Pan et al., 2019). Numerous studies have suggested that RSV acts on multiple cellular targets, namely, Nrf2, Sirt1, and AMPK, to control cellular processes and signaling pathways (Yang et al., 2018, 2019; Jiang et al., 2019). However, RSV has a high biotransformation rate in intestinal ecology, and a low dose of RSV is found in target tissues (Andres-Lacueva et al., 2012). A growing number of evidence has revealed that the health benefits of RSV could be associated with its capacity to alter the composition of the microbiota population, which was shown to have a profound impact on the health of organisms. For instance, supplementation of RSV could modulate gut microbiota, nutrient-sensing pathways, and oxidative stress to prevent the development of hypertension induced by maternal plus post-weaning high-fructose consumption (Tain et al., 2018). Therefore, RSV can act on gut microbiota to affect body metabolism.

Few studies have investigated the effects of dietary RSV on both the complex gut microbiota in mice programmed by post-weaning and the metabolism during juvenile phase. Therefore, the present study was conducted to explore the effects of RSV on growth performance, intestinal morphology, intestinal barrier functions, serum amino acid profiles, short-chain fatty acids (SCFAs), and microbiota community of C57BL/6 mice exposed to post-weaning juvenile stress. Our results will provide new insight into the mechanisms by which RSV regulates intestinal microecology in juvenile mice.

MATERIALS AND METHODS

Animals

All the procedures involving mice in this study were approved by the Animal Care and Use Committee of Hunan Normal University, Changsha City, Hunan, China. Three-week-old C57BL/6 mice (without received diet) were obtained from Hunan SLAC Laboratory Animal Co., Ltd. (Changsha, China) and were kept in an environmentally controlled room (temperature: 24 ± 2°C, humidity: 60 ± 5%) with a 12-h light–dark cycle. For all the experimental period, all the mice were housed in individual cages and had *ad libitum* access to food and water.

Experimental Design and Treatments

Three-week-old C57BL/6 mice (11 ± 1 g) were randomly assigned into four groups (n = 10/group): 1) control group (basal diet + vehicle solution), 2) RSV10 (basal diet + 10 mg/kg/day RSV), 3) RSV20 (basal diet + 20 mg/kg/day RSV), and 4) RSV50 (basal diet + 50 mg/kg/day RSV). The experiment was conducted for 4 weeks (28 days), and all the treatments were performed by gavage during the experimental period (28 days). The treatments of RSV10, RSV20, and RSV50 received RSV (Selleckchem, Houston, TX, United States) at a dose of 10, 20, and 50 mg/kg, respectively. Due to its low solubility in water, RSV was suspended into 0.5% (w/v) carboxymethylcellulose solution (Sigma-Aldrich, St. Louis, MO, United States) according to a previous study (Yang et al., 2019). During the experimental period, mice of all the treatments were daily recorded to calculate average daily feed intake and total body weight gain.

Sample Collection

After 4 weeks of RSV gavage daily, animals were then humanely sacrificed, and samples of blood were taken as in a previous report (Ren et al., 2018). For collection of the duodenum, jejunum, and ileum, the middle part of the duodenum, jejunum, and ileum samples was collected after washing with phosphate buffer saline (PBS, pH = 7.4). Samples of the ileum were collected for histological analysis, and cecum contents were collected for microbiota community analysis. Additionally, before sacrifice, the fresh feces from each group were collected. All methods and practical steps were in line with animal welfare rules in China.

Tissue Histological Examination

Ileums were stained with hematoxylin and eosin (H&E staining). Briefly, the cross-sections of ileum samples were preserved in 4% formaldehyde and then dehydrated and embedded using standard paraffin embedding techniques. Section of 5 μM was cut and stained with H&E staining. The villus height and crypt were measured under a microscope × 40 combined magnification using Image-Pro Plus for image processing and analysis system.

Determination of Serum Amino Acid Profiles

Free amino acid profiles in serum were determined according to our previous study (Ren et al., 2018). Briefly, the same volume of serum and 2.5% sulfosalicylic acid were added to a sealed centrifuge container. The two substances were shaken together and allowed to stand overnight at 4°C, and the containers were centrifuged at 1,000 rpm for 15 min at 4°C. Following this process, the supernatant was filtered through a 0.22-μM membrane and analyzed using Hitachi L-8900 automatic amino acid analyzer according to the manufacturer's instructions.

Determination of SCFAs

Fresh fecal samples were collected for determination of SCFAs (acetic acid, propionic acid, butyrate, isobutyric acid, valerate, and isovaleric acid) by using the Agilent 6890 gas chromatography (Agilent Technologies, Inc., Palo Alto, CA, United States) according to our previous study (Ren et al., 2018).

Quantitative Real-Time PCR

Total RNA of ileum samples from mice was extracted using TRIzol reagent (TaKaRa, Dalian, China), and first-stand cDNA was synthesized using a reverse transcription kit (TaKaRa, Dalian, China) following the manufacturer's instruction. Quantitative real-time PCR (qRT-PCR) was performed on QuantStudio™ 5 Real-Time PCR System analyzer (Applied Biosystems, Foster City, CA, United States) to quantify mRNA expression. The details of gene in this study are summarized in **Table 1** and synthesized by TsingKe Biological Technology (Changsha, China). The expression of β-actin was analyzed as an internal control for the normalization of the results. Relative expression levels were calculated using the $2^{-\Delta\Delta Ct}$ method according to a previous study (Yin et al., 2018).

Western Blot

Total cellular protein of IPEC-J2 cells was extracted by RIPA (Beyotime, Shanghai, China) with protease inhibitor and phosphatase inhibitor cocktail (Selleckchem, Houston, TX, United States). The content of protein was quantified using BCA protein assay kit (Beyotime, Shanghai, China) according to the instructions. And then the extracts of tissues were protein denaturation incubation with SDS-loading buffer at 100°C for 15 min. The denaturation protein was resolved over SDS-PAGE, transferred into 0.45 μM PVDF membranes, and then blocked with 5% non-fat dry milk for 2 h at room temperature, followed by incubation with primary antibodies for detection of claudin-1, zonula occludens-1 (ZO-1), and occludin-1. The membranes were probed by the secondary antibodies for 1.5 h at room temperature. And the blots were visualized by the enhancing chemiluminescence (ECL) method. The blots were quantified by measuring Image Lab™ Software (Bio-Rad, Hercules, CA, United States).

TABLE 1 | Sequences of target genes' primers.

Gene names	Genes No.	Sequence of primer	Length (bp)
Claudin-1	NM_016674.4	ACTGTGGATGTCCTGCGTTT	258
		ACTAATGTCGCCAGACCTGAA	
Occludin	NM_001360536.1	CAGGTGAATGGGTCACCGAG	163
		CCAAGATAAGCGAACCTGCC	
ZO-1	NM_009386.2	CTTCCCGGACTTTTGTCCCA	220
		CATTGCTGTGCTCTTAGCGG	
IL-6	NM_031168.2	CTCTGCAAGAGACTTCCATCCA	124
		GACAGGTCTGTTGGGAGTGG	
IL-1β	NM_008361.4	TGCCACCTTTTGACAGTGATG	220
		AAGGTCCACGGGAAAGACAC	
TNF-α	NM_001278601.1	AGGCACTCCCCCAAAAGATG	213
		CCACTTGGTGGTTTGTGAGTG	
MUC2	NM_023566.3	CCTGAAGACTGTCGTGCTGT	100
		GGGTAGGGTCACCTCCATCT	
MUC3	NM_010843.1	AGTGCTGTTGGTGATCCTCG	193
		AGAGTCCAGGGGCATGTAGT	
Retnlβ	NM_023881.4	TGGCTGTGGATCGTGGGATA	96
		TAAACCATTCGGCAGCAGCG	
Lyz	NM_013590.4	GAGACCGAAGCACCGACTATG	214
		CGGTTTTGACATTGTGTTCGC	
ang4	NM_177544.4	TGGCCAGCTTTGGAATCACTG	151
		GCTTGGCATCATAGTGCTGACG	
Defa3	NM_007850.2	TCCTCCTCTCTGCCCTCGT	240
		GACCCTTTCTGCAGGTCCC	
Defa5	NM_007851.2	GTCCAGGCTGATCCTATCCA	202
		GATTTCTGCAGGTCCAAAA	
Defa20	NM_183268.4	GACCTGCTCAGGACGACTTT	94
		GCCTCAGAGCTGATGGTTGT	
meprinβ	NM_008586.2	CAGGCAAGGAACACAACTTC	118
		TCTGTCCCGTTCTGGAAAG	
Mmp7	NM_010810.5	CTGCCACTGTCCCAGGAAG	175
		GGGAGAGTTTTCCAGTCATCG	
CFTR	NM_021050.2	AAGGCGGCCTATATGAGGTT	107
		AGGACGATTCCGTTGATGAC	
NKCC	NM_009194.3	CAAGGGTTTCTTTGGCTAT	144
		TCACCTGAGATATTTGCTCC	
SLC26A	NM_021353.3	TTCCCCTCAACATCACCATCC	111
		GTAAAATCGTTCTGAGGCCCC	
NHE3	NM_001033289.2	TGGCAGAGACTGGGATGATAA	145
		CGCTGACGGATTTGATAGAGA	
Ano1	NM_178642.5	AGCAGGCTTCTGACCATCAC	99
		CACGTCCAGACGACACAAGA	
PPARr	NM_001127330.2	CCAGCATTTCTGCTCCACAC	93
		ATTCTTGGAGCTTCAGGCCA	
GAPDH	XM_017321385.1	CTTATCAGGCCAAGTATGATG	96
		CAACCTGGTCCTCAGTGTAGC	

Microbial DNA Isolation and Microbiota Analysis Based on 16S RNA High-Throughput Sequencing

Total bacterial DNA of cecum content was extracted using a QIAamp DNA Stool Mini Kit (Qiagen, Hilden, Germany) according to the manufacturer's instructions. The diversity and composition of the bacterial community were determined by high-throughput sequencing of the

microbial 16S rRNA genes. The V3–V4 hypervariable region of the 16S rRNA genes was PCR amplified using primers, 338F: 5′-ACTCCTACGGGAGGCAGCA-3′ and 806R: 5′-GGACTACHVGGGTWTCTAAT-3′. Paired-end sequencing was performed on the Illumina HiSeq 2500 platform (BioMarker, Beijing, China). Raw 16S data sequences were obtained before being screened and assembled using the Trimmomatic (v 0.33) (Caporaso et al., 2010) and FLASH software packages. UCHIME (V4.2) was used to analyze the high-quality sequences and determine operational taxonomic units (OTUs). Subsequently, high-quality sequences were aligned against the SILVA reference database1 and clustered into OTUs at a 97% similarity level using the UCLUST algorithm2. Each OTU was assigned to a taxonomic level with the Ribosomal Database Project Classifier program v2.203.

Statistical Analyses

Results from a representative of three independent experiments were expressed as means ± standard error of the mean (SEM). Data among all treatments were analyzed by one-way analysis of variance (ANOVA) followed by Dunnett's multiple comparisons if the data were Gaussian distribution and had equal variance or analyzed by Kruskal–Wallis followed by Dunn's multiple comparisons if the data were not normally distributed. The Gaussian distribution of data was analyzed by D'Agostino–Pearson omnibus normality test, and Kolmogorov–Smirnov test was tested for multiple comparisons; a value of $p < 0.05$ was accepted as statistically significant. The statistical analyses were performed by GraphPad Prism 7. In addition, the statistical analyses of the microbial community were performed using the R package software (version 2.15.3; R Core Team, Auckland,

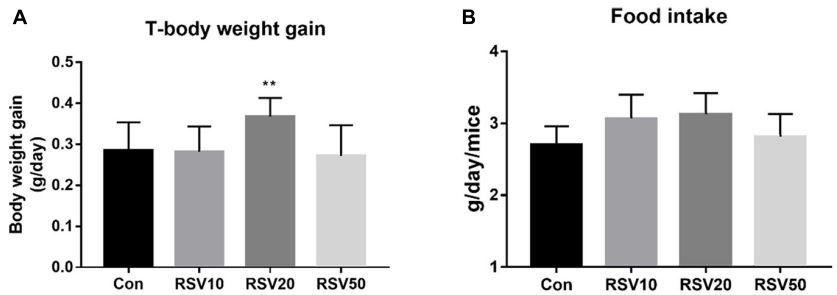

FIGURE 1 | Effect of RSV on body weight and feed intakes of weaned mice. **(A)** Average daily gain per mice in each group. **(B)** Average daily feed intake of mice in each group. Con = control group, RSV10 = 10 mg/kg RSV, RSV20 = 20 mg/kg RSV, RSV50 = 50 mg/kg RSV. **Means with double asterisks are significantly different ($p < 0.01$) from values of control group, and all the data are expressed as the means ± SEM.

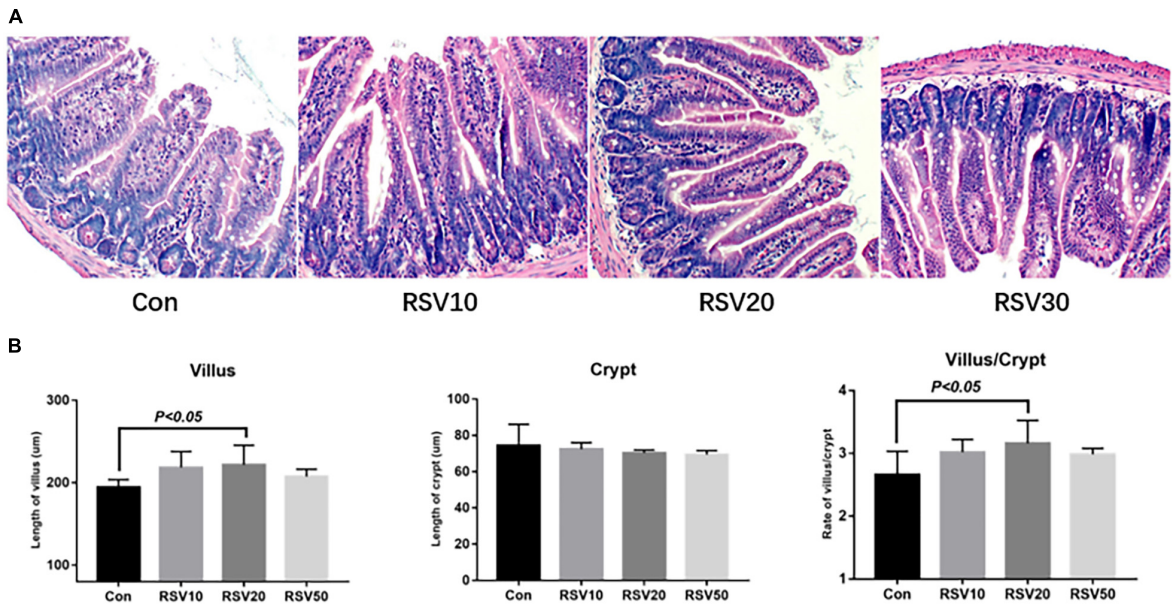

FIGURE 2 | Effect of RSV on intestinal morphology of weaned mice. **(A)** Ileum morphology of mice in each group was evaluated by hematoxylin and eosin (HE) staining. **(B)** Villus length, crypt depth, and the ratio of villus length to crypt depth of RSV-treated mice. Con = control group, RSV10 = 10 mg/kg RSV, RSV20 = 20 mg/kg RSV, RSV50 = 50 mg/kg RSV. All the data are expressed as the means ± SEM.

New Zealand), and the remaining data were performed using BMKCloud[1].

RESULTS

Growth Performance and Intestinal Morphology of Post-weaning Mice Fed With RSV

Mice fed with 20 mg/kg RSV had increased ($p < 0.05$) body weight gain compared with mice in the control group during the experimental period, while there was no significant difference ($p > 0.05$) in food intake among each group (**Figure 1**). In addition, mice fed with 20 mg/kg RSV had increased ($p < 0.05$) ileal villus height and ratio of villus height to crypt depth compared with those mice in the control, 10 and 50 mg/kg RSV groups. However, no differences were observed in crypt depth ($p > 0.05$) among each group (**Figure 2**).

Effects of Dietary RSV on Serum Amino Acids Profile, Intestinal Barrier Function, and Cytokine Expression in Post-weaning Mice

The contents of taurine (Tau), Gly, and Phe in the serum of mice fed with RSV were significantly increased ($p < 0.05$) compared with those in the control group. In contrast, the contents of Thr, Ser, Arg, and Glu in the serum of mice fed with RSV were significantly decreased ($p < 0.05$) compared with those in the control group. However, there were no significant differences ($p > 0.05$) in the contents of Ala, Val, Met, Leu, Ile, Lys, and Orn in the serum among each treatment (**Table 2**).

qRT-PCR and Western blot analysis showed that the expression of claudin-1 and occludin in mice fed with 20 mg/kg was significantly ($p < 0.05$) increased in the ileum compared with that in the control group (**Figures 3A,B**). In contrast, there was no difference ($p > 0.05$) in the expression of ZO-1 in the ileum among each treatment (**Figures 3A,B**). In addition, the mRNA expression of IL-6 and IL-1β in the ileum of mice fed with RSV was significantly decreased compared with that in the control group (**Figure 4**).

Effect of Dietary RSV on the Expression of Intestinal Ionic Transporter-Related Genes and Antimicrobial Peptide Genes

There were no differences ($p > 0.05$) in the mRNA expression of NKCC, SLC26A2, ANO1, and NHC3 in the ileum among each treatment (**Supplementary Figure 1**), while the mRNA expression of CFTR was significantly decreased ($p < 0.05$) in mice fed with RSV compared with that in the control group (**Supplementary Figure 1**).

The mRNA expression of Lyz, mmp7, Defa3, Defa5, and Defa20 in the ileum of mice fed with 20 and 50 mg/kg RSV was significantly ($p < 0.05$) increased compared with that in the control group. In addition, compared with mice in the control group, the mRNA expression of Memp-β and Retnl-β was significantly increased ($p < 0.05$) in the ileum of mice fed with 50 and 20 mg/kg RSV, respectively (**Figure 5**).

TABLE 2 | Effect of resveratrol on the serum amino acid profiles in weaned mice.

Items (mM)	CON[a]	RSV10[b]	RSV20[c]	RSV50[d]	*P*-value
Tau	0.4791	0.5928*	0.6256*	0.5331*	<0.001
Urea	5.164	5.985*	5.245	4.989	0.0117
Asp	0.0128	0.011	0.009143*	0.0115	0.0642
Thr	0.112	0.081*	0.07686*	0.0745*	0.0001
Ser	0.07667	0.0619*	0.05429*	0.0627*	0.0029
Glu	0.191*	0.1202	0.1848	0.1369*	0.0379
Gly	0.0738	0.0924*	0.08686	0.0997*	0.0130
Ala	0.211	0.1684	0.1724	0.1799	0.1152
Cit	0.028	0.036*	0.0332	0.02956	0.0172
Val	0.1133	0.1187	0.108	0.1213	0.5935
Met	0.047	0.0295	0.02457	0.0258	<0.0001
Ile	0.04	0.0444	0.04114	0.04943	0.5872
Leu	0.05267	0.0663	0.05629	0.07983*	0.0052
Tyr	0.0365	0.02967	0.03214	0.02538*	0.0008
Phe	0.05233	0.0629	0.1132*	0.0645*	<0.0001
Orn	0.051	0.0517	0.05314	0.053	0.9137
Lys	0.2603	0.1797	0.162	0.171	<0.0001
Arg	0.09533	0.0763*	0.06725*	0.0735*	<0.0001

[a]*Con = control group.*
[b]*RSV10 = 10 mg/kg RSV.*
[c]*RSV20 = 20 mg/kg RSV.*
[d]*RSV50 = 50 mg/kg RSV.*
**Means with single asterisks are significantly different ($p < 0.05$) from values of control group, and all the data are expressed as the means of six samples.*

Effect of Dietary RSV on the Production of Fecal SCFAs in Post-weaning Mice

The contents of propionic acid, isobutyric acid, butyric acid, and isovaleric acid in the feces of mice fed with RSV were significantly increased ($p < 0.05$) compared with those in the control group. The contents of valeric acid in mice fed with 20 mg/kg RSV were significantly increased ($p < 0.05$) compared with those in the control group, whereas there were no differences ($p > 0.05$) in the contents of acetic acid in the feces among each treatment (**Figure 6**).

Microbial Assessment and Metabolic Function Prediction in the Cecum Content of Post-weaning Mice Fed With RSV

Rarefaction curves of all the samples showed that the selected sequences were sufficient to determine the majority of bacterial diversity parameters (**Table 3**). The indices of Chao, ACE, and Simpson in mice fed with RSV were significantly increased compared with the control group, while the indices of Shannon in mice fed with RSV were significantly decreased compared with the control group. Meanwhile, the relative abundance of *Firmicutes*, *Proteobacteria*, and *Actinobacteria* was significantly increased in mice fed with RSV compared with the control group, whereas other phyla, namely, *Bacteroidetes*

[1]www.biocloud.net

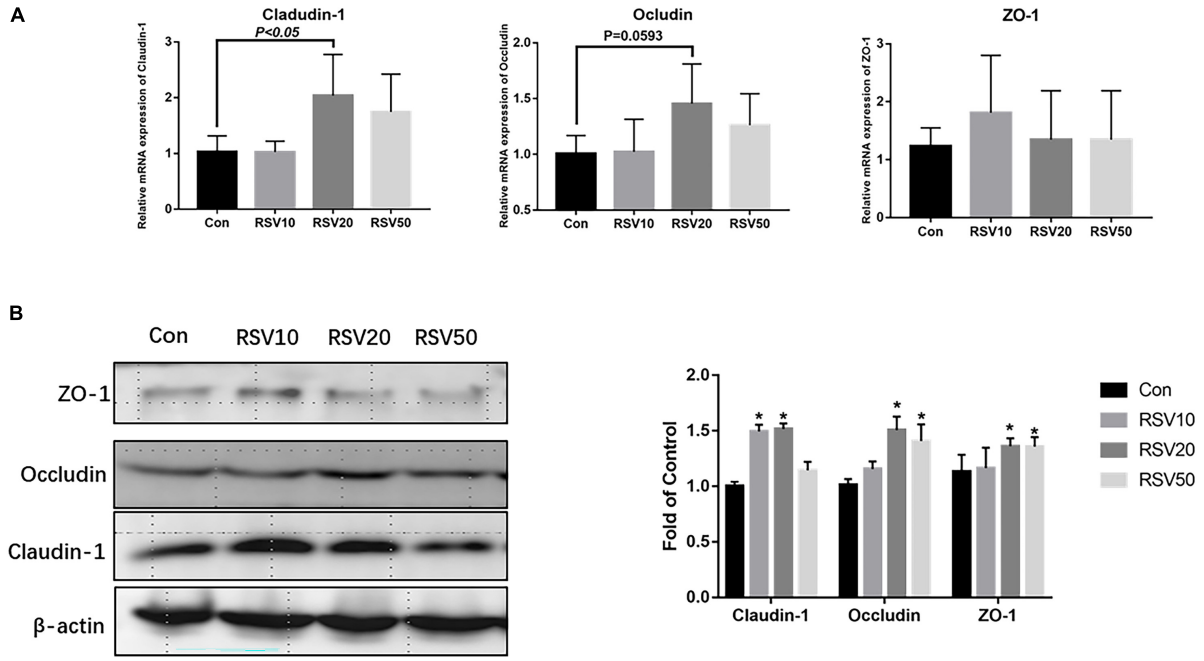

FIGURE 3 | Effect of RSV on the levels of intestinal barrier proteins in weaned mice. **(A)** The relative mRNA expression of claudin-1, occludin, and ZO-1 was detected by qRT-PCR. **(B)** The protein levels of Claudin-1, Occludin and ZO-1 were detected by Western blot with β-actin as the loading control. Con = control group, RSV10 = 10 mg/kg RSV, RSV20 = 20 mg/kg RSV, RSV50 = 50 mg/kg RSV. *Means with single asterisks are significantly different ($p < 0.05$) from values of control group, and all the data are expressed as the means ± SEM.

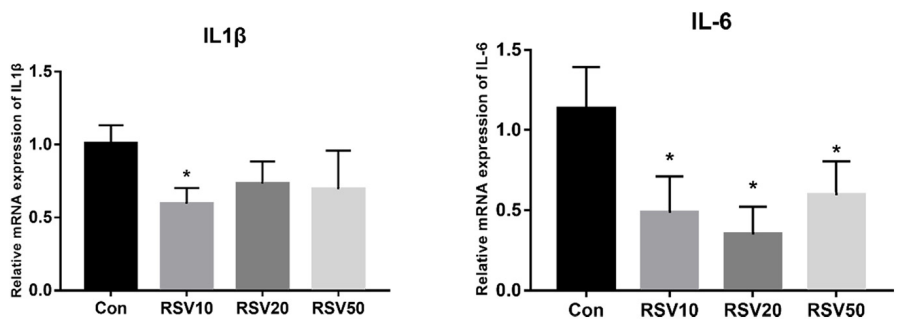

FIGURE 4 | Effect of RSV on the expression of IL-1β and IL-6 in weaned mice. The relative mRNA expression of IL1β and IL-6 was detected by qRT-PCR. Con = control group, RSV10 = 10 mg/kg RSV, RSV20 = 20 mg/kg RSV, RSV50 = 50 mg/kg RSV. *Means with single asterisks are significantly different ($p < 0.05$) from values of control group, and all the data are expressed as the means ± SEM.

and *Verrucomicrobia*, were significantly decreased in mice fed with RSV compared with the control group (**Supplementary Figure 2**). Principal component analysis (PCA), non-metric multidimensional scaling (NMDS) plots, and the two-tailed Student's *t*-test statistical analysis of β-diversity weighted Unifrac revealed obvious segregation between the control and RSV-treated groups (**Figure 7**). The relative abundance of microbial community genus analyzed by rank-sum test was shown in **Figure 8**. *Lactobacillus* (probiotics of genus), *Anaerotruncus*, and *Ruminococcus_1* (SCFA producers of genus) were significantly increased in mice fed with 20 mg/kg RSV compared with the control group. In addition, the fermentation genus of the SCFAs of *Butyricicoccus*, *Roseburia*, *Bifidobacterium*, and *Anaerotruncus* (beneficial genus) was significantly increased, whereas the *Streptococcus* (the harmful bacteria genus) in mice fed with RSV was significantly decreased compared with the control group (**Supplementary Table 1**).

To investigate further changes in microbial metabolic functions in the cecum microbiota induced by RSV treatment, we used PICRUSt to generate the metagenome based on 16S RNA sequencing results. We found that 31 metabolism pathways showed significant differences among the groups at KEGG level 3 (genus level), including those associated with amino acid metabolism, lipid metabolism, membrane transport, energy metabolism, cell growth and death, and metabolism of cofactors and vitamins (**Figure 9A**). Furthermore, 31 function enrichments

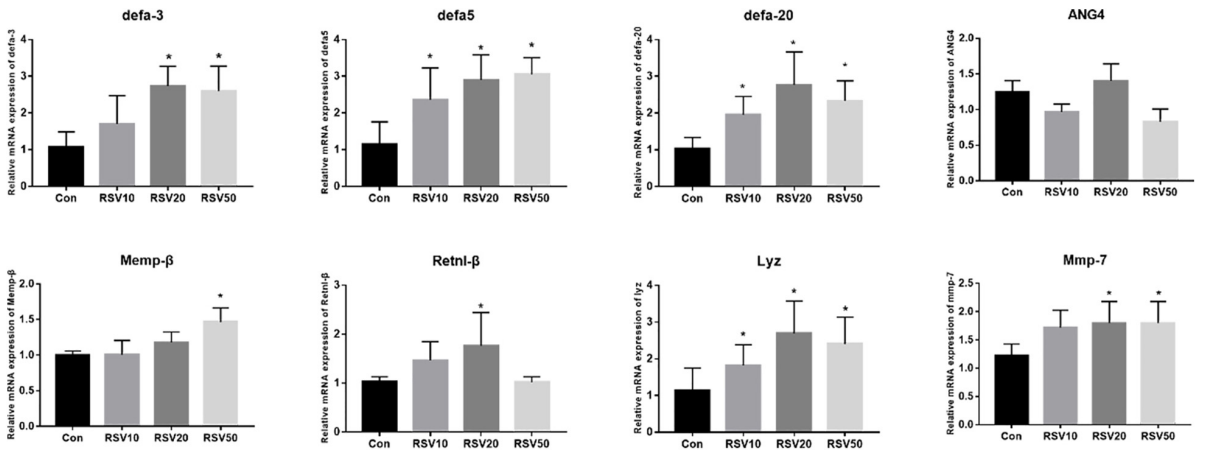

FIGURE 5 | Effect of RSV on the expression of AMP genes in the ileum of weaned mice. The relative mRNA expression of AMP related genes was detected by qRT-PCR. Con = control group, RSV10 = 10 mg/kg RSV, RSV20 = 20 mg/kg RSV, RSV50 = 50 mg/kg RSV. *Means with single asterisks are significantly different ($p < 0.05$) from values of control group, and all the data are expressed as the means ± SEM.

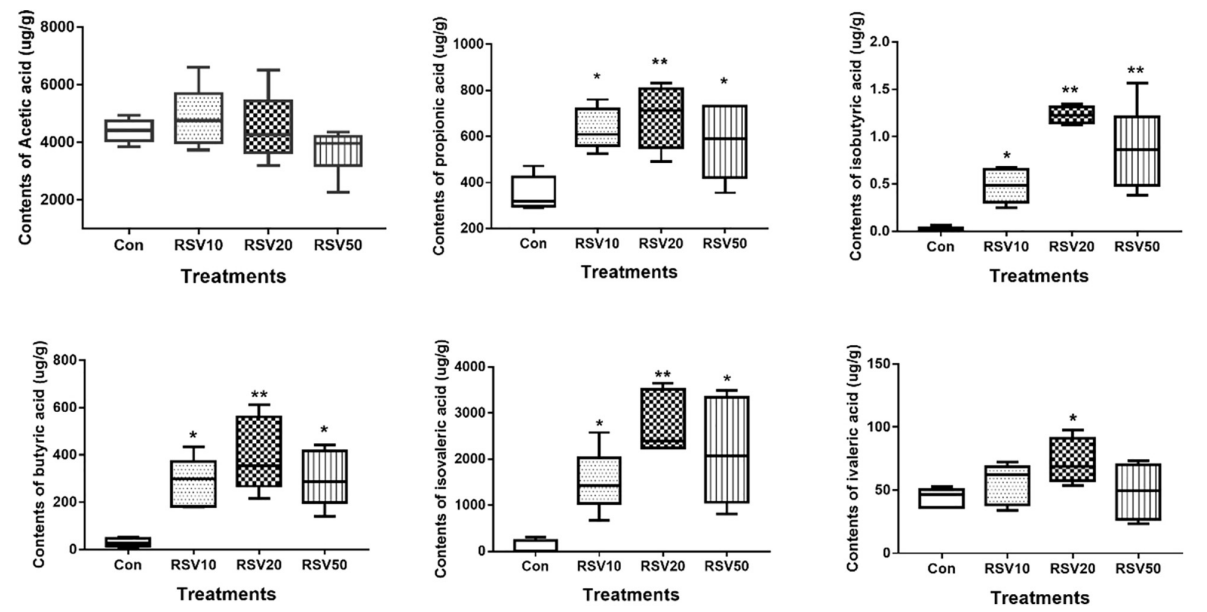

FIGURE 6 | Effect of RSV on the production of fecal SCFAs in weaned mice. The production of fecal SCFAs was determined using the Agilent 6890 gas chromatography. Con = control group, RSV10 = 10 mg/kg RSV, RSV20 = 20 mg/kg RSV, RSV50 = 50 mg/kg RSV. *Means with single asterisks are significantly different ($p < 0.05$) from values of control group, and **means with double asterisks are extremely significantly different ($p < 0.01$) from values of control group. All the data are expressed as the means ± SEM.

showed significant differences among the groups at KEGG level 3, including those associated with defense mechanisms, lipid transport and metabolism, carbohydrate transport and metabolism, nucleotide transport and metabolism, and amino acid transport and metabolism (**Figure 9B**).

DISCUSSION

Weaning is a critical period for newborn mammals, and this period deeply affects gut health and the immune system. During this phase, gut ecology tends to be mature and has a profound effect on host metabolism. Recent studies have shown that supplementation of RSV can modulate gut microbiota, nutrient-sensing pathways, and oxidative stress to prevent the development of hypertension programmed by maternal plus post-weaning high-fructose consumption in early life of newborn (Hsu et al., 2019; Zou et al., 2019). In the present study, our results showed that supplementation of RSV in weaned mice had better growth performance, higher SCFAs in feces, and increased expression of AMP genes.

TABLE 3 | Alpha diversity indices of bacterial communities in the cecum content of weaned mice.

Item	Experimental groups				*P*-value
	Con[a]	RSV10[b]	RSV20[c]	RSV50[d]	
Coverage	>99.9%	>99.9%	>99.9%	>99.9%	
Chao	142.8	331.8	331.8	316.9	<0.0001
ACE	170.9	323.3	328.4	315	<0.0001
Shannon	0.1956	0.4827	0.03617	0.06407	<0.0001
Simpson	2.152	4.089	4.169	3.867	<0.0001

[a]*Con = control group.*
[b]*RSV10 = 10 mg/kg RSV.*
[c]*RSV20 = 20 mg/kg RSV.*
[d]*RSV50 = 50 mg/kg RSV.*
All the data are expressed as the means of six samples.

The intestine is the first defense barrier against various stresses and also a selective barrier that absorbs small peptides, amino acids, vitamins, and so on. Given the improvement of growth performance in mice fed with RSV, it is reasonable to expect that the intestinal morphology of mice may be altered. The intestinal villus height and VH:CD ratio are widely used as important indicators to assess the capacity of nutrient digestion and absorption in the small intestine (Zou et al., 2019). The present study showed that supplementation of 20 mg/kg RSV had higher villus height and VH:CD ratio in the ileum than the control group, which is consistent with body weight increase in those groups. In addition, RSV could reduce oxidative stress-induced apoptosis of intestinal epithelial cells (Storniolo and Moreno, 2019); thus, the results of villus height and VH:CD ratio in mice fed with RSV are consistent with our expectation. Furthermore, Tau, as sulfamic acid, does not participate in protein synthesis and is widely considered to have antioxidant activity (Yamashita et al., 2019). In the present study, the contents of Tau were significantly increased in the serum of mice fed with RSV compared with those in the control group. Meanwhile, the contents of Gly and Phe in mice fed with RSV were also elevated. A previous study has revealed that Gly and Phe not only are building blocks of proteins but also have many physiological effects, including acting as antioxidants and regulation of hormone secretion and metabolism (Valdes et al., 2019). It should be noted that RSV can reduce the contents of Arg and Glu in serum possibly through affecting intestinal amino acid transporter and competing the absorption of amino acids.

Barrier is a fundamental function of intestinal epithelium to limit interactions between luminal contents, such as microbiota and antigens, and the host. Tight junctions are the principal determinants of barrier function in the intact epithelia and are composed of transmembrane and cytosolic proteins. Claudin-1, occludin, and ZO-1 are major transmembrane and cytosolic proteins (Hsu et al., 2019). Our data showed that supplementation of RSV had higher expression of claudin-1, occludin, and ZO-1 in the ileum than the control group. Many studies have shown that RSV can maintain gut barrier integrity and upregulate the expression of tight junction proteins *in vivo* and *in vitro* (Wang et al., 2016; Zhang et al., 2017). However, Muc-2, the large molecular weight glycoprotein secreted by

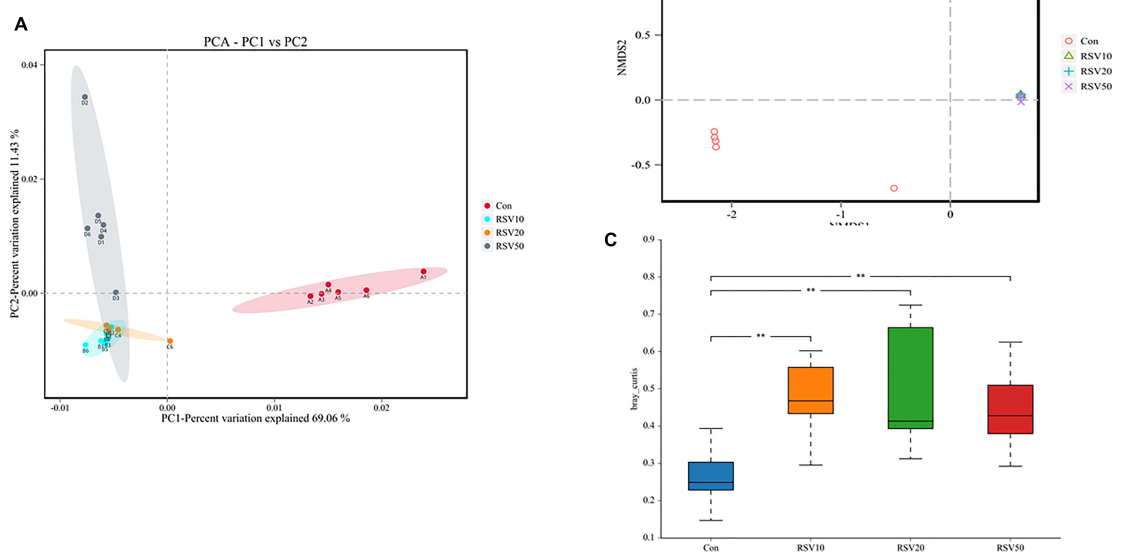

FIGURE 7 | Effect of RSV on Beta diversity indices of bacterial communities in the cecum content of weaned mice. **(A)** The principal component analysis (PCA) and **(B)** nonmetric multidimensional scaling (NMDS) plots were used to analyze bacterial communities. **(C)** Weighted Unifrac analysis was used to measure β-diversity. Con = control group, RSV10 = 10 mg/kg RSV, RSV20 = 20 mg/kg RSV, RSV50 = 50 mg/kg RSV. **Means with double asterisks are extremely significant different ($p < 0.01$) from values of control group.

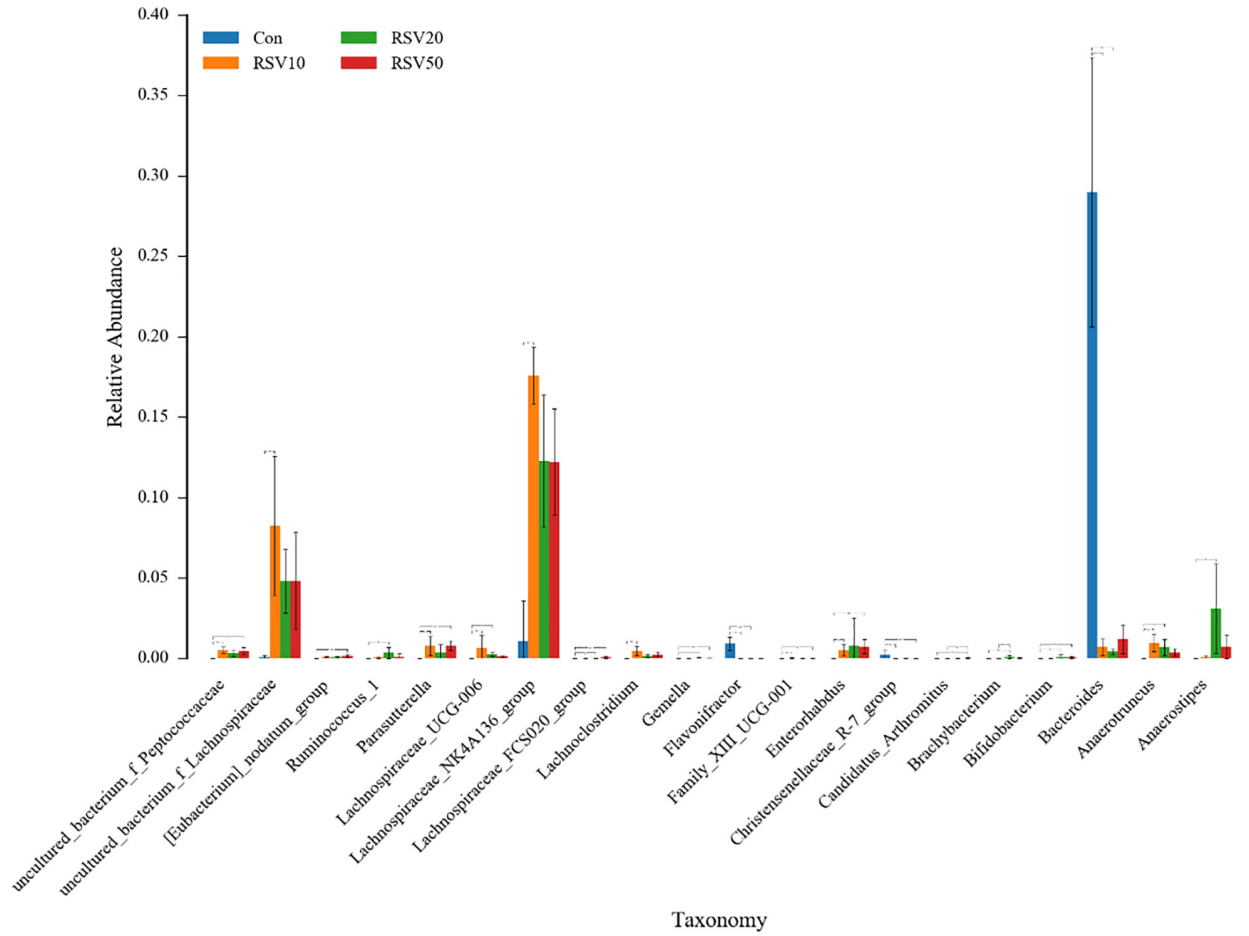

FIGURE 8 | Effect of RSV on the bacterial communities in the cecum content of weaned mice at the genus level. Con = control group, RSV10 = 10 mg/kg RSV, RSV20 = 20 mg/kg RSV, RSV50 = 50 mg/kg RSV. *Means with single asterisks are significantly different ($p < 0.05$) from values of control group, and **means with double asterisks are extremely significant different ($p < 0.01$) from values of control group.

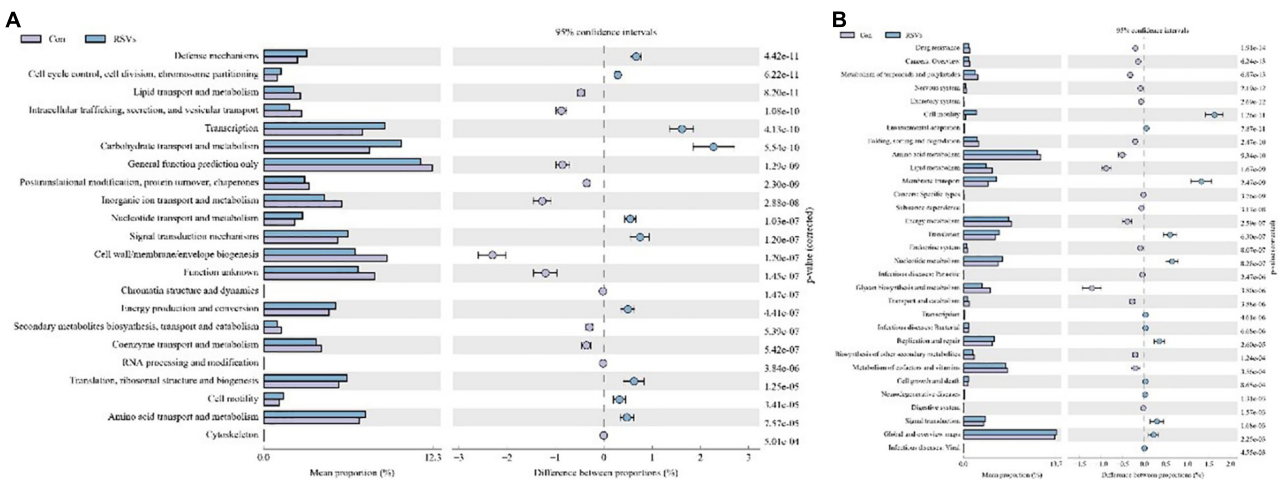

FIGURE 9 | Effect of RSV on predictive functional profiling of microbial communities in the cecum content of weaned mice at the genus level. **(A)** The KEEG genus level and **(B)** COG genus level were generated by OTU annotation by PICRUSt software analysis. Con = control group, RSVs = 10 mg/kg RSV, RSV20 = 20 mg/kg RSV and RSV50 = 50 mg/kg RSV group.

goblet cells, was not affected in our study. It suggests that RSV has no effect on intestinal chemical barrier, which is consistent with goblet cell results in the colon (data not shown).

Cytokines play important roles in the immune and inflammatory response. Previous studies have shown that dietary RSV has beneficial effects on regulating inflammatory response and innate immunity (Li et al., 2019; Meng et al., 2019; Yang et al., 2019). The present study showed that the expression of IL-1β and IL-6 was significantly inhibited by dietary RSV, which is consistent with previous studies on various pathological models *in vivo* and *in vitro* (Tain et al., 2018; Zhuang et al., 2019). In addition, the intestine functions as a main secretory organ, which maintains the homeostatic control of fluid and electrolytes balance and affects host defenses and microbiota in the gut. However, dietary RSV showed little effect on the expression of the genes regulating intestinal secretion, such as NKCC, SLC26A2, ANO1, and NHC3. The expression of CFTR, a cAMP-activated epithelial Cl^- and HCO_3^- channel, was significantly decreased in mice fed with RSV. CFTR plays a pivotal role in intestinal secretion and regulation of bacterial colonization in the intestine. Moreover, the expression of major AMP genes, such as defensins and Lyz, was significantly elevated in mice fed with RSV compared with the control group. In addition, the expression of Mmp-7, which is responsible for the maturation of AMP genes (Tomas et al., 2016; Cazorla et al., 2018), was correlated with the upregulation of AMP-coding genes tested in the ileum, such as defensins and Lyz. It seemed that dietary RSV induced a global increase in mucosal defense. Meanwhile, previous studies have revealed that the expression of AMP genes is correlated with spatial distribution of bacteria. Hence, intestinal microbe and their metabolites in mice fed with RSV have been assayed in our study.

Recent studies have revealed that microbiome and their metabolites are increasingly recognized to potentially impact host physiology by participating in digestion and absorption of nutrients, shaping of the mucosal immune response, and producing or modulating a plethora of potentially bioactive compounds, such as SCFAs (Rooks and Garrett, 2016; Bain and Cerovic, 2020). In the present study, our results showed that the contents of SCFAs, such as propionic acid, isobutyric acid, butyric acid, and isovaleric acid, were significantly increased in mice fed with RSV. Correspondingly, the composition of microbiome in mice fed with RSV also changed. SCFAs are mainly produced in the hindgut of animals (colon and cecum) and are metabolic end products produced by anaerobic microorganisms fermenting indigestible compounds through the glycolysis pathway and the pentose phosphate pathway. Previous studies have revealed that SCFAs play vital roles in regulating cell proliferation and differentiation and maintaining intestinal mucosal integrity (Rooks and Garrett, 2016). Juanola et al. (2018) revealed that SCFAs can regulate intestinal immune function and promote T cell differentiation and immune factor secretion through its G-protein coupled receptor (GPCR). Supplementation of berberine or other plant extracts in mice results in an increment of SCFA contents (Wang et al., 2017), which is consistent with our results. In addition, *Butyricicoccus*, *Ruminococcus_1*, and *Roseburia*, which are recognized as SCFA producers (Rooks and Garrett, 2016; Lv et al., 2018), were significantly increased in mice fed with RSV.

Newborn gut microbiota has a simple and distinct microbial composition. Furthermore, immature gut microbiota is sensitive to environmental factors and vulnerable to be disturbed. Using 16S rDNA high-throughput sequencing, we found that the dominant phylum of cecal contents was *Bacteroidetes*, *Firmicutes*, *Verrucomicrobia*, *Proteobacteria*, and *Actinobacteria*, which is in line with previous studies. Microbial diversity, evidenced by Chao1, ACE, Shannnon, and Simpson indexes, showed a significant change in mice fed with RSV. While the β-diversity, evidenced by PCA and NMDS, also indicated that differences in overall diversity among individual mice became greater with dietary RSV. As previous studies reported, higher microbial diversity indicates a better intestinal condition and physiological prevention of exogenous bacterial colonization and environmental stresses (Chen et al., 2017; Zhou et al., 2019). Furthermore, *Bifidobacterium* and *Anaerotruncus* showed a significant increase, but *Streptococcus* showed a remarkable decrease in the RSV group compared with the control group. Therefore, supplementation of RSV in mice showed a better intestinal condition to prevent the colonization of harmful bacteria. The PICRUSt analysis by KEGG and COG predicted that RSV may alter nutrient metabolism, such as energy production, lipid transport, and amino acid transport through changing intestinal microbial function of weaning mice. Meanwhile, the host defense was also altered in function prediction analysis, such as defense mechanisms, infectious diseases: parasitic, and infectious diseases: bacterial. Therefore, the results of PICRUSt analysis were highly consistent with current results of growth performance, SCFAs, and host defenses.

CONCLUSION

Collectively, our results indicate that mice supplemented with RSV show a greater growth performance and ileum morphology. In addition, supplementation of RSV induces the production of SCFA and the expression of AMP genes and decreases the expression of inflammatory genes. Meanwhile, supplementation of RSV also affects the bacterial community diversity and microbial function in mice cecum. This study will provide valuable guidance for the potential of using RSV as an additive against post-weaning juvenile stress.

DATA AVAILABILITY STATEMENT

The data presented in the study are deposited in the repository (https://www.ncbi.nlm.nih.gov/), accession number (PRJNA596657).

ETHICS STATEMENT

All procedures involving mice in this study were approved by the Animal care and Use Committee of Hunan Normal University, Changsha city, Hunan, China.

AUTHOR CONTRIBUTIONS

YZ, YY, and SH contributed to conception and design of the study. HH organized the database. SL performed the statistical analysis. YZ wrote the first draft of the manuscript. FL and QT wrote sections of the manuscript. All authors contributed to manuscript revision, read, and approved the submitted version.

FUNDING

This study was supported by the Key R&D Program of Hunan Province (2019NK2161), the Hunan Science and Technology Project (2017XK2020), the China Postdoctoral Science Foundation (2017M612562), the Key Research Project of Frontier Sciences of Chinese Academy of Sciences (QYZDY-SSW-SMC008), and the Xiaoxiang Scholar Distinguished Professor Fund of Hunan Normal University.

SUPPLEMENTARY MATERIAL

The Supplementary Material for this article can be found online at: https://www.frontiersin.org/articles/10.3389/fmicb.2021.726878/full#supplementary-material

REFERENCES

Andres-Lacueva, C., Macarulla, M. T., Rotches-Ribalta, M., Boto-Ordonez, M., Urpi-Sarda, M., Rodriguez, V. M., et al. (2012). Distribution of resveratrol metabolites in liver, adipose tissue, and skeletal muscle in rats fed different doses of this polyphenol. *J. Agric. Food Chem.* 60, 4833–4840. doi: 10.1021/jf3001108

Bain, C. C., and Cerovic, V. (2020). Interactions of the microbiota with the mucosal immune system. *Immunology* 159, 1–3. doi: 10.1111/imm.13159

Caporaso, J. G., Kuczynski, J., Stombaugh, J., Bittinger, K., Bushman, F. D. , Costello, E. K., et al. (2010). QIIME allows analysis of high-throughput community sequencing data. *Nat. Methods* 7, 335–336. doi: 10.1038/nmeth.f.303

Cazorla, S. I., Maldonado-Galdeano, C., Weill, R., De Paula, J., and Perdigon, G. (2018). Oral administration of probiotics increases paneth cells and intestinal antimicrobial activity. *Front. Microbiol.* 9:736. doi: 10.3389/fmicb.2018.00736

Chen, L., Xu, Y., Chen, X., Fang, C., Zhao, L., and Chen, F. (2017). The maturing development of gut microbiota in commercial piglets during the weaning transition. *Front. Microbiol.* 8:1688. doi: 10.3389/fmicb.2017.01688

Cruz-Lebron, A., D'Argenio, G. L., Talla, A., Joussef-Pina, S., Quinones-Mateu, M. E., Pierre, S. R., et al. (2019). Decreased enteric bacterial composition and diversity in South American Crohn's disease vary with the choice of treatment strategy and time since diagnosis. *J. Crohns. Colitis.* 14, 791-800.

Furbeyre, H., van Milgen, J., Mener, T., Gloaguen, M., and Labussiere, E. (2017). Effects of dietary supplementation with freshwater microalgae on growth performance, nutrient digestibility and gut health in weaned piglets. *Animal* 11, 183–192. doi: 10.1017/s1751731116001543

Heard-Garris, N., Sacotte, K. A., Winkelman, T., Cohen, A., Ekwueme, P. O., Barnert, E., et al. (2019). Association of childhood history of parental incarceration and juvenile justice involvement with mental health in early adulthood. *JAMA Netw. Open* 2:e1910465. doi: 10.1001/jamanetworkopen.2019.10465

Hsu, C. N., Hou, C. Y., Lee, C. T., Chan, J., and Tain, Y. L. (2019). The interplay between maternal and post-weaning high-fat diet and gut microbiota in the developmental programming of hypertension. *Nutrients* 11:1982, doi: 10.3390/nu11091982

Jiang, Q., Cheng, X., Cui, Y., Xia, Q., Yan, X., Zhang, M., et al. (2019). Resveratrol regulates skeletal muscle fibers switching through the AdipoR1-AMPK-PGC-1alpha pathway. *Food Funct.* 10, 3334–3343. doi: 10.1039/c8fo02518e

Juanola, O., Pinero, P., Gomez-Hurtado, I., Caparros, E., Garcia-Villalba, R., Marin, A., et al. (2018). Cells restrict permeability to bacterial antigen translocation and preserve short-chain fatty acids in experimental cirrhosis. *Hepatol. Commun.* 2, 1610–1623. doi: 10.1002/hep4.1268

Li, F., Han, Y., Cai, X., Gu, M., Sun, J., Qi, C., et al. (2019). Dietary resveratrol attenuated colitis and modulated gut microbiota in dextran sulfate sodium-treated mice. *Food Funct.* 11, 1063-1073

Lv, W. J., Wu, X. L., Chen, W. Q., Li, Y. F., Zhang, G. F., Chao, L. M., et al. (2019). The gut microbiome modulates the changes in liver metabolism and in inflammatory processes in the brain of chronic unpredictable mild stress rats. *Oxid. Med. Cell Longev.* 2019:7902874.

Lv, Y., Yan, Z., Zhao, X., Gang, X., He, G., Sun, L., et al. (2018). The effects of gut microbiota on metabolic outcomes in pregnant women and their offspring. *Food Funct.* 9, 4537–4547. doi: 10.1039/c8fo00601f

Melo, A. D., Silveira, H., Luciano, F. B., Andrade, C., Costa, L. B., and Rostagno, M. H. (2016). Intestinal alkaline phosphatase: potential roles in promoting gut health in weanling piglets and its modulation by feed additives - a review. *Asian-Australas. J. Anim. Sci.* 29, 16–22. doi: 10.5713/ajas.15.0120

Meng, Q., Sun, S., Luo, Z., Shi, B., Shan, A., and Cheng, B. (2019). Maternal dietary resveratrol alleviates weaning-associated diarrhea and intestinal inflammation in pig offspring by changing intestinal gene expression and microbiota. *Food Funct.* 10, 5626–5643. doi: 10.1039/c9fo00637k

Pan, M. H., Koh, Y. C., Lee, T. L., Wang, B., Chen, W. K., Nagabhushanam, K., et al. (2019). Resveratrol and oxyresveratrol activate thermogenesis via different transcriptional coactivators in high-fat diet-induced obese mice. *J. Agric. Food Chem.* 67, 13605–13616. doi: 10.1021/acs.jafc.9b05963

Patil, Y., Gooneratne, R., and Ju, X. H. (2019). Interactions between host and gut microbiota in domestic pigs: a review. *Gut. Microbes.* 11, 310-334.

Pohl, C. S., Medland, J. E., Mackey, E., Edwards, L. L., Bagley, K. D., DeWilde, M. P., et al. (2017). Early weaning stress induces chronic functional diarrhea, intestinal barrier defects, and increased mast cell activity in a porcine model of early life adversity. *Neurogastroenterol. Motil.* 29:10.1111/nmo.13118.

Rauf, A., Imran, M., Suleria, H., Ahmad, B., Peters, D. G., and Mubarak, M. S. (2017). A comprehensive review of the health perspectives of resveratrol. *Food Funct.* 8, 4284–4305. doi: 10.1039/c7fo01300k

Ren, W., Wang, P., Yan, J., Liu, G., Zeng, B., Hussain, T., et al. (2018). Melatonin alleviates weanling stress in mice: involvement of intestinal microbiota. *J. Pineal Res.* 64:12448,

Rooks, M. G., and Garrett, W. S. (2016). Gut microbiota, metabolites and host immunity. *Nat. Rev. Immunol.* 16, 341–352. doi: 10.1038/nri.2016.42

Ross, B. D., Verster, A. J., Radey, M. C., Schmidtke, D. T., Pope, C. E., Hoffman, L. R., et al. (2019). Human gut bacteria contain acquired interbacterial defence systems. *Nature* 575, 224–228. doi: 10.1038/s41586-019-1708-z

Shtoots, L., Richter-Levin, G., Hugeri, O., and Anunu, R. (2018). Juvenile stress leads to long-term immunological metaplasticity-like effects on inflammatory responses in adulthood. *Neurobiol. Learn. Mem.* 154, 12–21. doi: 10.1016/j.nlm.2017.09.008

Storniolo, C. E., and Moreno, J. J. (2019). Resveratrol analogs with antioxidant activity inhibit intestinal epithelial cancer caco-2 cell growth by modulating arachidonic acid cascade. *J. Agric. Food Chem.* 67, 819–828. doi: 10.1021/acs.jafc.8b05982

Tain, Y. L., Lee, W. C., Wu, K., Leu, S., and Chan, J. (2018). Resveratrol prevents the development of hypertension programmed by maternal plus post-weaning high-fructose consumption through modulation of oxidative stress, nutrient-sensing signals, and gut microbiota. *Mol. Nutr. Food Res.* 2018:e1800066.

Tomas, J., Mulet, C., Saffarian, A., Cavin, J. B., Ducroc, R., Regnault, B., et al. (2016). High-fat diet modifies the PPAR-gamma pathway leading to disruption of microbial and physiological ecosystem in murine small intestine. *Proc. Natl. Acad. Sci. USA* 113, E5934–E5943.

Valdes, M. E., Talaverano, M. I., Moreno, D., Prieto, M. H., Mancha, L. A., Uriarte, D., et al. (2019). Effect of the timing of water deficit on the must amino acid

profile of Tempranillo grapes grown under the semiarid conditions of SW Spain. *Food Chem.* 292, 24–31. doi: 10.1016/j.foodchem.2019.04.046

Wang, L. L., Guo, H. H., Huang, S., Feng, C. L., Han, Y. X., and Jiang, J. D. (2017). Comprehensive evaluation of SCFA production in the intestinal bacteria regulated by berberine using gas-chromatography combined with polymerase chain reaction. *J. Chromatogr. B Analyt. Technol. Biomed. Life Sci.* 1057, 70–80. doi: 10.1016/j.jchromb.2017.05.004

Wang, N., Han, Q., Wang, G., Ma, W. P., Wang, J., Wu, W. X., et al. (2016). Resveratrol protects oxidative stress-induced intestinal epithelial barrier dysfunction by upregulating heme oxygenase-1 expression. *Dig. Dis. Sci.* 61, 2522–2534. doi: 10.1007/s10620-016-4184-4

Yamashita, T., Kato, T., Isogai, T., Gu, Y., and Ma, N. (2019). Protective effects of taurine on the radiation exposure induced cellular damages in the mouse intestine. *Adv. Exp. Med. Biol.* 1155, 443–450. doi: 10.1007/978-981-13-8023-5_41

Yang, G., Chang, C. C., Yang, Y., Yuan, L., Xu, L., Ho, C. T., et al. (2018). Resveratrol alleviates rheumatoid arthritis via reducing ros and inflammation. inhibiting mapk signaling pathways, and suppressing angiogenesis. *J. Agric. Food Chem.* 66, 12953–12960. doi: 10.1021/acs.jafc.8b05047

Yang, J., Zhu, C., Ye, J., Lv, Y., Wang, L., Chen, Z., et al. (2019). Protection of porcine intestinal-epithelial cells from deoxynivalenol-induced damage by resveratrol via the nrf2 signaling pathway. *J. Agric. Food Chem.* 67, 1726–1735. doi: 10.1021/acs.jafc.8b03662

Yin, J., Li, Y., Han, H., Chen, S., Gao, J., Liu, G., et al. (2018). Melatonin reprogramming of gut microbiota improves lipid dysmetabolism in high-fat diet-fed mice. *J. Pineal Res.* 65:e12524. doi: 10.1111/jpi.12524

Zhang, C., Yang, L., Zhao, X., Chen, X., Wang, L., and Geng, Z. (2018). Effect of dietary resveratrol supplementation on meat quality, muscle antioxidative capacity and mitochondrial biogenesis of broilers. *J. Sci. Food Agric.* 98, 1216–1221. doi: 10.1002/jsfa.8576

Zhang, C., Zhao, X. H., Yang, L., Chen, X. Y., Jiang, R. S., Jin, S. H., et al. (2017). Resveratrol alleviates heat stress-induced impairment of intestinal morphology, microflora, and barrier integrity in broilers. *Poult. Sci.* 96, 4325–4332. doi: 10.3382/ps/pex266

Zhang, S., Asghar, S., Yu, F., Chen, Z., Hu, Z., Ping, Q., et al. (2019). BSA nanoparticles modified with n-acetylcysteine for improving the stability and mucoadhesion of curcumin in the gastrointestinal tract. *J. Agric. Food Chem.* 67, 9371–9381. doi: 10.1021/acs.jafc.9b02272

Zhou, J., Xiong, X., Yin, J., Zou, L., Wang, K., Shao, Y., et al. (2019). Dietary lysozyme alters sow's gut microbiota. serum immunity and milk metabolite profile. *Front. Microbiol.* 10:177. doi: 10.3389/fmicb.2019.00177

Zhuang, Y., Wu, H., Wang, X., He, J., He, S., and Yin, Y. (2019). Resveratrol attenuates oxidative stress-induced intestinal barrier injury through pi3k/akt-mediated nrf2 signaling pathway. *Oxid. Med. Cell Longev.* 2019:7591840.

Zou, L., Xiong, X., Liu, H., Zhou, J., Liu, Y., and Yin, Y. (2019). Effects of dietary lysozyme levels on growth performance, intestinal morphology, immunity response and microbiota community of growing pigs. *J. Sci. Food Agric.* 99, 1643–1650. doi: 10.1002/jsfa.9348

Conflict of Interest: FL and QT are employed by Yucheng Baolikang Biological Feed Company Limited.

The remaining authors declare that the research was conducted in the absence of any commercial or financial relationships that could be construed as a potential conflict of interest.

Publisher's Note: All claims expressed in this article are solely those of the authors and do not necessarily represent those of their affiliated organizations, or those of the publisher, the editors and the reviewers. Any product that may be evaluated in this article, or claim that may be made by its manufacturer, is not guaranteed or endorsed by the publisher.

frontiers in Microbiology

ORIGINAL RESEARCH
published: 10 September 2021
doi: 10.3389/fmicb.2021.695445

Effects of Dietary Energy Levels on Rumen Fermentation, Gastrointestinal Tract Histology, and Bacterial Community Diversity in Fattening Male Hu Lambs

Qiye Wang[1,2], Yutong Zeng[1], Xianglin Zeng[1], Xin Wang[1], Yancan Wang[1], Chunpeng Dai[2], Jianzhong Li[1], Pengfei Huang[1], Jing Huang[1], Tarique Hussain[3], Mingzhi Zhu[4] and Huansheng Yang[1,5]**

[1] Hunan Provincial Key Laboratory of Animal Intestinal Function and Regulation, Hunan International Joint Laboratory of Animal Intestinal Ecology and Health, Laboratory of Animal Nutrition and Human Health, College of Life Sciences, Hunan Normal University, Changsha, China, [2] Hubei Zhiqinghe Agriculture and Animal Husbandry Co., Ltd., Yichang, China, [3] Animal Sciences Division, Nuclear Institute for Agriculture and Biology, Faisalabad, Pakistan, [4] National Research Center of Engineering Technology for Utilization of Functional Ingredients from Botanicals, Co-Innovation Center of Education Ministry for Utilization of Botanical Functional Ingredients, College of Horticulture, Hunan Agricultural University, Changsha, China, [5] Hunan Provincial Key Laboratory of Animal Nutritional Physiology and Metabolic Process, Key Laboratory of Agro-Ecological Processes in Subtropical Region, Hunan Provincial Engineering Research Center of Healthy Livestock, Scientific Observing and Experimental Station of Animal Nutrition and Feed Science in South-Central, Ministry of Agriculture, Institute of Subtropical Agriculture, Chinese Academy of Sciences, Changsha, China

OPEN ACCESS

Edited by:
Peng Huang,
Hunan Agricultural University, China

Reviewed by:
Bingkun Zhang,
China Agricultural University, China
Qiuyue Liu,
Institute of Genetics and Developmental Biology, Chinese Academy of Sciences, China

***Correspondence:**
Mingzhi Zhu
mzzhucn@hotmail.com
Huansheng Yang
yhs@hunnu.edu.cn

Specialty section:
This article was submitted to Microbial Symbioses, a section of the journal Frontiers in Microbiology

Received: *15 April 2021*
Accepted: *02 August 2021*
Published: *10 September 2021*

Citation:
Wang Q, Zeng Y, Zeng X, Wang X, Wang Y, Dai C, Li J, Huang P, Huang J, Hussain T, Zhu M and Yang H (2021) Effects of Dietary Energy Levels on Rumen Fermentation, Gastrointestinal Tract Histology, and Bacterial Community Diversity in Fattening Male Hu Lambs. Front. Microbiol. 12:695445. doi: 10.3389/fmicb.2021.695445

This study investigated rumen fermentation and histological and microbial diversity in male Hu lamb fed diets with different metabolizable energy (ME) levels (MEA, 9.17 MJ/kg, MEB, 10.00 MJ/kg, and MEC, 10.82 MJ/kg). Thirty-six male Hu lambs were randomly allotted to three treatments, and the feeding trial lasted for 67 days. Rumen fermentation results suggest that the iso-valerate had a significant effect on dietary energy level. The papillary height (PH) of rumen was the highest in the MEB group, the crypt depth (CD) was significantly increased in the duodenum and jejunum, and the villus height (VH)-to-CD ratio (VH/CD) was significantly decreased in the duodenum by increasing dietary energy levels; the VH, villus width (VW), and VH/CD also had significant differences in the ileum. 16S rRNA sequencing results showed that the operational taxonomic units (OTUs) number, the ACE, and Chao1 indices were linearly decreased by increasing dietary energy level; 24 phyla including 124 genera were identified, and the relative abundance of *Papillibacter* and *Quinella* linearly decreased by increasing the dietary energy level. Compared to MEA and MEB groups, the relative abundance of *unidentified_Veillonellaceae* and *Anaerovibrio* was significantly increased in the MEC group at the genus level. The relative abundance of the carbohydrate metabolism pathway predicted by Phylogenetic Investigation of Communities by Reconstruction of Unobserved States (PICRUSt) was linearly increased by increasing the dietary energy levels. Three metabolic pathways identified in Kyoto

Encyclopedia of Genes and Genomes (KEGG) level 3 were significantly influenced as the dietary energy level increased. In summary, these results demonstrated that the dietary energy levels affected the rumen fermentation parameters, morphological structures of the gastrointestinal tract (GIT), and the composition and function of rumen microflora in male Hu sheep.

Keywords: rumen, bacteria, volatile fatty acid, high-throughput sequencing, Hu sheep

INTRODUCTION

The Hu sheep is a unique breed native to China, and is one of the several white lamb-skin sheep breeds in the world (Wang et al., 2020a). Commonly, Hu sheep are identified as an ideal choice for factory production in our country, especially in southern agricultural areas (Wang et al., 2020b). With the deterioration of ecological environments and the increasing demand for consumption of lamb, ruminant production with traditional grazing patterns is dominated instead by large-scale farming with stall-feeding. As ruminant farming patterns have transformed, animal diets are witnessing a change. Furthermore, performance traits such as daily gain and rumen micro-ecosystem have changed accordingly (Morand-Fehr et al., 2007; Wang H. R. et al., 2017).

The rumen of ruminants is a dynamic and complex microecosystem that consists mostly of bacteria, protozoa, archaea, and fungi (Mackie et al., 2000; Knoell et al., 2016). Bacteria are the dominant microorganism group (Pitta et al., 2016), and some of these microorganisms that are attached to feed particles participate in the transformation of plant ingredients into animal products (Preston and Leng, 1987; Han et al., 2015). Rumen bacterial diversity is influenced by diet, breed, host age, season, and geographic region (Lee et al., 2012), and diet is a key factor in determining its composition and function (Wang et al., 2020b). The energy and protein of dietary nutrition are the two determinants that most often limit microbial activity (Clark, 1975; Clark and Davis, 1980). For instance, protein-degrading bacteria can degrade true proteins to volatile fatty acids (VFAs) and ammonia, and the major source of nitrogen for microbial growth and protein synthesis is ammonia (Wang et al., 2015; Owens and Basalan, 2016). Bach et al. (2005) found that a diet of high energy level can promote the synthesis of microbial proteins due to it supplying only enough available energy for microbial growth and metabolism (Owens and Basalan, 2016). Carbohydrates are a predominant energy source for ruminants, which generally make up more than 70% of the ruminant diet. The rumen is the main site for carbohydrate digestion as dietary carbohydrates are fermented by rumen microbes into VFAs (such as acetate, propionate, and butyrate), which can provide nearly two-thirds of the energy requirements for the host and further digested and absorbed by the gastrointestinal tract (GIT) (Cunha et al., 2011; McGovern et al., 2018). Although the concentration of dietary energy is important for rumen microbial growth and protein synthesis, excessive energy intake not only increases the cost of feed but may also lead to a decrease in meat quality (Broderick, 2003). Thus, it is necessary to explore appropriate dietary energy levels for ruminants.

Applying high energy (or high grain, such as corn) diet to promote animal performance was considered as a popular strategy in modern factory fattening systems of ruminants. Furthermore, to elucidate the GIT histology and rumen microbial community diversity and function, appropriate high-energy (or high-grain) diets are very urgent, especially for improving animal performance in large-scale healthy farming. Several recent studies have focused on rumen microbial diversity associated with dietary nutrition levels in goats and bulls (Zhang et al., 2017; McGovern et al., 2018) and high-grain diets in sheep (Seddik et al., 2019). However, so far, systematically conducted studies on the dynamic effects of dietary energy levels on rumen microbiota and GIT histology of sheep have not been reported. Here, we hypothesize that the rumen fermentation, GIT histology, and ruminal microbiota would dynamically alter by increasing the dietary energy levels in fattening male Hu lambs. Therefore, the present study was conducted to explore the dynamic variation in rumen fermentation, GIT histology, and rumen microbial community and function in Hu sheep with different dietary energy levels.

MATERIALS AND METHODS

Animals, Diets, and Sampling Procedures

This experiment was performed in Hubei Zhiqinghe Agriculture and Animal Husbandry Co., Ltd., Yichang, Hubei, China. Thirty-six male Hu lambs (aged 4 months) with an average initial body weight (IBW) of 20.16 $\pm$ 0.38 kg were used in feeding trial. The lambs were allotted to one of three dietary treatments (groups MEA, MEB, and MEC), randomly based on their IBW. Each group included 12 lambs and fed in individual pens. All of the experimental diets met the nutritional requirements [National Research Council (NRC), 2007] for growing sheep with equivalent nutritional ingredients, except for energy. The dietary energy levels respectively were 9.17, 10.00, and 10.82 MJ/kg corresponding to 91, 99, and 107% of the energy levels that had been recommended by the Nutrient Requirements of Small Ruminants [National Research Council (NRC), 2007] for groups MEA to MEC, and the protein levels were all approximately 13% (**Table 1**). The experimental lambs feeding and management were referenced by Wang et al. (2020a); the trail lambs were fed their corresponding diets twice a day in the morning and afternoon and were subjected to free feeding and automatic drinking throughout the course of the experiment. At the end of the trial, five lambs close to the average weight from group

TABLE 1 | Diet ingredients and nutrition levels.

Item	Dietary energy, MJ/kg		
	MEA, 9.17	MEB, 10.00	MEC, 10.82
Ingredient, %			
Corn silage	40	25	10
Peanut seedling	30	30	30
Corn	5.44	22.25	39.06
Wheat bran	6.96	6.06	5.16
Soybean meal	14.60	13.69	12.78
Premix[1]	3	3	3
Total	100	100	100
Nutrient levels[2]			
Metabolic energy, MJ/kg	9.17	10.00	10.82
Crude fat, g/kg	20	22	23
Neutral-detergent fiber, g/kg	453	399	345
Acid-detergent fiber, g/kg	332	280	229
Crude ash, g/kg	67	61	54
Acid insoluble ash, g/kg	14	11	9
Crude protein, g/kg	132	130	129

[1]Premix provides the following per kg: vitamin A 120 KIU; vitamin D_3 60 KIU; vitamin E 200 mg; Cu 0.15 g; Fe 1 g; Zn 1 g; Mn 0.5 g; I 15 mg; Se 5 mg; Co 2.5 mg; Ca 20 g; NaCl 100–250 g; and P 10 g.
[2]Except for metabolic energy, which is a predicted value, the rest are measured values.

MEA, group MEB, and group MEC, respectively, were selected for slaughter after they were not fed for 12 h, with a total 15 lambs being exsanguinated according to veterinary police rules. The rumen was removed from each of the sheep, and 100 ml of rumen fluid was homogenized and then divided into two 50-ml sterile tubes and stored at −80°C for 16S rRNA sequencing and VFA content determination.

Rumen Fermentation Parameters

The concentrations of total VFA (TVFA) and individual VFA were detected by gas chromatography (Agilent 7890A, NYSE: A, Palo Alto, CL, United States), referring to the method of Wang et al. (2020b). A total of 0.15 ml of 25% metaphosphoric acid was added into 1.5 ml of rumen fluid samples and was properly mixed. Subsequently, the mixed samples were stored at −20°C for more than 24 h and then centrifuged at 15,000 × *g* for 10 min at 4°C to take 1.0 ml of supernatant to filter with a 0.45-μm membrane. Then, filter liquor was injected into a special gas-phase vial, in which 1 μl of the sample was injected into an Agilent DB-FFAP gas-phase capillary column (30 m × 0.25 mm × 0.25 μm) automatically. The injector and detector temperatures were respectively set at 250 and 280°C, with the split ratio set at 50:1. The column was heated from 60 to 220°C at a rate of 20°C/min.

Rumen and Intestinal Morphology

Hematoxylin–eosin (HE) staining and optical microscopy were used for the rumen and intestinal morphology analysis. According to the method described by Wang et al. (2020b) and Deng et al. (2020), paraffin sections of tissues were fixed. Formalin-immobilized duodenum, jejunum, ileum, and rumen samples were dehydrated and embedded in paraffin, subsequently embedded paraffin tissue was cut into cross sections of 5-μm thickness, and then the slices were stained with HE. The morphological structures of villus height (VH), villus width (VW), crypt depth (CD), and papillary height (PH) were acquired by using a microscope and an image processing and analysis system (Version 1, Leica Imaging Systems Ltd., Cambridge, United Kingdom). Using Image-Pro Plus 6.0 software, no fewer than 10 well-oriented intact villi and their corresponding crypts for each sample were measured; meanwhile, calculate the VH-to-CD ratio (VH/CD).

DNA Extraction and PCR Amplification

Total genomic DNA from the rumen fluid samples was extracted by the CTAB/SDS method. The concentration and purity of DNA were monitored with 1% agarose gels and then using sterile water diluted to 1 ng/μl. The V3–V4 regions of distinct 16S rRNA genes (16S) were amplified with specific primers V515F (5′-GTGYCAGCMGCCGCGGTA A-3′) and V806R (5′-GGACTACHVGGGTWTCTAAT-3′). PCR amplification reactions were carried out in 30-μl systems with 15 μl of Phusion® High-Fidelity PCR Master Mix (New England Biolabs), 10 ng of template DNA, and 0.2 μM of forward and reverse primers. PCR-amplified procedure initial denaturation was set at 98°C for 1 min, followed by 30 cycles of denaturation at 98°C for 10 s. Annealing was at 50°C for 30 s, and elongation was at 72°C for 30 s and finally at 72°C for 5 min. The amplified products were mixed with the same volume of 1× loading buffer (contained SYB green) and detected by 2% agarose gel electrophoresis. Then, using the GeneJET^{TM} Gel Extraction Kit (Thermo Scientific) to purify the mixture, PCR products were generated with the Ion Plus Fragment Library Kit 48 rxns (Thermo Scientific) to construct the sequencing libraries. The library quality was assessed on the Qubit@ 2.0 Fluorometer (Thermo Scientific). Finally, the Ion S5^{TM} XL platform was used to sequence the library and generate 407- to 412-bp single-end reads.

Sequencing Analyses

Under specific filtering conditions, the raw reads were performed according to the Cutadapt quality control process to obtain high-quality clean reads (Martin, 2011). The UCHIME algorithm (Edgar et al., 2011) was used to detect chimera sequences and remove the chimera sequences (Haas et al., 2011) to finally obtain the clean reads compared to the SILVA database (the reference database) (Quast et al., 2012). Sequence analysis was implemented by Uparse Software (Uparse v7.0.1001) (Edgar, 2013), and sequences with ≥97% similarity were assigned to the same operational taxonomic units (OTUs). The SILVA database was used to annotate taxonomic information for each representative sequence screened for each OTU; meanwhile, a standard of sequence number corresponding to the sample with the least sequences was used to normalize the OTUs' abundant information. Based on the output of normalized data, alpha diversity and beta diversity were analyzed subsequently. Alpha diversity was utilized to analyze the complexity of

species diversity for each sample, including Shannon, Simpson, Chao1, ACE, Good-coverage, and Observed-species indices, and which were calculated by QIIME (Version1.7.0) and displayed by R Software (Version 2.15.3). Beta diversity is implemented in the evaluation of the differences in samples of species complexity. The UniFrac distance was calculated and the unweighted pair-group method with arithmetic means (UPGMA) sample cluster tree was constructed by QIIME software (Version 1.7.0). The principal coordinate analysis (PCoA) was performed to obtain principal coordinates and visualizations from complex, multidimensional data and display with the WGCNA package, stat packages, and ggplot2 package in R software (Version 2.15.3); the Vegan software package of R software was used for non-metric multi-dimensional scaling (NMDS) analysis. UPGMA clustering was performed to interpret the distance matrix using average linkage and was conducted by QIIME software. The R software was used to analyze the differences between groups of beta diversity index.

Bacterial Metabolic Pathway and Function Predictions

Phylogenetic Investigation of Communities by Reconstruction of Unobserved States (PICRUSt) is based on the genetic information on the OTU and the Greengene database[1] to construct the archaeal and bacterial domain and predict the full spectrum of the gene function. This is achieved by extrapolating the gene function spectrum of their common ancestors and other untested species in the Greengene database. Finally, the sequence of the microbial composition map is imported into the database to predict the metabolic function of microbiota. Furthermore, PICRUSt2[2] was used to predict the metabolic function of rumen microorganisms; PICRUSt2 predictions based on the Integrated Microbial Genomes (IMG) database, including the Kyoto Encyclopedia of Genes and Genomes (KEGG) orthologs (KO) and Enzyme Commission numbers (EC numbers) and other several gene family databases, are supported by IMG (Douglas et al., 2020).

Statistical Analysis

Preliminary experimental data were processed by Excel (Microsoft, Seattle, Washington, DC, United States), and SPSS 22 software (SPSS, Chicago, IL, United States) was performed for further statistical analysis. One-way ANOVA and *t*-tests were used to test the significance of rumen fermentation parameters and morphological indices. The microbial diversity, bacterial relative abundance, and function prediction analyses were carried out by the non-parametric test. The final results were expressed as means ± SEM. A p-value of <0.10 shows a trend, a p-value of <0.05 is significant, and $p < 0.01$ is extremely significant.

[1]https://picrust.github.io/picrust/

[2]https://github.com/picrust/picrust2/wiki

RESULTS

Rumen Fermentation Parameters

The results of VFAs in the rumen are shown in **Table 2**. There was no significant difference linearly in the concentrations of acetate, propionate, butyrate, iso-butyrate, iso-valerate, valerate, and TVFA, and the ratio of acetate/propionate (Ac/Pr) in the rumen of fattening male Hu lambs with the increase of dietary energy level (one-way ANOVA and *t*-tests $p > 0.05$). The molar concentration of iso-valerate in the MEB group was significantly higher than the other two groups (quadratic, one-way ANOVA and *t*-tests $p = 0.041$). The molar proportion of iso-valerate in the MEB group was significantly higher than the other two groups (quadratic, one-way ANOVA and *t*-tests $p = 0.033$), while the molar proportion of acetate in the MEB group was dramatically lower than other two groups (quadratic, one-way ANOVA and *t*-tests $p = 0.044$) (**Table 2**). Actually, our previous research has found that the daily weight gain (ADG) and dry matter intake (DMI) are significantly increased, and feed conversion ratio (FCR) is dramatically decreased by increasing the dietary ME level in growth performance (Wang et al., 2020a).

Rumen and Intestinal Morphology

The rumen and intestinal morphology are shown in **Table 3** and **Figure 1**. By increasing the dietary energy level, the CD (linear, one-way ANOVA and *t*-tests $p = 0.000$ and quadratic, one-way ANOVA and *t*-tests $p = 0.002$) was dramatically increased, while the VH/CD was significantly decreased (linear, one-way ANOVA and *t*-tests $p = 0.002$) in the duodenum. In the jejunum, the CD (linear, one-way ANOVA and *t*-tests $p = 0.012$ and quadratic, one-way ANOVA and *t*-tests $p = 0.033$) was also significantly increased. There were significant differences in the VH (linear,

TABLE 2 | Effects of dietary energy levels on rumen fermentation parameters.

Item	Groups			SEM[2]	*p*-Value	
	MEA	MEB	MEC		Linear	Quadratic
Molar concentration (mM)						
Acetate	39.49	35.04	35.35	1.68	0.369	0.517
Propionate	9.59	8.92	8.47	0.49	0.419	0.922
Butyrate	4.84	4.34	4.30	0.23	0.402	0.654
Iso-butyrate	1.59	1.82	1.65	0.06	0.717	0.127
Iso-valerate	2.47^{b}	2.98^{a}	2.52^{b}	0.11	0.865	0.041
Valerate	0.79	0.81	0.79	0.03	0.967	0.735
TVFA[1]	58.77	53.91	53.08	2.40	0.408	0.773
Ac/Pr	4.10	4.02	4.23	0.11	0.671	0.571
Molar proportion (mol/100 mol)						
Acetate	66.99^{a}	65.05^{b}	66.70^{a}	0.46	0.695	0.044
Propionate	16.36	16.38	15.86	0.36	0.574	0.878
Butyrate	8.16	8.13	8.06	0.16	0.765	0.877
Iso-butyrate	2.78	3.38	3.13	0.12	0.229	0.091
Iso-valerate	4.34^{b}	5.54^{a}	4.77^{b}	0.23	0.389	0.033
Valerate	1.36	1.52	1.48	0.04	0.298	0.348

Values within a row with different superscripts (a,b) differ significantly at $p < 0.05$.
[1]Total volatile fatty acids. [2]SEM, standard error of the mean.

TABLE 3 | Effects of dietary energy levels on GIT morphology.

Item	Measured index (μm)	Groups			SEM	*p*-Value	
		MEA	MEB	MEC		Linear	Quadratic
Duodenum	Villus height	362.12	390.08	354.57	12.75	0.825	0.264
	Crypt depth	156.53^{b}	239.48^{a}	229.13^{a}	11.66	0.000	0.002
	Villus width	127.34	133.44	123.79	2.86	0.636	0.210
	VH/CD	2.34^{a}	1.64^{b}	1.55^{b}	0.12	0.002	0.072
Jejunum	Villus height	363.75	338.43	428.97	19.00	0.125	0.165
	Crypt depth	184.94^{b}	163.8^{b}	254.59^{a}	14.86	0.012	0.033
	Villus width	131.76	129.64	141.25	2.83	0.152	0.285
	VH/CD	1.99	2.10	1.70	0.08	0.079	0.113
Ileum	Villus height	355.73^{b}	362.09^{b}	463.45^{a}	15.12	0.000	0.018
	Crypt depth	195.12	175.59	177.05	8.91	0.455	0.600
	Villus width	156.83^{a}	137.13^{b}	142.67^{b}	2.76	0.004	0.002
	VH/CD	1.86^{b}	2.12^{b}	2.66^{a}	0.12	0.005	0.470
Rumen	Papillary height	1,648.41^{b}	2,000.15^{a}	1,706.07^{b}	70.76	0.693	0.043

Values within a row with different superscripts (a,b) differ significantly at $p < 0.05$.

one-way ANOVA and *t*-tests $p = 0.000$ and quadratic, one-way ANOVA and *t*-tests $p = 0.018$), VW (linear, one-way ANOVA and *t*-tests $p = 0.004$ and quadratic, one-way ANOVA and *t*-tests $p = 0.002$), and VH/CD (linear, one-way ANOVA and *t*-tests $p = 0.005$) in the ileum; the VH and VH/CD increased as the diet energy level increases, while the VW in the MEA group was significantly higher than the other two groups. The rumen PH was the highest in the MEB (medium energy) group (quadratic, one-way ANOVA and *t*-tests $p = 0.043$).

Sequences Across Different Diet Groups

Sequencing results showed that the average of 84,736 reads for each sample was measured through shearing and filtration, and an average of 80,128 valid data reads was obtained through quality control, and the quality control efficiency was 94.61%. A total of 2,456 OTUs were acquired for all samples. Among them, 2,453 (99.88%) OTUs were annotated at the kingdom level, 2,365 (96.29%) at the phylum level, 2,310 (94.06%) at the phylum level, 2,171 (88.40%) at the order level, 1,856 (75.57%) at the family level, 603 (24.55%) at the genus level, and 197 (8.02%) OTUs annotated at the species level (**Supplementary Table 1**). The OTU number, which reflects the rumen microbial diversity, was significantly (non-parametric test $p = 0.013$) decreased by increasing the dietary energy level. The richness estimator indices of ACE (non-parametric test $p = 0.085$) and Chao1 (non-parametric test $p = 0.063$) showed a downward trend as dietary energy level increased, whereas there were no significant differences in the alpha diversity indices of Shannon and Simpson and the phylogenetic diversity index of PD-whole-tree (non-parametric test $p > 0.05$). Additionally, the goods-coverage index was greater than 99%, indicating that the sequencing depth basically covered all the species in all the samples and accurately reflected the microbial community (**Table 4**). The rarefaction curves tended to be flat at 3% divergence and also showed that the sequencing data were reasonable and that the sequencing depth sufficiently covered the majority of bacterial diversity in all samples (**Supplementary Figure 1**).

Rumen Microbial Diversity

The taxonomic analysis results showed that 24 phyla were detected and that unclassified bacteria were excluded. The five phyla with the highest relative abundance were *Firmicutes*, *Bacteroidetes*, *Euryarchaeota*, *Proteobacteria*, and *Gracilibacteria* (**Figure 2A**). As expected, the relative abundance of *Firmicutes*, *Bacteroidetes*, and *Euryarchaeota* was the richest in the three experimental groups, accounting for about 95% of the total abundance. The relative abundance of *Synergistetes* first increased and then decreased (non-parametric test $p = 0.077$) with the increase in dietary energy levels (**Figure 2B**).

At the genus level, 124 genera were identified and the 10 most relatively abundant genera were elucidated in all the samples (**Supplementary Table 2** and **Figure 2C**). Within three groups, the five dominant relative genera were *unidentified Ruminococcaceae*, *unidentified Lachnospiraceae*, *unidentified Bacteroidales*, *Saccharofermentans*, and *Papillibacter*. Among the rest, *unidentified Ruminococcaceae* and *unidentified Lachnospiraceae* were members of *Firmicutes* in the phylum, *unidentified Bacteroidales* is from *Bacteroidetes*, and *Saccharofermentans* and *Papillibacter* belonged to *Clostridiales* of *Firmicutes*.

The relative abundance of *Papillibacter* (non-parametric test $p = 0.021$) and *Quinella* (non-parametric test $p = 0.008$) was significantly decreased by increasing dietary energy, while the relative abundance of *unidentified_Veillonellaceae* (non-parametric test $p = 0.022$) and *Anaerovibrio* (non-parametric test $p = 0.018$) increased significantly with the increase in dietary energy level (**Figure 2D**). The relative abundance of *Oribacterium* showed an upward tendency (non-parametric test $p = 0.059$), the relative abundance of *Mycoplasma* presented a downward trend (non-parametric test $p = 0.065$), the relative abundance of *Fretibacterium* showed a tendency of rising after falling (non-parametric test $p = 0.065$), and the relative abundance of *Saccharofermentans* (non-parametric test $p = 0.085$), *Shuttleworthia* (non-parametric test $p = 0.057$), *Moryella* (non-parametric test $p = 0.061$), *Acetitomaculum*

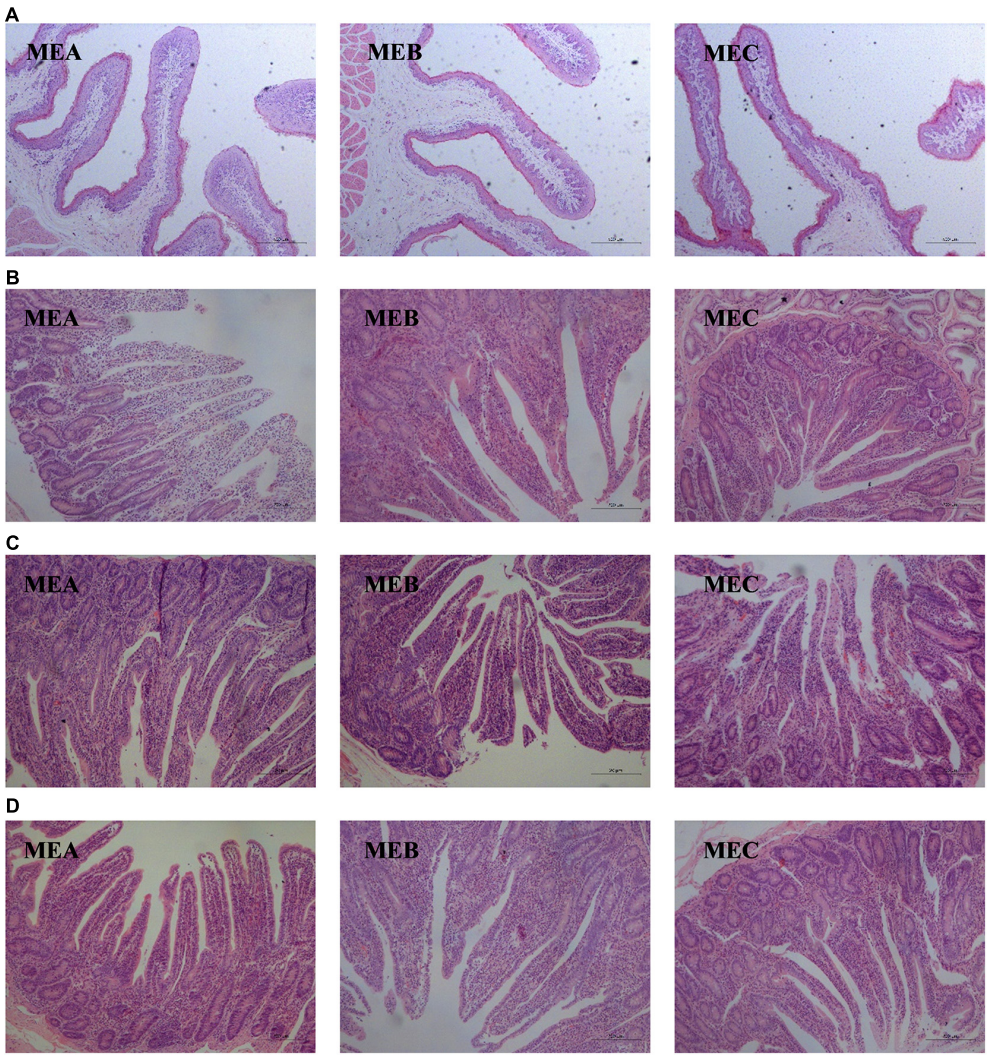

FIGURE 1 | Effects of low-, medium-, and high-energy diets on rumen and small intestinal morphology of male Hu lambs. **(A)** Papillary height of rumen. Scale bar, 500 μm. **(B)** Duodenum. Scale bar, 200 μm. **(C)** Jejunum. Scale bar, 20 μm. **(D)** Ileum. Scale bar, 200 μm.

(non-parametric test p = 0.054), and *Desulfobulbus* (non-parametric test p = 0.057) first decreased and then increased with the increase in dietary energy levels (**Figure 2D**). Additionally, the relative abundance of *Oscillibacter*_sp_ER4 (non-parametric test p = 0.040) in both MEB and MEC groups was significantly higher than the MEA group, the relative abundance of *Lachnospiraceae*_bacterium_AC2029 (non-parametric test p = 0.005) and *Lachnospiraceae_bacterium*_RM66 (non-parametric test p = 0.035) in the MEC group was significantly higher than that in MEA and MEB groups at the species level (**Figure 2E**), and the three kinds of bacteria all belonged to *Firmicutes*.

Rumen Bacteria Clustering Dissimilarities

The PCoA showed that the rumen microbial diversity accounted for 16.92% variation in the MEC group, distinguished from both MEA and MEB groups by PC1, and that the microbial diversity between MEA and MEB groups represented 14.67% variation of PC2 (**Figure 3**). The NMDS analysis also verified that the rumen bacterial diversity in the MEC group was clustered discretely with the other two groups (Stress = 0.098), which could accurately reflect the degree of variation for all samples (**Supplementary Figure 2**).

Rumen Microbial Function Prediction

"Metabolism" with more than 47% of the total reads has the highest relative abundance among the three groups at KEGG level 1 (**Supplementary Figure 3**). The 35 gene families of the most relative abundant (relative abundance >0.08%) from each rumen sample were present at KEGG level 2 (**Supplementary Table 3**). The genes related to membrane transport, amino acid metabolism, carbohydrate metabolism, replication and repair, and energy metabolism

TABLE 4 | Rumen microbiota diversity indices of different dietary energy levels.

Item	Groups			SEM[6]	*p*-Value
	MEA	MEB	MEC		
OTUs[1]	1,514.60[a]	1,450.20[ab]	1,365.40[b]	26.32	0.013
Shannon indices[2]	8.27	8.11	8.11	0.08	0.932
Simpson indices[2]	0.99	0.99	0.99	0.00	0.704
ACE value[3]	1,606.07	1,532.01	1,467.62	27.83	0.085
Chao1 value[3]	1,605.26	1,530.87	1,578.59	51.36	0.063
Goods-coverage[4]	0.997	0.997	0.997	0.00	0.985
PD-whole-tree[5]	103.82	102.26	94.84	2.09	0.134

Values within a row with different superscripts (a,b) differ significantly at $p < 0.05$. OTU, operational taxonomic units; ACE, abundance-based coverage estimator. [1]Number of operational taxonomic units. [2]Shannon and Simpson indices. [3]ACE and Chao species richness estimators. [4]Sequencing depth index. [5]Phylogenetic diversity index. [6]SEM, standard error of the mean.

exhibited the most relative abundance among the three groups (**Figure 4A**), in which carbohydrate metabolism showed an obviously increased trend (non-parametric test $p = 0.063$) by increasing the dietary energy level (**Figure 4B**). At KEGG level 3, the pathways referring to transporters, general function prediction only, DNA repair and recombination proteins, ATP-binding cassette (ABC) transporter and ribosome, purine metabolism, and pyrimidine metabolism were highly represented (**Supplementary Table 4**). With an increase in the dietary energy level, three pathways showed significant variation; the relative abundance of phenylalanine tyrosine and tryptophan biosynthesis (non-parametric test $p = 0.009$) had notably increased, the relative abundance of arginine and proline metabolism significantly increased after falling (non-parametric test $p = 0.038$), whereas the abundance of the transcription machinery (non-parametric test $p = 0.015$) pathway had dramatically decreased (**Figure 4C**). Results of rumen microbial function prediction by PICRUSt2 are shown in **Figures 4D–I**. The top 10 relative abundance pathways are shown in **Figure 4D**, but there was no significant difference among the three groups, including the top 35 relative abundance pathways, whereas there were nine predictive metabolic pathways that were significantly affected by dietary energy levels and two other pathways showed a certain trend (**Figure 4F**). In addition, the NSTI (Nearest Sequenced Taxon Index) values are evaluated in **Figure 4E**, and the NSTI values were lower than 0.18 among different groups. The results of COG (Clusters of Orthologous Groups) functional annotation analysis showed that the relative abundance of NAD(P)-dependent dehydrogenase, short-chain alcohol dehydrogenase family was significantly higher (non-parametric test $p = 0.009$) in MEA and MEB than in MEC (**Figure 4G**). The results showed that the top 35 relative abundance based on KO analysis had no significant difference among the three groups (**Figure 4H**). The EC analysis results showed that the relative abundance of Type I site-specific deoxyribonuclease (non-parametric test $p = 0.015$) was significantly affected by different dietary energy levels (**Figure 4I**).

DISCUSSION

The rumen is a unique digestive organ, which is known to be the most powerful natural fermentation tank to degrade fiber materials, and plays an extremely crucial role in nutrient digestion and metabolism in ruminants. The complex microbiota in the rumen played a critical role in feed fermentation and energy metabolism (Flint et al., 2007). The fermentation and degradation of feed in the rumen are closely related to the composition of rumen microbiota. About 70% of the energy required by rumen fermentation is provided by VFAs to ensure the maintenance, growth, and production performance of the host. Therefore, the rumen microbial composition and structure affected the nutritional health and growth of ruminants (Pokharel et al., 2018). On the contrary, the host provided fermentation substrates and a suitable anaerobic environment for the survival of rumen microorganisms (Guan et al., 2008). In the present study, the experimental population was assigned to three groups according to the dietary energy level: low (MEA), medium (MEB), and high (MEC) energy.

Previous studies have demonstrated that the feed type and nutrient level can influence the proportion of acetate, propionate, and butyrate; in particular, a concentrate-based or a high-energy diet is capable of increasing the proportion of propionate in the rumen (van Soest, 1994; Keady et al., 2001; Agle et al., 2010). In the present study, different dietary energy levels had no significant effect on the molar concentration of acetate, propionate, butyrate, and TVFA, and these results were in agreement with other studies (Murphy et al., 2000). Interestingly, the medium energy level significantly increased the molar concentration and proportion of iso-valerate at the quadratic level, while quadratically decreasing the proportion of acetate compared to the low- and high-energy groups; these results were not completely consistent with previous studies (Shabat et al., 2016), whether these findings had beneficial effects on the composition and function of rumen microbiota remained to be explored. Unexpectedly, the concentrations of acetate, propionate, butyrate, and TVFA were lower in the medium- and high-energy groups compared with the low-energy group in the present study, which might be related to the increase of high corn content in the medium- and high-energy diet and excessive fasting times during sampling (more than 12 h). Guan et al. (2008) and Ellison et al. (2017) found that the feed composition and rumen environment could affect the feed conversion efficiency in ruminants, and high-grain diets might be easier to digest and absorb. Accordingly, the concentration of VFAs in rumen fluid would decrease faster. Thus, it can be seen that iso-valerate and acetate responded to alter dietary energy levels.

The primary site of nutrient digestion and absorption is the GIT of ruminants. Steele et al. (2016) and Wester et al. (1995) found that the dietary energy density and ME intake can affect the GIT tissues, such as the height and width of rumen papillae, which are generally used to estimate the rumen epithelium growth (Steele et al., 2014). Khan et al. (2011) found that the particle size and diet composition can affect the morphological structure of rumen papillae. A previous study has also shown that the high-energy diet could stimulate the proliferation of rumen

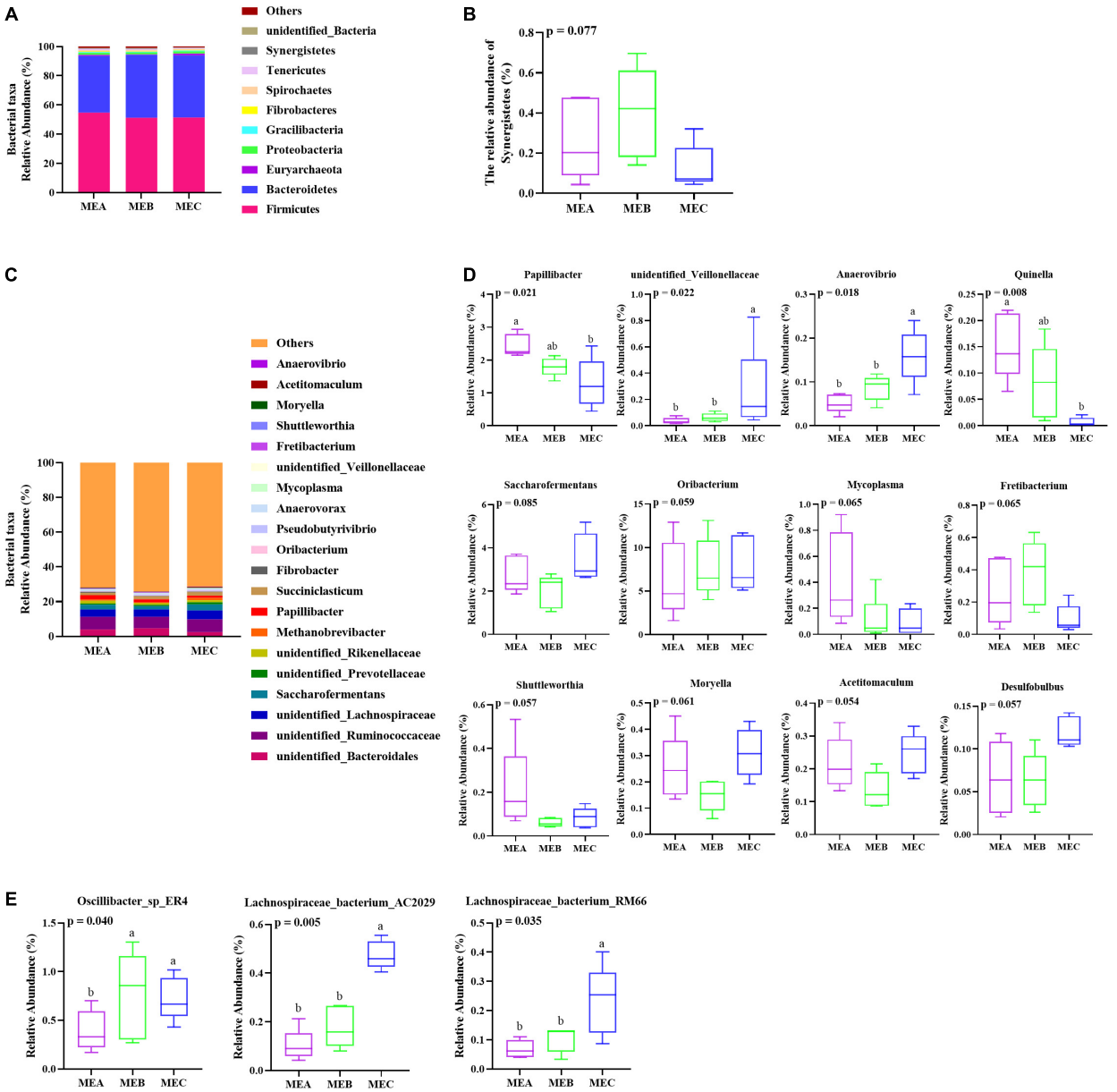

FIGURE 2 | Effects of low-, medium-, and high-energy diets on rumen microbiota in male Hu lambs. **(A)** Bacterial taxonomic profile of the rumen microbiota at the phylum level. **(B)** Relative abundances of *Synergistetes*. **(C)** Relative abundances of the dominant genera in the rumen. **(D)** Relative abundance of representative genera. **(E)** Relative abundance of representative species. Values with different superscripts (a,b) differ significantly at $p < 0.05$.

papillae of goats (Shen et al., 2004). Papillae height was the highest in the medium-energy group compared with the low- and high-energy groups in this study, which suggested that an appropriate increase in dietary energy level might contribute to the growth and development of rumen papilla. This result was consistent with that of a previous experiment (Kim et al., 2012).

Villus height, VW, CD, and VH/CD are acknowledged as key histomorphology figures to reflect the digestive and absorption functions of the small intestine (Hedemann et al., 2003; Yang et al., 2013, 2016). Intestinal epithelial cell proliferation has a positive impact on VH and CD. Wang et al. (2019) found that VH was positively correlated with the absorption capacity of nutrients and CD had a synergistic effect on villus cell renewal. In the present study, the VH of ileum significantly increased in the high-energy group, and the CD of the duodenum and jejunum significantly increased in the medium- and high-energy groups, while a significant decrease was observed in the VH/CD of the duodenum and the VW of the ileum in the medium- and high-energy groups. Previous studies have found that nutritional restriction in weaned lambs could reduce the CD of jejunum (Lingyan et al., 2014), while supplementary concentration could promote the VH of grazing calves (Azim et al., 2011), and our

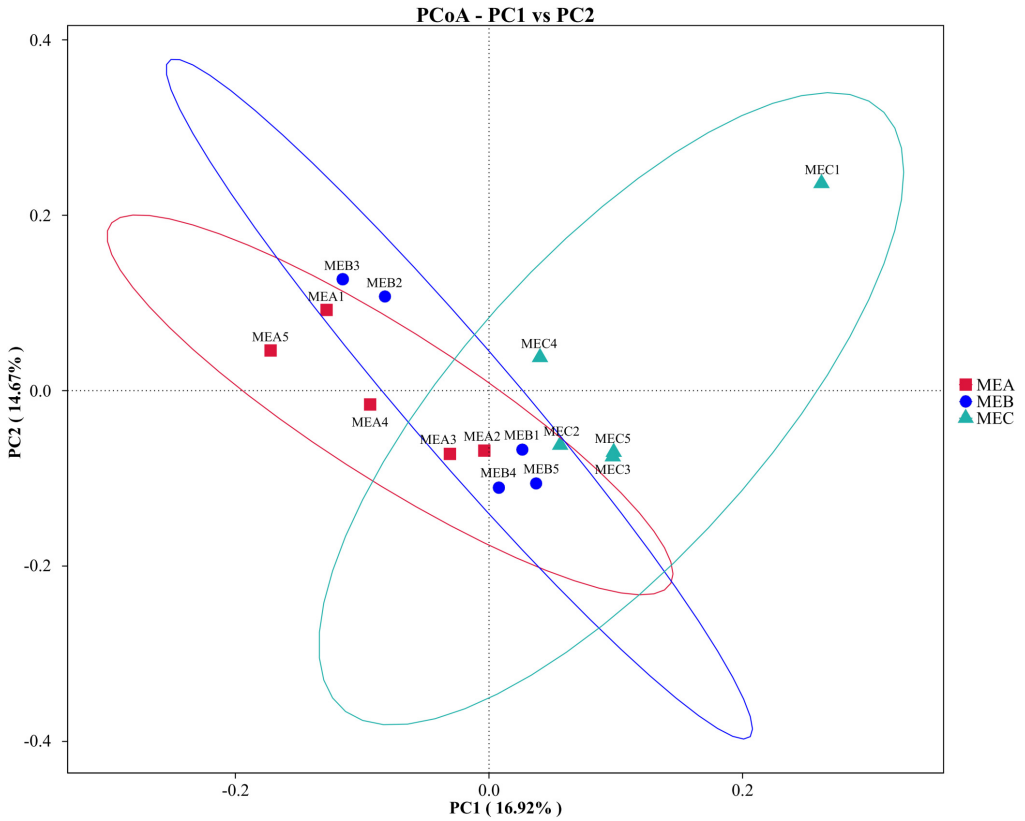

FIGURE 3 | Principal coordinate analysis (PCoA) of low-, medium-, and high-energy diets based on unweighted UniFrac distances. MEA1 to MEA5 in group MEA (red); MEB1 to MEB5 in group MEB (blue); and MEC1 to MEC5 in group MEC (green). PC, percent variation explained by the axis.

study showed similar results. Wang et al. (2009) and Mcleod and Baldwin (2000) found that increasing dietary ME could strengthen Na^+-K^+-ATPase activity in the small intestine, which contributed to promote the proliferation of intestinal epithelial cells and VH formation of ruminants. These results demonstrated that dietary energy levels might lead to a dynamic effect on the intestinal morphology of male Hu lambs, and there are many similarities between our results and those of previous studies; the high-energy group was recommended as an appropriate dietary energy level to promote the intestinal development and improve intestinal digestion and absorption function.

The correlation between dietary energy levels and rumen microbiota in fattening male Hu lambs was investigated by using an Ion S5TMXL sequencing platform to sequence the V3–V4 regions of the rumen microbial 16S rDNA gene. The alpha diversity index mainly reflects the richness and evenness of the species in the samples. A previous study has shown that a high-grain diet could notably decrease the OTUs number (Zhang et al., 2017). The present study also revealed that OTUs significantly decreased as the dietary energy level increased, which implies that the high energy level (or a concentrated level of diet) might affect rumen microbial diversity and the relative abundance of some microorganisms. The chao1 and ACE values observed in the low energy level were higher than those in the medium and high energy levels. Our results indicated that the relative abundance of rumen microbial communities was influenced by the different energy levels in the diets, and the rumen microecological environment was relatively stable and microbial communities were rich and diverse in low and medium energy level, which might be conducive to rumen health and the absorption and transformation of nutrients in ruminants (Liu et al., 2013).

From the composition of the rumen microorganisms, the types and proportions of the dominant microbiota in the rumen of lambs were similar among the three groups (low, medium, and high energy level), indicating that the rumen microbial communities of male Hu lambs in the fattening stage were relatively stable, and dietary energy levels had no significant impact on the dominant microbial community in rumen. At the phylum level, the three dominant microbial phyla were *Firmicutes*, *Bacteroidetes*, and *Proteobacteria* in three experimental groups, and this result was consistent with previous research findings in goats (Zhang et al., 2017) and cattle (Plaizier et al., 2017; Wetzels et al., 2017). The relative abundance of the dominant genera also did not change significantly at the genus level, which was in agreement with the results of Wang et al. (2016). Notably, the present study revealed large numbers of bacteria related to unclassified and uncultured genera in the rumen of Hu sheep. Wang Y. et al. (2017) found a similar pattern in Tan sheep. This result suggested that sheep might have a

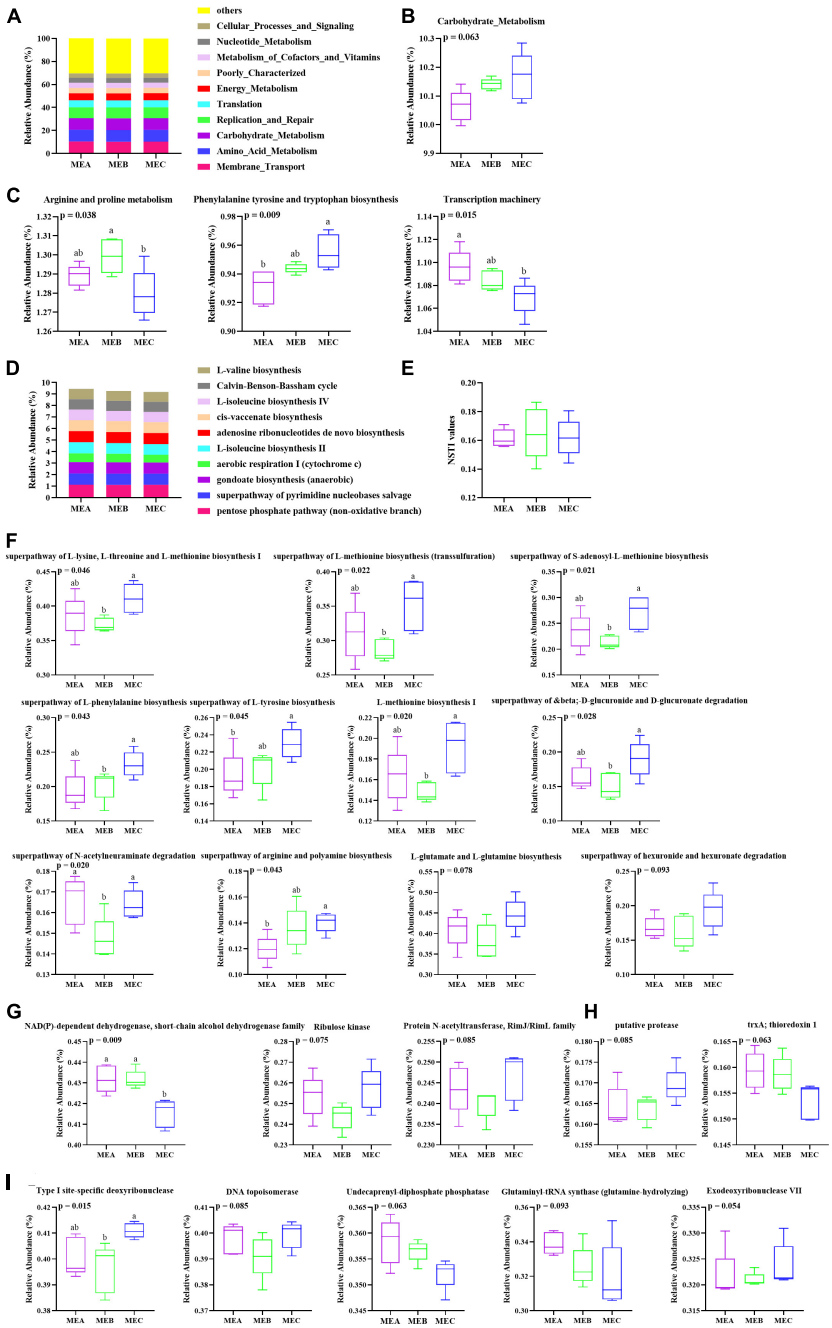

FIGURE 4 | Functional prediction of low, medium, and high dietary energy of rumen microbial community and related pathways. **(A)** Relative abundance of the dominant pathways annotated to KEGG level 2. **(B)** Relative abundance of carbohydrate metabolism. **(C)** Relative abundance of representative pathways at KEGG level 3. **(D)** The top 10 relative abundance of KEGG pathways by PICRUSt2. **(E)** The NSTI values. **(F)** The differential metabolic pathways by PICRUSt2. **(G)** The variation in top 35 relative abundances of COG analysis. **(H)** The variation in top 35 relative abundances of KO analysis. **(I)** The variation in top 35 relative abundances of EC analysis. Values with different superscripts (a,b) differ significantly at $p < 0.05$.

more diverse rumen microbiome and exhibit great differences among different breeds. Hook et al. (2011) and Wang Y. et al. (2017) also have reported that *Firmicutes* and *Bacteroidetes* were the dominant phyla in rumen, which were closely associated with carbohydrate and protein metabolism. *Firmicutes* and *Bacteroidetes* were also the most dominant phyla in the current study, and our results further verified that dietary energy level had no significant effect on the dominant rumen microbiota in Hu sheep. Additionally, the different dietary treatments can affect the ratios of *Firmicutes* and *Bacteroidetes*, which might obstruct the rumen bacterial function. Pitta et al. (2016) found that *Bacteroidetes*, compared to *Proteobacteria*, has a stronger

ability to degrade carbohydrates and can efficiently degrade polysaccharides and protein (Huo et al., 2014). Previous studies also reported that dietary nutrient level could influence the rumen bacterial composition of sheep (Wang Y. et al., 2017; Seddik et al., 2019). Golder et al. (2014) and Metzler-Zebeli et al. (2015) have shown that the relative abundance of *Proteobacteria* was the third highest at the phylum level, unexpectedly much lower than *Firmicutes* and *Bacteroidetes*, and the present study obtained the same consistent result as above. However, Pitta et al. (2016) found that *Proteobacteria* plays an important role in rumen metabolism, such as insoluble sugar digestion and biofilm formation. Besides, in the current study, *Fibrobacteres* was less abundant at the phylum level, but this observation was confirmed by the previous result of Pitta et al. (2014).

At the genus level, the variations of the rumen microbiome population within the represented genera were identified among three groups with different dietary energy levels in the present study, such as *unidentified Ruminococcaceae* comprising 6.68–7.36% of the total bacteria, which is clearly inconsistent with previous studies (Wang Y. et al., 2017; Seddik et al., 2019). Additionally, breed, age, feeding, management, season, herding, and geographic regions may also influence the characteristics of rumen microbial communities in ruminants (de Menezes et al., 2011). Recent research has shown that *Ruminococcaceae* bacteria played a critical role in dietary energy and lipid metabolism. Menni et al. (2018) found that diversity was negatively correlated with vascular hardness. The present study indicated that *unidentified Ruminococcaceae* was the most relatively abundant genus in all three treatments. *Papillibacter* is a butyrate-producing bacterium; restricted feeding could increase its abundance in sheep (Hu et al., 2018), whose relative abundance was markedly decreased and the butyrate concentration was decreased with increasing dietary energy. The relative abundance of propionate producing *Quinella* also significantly decreased, and the concentration of propionate showed a corresponding decline by increasing dietary energy level. Previous research found that *Veillonellaceae* was positively associated with inflammatory bowel disease (Atarashi et al., 2017), while in the present study, the relative abundance of *unidentified_Veillonellaceae* in the high-energy group was dramatically higher than that in both low- and medium-energy groups. *Anaerovibrio* are typically fat decomposers, which can hydrolyze triglycerides to glycerol and fatty acids, and further convert glycerol to propionate and succinate (Ren et al., 2019); the relative abundance of *Anaerovibrio* was highest in the high-energy group in the present study. These results indicated that high dietary energy altered bacterial community and damaged the rumen development. Long-term feeding of high-energy diet might affect the gastrointestinal health of lambs and lead to excessive fat deposition. Furthermore, beta diversity analysis of PCoA and NMDS revealed the distinct bacterial compositions with three diets of different energy.

Functional prediction of rumen bacteria by PICRUSt showed that the number of metabolism-related pathways was enriched at KEGG level 2, in which the membrane transporter was the most relatively abundant; carbohydrate metabolism, energy metabolism, amino acid metabolism, replication and repair, and translation were all general metabolic functions and essential for survival, reproduction, and growth of GIT microorganisms (Lamendella et al., 2011). These results are consistent with previous studies (Wang Y. et al., 2017). In particular, the relative abundance of carbohydrate metabolism-related genes showed a clear upward trend as dietary energy increases. Gifford et al. (2013) found that ribosomes played a crucial role in protein synthesis, and Yan et al. (2016) showed that ABC transporters were closely related to nutrient uptake. In the current study, the pathways of both ABC transporter and ribosome were enriched and all the related genes showed high relative abundance in the three groups at KEGG level 3. The present study also showed that the genes responsible for phenylalanine, tyrosine, and tryptophan biosynthesis were up-regulated by increasing dietary energy, which indicated enhanced fermentation and metabolic activities of rumen microorganisms, whereas the decrease in the arginine and proline metabolism and transcription machinery-related genes could be indicators of the high-energy diet influencing the function of the rumen. Furthermore, the rumen microbial functions predicted by PICRUSt2 showed that the relative abundances of KEGG pathways were significantly affected by dietary energy levels, but the top 35 relative abundance pathways had no significant difference in the three groups. Results of COG analysis showed that only the relative abundance of NAD(P)-dependent dehydrogenase, a short-chain alcohol dehydrogenase family, was significantly affected by different dietary energy levels, such as in the high-energy group, but lower in the low- and medium-energy groups. NAD(P)-dependent dehydrogenase, a short-chain alcohol dehydrogenase, is known to play critical roles in amino acid, carbohydrate, and lipid metabolism (Kavanagh et al., 2008). There were no significant differences in the top 35 relative abundances based on KO functional analysis with different dietary energy levels, while the relative abundance of Type I site-specific deoxyribonuclease was significantly affected by low, medium, and high dietary energy levels. Additionally, the NSTI values did not exceed 0.18, indicating the prediction reliability of rumen microbial metabolism by PICRUSt2. These results were inconsistent with the results of previous studies (Seddik et al., 2019). It is also implied that increasing the dietary energy level could alter the rumen microbial diversity and also influenced their corresponding metabolic function.

CONCLUSION

In conclusion, this study primarily investigated rumen fermentation and histological and microbial diversity in fattening male Hu lambs fed diets with different energy levels. The results suggested that the concentration and molar proportion of rumen iso-valerate were significantly higher in the medium-energy group; also, the molar proportion of iso-butyrate was higher in the medium-energy group than in both low- and high-energy groups. The rumen PH was significantly higher in the medium-energy group than in both low- and high-energy groups. In addition, the duodenum CD and VH/CD, jejunum CD, and ileum VH, VW, and VH/CD were dramatically affected by dietary ME levels; a high energy level might be better for digestion and

absorption in the small intestine. The diversity index of OTUs was significantly lower in the high-energy group compared to the low- and medium-energy groups. The dietary energy level significantly affected the relative abundance of *Papillibacter*, *Quinella*, *unidentified_Veillonellaceae*, and *Anaerovibrio*, while the majority of rumen microbial community and corresponding functions were consistent and were not affected by dietary ME. Taking the above points into consideration, the medium-energy group (metabolizable energy of 10.00 MJ/kg) was recommended as the appropriate dietary energy level in intensive fattening of Hu lambs, and these findings provided important theory reference and production practice guidance.

DATA AVAILABILITY STATEMENT

The datasets presented in this study can be found in online repositories. The names of the repository/repositories and accession number(s) can be found below: https://www.ncbi.nlm.nih.gov/, SRR11829336–SRR11829350.

ETHICS STATEMENT

The animal study was reviewed and approved by the Animal Care Committee of Hunan Normal University in reference to the Administration of Affairs Concerning Experimental Animals.

AUTHOR CONTRIBUTIONS

HY and QW: conceptualization. XW and YW: methodology. PH and XZ: software. MZ: validation. YZ: formal analysis. QW: investigation and writing—original draft preparation. CD: resources. JH: data curation. TH: writing—review and editing. MZ: visualization. JL: supervision. HY: project administration and funding acquisition. All authors have read and agreed to the published version of the manuscript.

FUNDING

This research was funded by the Hunan Province's Changsha-Zhuzhou-Xiangtan National Independent Innovation Demonstration Zone Projects, grant number 2017XK2058 and Hunan Provincial Key Laboratory of Animal Nutritional Physiology and Metabolic Process Open Fund Projects, grant number ISA2020113.

ACKNOWLEDGMENTS

The authors are grateful to the Hubei Zhiqinghe Agriculture and Animal Husbandry Co., Ltd. of Yichang (China) for the experimental animals and Hunan Normal University of Changsha (China) for the research infrastructure.

SUPPLEMENTARY MATERIAL

The Supplementary Material for this article can be found online at: https://www.frontiersin.org/articles/10.3389/fmicb.2021.695445/full#supplementary-material

Supplementary Figure 1 | Rarefaction analyses of the different samples. Rarefaction curves of all samples and OTUs clustered at 97% similarity.

Supplementary Figure 2 | NMDS analysis results based on OTU level from different dietary energy levels.

Supplementary Figure 3 | The relative abundance of different functional taxa at level 1, annotated based on the KEGG orthologs datasets at different dietary nutrient levels.

Supplementary Table 1 | Overview of species annotation for all samples.

Supplementary Table 2 | Variance analysis of taxonomic composition of the 10 most abundance in phylum level and genus level of rumen bacterial community fed different dietary energy levels.

Supplementary Table 3 | Predicted functions at level 2 of the rumen bacterial microbiota of male Hu lambs fed different dietary energy levels.

Supplementary Table 4 | The 35 most abundant KEGG pathways at level 3 in the rumen bacteria of male Hu lambs fed different dietary energy levels.

REFERENCES

Agle, M., Hristov, A. N., Zaman, S., Schneider, C., Ndegwa, P. M., and Vaddella, V. K. (2010). Effect of dietary concentrate on rumen fermentation, digestibility, and nitrogen losses in dairy cows. *J. Dairy Sci.* 93, 4211–4222. doi: 10.3168/jds.2009-2977

Atarashi, K., Suda, W., Luo, C., Kawaguchi, T., Motoo, I., Narushima, S., et al. (2017). Ectopic colonization of oral bacteria in the intestine drives TH1 cell induction and inflammation. *Science* 358, 359–365. doi: 10.1126/science.aan4526

Azim, A., Khan, A. G., Anjum, M. I., and Nadeem, M. A. (2011). Effect of milk replacer and early weaning diets on growth performance of buffalo calves during weaning period. *Pak. Vet. J.* 31, 23–26.

Bach, A., Calsamiglia, S., and Stern, M. D. (2005). Nitrogen metabolism in the rumen. *J. Dairy Sci.* 88, E9–E21. doi: 10.3168/jds.S0022-0302(05)73133-7

Broderick, G. A. (2003). Effects of varying dietary protein and energy levels on the production of lactating dairy cows. *J. Dairy Sci.* 86, 1370–1381. doi: 10.3168/jds.S0022-0302(03)73721-7

Clark, J. H. (1975). Lactational responses to post ruminal administration of proteins and amino acids. *J. Dairy Sci.* 58, 1178–1197. doi: 10.3168/jds.S0022-0302(75)84696-0

Clark, J. H., and Davis, C. L. (1980). Some aspects of feeding high producing dairy cows. *J. Dairy Sci.* 63, 873–885. doi: 10.3168/jds.S0022-0302(80)83021-9

Cunha, I. S., Barreto, C. C., Costa, O. Y., Bomfim, M. A., Castro, A. P., Kruger, R. H., et al. (2011). *Bacteria* and *Archaea* community structure in the rumen microbiome of goats (*Capra hircus*) from the semiarid region of Brazil. *Anaerobe* 17, 118–124. doi: 10.1016/j.anaerobe.2011.04.018

de Menezes, A. B., Lewis, E., O'Donovan, M., O'Neill, B. F., Clipson, N., and Doyle, E. M. (2011). Microbiome analysis of dairy cows fed pasture or total mixed ration diets. *FEMS Microbiol. Ecol.* 78, 256–265. doi: 10.1111/j.1574-6941.2011.01151.x

Deng, Q., Tan, X., Wang, H., Wang, Q., Huang, P., Li, Y., et al. (2020). Changes in cecal morphology, cellproliferation, antioxidant enzyme, volatile fatty acids, lipopolysaccharide, and cytokines in piglets during the postweaning period. *J. Anim. Sci.* 98:skaa046. doi: 10.1093/jas/skaa046

Douglas, G. M., Maffei, V. J., Zaneveld, J. R., Yurgel, S. N., Brown, J. R., Taylor, C. M., et al. (2020). PICRUSt2 for prediction of metagenome functions. *Nat. biotechnol.* 38, 685–688. doi: 10.1038/s41587-020-0548-6

Edgar, R. C. (2013). UPARSE: highly accurate OTU sequences from microbial amplicon reads. *Nat. Methods* 10, 996–998. doi: 10.1038/nmeth.2604

Edgar, R. C., Haas, B. J., Clemente, J. C., Quince, C., and Knight, R. (2011). UCHIME improves sensitivity and speed of chimera detection. *Bioinformatics* 27, 2194–2200. doi: 10.1093/bioinformatics/btr381

Ellison, M. J., Conant, G. C., Lamberson, W. R., Cockrum, R. R., Austin, K. J., Rule, D. C., et al. (2017). Diet and feed efficiency status affect rumen microbial profiles of sheep. *Small Ruminant Res.* 156, 12–19. doi: 10.1016/j.smallrumres.2017.08.009

Flint, H. J., Duncan, S. H., Scott, K. P., and Louis, P. (2007). Interactions and competition within the microbial community of the human colon: links between diet and health. *Environ. Microbiol.* 9, 1101–1111. doi: 10.1111/j.1462-2920.2007.01281.x

Gifford, S. M., Sharma, S., Booth, M., and Moran, M. A. (2013). Expression patterns reveal niche diversification in a marine microbial assemblage. *ISME J.* 7, 281–298. doi: 10.1038/ismej.2012.96

Golder, H. M., Denman, S. E., McSweeney, C., Wales, W. J., Auldist, M. J., and Wright, M. M. (2014). Effects of partial mixed rations and supplement amounts on milk production and composition, ruminal fermentation, bacterial communities, and ruminal acidosis. *J. Dairy Sci.* 97, 5763–5785. doi: 10.3168/jds.2014-8049

Guan, L. L., Nkrumah, J. D., Basarab, J. A., and Moore, S. S. (2008). Linkage of microbial ecology to phenotype: correlation of rumen microbial ecology to cattle's feed efficiency. *FEMS Microbiol. Lett.* 288, 85–91. doi: 10.1111/j.1574-6968.2008.01343.x

Haas, B. J., Gevers, D., Earl, A. M., Feldgarden, M., Ward, D. V., Giannoukos, G., et al. (2011). Chimeric 16S rRNA sequence formation and detection in Sanger and 454-pyrosequenced PCR amplicons. *Genome Res.* 21, 494–504. doi: 10.1101/gr.112730.110

Han, X., Yang, Y., Yan, H., Wang, X., Qu, L., and Chen, Y. (2015). Rumen bacterial diversity of 80 to 110-day old goats using 16S rRNA sequencing. *PLoS One* 10:e0117811. doi: 10.1371/journal.pone.0117811

Hedemann, M. S., Højsgaard, S., and Jensen, B. B. (2003). Small intestinal morphology and activity of intestinal peptidases in piglets around weaning. *J. Anim. Physiol. Anim. Nutr.* 87, 32–41. doi: 10.1046/j.1439-0396.2003.00405.x

Hook, S. E., Steele, M. A., Northwood, K. S., Dijkstra, J., France, J., Wright, A. D. G., et al. (2011). Impact of subacute ruminal acidosis (SARA) adaptation and recovery on the density and diversity of bacteria in the rumen of dairy cows. *FEMS Microbiol. Ecol.* 78, 275–284. doi: 10.1111/j.1574-6941.2011.01154.x

Hu, F., Xue, Y., Guo, C., Liu, J., and Mao, S. (2018). The response of ruminal fermentation, epithelium-associated microbiota, and epithelial barrier function to severe feed restriction in pregnant ewes. *J. Anim. Sci.* 96, 4293–4305. doi: 10.1093/jas/sky306

Huo, W., Zhu, W., and Mao, S. (2014). Impact of subacute ruminal acidosis on the diversity of liquid and solid-associated bacteria in the rumen of goats. *World J. Microb. Biot.* 30, 669–680. doi: 10.1007/s11274-013-1489-8

Kavanagh, K. L., Jörnvall, H., Persson, B., and Oppermann, U. (2008). Medium- and short-chain dehydrogenase/reductase gene and protein families: the SDR superfamily: functional and structural diversity within a family of metabolic and regulatory enzymes. *Cell Mol. Life Sci.* 65, 3895–3906. doi: 10.1007/s00018-008-8588-y

Keady, T. W., Mayne, C. S., Fitzpatrick, D. A., and McCoy, M. A. (2001). Effect of concentrate feed level in late gestation on subsequent milk yield, milk composition, and fertility of dairy cows. *J. Dairy Sci.* 84, 1468–1479. doi: 10.3168/jds.S0022-0302(01)70180-4

Khan, M. A., Weary, D. M., and von Keyserlingk, M. A. (2011). Invited review: effects of milk ration on solid feed intake, weaning, and performance in dairy heifers. *J. Dairy Sci.* 94, 1071–1081. doi: 10.3168/jds.2010-3733

Kim, W. Y., Lee, S. H., Hwang, J. H., Kim, S. K., Lee, S. S., and Yeo, J. M. (2012). Effects of Concentrate Feeding on Rumen Papillae Development in Hanwoo Calves before Weaning. *J. Anim. Sci. Technol.* 54, 355–361. doi: 10.5187/JAST.2012.54.5.355

Knoell, A. L., Anderson, C. L., Pesta, A. C., Erickson, G. E., Klopfenstein, T. J., and Fernando, S. C. (2016). 114 Alterations of the rumen bacterial and archaeal communities in growing and finishing beef cattle and its effects on methane emissions. *J. Anim. Sci.* 94, 53–54. doi: 10.2527/msasas2016-114

Lamendella, R., Santo Domingo, J. W., Ghosh, S., Martinson, J., and Oerther, D. B. (2011). Comparative fecal metagenomics unveils unique functional capacity of the swine gut. *BMC Microbiol.* 11:103. doi: 10.1186/1471-2180-11-103

Lee, H. J., Jung, J. Y., Oh, Y. K., Lee, S. S., Madsen, E. L., and Jeon, C. O. (2012). Comparative survey of rumen microbial communities and metabolites across one caprine and three bovine groups, using bar-coded pyrosequencing and 1H nuclear magnetic resonance spectroscopy. *Appl. Environ. Microb.* 78, 5983–5993. doi: 10.1128/AEM.00104-12

Lingyan, L., Yang, H., Azizurrahman, M., and Binghai, C. (2014). Effects of different dietary energy and rumen-degradable protein levels on rumen fermentation, nutrients apparent digestibility and blood biochemical constituents of Chinese crossbred yellow bulls. *Pak. Vet. J.* 34, 367–371.

Liu, J. H., Xu, T. T., Liu, Y. J., Zhu, W. Y., and Mao, S. Y. (2013). A high-grain diet cause massive disruption of ruminal epithelial tight junctions in goats. *Am. J. Physiol. Integr. Comp. Physiol.* 305, R232–R241. doi: 10.1152/ajpregu.00068.2013

Mackie, R. I., Aminov, R. I., White, B. A., and McSweeney, C. S. (2000). "Molecular ecology and diversity in gut microbial ecosystems," in *Ruminant Physiology: Digestion, Metabolism, Growth and Reproduction*, ed. P. B. Cronjé (Wallingford: CAB International).

Martin, M. (2011). Cutadapt removes adapter sequences from high-throughput sequencing reads. *EMBnet. J.* 17, 10–12. doi: 10.14806/ej.17.1.200

McGovern, E., Kenny, D. A., McCabe, M. S., Fitzsimons, C., McGee, M., et al. (2018). 16S rRNA Sequencing Reveals Relationship Between Potent Cellulolytic Genera and Feed Efficiency in the Rumen of Bulls. *Front. Microbiol.* 9:1842. doi: 10.3389/fmicb.2018.01842

Mcleod, K. R., and Baldwin, R. L. (2000). Effects of diet forage: concentrate ratio and metabolizable energy intake on visceral organ growth and in vitro oxidative capacity of gut tissues in sheep. *J. Anim. Sci.* 78, 760–770. doi: 10.2527/2000.783760x

Menni, C., Lin, C., Cecelja, M., Mangino, M., Matey-Hernandez, M. L., Keehn, L., Mohney, R. P., et al. (2018). Gut microbial diversity is associated with lower arterial stiffness in women. *Eur. Heart J.* 39, 239–2397. doi: 10.1093/eurheartj/ehy226

Metzler-Zebeli, B. U., Khol-Parisini, A., Gruber, L., and Zebeli, Q. (2015). Microbial populations and fermentation profiles in rumen liquid and solids of Holstein cows respond differently to dietary barley processing. *J. Appl. Microbiol.* 119, 1502–1514. doi: 10.1111/jam.12958

Morand-Fehr, P., Fedele, V., Decandia, M., and Frileux, Y. L. (2007). Influence of farming and feeding systems on composition and quality of goat and sheep milk. *Small Ruminant Res.* 68, 20–34. doi: 10.1016/j.smallrumres.2006.09.019

Murphy, M., Akerlind, M., and Holtenius, K. (2000). Rumen fermentation in lactating cows selected for milk fat content fed two forage to concentrate ratios with hay or silage. *J. Dairy Sci.* 83, 756–764. doi: 10.3168/jds.S0022-0302(00)74938-1

National Research Council (NRC) (2007). *Nutrient Requirements of Small Ruminants. Sheep, Goats, Cervids, and New World Camelids*. Washington: National Academies Press.

Owens, F. N., and Basalan, M. (2016). "Ruminal fermentation," in *Rumenology*, eds D. D. Millen, M. D. B. Arrigoni, and R. D. L. Pacheco (Cham: Springer International Publishing).

Pitta, D. W., Indugu, N., Kumar, S., Vecchiarelli, B., Sinha, R., Baker, L. D., et al. (2016). Metagenomic assessment of the functional potential of the rumen microbiome in Holstein dairy cows. *Anaerobe* 38, 50–60. doi: 10.1016/j.anaerobe.2015.12.003

Pitta, D. W., Kumar, S., Vecchiarelli, B., Shirley, D. J., Bittinger, K., Baker, L. D., et al. (2014). Temporal dynamics in the ruminal microbiome of dairy cows during the transition period. *J. Anim. Sci.* 92, 4014–4022. doi: 10.2527/jas.2014-7621

Plaizier, J. C., Li, S., Tun, H. M., and Khafipour, E. (2017). Nutritional models of experimentally-induced subacute ruminal acidosis (SARA) differ in their impact on rumen and hindgut bacterial communities in dairy cows. *Front. Microbiol.* 7:2128. doi: 10.3389/fmicb.2016.02128

Pokharel, K., Peippo, J., Honkatukia, M., Seppälä, A., Rautiainen, J., Ghanem, N., et al. (2018). Integrated ovarian mRNA and miRNA transcriptome profiling

characterizes the genetic basis of prolificacy traits in sheep (*Ovis aries*). *BMC Genomics* 19:104. doi: 10.1186/s12864-017-4400-4

Preston, T. R., and Leng, R. A. (1987). "Digestive physiology of ruminants," in *Matching Ruminant Production Systems with Available Resources in the Tropics and Subtropics*, eds J. W. Hansen, P. K. Thornton, and P. B. M. Berentsen (Armidale: Penambul books).

Quast, C., Pruesse, E., Yilmaz, P., Gerken, J., Schweer, T., Yarza, P., et al. (2012). The SILVA ribosomal RNA gene database project: improved data processing and web-based tools. *Nucleic Acids Res.* 41, D590–D596. doi: 10.1093/nar/gks1219

Ren, Z., Yao, R., Liu, Q., Deng, Y., Shen, L., Deng, H., et al. (2019). Effects of antibacterial peptides on rumen fermentation function and rumen microorganisms in goats. *PLoS One* 14:e0221815. doi: 10.1371/journal.pone.0221815

Seddik, H., Xu, L., Wang, Y., and Mao, S. Y. (2019). A rapid shift to high-grain diet results in dynamic changes in rumen epimural microbiome in sheep. *Animal* 13, 1614–1622. doi: 10.1017/S1751731118003269

Shabat, S. K., Sasson, G., Doron-Faigenboim, A., Durman, T., Yaacoby, S., Berg Miller, et al. (2016). Specific microbiome-dependent mechanisms underlie the energy harvest efficiency of ruminants. *ISME J.* 10, 2958–2972. doi: 10.1038/ismej.2016.62

Shen, Z., Seyfert, H. M., Löhrke, B., Schneider, F., Zitnan, R., Chudy, A., et al. (2004). An energy-rich diet causes rumen papillae proliferation associated with more IGF type 1 receptors and increased plasma IGF-1 concentrations in young goats. *J. Nutr.* 134, 11–17. doi: 10.1093/jn/134.1.11

Steele, M. A., Garcia, F., Lowerison, M., Gordon, K., Metcalf, J. A., and Hurtig, M. (2014). Technical note: Three-dimensional imaging of rumen tissue for morphometric analysis using micro-computed tomography. *J. Dairy Sci.* 97, 7691–7696. doi: 10.3168/jds.2014-8374

Steele, M. A., Penner, G. B., Chaucheyras-Durand, F., and Guan, L. L. (2016). Development and physiology of the rumen and the lower gut: Targets for improving gut health. *J. Dairy Sci.* 99, 4955–4966. doi: 10.3168/jds.2015-10351

van Soest, P. J. (1994). *Nutritional Ecology of the Ruminant*, 2nd Edn. Ithaca, NY: Cornell University Press.

Wang, H. R., Chen, Q., Chen, L. M., Ge, R. F., Wang, M. Z., Yu, L. H., et al. (2017). Effects of dietary physically effective neutral detergent fiber content on the feeding behavior, digestibility, and growth of 8-to10-month-old Holstein replacement heifers. *J. Dairy Sci.* 100, 1161–1169. doi: 10.3168/jds.2016-10924

Wang, L., Yan, S., Li, J., Li, Y., Ding, X., Yin, J., et al. (2019). Rapid Communication: The relationship of enterocyte proliferation with intestinal morphology and nutrient digestibility in weaning piglets. *J. Anim. Sci.* 97, 353–358. doi: 10.1093/jas/sky388

Wang, P., Tan, Z., Guan, L., Tang, S., Zhou, C., Han, X., et al. (2015). Ammonia and amino acids modulate enzymes associated with ammonia assimilation pathway by ruminal microbiota in vitro. *Livest. Sci.* 178, 130–139. doi: 10.1016/j.livsci.2015.05.033

Wang, Q., Wang, Y., Hussain, T., Dai, C., Li, J., Huang, P., et al. (2020a). Effects of dietary energy level on growth performance, blood parameters and meat quality in fattening male Hu lambs. *J. Anim. Physiol. Anim. Nutr.* 104, 418–430. doi: 10.1111/jpn.13278

Wang, Q., Wang, Y., Wang, X., Dai, C., Tang, W., Li, J., et al. (2020b). Effects of dietary energy levels on rumen fermentation, microbiota, and gastrointestinal morphology in growing ewes. *Food Sci. Nutr.* 8, 6621–6632. doi: 10.1002/fsn3.1955

Wang, W., Li, C., Li, F., Wang, X., Zhang, X., Liu, T., et al. (2016). Effects of early feeding on the host rumen transcriptome and bacterial diversity in lambs. *Sci. Rep.* 6:32479. doi: 10.1038/srep32479

Wang, Y. J., Holligan, S., Salim, H., Fan, M. Z., Mcbride, B. W., and Swanson, K. C. (2009). Effect of dietary crude protein level on visceral organ mass, cellularity, and the protein expression of ATP synthase, Na+/K+-ATPase, proliferating cell nuclear antigen and ubiquitin in feedlot steers. *Can. J. Anim. Sci.* 89, 253–262. doi: 10.4141/CJAS08078

Wang, Y., Cao, P., Wang, L., Zhao, Z., Chen, Y., and Yang, Y. (2017). Bacterial community diversity associated with different levels of dietary nutrition in the rumen of sheep. *Appl. Microbiol. Biot.* 101, 3717–3728. doi: 10.1007/s00253-017-8144-5

Wetzels, S. U., Mann, E., Pourazad, P., Qumar, M., Pinior, B., Metzler-Zebeli, B. U., et al. (2017). Epimural bacterial community structure in the rumen of Holstein cows with different responses to a long-term subacute ruminal acidosis diet challenge. *J. Dairy Sci.* 100, 1829–1844. doi: 10.3168/jds.2016-11620

Wester, T. J., Britton, R. A., Klopfenstein, T. J., Ham, G. A., Hickok, D. T., and Krehbiel, C. R. (1995). Differential effects of plane of protein or energy nutrition on visceral organs and hormones in lambs. *J. Anim. Sci.* 73, 1674–1688. doi: 10.2527/1995.7361674x

Yan, X., Luo, X., and Zhao, M. (2016). Metagenomic analysis of microbial community in uranium-contaminated soil. *Appl. Microbiol. Biot.* 100, 299–310. doi: 10.1007/s00253-015-7003-5

Yang, H. S., Fu, D. Z., Kong, X. F., Wang, W. C., Yang, X. J., Nyachoti, C. M., et al. (2013). Dietary supplementation with N-carbamylglutamate increases the expression of intestinal amino acid transporters in weaned Huanjiang mini-pig piglets. *J. Anim. Sci.* 91, 2740–2748. doi: 10.2527/jas.2012-5795

Yang, H., Xiong, X., Wang, X., Li, T., and Yin, Y. (2016). Effects of weaning on intestinal crypt epithelial cells in piglets. *Sci. Rep.* 6:36939. doi: 10.1038/srep36939

Zhang, R., Ye, H., Liu, J., and Mao, S. (2017). High-grain diets altered rumen fermentation and epithelial bacterial community and resulted in rumen epithelial injuries of goats. *Appl. Microbiol. Biot.* 101, 6981–6992. doi: 10.1007/s00253-017-8427-x

Conflict of Interest: QW and CD were employed by the company Hubei Zhiqinghe Agriculture and Animal Husbandry Co., Ltd.

The remaining authors declare that the research was conducted in the absence of any commercial or financial relationships that could be construed as a potential conflict of interest.

Publisher's Note: All claims expressed in this article are solely those of the authors and do not necessarily represent those of their affiliated organizations, or those of the publisher, the editors and the reviewers. Any product that may be evaluated in this article, or claim that may be made by its manufacturer, is not guaranteed or endorsed by the publisher.

frontiers in Microbiology

ORIGINAL RESEARCH
published: 16 September 2021
doi: 10.3389/fmicb.2021.706424

Black Soldier Fly (*Hermetia illucens*) Larvae Meal Modulates Intestinal Morphology and Microbiota in Xuefeng Black-Bone Chickens

Changqing He[1,2], Jiaxing Lei[1,2], Yaling Yao[3], Xiangyong Qu[1,2], Jifa Chen[2,4], Kailai Xie[1], Xingju Wang[1], Qi Yi[1], Bing Xiao[5], Songchang Guo[1,2] and Xiaoyan Zou[6]**

[1] Hunan Engineering Research Center of Poultry Production Safety, Hunan Agricultural University, Changsha, China, [2] College of Animal Science and Technology, Hunan Agricultural University, Changsha, China, [3] Huaihua Animal Husbandry and Fishery Affairs Center, Huaihua, China, [4] College of Life Science and Resources and Environment, Yichun University, Yichun, China, [5] Hunan Yunfeifeng Agricultural Co., Ltd., Huaihua, China, [6] College of Veterinary Medicine, Hunan Agricultural University, Changsha, China

OPEN ACCESS

Edited by:
Jia Yin,
Hunan Normal University, China

Reviewed by:
Vahid Rezaeipour,
Qaemshahr Islamic Azad University, Iran
Rejun Fang,
Hunan Agricultural University, China
Kai Qiu,
Chinese Academy of Agricultural Sciences (CAAS), China

***Correspondence:**
Songchang Guo
guo_ast@126.com
orcid.org/0000-0001-6067-3475
Xiaoyan Zou
dayan2200@163.com
orcid.org/0000-0003-1590-4179

Specialty section:
This article was submitted to Microbial Symbioses, a section of the journal Frontiers in Microbiology

Received: *07 May 2021*
Accepted: *26 July 2021*
Published: *16 September 2021*

Citation:
He C, Lei J, Yao Y, Qu X, Chen J, Xie K, Wang X, Yi Q, Xiao B, Guo S and Zou X (2021) Black Soldier Fly (Hermetia illucens) Larvae Meal Modulates Intestinal Morphology and Microbiota in Xuefeng Black-Bone Chickens. Front. Microbiol. 12:706424. doi: 10.3389/fmicb.2021.706424

The addition of *Hermetia illucens* larvae meal (HILM) to the feed could contribute to particular antimicrobial and intestinal health in animal husbandry. This study was conducted to investigate the effects of HILM on intestinal morphology and microbial diversity in different intestinal segments of Xuefeng black-bone chickens. All of 432 birds (45 weeks old) were randomly assigned to four equal groups with six replicates and 18 hens in each replicate: (A) basal diet, (B) basal diet with 1% HILM, (C) basal diet with 3% HILM, and (D) basal diet with 5% HILM. The results showed that, compared with the basal diet group, the HILM supplement significantly increased the abundance-based coverage estimator (ACE) and Chao index in cecum ($p < 0.05$). Diet with 1% HILM significantly increased the villus height (VH) of the duodenum ($p < 0.05$) and cecum microbial diversity as represented by the Simpson index ($p < 0.05$). In particular, 1% HILM displayed a markedly increase in the genus unclassified Bacteroidales (cecum, $p < 0.05$). A basal diet with 3% HILM markedly increased the beneficial genus *Romboutsia* (jejunum, $p < 0.05$). Also, principal component analysis (PCA) cluster analysis showed that 3% of HILM was more individual than other groups ($p < 0.05$). However, 5% HILM decreased the VH and the ratio of villus height to crypt depth (VH/CD) of the jejunum and increased beneficial bacteria such as *Staphylococcus* ($p < 0.05$), which was regarded as pathogenetic genera. In conclusion, we found that HILM improved intestinal morphology and increased microbiological diversity and species abundance. Together, dietary supplementation of 1 or 3% HILM might benefit the intestinal morphology and intestinal microbiota of Xuefeng black-bone chicken. However, the addition of 5% HILM could decrease VH and the ratio of VH/CD of the jejunum and increased pathogenetic genera. HILM was an excellent protein substitute for Xuefeng black-bone chickens, which could meet the nutritional requirements under the condition of less feed. These results provide information for HILM meal as an alternative source of soybean meal in Xuefeng black-bone chickens' feed.

Keywords: *Hermetia illucens* larvae meal, Xuefeng black-boned chicken, intestinal morphology, intestinal microbial diversity, gut health

INTRODUCTION

In recent years, the demand for high-quality protein in the world has grown tremendously. Being one of the sources with high-quality protein, it has been reported that human demand for poultry meat would increase more rapidly than any other meat product between 2030 and 2050 (the 25th World's Poultry Congress, 2016). With this upcoming expansion, the resources needed to grow food and feed were becoming increasingly strained because the production of animal and plant proteins required the use of large amounts of land, water, and energy (Kim et al., 2019; Rathnayaka et al., 2021). Therefore, existing feed resources might not be able to support the current growth in poultry production; alternative feeds and feed protein supplements were absolutely needed to replace the current supply and meet the growing demand (De Smet et al., 2018).

Insect, compared with conventional proteins, seemed to be one of the most promising alternatives (Henry et al., 2015; DiGiacomo et al., 2019; Gravel and Doyen, 2020). *Hermetia illucens* larvae meal (HILM) was characterized by being rich in protein (dry matter >37%) and fat (up to 49%), as well as several macronutrients and micronutrients, which were important for animal development (Smetana et al., 2019). The amino acids of HILM are balanced; most of the amino acid content is similar to fish meals and soybean meals (Barroso et al., 2014). Different from other insects, it was indicated in the prevailing view that HILM products could have particular antimicrobial attributes (Elhag et al., 2017; Fawole et al., 2020; Wang et al., 2020), which might profit from the antimicrobial peptides and chitin in HILM. Furthermore, HILM had a lower environmental impact than other protein sources, making it a potential alternative to regular feed resources for animal production (Wang and Shelomi, 2017). Recently, HILM had been used in the production of livestock (poultry, rabbits, and pigs) and aquaculture species (Gasco et al., 2019).

Xuefeng black-bone chickens, originating from Xuefengshan Mountain and the adjacent region, were the most famous local breed in the Hunan province of China and had been listed as one of the national livestock and poultry genetic resources in China. Being classified into the type of meat-and-egg chicken, Xuefeng black-bone chicken was commonly believed to have medicinal properties and has been used as remedies to enhance the human immune system by providing protein, vitamins, and amino acids (Xie et al., 2020). At present, induced by the switch from quantity to quality of consumers, the market demand for Xuefeng black-bone chicken is increasing (Guo et al., 2021). Moreover, the shortage of protein resources for livestock and poultry feeding drove up the rise of the cost of animal husbandry, which required seeking potential substitutes. Studies have revealed that HILM could be a suitable protein substitution for poultry (Marono et al., 2017; Cutrignelli et al., 2018; Moniello et al., 2019). Nonetheless, its application on Xuefeng black-bone chicken remained poorly understood. In this context, we conducted to explore the effects of HILM on intestinal morphology and microbial diversity in different intestinal segments of the Xuefeng black-bone chicken and provide more detailed information about the capability of HILM as an ideal protein replacement in feed and inform the future diagnosis and therapy of insect meal as a sustainable protein source.

MATERIALS AND METHODS

All the animals were humanely conducted in accordance with the principles stated by the Chinese guidelines for animal welfare. The experimental procedures received approval from the animal welfare standards of the College of Animal Science and Technology, Hunan Agricultural University.

Animals, Diets, and Experimental Design

A total of 432 female Xuefeng black-bone chickens were randomly divided into four groups (6 replicas of 18 hens) and fed for 56 days. The diets based on corn and soybean meal of the chickens were supplemented with 0, 1, 3, or 5% HILM to partly replace soybean meal and designated as A, B, C, and D groups, respectively. The feeding experiment was the same as our previous study (Liu et al., 2021). The experimental diets were isonitrogenous and isoenergetic, but the proportion of HILM was different.

Sample Collection

At the end of the experiment, three chickens from each group were randomly chosen and killed by cervical dislocation. After killing, the digesta samples from the jejunum and cecum were collected in sterilized plastic tubes and then immediately stored in liquid nitrogen to investigate intestinal microflora. Additionally, segments (10 cm in length) of the middle of the duodenum and jejunum were excised and washed with phosphate-buffered saline until no digesta were visible. The segments were fixed with 4% paraformaldehyde for more than 24 h to make intestinal sections.

Experimental Parameters Analysis

Intestinal Morphology

Five-μm sections were cut from the paraffin-embedded intestinal segments after removing the fixation solution and then stained with hematoxylin and eosin for light microscopy. Zeiss microscope (Axio Imager, A1) and the MShot Image Analysis System were used to take photographs for sections. The villus height (VH) and the crypt depth (CD) were used in five typical fields to measure (Wang and Hogan, 2019).

Intestinal Microflora

Genomic DNA was extracted from chyme samples using a kit (DP328, Tiangen Biochemical Technology Co., Ltd., China) (Xia et al., 2020). The samples of qualified DNA were sent to Shanghai Majorbio Bio-pharm Technology Co., Ltd. (China) for polymerase chain reaction amplification and sequencing analysis.

Using quantitative DNA as a template, the 16S rRNA gene V3–V4 region was amplified by primer pairs 338F (5′-ACTCCTACGGGAGCAGAC-3′) and 806R (5′-GGACTACHVGGGTWTCTA-3′). The purified, amplified products were sequenced on the Novaseq PE250 platform

(Illumina, San Diego, United States) using equimolar and paired-end sequencing according to MajorBio Biopharma Technologies, Inc. (Shanghai, China) standard protocol.

The original sequence was demultiplexed and quality filtered using FASTP version 0.20.0 (Chen et al., 2018) and merged using Flash version 1.2.7 (Magoc and Salzberg, 2011). The criteria are as follows: (a) the 300-bp reads were truncated at any site receiving an average quality score of <20 over a 50-bp sliding window, and the truncated reads shorter than 50 bp were discarded; reads containing ambiguous characters were also discarded; (b) Only overlap sequences greater than 10 bp are spliced according to overlapping sequences. The maximum mismatch in the overlapping area is 0.2. Reads that cannot be assembled are discarded; (c) samples were distinguished according to the barcode and primers, and the sequence direction was adjusted. The barcode matching was accurate, and the two nucleotides in the primer matching did not match. UPARSE version 7.1 was used to cluster operational taxonomic units (OTU) with a similarity cutoff rate of 97% (Edgar, 2013). RDP Classifier version 2.2 was used to classify each OTU representative sequence, and Silva V132 was used for classification and identification.

Statistical Analysis

One-way analysis of variance in SPSS 22.0 software (IBM SPSS, United States) was used for the statistical analyses. The analysis results were expressed as the arithmetic mean and standard error. Differences were considered to be significant at $p < 0.05$ and highly significant at $p < 0.01$. The Majorbio Cloud Platform [1] was used to analyze intestinal microflora.

RESULTS

Intestinal Morphology

To determine whether HILM diets were associated with the intestinal morphology of Xuefeng black-bone chickens, we measured the VH and CD of the duodenum and jejunum (**Figure 1**). In the duodenum, the VH of group B was significantly higher than groups A and D ($p < 0.05$). However, no significant difference was observed in the CD and the ratio of VH to CD (VH/CD) among four treatments ($p > 0.05$). In the jejunum, the VH of group B was the highest, which was markedly higher than groups C and D ($p < 0.05$). The CD decreased significantly in group D, compared with group A ($p < 0.05$).

Production Performance

The production performance was shown in Table 2 of our previous study (Liu et al., 2021). In the overall period (from day 1 to 56 of the experiment), 3% HILM increased the egg weight ($p < 0.05$), feed intake ($p < 0.05$), and egg production ($p < 0.05$), meanwhile decreased the feed conversion ratio ($p < 0.05$) in a linear or quadratic manner.

[1] www.majorbio.com

Operational Taxonomic Unit Analysis and Venn Diagram of the Difference in Operational Taxonomic Unit Distributions Between Groups

In our study, a total of four groups (each group with two intestinal segments) were investigated, and each sample contained large numbers of enriched OTUs (**Figure 2**). According to OTU classification, we calculated the same number of OTUs between groups and then pointed them in the Venn graph. Each color block in the Venn graph represents a group, intersecting sections represent OTUs shared with adjacent groups, and one number means one group. The OTUs of the jejunum were as follows (**Figure 2A**): JA, 53; JB, 64; JC, 92; and JD, 85. Uniform OTUs in the jejunum among groups were as follows: JA and JB, 32; JA and JC, 59; JA and JD, 13; JB and JC, 44; JB and JD, 30; JC and JD, 54; JA, JB, and JC, 83; JA, JB, and JD, 36; JA, JC, and JD, 32; JB, JC, and JD, 53; and JA, JB, JC, and JD, 627. The OTUs in the duodenum were as follows (**Figure 2B**): CA, 23; CB, 16; CC, 24; and CD, 46. Uniform OTUs in the duodenum among groups were as follows: CA and CB, 8; CA and CC, 10; CA and CD, 28; CB and CC, 20; CB and CD, 22; CC and CD, 44; CA, CB, and CC, 24; CA, CB, and CD, 20; CA, CC, and CD, 42; CB, CC, and CD, 77; and CA, CB, CC, and CD, 733.

Alpha Diversity

The abundance-based coverage estimator (ACE) index, Chao index, Shannon index, and Simpson index were selected to analyze diversity (**Figure 3**). Although dietary HILM did not influence bacterial diversity in the jejunum, the richness of the intestinal microbiota increased in group C, but the community richness and diversity decreased in group D (**Figure 3A**, $p > 0.05$). However, in the cecum, the ACE index and Chao index of group D were significantly higher than those of group A ($p < 0.05$) and group B ($p < 0.01$). The Simpson index was the lowest, which was significantly higher than that of group A ($p < 0.05$). There were no significant differences observed among the groups in the Shannon index ($p > 0.05$).

Heatmap Analysis–Phylum Level

To analyze the effects of HILM on the microbial community, a heatmap was used to assess the composition of microorganisms by color shades among the four groups (each group with two intestinal segments). The results showed that *Firmicutes, Bacteroidetes, Proteobacteria, Actinobacteria, Spirochaetota, Desulfobacterota, Campilobacterota, WPS-2*, and *Synergistetes* accounted for 98.58% of the microbial population (**Figure 4A**). Among those, *Bacteroidetes* and *Firmicutes* were the main phyla in the jejunum, accounting for 83.37%. As shown in **Figure 4C**, the *Deferribacterota* and *Fusobacteriota* phyla of group A were markedly improved ($p < 0.05$).

As shown in **Figure 4B**, the dominant bacterial phyla of the cecum were *Firmicutes, Bacteroidetes, Desulfobacterota, Synergistetes, Spirochaetota,* and *WPS-2*, accounting for 99.12% of the microbial population. Among those, *Bacteroidetes* and Firmicutes were the main phyla in the jejunum, accounting for 91.78%. The *Campilobacterota* phylum of group C was

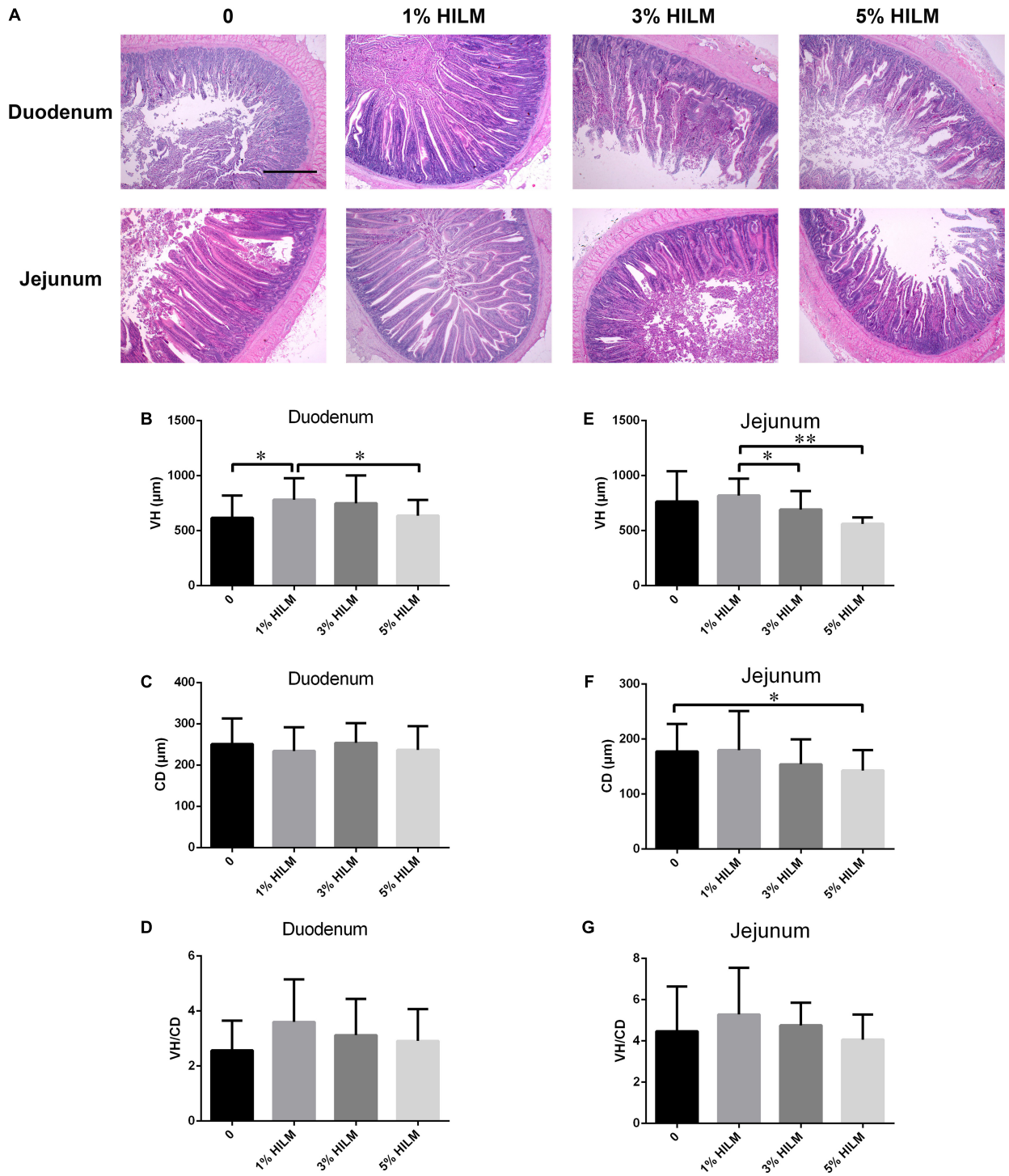

FIGURE 1 | Effects of HILM on intestinal morphology of Xuefeng black-bone chicken. **(A)** Representative pictures of hematoxylin and eosin staining (40×, scale bar: 20 μm); VH of duodenum **(B)** and jejunum **(E)**; CD of duodenum **(C)** and jejunum **(F)**; VH/CD of duodenum **(D)** and jejunum **(G)**. Results shown are means ± SEM ($n = 12$). *$p < 0.05$, **$p < 0.01$. VH, villus height; CD, crypt depth; VH/CD, ratio of villus height to crypt depth; HILM, *Hermetia illucens* larvae meal.

significantly elevated ($p < 0.05$); however, there were no significant differences among other microorganisms ($p > 0.05$, **Figure 4D**).

Heatmap Analysis–Genus Level

As shown in **Figure 5A**, the dominant genus of the jejunum was *Bacteroides*, and the second genus was *Lactobacillus*. At the genus

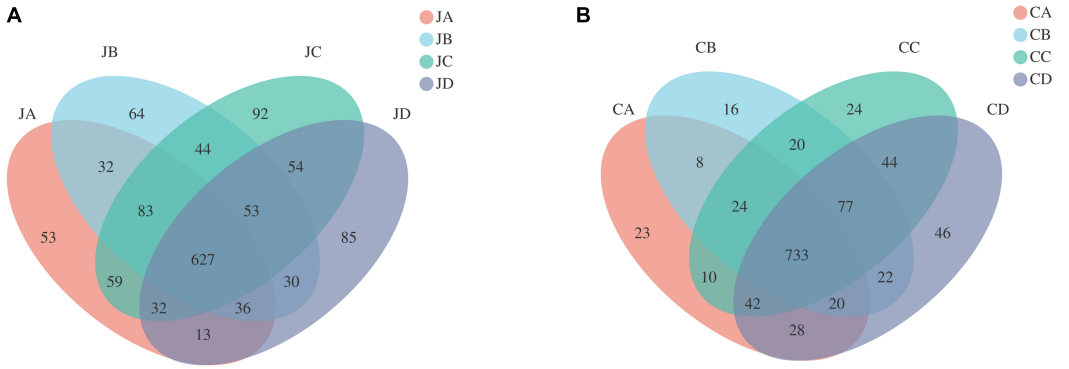

FIGURE 2 | Shared and specific operational taxonomic unit (OTUs) in different intestinal sections of different groups (**A**: jejunum; **B**: cecum). JA, jejunum of 0% HILM; JB, jejunum of 1% HILM; JC, jejunum of 3% HILM; JD, jejunum of 5% HILM; CA, cecum of 0% HILM; CB, cecum of 1% HILM; CC, cecum of 3% HILM; CD, cecum of 5% HILM.

level, the analysis results showed that compared with groups A, B, and C, the abundances of *Staphylococcus* in group D significantly increased. The abundances of *Romboutsia* increased in group C ($p < 0.05$, **Figure 5C**). However, in group A, we found that the abundances of *Megamonas* were significantly higher than others ($p < 0.05$).

As shown in **Figure 5B**, the dominant genus of the cecum was *Bacteroides*, and the next genus was *Rikenellaceae*. In group B, we found that the abundances of the unclassified *Bacteroidales* were significantly higher than the other groups ($p < 0.05$, **Figure 5D**). However, there was no significant change in the intestinal microflora in the cecum ($p > 0.05$).

Principal Component Analysis Cluster Analysis

To analyze the effects of HILM on the microbial community, principal component analysis (PCA) used weighted UniFrac distances, which were calculated based on the OTU species and relative abundance of the samples (**Figure 6**). The results displayed significant differences between microbial communities in group C and group D of the jejunum but no significant differences between the microbial communities of groups A and B (**Figure 6A**). It suggested that the feed additives significantly influenced the gut microbiota distribution in chicken. **Figure 6B** showed that the degree of clustering of individuals in groups A and B was high, whereas the degree of clustering of individuals in groups C and D was low, indicating that the similarity within groups A and B was higher than in other groups. There were no significant differences among the microbial communities in the cecum ($p > 0.05$).

DISCUSSION

HILM contains higher or similar protein content and richer essential amino acid content (Yu et al., 2020). During recent decades, many studies indicated that the significant effects of HILM on intestinal health (Weththasinghe et al., 2021). Intestinal morphology and intestinal microbiota are critical to maintaining ecosystem stability and performance. HILM is a reasonable protein feed additive. The current study evaluated the effect of HILM on villus morphology of the jejunum and duodenum and the comparison of OTUs of microorganisms, alpha diversity, PCA cluster analysis, and microbial species composition analysis of the jejunum and cecum.

The rapid growth of broilers was due to the great potential of the small intestinal cells to absorb nutrients and the efficient conversion of nutrients to muscles (Mishra and Jha, 2019; Liu et al., 2020). Modifications of intestinal morphology, mainly increasing VH and the VH/CD in the duodenum and jejunum, could improve nutrient absorption (Schiavone et al., 2018; Hajimohammadi et al., 2020). Small intestinal VH determined the functional maturity of villus absorptive cells while the VH increases; the intestinal surface area enabled more efficient absorption of available nutrients (Li et al., 2019; Ramlucken et al., 2019). In this study, the supplementation of 1% HILM significantly increased the VH of the duodenum, and dietary 1 and 3% HILM supplementation had no damage effect in the duodenum and jejunum. In conclusion, dietary supplementation of HILM could improve nutrient absorption, maintain the normal intestinal morphology, and had effects on VH, CD, and VH/CD. However, dietary supplementation of 5% HILM reduced the VH of the jejunum and duodenum and VH/CD of the jejunum, consistent with the adverse effects of protein source substitution on small intestinal morphology in broilers (Biasato et al., 2018b). Interestingly, the CD of dietary 5% HILM supplementation in the jejunum decreased, which contrasted with earlier studies (Ibitoye et al., 2019). This might be related to the high chitin content in HILM, which may cause damage to the intestinal structure and reduce nutrient digestibility (Kroeckel et al., 2012). The supplementation of chitinase in diets supplemented with HILM might improve the effect, which needed to be studied in the future.

The intestinal tracts of poultry were complex, diverse, and dynamic microbial communities, which played an important role in host health and production performance. In the process of nutrition, metabolism, physiology, and immunity, the microbial community could promote digestion and absorption of nutrients,

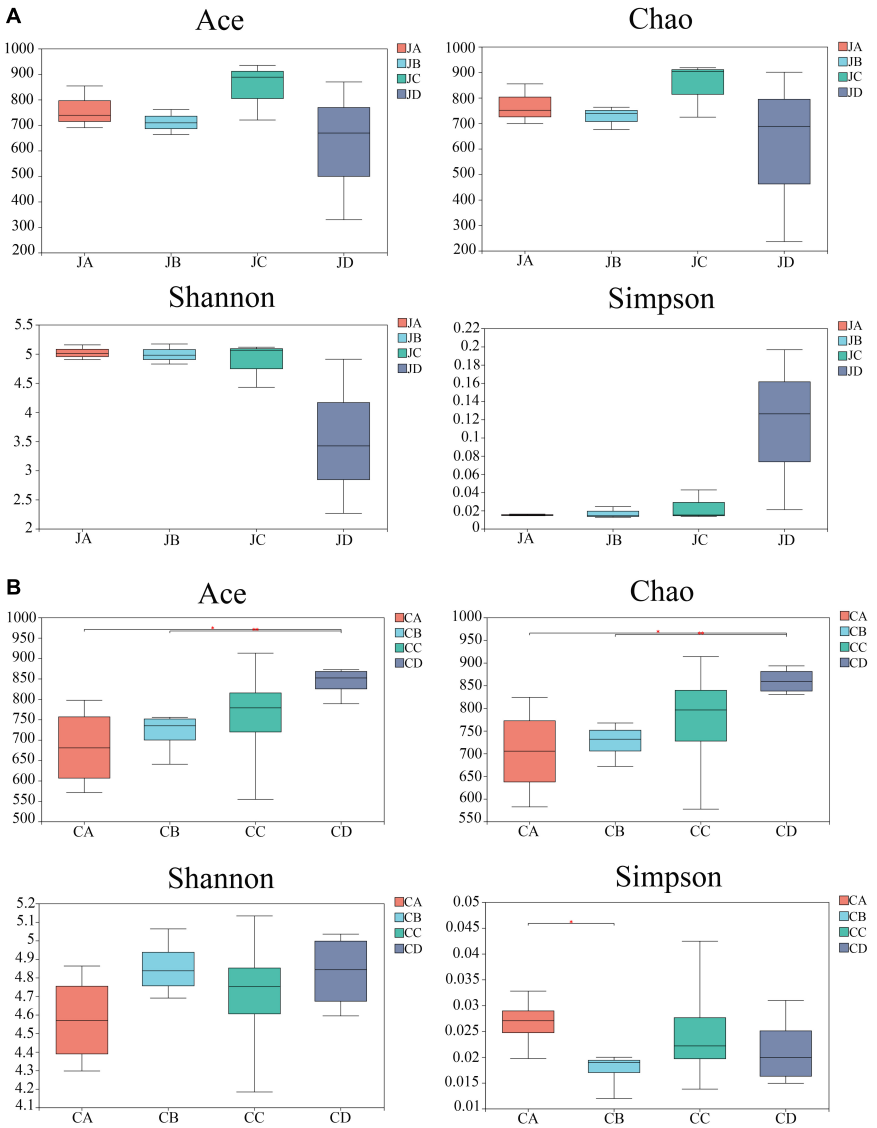

FIGURE 3 | Alpha diversity of four groups in jejunum **(A)** and cecum **(B)**. Significant difference between samples and marks with significant differences between two groups. JA, jejunum of 0% HILM; JB, jejunum of 1% HILM; JC, jejunum of 3% HILM, JD: jejunum of 5% HILM; CA, cecum of 0% HILM; CB, cecum of 1% HILM; CC, cecum of 3% HILM; CD, cecum of 5% HILM.

stimulate the immune response of the host, and enhance resistance to infection (Shi et al., 2020). However, gut microbiota also had direct and indirect harmful effects on decreased digestibility, increased cell turnover rate, and production of toxic metabolites, which might also lead to the decreased growth performance of chickens (Wang et al., 2017; Yadav and Jha, 2019). It was necessary to sufficiently understand the composition and diversity of the intestinal microbiome to further promote poultry growth and intestinal health. In this study, 16S recombinant DNA gene sequencing was used to detect the microbial diversity and community compositions of bacteria in the jejunum and cecum of Xuefeng black-bone chickens fed with different doses of HILM diets. The OTU number of dietary 3% HILM supplementation was the highest in the jejunum, which implied that the 3% HILM to the diet increased the microbial diversity of the jejunum. However, none of the groups in both the jejunum and cecum had the unique OTU number, indicating that dietary HILM had no effect but maintained species richness.

In different parts of the intestine, due to different intestinal structures, pH values, and diet status, bacterial populations vary greatly. Alpha diversity analysis analyzed species diversity in independent samples (Cui et al., 2021). The high diversity of intestinal bacteria is conducive to maintaining intestinal stability. In this study, we investigated the ACE, Chao, Shannon, and Simpson indexes in the jejunum and cecum of the dietary HILM to Xuefeng black-bone chickens. The results showed that dietary 3 and 5% HILM supplementation significantly increased the ACE and Chao indexes, and 1% HILM supplementation significantly

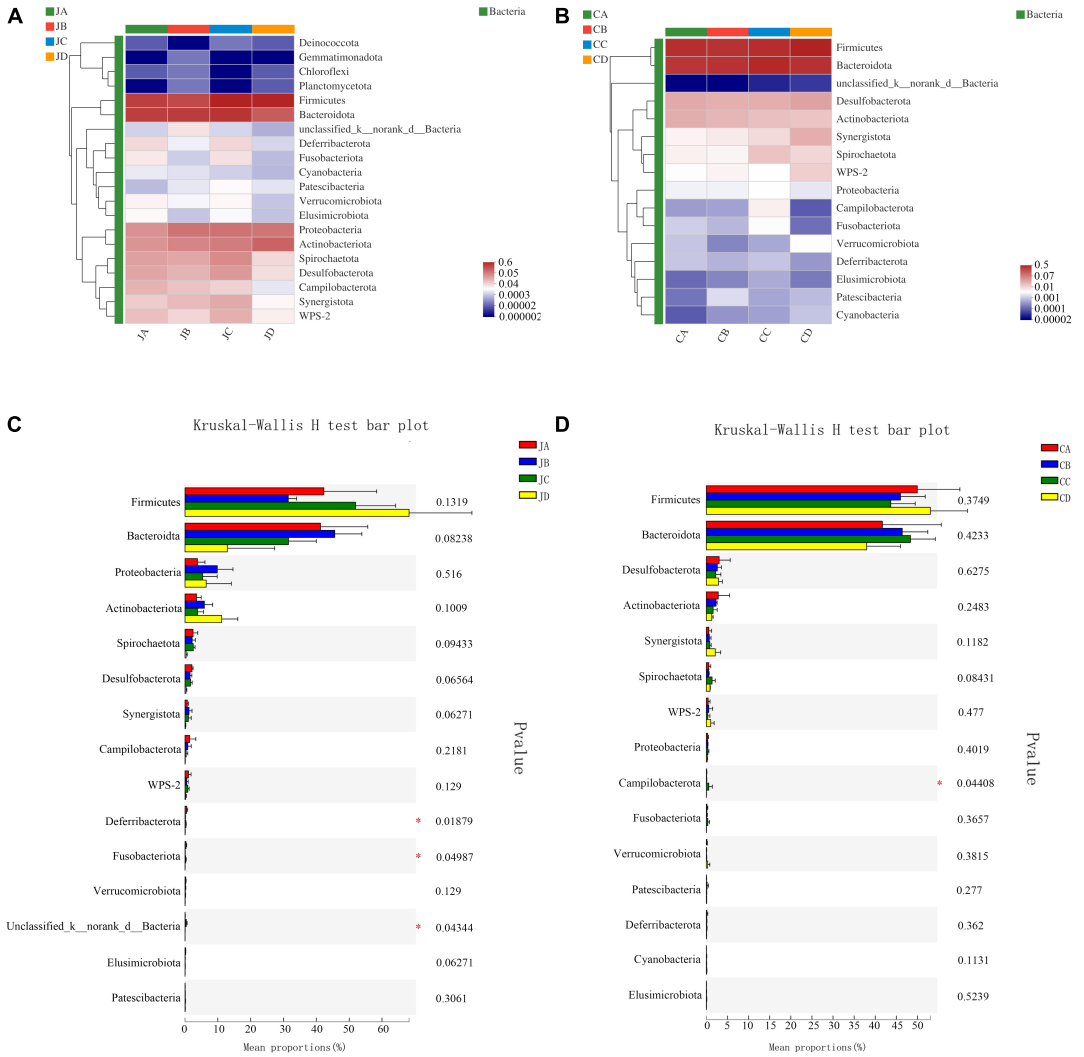

FIGURE 4 | Heatmap chart of top 20 phyla in different intestinal segments (**A**: jejunum; **B**: cecum) and comparison of differences between groups of top 20 phyla (**C**: jejunum; **D**: cecum). One-way analysis of variance, JA, jejunum of 0% HILM; JB, jejunum of 1% HILM; JC, jejunum of 3% HILM; JD, jejunum of 5% HILM; CA, cecum of 0% HILM; CB, cecum of 1% HILM; CC, cecum of 3% HILM; CD, cecum of 5% HILM.

decreased the Simpson index in the cecum, consistent with the report that highly nutritious diets could increase diversity indexes (He et al., 2020). Although there were no significantly differences of alpha diversity index in the jejunum, 3% HILM had the highest ACE, Chao, and Shannon indexes and the lowest Simpson index. Accordingly, the alpha diversity index was used as the community richness index. The higher the ACE, Chao, and Shannon indexes, the higher the community richness, whereas the Simpson index was the opposite. Improving the alpha index of dietary HILM might increase the stability between communities and closer the connections between communities.

Robust and balanced compositions of intestinal microflora were required to support health and growth. Microorganisms could benefit the host by affecting nutrient digestion and disease resistance, but an overgrowth of gut microbial could affect ecosystem balance and destroy gut integrity to initiate intestinal inflammation (Saracila et al., 2018). HILM, as a kind of feed resource based on insects, which could maintain intestinal microorganism health, has been reported in animal feed production (Leni et al., 2020). Based on the results of species annotation, we analyzed the microbial composition of the cecum and jejunum at the phylum and genus levels to evaluate the role of HILM in maintaining homeostasis.

At the phylum level of the jejunum and cecum microbial composition, both *Bacteroidetes* and *Firmicutes* were the largest phyla, which accounted for >80% of all the microbial community detected in our study, and *Bacteroidetes* and *Firmicutes* accounted for >90% in the cecum. This was consistent with many previous studies suggesting that *Firmicutes* and *Bacteroidetes* made up the majority of the microbial communities in chickens (accounting for >80%) at the phylum level, and these bacteria affected energy production and metabolism (Shang et al., 2018;

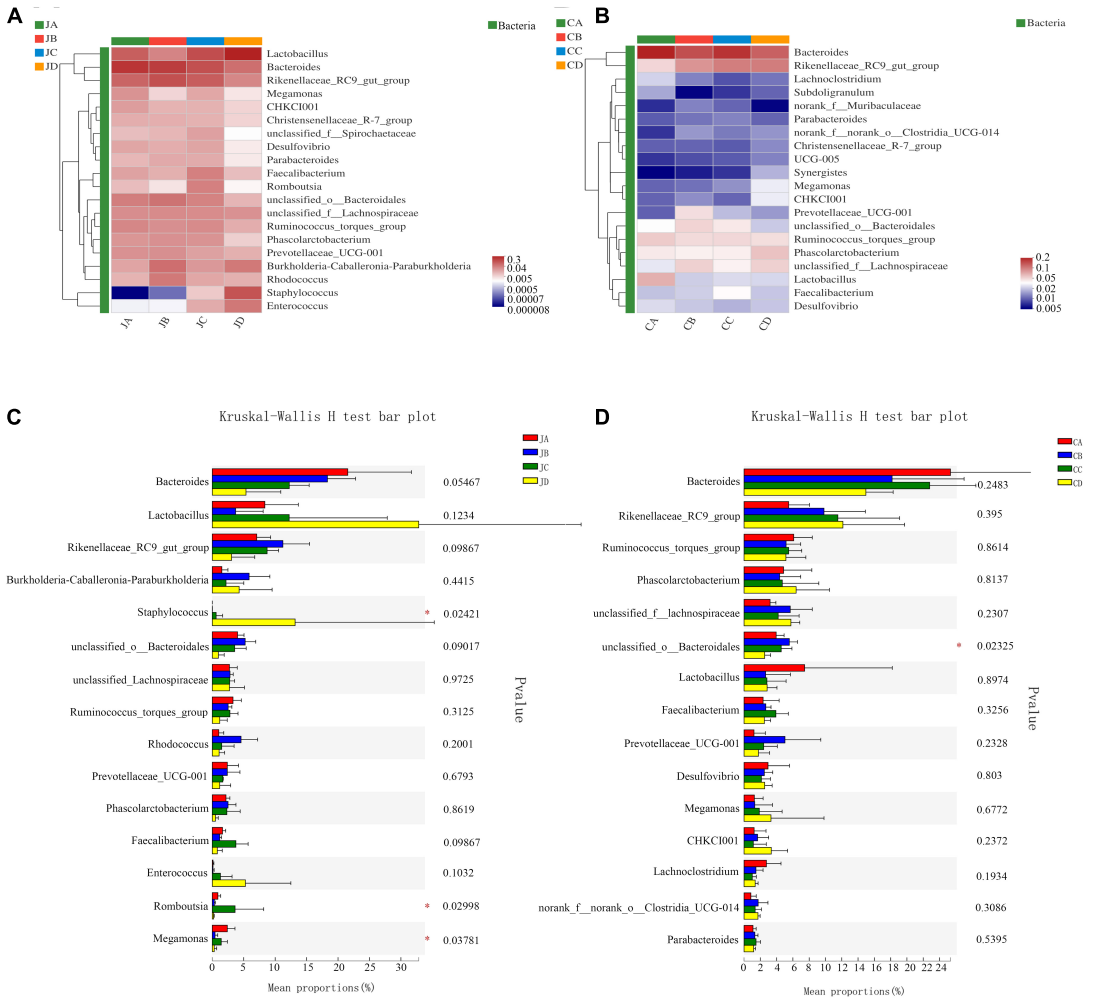

FIGURE 5 | Heatmap chart of the top 20 genera in different intestinal segments (**A**: jejunum; **B**: cecum) and comparison of differences between groups of the top 20 phyla (**C**: jejunum; **D**: cecum). One-way analysis of variance, JA, jejunum of 0% HILM; JB, jejunum of 1% HILM; JC, jejunum of 3% HILM; JD, jejunum of 5% HILM; CA, cecum of 0% HILM; CB, cecum of 1% HILM; CC, cecum of 3% HILM; CD, cecum of 5% HILM.

Herrero-Encinas et al., 2020). *Bacteroidetes* and *Firmicutes* were the common colonizers of the chicken intestinal, which were considered to be potentially beneficial autochthonous bacteria (Borda-Molina et al., 2020). Cui et al. (2021) found that these two kinds of a dominant phylum of the gut community played an important role in improving intestinal diseases, inhibiting the proliferation of harmful intestinal bacteria, and producing short-chain fatty acids, which reduced luminal pH and regulated the microbial composition (stimulating the growth of beneficial bacteria, such as *Bifidobacterium*) (Dong et al., 2017; Ratajczak et al., 2019). At the phylum level of the jejunum, we found that HILM supplementation decreased the number of *Deferribacterota* and *Fusobacteriota* phyla. *Deferribacterota* has been found in healthy mice and humans. However, the relatively small proportion of intestinal microorganisms and their role and function have been rarely reported (Lewis et al., 2021). Also, Fusobacteria, anaerobic Gram-negative rods, were rare agents of severe human diseases that had repeatedly noted their link to colorectal cancer. It was indicated that HILM supplementation to the diet could alleviate damage and improve the intestinal microbiota disorders caused by the disease. At the phylum level of the cecum, the *Campilobacterota* phyla were greatly improved with 3% HILM supplementation, which was not a usual report with the phylum by poultry studies under natural or captivity conditions. Although some members of this phylum might cause diseases in wild and domestic animals, they were considered to be nonpathogenic and were frequently isolated from healthy birds (Zhao Y. et al., 2019; Chen et al., 2020; Maraci et al., 2021). It was showed that HILM could affect intestinal microbiota, either directly or indirectly, by modulating jejunal and cecal microbial compositions at the phylum level, especially a diet with 3% HILM supplementation.

At the genus level, the dominant bacteria in the gut were remodeled. Different from phyla, the dominant taxa in chicken cecal microbiota was controversial (Biasato et al., 2018a). Costa et al. (2017) found that the most predominant genera in the

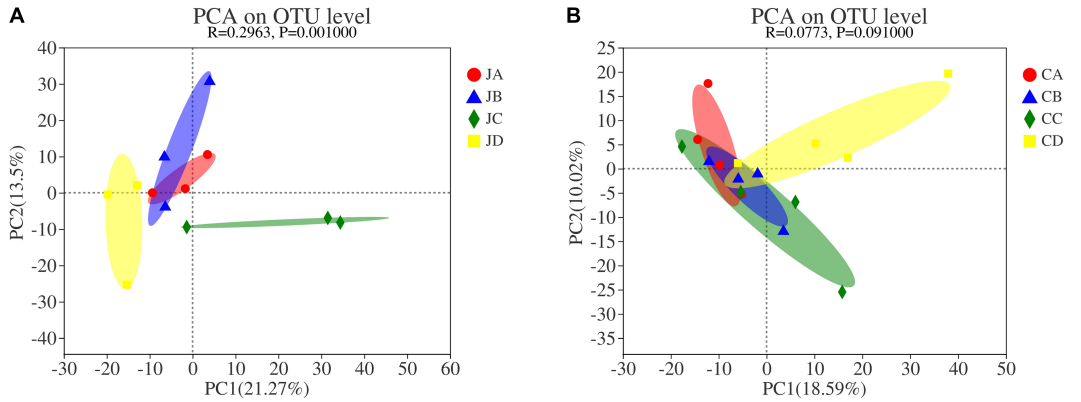

FIGURE 6 | Cluster analysis by principal coordinate analysis. **(A)** jejunum; **(B)** cecum. JA, jejunum of 0% HILM; JB, jejunum of 1% HILM; JC, jejunum of 3% HILM; JD, jejunum of 5% HILM; CA, cecum of 0% HILM; CB, cecum of 1% HILM; CC, cecum of 3% HILM; CD, cecum of 5% HILM. X- and Y-axes represent two selected main coordinate axes, and percentage represents interpretation value of main coordinate axis to difference of sample composition; scales of the X- and Y-axes are relative distances and have no practical significance; points of different colors or shapes represent samples of different groups; the closer the two sample points are, the more similar the species composition of the two samples.

cecum of broilers were *Clostridium*, *Ruminococcus*, *Lactobacillus*, and *Bacteroides*. Callaway et al. (2009) found that *Prevotella* was the most abundant genus. In particular, the *Bacteroides* genus has been reported as the most predominant member of the cecal microbiota of Bermuda free-range broilers. In this study, the genus *Bacteroides* was the positive bacterium in the jejunum and cecum, which is in line with the previous finding that a higher number of *Bacteroides* enables larger efficiency of gut microbiota in extracting energy from the diet (Yue et al., 2019). Of interest, in our findings, the genus *Lactobacillus* was the second leading bacterium in the jejunum. Li et al. (2020) also found that *Lactobacillus* consisted in the gut of healthy pigs. *Lactobacillus* had a strong antibacterial activity, which enhanced the health of the chickens by inhibiting the growth of pathogens through competitive exclusion in the gastrointestinal tract (Ahmed et al., 2019). In addition, dietary 3% HILM increased the genus *Romboutsia*, a valuable intestinal biomarker in maintaining the health of the host (Mangifesta et al., 2018; Zhang et al., 2021). However, the 5% HILM supplementation increased the genus *Staphylococcus* and decreased the genus *Megamonas* in the jejunum. *Megamonas* was a genus of Firmicutes bacteria, which has been reported that it acted as a hydrogen sink in the gut of broilers by increasing the production of short-chain fatty acids (Chen et al., 2019). In general, most *Staphylococcus* were nonpathogenic bacteria, but a few might cause disease. The result showed that high-level protein might result in the decrease of beneficial microbes, leading to an imbalance of the jejunum microbiota. Diet was one of the most important factors that affected the gut microbiota (Makki et al., 2018). The components of dietary protein affected the composition of gut microbiota, and higher levels could lead to an increase in pathogenic microorganisms, thereby increasing the associated risk of metabolic diseases (Zhao J. et al., 2019; Sedgh-Gooya et al., 2021). Moreover, in the cecum, the genus *Lactobacillus* was the second leading bacterium. Dalle Zotte et al. (2021) fattened quails with full-fat or defatted silkworm pupa meal to observe the cecal microbiome and found that the genus *Rikenellaceae* was increased, which was consistent with our results. *Rikenellaceae* has been reported to promote starch decomposition in raw potato starch-fed mice (Bang et al., 2019). Meanwhile, we observed that the genus unclassified *Bacteroidales* in 1% HILM of the cecum was significantly increased. The results showed that dietary 1 or 3% HILM could increase the number of beneficial microflora, maintaining the jejunal and cecal microflora stability. However, 5% HILM supplementation might have no beneficial effect on the intestine.

The main intention of PCA cluster analysis was to investigate the similarity of community structure among varied samples, to observe the differences among samples by sorting the samples by decomposing the community data structure (Fang et al., 2016). In this study, the weighted UniFrac plot showed that the jejunal microbial community of groups C and D was highly isolated from groups A and B. Cui et al. (2021) reported that the grouping effect was obvious and could effectively stabilize the progenitor of intestinal flora. It indicated that a diet supplemented with 3 and 5% HILM could change the species and abundance of main intestinal microflora and stabilize the composition of intestinal microflora. In addition, diet HILM had little effect on the difference of community members and the abundance of community members of the cecum.

Our previous data demonstrated that dietary supplementation of 3% HILM in broiler breeders could significantly increase feed intake and egg weight. Additionally, HILM could strengthen the activity of total-superoxide dismutase and the level of antibody to avian influenza virus of plasma. The data of this study displayed that dietary supplementation of 1 or 3% HILM benefited the intestinal morphology and intestinal microbiota of Xuefeng black-bone chicken. Together, 3% HILM dietary supplementation might improve intestinal morphology and regulate microbiota, increasing feed intake, egg weight, and disease resistance. Hence, HILM would be a suitable substitute for plant protein in the diet of Xuefeng black-bone chicken.

CONCLUSION

Dietary supplementation of HILM to Xuefeng black-bone chicken diets improved intestinal morphology, alpha diversity, and beneficial flora content (*Campilobacterota*, *Romboutsia*, unclassified *Bacteroidales*). Among the three additive quantities, the addition of 1% HILM increased the VH of the duodenum and decreased the Simpson index of the cecum, and the addition of 3% HILM stabilized the composition of the jejunum. However, the addition of 5% HILM decreased the VH and the ratio of VH/CD of the jejunum and increased pathogenetic genera (*Staphylococcus*). Dietary 1 or 3% HILM might benefit intestinal morphology and intestinal microbiota of Xuefeng black-bone chicken. HILM could be an alternative protein supplement to meet the growing demand in poultry production.

DATA AVAILABILITY STATEMENT

The datasets presented in this study can be found in online repositories. The names of the repository/repositories and accession number(s) can be found below: https://www.ncbi.nlm.nih.gov/bioproject/PRJNA747901/.

ETHICS STATEMENT

The animal study was reviewed and approved by the Animal Care and Use Committee of Hunan Agricultural University (HUNAU2020005).

AUTHOR CONTRIBUTIONS

CH, JC, and XZ designed the experiment. JL and YY performed the experiment. KX and XW collected the samples. QY, BX, XQ, and SG analyzed the samples and data. SG, CH, and XZ conceptualized the manuscript, compiled all of the information, and prepared the manuscript. All authors read and approved the final manuscript.

FUNDING

This study was funded by the start-up funds from Hunan Agricultural University, the National Innovation Training Program for College Students (G)SCX1802, the Hunan Science and Technology Correspondent Innovation and Entrepreneurship Project (2020NK4155), and the National Natural Science Foundation of China (32072711).

REFERENCES

Ahmed, Z., Vohra, M. S., Khan, M. N., Ahmed, A., and Khan, T. A. (2019). Antimicrobial role of *Lactobacillus* species as potential probiotics against enteropathogenic bacteria in chickens. *J. Infect. Dev. Ctries.* 13, 130–136. doi: 10.3855/jidc.10542

Bang, S. J., Lee, E. S., Song, E. J., Nam, Y. D., Seo, M. J., Kim, H. J., et al. (2019). Effect of raw potato starch on the gut microbiome and metabolome in mice. *Int. J. Biol. Macromol.* 133, 37–43. doi: 10.1016/j.ijbiomac.2019.04.085

Barroso, F. G., de Haro, C., Sanchez-Muros, M. J., Venegas, E., Martinez-Sanchez, A., and Perez-Banon, C. (2014). The potential of various insect species for use as food for fish. *Aquaculture* 422, 193–201. doi: 10.1016/j.aquaculture.2013.12.024

Biasato, I., Ferrocino, I., Biasibetti, E., Grego, E., Dabbou, S., Sereno, A., et al. (2018a). Modulation of intestinal microbiota, morphology and mucin composition by dietary insect meal inclusion in free-range chickens. *BMC Vet. Res.* 14:383. doi: 10.1186/s12917-018-1690-y

Biasato, I., Gasco, L., De Marco, M., Renna, M., Rotolo, L., Dabbou, S., et al. (2018b). Yellow mealworm larvae (*Tenebrio molitor*) inclusion in diets for male broiler chickens: effects on growth performance, gut morphology, and histological findings. *Poult. Sci.* 97, 540–548. doi: 10.3382/ps/pex308

Borda-Molina, D., Matis, G., Mackei, M., Neogrady, Z., Huber, K., Seifert, J., et al. (2020). Caeca microbial variation in broiler chickens as a result of dietary combinations using two cereal types, supplementation of crude protein and sodium butyrate. *Front. Microbiol.* 11:617800. doi: 10.3389/fmicb.2020.617800

Callaway, T. R., Dowd, S. E., Wolcott, R. D., Sun, Y., McReynolds, J. L., Edrington, T. S., et al. (2009). Evaluation of the bacterial diversity in cecal contents of laying hens fed various molting diets by using bacterial tag-encoded FLX amplicon pyrosequencing. *Poult. Sci.* 88, 298–302. doi: 10.3382/ps.2008-00222

Chen, C. Y., Chen, C. K., Chen, Y. Y., Fang, A., Shaw, G. T., Hung, C. M., et al. (2020). Maternal gut microbes shape the early-life assembly of gut microbiota in passerine chicks via nests. *Microbiome* 8:129. doi: 10.1186/s40168-020-00896-9

Chen, S., Zhou, Y., Chen, Y., and Gu, J. (2018). fastp: an ultra-fast all-in-one FASTQ preprocessor. *Bioinformatics* 34, 884–890. doi: 10.1093/bioinformatics/bty560

Chen, Y., Ni, J., and Li, H. (2019). Effect of green tea and mulberry leaf powders on the gut microbiota of chicken. *BMC Vet Res* 15:77. doi: 10.1186/s12917-019-1822-z

Costa, M. C., Bessegatto, J. A., Alfieri, A. A., Weese, J. S., Filho, J. A., and Oba, A. (2017). Different antibiotic growth promoters induce specific changes in the cecal microbiota membership of broiler chicken. *PLoS One* 12:e0171642. doi: 10.1371/journal.pone.0171642

Cui, Y., Han, C., Li, S., Geng, Y., Wei, Y., Shi, W., et al. (2021). High-throughput sequencing-based analysis of the intestinal microbiota of broiler chickens fed with compound small peptides of Chinese medicine. *Poult. Sci.* 100:100897. doi: 10.1016/j.psj.2020.11.066

Cutrignelli, M. I., Messina, M., Tulli, F., Randazzo, B., Olivotto, I., Gasco, L., et al. (2018). Evaluation of an insect meal of the Black Soldier Fly (*Hermetia illucens*) as soybean substitute: intestinal morphometry, enzymatic and microbial activity in laying hens. *Res. Vet. Sci.* 117, 209–215. doi: 10.1016/j.rvsc.2017.12.020

Dalle Zotte, A., Singh, Y., Squartini, A., Stevanato, P., Cappellozza, S., Kovitvadhi, A., et al. (2021). Effect of a dietary inclusion of full-fat or defatted silkworm pupa meal on the nutrient digestibility and faecal microbiome of fattening quails. *Animal* 15:100112. doi: 10.1016/j.animal.2020.100112

De Smet, J., Wynants, E., Cos, P., and Van Campenhout, L. (2018). Microbial community dynamics during rearing of black soldier fly larvae (*Hermetia illucens*) and impact on exploitation potential. *Appl. Environ. Microbiol.* 84:e02722–17. doi: 10.1128/AEM.02722-17

DiGiacomo, K., Akit, H., and Leury, B. J. (2019). Insects: a novel animal-feed protein source for the Australian market. *Anim. Prod. Sci.* 59, 2037–2045. doi: 10.1071/an19301

Dong, X. Y., Azzam, M. M. M., and Zou, X. T. (2017). Effects of dietary threonine supplementation on intestinal barrier function and gut microbiota of laying hens. *Poult. Sci.* 96, 3654–3663. doi: 10.3382/ps/pex185

Edgar, R. C. (2013). UPARSE: highly accurate OTU sequences from microbial amplicon reads. *Nat. Methods* 10, 996–998. doi: 10.1038/nmeth.2604

Elhag, O., Zhou, D., Song, Q., Soomro, A. A., Cai, M., Zheng, L., et al. (2017). Screening, expression, purification and functional characterization of novel antimicrobial peptide genes from *Hermetia illucens* (L.). *PLoS One* 12:e0169582. doi: 10.1371/journal.pone.0169582

Fang, X., Wang, X., Yang, S., Meng, F., Wang, X., Wei, H., et al. (2016). Evaluation of the microbial diversity in amyotrophic lateral sclerosis using

high-throughput sequencing. *Front. Microbiol.* 7:1479. doi: 10.3389/fmicb.2016.01479

Fawole, F. J., Adeoye, A. A., Tiamiyu, L. O., Ajala, K. I., Obadara, S. O., and Ganiyu, I. O. (2020). Substituting fishmeal with *Hermetia illucens* in the diets of African catfish (*Clarias gariepinus*): effects on growth, nutrient utilization, haemato-physiological response, and oxidative stress biomarker. *Aquaculture* 518:734849. doi: 10.1016/j.aquaculture.2019.734849

Gasco, L., Biasato, I., Dabbou, S., Schiavone, A., and Gai, F. (2019). Animals fed insect-based diets: state-of-the-art on digestibility, performance and product quality. *Animals (Basel)* 9:170. doi: 10.3390/ani9040170

Gravel, A., and Doyen, A. (2020). The use of edible insect proteins in food: challenges and issues related to their functional properties. *Innov. Food Sci. Emerg. Technol.* 59:102272. doi: 10.1016/j.ifset.2019.102272

Guo, S. C., Lei, J. X., Liu, L. L., Qu, X. Y., Li, P., Liu, X., et al. (2021). Effects of *Macleaya cordata* extract on laying performance, egg quality, and serum indices in Xuefeng black-bone chicken. *Poult. Sci.* 100:9. doi: 10.1016/j.psj.2021.101031

Hajimohammadi, A., Mottaghitalab, M., and Hashemi, M. (2020). Effects of microbial fermented sesame meal and enzyme supplementation on the intestinal morphology, microbiota, pH, tibia bone and blood parameters of broiler chicks. *Ital. J. Anim. Sci.* 19, 457–467. doi: 10.1080/1828051x.2020.1755378

He, Y., Yang, Y., Dong, Y., Ito, K., and Zhang, B. (2020). Highly nutritious diet resists *Salmonella typhimurium* infections by improving intestinal microbiota and morphology in broiler chickens. *Poult. Sci.* 99, 7055–7065. doi: 10.1016/j.psj.2020.09.073

Henry, M., Gasco, L., Piccolo, G., and Fountoulaki, E. (2015). Review on the use of insects in the diet of farmed fish: past and future. *Anim. Feed Sci. Technol.* 203, 1–22. doi: 10.1016/j.anifeedsci.2015.03.001

Herrero-Encinas, J., Blanch, M., Pastor, J. J., Mereu, A., Ipharraguerre, I. R., and Menoyo, D. (2020). Effects of a bioactive olive pomace extract from *Olea europaea* on growth performance, gut function, and intestinal microbiota in broiler chickens. *Poult. Sci.* 99, 2–10. doi: 10.3382/ps/pez467

Ibitoye, E. B., Lokman, I. H., Hezmee, M. N. M., Goh, Y. M., Zuki, A. B. Z., Jimoh, A. A., et al. (2019). Gut health and serum growth hormone levels of broiler chickens fed dietary chitin and chitosan from cricket and shrimp. *Poult. Sci.* 98, 745–752. doi: 10.3382/ps/pey419

Kim, S. W., Less, J. F., Wang, L., Yan, T., Kiron, V., Kaushik, S. J., et al. (2019). Meeting global feed protein demand: challenge, opportunity, and strategy. *Annu. Rev. Anim. Biosci.* 7, 221–243. doi: 10.1146/annurev-animal-030117-014838

Kroeckel, S., Harjes, A. G. E., Roth, I., Katz, H., Wuertz, S., Susenbeth, A., et al. (2012). When a turbot catches a fly: evaluation of a pre-pupae meal of the black soldier fly (*Hermetia illucens*) as fish meal substitute–growth performance and chitin degradation in juvenile turbot (*Psetta maxima*). *Aquaculture* 364, 345–352. doi: 10.1016/j.aquaculture.2012.08.041

Leni, G., Prandi, B., Varani, M., Faccini, A., Caligiani, A., and Sforza, S. (2020). Peptide fingerprinting of *Hermetia illucens* and *Alphitobius diaperinus*: identification of insect species-specific marker peptides for authentication in food and feed. *Food Chem.* 320:126681. doi: 10.1016/j.foodchem.2020.126681

Lewis, W. H., Tahon, G., Geesink, P., Sousa, D. Z., and Ettema, T. J. G. (2021). Innovations to culturing the uncultured microbial majority. *Nat. Rev. Microbiol.* 19, 225–240. doi: 10.1038/s41579-020-00458-8

Li, X. J., Wang, M., Xue, Y., Duan, D., Li, C., Han, X., et al. (2020). Identification of microflora related to growth performance in pigs based on 16S rRNA sequence analyses. *AMB Express* 10:192. doi: 10.1186/s13568-020-01130-3

Li, Y., Lu, X., Wu, H., Xia, M., Hou, Q., Hu, W., et al. (2019). The effect of dietary supplementation of low crude protein on intestinal morphology in pigs. *Res. Vet. Sci.* 122, 15–21. doi: 10.1016/j.rvsc.2018.11.013

Liu, J. B., Yan, H. L., Zhang, Y., Hu, Y. D., and Zhang, H. F. (2020). Effects of stale maize on growth performance, immunity, intestinal morphology and antioxidant capacity in broilers. *Asian-Australas. J. Anim. Sci.* 33, 605–614. doi: 10.5713/ajas.19.0224

Liu, X., Liu, X., Yao, Y., Qu, X., Chen, J., Xie, K., et al. (2021). Effects of different levels of *Hermetia illucens* larvae meal on performance, egg quality, yolk fatty acid composition and oxidative status of laying hens. *Ital. J. Anim. Sci.* 20, 256–266. doi: 10.1080/1828051x.2021.1878946

Magoc, T., and Salzberg, S. L. (2011). FLASH: fast length adjustment of short reads to improve genome assemblies. *Bioinformatics* 27, 2957–2963. doi: 10.1093/bioinformatics/btr507

Makki, K., Deehan, E. C., Walter, J., and Backhed, F. (2018). The impact of dietary fiber on gut microbiota in host health and disease. *Cell Host Microbe* 23, 705–715. doi: 10.1016/j.chom.2018.05.012

Mangifesta, M., Mancabelli, L., Milani, C., Gaiani, F., de'Angelis, N., de'Angelis, G. L., et al. (2018). Mucosal microbiota of intestinal polyps reveals putative biomarkers of colorectal cancer. *Sci. Rep.* 8:13974. doi: 10.1038/s41598-018-32413-2

Maraci, O., Antonatou-Papaioannou, A., Junemann, S., Castillo-Gutierrez, O., Busche, T., Kalinowski, J., et al. (2021). The gut microbial composition is species-specific and individual-specific in two species of estrildid finches, the bengalese finch and the zebra finch. *Front. Microbiol.* 12:619141. doi: 10.3389/fmicb.2021.619141

Marono, S., Loponte, R., Lombardi, P., Vassalotti, G., Pero, M. E., Russo, F., et al. (2017). Productive performance and blood profiles of laying hens fed *Hermetia illucens* larvae meal as total replacement of soybean meal from 24 to 45 weeks of age. *Poult. Sci.* 96, 1783–1790. doi: 10.3382/ps/pew461

Mishra, B., and Jha, R. (2019). Oxidative stress in the poultry gut: potential challenges and interventions. *Front. Vet. Sci.* 6:60. doi: 10.3389/fvets.2019.00060

Moniello, G., Ariano, A., Panettieri, V., Tulli, F., Olivotto, I., Messina, M., et al. (2019). Intestinal morphometry, enzymatic and microbial activity in laying hens fed different levels of a *Hermetia illucens* larvae meal and toxic elements content of the insect meal and diets. *Animals (Basel)* 9:86. doi: 10.3390/ani9030086

Ramlucken, U., Ramchuran, S. O., Moonsamy, G., Lalloo, R., Thantsha, M. S., and Jansen van Rensburg, C. (2019). A novel *Bacillus* based multi-strain probiotic improves growth performance and intestinal properties of *Clostridium perfringens* challenged broilers. *Poult. Sci.* 99, 331–341. doi: 10.3382/ps/pez496

Ratajczak, W., Ryl, A., Mizerski, A., Walczakiewicz, K., Sipak, O., and Laszczynska, M. (2019). Immunomodulatory potential of gut microbiome-derived short-chain fatty acids (SCFAs). *Acta Biochim. Pol.* 66, 1–12. doi: 10.18388/abp.2018_2648

Rathnayaka, S. D., Selvanathan, S., and Selvanathan, E. A. (2021). Demand for animal-derived food in selected Asian countries: a system-wide analysis. *Agric. Econ.* 52, 97–122. doi: 10.1111/agec.12609

Saracila, M., Criste, R. D., Panaite, T. D., Vlaicu, P. A., Tabuc, C., Turcu, R. P., et al. (2018). *Artemisia annua* as phytogenic feed additive in the diet of broilers (14-35 Days) reared under heat stress (32 °C). *Braz. J. Poult. Sci.* 20, 825–832. doi: 10.1590/1806-9061-2018-0772

Schiavone, A., Dabbou, S., De Marco, M., Cullere, M., Biasato, I., Biasibetti, E., et al. (2018). Black soldier fly larva fat inclusion in finisher broiler chicken diet as an alternative fat source. *Animal* 12, 2032–2039. doi: 10.1017/S1751731117003743

Sedgh-Gooya, S., Torki, M., Darbemamieh, M., Khamisabadi, H., Karimi Torshizi, M. A., and Abdolmohamadi, A. (2021). Yellow mealworm, *Tenebrio molitor* (Col: Tenebrionidae), larvae powder as dietary protein sources for broiler chickens: Effects on growth performance, carcass traits, selected intestinal microbiota and blood parameters. *J. Anim. Physiol. Anim. Nutr. (Berl.)* 105, 119–128. doi: 10.1111/jpn.13434

Shang, Y., Kumar, S., Thippareddi, H., and Kim, W. K. (2018). Effect of dietary fructooligosaccharide (FOS) supplementation on ileal microbiota in broiler chickens. *Poult. Sci.* 97, 3622–3634. doi: 10.3382/ps/pey131

Shi, J., Zhao, D., Song, S., Zhang, M., Zamaratskaia, G., Xu, X., et al. (2020). High-meat-protein high-fat diet induced dysbiosis of gut microbiota and tryptophan metabolism in wistar rats. *J. Agric. Food Chem.* 68, 6333–6346. doi: 10.1021/acs.jafc.0c00245

Smetana, S., Schmitt, E., and Mathys, A. (2019). Sustainable use of *Hermetia illucens* insect biomass for feed and food: attributional and consequential life cycle assessment. *Resour. Conserv. Recycl.* 144, 285–296. doi: 10.1016/j.resconrec.2019.01.042

Wang, A. H., and Hogan, N. S. (2019). Performance effects of feed-borne *Fusarium mycotoxins* on broiler chickens: Influences of timing and duration of exposure. *Anim. Nutr.* 5, 32–40. doi: 10.1016/j.aninu.2018.08.001

Wang, J., Fan, H., Han, Y., Wei, J. P., Zhao, J. Z., and Zhou, Z. J. (2017). Pyrosequencing of the broiler chicken gastrointestinal tract reveals the regional

similarity and dissimilarity of microbial community. *Can. J. Anim. Sci.* 97, 302–313. doi: 10.1139/cjas-2015-0120

Wang, T., Shen, Q., Feng, W., Wang, C., and Yang, F. (2020). Aqueous ethyl acetate as a novel solvent for the degreasing of black soldier fly (*Hermetia illucens* L.) larvae: degreasing rate, nutritional value evaluation of the degreased meal, and thermal properties. *J. Sci. Food Agric.* 100, 1204–1212. doi: 10.1002/jsfa.10131

Wang, Y. S., and Shelomi, M. (2017). Review of black soldier fly (*Hermetia illucens*) as animal feed and human food. *Foods* 6:91. doi: 10.3390/foods6100091

Weththasinghe, P., Lagos, L., Cortes, M., Hansen, J. O., and Overland, M. (2021). Dietary inclusion of black soldier fly (*Hermetia illucens*) larvae meal and paste improved gut health but had minor effects on skin mucus proteome and immune response in Atlantic salmon (*Salmo salar*). *Front. Immunol.* 12:599530. doi: 10.3389/fimmu.2021.599530

Xia, Y., Wang, M., Gao, F., Lu, M., and Chen, G. (2020). Effects of dietary probiotic supplementation on the growth, gut health and disease resistance of juvenile Nile tilapia (*Oreochromis niloticus*). *Anim. Nutr.* 6, 69–79. doi: 10.1016/j.aninu.2019.07.002

Xie, Y., Liu, J., Wang, H., Luo, J., Chen, T., Xi, Q., et al. (2020). Effects of fermented feeds and ginseng polysaccharides on the intestinal morphology and microbiota composition of Xuefeng black-bone chicken. *PLoS One* 15:e0237357. doi: 10.1371/journal.pone.0237357

Yadav, S., and Jha, R. (2019). Strategies to modulate the intestinal microbiota and their effects on nutrient utilization, performance, and health of poultry. *J. Anim. Sci. Biotechnol.* 10:2. doi: 10.1186/s40104-018-0310-9

Yu, M., Li, Z., Chen, W., Wang, G., Rong, T., Liu, Z., et al. (2020). *Hermetia illucens* larvae as a fishmeal replacement alters intestinal specific bacterial populations and immune homeostasis in weanling piglets. *J. Anim. Sci.* 98:skz395. doi: 10.1093/jas/skz395

Yue, S., Zhao, D., Peng, C., Tan, C., Wang, Q., and Gong, J. (2019). Effects of theabrownin on serum metabolites and gut microbiome in rats with a high-sugar diet. *Food Funct.* 10, 7063–7080. doi: 10.1039/c9fo01334b

Zhang, S., Zhong, G., Shao, D., Wang, Q., Hu, Y., Wu, T., et al. (2021). Dietary supplementation with *Bacillus subtilis* promotes growth performance of broilers by altering the dominant microbial community. *Poult. Sci.* 100:100935. doi: 10.1016/j.psj.2020.12.032

Zhao, J., Zhang, X., Liu, H., Brown, M. A., and Qiao, S. (2019). Dietary protein and gut microbiota composition and function. *Curr. Protein Pept. Sci.* 20, 145–154. doi: 10.2174/1389203719666180514145437

Zhao, Y., Li, K., Luo, H., Duan, L., Wei, C., Wang, M., et al. (2019). Comparison of the intestinal microbial community in ducks reared differently through high-throughput sequencing. *Biomed. Res. Int.* 2019:9015054. doi: 10.1155/2019/9015054

Conflict of Interest: BX was employed by Hunan Yunfeifeng Agricultural Co. Ltd.

The remaining authors declare that the research was conducted in the absence of any commercial or financial relationships that could be construed as a potential conflict of interest.

The reviewer RF declared a shared affiliation, with no collaboration, with the authors, to the handling editor at the time of the review.

Publisher's Note: All claims expressed in this article are solely those of the authors and do not necessarily represent those of their affiliated organizations, or those of the publisher, the editors and the reviewers. Any product that may be evaluated in this article, or claim that may be made by its manufacturer, is not guaranteed or endorsed by the publisher.

frontiers in Microbiology

ORIGINAL RESEARCH
published: 05 October 2021
doi: 10.3389/fmicb.2021.739572

Effects of Supplementing Intestinal Autochthonous Bacteria in Plant-Based Diets on Growth, Nutrient Digestibility, and Gut Health of Bullfrogs (*Lithobates catesbeianus*)

Zhe Wang[1], Chunxiao Zhang[1], Kangle Lu[1], Kai Song[1], Xueshan Li[1], Ling Wang[1] and Samad Rahimnejad[2]*

[1] Xiamen Key Laboratory for Feed Quality Testing and Safety Evaluation, Fisheries College, Jimei University, Xiamen, China, [2] South Bohemian Research Center of Aquaculture and Biodiversity of Hydrocenoses, Faculty of Fisheries and Protection of Waters, University of South Bohemia in České Budějovice, České Budějovice, Czechia

OPEN ACCESS

Edited by:
Jia Yin,
Hunan Normal University, China

Reviewed by:
Sun Yun,
Hainan University, China
Sergio Enrique Pasteris,
Universidad Nacional de Tucumán, Argentina

***Correspondence:**
Ling Wang
lingwang@jmu.edu.cn

Specialty section:
This article was submitted to Microbial Symbioses, a section of the journal Frontiers in Microbiology

Received: *11 July 2021*
Accepted: *10 September 2021*
Published: *05 October 2021*

Citation:
Wang Z, Zhang C, Lu K, Song K, Li X, Wang L and Rahimnejad S (2021) Effects of Supplementing Intestinal Autochthonous Bacteria in Plant-Based Diets on Growth, Nutrient Digestibility, and Gut Health of Bullfrogs (Lithobates catesbeianus). Front. Microbiol. 12:739572. doi: 10.3389/fmicb.2021.739572

Poor utilization efficiency of plant protein diets always leads to intestinal barrier dysfunction and growth inhibition in animals. Probiotics have shown promise in improving growth performance and gut health of the host. However, obtaining the host-beneficial probiotic from thousands of bacterial phylotypes is challenging. Here, four intestinal autochthonous bacteria were isolated from fast-growing bullfrog after a 60-day feeding on a soybean meal (SM)-based diet. Another feeding trial was conducted to evaluate the effects of supplementing these strains in an SM-based diet on growth, nutrient digestibility, immunity, and gut health of bullfrog. A high-SM basal diet was used as a non-supplemented control group (NC), and four other diets were prepared by supplementing the basal diet with 1×10^7 CFU/g of *Bacillus siamensis*, *Bacillus tequilensis* (BT), *Bacillus velezensis*, and *Lactococcus lactis* (LL). Results showed that weight gain, feed efficiency, nitrogen retention, and apparent digestibility coefficients of dry matter and protein were significantly higher in the LL group compared with the NC group ($p < 0.05$). Furthermore, compared with the NC group, both BT and LL groups showed markedly higher jejunal protease and amylase activities, serum complement 4 and immunoglobulin M levels, jejunal muscularis thickness ($p < 0.05$), and up-regulated expression of *il-10* and *zo-1* genes ($p < 0.05$). High-throughput sequencing revealed higher abundances of *Bacillus* and *Cetobacterium* in BT and LL groups, respectively, accompanied with decreased abundances of *Enterobacter* and *Escherichia–Shigella*. Besides, KEGG pathways related to metabolisms were significantly enhanced by the LL diet relative to the NC diet ($p < 0.05$). Overall, the beneficial effects of two frog-derived probiotics were determined: supplementation of *L. lactis* in SM-based diet promoted growth and nutrient digestibility; both *B. tequilensis* and *L. lactis* supplementation improved immune response and intestinal barrier function of bullfrogs.

Keywords: *Lithobates catesbeianus*, autochthonous bacteria, gut structure, gut microbiota, soybean meal-based diet

INTRODUCTION

Plant proteins are widely used as substitutes for expensive animal-derived protein sources in aquaculture and livestock sectors (Li Z.C. et al., 2017; Naylor et al., 2021). However, due to their general drawbacks such as low palatability, imbalanced amino acid profile, and presence of anti-nutritional factors (Liu et al., 2019; Peng et al., 2019; Yao et al., 2019), an excess proportion of plant proteins in diets usually induce immune dysfunction, gut inflammation, and subsequent growth inhibition in animals (Sahlmann et al., 2013; Wang et al., 2020).

Recently, probiotics have garnered significant attraction for disease prevention and growth promotion in aquaculture (Melo-Bolivar et al., 2021). Efficacy of probiotics is dictated by genetic, nutritional, and environmental factors, and the origin of the probiotic strains, accordingly some probiotics are only effective in specific animals (Sun et al., 2009). To avoid potentially harmful effects on the host and endogenous microbiota, intestinal autochthonous bacteria have more advantages over allochthonous bacteria in colonizing host's intestinal mucosa and exerting physiological effects (Ringø et al., 2018). In addition, it has been reported that bacteria attached to the intestinal epithelial surfaces are more likely to be the real autochthonous bacteria (Denev et al., 2009). Bullfrog (*Lithobates catesbeianus*) has become one of the most economically valuable farmed amphibians worldwide. The evaluation of the cultivable indigenous microbiota from bullfrog specimens has already been performed as well as the study of the beneficial properties of some bacterial groups to advance in the design of probiotics to control both bacterial and fungal diseases (Montel Mendoza et al., 2012; Niederle et al., 2019). Some *in vivo* studies proposed the use of native or commercial lactic acid bacteria as potential probiotics for bullfrog hatcheries (de Clarla Dias et al., 2010; Pereira et al., 2016, 2018). However, information about the application of autochthonous probiotics isolated from intestinal mucosa of bullfrogs is scarce.

Growth rate of animals is determined by a series of factors such as ambient temperature, stocking density, available nutrients, etc. (Baltz et al., 1998; Nielsen, 2012). In addition, increasing studies showed that gut microbiota is deeply involved in various host physiological processes (Gao et al., 2018). Thus, it can be regarded as an "internal factor," which confers multifaceted effects on the host. Remarkable growth difference usually occurs in farmed animals in breeding industry although they might be reared under the same environmental and dietary conditions. Sun et al. (2009) found that gut microbial composition differs in fast-growing (FG) and slow-growing (SG) groupers where higher abundances of potential pathogens were recorded in SG individuals. Similarly, Gui et al. (2017) reported that gut microbiota of FG chicken showed higher diversity and richness compared with the slow- and medium-growing chicken. Furthermore, a research on sea cucumber (*Apostichopus japonicus*) revealed that the differences in *Actinobacteria* abundance might be associated with the remarkable difference in body weight (Sha et al., 2016). These studies indicated that the growth of animals is closely linked to the gut microbiota. Although gut microbiota has long been researched through traditional and molecular techniques, information on intestinal microbiota–host crosstalk is scarce. Thus, recognition of the host-beneficial probiotics from thousands of bacterial phylotypes is challenging. Besides, as diet plays a key role in animals' gut community, whether some sort of bacterial species enriched by a specific diet could in turn contribute to utilization of the same diet is uncertain.

Soybean meal (SM) has been widely used as a typical plant protein source in aquafeed. Previous studies conducted in our laboratory showed that high-SM diet caused intestine inflammation in bullfrog referred to as SM-induced enteritis (SBMIE), accompanied with poor growth and feed utilization (Ding et al., 2019; Yang et al., 2019). In the present study, initially a high-SM diet was fed to bullfrogs for 60 days. Presumably, the FG individuals might harbor a more favorable gut microbiota, which could adapt to the gut environment established by the SM-based diet, and this in turn contributes to the host's growth. Then, the dominant gut bacterial species enriched in FG bullfrogs were isolated. A 58-day feeding trial was conducted to investigate the effects of supplementing these bacterial strains in a high-SM diet on growth performance, feed utilization, nutrient digestibility, immune function, and gut health of bullfrog.

MATERIALS AND METHODS

Preparation of Candidate Bacterial Strains

A high-SM diet (**Supplementary Table 1**) was used to feed 108 bullfrogs of similar size (26.14 ± 0.21 g) for 60 days. After the feeding trial, bullfrogs were euthanized by destroying the spinal cord with a pin and weighed (Wang et al., 2020). Then, 12 heaviest bullfrogs and 12 lightest bullfrogs were sampled and grouped into FG and SG groups, respectively. The gut brush border membranes (mucosa) of bullfrogs from two groups were scraped with a coverslip on ice under sterile conditions, and then moved into sterile tubes. The mucosa samples were homogenized in normal saline solution (NSS, 0.7% NaCl). After gradient dilution, each dilution was evenly spread onto three different plates in triplicate, including nutrient agar (pH 7.3 ± 0.1), Man Rogosa Sharpe (pH 6.5 ± 0.2) agar, and Bacillus agar (pH 7.0 ± 0.2; Hopebio Technology Co. Ltd, China). The plates were incubated in normoxic incubator (33°C for 24 h) for growth of aerobic and facultative anaerobic bacteria. Then, the bacterial colonies were divided into different types based on the colony characteristics of shape, structure, size, opacity, and color, and the colonies of each recognizable type was counted for determining number and occurrence rate [(the number of plates containing the strain)/(the number of all plates) × 100]. Then, three to five representatives of each colony type were streaked on corresponding plates repeatedly until pure cultures were obtained. Finally, a total of 35 representative isolates with different types were successfully isolated from agar plates, and the isolates with higher occurrence rates and numbers in the plates of the FG group compared with those of the SG group (**Table 1**) were picked up for gene sequencing. The bacterial DNA was extracted using bacterial genome DNA extraction kits (SBS

Genetech, China) and sent for sequence analysis of the 16S rRNA gene by Majorbio Bio-pharm Technology Co., Ltd. (Shanghai, China). The 16S rRNA sequences were blast in Ezbiocloud to determine genetic homology.

Preparation of Experimental Diets

Bacillus species and a lactic acid bacterium were cultured in nutrient broth or MRS broth overnight. These cultures were then centrifuged at 4,000 × *g* for 5 min, and the bacterial pellets were suspended in sterile NSS after washing twice with NSS. The number of alive bacterial cells in the suspensions was determined by plate-counting method (Balestra and Misaghi, 1997). A basal diet (**Supplementary Table 1**) containing 55% SM was produced following the protocol described by Li et al. (2019). Four treated diets were prepared by supplementing the basal diet with 1×10^7 CFU/g feed of bacterial suspension of *Bacillus siamensis* (BS diet), *Bacillus tequilensis* (BT diet), *Bacillus velezensis* (BV diet), and *Lactococcus lactis* (LL diet). The non-supplemented control diet (NC diet) was supplemented with equivalent sterile NSS, then all diets were encapsulated with a

TABLE 1 | Species with a higher occurrence rate or number in plates of fast-growing (FG) group compared with those of slow-growing (SG) group.

Species	FG		SG	
	Occurrence rate (%)	CFU/g	Occurrence rate (%)	CFU/g
Lactococcus lactis subsp. *lactis*[a]	100.00	4.76×10^6	50.00	5.93×10^5
Chryseobacterium pennipullorum[b]	75.00	3.93×10^6	83.00	4.31×10^5
Bacillus velezensis[c]	66.67	2.12×10^6	50.00	1.99×10^6
Bacillus siamensis[d]	50.00	4.75×10^4	41.60	2.25×10^4
Escherichia fergusonii[e]	34.00	7.5×10^3	–	–
Bacillus tequilensis[f]	50.00	–[h]	–	–
Microbacterium lacticum[g]	50.00	–	–	–

Species were generally recorded in [a,g]Man Rogosa Sharpe plates, [b,c,e]Nutrient agar plates, and [d,f]Bacillus agar plates; [h]invalid data.

TABLE 2 | Growth performance, feed utilization, organosomatic indices, and survival of bullfrog.

	NC	BS	BT	BV	LL
FBW (g)	160.27 ± 2.01^{a}	165.82 ± 4.69^{ab}	172.33 ± 3.68^{ab}	160.64 ± 1.87^{a}	180.09 ± 2.06^{b}
WG (%)	443.87 ± 9.54^{a}	463.08 ± 15.90^{ab}	487.88 ± 12.07^{ab}	440.26 ± 6.21^{a}	503.55 ± 6.14^{b}
FR (%/day)	2.44 ± 0.01^{ab}	2.46 ± 0.02^{b}	2.45 ± 0.00^{b}	2.45 ± 0.01^{b}	2.40 ± 0.01^{a}
FE	0.97 ± 0.00^{a}	0.98 ± 0.00^{ab}	1.00 ± 0.01^{b}	0.97 ± 0.00^{a}	1.03 ± 0.00^{c}
NRR (%)	33.81 ± 1.12^{a}	35.93 ± 0.30^{ab}	35.97 ± 1.13^{ab}	31.75 ± 1.24^{a}	39.55 ± 0.25^{b}
Survival (%)	100.00 ± 0.00^{a}	100.00 ± 0.00^{a}	100.00 ± 0.00^{a}	100.00 ± 0.00^{a}	100.00 ± 0.00^{a}
HSI (%)	4.73 ± 0.54^{a}	5.52 ± 0.04^{a}	5.36 ± 0.28^{a}	5.33 ± 0.57^{a}	5.09 ± 0.74^{a}
HLI (%)	33.90 ± 3.97^{a}	38.66 ± 0.50^{a}	38.13 ± 0.09^{a}	38.05 ± 0.51^{a}	40.65 ± 0.41^{a}

[a–c]Mean values in the same row with different superscripts differ significantly ($p < 0.05$).
NC, control diet; BS, control diet containing 1×10^7 CFU/g of Bacillus siamensis; BT, control diet containing 1×10^7 CFU/g of Bacillus tequilensis; BV, control diet containing 1×10^7 CFU/g of Bacillus velezensis; LL, control diet containing 1×10^7 CFU/g of Lactococcus lactis; FBW, final body weight; WG, weight gain; FR, feeding rate; FCR, feed efficiency; NRR, nitrogen retention ratio; HSI, hepatosomatic index; and HLI, hind leg index.

TABLE 3 | Body composition analysis (%, wet weight) of bullfrog.

	NC	BS	BT	BV	LL
Whole body					
Moisture	75.63 ± 0.65^{ab}	74.73 ± 0.29^{ab}	73.85 ± 0.68^{ab}	75.99 ± 0.53^{b}	73.24 ± 0.38^{a}
Protein	14.31 ± 0.34^{a}	15.12 ± 0.10^{ab}	14.94 ± 0.48^{ab}	13.71 ± 0.40^{a}	15.95 ± 0.12^{b}
Lipid	6.14 ± 0.14^{a}	6.24 ± 0.08^{a}	6.08 ± 0.12^{a}	6.01 ± 0.14^{a}	6.30 ± 0.16^{a}
Ash	2.65 ± 0.08^{a}	2.65 ± 0.06^{a}	2.71 ± 0.07^{a}	2.73 ± 0.12^{a}	2.67 ± 0.04^{a}
Muscle					
Moisture	77.75 ± 0.62^{ab}	78.16 ± 0.42^{ab}	76.37 ± 0.30^{a}	78.54 ± 0.38^{b}	76.77 ± 0.19^{ab}
Protein	20.36 ± 0.57^{ab}	19.92 ± 0.38^{ab}	21.34 ± 0.28^{b}	19.39 ± 0.37^{a}	20.49 ± 0.23^{ab}
Lipid	0.55 ± 0.02^{a}	0.53 ± 0.02^{a}	0.56 ± 0.00^{a}	0.52 ± 0.01^{a}	0.56 ± 0.01^{a}

[a,b]Mean values in the same row with different superscripts differ significantly ($p < 0.05$).
NC, control diet; BS, control diet containing 1×10^7 CFU/g of Bacillus siamensis; BT, control diet containing 1×10^7 CFU/g of Bacillus tequilensis; BV, control diet containing 1×10^7 CFU/g of Bacillus velezensis; and LL, control diet containing 1×10^7 CFU/g of Lactococcus lactis.

mixture of fish oil and soybean oil and dried in the shade. To ensure the viability of bacterial cells, diets were prepared every 2 weeks and stored at −20°C until used.

Feeding Trial

Bullfrogs were obtained from a commercial farm and transported to the fisheries laboratory of Jimei University (Xiamen, China). Before starting the experiment, bullfrogs were reared in an indoor aquarium (π × 160 × 80 cm) supplied with 4–6 cm of freshwater. All bullfrogs were fed the basal diet twice daily for 3 weeks to acclimate them to experimental conditions. Then, a total of 195 disease-free bullfrogs with homogenous size (initial mean body weight 29.61 ± 0.28 g) were equally divided into five groups with triplicates per group (13 bullfrogs per tank), and they were allocated into fifteen 10-L tanks. Bullfrogs within three tanks were randomly assigned to each dietary treatment and hand-fed to apparent satiation twice daily (8:00 and 18:00) for 58 days. After each feeding, the uneaten feeds were siphoned out and the water in each tank was entirely renewed with fresh water. Feces samples in each tank were collected as described by Lin et al. (2020) over the last 2 weeks for digestibility analysis. During the feeding period, a 12 h light/12 h dark photoperiod was maintained by fluorescent lamp, air temperature ranged from 28 to 32°C, and water temperature ranged from 27 to 31°C.

Sample Collection

At the end of the feeding trial, bullfrogs were fasted for 24 h and euthanized by destroying the spinal cord with a pin. The number and total weight of bullfrogs in each tank were recorded for analyses of survival and final body weight. Three bullfrogs per tank were randomly sampled and frozen at −20°C for body composition analysis. The abdomen of 10 additional bullfrogs in each tank was opened immediately with sterile scissors. Blood samples of the aforementioned bullfrogs were collected from ductus arteriosus using a sterile syringe, transported into sterile tubes, and kept at 4°C overnight. Then, serum was separated after centrifugation (3,000 × *g*, 10 min, 4°C) and stored at −80°C for further analyses. Liver and hind legs were dissected from three bullfrogs per tank and weighed for calculations of hepatosomatic index (HSI) and hind leg index (HLI). The jejunum samples were collected from two bullfrogs per tank and fixed in Bouin's solution for morphology analysis. Jejunum samples were collected from three bullfrogs per tank and kept at −80°C for tissue RNA extraction and analysis of enzyme activity. Jejunum samples of

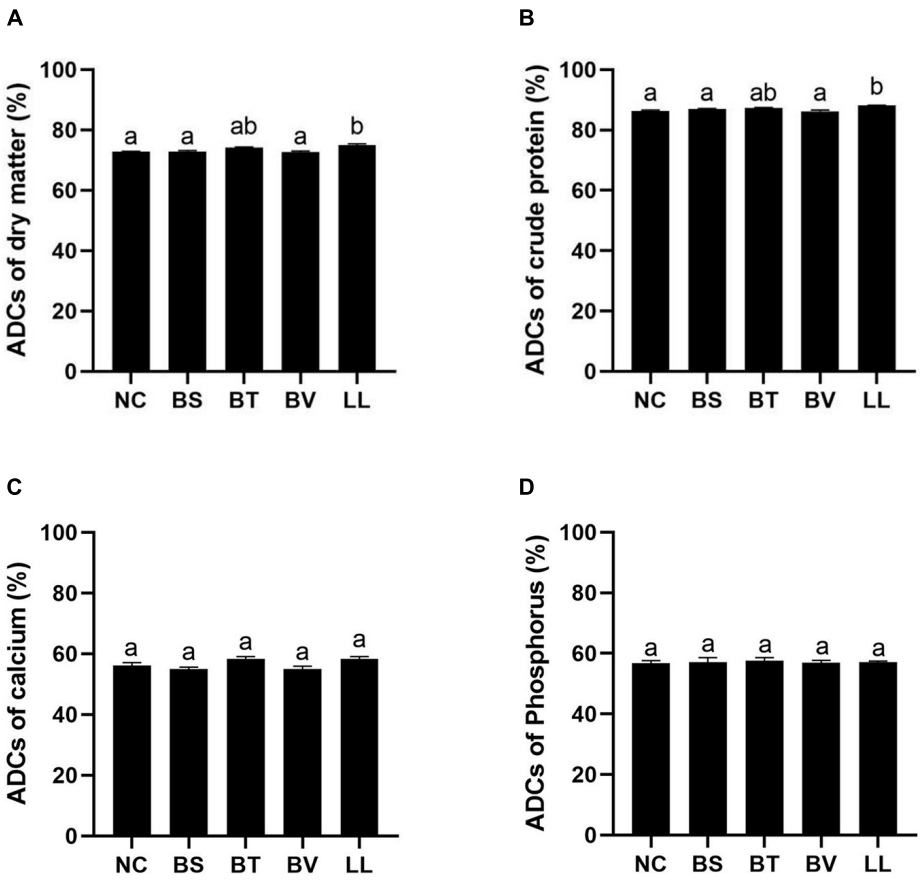

FIGURE 1 | Apparent digestibility coefficients (ADCs) of nutrients: **(A)** dry matter, **(B)** protein, **(C)** calcium, and **(D)** phosphorus. Bars with different letters were significantly different ($p < 0.05$). NC, control diet; BS, control diet containing 1×10^7 CFU/g of *Bacillus siamensis*; BT, control diet containing 1×10^7 CFU/g of *Bacillus tequilensis*; BV, control diet containing 1×10^7 CFU/g of *Bacillus velezensis*; and LL, control diet containing 1×10^7 CFU/g of *Lactococcus lactis*.

two bullfrogs per tank were sampled and pooled for intestinal microbiota analysis.

Chemical Composition

The crude protein, crude lipid, moisture, and ash contents in diet, whole body, muscle, and feces samples were analyzed according to the standard method of AOAC (2002). Moisture content was estimated by drying in an oven at 105°C until a constant weight was reached. Crude protein (N × 6.25) was determined by the Dumas method (Gerhardt, Germany). Crude lipid content was quantified by ether extraction, and ash content was measured by the combustion method in a muffle furnace at 550°C for 8 h. The mineral element content of samples was determined by inductively coupled plasma atomic emission spectroscopy (ICP-OES; Leeman, United States).

Digestive Enzymes

Intestine samples were homogenized in 10 volumes (w/v) of NSS and centrifuged at 3,000 × *g* for 10 min. Then, the homogenized solution was collected and stored at 4°C. The protease activity was measured by Folin-phenol method (Lowry et al., 1951). One unit of protease activity was defined as the amount of the hydrolysis of casein that liberated 1 μg of tyrosine per minute. Lipase and amylase activities were quantified using commercial kits (Nanjing Jiancheng Biological Company, China). One unit of lipase activity was defined as the amount of enzyme that hydrolyzes 1 μmol substrate per minute at 37°C. One unit of amylase activity was defined as the amount of protein that hydrolyzed 10 mg starch per 30 min at 37°C.

Gut Barrier Function and Immune Parameters

Serum D-lactate concentration, complement 3 (C3), complement 4 (C4), and IgM levels were measured by competition method according to Syedbasha et al. (2016) using amphibian ELISA kits from Nanjing Jiancheng Biological Company (Nanjing, China). Serum diamine oxidase (DAO) and lysozyme (LZM) activities were determined by colorimetric method using commercial assay kits (Nanjing Jiancheng Bioengineering Institute, China). One unit of LZM activity was defined as the amount of enzyme needed to decrease absorbance at a rate of 0.001 $min^{-1} \cdot ml^{-1}$ at 37°C, and one unit of DAO activity was defined as 1 mmol ammonia formed per minute per milliliter of serum at 37°C.

Quantitative Real-Time PCR

Total RNA was extracted from jejunum of bullfrogs using FastPure Tissue Total RNA Isolation Kit (Vazyme Biotech Co., Ltd, China). The purity of the total RNA was analyzed in 1% agarose gel electrophoresis, and the concentration of the total RNA was quantitated using NanoDrop One Ultramicro spectrophotometer (Thermo Fisher, United States). Total RNA was reversely transcribed to cDNA by TransScript ALL-in-one First-Strand cDNA Synthesis Kit (TransGen Biotech Co., Ltd., China). Quantitative PCR was performed on ABI StepOne Plus (Thermal Cycler, United States). The primers of the gene (**Supplementary Table 2**) and PCR amplification program were designed as our previous research on bullfrogs (Ding et al., 2019; Lin et al., 2021). The relative expression levels of genes were calculated using $2^{-\Delta\Delta Ct}$ method.

Gut Histology

Jejunal samples were stained with H&E following the standard histological procedures conducted by Servicebio Biotechnology Co., Ltd. (Wuhan, China). The micrographs were observed with

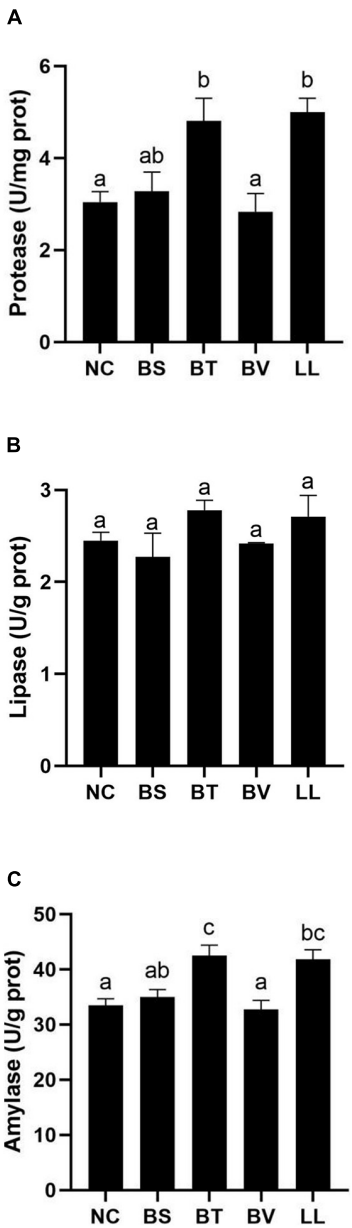

FIGURE 2 | Digestive enzymes activity in jejunum of bullfrog: **(A)** protease, **(B)** lipase, and **(C)** amylase. Bars with different letters were significantly different ($p < 0.05$). NC, control diet; BS, control diet containing 1 × 10^7 CFU/g of *Bacillus siamensis*; BT, control diet containing 1 × 10^7 CFU/g of *Bacillus tequilensis*; BV, control diet containing 1 × 10^7 CFU/g of *Bacillus velezensis*; and LL, control diet containing 1 × 10^7 CFU/g of *Lactococcus lactis*.

a light microscope (Leica DM5500B, Germany), and Image J software was used for morphometric analysis.

Illumina High-Throughput Sequencing

Bacterial DNA was extracted from bullfrog jejunum using HiPure Soil DNA Kits (Magen, China). The DNA yield was detected using Nanodrop 2000 (Thermo Scientific, United States). The amplicons of 16S rRNA gene V3–V4 region were extracted from 2% agarose gel, purified by the AxyPrep DNA Gel Extraction Kit (Axygen Biosciences, United States), and quantified using ABI StepOnePlus Real-Time PCR System (Life Technologies, United States). Then, the purified amplicons were paired-end sequenced on Illumina MiSeq PE 250 (Gene *Denovo* Biotechnology Co., Ltd., China).

Noisy sequences of raw tags were filtered by QIIME software to obtain high-quality clean tags. Clean tags were searched against the reference database to perform reference-based chimera checking using UCHIME algorithm. All chimeric tags were removed and finally obtained effective tags were used for further analysis. The effective tags were clustered into operational taxonomic units (OTUs) of ≥97% similarity using UPARSE software. The tag sequence with the highest abundance was selected as a representative sequence within each cluster. Venn analysis and principal coordinates analysis (PCoA) based on Jaccard distance matrix were performed in R project package. The representative sequences were classified into organisms using RDP classifier based on SILVA database with the confidence threshold value of 80%. The abundance statistics of each taxonomy were visualized using Krona. The KEGG pathway analysis of the OTUs was inferred using PICRUSt2 (Douglas et al., 2020). Analysis of function difference between groups was calculated by Welch's *t*-test in R project package. The raw reads were uploaded to NCBI Sequence Read Archive database (accession number PRJNA747862).

Calculation and Statistical Analysis

Weight gain (WG, %) = $(W_1 - W_0)/W_0 \times 100$

Feeding rate (FR, %/day) = $W_D/(W_1/2 + W_0/2)/t \times 100$

Feed efficiency (FE) = $(W_1 - W_0)/W_D$

Nitrogen retention ratio (NRR, %) = $(W_1 \times P_1 - W_0 \times P_0)/(W_D \times P_D) \times 100$

Survival (%) = $N_1/N_0 \times 100$

Hepatosomatic index (%) = liver weight/$W_1 \times 100$

Hind leg index (%) = hind leg weight/$W_1 \times 100$

Apparent digestibility coefficients (ADCs, %) = $(1 - F_0/D_0 \times (D_Y/F_Y)) \times 100$

Where W_1 and W_0 are the mean final and initial wet body weights, respectively; W_D is dry feed intake; t is feeding days; P_D, P_0, and P_1 are the concentrations of crude protein in the diet, initial body, and final body, respectively; N_0 and N_1 are the initial and final number of bullfrogs, respectively; D_Y and F_Y are the concentration of yttrium in diet and feces, respectively; and D_0 and F_0 are the quantities of compositions in diets and feces, respectively.

The homogeneity of variances of data was tested before further analysis. The significance of difference between the FG group and the SG group was analyzed by Student's *t*-test using SPSS 22.0. One-way ANOVA followed by Tukey multiple comparison test was used to identify differences among NC, BT, BV, BS, and LL groups. The values are presented as mean ± SEM and the differences were considered significant at $p < 0.05$.

RESULTS

Preparation of Candidate Bacterial Strains

After the 60-day feeding on the SM-based diet, the FG group showed significantly higher WG than the SG group ($p < 0.05$; **Supplementary Figure 1**). Some species enriched in the gut of the FG group, but scarce in the gut of the SG group, and the species with higher occurrence rate and numbers in the FG group compared with the SG group are listed in **Table 1**. Three *Bacillus* species (*B. siamensis*, *B. tequilensis*, and *B. velezensis*) and a lactic acid bacterium (*L. lactis* subsp. *lactis*) were then selected for the subsequent feeding trial.

Growth Performance, Feed Utilization, and Organosomatic Indices

Compared with the NC group, WG was significantly increased in bullfrogs fed the LL diet ($p < 0.05$), and intermediary WG values were observed in BS and BT groups ($p > 0.05$; **Table 2**). No marked difference was found in FR between the NC group and each treated group ($p > 0.05$). LL supplementation led to a remarkable increment of FE compared with the other groups ($p < 0.05$). Moreover, the highest NRR was found in the LL group, which was significantly higher than that in NC and BV groups

TABLE 4 | Humoral immune parameters including LZM, IgM, C3, and C4 of bullfrog.

	NC	BS	BT	BV	LL
LZM (U/ml)	632.96 ± 52.83^{a}	651.68 ± 76.48^{a}	812.73 ± 52.83^{ab}	573.03 ± 45.41^{a}	996.25 ± 103.86^{b}
IgM (μg/ml)	359.88 ± 25.12^{a}	394.18 ± 10.40^{ab}	466.22 ± 10.49^{b}	316.71 ± 10.76^{a}	547.56 ± 22.33^{c}
C3 (μg/ml)	141.26 ± 10.06^{a}	155.4 ± 10.05^{ab}	178.26 ± 12.09^{ab}	138.27 ± 12.56^{a}	202.28 ± 6.29^{b}
C4 (μg/ml)	107.23 ± 4.04^{a}	113.80 ± 5.42^{a}	135.80 ± 3.86^{b}	100.40 ± 6.21^{a}	156.18 ± 2.60^{b}

$^{a-c}$*Mean values in the same row with different superscripts differ significantly ($p < 0.05$).*

NC, control diet; BS, control diet containing 1 × 10^7 CFU/g of Bacillus siamensis; BT, control diet containing 1 × 10^7 CFU/g of Bacillus tequilensis; BV, control diet containing 1 × 10^7 CFU/g of Bacillus velezensis; LL, control diet containing 1 × 10^7 CFU/g of Lactococcus lactis; LZM, lysozyme; IgM, immunoglobulin M; C3, complement 3; and C4, complement 4.

($p < 0.05$). No significant difference was observed in survival, HSI, and HLI among all groups ($p > 0.05$).

Body Composition

Bullfrogs fed the LL diet exhibited markedly higher whole-body protein content than both NC and BV groups ($p < 0.05$; **Table 3**). Whole-body moisture content significantly decreased in the LL group compared with that in the BV group ($p < 0.05$). Higher protein but lower moisture contents were found in the muscle of the BT group compared with that of the BV group ($p < 0.05$). No significant changes were found in whole-body lipid and ash, and muscle lipid contents ($p > 0.05$).

Nutrient Digestibility and Digestive Enzyme Activity

Apparent digestibility coefficients of dry matter and crude protein were significantly increased in the LL group compared with those in NC, BS, and BV groups ($p < 0.05$; **Figures 1A,B**). There were no marked changes in ADCs of calcium and phosphorus among all groups ($p > 0.05$; **Figures 1C,D**). In addition, LL and BT groups exhibited profoundly higher jejunal protease and amylase activities than NC and BV groups ($p < 0.05$; **Figures 2A,C**). Bacteria supplementation did not significantly affect jejunal lipase activity ($p > 0.05$; **Figure 2B**).

Humoral Immunity

Bullfrogs fed LL diet showed significantly higher serum LZM activity and C3 level compared with the NC group ($p < 0.05$; **Table 4**). Moreover, serum C4 and IgM levels were remarkably increased in both BT and LL groups relative to NC and BV groups ($p < 0.05$). BS and BV diets did not affect the aforementioned immune parameters in bullfrogs ($p > 0.05$).

Jejunal Morphology, Tight Junction Proteins, and Epithelial Permeability

A typical SBMIE phenomenon was detected in the jejunal epithelium of NC, BS, and BV groups, including shrunken mucosal folds, narrow muscularis, and partial separation of tissue (**Figure 3A**). Conversely, the mucosal folds in the LL group were longer and curlier, accompanied by more branches. Besides, no obvious separation of tissue or degenerative changes were found in the BT and LL groups. Morphometric analysis of jejunum showed increased number ($p < 0.05$) and height ($p > 0.05$) of mucosal folds in the LL group compared with the NC group (**Table 5**). Furthermore, muscularis thickness in BT and LL groups was significantly higher than that in the other groups ($p < 0.05$). There was no significant difference in mucosal fold width and lamina propria thickness among groups ($p > 0.05$). In addition, the mRNA expression of tight junction protein *zo-1* ($p < 0.05$) and *occludin* ($p > 0.05$) increased in BT and LL groups compared with the NC group (**Figures 3B,C**). Moreover, compared with the NC group, BT and LL diets resulted in a significant reduction of serum DAO activity ($p < 0.05$; **Figure 3D**). However, no significant difference was found in serum D-lactate concentration among all groups ($p > 0.05$; **Figure 3E**).

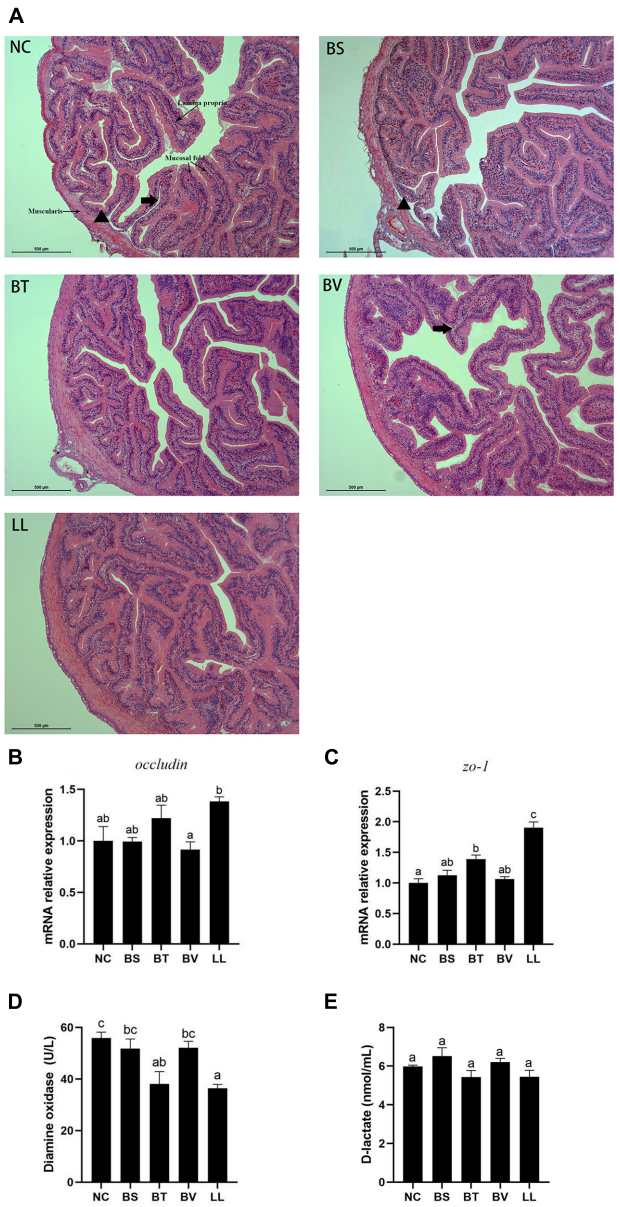

FIGURE 3 | (A) Jejunal morphology of bullfrog using H&E staining. The arrow pointed to the separation between lamina propria and mucosa. The triangle pointed to the separation between submucosa and muscularis. **(B,C)** Expression of tight junction proteins genes (*occludin* and *zo-1*) in jejunum of bullfrog. **(D,E)** Intestinal epithelial permeability indicators (diamine oxidase and D-lactate) in serum of bullfrog. Bars with different letters were significantly different ($p < 0.05$). *zo*, zonula occludens; NC, control diet; BS, control diet containing 1×10^7 CFU/g of *Bacillus siamensis*; BT, control diet containing 1×10^7 CFU/g of *Bacillus tequilensis*; BV, control diet containing 1×10^7 CFU/g of *Bacillus velezensis*; and LL, control diet containing 1×10^7 CFU/g of *Lactococcus lactis*.

Jejunal Inflammatory Cytokines

Compared with the NC group, BT and LL supplementation led to up-regulated expression of anti-inflammatory cytokines including *il-10* ($p < 0.05$) and *il-4* ($p > 0.05$) genes

TABLE 5 | Jejunum morphological indices of bullfrog.

	NC	BS	BT	BV	LL
Number of mucosal folds	28.83 ± 1.45^{ab}	30.0 ± 1.21^{ab}	33.33 ± 1.86^{bc}	25.67 ± 0.84^{a}	36.17 ± 1.01^{c}
Mucosal fold height (μm)	526.00 ± 21.34^{ab}	517.83 ± 20.53^{a}	572.00 ± 26.20^{ab}	507.67 ± 21.62^{a}	619.00 ± 22.39^{b}
Mucosal fold width (μm)	157.00 ± 8.25^{a}	168.83 ± 4.89^{a}	166.33 ± 7.06^{a}	148.67 ± 4.13^{a}	169.17 ± 9.18^{a}
Muscularis thickness (μm)	34.83 ± 3.46^{a}	38.67 ± 2.23^{a}	58.17 ± 2.36^{b}	38.00 ± 4.86^{a}	84.83 ± 7.42^{c}
Lamina propria thickness (μm)	21.95 ± 1.76^{a}	21.35 ± 1.60^{a}	20.31 ± 0.96^{a}	22.13 ± 2.53^{a}	20.88 ± 1.88^{a}

$^{a-c}$*Mean values in the same row with different superscripts differ significantly ($p < 0.05$).*
NC, control diet; BS, control diet containing 1×10^7 CFU/g of Bacillus siamensis; BT, control diet containing 1×10^7 CFU/g of Bacillus tequilensis; BV, control diet containing 1×10^7 CFU/g of Bacillus velezensis; and LL, control diet containing 1×10^7 CFU/g of Lactococcus lactis.

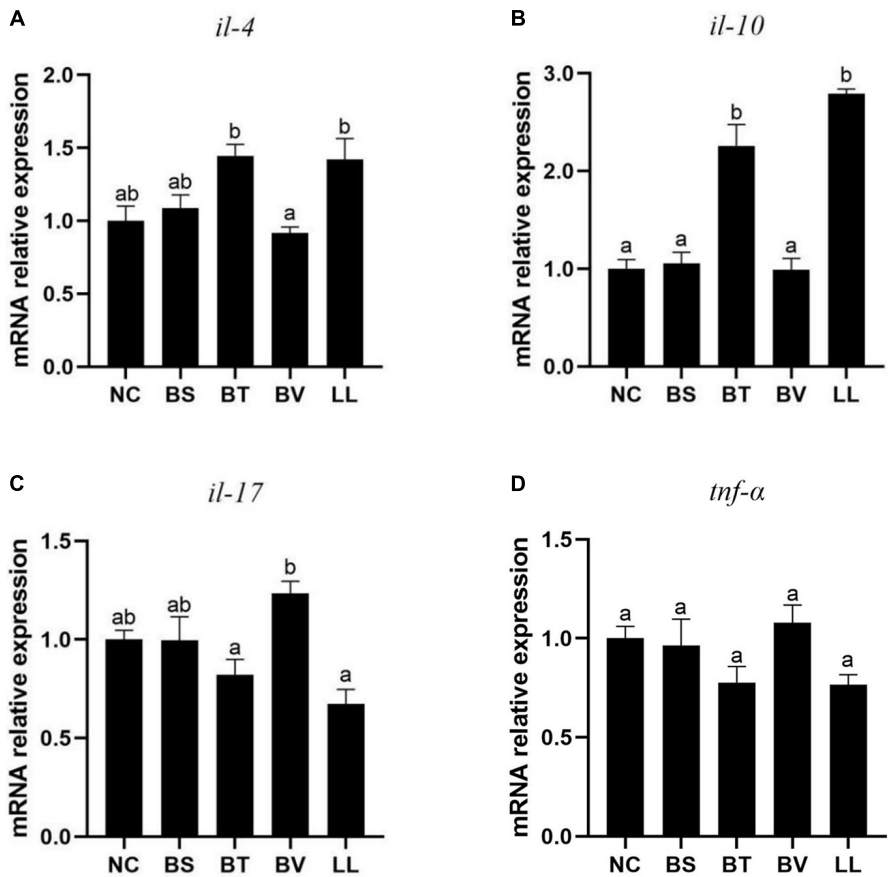

FIGURE 4 | Expression of jejunal inflammatory cytokines of bullfrog, including **(A)** *il-4*, **(B)** *il-10*, **(C)** *il-17*, and **(D)** *tnf-α*. Bars with different letters were significantly different ($p < 0.05$). *il*, interleukin; *tnf*, tumor necrosis factor; NC, control diet; BS, control diet containing 1×10^7 CFU/g of *Bacillus siamensis*; BT, control diet containing 1×10^7 CFU/g of *Bacillus tequilensis*; BV, control diet containing 1×10^7 CFU/g of *Bacillus velezensis*; and LL, control diet containing 1×10^7 CFU/g of *Lactococcus lactis*.

(**Figures 4A,B**). No significant difference was found in the expression of pro-inflammatory cytokines (*il-17* and *tnf-α* genes) between the NC group and each of the treated groups ($p > 0.05$; **Figures 4C,D**).

Jejunum Microbial Communities

A total of 2,160,089 effective tags were obtained from five groups, with an average of 108,004 ± 1,024 per sample. The resulting sequences were clustered into OTUs at 97% sequence identity. Thus, a total of 2,457 OTUs were found in five groups, with an average of 123 ± 5 per sample. Venn diagram of bacterial communities showed that the core OTUs of all groups was 45, and total OTUs of NC, BS, BT, BV, and LL groups were 199, 108, 140, 95, and 98, respectively, (**Figure 5A**). PCoA plot based on Jaccard distance matrix was executed to indicate the similarity of intestinal microbial communities among experimental groups. Some data points of NC, BS, and BV groups had overlap regions (**Figure 5B**), which were distinct from those of BT and LL groups.

In general, Proteobacteria, Fusobacteria, and Firmicutes were the three most dominant bacterial phyla in the jejunum

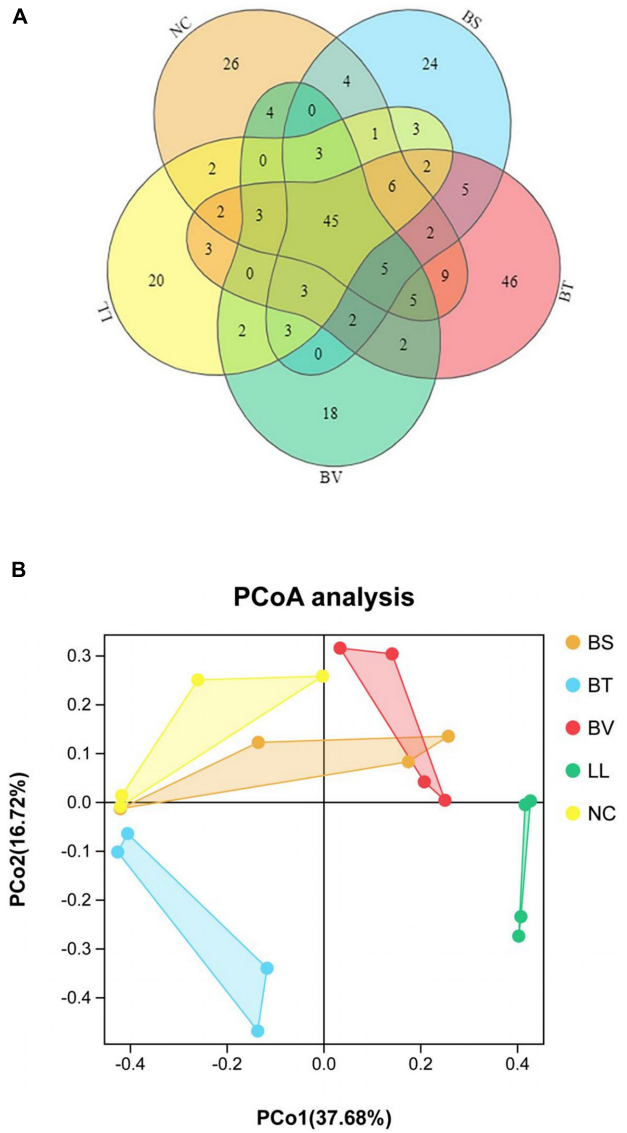

FIGURE 5 | (A) Venn diagram and **(B)** principal component analysis (PCoA) based on Jaccard distance matrix of jejunal microbiota. NC, control diet; BS, control diet containing 1×10^7 CFU/g of *Bacillus siamensis*; BT, control diet containing 1×10^7 CFU/g of *Bacillus tequilensis*; BV, control diet containing 1×10^7 CFU/g of *Bacillus velezensis*; and LL, control diet containing 1×10^7 CFU/g of *Lactococcus lactis*.

of bullfrog (**Figure 6A**), and their relative abundance was different among experimental groups. The relative abundance of Proteobacteria (the dominant phylum) in NC, BS, BT, and BV groups was 81.84, 61.75, 55.91, and 70.94%, respectively, whereas the dominant phylum in the LL group was Fusobacteria (67.57%). The LL group showed significantly lower abundance of Proteobacteria and higher abundance of Fusobacteria than the NC group ($p < 0.05$; **Figure 6B**). The highest abundance of Firmicutes was found in the BT group (41.82%) which significantly differed from that of BS, BV, and LL groups ($p < 0.05$). The major genera in the NC group were *Enterobacter* (50.27%), *Plesiomonas* (12.10%), and *Escherichia–Shigella* (6.59%; **Figure 7A**), and the dominant genera in treated groups were *Enterobacter* (BS, 48.62%), *Bacillus* (BT, 33.86%), *Escherichia–Shigella* (BV, 26.53%), and *Cetobacterium* (LL, 67.20%). The LL group exhibited significantly lower abundance of *Enterobacter* and higher abundance of *Cetobacterium* compared with the NC group ($p < 0.05$; **Figure 7B**). Moreover, the highest abundance of *Bacillus* and *Escherichia–Shigella* were recorded in the BT and BV groups, respectively.

Predicted functional analysis of intestinal microbiota by PICRUSt2 revealed the top 20 level-2 KO groups. The KEGG pathways enriched in BS and BV groups were similar to that in the NC group (**Figure 8A**), whereas BT and LL groups showed a higher abundance of partial KEGG pathways than the NC group. Lipid metabolism was markedly enhanced by the BT diet compared with the NC diet ($p < 0.05$; **Figure 8B**). Moreover, 14 KEGG pathways including carbohydrate metabolism, metabolism of cofactors and vitamins, metabolism of terpenoids and polyketides, metabolism of other amino acids, energy metabolism, replication and repair, folding, sorting and degradation, glycan biosynthesis and metabolism, membrane transport, translation, biosynthesis of other secondary metabolites, nucleotide metabolism, cell growth and death, and transcription were significantly enriched in the LL group compared with the NC group ($p < 0.05$; **Figure 8C**).

DISCUSSION

In the current study, remarkable growth differences were observed among bullfrogs that received SM-based diet for 60 days and reared under the same conditions. Several representative bacterial strains enriched in FG bullfrogs were isolated by standard spread plate method. Presumably, those strains could be adaptive to the gut environment established by a long-term feeding on plant-based diet and might be associated with the growth of bullfrogs. Then, three *Bacillus* species (*B. siamensis*, *B. tequilensis*, and *B. velezensis*) and a lactic acid bacterium (*L. lactis*) were selected as feed additives since the two bacterial categories were among the most common probiotics used in breeding production and experimental research.

In livestock industry and aquaculture, it is challenging to improve the feed utilization of plant-sourced proteins and alleviate their adverse effects on animals. *Bacillus* spp. and lactic acid bacteria are among the most widely used probiotics which exert diverse host-beneficial properties including growth promotion (Yu et al., 2016), immune modulation (Sun et al., 2012), mucosal barrier repair (Lin et al., 2020), disease resistance, etc. (Xia et al., 2019). In the current study, *L. lactis* supplementation improved growth performance, feed efficiency, and nitrogen retention of bullfrogs, and the increase in nitrogen retention was consistent with the trend in whole-body protein content, which agrees with our previous bullfrog study (Lin et al., 2021). This result indicated that the protein synthesis in bullfrogs might be stimulated by *L. lactis* treatment. Similarly, Xia et al. (2018) showed that dietary supplementation of *L. lactis* JCM5805 led to improved weight gain and feed utilization in

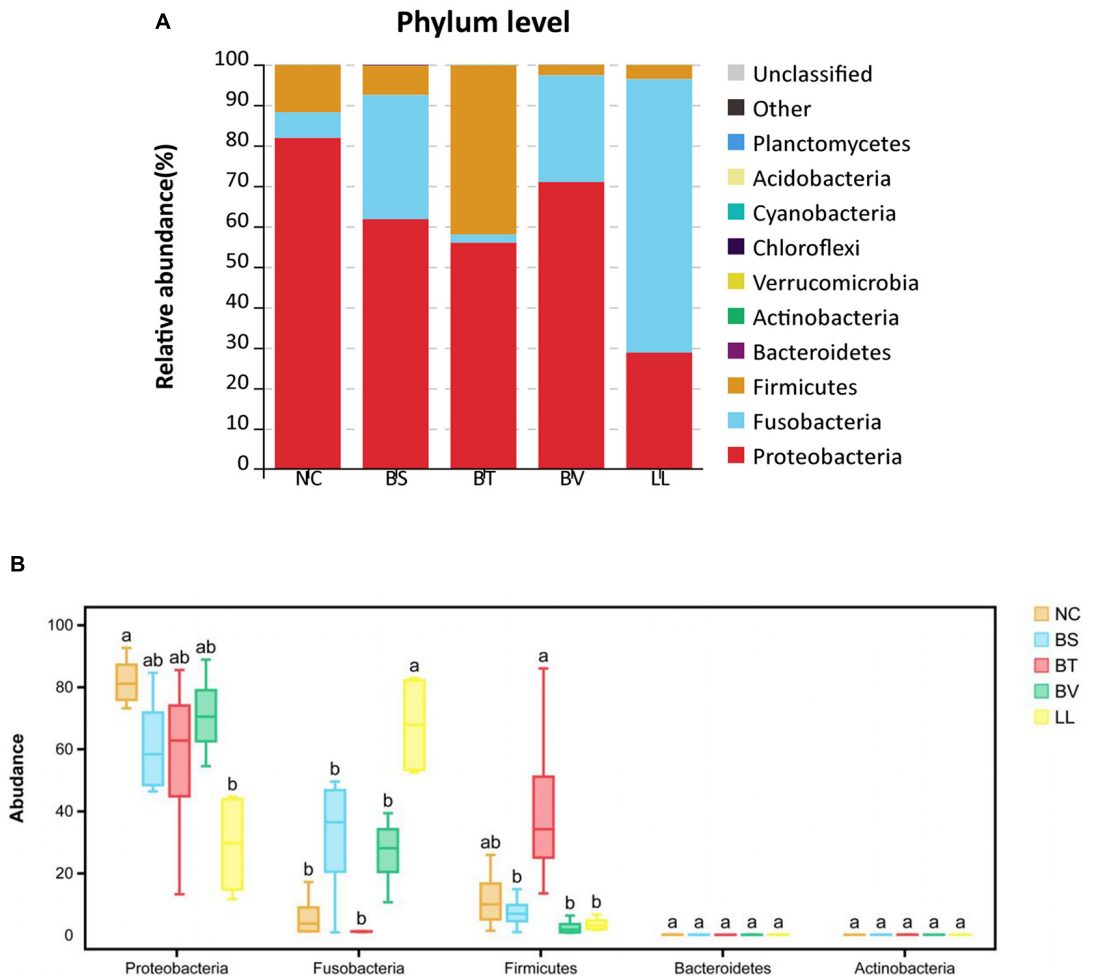

FIGURE 6 | The relative abundance of major bacterial phyla in **(A)** barplot and **(B)** boxplot. Bars with different letters were significantly different ($p < 0.05$). NC, control diet; BS, control diet containing 1×10^7 CFU/g of *Bacillus siamensis*; BT, control diet containing 1×10^7 CFU/g of *Bacillus tequilensis*; BV, control diet containing 1×10^7 CFU/g of *Bacillus velezensis*; and LL, control diet containing 1×10^7 CFU/g of *Lactococcus lactis*.

Nile tilapia (*Oreochromis niloticus*). Also, Li C. et al. (2017) reported enhanced growth of sea cucumber by dietary *L. lactis* LH8 application. However, several researches indicated the lack of growth-promoting effect of *Bacillus* spp. (Reda and Selim, 2015; Yi et al., 2018). In the current study, the three tested *Bacillus* strains (*B. siamensis*, *B. tequilensis*, and *B. velezensis*) had a slight effect on growth of bullfrog, which might be associated with their antibiosis activity, action mechanism, application dosage, and the complex microbiota–host crosstalk (Sahu et al., 2008).

Humoral immunity is a part of innate immune system in aquatic animals, which consisted of complement, LZM, phagocytosis, etc. (Jia et al., 2016). IgM is the key molecule involved in systemic immunity and immune response mechanisms (Liu et al., 2021). C3 and C4 participate in complement pathways, which are crucial to the elimination of pathogens (Alexander and Ingram, 1992). Excessive levels of dietary plant-protein diets increase the risk of immune homeostasis disruption in animals, especially in aquatic animals (Sahlmann et al., 2013). *Bacillus* species and lactic acid bacteria have been proven to stimulate the immune system and maintain the immune homeostasis in animals (Ringø et al., 2018). In this study, *L. lactis* and *B. tequilensis* diets resulted in elevated serum LZM, IgM, and complement levels in bullfrog. Similar results have also been found in olive flounder (*Paralichthys olivaceus*) through dietary supplementation of *L. lactis* I2 (Heo et al., 2013) and in grouper by *L. lactis* application (Sun et al., 2012). Overall, the current study indicated that the immune response of bullfrog might be improved by dietary supplementation of *B. tequilensis* and *L. lactis*.

Intestine morphology is widely used for assessing the intestine development. In the present study, bullfrogs fed the high-SM diet showed a typical SBMIE phenomenon in the jejunum: few and shrunken mucosal folds, as well as narrow muscularis. These degenerative changes might be associated with the inflammatory reaction (Yu et al., 2021). Besides, plant-protein-based diet was proven to induce mucosa damage and infiltration of leukocytes in the lamina propria (Li Y. et al., 2017). In this context, partial separations of tissue were detected in the jejunum

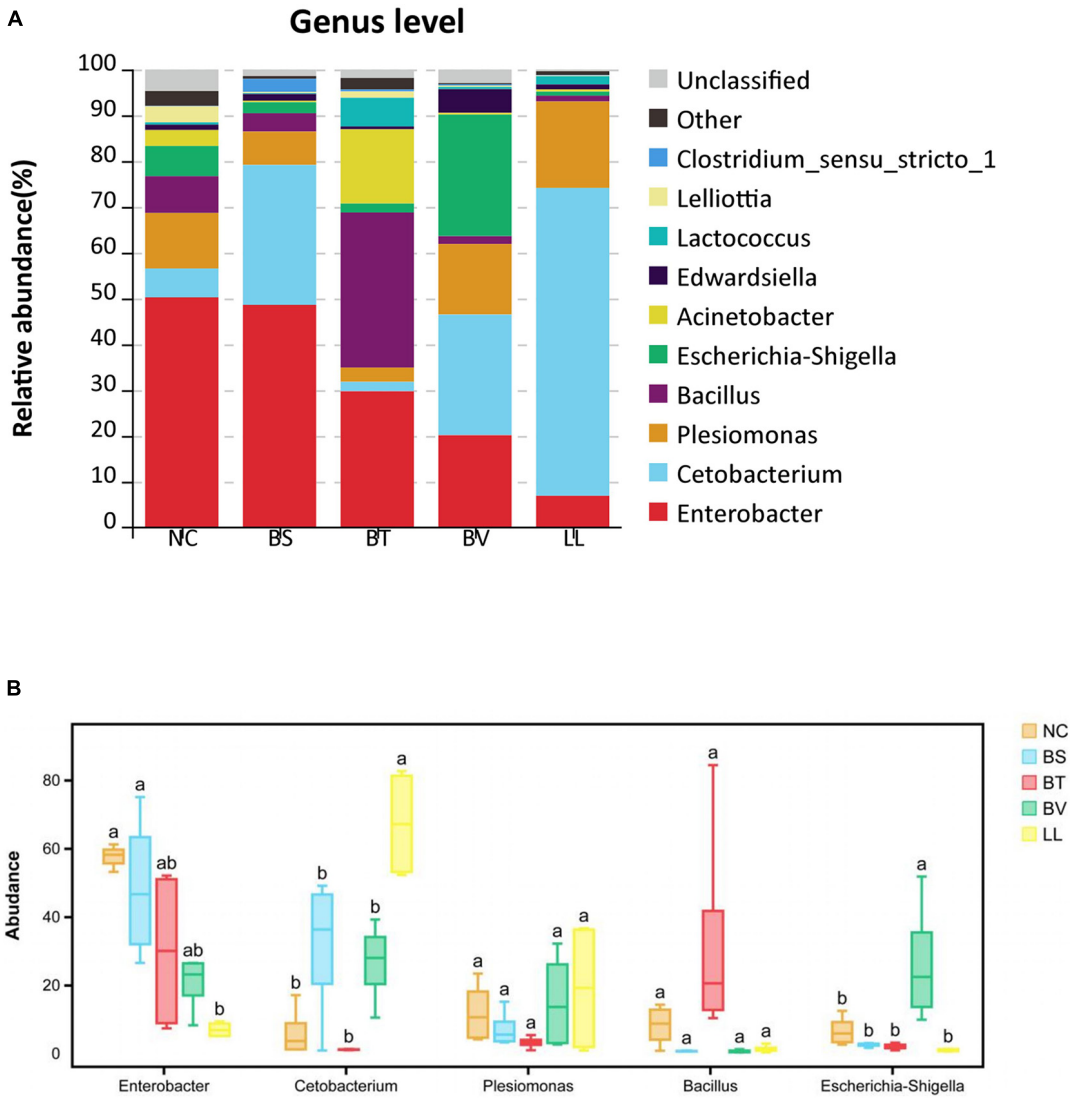

FIGURE 7 | The relative abundance of major bacterial genera in **(A)** barplot and **(B)** boxplot. Bars with different letters were significantly different ($p < 0.05$). NC, control diet; BS, control diet containing 1×10^7 CFU/g of *Bacillus siamensis*; BT, control diet containing 1×10^7 CFU/g of *Bacillus tequilensis*; BV, control diet containing 1×10^7 CFU/g of *Bacillus velezensis*; and LL, control diet containing 1×10^7 CFU/g of *Lactococcus lactis*.

of NC, BS, and BV groups. Probiotics have been reported to promote intestinal barrier function through modulation of cytokine production, mucus secretion, macrophage activation, etc. (Anderson et al., 2012). Thus, making use of probiotics conferred a compelling strategy to alleviate adverse impacts caused by plant-protein diet in the gut. For example, Navarrete et al. (2013) reported that dietary *L. lactis* supplementation aided in the restoration of intestinal morphology impaired by SM-based diet in Atlantic salmon (*Salmo salar*). Furthermore, a bullfrog study showed an increase in villus height and thickness by *B. subtilis* application (Lin et al., 2020). Similarly, in the current study, LL and BT diets alleviated the intestinal structural damage caused by high-SM diet. The integrity of intestinal structure is associated with intestinal epithelial permeability (Anderson et al., 2012). Serum DAO activity and D-lactate concentration are two well-established markers for the intestinal mucosal damage (Anderson et al., 2012). In the present study, decreased serum DAO activity indicated the improvement in intestinal integrity and permeability. In addition, intestinal tight junction protein (*zo-1* and *occludin*) were also important components contributing to intestinal physical barrier function (Anderson et al., 2012), and their mRNA expression were up-regulated in bullfrogs fed BT or LL diets as expected. Generally, the results of intestinal morphology, gut permeability, and tight junction proteins collectively indicated that both *B. tequilensis* and *L. lactis* aided in maintaining the intestinal barrier functions and preventing SBMIE.

The intestine epithelium is the main site of nutrient digestion and absorption, the longer and thicker intestinal mucosal folds corresponded to enhanced absorptive surface area

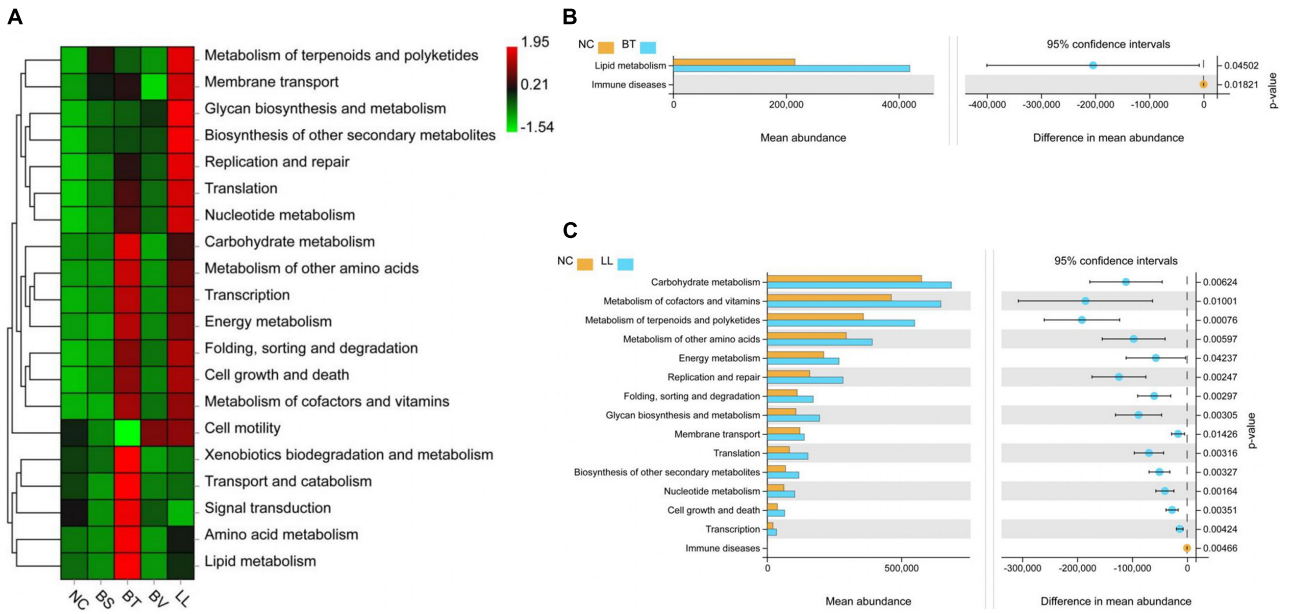

FIGURE 8 | Predicted functional profiles of jejunal microbiota using PICRUSt2 at level 2. **(A)** The heat map analysis among all groups. **(B,C)** Analysis of function difference between NC group and BT (or LL) group. Differences were calculated by Welch's *t*-test ($p < 0.05$). NC, control diet; BS, control diet containing 1×10^7 CFU/g of *Bacillus siamensis*; BT, control diet containing 1×10^7 CFU/g of *Bacillus tequilensis*; BV, control diet containing 1×10^7 CFU/g of *Bacillus velezensis*; and LL, control diet containing 1×10^7 CFU/g of *Lactococcus lactis*.

(Standen et al., 2016), which could be partially responsible for the increased feed efficiency determined in LL and BT groups. Besides, some probiotics could alter intestinal motility and stimulate the digestive enzyme production, leading to greater digestion efficiency (Anderson et al., 2012), as reported in gibel carp (*Carassius auratus gibelio*) following *B. coagulans* supplementation (Yu et al., 2016), and in Pacific white shrimp after *L. plantarum* application (Zheng et al., 2017). Consistently, in the current study, both jejunal protease and amylase activities of bullfrog were increased by both *B. tequilensis* and *L. lactis* diets, while feed digestibility was increased by *L. lactis* treatment. It has been reported that multiple non-digestible ingredients, including oligosaccharides, disaccharide components, and sugar alcohols, were the main substrates for probiotic growth, and many of these ingredients could be fermented by specific bacteria to short-chain fatty acids, which also conferred health benefits for animals (Sahu et al., 2008). Overall, it could be concluded that intestinal digestive and absorptive functions of bullfrog were improved by both *B. tequilensis* and *L. lactis* supplementation.

The intestinal microbiota is closely tied to the host's physiological function, nutrient metabolism, and immune homeostasis (Gao et al., 2018; Xia et al., 2018). Diet intake constitutes a pivotal determinant of the compositions of trillions of microorganisms residing in the gut. In the present study, high-SM diet led to the dominance of Proteobacteria, Firmicutes, and Fusobacteria in the jejunum of bullfrog, which was consistent with previous studies on bullfrog (Wang et al., 2020) and freshwater fish species (Desai et al., 2012; Ni et al., 2012). Reportedly, intestinal microbiota disorder was one of the characteristics of enteritis including SBMIE (Merrifield et al., 2010). In the current study, *Enterobacter* or *Escherichia–Shigella* were the major bacterial genera in NC, BS, and BV groups, whereas most bacterial species affiliated to the two genera had been determined as pathogenic bacteria and associated with the inflammatory disorders of animals (Hung et al., 2015; Cao et al., 2017). These results indicated that the long-term SM-based diet might establish favorable conditions for colonization of pathogenic bacteria in bullfrog gut, which might be the main factor that caused intestinal structural damage and microbiota disorder. Probiotics are widely used to modulate the host's intestinal microbial community; their modes of action include the inhibition of pathogens' growth by competition for nutrients and adhesion sites, secretion of antibacterial peptides, etc. (Rengpipat et al., 1998; Verschuere et al., 2000). To effectively confer health benefits on the host, it is vitally important for probiotics to adhere and colonize on intestinal mucosa (Alander et al., 1999). In the current study, the BT-fed bullfrogs exhibited an increased abundance of *Bacillus* and decreased abundance of potential pathogens including *Enterobacter*, *Plesiomonas*, and *Escherichia–Shigella*. However, *B. siamensis* and *B. velezensis* diets had a weak effect on the abundance of *Bacillus* in bullfrog jejunum; it suggested that the ability of *Bacillus* species to colonize the intestine varied from strain to strain. Interestingly, the intestinal microbiota in the LL-fed bullfrog was characterized by a bloom of *Cetobacterium*. It was reported that the main components of *L. lactis* were glycerol phosphate, teichoic acid, and some polysaccharides (Vinogradov et al., 2018), which might serve as substrates for *Cetobacterium* growth. However, the concrete mechanism of the symbiotic relationship among

microorganisms needs to be further studied. *Cetobacterium* was able to produce vitamin B_{12} and short-chain fatty acids by fermenting carbohydrates and peptides, and thereby promoting the nutrients' utilization (Finegold et al., 2003; Tsuchiya et al., 2008; Li et al., 2015), as confirmed by the fact that increased nutrient digestibility was obtained in bullfrogs fed *L. lactis* diet.

As an added metabolic "organ" of the host, intestinal microbiota participates in a series of host metabolism steps (Backhed et al., 2004; Zhang et al., 2014). In the current study, analyses of predicted functions of gut microbial communities showed that the pathway of lipid metabolism was stimulated by *B. tequilensis* diet. Zhou et al. (2016) reported that a *Bacillus* strain contributed to decompose cholesterol into coprostanol, and reduced lipid accumulation by stimulating fecal-lipid and bile-acid output. Besides, pathways of metabolisms, including that of carbohydrate, amino acids, energy, cofactors, and vitamins, were significantly enhanced by *L. lactis* diet, and they might be attributed to the effects of *Cetobacterium* on fermenting carbohydrates and peptides as mentioned earlier. Excessive levels of dietary carbohydrate induced metabolic load and stress responses in aquatic animals since most of them were generally considered to be glucose intolerant and poor at utilizing carbohydrates (Qiao et al., 2016; Boonanuntanasarn et al., 2018; Gao et al., 2018). Thus, it is of great significance that gut microbes aid the host in the utilization of carbohydrate and non-digestible ingredients. Collectively, after feeding the SM-based diet supplemented with *L. lactis* for 58 days, the changes in intestinal structure and digestive function, as well as the alterations in gut microbiota, collaborated to promote the gut health, resulting in improved feed utilization and growth performance of bullfrog.

CONCLUSION

The beneficial effects of two frog-derived probiotics were determined. Dietary supplementation of *L. lactis* significantly promoted feed utilization and growth performance of bullfrog, and both *L. lactis* and *B. tequilensis* supplementation improved the immune response and alleviated enteritis caused by the high-SM diet. These beneficial effects could be attributed to the improvement in intestinal epithelial integrity and digestive function, as well as the alterations in gut microbiota.

DATA AVAILABILITY STATEMENT

The datasets presented in this study can be found in online repositories. The names of the repository/repositories and accession number(s) can be found below: GenBank MZ573378, MZ573379, MZ573380, and MZ573381; BioProject PRJNA747862.

ETHICS STATEMENT

The animal study was reviewed and approved by The Committee on the Ethics of Animal Experiments of Jimei University.

AUTHOR CONTRIBUTIONS

LW and CZ designed the study. ZW performed the experiment, analyzed data, and wrote the manuscript. KL and KS participated in the experiment design and gave valuable advice. XL and SR contributed to revision of the manuscript. All authors have read and approved the final version of this article.

FUNDING

This study was supported by National Natural Science Foundation of China (Grant No. 31602172) and the Science, Technology Leading Project of Fujian Province (Grant No. 2017N0021). SR was supported by NAZV project (Grant No. QK1710310).

SUPPLEMENTARY MATERIAL

The Supplementary Material for this article can be found online at: https://www.frontiersin.org/articles/10.3389/fmicb.2021.739572/full#supplementary-material

REFERENCES

Alander, M., Satokari, R., and Korpela, R. (1999). Persistence of colonization of human colonic mucosa by a probiotic strain, *Lactobacillus rhamnosus* GG, after oral consumption. *Appl. Environ. Microbiol.* 65, 351–354. doi: 10.1128/aem.65.1.351-354.1999

Alexander, J. B., and Ingram, G. A. (1992). Noncellular nonspecific defence mechanisms of fish. *Ann. Rev. Fish Dis.* 2, 249–279. doi: 10.1016/0959-8030(92)90066-7

Anderson, R. C., Dalziel, J. E., Gopal, P. K., Bassett, S., Ellis, A., and Roy, N. C. (2012). "The role of intestinal barrier function in early life in the development of colitis," in *Colitis*, ed. M. Fukata (London: InTechOpen), 1–30.

AOAC (2002). *Official Methods of Analysis of the Association of Analytical Chemistry*, 17th Edn. Arlington: AOAC.

Backhed, F., Ding, H., Wang, T., Hooper, L. V., Koh, G. Y., Nagy, A., et al. (2004). The gut microbiota as an environmental factor that regulates fat storage. *Proc. Natl. Acad. Sci. U.S.A.* 101, 15718–15723. doi: 10.1073/pnas.0407076101

Balestra, G. M., and Misaghi, I. J. (1997). Increasing the efficiency of the plate counting method for estimating bacterial diversity. *J. Microbiol. Meth.* 30, 111–117. doi: 10.1016/s0167-7012(97)00056-0

Baltz, D. M., Fleeger, J. W., Rakocinski, C. F., and McCall, J. N. (1998). Food, density, and microhabitat: factors affecting growth and recruitment potential of juvenile saltmarsh fishes. *Environ. Biol. Fish.* 53, 89–103. doi: 10.1023/a:1007471724608

Boonanuntanasarn, S., Jangprai, A., Kumkhong, S., Plagnes-Juan, E., Veron, V., Burel, C., et al. (2018). Adaptation of Nile tilapia (*Oreochromis niloticus*) to different levels of dietary carbohydrates: new insights from a long term nutritional study. *Aquaculture* 496, 58–65.

Cao, H., An, J., Ou, R., Lu, L., Ai, X., and Yang, Y. (2017). Enterobacter aerogenes: an emerging pathogen for enteritis in farmed channel catfish *Ictalurus punctatus*. *Isr. J. Aquacult. Bamid.* 69, 1–7.

de Clarla Dias, D., De Stefani, M. V., Ferreira, C. M., Franca, F. M., Tavares Ranzani-Paiva, M. J., and Santos, A. A. (2010). Haematologic and immunologic parameters of bullfrogs, *Lithobates catesbeianus*, fed probiotics. *Aquac. Res.* 41, 1064–1071.

Denev, S., Staykov, Y., Moutafchieva, R., and Beev, G. (2009). Microbial ecology of the gastrointestinal tract of fish and the potential application of probiotics and prebiotics in finfish aquaculture. *Int. Aquatic Res.* 1, 1–29. doi: 10.1002/9781118897263.ch1

Desai, A. R., Links, M. G., Collins, S. A., Mansfield, G. S., and Hill, J. E. (2012). Effects of plant-based diets on the distal gut microbiome of rainbow trout (*Oncorhynchus mykiss*). *Aquaculture* 35, 134–142. doi: 10.1016/j.aquaculture.2012.04.005

Ding, L., Wang, L., Lu, K. L., Song, K., and Zhang, C. X. (2019). Effects of replacement of fish meal with soybean meal on growth performance, digestive enzyme activity and intestinal health of *Rana catesbeiana*. *Freshw. Fish.* 49, 69–75.

Douglas, G. M., Maffei, V. J., Zaneveld, J. R., Yurgel, S. N., Brown, J. R., Taylor, C. M., et al. (2020). PICRUSt2 for prediction of metagenome functions. *Nat. Biotechnol.* 38, 685–688. doi: 10.1038/s41587-020-0548-6

Finegold, S. M., Vaisanen, M. L., Molitoris, D. R., Tomzynski, T. J., Song, Y., Liu, C., et al. (2003). Cetobacterium somerae sp. nov. from human feces and emended description of the genus *Cetobacterium*. *Syst. Appl. Microbiol.* 26, 177–181. doi: 10.1078/072320203322346010

Gao, S., Pan, L. Q., Huang, F., Song, M. S., and Zhang, M. Y. (2018). Metagenomic insights into the structure and function of intestinal microbiota of the farmed Pacific white shrimp (*Litopenaeus vannamei*). *Aquaculture* 499, 109–118. doi: 10.1016/j.aquaculture.2018.09.026

Gui, G., Xiao, Y., Dai, B., Chen, X., Yang, H. L., and Xu, E. (2017). Alteration of intestinal archaeal community composition in broilers with different growth rates. *Anim. Husb. Feed Sci.* 9, 335–359.

Heo, W. S., Kim, Y. R., Kim, E. Y., Bai, S. C., and Kong, I. S. (2013). Effects of dietary probiotic, *Lactococcus lactis* subsp. lactis I2, supplementation on the growth and immune response of olive flounder (*Paralichthys olivaceus*). *Aquaculture* 376, 20–24. doi: 10.1016/j.aquaculture.2012.11.009

Hung, L. D., Hirayama, M., Ly, B. M., and Hori, K. (2015). Biological activity, cDNA cloning and primary structure of lectin KSA-2 from the cultivated red alga *Kappaphycus striatum* (Schmitz) Doty ex Silva. *Phytochem. Lett.* 14, 99–105. doi: 10.1016/j.phytol.2015.09.012

Jia, R., Liu, B. L., Han, C., Huang, B., and Lei, J. L. (2016). The physiological performance and immune response of juvenile turbot (*Scophthalmus maximus*) to nitrite exposure. *Comp. Biochem. Phys. C* 18, 40–46. doi: 10.1016/j.cbpc.2016.01.002

Li, C., Ren, Y. C., Jiang, S. H., Zhou, S., Zhao, J. S., Wang, R. J., et al. (2017). Effects of dietary supplementation of four strains of lactic acid bacteria on growth, immune-related response and genes expression of the juvenile sea cucumber *Apostichopus japonicus* Selenka. *Fish Shellfish Immun.* 74, 69–75. doi: 10.1016/j.fsi.2017.12.037

Li, T. T., Long, M., Gatesoupe, F. J., Zhang, Q., Li, A. H., and Gong, X. N. (2015). Comparative analysis of the intestinal bacterial communities in different species of carp by pyrosequencing. *Microb. Ecol.* 69, 25–36. doi: 10.1007/s00248-014-0480-8

Li, X., Rahimnejad, S., Wang, L., Lu, K., Song, K., and Zhang, C. (2019). Substituting fish meal with housefly (*Musca domestica*) maggot meal in diets for bullfrog *Rana (Lithobates) catesbeiana*: effects on growth, digestive enzymes activity, antioxidant capacity and gut health. *Aquaculture* 499, 295–305. doi: 10.1016/j.aquaculture.2018.09.053

Li, Y., Hu, H., Liu, J., Yang, P., Zhang, Y., Ai, Q., et al. (2017). Dietary soya allergen β-conglycinin induces intestinal inflammatory reactions, serum-specific antibody response and growth reduction in a carnivorous fish species, turbot *Scophthalmus maximus* L. *Aquac. Res.* 48, 4022–4037. doi: 10.1111/are.13224

Li, Z. C., Li, Y. K., Lv, Z. Q., Liu, H., Zhao, J. B., Noblet, J., et al. (2017). Net energy of corn, soybean meal and rapeseed meal in growing pigs. *J. Anim. Sci. Biotechno.* 8:44.

Lin, J. B., Zeng, Q. H., Zhang, C. X., Song, K., Lu, K. L., Wang, L., et al. (2020). Effects of *Bacillus subtilis* supplementation in soybean meal-based diets on growth performance, diet digestibility and gut health in bullfrog *Lithobates catesbeianus*. *Aquac. Rep.* 16:100273. doi: 10.1016/j.aqrep.2020.100273

Lin, J. B., Zhang, C. X., Lu, K. L., Song, K., and Wang, L. (2021). Effect of guanidinoacetic acid and betaine supplementation in soybean meal-based diets on growth performance, muscle energy metabolism and methionine utilization in the bullfrog *Lithobates catesbeianus*. *Aquaculture* 533:736167. doi: 10.1016/j.aquaculture.2020.736167

Liu, T., Zhang, G. G., Feng, Y., Kong, C., Ayisi, C. L., Huang, X. X., et al. (2019). Dietary soybean antigen impairs growth and health through stress-induced non-specific immune responses in Pacific white shrimp, *Litopenaeus vannamei*. *Fish Shellfish Immun.* 84, 124–129. doi: 10.1016/j.fsi.2018.09.062

Liu, Z. N., Liao, L. Y., Chen, Q., Lin, S. Q., and Wu, Y. J. (2021). Effects of *Hericium erinaceus* polysaccharide on immunity and apoptosis of the main immune organs in Muscovy duck reovirus-infected ducklings. *Int. J. Biol. Macromol.* 171, 448–456. doi: 10.1016/j.ijbiomac.2020.12.222

Lowry, O. H., Rosebrough, N. J., Farr, A. L., and Randall, R. J. (1951). Protein measurement with the folin phenol reagent. *J. Biol. Chem.* 193, 265–275. doi: 10.1016/s0021-9258(19)52451-6

Melo-Bolivar, J. F., Ruiz Pardo, R. Y., Hume, M. E., and Villamil Diaz, L. M. (2021). Multistrain probiotics use in main commercially cultured freshwater fish: a systematic review of evidence. *Rev. Aquacult.* 13, 1758–1780. doi: 10.1111/raq.12543

Merrifield, D. L., Dimitroglou, A., Bradley, G., Baker, R. T., and Davies, S. J. (2010). Soybean meal alters autochthonous microbial populations, microvilli morphology and compromises intestinal enterocyte integrity of rainbow trout, *Oncorhynchus mykiss* (Walbaum). *J. Fish Dis.* 32, 755–766. doi: 10.1111/j.1365-2761.2009.01052.x

Montel Mendoza, G., Pasteris, S. E., Ale, C. E., Otero, M. C., Buehler, M. I., and Fatima Nader-Macias, M. E. (2012). Cultivable microbiota of *Lithobates catesbeianus* and advances in the selection of lactic acid bacteria as biological control agents in raniculture. *Res. Vet. Sci.* 93, 1160–1167.

Navarrete, P., Fuentes, P., Fuente, L. D. L., Barros, L., Magne, F., Opazo, R., et al. (2013). Short-term effects of dietary soybean meal and lactic acid bacteria on the intestinal morphology and microbiota of Atlantic salmon (*Salmo salar*). *Aquacult. Nutr.* 19, 827–836. doi: 10.1111/anu.12047

Naylor, R. L., Hardy, R. W., Buschmann, A. H., Bush, S. R., Cao, L., Klinger, D. H., et al. (2021). A 20-year retrospective review of global aquaculture. *Nature* 591, 551–563. doi: 10.1038/s41586-021-03308-6

Ni, J. J., Yu, Y. H., Zhang, T. L., and Gao, L. (2012). Comparison of intestinal bacterial communities in grass carp, *Ctenopharyngodon idellus*, from two different habitats. *Chin. J. Oceanol. Limn.* 30, 757–765. doi: 10.1007/s00343-012-1287-4

Niederle, M. V., Bosch, J., Ale, C. E., Nader-Macias, M. E., Aristimuno Ficoseco, C., Toledo, L. F., et al. (2019). Skin-associated lactic acid bacteria from North American bullfrogs as potential control agents of *Batrachochytrium dendrobatidis*. *PLoS One* 14:e0223020. doi: 10.1371/journal.pone.0223020

Nielsen, B. L. (2012). Effects of ambient temperature and early open-field response on the behaviour, feed intake and growth of fast- and slow-growing broiler strains. *Animal* 6, 1460–1468. doi: 10.1017/s1751731112000353

Peng, C., Tang, X., Shu, Y., He, M., Xia, X., Zhang, Y., et al. (2019). Effects of 7S and 11S on the intestine of weaned piglets after injection and oral administration of soybean antigen protein. *Anim. Sci. J.* 90, 393–400. doi: 10.1111/asj.13130

Pereira, S. A., Jeronimo, G. T., da Costa Marchiori, N., de Oliveira, H. M., Owatari, M. S., Jesus, G. F. A., et al. (2016). Autochthonous probiotic *Lactobacillus* sp. in the diet of bullfrog tadpoles *Lithobates catesbeianus* improves weight gain, feed conversion and gut microbiota. *Aquacult. Nutr.* 23, 910–916. doi: 10.1111/anu.12458

Pereira, S. A., Jeronimo, G. T., Marchiori, N. C., Oliveira, H. M., Jesus, G. F. A., Schmidt, E. C., et al. (2018). Tadpoles fed supplemented diet with probiotic bacterium isolated from the intestinal tract of bullfrog *Lithobates catesbeianus*: haematology, cell activity and electron microscopy. *Microb. Pathog.* 114, 255–263. doi: 10.1016/j.micpath.2017.11.033

Qiao, F., Liu, Y. K., Sun, Y. H., Wang, X. D., and Zhang, M. L. (2016). Influence of different dietary carbohydrate sources on the growth and intestinal microbiota of *Litopenaeus vannamei* at low salinity. *Aquac. Nutr.* 23, 444–542. doi: 10.1111/anu.12412

Reda, R. M., and Selim, K. M. (2015). Evaluation of *Bacillus amyloliquefaciens* on the growth performance, intestinal morphology, hematology and body composition of Nile tilapia, *Oreochromis niloticus*. *Aquacult. Int.* 23, 203–217. doi: 10.1007/s10499-014-9809-z

Rengpipat, S., Phianphak, W., Piyatiratitivorakul, S., and Menasveta, P. (1998). Effects of a probiotic bacterium on black tiger shrimp *Penaeus monodon* survival and growth. *Aquaculture* 167, 301–313. doi: 10.1016/s0044-8486(98)00305-6

Ringø, E., Hoseinifar, S. H., Ghosh, K., Doan, H. V., Beck, B. R., and Song, S. K. (2018). Lactic acid bacteria in finfish—an update. *Front. Microbiol.* 9:1818. doi: 10.3389/fmicb.2018.01818

Sahlmann, C., Sutherland, B. J. G., Kortner, T. M., Koop, B. F., Krogdahl, Å, and Bakke, A. M. (2013). Early response of gene expression in the distal intestine of Atlantic salmon (*Salmo salar* L.) during the development of soybean meal induced enteritis. *Fish. Shellfish Immun.* 34, 599–609. doi: 10.1016/j.fsi.2012.11.031

Sahu, M. K., Swarnakumar, N. S., Sivakumar, K., Thangaradjou, T., and Kannan, L. (2008). Probiotics in aquaculture: importance and future perspectives. *Indian J. Microbiol.* 48, 299–308. doi: 10.1007/s12088-008-0024-3

Sha, Y., Liu, M., Wang, B., Jiang, K., Sun, G., and Wang, L. (2016). Gut bacterial diversity of farmed sea cucumbers *Apostichopus japonicus* with different growth rates. *Microbiology* 85, 109–115. doi: 10.1134/s0026261716010112

Standen, B. T., Peggs, D. L., Rawling, M. D., Foey, A., Davies, S. J., Santos, G. A., et al. (2016). Dietary administration of a commercial mixed-species probiotic improves growth performance and modulates the intestinal immunity of tilapia, *Oreochromis niloticus*. *Fish Shellfish Immun.* 49, 427–435. doi: 10.1016/j.fsi.2015.11.037

Sun, Y. Z., Yang, H. L., Ma, R. L., and Song, K. (2012). Effect of *Lactococcus lactis* and *Enterococcus faecium* on growth performance, digestive enzymes and immune response of grouper *Epinephelus coioides*. *Aquacult. Nutr.* 18, 281–289. doi: 10.1111/j.1365-2095.2011.00894.x

Sun, Y., Yang, H., Ling, Z., Chang, J., and Ye, J. (2009). Gut microbiota of fast and slow growing grouper *Epinephelus coioides*. *Afr. J. Microbiol. Res.* 3, 713–720.

Syedbasha, M., Linnik, J., Santer, D., O'Shea, D., Barakat, K., Joyce, M., et al. (2016). An ELISA based binding and competition method to rapidly determine ligand-receptor interactions. *J. Vis. Exp.* 109:e53575.

Tsuchiya, C., Sakata, T., and Sugita, H. (2008). Novel ecological niche of *Cetobacterium somerae*, an anaerobic bacterium in the intestinal tracts of freshwater fish. *Lett. Appl. Microbiol.* 46, 43–48.

Verschuere, L., Rombaut, G., Sorgeloos, P., and Verstraete, W. (2000). Probiotic bacteria as biological control agents in aquaculture. *Microbiol. Mol. Biol. Rev.* 64, 655–671. doi: 10.1128/mmbr.64.4.655-671.2000

Vinogradov, E., Sadovskaya, I., Courtin, P., Kulakauska, S., Grard, T., Mahonyet, J., et al. (2018). Determination of the cell wall polysaccharide and teichoic acid structures from *Lactococcus lactis* IL1403. *Carbohydr. Res.* 462, 39–44. doi: 10.1016/j.carres.2018.04.002

Wang, L., Wang, J., Lu, K. L., Song, K., and Rahimnejad, S. (2020). Total replacement of fish meal with soybean meal in diets for bullfrog (*Lithobates catesbeianus*): effects on growth performance and gut microbial composition. *Aquaculture* 524:735236. doi: 10.1016/j.aquaculture.2020.735236

Xia, Y., Gao, J. M., Wang, M., Lu, M. X., Chen, G., Gao, F. Y., et al. (2019). Effects of *Lactococcus lactis* subsp. *lactis* JCM5805 on colonization dynamics of gut microbiota and regulation of immunity in early ontogenetic stages of tilapia. *Fish Shellfish Immun.* 86, 53–63. doi: 10.1016/j.fsi.2018.11.022

Xia, Y., Lu, M. X., Chen, G., Cao, J. M., Gao, F. Y., Wang, M., et al. (2018). Effects of dietary *Lactobacillus rhamnosus* JCM1136 and *Lactococcus lactis* subsp. *lactis* JCM5805 on the growth, intestinal microbiota, morphology, immune response and disease resistance of juvenile Nile tilapia, *Oreochromis niloticus*. *Fish Shellfish Immun.* 76, 368–379. doi: 10.1016/j.fsi.2018.03.020

Yang, M. Q., Rahimnejad, S., Zhang, C. X., Song, K., Lu, K. L., and Wang, L. (2019). Histomorphology of gastrointestinal tract in bullfrog *Rana (Lithobates) catesbeiana* and evaluation of the changes induced by a soybean meal-based diet. *Aquacult. Res.* 51, 164–174. doi: 10.1111/are.14361

Yao, J. T., Kong, C., Hua, X. M., Yang, J. F., Liu, T., Wang, G., et al. (2019). T1R1 expression in obscure puffer (*Takifugu fasciatus*) is associated with effect of dietary soybean antigenic protein on intestinal health. *Aquaculture* 501, 202–212. doi: 10.1016/j.aquaculture.2018.11.010

Yi, Y. L., Zhang, Z. H., Zhao, F., Liu, H., and Wang, G. X. (2018). Probiotic potential of *Bacillus velezensis* JW: antimicrobial activity against fish pathogenic bacteria and immune enhancement effects on *Carassius auratus*. *Fish Shellfish Immun.* 78, 322–330. doi: 10.1016/j.fsi.2018.04.055

Yu, G., Liu, Y., Ou, W., Dai, J., Ai, Q., Zhang, W., et al. (2021). The protective role of daidzein in intestinal health of turbot (*Scophthalmus maximus* L.) fed soybean meal-based diets. *Sci. Rep.* 11:3352. doi: 10.1038/s41598-021-82866-1

Yu, Y. B., Lv, F., Wang, C. H., Wang, A. M., Zhao, W. H., and Yang, W. P. (2016). Effects of *Bacillus coagulans* on growth performance, disease resistance, and HSP70 gene expression in Juvenile gibel carp, *Carassius auratus gibelio*. *J. World Aquacult. Soc.* 47, 729–740. doi: 10.1111/jwas.12308

Zhang, M. L., Chekan, J. R., Dodd, D., Hong, P. Y., and Cann, I. (2014). Xylan utilization in human gut commensal bacteria is orchestrated by unique modular organization of polysaccharide-degrading enzymes. *Proc. Natl. Acad. Sci. U.S.A.* 111, E3708–E3717.

Zheng, X. T., Duan, Y. F., Dong, H. B., and Zhang, J. S. (2017). Effects of dietary *Lactobacillus plantarum* on growth performance, digestive enzymes and gut morphology of *Litopenaeus vannamei*. *Probiotics. Antimicro.* 10, 504–510. doi: 10.1007/s12602-017-9300-z

Zhou, M., Zeng, D., Ni, X., Tu, T., Yin, Z., Pan, K., et al. (2016). Effects of *Bacillus licheniformis* on the growth performance and expression of lipid metabolism-related genes in broiler chickens challenged with *Clostridium perfringens*-induced necrotic enteritis. *Lipids Health Dis.* 15:48.

Conflict of Interest: The authors declare that the research was conducted in the absence of any commercial or financial relationships that could be construed as a potential conflict of interest.

Publisher's Note: All claims expressed in this article are solely those of the authors and do not necessarily represent those of their affiliated organizations, or those of the publisher, the editors and the reviewers. Any product that may be evaluated in this article, or claim that may be made by its manufacturer, is not guaranteed or endorsed by the publisher.

frontiers in Microbiology

ORIGINAL RESEARCH
published: 29 October 2021
doi: 10.3389/fmicb.2021.768767

Comparative Effects of Compound Enzyme and Antibiotics on Growth Performance, Nutrient Digestibility, Blood Biochemical Index, and Intestinal Health in Weaned Pigs

*Zhiqing Li, Lizi Tang, Nian Liu, Fan Zhang, Xiang Liu, Qian Jiang, Jiashun Chen and Xiaokang Ma**

College of Animal Science and Technology, Hunan Agricultural University, Changsha, China

OPEN ACCESS

Edited by:
Jia Yin,
Hunan Normal University, China

Reviewed by:
Shiyu Tao,
Huazhong Agricultural University, China
Tarique Hussain,
Nuclear Institute for Agriculture and Biology, Pakistan
Dandan Han,
China Agricultural University, China

***Correspondence:**
Xiaokang Ma
maxiaokang@hunau.edu.cn

Specialty section:
This article was submitted to Microbial Symbioses, a section of the journal Frontiers in Microbiology

Received: *01 September 2021*
Accepted: *23 September 2021*
Published: *29 October 2021*

Citation:
Li ZQ, Tang LZ, Liu N, Zhang F, Liu X, Jiang Q, Chen JS and Ma XK (2021) Comparative Effects of Compound Enzyme and Antibiotics on Growth Performance, Nutrient Digestibility, Blood Biochemical Index, and Intestinal Health in Weaned Pigs. Front. Microbiol. 12:768767. doi: 10.3389/fmicb.2021.768767

This experiment aims to explore the effects of compound enzyme preparation substituting chlortetracycline on growth performance, serum immune markers, and antioxidant capacity and intestinal health in weaned piglets. A total of twenty-four 28-day-old "Duroc × Landrace × Yorkshire" weaned piglets with an average initial weight of 7.25 ± 0.25 kg were randomly divided into three groups according to their body weight, with eight replicates in each group and one pig in each replicate. The three dietary treatments were basal diet (CON), basal diet + 1,000 mg/kg compound enzyme preparation (cellulase 4,000 IU/g, α-amylase 1,000 IU/g, β-glucanase 150 IU/g, and neutral protease 3,000 IU/g, CE), and basal diet + 75 mg/kg chlortetracycline (CTC). The animal experiment lasted for 28 days and was divided into two stages: the early stage (0–14 days) and the late stage (15–28 days). The results showed that (1) compared with the CON, the CE and CTC significantly increased the ADG of weaned piglets during the early and whole period of experiment ($p < 0.05$), decreased the F:G in the whole experiment period ($p < 0.05$), and diarrhea rate in the early stage ($p < 0.01$). (2) Compared with the CON, the apparent total tract digestibility of ADF and NDF was significantly increased in pigs fed the CE diet in the early and late stages of experiment ($p < 0.05$) with no significant difference compared with the CTC. (3) Compared with the CON, the concentrations of serum IgA and SOD in weaned piglets were significantly increased in the CE group in the early stage of the experiment ($p < 0.05$). (4) Compared with the CON group, the acetic acid, propionic acid, and total VFA contents in cecum and colon segments were elevated in the CE group ($p < 0.05$) with no significant difference compared with the CTC. (5) Compared with the CON group, the villus height of duodenum and jejunum and the ratio of villus height to recess depth of ileum were increased in the CE and CTC group ($p < 0.05$). (6) Compared with the CON group, the abundance of *Lactobacillus* significantly increased ($p < 0.01$) while the abundance of

Escherichia coli decreased in the CE group and CTC group ($p < 0.01$). In conclusion, CE preparation instead of CTC can significantly improve the nutrient digestibility, the immunity, antioxidant capacity, and intestinal health of pigs, which may contribute to the improved growth performance of piglets.

Keywords: compound enzymes, growth performance, nutrient digestibility, serum biochemical profiles, intestinal health, weaned piglets

INTRODUCTION

In the pig industry, weaning stress of piglets has always been a huge problem. Piglets have a series of problems such as diarrhea, anorexia, and decreased growth performance due to immature digestive tract, low immune function, and dietary changes (Li et al., 2021). In the past, antibiotics were commonly used in piglets to reduce weaning stress, but bacterial resistance to antibiotics has become a global threat to animals and public health (Teale and Borriello, 2021). The inclusion of antibiotics in animal diets is a controversial issue worldwide (Zainab et al., 2020). China stopped using antibiotics as feed additives in July 2020. Therefore, it is necessary to develop new feed additives to replace antibiotics and improve the health condition of pigs and its product quality.

Since antibiotics were banned, enzymes used in pig diets have been widely accepted (Willamil et al., 2012). It has been reported that dietary supplementation of compound enzyme containing amylase, protease, and xylanase can promote the growth of piglets by improving nutrient digestibility and regulating intestinal flora (Yi et al., 2013). Since cereal feeds contain large amounts of soluble non-starch polysaccharides (NSP), it not only reduced nutrient digestibility but also induced inflammation in pigs (Woyengo et al., 2009; Vila et al., 2018). Moreover, starch particles embedded in cereal protein matrix are not easily decomposed by starch degrading enzymes (Zaefarian et al., 2015). The adverse effects of NSP and cellulose could be alleviated by adding cellulase, α-amylase, and β-glucanase to cereal grain-based diets. In addition, supplementation of cereal grain-based diets with protease for pigs may increase the degradation of protein that interacts with NSP and starch, thereby increasing nutrient digestibility.

At present, most studies mainly explore the effects of different enzyme preparations on barley, oats, or Distillers Dried Grains with Solubles (DDGS) as the basic diet, while there are few studies investigating whether enzyme preparations can improve the utilization efficiency of corn–soybean meal diet. Therefore, this experiment was conducted to evaluate the effects of adding a compound enzyme preparation composed of NSP enzyme, amylase and protease to replace antibiotics in corn-soybean meal diet on growth performance, serum immune markers, and antioxidant capacity and intestinal health of weaned piglets. It provides scientific basis and theoretical basis for the application of compound enzyme preparation to replace antibiotics in animal production.

Abbreviations: BW, body weight; ADG, average daily gain; ADFI, average daily feed intake; G:F, gain-to-feed ratio; DM, dry matter; OM, organic matter; CP, crude protein; GE, gross energy; ADF, acid detergent fiber; NDF, neutral detergent fiber; IgA, immunoglobulin A; IgG, immunoglobulin G; IgM, immunoglobulin M; SOD, superoxide dismutase; GSH-Px, glutathione peroxidase; T-AOC, total antioxidant capacity; MDA, malondialdehyde; VFAs, volatile fatty acids; SCFAs, short-chain fatty acids; BCFAs, branched-chain fatty acids; PCR, polymerase chain reaction; OTUs, operational taxonomic units; PCoA, principal coordinate analysis; LDA, linear discriminant analysis; LEfSe, linear discriminant analysis effect size.

MATERIALS AND METHODS

The compound enzyme used in this study contained amylase, protease, and xylanase. The compound enzyme preparation is provided by DuPont, Inc. The main components are cellulase (4,000 IU/g), α-amylase (1,000 IU/g), β-glucanase (150 IU/g), and neutral protease (3,000 IU/g). According to the results of *in vitro* test (Long et al., 2021) and the company's recommendation, the supplemental amount was 1,000 mg/kg.

Animal Treatment and Experimental Design

Twenty-four 28-day-old weaned piglets (Duroc × Landrace × Large White) with an average initial body weight of 7.25 kg were randomly allocated to three groups with eight replicates per group and one piglet per replicate according to gender and body weight in a randomized complete block design. The three experimental diets were a corn–soybean meal basal diet (CON), a basal diet supplemented with 1,000 mg/kg compound enzyme preparation (CE) and a basal diet supplemented with 75 mg/kg chlorotetracycline preparation (CTC). The animal experiment lasted for 28 days, which was divided into early (0–14 days) and late (15–28 days) stages. The nutrient composition of diets (**Table 1**) met or exceeded the requirements of NRC (2012).

These experiments were conducted in accordance with Chinese guidelines for animal welfare and experimental protocols, and all animal procedures were approved by the Committee of Animal Care at Hunan Agricultural University (Changsha, China) (Permit Number: CACAHU 2021-01106). The animal experiments were carried out in the Animal Test Base of Hunan Agricultural University. All the piglets were housed on a net bed with a leaky floor and had free access to feed and water. The piglets were dewormed and immunized according to routine procedures and pig houses were cleaned and disinfected regularly. The ambient temperature is automatically adjusted by the thermostatic controller and windows are regularly opened for ventilation.

DETECTION INDICATORS

Growth Performance and Diarrhea Rate

On days 0, 14, and 28, the body weight and feed intake of pigs were recorded to calculate average daily gain (ADG), average daily feed intake (ADFI), and feed to weight gain ratio (F:G). From days 0 to 28, the health status and mortality of each piglet were recorded. The occurrence of diarrhea and fecal score of each pig was visually assessed and evaluated twice a day by trained observers blinded to the treatments according to the method of Long et al. (2017). In brief, the severity of diarrhea was assessed using a scoring system as shown below: 1 = hard stool; 2 = slightly soft feces; 3 = partially formed soft feces; 4 = loose semi-liquid feces; 5 = watery mucous feces. Pigs are identified as having diarrhea when the average score exceeds 3 points. Diarrhea rate was determined mainly based on the average score of feces and the formula was: diarrhea rate (%) = days of diarrhea number of pigs with diarrhea/(test days × total number of pigs).

Nutrient Digestibility

During this experiment, a total of 1 kg of feed samples were collected weekly. The dry matter (DM), crude protein (CP), acid detergent fiber (ADF), and neutral detergent fiber (NDF) in feed and fecal samples were measured according to AOAC (2012). The apparent total tract digestibility (ATTD) was calculated as follows:

$$\text{ATTD nutrient} = 1 - (\text{Cr}_{\text{diet}} \cdot \text{Nutrient}_{\text{feces}})/(Cr_{\text{feces}} \cdot Nutrient_{\text{diet}}).$$

Serum Assays

On days 14 and 28, blood samples were collected by anterior vena cava puncture in each treatment, centrifuged at 3,000 *g* at 4°C for 15 min to obtain the serum, and stored at –20°C until analysis. Serum immunoglobulin concentration was determined by using an ELISA kit (A) following the manufacturer's instructions (Cusabio Biotechnology Co., Ltd., Wuhan, China). Moreover, the contents of total antioxidant capacity (T-AOC), superoxide dismutase (SOD), glutathione peroxidase (GSH-Px), and malondialdehyde (MDA) in serum were determined using a spectrophotometer (Leng Guang SFZ1606017568, Shanghai, China) following the manufacturer's instructions (Nanjing Jiancheng Bioengineering Institute, Nanjing, China).

Volatile Fatty Acids Analysis

Digesta samples from cecal, colonic, and ileum segments were collected on day 28 to determine volatile fatty acid (VFA) content (n = 8). All samples were frozen in a –80°C freezer immediately after collection. VFA content of digesta was determined using a HP 5, 890 gas chromatograph (HP, Pennsylvania, United States) according to the method of Long et al. (2017).

Morphology of Small Intestine

At the end of the animal experiment, 24 pigs (8 pigs per treatment) were slaughtered and the proximal, middle, and distal part of the small intestine from the gastric pylorus to the ileo-cecal valve were obtained to analyze the morphological changes of duodenum, jejunum, and ileum. The samples of small intestine were fixed in neutral-buffered formalin and processed by the standard paraffin method. Small intestine sections (9–10 cm) were stained with hematoxylin and eosin. Measurements of villus height and crypt depth were taken only from sections where the plane of section ran vertically from the tip of villus to the base of an adjacent crypt by using a light microscope. Ten well-oriented villus × 3 sections of each pig were used to determine these indices (Wang et al., 2021).

Microbiota Analysis by 16S RNA

Total genome DNA was extracted from cecal digesta samples using the QIAamp Fast DNA Stool mini kit (Qiagen, Hilden, Germany) and checked with 1% agarose gel. The DNA concentration and purity were determined with Nano Drop 2,000 UV-vis spectrophotometer (Thermo Fisher Scientific, Wilmington, United States). The specific primer with the barcode

TABLE 1 | Ingredient composition and nutrient levels of the experimental diets (%, as-fed basis).

Items	Content (%)
Ingredients	
Corn	54.75
Soybean meal	19.00
Full-fat soybean powder	10.00
Fish meal	5.00
Whey powder	6.15
Soybean oil	1.50
Dicalcium phosphate	0.90
L-Lysine-HCl	0.48
L-Threonine	0.05
DL-Methionine	0.10
L-Tryptophan	0.02
Salt	0.30
Limestone	0.50
Premix[a]	1.00
Cr_2O_3	0.25
Total	100.00
Calculated nutrients	
Digestible energy (MJ/kg)	14.64
Crude protein	20.15
Lysine	1.38
Methionine	0.82
Methionine + cysteine	1.01
Threonine	0.97
Tryptophan	0.25
Calcium	0.80
Total phosphorus	0.73

[a]*The premix provided the following (per kilogram of complex feed): Vitamin A, 12,000 IU; Vitamin D, 2,500 IU; Vitamin E, 30 IU; Vitamin B12, 12 μg; Vitamin K, 3 mg; d-pantothenic acid, 15 mg; nicotinic acid, 40 mg; choline chloride, 400 mg; Mn, 40 mg; Zn, 100 mg; Fe, 90 mg; Cu, 8.8 mg; I, 0.35 mg; Se, 0.3 mg.*

(16S V3-V4) were amplified by an ABI Gene Amp® 9,700 PCR thermocycler (ABI, CA, United States). Then, the PCR products were extracted, purified, and quantified.

Paired-end sequencing was performed on an Illumina MiSeq PE300 platform/NovaSeq PE250 platform (Illumina, San Diego, United States). The raw 16S rRNA gene sequencing reads were demultiplexed, quality-filtered and merged according to previous studies (Magoč and Salzberg, 2011; Chen et al., 2018). The complexity of species diversity was evaluated with ACE and Chao richness estimators and diversity indices of Shannon and Simpson (Edgar, 2013). β-diversity was evaluated using principal component analysis (PCA) based on the Euclid distance. The significant differences between samples were evaluated by analysis of similarities (ANOSIM).

OTUs representing < 0.005% of the population were removed and taxonomy was assigned using the RDP classifier. The relative abundance of each OTU was counted at different taxonomic levels. Then, bioinformatics analysis was mainly performed using QIIME (v1.7.0) and R packages (v3.2.0). The OTU table in QIIME was used to calculate OTU-level and β-diversity was assessed by principal coordinate analysis (PCoA). Cluster analysis and significant differences between samples were tested by ANOSIM.

Statistical Analysis

Differences in the diarrhea incidence were tested by the χ^2 contingency test. All other data were analyzed by ANOVA method using the GLM model in SAS 9.2 statistical software with repetition (cycle) as the statistical unit. A very significant difference between the means was defined as $p \leq 0.01$ and significant difference between the means was defined at $p \leq 0.05$, while a trend for the significance between the means was designated at $0.05 < p \leq 0.10$.

RESULTS

Growth Performance and Diarrhea Rate

As shown in **Table 2**, pigs in the CE group had higher ADG during days 0–14 and days 0–28 and higher body weight at days 14 and 28 than pigs in the CON group ($p < 0.05$) without significant difference compared with the CTC. The CE diet did not significantly change the ADFI of pigs, but in the early stage and the whole period of the experiment, the F:G ratio and the diarrhea rate from days 0 to 14 were significantly reduced compared with the CON diet ($p < 0.05$). However, there was no differences in growth performance or diarrhea rate between CE and CTC.

Nutrient Digestibility

The effects of CE on nutrients in weaned piglets are shown in **Table 3**. Compared with the CON, the apparent total tract digestibility of ADF and NDF was significantly increased in pigs fed CE diet in the early and late stages of experiment ($p < 0.05$), and there was no significant difference between the CE and CTC groups.

Immunity and Antioxidant Properties

As shown in **Table 4** that compared with the CON, CE induced higher serum IgA concentrations in weaned piglets on day 14 ($p < 0.05$) and higher IgG on day 28, which was not significantly different from the CTC. **Table 5** shows that pigs fed CE had higher serum SOD concentration on day 14 ($p < 0.05$) compared with the CON and was not significantly different from the CTC. The CE group showed increased serum GSH-Px concentration of pigs on day 28 compared with the CON ($p < 0.05$) without

TABLE 2 | Effect of CE on growth performance and diarrhea rate of weaned piglets.

Items	CON	CE	CTC	SEM	*p*-value
Day 0 BW (kg)	7.25	7.24	7.25	0.04	0.97
Day 14 BW (kg)	10.97^b	11.45^a	11.34^a	0.12	0.03
Day 28 BW (kg)	15.88^b	16.80^a	16.66^a	0.21	0.01
Days 0–14					
ADG (g)	265.71^b	300.98^a	292.14^a	7.54	0.01
ADFI (g)	441.43	456.09	460.01	9.33	0.20
F:G	1.66^a	1.51^b	1.57^b	0.02	< 0.01
Diarrhea rate (%)	3.46^a	1.34^b	1.23^b	0.39	< 0.01
Days 15–28					
ADG (g)	351.07	382.32	379.91	17.24	0.39
ADFI (g)	658.21	655.27	660.45	15.47	0.97
F:G	1.89	1.73	1.74	0.06	0.13
Diarrhea rate (%)	1.00	1.00	1.23	0.57	0.95
Days 0–28					
ADG (g)	308.39^b	341.65^a	336.03^a	7.52	0.02
ADFI (g)	549.82	560.18	560.22	5.30	0.31
F:G	1.79^a	1.65^b	1.67^b	0.03	0.01
Diarrhea rate (%)	2.23	1.17	1.23	0.39	0.13

SEM, standard error of the mean (n = 8).
^{a,b}Different superscripts within a row indicate a significant difference ($p < 0.05$).

TABLE 3 | Effects of CE on total intestinal apparent digestibility of nutrients in weaned piglets (%).

Items	CON	CE	CTC	SEM	*p*-value
Days 0–14					
DM	81.51	81.16	82.01	0.40	0.34
OM	83.93	83.18	83.53	0.33	0.31
CP	76.14	75.12	76.87	0.55	0.12
GE	81.61	81.11	82.08	0.32	0.13
ADF	56.82^b	65.20^a	65.99^a	1.75	< 0.01
NDF	40.92^b	54.74^a	51.05^a	2.44	< 0.01
Days 15–28					
DM	81.17	80.36	80.58	0.27	0.13
OM	83.29	82.72	82.54	0.29	0.19
CP	75.19	76.31	76.22	0.57	0.33
GE	81.28	80.39	80.46	0.35	0.17
ADF	59.81^b	64.38^a	64.44^a	1.25	0.03
NDF	46.90^b	54.86^a	55.87^a	2.01	0.01

SEM, standard error of the mean (n = 8).
^{a,b}Different superscripts within a row indicate a significant difference ($p < 0.05$).

significant difference compared with the CTC group. Moreover, the CE diet tended to decrease the serum MDA concentration in weaned piglets compared with the CON diet ($0.05 < p \leq 0.10$).

Volatile Fatty Acid Composition

VFA profiles of ileal, cecal, and colonic segments are shown in **Table 6**. Pigs fed CE diet had increased acetic acid, propionic acid, and total VFA contents in the cecum and colon compared with CON ($p < 0.05$) with no significant difference compared with the CTC.

Intestinal Morphology

As shown in **Table 7**, pigs in CE group had lower crypt depth and higher villus height and villus height-to-crypt depth ratio in jejunum compared with that of CON ($p < 0.01$). The duodenum villus height of pigs in the CE group was significantly higher than that in the CON ($p < 0.05$) with no significant difference compared with the CTC.

Cecal Microbiota

Venn diagrams showed that there were 684, 543, and 755 OTUs in cecal digesta samples of CE, CON, and CTC groups, respectively, of which 423 OTUs were shared and 201 OTUs were unique (**Figure 1A**). The β-diversity of bacterial community between CON, CTC, and CE groups was presented with PCoA (**Figure 1B**). The PCoA with the Bray–Curtis distance indicated that the samples of the CON group gathered together and clearly separated from the samples of the CE and CTC groups.

At the phylum level (**Figure 2A**), the dominant phyla of cecum in three groups were *Firmicutes* and *Proteobacteria*. The

TABLE 4 | Effects of dietary CE supplementation on serum immunological traits of weaned pigs.

Items	CON	CE	CTC	SEM	*p*-value
Day 14					
IgA (g/L)	1.00^{b}	1.17^{a}	1.14^{a}	0.04	0.01
IgG (g/L)	6.93	7.36	7.99	0.33	0.11
IgM (g/L)	0.57	0.57	0.64	0.02	0.09
Day 28					
IgA (g/L)	2.81	2.59	2.73	0.08	0.23
IgG (g/L)	8.34^{b}	9.73^{a}	9.85^{a}	0.40	0.03
IgM (g/L)	0.10	0.11	0.12	0.01	0.16

SEM, standard error of the mean (n = 8).
^{a,b}Different superscripts within a row indicate a significant difference ($p < 0.05$).

TABLE 5 | Effect of CE on antioxidant parameters of weaned piglets.

Items	CON	CE	CTC	SEM	*p*-value
Day 14					
GSH-Px (U/ml)	748.05	752.22	768.75	24.47	0.82
MDA (nmol/ml)	4.02	3.32	2.87	0.30	0.05
SOD (U/ml)	119.78^{b}	133.13^{a}	140.16^{a}	4.03	< 0.01
T-AOC (U/ml)	8.48	9.40	10.11	0.62	0.21
Day 28					
GSH-Px (U/ml)	297.68^{b}	319.53^{a}	320.37^{a}	5.44	0.02
MDA (nmol/ml)	5.84	4.38	4.28	0.49	0.07
SOD (U/ml)	180.43	180.87	180.29	5.70	0.76
T-AOC (U/ml)	7.75	7.80	8.08	0.34	0.76

SEM, standard error of the mean (n = 8).
^{a,b}Different superscripts within a row indicate a significant difference ($p < 0.05$).

TABLE 6 | Effect of CE on VFA content in different intestinal segments of weaned piglets (mg/kg).

Items	CON	CE	CTC	SEM	*p*-value
Ileum					
Acetic acid	489.06	481.36	491.70	43.59	0.98
Propionic acid	129.42	136.85	144.32	16.67	0.82
Isobutyric acid	16.98	17.45	15.97	0.68	0.32
Butyric acid	62.86	68.16	69.00	5.70	0.72
Isovaleric acid	7.13	8.83	7.49	1.45	0.69
Valeric acid	8.09	8.24	8.91	0.80	0.74
Total VFA	713.51	720.89	737.45	44.56	0.93
Caecum					
Acetic acid	$3,433.76^{b}$	$4,514.55^{a}$	$4,449.69^{a}$	309.32	0.04
Propionic acid	$2,014.41^{b}$	$2,792.03^{a}$	$2,809.36^{a}$	223.22	0.04
Isobutyric acid	82.18	55.62	91.19	13.09	0.17
Butyric acid	1,056.40	1,194.49	1,233.27	94.99	0.41
Isovaleric acid	90.29	70.91	90.73	9.92	0.30
Valeric acid	193.99	180.81	210.94	22.67	0.65
Total VFA	$6,871.04^{b}$	$8,808.40^{a}$	$8,885.18^{a}$	564.34	0.04
Colon					
Acetic acid	$2,538.82^{b}$	$3,141.48^{a}$	$3,305.58^{a}$	186.45	0.03
Propionic acid	$1,616.77^{b}$	$2,083.41^{a}$	$2,207.99^{a}$	140.07	0.02
Isobutyric acid	90.24	120.99	113.61	12.31	0.22
Butyric acid	1,142.52	1,222.97	1,295.80	118.56	0.67
Isovaleric acid	161.77	192.08	185.77	11.10	0.16
Valeric acid	306.73	327.35	300.58	22.84	0.69
Total VFA	$5,856.84^{b}$	$7,088.28^{a}$	$7,409.33^{a}$	326.98	0.01

SEM, standard error of the mean (n = 8).
^{a,b}Different superscripts within a row indicate a significant difference ($p < 0.05$).
Total VFAs = Acetate + Propionate + Butyrate + Valerate + Isobutyrate + Isovalerate.

TABLE 7 | Effect of CE on intestinal morphology of weaned piglets.

Items	CON	CE	CTC	SEM	*p*-value
Duodenum					
Villus height (μm)	258.58^{b}	302.41^{a}	302.18^{a}	12.16	0.03
Crypt depth (μm)	252.26	220.42	246.12	16.26	0.37
Villus height/Crypt depth	1.08	1.40	1.26	0.10	0.10
Jejunum					
Villus height (μm)	271.33^{b}	356.53^{a}	296.00^{b}	11.52	< 0.01
Crypt depth (μm)	200.69^{a}	159.42^{b}	183.48^{a}	7.45	< 0.01
Villus height/Crypt depth	1.37^{b}	2.25^{a}	1.62^{b}	0.11	< 0.01
Ileum					
Villus height (μm)	255.62	291.54	264.89	11.78	0.11
Crypt depth (μm)	151.08	141.07	150.93	4.97	0.29
Villus height/Crypt depth	1.70	2.07	1.76	0.11	0.06

SEM, standard error of the mean (n = 8).
^{a,b}Different superscripts within a row indicate a significant difference ($p < 0.05$).

relative abundance of *Firmicutes* in cecum was significantly increased in piglets fed CE and CTC diets compared with CON diet ($p < 0.01$). Feeding CE and CTC diet significantly decreased the relative abundance of *Proteobacteria* and *Actinobacteriota* in cecum ($p < 0.01$). On day 28, the top three genera in the CON group were *Escherichia-Shigella*, *Lactobacillus*, and *Succiniclasticum* (**Figure 2B**), while those in CTC group were *Lactobacillus*, *Clostridium_sensu_stricto_1*, and *Streptococcus*, and *Lactobacillus*, *norank_f_T34*, and *Clostridium_sensu_stricto_1* in CE group. At the genus level, the CE supplementation significantly decreased the relative abundance of *Escherichia_Shigella*, *Collinsella*, and *Syntrophococcus* in cecum compared with CON ($p < 0.01$). Piglets fed CE diet had greater relative abundance of *Lactobacillus* than those fed the other two diets ($p < 0.001$). In addition, supplementation of CE and CTC diet reduced ($p < 0.05$) the relative abundance of *Succiniclasticum* in cecum when compared with the CON diet.

The LEfSe analysis was used to identify the significantly different bacteria at the genus level between the three treatments (**Figure 3A**). A total of 15 cecal genera were identified to be significantly different between the three groups, namely, 3 genera from CE, 8 genera from CON, and 4 genera from CTC. The relative abundance of *g_Lactobacillus, g_Clostridium_sensu_stricto*, and *g_Terrisporobacter* in cecum was increased in piglets fed with the CE diet; the relative abundance of *g_Escherichia-Shigella, g_Succiniclasticum, g_Collinsella, g_Syntrophococcus, g_Bifidobacterium, g_Erysipelotrichaceae_UCG006, g_Ruminococcus_gauvreauii_group*, and *g_Catenisphaera* was increased in piglets fed with the CON diet, whereas the relative abundance of *g_Streptococcus*, *g_Treponema, g_UCG-005,* and *g_Lachnospiraceae_XPB1014_group* was increased in cecum of piglets fed with the CON diet.

Correlation analysis between serum biochemical parameters and cecal microorganisms has been shown in **Figure 3B**, wherein the bacteria including *g_Lactobacillus, g_Escherichia-Shigella, g_Clostridium_sensu_stricto_1, g_Streptococcus, g_ UCG-005, g_Succiniclasticum, g_Collinsella, g_Treponema, g_Bifidobacterium, g_Syntrophococcus, g_Erysipelotrichaceae_UCG006, g_Ruminococcus_gauvreauii_ group, g__Lachnospiraceae_XPB1014_group,* and *g_Catenisphaeras* had a strong positive correlation with the concentration of IgG ($p < 0.01$). In addition, the bacteria including *g_Lactobacillus* and *g_Escherichia___Shigellag_Succiniclasticum* had a strong positive correlation with the GSH-Px ($p < 0.01$); the bacteria including g_Clostridium_sensu_stricto_1, g_Treponema, and g_Ruminococcus_gauvreauii_group had a strong positive correlation with the MDA ($p < 0.01$).

DISCUSSION

Adding multi-enzyme in the corn–soybean meal diet not only increased the ADG and G:F, but also increased the ATTD of ADF and NDF in the early and late stages of the experiment. However, dietary treatments had no significant effect on the ATTD of GE and the reason could be that the NSP enzyme acting as fiber-degrading enzyme has greater effects on fiber digestibility in ileum but no other nutrients such as fat and protein digestibility; therefore, no change in ATTD of GE was detected (Li et al., 2018). However, NSP can release more nutrients from the cell wall of grain, while neutral protease can decompose soybean antigen proteins in soybean meal, which are difficult for mammals to decompose into small peptides and amino acids (Meinlschmidt et al., 2016; Munyaka et al., 2016). Since the small peptides and amino acids are easily absorbed, the supplementation of compund enzyme consequently induced improved utilization efficiency of feed and promoted growth of piglets. Our study is consistent with previous studies in that CE promoted the growth of piglets by increasing the conversion rate of nutrients in the feed (Zhang et al., 2014; Li et al., 2018). Tsai et al. (2017) reported that adding both xylanase and β-glucanase into nursery diets with 30% corn DDGS improved ADG from days 7 to 35. However, according to the meta-analysis of Torres-Pitarch et al. (2017), 39% of studies showed that CE had no effects on pig growth performance, while 61% of studies showed that CE could improve pig growth performance. There are many factors affecting the growth performance of pigs, such as the proportion of CE, active ingredients, ages and breeds of pigs, feeding environment, and so on. In the future, it will be important to accurately predict the type and concentration of enzymes added to the diet according to different diets and growth stages of pigs.

Immunoglobulins are abundant in serum, have antibody activity or chemical structure similar to antibody molecules, and consist of two identical light and heavy chains linked by disulfide interchain bonds (Schroeder and Cavacini, 2010). Immunoglobulins play an important role in participating in antigen response and improving anti-immune function of weaned piglets. Long et al. (2021) found that CE increased serum immunoglobulins (IgA, IgG, and IgM) of pigs, indicating that CE could enhance the immune function of weaned pigs. He et al. (2020) reported that the CE could enhance the sIgA content in jejunal mucosa, which indicated that CE could help improve intestinal immune function of weaned pigs. Our study is also consistent with the results of previous studies in that CE increased serum IgA and IgG levels of piglets, reflecting that CE can improve the disease resistance of piglets. The CE could probably decompose the NSP in the soybean diet into oligosaccharides, which could help improve the immune function in pigs (Agyekum et al., 2015). The normal growth of animals can be guaranteed by maintaining the relative stability between systematic oxidation and antioxidant status. As the main product of lipid peroxidation, MDA will induce oxidative stress response when it was excessively produced and deposited (Ozdemir et al., 2007). SOD, GSH-Px, and other antioxidant enzymes can use the chain reaction mechanism to reduce the free radical reaction and protect animal from the damage of pro-oxidants (Benzie, 2003; Minelli et al., 2009; Yin et al., 2013). In the present study, dietary CE supplementation showed increased concentrations of antioxidant enzymes including SOD and GSH-Px in serum and decreased serum MDA concentration, which indicated that CE

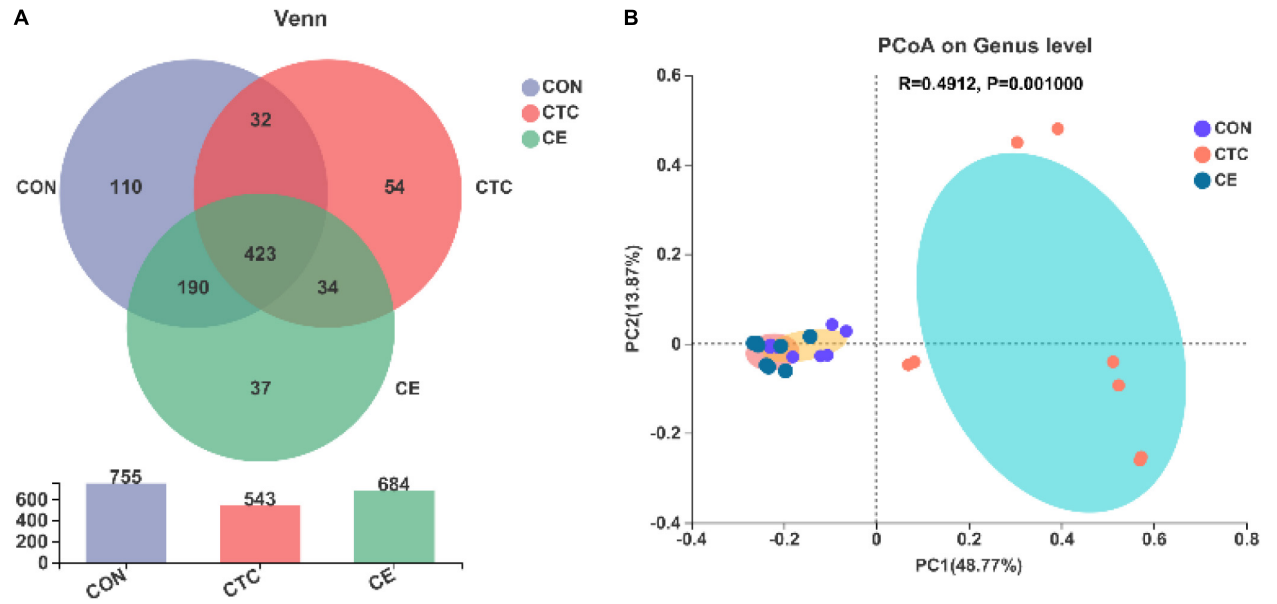

FIGURE 1 | Effect of compund enzymes on cecal OTU of pigs **(A)**. β-diversity of cecal microbes in piglets **(B)**. The individual minipig was regarded as the experimental unit, n = 8 for CE, n = 8 for CON, and n = 8 for CTC. CE, compund enzyme group; CON, basal diet group; CTC, chlortetracycline group.

may play an important role in eliminating reactive free radicals and alleviating oxidative stress response. This finding was partly consistent with the study of Long et al. (2021) who reported that dietary CE supplementation showed increased serum SOD and CAT content, and reduced serum MDA content. Additionally, Han et al. (2017) found that adding CE containing NSP enzyme and acid protease to piglet diet with antibiotics could significantly increase serum GSH-Px activity and significantly reduce MDA levels. Obviously, the improved antioxidant capacity may lead to reduced damage in intestinal barrier and alleviation of diarrhea (Huang et al., 2015). The positive effects of CE could be explained by reduced anti-nutritional factors in soybean meals due to the neutral protease addition, which may promote the healthy development of the intestinal tract, increase the colonization of beneficial bacteria in the intestinal tract, and reduce the post-intestinal fermentation, thereby improving the antioxidant capacity of piglets.

Microbial fermentation mainly occurs in the cecum and colon of pigs and play an important role in the intestinal health of pigs. It can produce a variety of VFAs, mainly including formic acid, acetic acid, propionic acid, and butyric acid, which can effectively inhibit the reproduction of harmful bacteria and enhance the absorption of intestinal nutrients (Högberg and Lindberg, 2006). In our study, the acetic acid, propionic acid, and total VFA concentrations in cecum and colon were significantly increased in pigs fed the diet supplemented with compound enzyme than those without enzymes. Similarly, Long et al. (2021) reported that dietary CE supplementation tended to increase acetic acid content in colon. Yi et al. (2013) also found that dietary CE supplementation could effectively enhance the VFA contents and improve the health status in weaned pigs. According to the previous studies, acetic acid and propionic acid contents in the large intestine of piglets increased due to dietary CE supplementation; one explanation could be the improved microflora profiles since acetic acid and propionic acid are the main metabolites of microflora in the large intestine (Yi et al., 2013; Zhang et al., 2014). Since VFA has been linked with intestinal health of animals, a higher VFA concentration also explained the improvement in growth performance of piglets.

The integrity of intestinal morphology and structure is a necessary condition to maintain the growth and healthy status of piglets. The ratio of intestinal villus height to crypt depth can directly reflect nutrient digestibility and gastrointestinal absorption function. A higher villus height-to-crypt depth ratio was more favorable for pigs to digest and absorb nutrient (Lm et al., 2003). However, weaning stress can significantly reduce intestinal villus height and villus atrophy can lead to intestinal cell death and reduce cell renewal rate (Wang et al., 2011). In our study, supplementation of CE increased the villus height of duodenum and jejunum as well as the villus height-to-crypt depth ratio in ileum. This finding was in agreement with the study of Long et al. (2021), who reported that CE could increase the villus height and the villus height-to-crypt depth ratio in ileum of weaned pigs. Jiang et al. (2015) also found that CE could improve ileal histology and intestinal health of weaning piglets. The reason for the current finding might be that CE can improve nutrient digestion and absorption in the small intestine and improve the intestinal integrity due to the increased nutrient supply to the intestinal tract (Wijtten et al., 2011).

This study also found that CE increased the relative abundance of *Firmicutes* and *Lactobacillus* in cecum, while the relative abundance of *Proteobacteria* and *Actinobacteriota* and *Escherichia-Shigella* were reduced by CE. These results

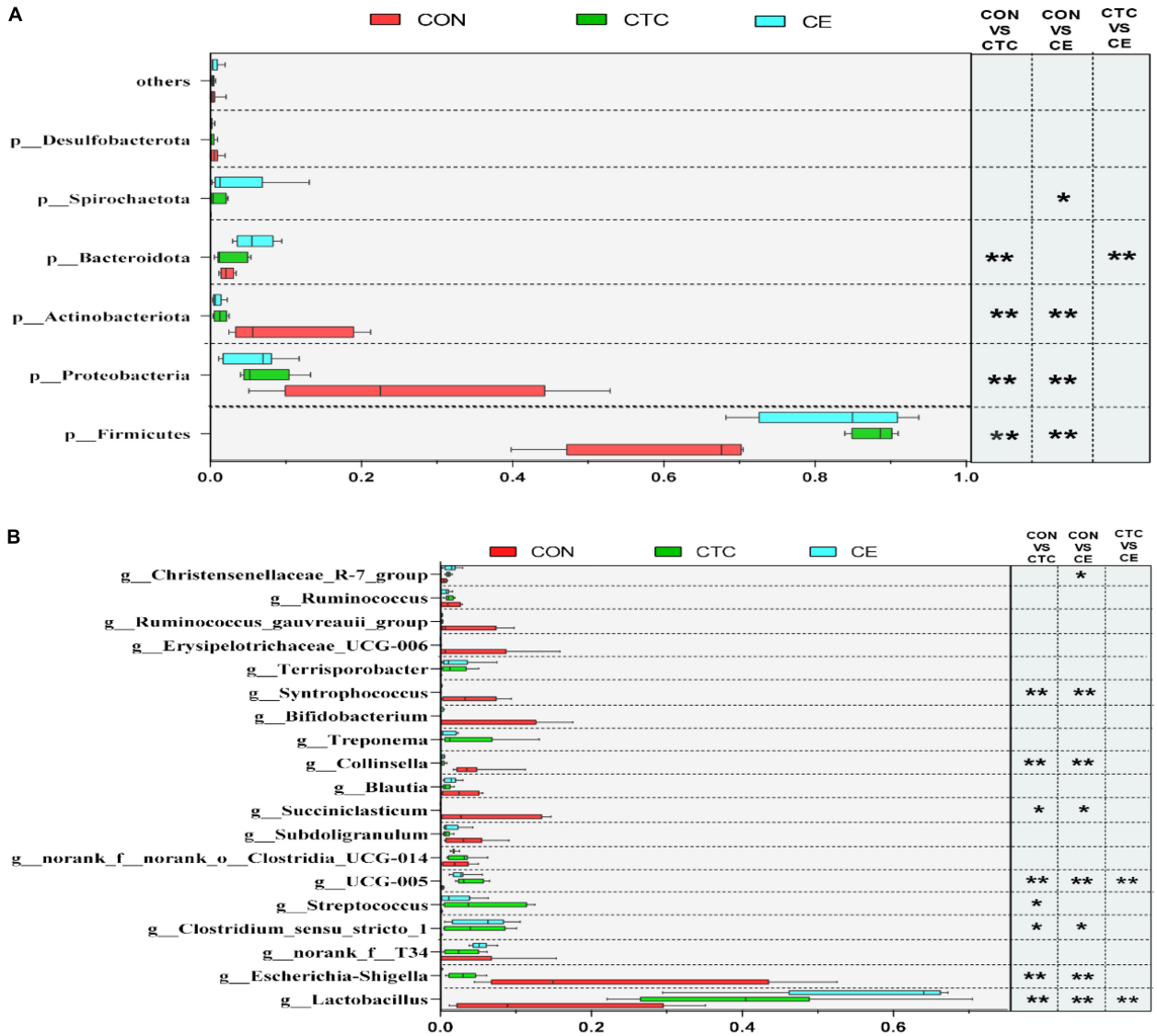

FIGURE 2 | Different microbiota comparison by the Student's *t*-test on phylum **(A)** and genus **(B)** of cecum. LEfSe analysis showed significantly changed bacteria between CON, CE, and CTC group. The individual minipig was regarded as the experimental unit ($n = 8$). CE, compund enzyme group; CON, basal diet group; CTC, chlortetracycline group. $^{*}p < 0.05$ and $^{**}p < 0.01$ represent significant difference, respectively.

indicated that CE had a good regulatory effect on the intestinal microflora of piglets. Moreover, an increase in the relative abundance of lactic acid bacteria or a decrease in the relative abundance of *Escherichia-Shigella* may be more beneficial for the intestinal health of weaned piglets and contributed to an improved growth performance in the CE group. Similar to our results, Long et al. (2021) found that dietary CE supplementation increased the relative abundance of *Firmicutes*, *Bacilli*, and *Lactobacillus* in cecum and colon. The changed microbial profiles induced by dietary treatments could be that the combination of protease, amylase, and cellulase reduced the posterior intestinal fermentation of piglets, inhibited the reproduction of harmful bacteria, and increased the abundance of beneficial bacteria. At the same time, the combination of exogenous amylase or β-glucanase with other enzymes can also reduce the relative abundance of harmful bacteria such as *Escherichia coli* in the intestinal tract of weaned piglets, which helps to reduce the diarrhea rate (Zhang et al., 2014; Jiang et al., 2015). Overall, these findings revealed that CE could be used to replace CTC to achieve a growth-promoting effect in some extent and may be even better than antibiotics in improving intestinal microflora in weaned piglets.

Members of *Firmicutes* can produce short-chain fatty acids by degrading carbohydrate, which are closely related to energy acquisition and immune response regulation in the body (Atarashi et al., 2011; Zhang et al., 2015). *Clostridium* has been reported to affect the accumulation of $CD8^{+}$ IELs (intraepithelial lymphocytes) in the colon (Umesaki et al., 1999). Based on

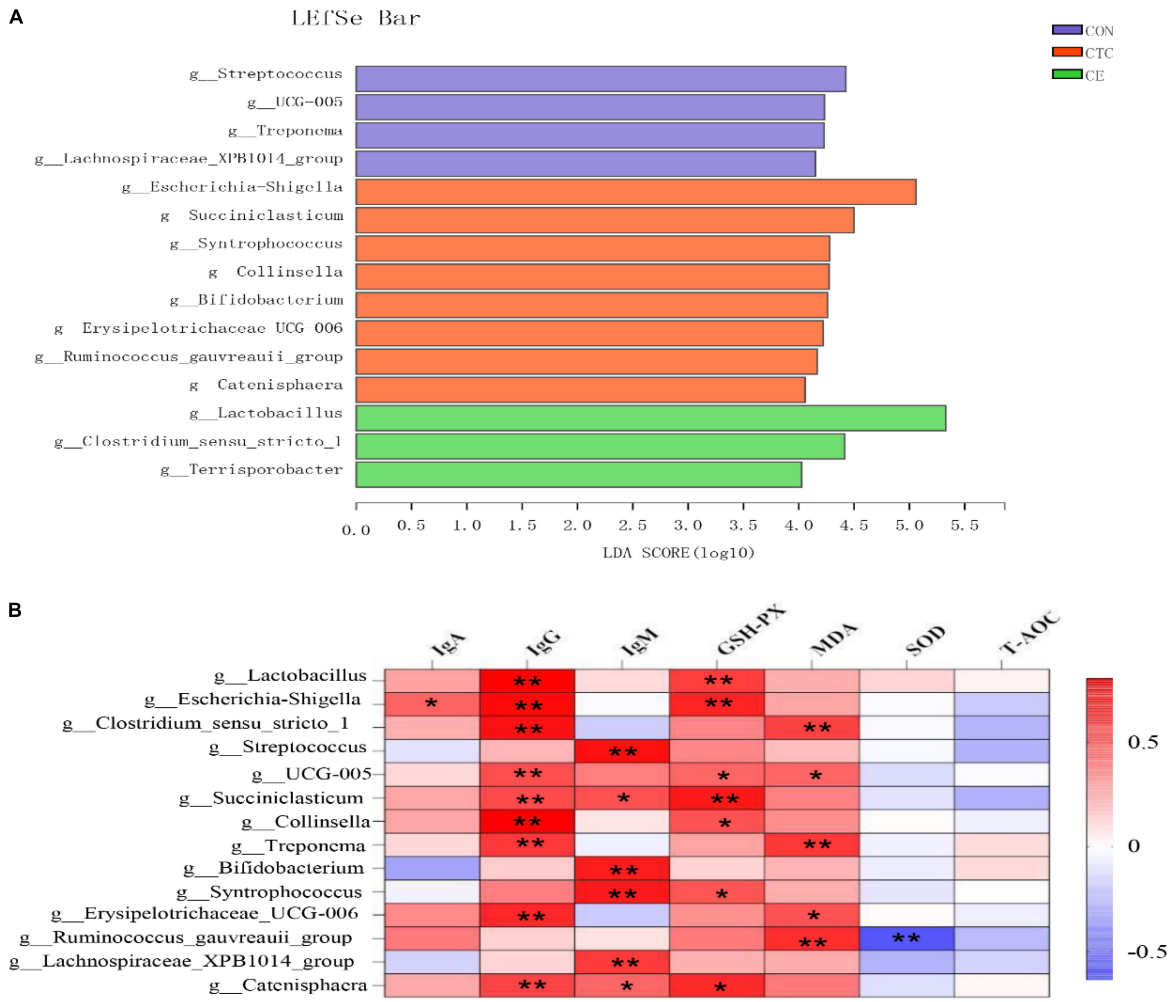

FIGURE 3 | Identification of the most differentially abundant genera in cecum **(A)**. The plot is generated from Linear Discriminant Analysis Effect Size (LEfSe) analysis with CSS-normalized OTU table and displays taxa with LDA scores above 4 and *p*-values below 0.05. Genera enriched in the samples with CTC diet are indicated with red bars, genera enriched in the samples with CON diet are indicated with blue bars, and genera enriched in the samples with CE diet are indicated with green bars. The individual minipig was regarded as the experimental unit ($n = 8$). CE, compund enzyme group; CON, basal diet group; CTC, chlortetracycline group. Correlation analysis between serum biochemical parameters and cecal microorganisms **(B)**. $^{*}p < 0.05$ and $^{**}p < 0.01$ represent significant difference, respectively.

these studies, it is not hard to find that microbes can modulate various aspects of the immune system function. In our study, the correlation analysis between serum biochemical indexes and cecal microorganisms showed that *g_Lactobacillus*, *g_UCG-005*, *g_Succiniclasticum*, *g_Collinsella*, and *g__Catenisphaeras* had a positive correlation with the concentration of IgG and GSH-Px, while *g_Ruminococcus-gauvreauii-group* had a negative correlation with the concentration of MDA and SOD. Some families and genera of *Clostridiales* cannot only degrade oligosaccharides into butyrate, but also regulate the balance of intestinal microflora (Louis and Flint, 2009) and are mediated by G-protein-coupled receptors in immune cells. Some members of the *Lactobacillales*, *Clostridiales*, and *Bifidobacteriales* are metabolically capable of producing conjugated linoleic acid (Devillard et al., 2007), which has an ability to enhance animal immunity by increasing the activity of immunoglobulin in serum and antioxidant enzymes in liver of animals (Ramírez-Santana et al., 2011; Huang et al., 2017). Besides lactic acid and acetic acid production (Mitsuoka, 1990), *Bifidobacterium* can promote the production of cytokines, specific antibodies, and non-specific antibodies, which induced activated immunity and enhanced disease resistance (Moya-Pérez et al., 2017). Its mechanism of action may be that *Bifidobacterium* forms a defensive barrier through competitive inhibition, and its metabolites can increase the content of free cholic acid and inhibit the growth of pathogenic microorganisms by activating the body to produce catalase (Zuo et al., 2013). The study of Liu et al. (2017) showed that *Lactoales* and *Enterococcus faecalis* could increase the intestinal immune function of piglets and reduce the incidence of diarrhea and mortality of piglets. Similarly, studies have shown that daily probiotic strains containing *Bifidobacterium* and

Lactobacillus treatment in mice can alter the inflammatory state of mice (Giacinto et al., 2005; Lyons et al., 2010; Karimi et al., 2012).

CONCLUSION

In summary, supplementation of CE in diets effectively improved nutrient digestibility and immunity function in weaned piglets and increased relative abundance of *Lactobacillus* species in the cecum, which could contribute to the improved intestinal health, and consequently was associated with improved growth performance and reduced diarrhea rate of pigs. Overall, CE had comparative effects on growth performance, immunity, antioxidant capacity, and intestinal health of weaned piglets.

DATA AVAILABILITY STATEMENT

The datasets presented in this study can be found in online repositories. The names of the repository/repositories and accession number(s) can be found below: NCBI SRA database and Bioproject accession number: PRJNA760807 (https://www.ncbi.nlm.nih.gov/bioproject/PRJNA760807).

ETHICS STATEMENT

The animal study was reviewed and approved by the Committee of Animal Care at Hunan Agricultural University (Changsha, China) (Permit Number: CACAHU 2021-01106).

AUTHOR CONTRIBUTIONS

ZL and XM: conceptualization, methodology, and software. LT, NL, XL, and FZ: literature collection. ZL and QJ: writing—original draft preparation. JC: writing—reviewing and editing. XM: funding acquisition. All authors contributed to the article and approved the submitted version.

FUNDING

This review was funded by the Scientific Research Fund of Hunan Provincial Education Department (19B267), the Youth Science Foundation Project of Hunan Agricultural University (19QN01), and the Open Foundation of CAS Key Laboratory of Agro-ecological Processes in Subtropical Region, Institute of Subtropical Agriculture (ISA2020101).

REFERENCES

Agyekum, A. K., Sands, J. S., Regassa, A., Kiarie, E., Weihrauch, D., Kim, W. K., et al. (2015). Effect of supplementing a fibrous diet with a xylanase and β-glucanase blend on growth performance, intestinal glucose uptake, and transport-associated gene expression in growing pigs. *J. Anim. Sci.* 93, 3483–3493. doi: 10.2527/jas.2015-9027

Atarashi, K., Tanoue, T., Shima, T., Itoh, Y., and Honda, K. (2011). Induction of colonic regulatory T cells by indigenous *Clostridium* species. *Science (New York, N.Y.)* 331, 337–341. doi: 10.1126/science.1198469

Benzie, I. F. (2003). Evolution of dietary antioxidants. *Comp. Biochem. Physiol. Part A Mol. Integr. Physiol.* 136, 113–126. doi: 10.1016/s1095-6433(02)00368-9

Chen, S., Zhou, Y., Chen, Y., and Gu, J. (2018). fastp: an ultra-fast all-in-one FASTQ preprocessor. *Bioinformatics (Oxford, England)* 34, i884–i890. doi: 10.1093/bioinformatics/bty560

Devillard, E., Mcintosh, F. M., Duncan, S. H., and Wallace, R. J. (2007). Metabolism of linoleic acid by human gut bacteria: different routes for biosynthesis of conjugated linoleic acid. *J. Bacteriol.* 189, 2566–2570. doi: 10.1128/JB.01359-06

Edgar, R. C. (2013). UPARSE: highly accurate OTU sequences from microbial amplicon reads. *Nat. Methods* 10, 996−998. doi: 10.1038/nmeth.2604

Giacinto, C. D., Marinaro, M., Sanchez, M., Strober, W., and Boirivant, M. (2005). Probiotics ameliorate recurrent th1-mediated murine colitis by inducing il-10 and il-10-dependent tgf-β-bearing regulatory cells. *J. Immunol.* 174:3237. doi: 10.4049/jimmunol.174.6.3237

Han, X. Y., Yan, F. Y., Nie, X. Z., Xia, W., Chen, S., Zhang, X. X., et al. (2017). Effect of replacing antibiotics using multi-enzyme preparations on production performance and antioxidant activity in piglets. *J. Integr. Agric.* 16, 640–647. doi: 10.1016/S2095-3119(16)61425-9

He, X., Yu, B., He, J., Huang, Z., Mao, X., and Zheng, P. (2020). Effects of xylanase on growth performance, nutrients digestibility and intestinal health in weaned piglets - sciencedirect. *Livest. Sci.* 233:103940.

Högberg, A., and Lindberg, J. E. (2006). The effect of level and type of cereal non-starch polysaccharides on the performance, nutrient utilization and gut environment of pigs around weaning. *Anim. Feed Sci. Technol.* 127, 200–219. doi: 10.1016/j.anifeedsci.2005.09.004

Huang, C., Song, P., Fan, P., Hou, C., Thacker, P., and Ma, X. (2015). Dietary sodium butyrate decreases postweaning diarrhea by modulating intestinal permeability and changing the bacterial communities in weaned piglets. *J. Nutr.* 145, 2774–2780. doi: 10.3945/jn.115.217406

Huang, Y. S., Lin, Z. D., Rong, H., Hao, M. L., Zhu, D. S., Li, S. K., et al. (2017). Effects of conjugated linoleic acid on growth, body composition, antioxidant status, lipid metabolism and immunity parameters of juvenile chu's croaker, nibea coibor. *Aquacul. Res.* 49, 546–556. doi: 10.1111/are.13486

Jiang, X. R., Awati, A., Agazzi, A., Vitari, F., Ferrari, A., Bento, H., et al. (2015). Effects of a blend of essential oils and an enzyme combination on nutrient digestibility, ileum histology and expression of inflammatory mediators in weaned piglets. *Animal* 9, 417–426. doi: 10.1017/S1751731114002444

Karimi, K., Inman, M. D., Bienenstock, J., and Forsythe, P. (2012). *Lactobacillus* reuteri-induced regulatory t cells protect against an allergic airway response in mice. *Am. J. Respir. Crit. Care Med.* 179, 186–193. doi: 10.1164/rccm.200806-951OC

Li, H., Yin, J., He, X., Li, Z., Tan, B., Jiang, Q., et al. (2021). Enzyme-treated soybean meal replacing extruded full-fat soybean affects nitrogen digestibility, cecal fermentation characteristics and bacterial community of newly weaned piglets. *Front. Vet. Sci.* 8:639039. doi: 10.3389/fvets.2021.639039

Li, Q., Gabler, N. K., Loving, C. L., Gould, S. A., and Patience, J. F. (2018). A dietary carbohydrase blend improved intestinal barrier function and growth rate in weaned pigs fed higher fiber diets. *J. Anim. Sci.* 96, 5233–5243. doi: 10.1093/jas/sky383

Liu, C., Zhu, Q., Chang, J., Yin, Q., Song, A., Li, Z., et al. (2017). Effects of *Lactobacillus casei* and enterococcus faecalis on growth performance, immune function and gut microbiota of suckling piglets. *Arch. Anim. Nutr.* 71, 120–133. doi: 10.1080/1745039X.2017.1283824

Lm, A., Jrp, B., and Djh, B. (2003). A review of interactions between dietary fibre and the intestinal mucosa, and their consequences on digestive health in young non-ruminant animals - sciencedirect. *Anim. Feed Sci. Technol.* 108, 95–117.

Long, S., Hu, J., Mahfuz, S., Ma, H., and Piao, X. (2021). Effects of dietary supplementation of compound enzymes on performance, nutrient digestibility, serum antioxidant status, immunoglobulins, intestinal morphology and microbiota community in weaned pigs. *Arch. Anim. Nut.* 75, 31–47. doi: 10.1080/1745039X.2020.1852008

Long, S. F., Xu, Y. T., Pan, L., Wang, Q. Q., Wang, C. L., Wu, J. Y., et al. (2017). Mixed organic acids as antibiotic substitutes improve performance, serum

immunity, intestinal morphology and microbiota for weaned piglets. *Anim. Feed Sci. Technol.* 235, 23–32. doi: 10.1016/j.anifeedsci.2017.08.018

Louis, P., and Flint, H. J. (2009). Diversity, metabolism and microbial ecology of butyrate-producing bacteria from the human large intestine. *FEMS Microbiol. Lett.* 294, 1–8. doi: 10.1111/j.1574-6968.2009.01514.x

Lyons, A., O'Mahony, D., O'Brien, F., Macsharry, J., and O'Mahony, L. (2010). Bacterial strain-specific induction of foxp3+t regulatory cells is protective in murine allergy models. *Clin. Exp. Allergy* 40, 811–819. doi: 10.1111/j.1365-2222.2009.03437.x

Magoč, T., and Salzberg, S. L. (2011). FLASH: fast length adjustment of short reads to improve genome assemblies. *Bioinformatics* 27, 2957-2963. doi: 10.1093/bioinformatics/btr507

Meinlschmidt, P., Schweigee, U., and Rode, V. (2016). Enzyme assisted degradation of po-tential soy protein allergens with special emphasis onthe technofunctionality and the avoidance of a bitter taste formation. *LWT Food Sci. Technol.* 68, 707-716. doi: 10.2767/jas.2000-5598

Minelli, A., Bellezza, I., Conte, C., and Culig, Z. (2009). Oxidative stress-related aging: a role for prostate cancer? *Biochim. Biophys. Acta* 1795, 83–91. doi: 10.1016/j.bbcan.2008.11.001

Mitsuoka, T. (1990). Bifidobacteria and their role in human health. *J. Ind. Microbiol.* 6, 263–267. doi: 10.1007/BF01575871

Moya-Pérez, A., Perez-Villalba, A., Benítez-Páez, A., Campillo, I., and Sanz, Y. (2017). Bifidobacterium cect 7765 modulates early stress-induced immune, neuroendocrine and behavioral alterations in mice. *Brain Behav. Immun.* 65, 43–56. doi: 10.1016/j.bbi.2017.05.011

Munyaka, P. M., Nandha, N. K., Kiarie, E., Nyachoti, C. M., and Khafipour, E. (2016). Impact of combined β-glucanase and xylanase enzymes on growth performance, nutrients utilization and gut microbiota in broiler chickens fed corn or wheat-based diets. *Poult. Sci.* 95, 528–540. doi: 10.3382/ps/pev333

NRC (2012). *Nutrient Requirements of Swine*, 11th Edn. Washington, DC: National Academies Press.

Ozdemir, D., Uysal, N., Tugyan, K., Gonenc, S., Acikgoz, O., Aksu, I., et al. (2007). The effect of melatonin on endotoxemia-induced intestinal apoptosis and oxidative stress in infant rats. *Intensive Care Med.* 33, 511–516. doi: 10.1007/s00134-006-0492-z

Ramírez-Santana, C., Castellote, C., Castell, M., Moltó-Puigmartí, C., Rivero, M., Pérez-Cano, F. J., et al. (2011). Enhancement of antibody synthesis in rats by feeding cis-9,trans-11 conjugated linoleic acid during early life. *J. Nutr. Biochem.* 22, 495–501. doi: 10.1016/j.jnutbio.2010.04.005

Schroeder, H. W. Jr., and Cavacini, L. (2010). Structure and function of immunoglobulins. *J. Allergy Clin. Immunol.* 125(2 Suppl 2), S41–S52.

Teale, C., and Borriello, P. (2021). A proposed scheme for the monitoring of antibiotic resistance in veterinary pathogens of food animals in the uk. *Vet. Rec.* 189:e201. doi: 10.1002/vetr.201

Torres-Pitarch, A., Hermans, D., Manzanilla, E. G., Bindelle, J., Everaert, N., Beckers, Y., et al. (2017). Effect of feed enzymes on digestibility and growth in weaned pigs: a systematic review and meta-analysis. *Anim. Feed Sci. Technol.* 233, 145–159. doi: 10.1016/j.anifeedsci.2017.04.024

Tsai, T., Dove, C. R., Cline, P. M., Owusu-Asiedu, A., Walsh, M. C., and Azain, M. (2017). The effect of adding xylanase or β-glucanase to diets with corn distillers dried grains with solubles (cddgs) on growth performance and nutrient digestibility in nursery pigs. *Livest. Sci.* 197, 46–52. doi: 10.1016/j.livsci.2017.01.008

Umesaki, Y., Setoyama, H., Matsumoto, S., Imaoka, A., and Itoh, K. (1999). Differential roles of segmented filamentous bacteria and clostridia in development of the intestinal immune system. *Infect. Immun.* 67:3504. doi: 10.1111/j.1574-695X.1999.tb01309.x

Vila, M. F., Trudeau, M. P., Hung, Y. T., Zeng, Z., Urriola, P. E., Shurson, G. C., et al. (2018). Dietary fiber sources and non-starch polysaccharide-degrading enzymes modify mucin expression and the immune profile of the swine ileum. *PLoS One* 13:e0207196. doi: 10.1371/journal.pone.0207196

Wang, D., Piao, X. S., Zeng, Z. K., Lu, T., Zhang, Q., Li, P. F., et al. (2011). Effects of keratinase on performance, nutrient utilization, intestinal morphology, intestinal ecology and inflammatory response of weaned piglets fed diets with different levels of crude protein. *Asian Australas. J. Anim. Sci.* 24, 1718–1728. doi: 10.5713/ajas.2011.11132

Wang, F., Yin, Y., Yang, M., Chen, J., Fu, C., and Huang, K. (2021). Effects of combined supplementation of *Macleaya cordata* extract and benzoic acid on the growth performance, immune responses, antioxidant capacity, intestinal morphology, and microbial composition in weaned piglets. *Front. Vet. Sci.* 8:708597. doi: 10.3389/fvets.2021.708597

Wijtten, P. J., van der Meulen, J., and Verstegen, M. W. (2011). Intestinal barrier function and absorption in pigs after weaning: a review. *Br. J. Nutr.* 105, 967–981. doi: 10.1017/S0007114510005660

Willamil, J., Badiola, I., Devillard, E., Geraert, P. A., and Torrallardona, D. (2012). Wheat-barley-rye- or corn-fed growing pigs respond differently to dietary supplementation with a carbohydrase complex. *J. Anim. Sci.* 90, 824–832. doi: 10.2527/jas.2010-3766

Woyengo, T. A., Cowieson, A. J., Adeola, O., and Nyachoti, C. M. (2009). Ileal digestibility and endogenous flow of minerals and amino acids: responses to dietary phytic acid in piglets. *Br. J. Nutr.* 102, 428–433. doi: 10.1017/S0007114508184719

Yi, J. Q., Piao, X. S., Li, Z. C., Zhang, H. Y., and Dong, B. (2013). The effects of enzyme complex on performance, intestinal health and nutrient digestibility of weaned pigs. *Asian Australas. J. Anim. Sci.* 26, 1181–1188. doi: 10.5713/ajas.2013.13129

Yin, J., Ren, W., Wu, X., Yang, G., and Su, D. (2013). Oxidative stress-mediated signaling pathways: a review. *J. Food Agric. Environ.* 11, 132–139.

Zaefarian, F., Abdollahi, M. R., and Ravindran, V. (2015). Starch digestion in broiler chickens fed cereal diets. *Anim. Feed Sci. Technol.* 209, 16–29. doi: 10.1016/j.anifeedsci.2015.07.020

Zainab, S. M., Junaid, M., Xu, N., and Malik, R. N. (2020). Antibiotics and antibiotic resistant genes (ARGs) in groundwater: a global review on dissemination, sources, interactions, environmental and human health risks. *Water Res.* 187:116455. doi: 10.1016/j.watres.2020.116455

Zhang, G. G., Yang, Z. B., Wang, Y., Yang, W. R., and Zhou, H. J. (2014). Effects of dietary supplementation of multi-enzyme on growth performance, nutrient digestibility, small intestinal digestive enzyme activities, and large intestinal selected microbiota in weanling pigs. *J. Anim. Sci.* 92, 2063–2069. doi: 10.2527/jas.2013-6672

Zhang, J., Guo, Z., Xue, Z., Sun, Z., Zhang, M., Wang, L., et al. (2015). A phylo-functional core of gut microbiota in healthy young chinese cohorts across lifestyles, geography and ethnicities. *ISME J. Multidiscip. J. Microb. Ecol.* 9, 1979–1990. doi: 10.1038/ismej.2015.11

Zuo, Q. R., Mai, K., and Xu, W. (2013). *Effects of Conjugated Linoleic Acid on Growth, Non-Specific Immunity, Antioxidant Capacity, Lipid Deposition And Related Gene Expression in Juvenile Large Yellow Croaker*. Cambridge: Cambridge University Press.

Conflict of Interest: The authors declare that the research was conducted in the absence of any commercial or financial relationships that could be construed as a potential conflict of interest.

Publisher's Note: All claims expressed in this article are solely those of the authors and do not necessarily represent those of their affiliated organizations, or those of the publisher, the editors and the reviewers. Any product that may be evaluated in this article, or claim that may be made by its manufacturer, is not guaranteed or endorsed by the publisher.

frontiers in Microbiology

ORIGINAL RESEARCH
published: 03 November 2021
doi: 10.3389/fmicb.2021.762689

Effects of Dietary *Phaffia rhodozyma* Astaxanthin on Growth Performance, Carotenoid Analysis, Biochemical and Immune-Physiological Parameters, Intestinal Microbiota, and Disease Resistance in *Penaeus monodon*

Weilong Wang[1,2,3,4†], Mengting Liu[1†], Samia Fawzy[1], Yucai Xue[1], Meiqin Wu[5], Xuxiong Huang[1,3,4], Ganfeng Yi[1,6*] and Qian Lin[2*]*

[1] Centre for Research on Environmental Ecology and Fish Nutrition of the Ministry of Agriculture, Shanghai Ocean University, Shanghai, China, [2] Institute of Bast Fiber Crops, Chinese Academy of Agricultural Sciences, Changsha, China, [3] Shanghai Collaborative Innovation for Aquatic Animal Genetics and Breeding, Shanghai Ocean University, Shanghai, China, [4] National Demonstration Center for Experimental Fisheries Science Education, Shanghai Ocean University, Shanghai, China, [5] College of Marine Ecology and Environment, Shanghai Ocean University, Shanghai, China, [6] Beijing Dabeinong Technology Group Co., Ltd., Beijing, China

The present study aimed to investigate the effect of dietary astaxanthin (Ast) from *Phaffia rhodozyma* on growth performance, survival, carotenoid content, the activity of antioxidant and immune-related enzymes, intestinal microbiota comparison, and disease resistance against *Vibrio parahaemolyticus* in *Penaeus monodon*. Juveniles (average weight 3.15 ± 0.12 g) were fed with six experimental diets supplemented with 0 (Control), 20.5, 41, 61.5, 82, and 102.5 mg/kg of Ast (defined as diet A–D) in triplicate for 56 days. The results indicated that shrimp fed with Ast supplementation significantly ($p < 0.05$) improved growth performance compared with the control. Furthermore, significantly ($p < 0.05$) increased survival and decreased feed conversion ratio (FCR) demonstrated the beneficial effects of dietary Ast on enhancing nutrient utilization and ultimately improving the growth and survival of shrimp. Furthermore, shrimp fed with Ast including diet developed a deeper red color than the control, consistent with the significantly ($p < 0.05$) increased Ast deposition in the shrimp shell. Hemolymph-immunological parameters [aspartate aminotransferase (AST), alanine aminotransferase (ALT), and alkaline phosphatase (AKP)] and hepatopancreatic antioxidant status [total antioxidant capacity (T-AOC), malondialdehyde (MDA), catalase (CAT), and superoxide dismutase (SOD)] were significantly ($p < 0.05$) affected by dietary Ast supplementation. Dietary increasing Ast levels significantly ($p < 0.05$) increased shrimp resistance performance to *V. parahaemolyticus* according to the LT_{50} results in the current study, which may be caused by increased total carotenoid contents in shrimp tissues from all the Ast-supplemented treatments. Conversely, intestinal microbiota biodiversity and

OPEN ACCESS

Edited by:
Jia Yin,
Hunan Normal University, China

Reviewed by:
Min Jin,
Ningbo University, China
Yuzhe Han,
Dalian Ocean University, China
Md. Sakhawat Hossain,
Sylhet Agricultural University, Bangladesh

***Correspondence:**
Xuxiong Huang
xxhuang@shou.edu.cn
Ganfeng Yi
2683763570@qq.com
Qian Lin
linqian@caas.cn

[†] These authors have contributed equally to this work and share first authorship

Specialty section:
This article was submitted to Microbial Symbioses, a section of the journal Frontiers in Microbiology

Received: *22 August 2021*
Accepted: *14 September 2021*
Published: *03 November 2021*

Citation:
Wang W, Liu M, Fawzy S, Xue Y, Wu M, Huang X, Yi G and Lin Q (2021) Effects of Dietary Phaffia rhodozyma Astaxanthin on Growth Performance, Carotenoid Analysis, Biochemical and Immune-Physiological Parameters, Intestinal Microbiota, and Disease Resistance in Penaeus monodon. Front. Microbiol. 12:762689. doi: 10.3389/fmicb.2021.762689

richness were not affected by dietary Ast. The best performances of growth, antioxidant status, immunological response, and carotenoid deposition were observed in diets E and F among all the Ast-supplemented treatments. Overall, all the data suggested that dietary *P. rhodozyma* Ast played a critical role in improving growth performance, achieving the desired coloration, increasing carotenoid content, and keeping better health status of shrimp. Based on these positive performances, *P. rhodozyma* Ast could gain the trust of the consumers as a natural source and provide a potential alternative for synthetic Ast using in the *Penaeus monodon* culture industry.

Keywords: astaxanthin, *Phaffia rhodozyma*, *Penaeus monodon*, shrimp health, intestinal microbiota

INTRODUCTION

The black tiger shrimp *Penaeus monodon*, one of the primary farmed penaeid shrimp species worldwide, is widely distributed on the southeastern coast of China. Consumers greatly favor *P. monodon* due to its rich nutrition and delicious taste, increasing the demand gradually. In recent years, due to the shortage of water and land resources, intensive farming has developed rapidly to meet the needs of the market (Biao and Yu, 2007; Zhang et al., 2017). However, higher feeding densities and more significant feed inputs come with a series of problems, such as water deterioration, disease outbreaks, and lightening of body color (Chien and Jeng, 1992; Verdegem, 2013; Bossier and Ekasari, 2017; Dauda, 2020). During intensive cultivation, the fluctuating pond environments may produce various environmental stressors (e.g., hypoxia, high concentration of ammonia, and nitrite), suppressing the antioxidant defense system and rendering shrimp susceptible to different diseases (Zhang et al., 2013). Meanwhile, outbreaks of pathogenic bacteria and viral diseases would negatively affect the growth and survival, led to massive economic losses, and impede the development of *P. monodon* aquaculture (Soonthornchai et al., 2009; Han et al., 2015). The color of shrimp flesh is an important indicator that could evaluate the health status and quality, directly affecting the choices of customers in the supermarket (Brun and Vidal, 2006). Since crustaceans themselves cannot synthesize pigment, the type, amount, and duration of pigments in the feed determine the color of the flesh and surface (Wade et al., 2017). Therefore, it is crucial to supplement antioxidants and pigments to prevent and manage the possible industrial problems during intensive aquaculture.

Astaxanthin (Ast) is a kind of symmetric ketocarotenoid, referred to as xanthophyll carotenoid, the end product of carotenoid synthesis, and distributes widely throughout nature (Pashkow et al., 2008). Because of containing ketone functional groups and hydroxyl, this compound owns several biological properties, including antioxidant action, immunomodulatory effects, anti-inflammatory properties, disease prevention, and coloration effects (Pashkow et al., 2008; Takahashi et al., 2011). Early studies found that dietary Ast could increase survival, enhance the antioxidant capacity, and improve the growth performance of *P. monodon* (Torrissen, 1995; Chien et al., 2003). Several reports had demonstrated that dietary Ast could significantly enhance shrimp tolerance to low temperature, low salinity, hypoxia, and ammonia stress (Chien et al., 2003; Pan et al., 2003; Chien and Shiau, 2005; Flores et al., 2007; Niu et al., 2009). In addition, supplementation of Ast in feed can darken the body color of aquatic animals, such as *Oncorhynchus mykiss* (Mora et al., 2006), *Amphilophus citrinellus* × *Cichlasoma synspilum* (Li et al., 2018), *Portunus trituberculatus* (Han et al., 2018), and *Marsupenaeus japonicus* (Wang et al., 2018b).

Ast is synthesized *de novo* by microbes, microalgae, and some plants in nature. Commercial products are mainly derived from natural sources and chemical synthesis (Ho et al., 2018; Jin et al., 2018). *Phaffia rhodozyma*, a red yeast, is one of the important natural sources of Ast (Andrewes et al., 1976; Lorenz and Cysewski, 2000). Because of the advantages of having a culture cycle, primarily utilizing sucrose, glucose as carbon sources, fermentation in high-density conditions, and not turn into toxic vitamin A in the body, *P. rhodozyma* is a potential Ast source with a commercial value that would be widely used in aquaculture (Mata-Gomez et al., 2014). In recent years, Ast from *P. rhodozyma* has been utilized to promote growth performance, antioxidant activities, quality of the meat, and the anti-inflammatory response of animals (Takahashi et al., 2011; Perenlei et al., 2015), such as finishing pigs (Yang, 2006), laying hens (Lorenz and Cysewski, 2000; Akiba et al., 2008), rainbow trout (Nakano et al., 1999). Nevertheless, no studies have focused on the effects of dietary *P. rhodozyma* on *P. monodon*. Therefore, the purpose of the present work was to investigate the effect of Ast from *P. rhodozyma* on growth performance, non-specific immune response, intestinal microbiota, and disease resistance against *Vibrio parahaemolyticus* in *P. monodon*.

MATERIALS AND METHODS

Preparation of Astaxanthin and Experimental Diet Formulation

Phaffia rhodozyma (Ast containing: 0.41% of dry matter, produced by Lida Biotechnology Co., Ltd, Weihai, China) was used as natural Ast source for the current study.

Six iso-nitrogenous and iso-lipidic experimental diets were formulated with graded levels (0, 20.5, 41, 61.5, 82, and 102.5 mg/kg diet) of Ast (**Table 1**, defined as A–D, respectively). Fish meal, soybean meal, and peanut meal were added to cover the protein requirements of juveniles. Fish oil provided the

TABLE 1 | Formulation and composition of the experimental diets (%, dry matter basis).

Ingredients	Treatments (Ast contents, mg/kg diet)					
	Control (A)	$Ast_{20\cdot5}$ (B)	Ast_{41} (C)	$Ast_{61\cdot5}$ (D)	Ast_{82} (E)	$Ast_{102\cdot5}$ (F)
Fish meal[a]	29	29	29	29	29	29
Soybean meal[a]	25	25	25	25	25	25
Peanut meal[a]	18	18	18	18	18	18
α-Starch[a]	5	5	5	5	5	5
Squid paste[a]	3	3	3	3	3	3
Fish oil[a]	2	2	2	2	2	2
Soybean lecithin[a]	2	2	2	2	2	2
Vitamin mixture[b]	0.4	0.4	0.4	0.4	0.4	0.4
Mineral mixture[c]	0.5	0.5	0.5	0.5	0.5	0.5
Vitamin C phosphate[a]	0.1	0.1	0.1	0.1	0.1	0.1
Monocalcium phosphate[a]	1	1	1	1	1	1
Wheat flour[a]	14	13.5	13	12.5	12	11.5
Phaffia rhodozyma[d]	0	0.5	1	1.5	2	2.5
Total	100	100	100	100	100	100

[a] *Dabeinong Technology Group Co., Ltd, Beijing, China.*
[b] *Vitamin mixture: vitamin A (IU/kg), 1,200,000–6,800,000; vitamin D_3, 500,000–1,000,000; vitamin E, 25,000–130,000; vitamin K_3 (g/kg), ≥10; nicotinamide, ≥18.5; inositol, 100; folic acid, 2; vitamin B_{12} (mg/kg), 21; biotin, ≥ 240.*
[c] *Mineral mixture: calcium pantothenate (g/kg),12.5; Cu, 5–16.6; Fe, 25–100; Zn, 15–50; Mn, 2–20; Mg, 30–100; I (mg/kg), 100–1,000; Se, 10–166; Co, 100–166.*
[d] *Phaffia rhodozyma powder: Bairihong® containing 0.41% (measured value) astaxanthin made by Lida Biotechnology Co., Ltd, Weihai, China. Astaxanthin comprised 83% of the total carotenoids.*

primary lipid. Squid paste and soybean lecithin oil were used as the source of cholesterol and phospholipids. In addition, other ingredients were added to meet the essential requirements for juvenile shrimp. The basal composition (9.51% moisture, 45.68% crude protein, 5.50% crude lipid, and 11.52% ash) and Ast contents (1.41%) of the experimental diets were described in **Table 2**. All the dry ingredients for the experimental diets were mixed thoroughly after being ground and passed through an 80-mesh sieve. Lipid substances were added while blending to form a homogeneous mixture. After that, an appropriate amount of water was added to form a homogeneous dough. Then, the dough was made into pellets by passing through a 1.5 mm orifice and oven-dried at 40°C until the moisture content was reduced to 10%. The dried experimental diets were stored in a −20°C freezer until use.

Shrimp and Experimental Conditions

Penaeus monodon was supplied by Dabeinong Technology Group Co., Ltd, Beijing, China. Before the experiments, juveniles were maintained at an ambient water temperature (29 ± 0.5°C) in a cement pool (Length = 10 m, Width = 5m, and Height = 1.5 m), and fed with a commercial diet (40% crude protein and 8% crude lipid) to acclimatize the laboratory environment for 2 weeks. At the start of the feeding trial, 900 juveniles of similar size (3.15 ± 0.12 g) were randomly distributed into 18 polyethylene circular tanks (H = 117 cm and R = 50 cm), connected with a recirculating aquaculture system. During the feeding trial, experimental tanks were continuously aerated. The rearing water was supplied directly from the sea with salinity 28–30‰ after filtered and UV sterilized before use. Each tank was covered with a net to prevent the shrimp from jumping out. Juveniles were fed five times a day (7:00, 11:00, 15:00, 19:00, and 23:00) at a daily ration of 5–8% of body weight for 8 weeks. Uneaten feed was collected 3 h after feeding to calculate feed intake and feed efficiency ratio, while fecal matter was siphoned from the tanks. The experimental water was changed about 20% every 3 days to keep the water quality, including temperature, ammonia nitrogen, pH, and dissolved oxygen, were measured every day and kept at 28–31°C, < 0.05 mg/L, 8.0–8.5, and > 5 mg/L, respectively.

Sampling Techniques

After the 8-week culture experiment, all the shrimp were fasted for 1 day before final sampling, recorded, and weighed all surviving shrimp and body weight from each tank. Five juveniles from each tank were obtained for whole-body composition and carotenoid analysis. Hemolymph was drawn with 1 ml sterile syringes from the first abdominal segment of 10 juveniles per tank; hepatopancreas was collected separately in 5 ml tubes from the 10 shrimp and stored at −80°C together with hemolymph samples for enzymatic activity analysis. Three mid-guts were randomly sampled, loaded into dividual 1.2 ml RNase-free cryogenic vials, and immediately stored in liquid nitrogen for intestinal microflora analysis.

Biochemical Analysis

Moisture, crude protein, ash, and total lipid contents of experimental diets and whole-body shrimp were quantified per the Association of Official Analytical Chemists (AOAC, 2006). To measure the moisture content, each sample was dried in an oven to a constant weight at 105°C. The crude protein of the samples was determined by the Kjeldahl method using an Auto Kjeldahl

TABLE 2 | Proximate and carotenoid composition of the experimental diets.

Parameters[a]	Treatments					
	A	B	C	D	E	F
Basal composition (%)						
Crude protein	45.68 ± 0.43	44.86 ± 0.27	45.11 ± 0.18	46.05 ± 0.06	45.58 ± 0.24	45.99 ± 0.16
Crude lipid	5.50 ± 0.16	4.95 ± 0.31	5.03 ± 0.12	5.19 ± 0.11	5.38 ± 0.16	5.24 ± 0.07
Ash	11.52 ± 0.88	11.15 ± 0.05	10.60 ± 0.53	11.78 ± 0.29	12.43 ± 0.22	10.23 ± 0.75
Moisture	9.51 ± 0.61	10.15 ± 0.06	9.89 ± 0.05	10.89 ± 0.14	11.34 ± 0.09	11.65 ± 0.21
Astaxanthin (mg/kg)	1.41 ± 0.14	21.82 ± 0.37	40.37 ± 0.59	63.73 ± 0.19	83.15 ± 1.15	105.32 ± 0.31

[a]*Data are expressed as mean ± SEM from triplicate groups.*
ND, not detected.

System (2300-Auto-analyzer, Foss Tecator, Sweden). Ash content of the samples was carried out by using a muffle furnace at 550°C for 8 h. The crude lipid was determined by the ether extraction method using Soxtec System HT (Soxtec System HT6, Sweden) (Wang et al., 2018b).

Hemolymph samples were centrifuged at 4,000 rpm, at 4°C for 10 min, and the serum was separated and collected from supernatants. Weighted hepatopancreas samples were homogenized with shrimp saline solution in an ice-water bath (Wang et al., 2019). After total protein (TP) content was quantified, serum and hepatopancreas samples were used to determine the activities of antioxidant (superoxide dismutase SOD, catalase CAT, total antioxidant capacity T-AOC, and malondialdehyde MDA), and non-specific immune enzymes (aspartate aminotransferase AST, alanine aminotransferase ALT, and alkaline phosphatase AKP). According to the instructions of the manufacturer, all parameters were measured using the corresponding reagent kits purchased from Nanjing Jiancheng Biological Company Research Institute.

Carotenoid Analysis

The shrimp samples were prepared into the shell (including carapace, telson, and uropod), muscle, and whole body. The samples were freeze dried and ground into a powder. Dried powder of shell (1 g), muscle (2 g), and whole body (1.5 g) per each treatment were weighed and placed into a 50-ml polypropylene centrifuge tube in triplicate. The carotenoid extraction process was conducted with chloroform by shaking for 10 min, then centrifuged at 4°C at 10,000 rpm for 5 min. All extraction steps were repeated three times for each sample until no more color was extracted. The extracts were collected and combined into new tubes, then dried in a rotary vacuum evaporator (Eyela SB 1100, Japan). After that, the carotenoids were dissolved in 8 ml acetone solution. Three milliliters of the solution was used for determining the total carotenoid concentration with a spectrophotometer (Puxi T6, China) at 475 nm (Johnston et al., 2000). The leftover 5 ml was dried by N_2 and redissolved in 2 ml of mobile phase solution (Acetonitrile: Methanol, 70:30 v/v) for Ast analysis. After being filtered through 0.2-μm hydrophilic polypropylene disks (Pall Corp), all samples were analyzed with an Ultra Performance Liquid Chromatography (UPLC, Waters ACQUITY, United States) system at the same time. Ten microliters of the sample was injected into a Waters ACQUITY H-Class BEH C18 column (1.7 μm, 2.1 mm × 150 mm). The sample was delivered to the column using a linear gradient mobile phase consisting of A (100% dH_20), B (acetonitrile: methanol, 70:30 v/v), and C (100% methyl tert-butyl ether) at a flow rate of 0.2 ml/min. Relative amounts of carotenoids were identified by an ultraviolet/visible detector set to 475 nm and quantified based on commercially available standards (Ast, zeaxanthin, canthaxanthin, β-cryptoxanthin, echinenone, and β-carotene) by calculating the area under the curve of each peak. The Ast, canthaxanthin, zeaxanthin, echinenone, and β-carotene standards were purchased from Sigma-Aldrich (United States), and the β-cryptoxanthin standard was purchased from CaroteNature (Swit).

Microbial Diversity Analysis of Intestines in the Shrimp

DNA was extracted from all samples using the MagPure Soil DNA LQ Kit (Magen D6356-02, China) following the instructions of the manufacturer. To amplify the V3–V4 hypervariable regions of the bacterial 16S rRNA gene for Illumina deep sequencing, universal primer pairs (343F: 5′-TACGGRAGGCAGCAG-3′ and 798R: 5′-AGGGTATCTAATCCT-3′) were used. PCR (Bio-Rad 580BR10905, United States) was performed in triplicate 30-μl reactional mixtures (containing 15 μl 2 × Gflex PCR Buffer, 1 μl of each primer, 2 μl template DNA, 0.6 μl of Tks Gflex DNA Polymerase, and ddH_2O) at 94°C for 5 min, followed by 26 cycles at 94°C for 30 s, 56°C for 30 s, 72°C for 20 s, and a final extension at 72°C for 5 min. After checking the amplicon quality using gel electrophoresis, the PCR products were purified with Agencourt AMPure XP beads (Beckman Coulter Co., United States) and quantified using Qubit dsDNA assay kit (Life Technologies Q32854, United States). Sequencing was performed after adjusting the concentration using an Illumina MiSeq platform (OE Biotech Company, China) with two paired-end read cycles of 250 bases. The raw reads were deposited into the NCBI Sequence Read Archive (SRA) database (Accession Number: PRJNA761235).

The bioinformatic analysis in the current study was completed using the Oe-biotech bio-cloud platform[1]. Raw FASTQ files

[1]www.oebiotech.com

were preprocessed using Trimmomatic software (Bolger et al., 2014) to detect and cut off ambiguous bases (N) by cutting off low-quality sequences with an average quality score below 20 using a sliding window trimming approach. After trimming, FLASH (version 1.2.7) merged with paired-end reads: 10 bp of minimal overlapping, 200 bp of maximum overlapping, and 20% of maximum mismatch rate. After that, sequences were performed further denoising with the following criteria: abandoning ambiguous, homologous sequences or below 200 bp; retaining reads above 75% of Q20 using QIIME software (version 1.8.0); detecting and removing the reads with chimera using UCHIME (Edgar et al., 2011). Subsequently, the sequences were subjected to primer sequences for removing and clustering to generate operational taxonomic units (OTUs) using VSEARCH software at 97% similarity (Rognes et al., 2016). Taxonomy was assigned to all OUTs by annotated and blasted against the Sliva database (version 132) using the RDP classifier (confidence threshold was 70%).

Susceptibility to *Vibrio parahaemolyticus*

The *V. parahaemolyticus* strains were obtained from Beijing Dabeinong Technology Group Co., Ltd. The bacteria were activated by infecting the *P. monodon*. Hemolymph samples from diseased juveniles were inoculated on TCBS agar culture medium plates to obtain virulent clones for the formal infection test per Yan et al. (2020). After a 56-day feeding trial, 10 juveniles with similar size from each tank were selected and injected with 20 μl of activated *V. parahaemolyticus* (1.2×10^8 CFU/ml). Continuous aeration and constant water temperature (29–30°C) were kept during the stress test that lasted for 1 week. The time to death was recorded, and mortality values were expressed as the LT_{50} per the method of Wang et al. (2018b).

Calculations and Statistical Analysis

The indexes were calculated using the following formulas:

Survival (%) = (final number of shrimp/initial number of shrimp) × 100

Body weight gain (BWG,%) = [(final weight–initial weight)/initial weight] × 100

Feed conversion ratio (FCR) = dry weight of feed consumed (g)/live weight gain (g).

Specific growth rate (SGR,% day^{-1}) = [(Ln final weight–Ln initial weight)/duration] × 100

The statistical analyses were performed using the software SPSS 20.0. All data were presented by means ± standard error of the mean (SEM, $n = 3$). One-way ANOVA was used to detect the differences among the treatments. When significant differences ($p < 0.05$) were identified among treatments, Duncan's multiple range test was used to compare the means of the treatments.

Ethics Statement

The present study was carried out in strict accordance with the recommendations in the ethical guidelines of EU Directive 2010/63/EU for animal experiments.

RESULTS

Growth Performance, Survival, and Feed Utilization

Growth performance, including final body weight (FBW), body weight gain (BWG), as well as the specific growth rate (SGR), was significantly affected by dietary Ast supplementation levels (**Table 3**). FBW, BWG, and SGR of shrimp fed with Ast including diets (B, C, D, E, and F), were significantly ($p < 0.05$) higher than the one fed the control diet, but without significant difference ($p > 0.05$) with shrimp fed with high Ast levels (E and F). The increasing dietary Ast levels improved shrimp survival and nutrient utilization of diet (FCR), and there were significant ($p < 0.05$) differences in D, E, and F treatments compared with the control.

Shrimp Whole-Body Composition

The effect of different dietary levels of Ast on proximate composition of shrimp whole body (% dry basis) is shown in **Table 4**. The crude protein, crude lipid, ash, and moisture contents in the whole body did not show any statistical differences among all the treatments ($p > 0.05$).

Total Carotenoid Contents and Carotenoid Composition Analysis in Different Tissues

Total carotenoid contents in whole-body, shell, and muscle samples of the studied shrimp are presented in **Figure 1**. The highest total carotenoid content of the whole body, shell, and muscle tissues was determined in the F treatment, while the lowest was observed in the control ($p < 0.05$).

The contents of six main kinds of carotenoids, including Ast, zeaxanthin, canthaxanthin, β-cryptoxanthin, echinenone, and β-carotene detected in the shrimp whole body, shell, and muscle are listed in **Table 5**. The shrimp fed the Ast-supplemented diets (B–F) showed markedly ($p < 0.05$) increasing trends in Ast concentrations with dietary Ast supplementation in the whole body, shell, and muscle tissues. The contents of canthaxanthin and β-cryptoxanthin showed continuous increasing trends with the increase in dietary Ast levels in different tissues. Zeaxanthin was only detected in the muscle, and the whole body belongs to the treatment with high-level Ast supplementation.

Antioxidant Parameters

The results obtained from the determination of antioxidant activities in shrimp hepatopancreas are shown in **Table 6**. The T-AOC significantly increased in Ast-supplemented treatments compared with the control, while SOD, CAT, and MDA decreased significantly ($p < 0.05$).

Hemolymph-Immunological Parameters

The hemolymph-immunological results of *P. monodon* are presented in **Table 7**. AKP increased significantly ($p < 0.05$) in dietary Ast treatments, while no more significance ($p > 0.05$) was detected among D–F treatments. The AST showed a continuous

TABLE 3 | Growth parameters and nutrient utilization of *P. monodon* fed with experimental diets for 56 days.[#]

Parameters	Treatments					
	A	B	C	D	E	F
Survival (%)	80.00 ± 0.81^{a}	81.00 ± 0.57^{ab}	82.5 ± 0.95^{abc}	83.00 ± 0.57^{bc}	83.00 ± 1.29^{bc}	84.5 ± 0.50^{c}
FBW (g)	13.55 ± 0.16^{a}	14.54 ± 0.09^{b}	15.30 ± 0.06^{c}	15.59 ± 0.15^{c}	16.16 ± 0.13^{d}	16.46 ± 0.05^{d}
BWG (%)	351.58 ± 5.51^{a}	384.67 ± 3.28^{b}	409.92 ± 2.17^{c}	419.58 ± 5.03^{c}	438.75 ± 4.41^{d}	448.67 ± 1.90^{d}
SGR (%/day)	2.51 ± 0.02^{a}	2.63 ± 0.01^{b}	2.72 ± 0.01^{c}	2.75 ± 0.01^{c}	2.81 ± 0.01^{d}	2.84 ± 0.01^{d}
FCR	1.79 ± 0.02^{c}	1.76 ± 0.02^{c}	1.64 ± 0.01^{b}	1.61 ± 0.02^{b}	1.53 ± 0.02^{a}	1.49 ± 0.01^{a}

[#]*FBW, final body weight; BWG, body weight gain; SGR, specific growth rate; FCR, feed conversion ratio. Data are expressed as mean ± SEM from triplicate groups. Mean values in the same row with different letters are significantly different ($p < 0.05$).*

TABLE 4 | Proximate composition of shrimp whole body.

Parameters[a]	Treatments					
	A	B	C	D	E	F
Basal composition (%)						
Crude protein	61.12 ± 0.45	61.51 ± 0.80	62.60 ± 0.41	60.55 ± 0.82	60.34 ± 0.37	60.07 ± 0.14
Crude lipid	4.67 ± 0.07	4.39 ± 0.05	4.95 ± 0.17	4.41 ± 0.03	4.11 ± 0.10	4.60 ± 0.18
Ash	12.54 ± 0.45	13.37 ± 0.23	12.77 ± 0.10	12.36 ± 0.44	12.87 ± 0.33	13.04 ± 0.29
Moisture	78.67 ± 0.32	78.12 ± 0.75	78.30 ± 0.41	79.03 ± 0.36	79.06 ± 0.52	79.28 ± 0.65

[a]*Data are expressed as mean ± SEM from triplicate groups.*

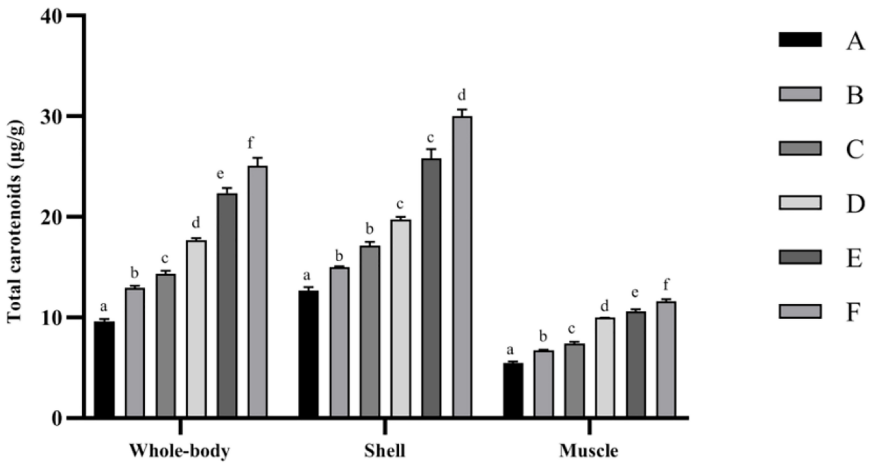

FIGURE 1 | Total carotenoid contents of *Penaeus monodon* fed with different astaxanthin levels for 56 days. Data are expressed as mean ± SEM from triplicate groups. Different letters indicate significant ($p < 0.05$) differences among various bars. S.E.M., standard error of mean.

decreasing trend with the increase in dietary Ast levels. Ast-supplemented levels over 61.5 mg/kg diet (D treatment) showed significantly higher values compared with the control. By contrast, dietary Ast significantly ($p < 0.05$) decreased ALT activities in the hemolymph of shrimp.

Stress Resistance Test

The LT_{50} values for the *Vibrio parahaemolyticus* infecting stress resistance test are shown in **Figure 2**. The LT_{50} values were significantly ($p < 0.05$) increased by dietary supplementation of Ast. The best performance was given by F treatment, while no significant ($p > 0.05$) difference was observed compared with treatment E.

Intestinal Microbiota Comparison

The alpha diversity statistics and OTUs of the intestinal microbiota in *P. monodon* are shown in **Figure 3**. The mean of Good's coverage (**Figure 3A**) for each treatment approached 99%. The Shannon and Chao 1 results could reflect the bacterial diversity and richness information of the intestine samples (**Figures 3B,C**). These two parameters did not show any significant ($p > 0.05$) differences

TABLE 5 | Carotenoid contents (μg/g) analysis in tissues of *Penaeus monodon.*[#]

Parameters	Treatments					
	A	B	C	D	E	F
Whole body						
Astaxanthin	4.2 ± 0.15^{a}	5.13 ± 0.24^{ab}	6.24 ± 0.08^{b}	8.88 ± 0.12^{c}	11.35 ± 0.40^{d}	12.01 ± 0.84^{d}
Zeaxanthin	ND	ND	ND	0.13 ± 0.02^{a}	0.33 ± 0.01^{b}	0.26 ± 0.06^{b}
Canthaxanthin	0.44 ± 0.03^{a}	0.68 ± 0.08^{ab}	0.80 ± 0.04^{b}	0.88 ± 0.09^{b}	1.03 ± 0.02^{bc}	1.42 ± 0.17^{c}
β-cryptoxanthin	0.38 ± 0.03^{a}	0.50 ± 0.11^{ab}	0.60 ± 0.23^{ab}	0.64 ± 0.07^{ab}	0.76 ± 0.03^{b}	1.30 ± 0.02^{c}
Echinenone	0.68 ± 0.08^{a}	1.18 ± 0.20^{ab}	0.89 ± 0.01^{a}	1.26 ± 0.02^{ab}	2.06 ± 0.16^{b}	2.76 ± 0.35^{c}
β-carotene	1.06 ± 0.40^{a}	1.46 ± 0.23^{ab}	1.92 ± 0.07^{bc}	2.58 ± 0.19^{cd}	3.05 ± 0.13^{d}	5.32 ± 0.01^{e}
Shell						
Astaxanthin	5.13 ± 0.10^{a}	6.78 ± 0.13^{b}	7.65 ± 0.03^{c}	8.81 ± 0.04^{d}	11.21 ± 0.20^{e}	12.01 ± 0.38^{e}
Zeaxanthin	ND	ND	ND	ND	ND	ND
Canthaxanthin	0.66 ± 0.03^{a}	0.66 ± 0.02^{a}	0.87 ± 0.03^{ab}	1.02 ± 0.03^{b}	1.50 ± 0.02^{c}	1.54 ± 0.03^{c}
β-cryptoxanthin	0.57 ± 0.15^{a}	1.20 ± 0.16^{b}	1.80 ± 0.05^{b}	2.28 ± 0.04^{c}	2.52 ± 0.09^{c}	2.85 ± 0.08^{c}
Echinenone	1.38 ± 0.27^{a}	1.47 ± 0.07^{a}	1.95 ± 0.08^{ab}	2.88 ± 0.06^{b}	3.39 ± 0.03^{c}	4.27 ± 0.28^{d}
β-carotene	2.79 ± 0.40^{ab}	2.19 ± 0.11^{a}	3.66 ± 0.07^{b}	4.25 ± 0.21^{b}	5.34 ± 0.41^{c}	6.73 ± 0.10^{d}
Muscle						
Astaxanthin	1.34 ± 0.04^{a}	1.75 ± 0.04^{a}	2.51 ± 0.01^{b}	3.18 ± 0.04^{c}	3.38 ± 0.07^{c}	3.70 ± 0.45^{c}
Zeaxanthin	ND	ND	ND	ND	0.08 ± 0.01^{a}	0.27 ± 0.03^{b}
Canthaxanthin	0.18 ± 0.01^{a}	0.21 ± 0.04^{a}	0.33 ± 0.01^{ab}	0.39 ± 0.04^{ab}	0.42 ± 0.03^{ab}	0.54 ± 0.39^{b}
β-cryptoxanthin	0.56 ± 0.04^{a}	0.65 ± 0.16^{a}	0.70 ± 0.13^{ab}	0.79 ± 0.04^{ab}	1.03 ± 0.06^{b}	1.11 ± 0.08^{b}
Echinenone	0.85 ± 0.08^{a}	1.17 ± 0.10^{ab}	1.44 ± 0.03^{ab}	2.03 ± 0.01^{ab}	2.31 ± 0.25^{b}	2.57 ± 0.12^{b}
β-carotene	0.85 ± 0.23^{a}	1.44 ± 0.10^{b}	1.49 ± 0.14^{b}	2.26 ± 0.17^{c}	2.70 ± 0.06^{c}	2.78 ± 0.20^{c}

[#]*Data are expressed as mean ± SEM from triplicate groups. Mean values in the same row with different letters are significantly different ($p < 0.05$). ND, not detected. Shell: including shrimp carapace, telson, and uropod.*

TABLE 6 | Hepatopancreatic antioxidant status of *P. monodon* fed with different astaxanthin levels.[#]

Parameters	Treatments					
	A	B	C	D	E	F
SOD (U/mg protein)	39.62 ± 0.97^{b}	37.83 ± 0.88^{b}	32.29 ± 0.89^{a}	32.05 ± 1.34^{a}	31.57 ± 0.55^{a}	30.74 ± 0.59^{a}
T-AOC (U/mg protein)	1.19 ± 0.01^{a}	1.31 ± 0.06^{b}	1.32 ± 0.01^{b}	1.39 ± 0.04^{bc}	1.45 ± 0.05^{c}	1.48 ± 0.02^{c}
MDA (nmol/mg protein)	30.01 ± 0.19^{d}	24.90 ± 0.76^{c}	24.00 ± 0.45^{bc}	22.07 ± 0.87^{b}	18.38 ± 0.64^{a}	17.29 ± 0.64^{a}
CAT (U/mg protein)	9.20 ± 0.39^{d}	8.85 ± 0.03^{d}	7.26 ± 0.08^{c}	5.57 ± 0.12^{b}	5.09 ± 0.18^{b}	4.03 ± 0.07^{a}

[#]*Data are expressed as mean ± SEM from triplicate groups. Mean values in the same row with different letters are significantly different ($p < 0.05$). SOD, superoxide dismutase; T-AOC, total antioxidant capacity; MDA, malondialdehyde; CAT, catalase.*

TABLE 7 | Hemolymph-immunological parameters of *P. monodon* fed with experimental diets.[#]

Parameters	Treatments					
	A	B	C	D	E	F
AST (U/mg protein)	18.74 ± 0.89^{d}	17.92 ± 0.49^{cd}	17.52 ± 0.63^{bcd}	15.31 ± 0.60^{abc}	15.08 ± 1.29^{ab}	14.42 ± 0.85^{a}
ALT (U/mg protein)	26.12 ± 1.17^{d}	15.25 ± 0.31^{c}	14.89 ± 0.47^{c}	12.18 ± 1.05^{b}	10.40 ± 0.49^{ab}	8.79 ± 0.73^{a}
AKP (U/mg protein)	5.66 ± 0.07^{a}	7.38 ± 0.14^{b}	8.56 ± 0.22^{bc}	9.67 ± 0.12^{cd}	10.62 ± 0.73^{d}	10.93 ± 0.63^{d}

[#]*Data are expressed as mean ± SEM from triplicate groups. Mean values in the same row with different letters are significantly different ($p < 0.05$). AST, aspartate aminotransferase; ALT, alanine aminotransferase; AKP, alkaline phosphatase.*

among all the treatments. Although OTUs (**Figure 3D**) decreased with the increase in dietary Ast levels, no significant ($p > 0.05$) difference was detected among all the treatments.

The microbial community composition and abundance of all intestinal samples at the phylum level are presented in **Figure 4**. The most dominant microbial community members at the phylum level, Firmicutes, Bacteroidetes,

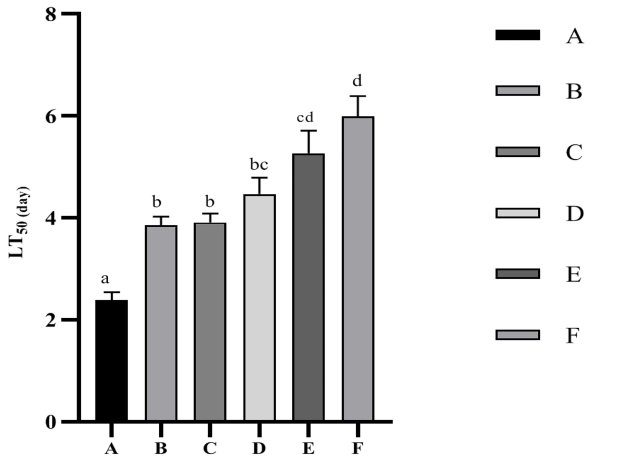

FIGURE 2 | Time to 50% mortality (LT_{50}) of *P. monodon* after infected with *Vibrio parahaemolyticus*. Data are expressed as mean ± SEM from triplicate groups. Different letters indicate significant ($p < 0.05$) differences among various bars.

Proteobacteria, and Actinobacteria accounted for 45.23, 31.66, 15.82, and 4.87% of the total microbial community, respectively (**Figure 4A**). No significant differences were observed in relative abundance of Firmicutes ($p = 0.67$), Bacteroidetes ($p = 0.27$), Proteobacteria ($p = 0.41$), and Actinobacteria ($p = 0.61$) among all treatments (**Figure 4B**).

The microbial community composition and abundance of all intestinal samples at the genus level are presented in **Figure 5**. The top 15 genera in classifiable sequences were *Clostridium*, *Ruminococcus*, *Bacteroides*, *Bifidobacterium*, *Escherichia–Shigella*, *Klebsiella*, *Sutterella*, *Prevotella*, *Prevotella*, *Eubacterium*, *Lachnospiraceae*, *Rikenellaceae*, *Blautia*, *Haemophilus*, and *Lactobacillus* (**Figure 5A**). The ANOVA test analysis results did not show any significant differences ($p > 0.05$) in the relative abundance of these genera (**Figure 5B**) among all the treatments.

DISCUSSION

Biological Performance

Carotenoids are primarily used as pigments sources in aquaculture for improving product quality (Shahidi and Brown, 1998). Besides this crucial role, carotenoids also play an essential role in enhancing nutrient utilization and ultimately improving the growth and survival of aquatic animals (Niu et al., 2012; Zhang et al., 2013). In the aquaculture industry, the cost of feed represents about 50–60% of a total operational cost depending on production scale and cultivation methods (Lim et al., 2017). Therefore, the beneficial role of Ast as a critical nutritive additive for tremendous growth and survival is necessary to minimize the production cost fluctuation caused by its high price (Niu et al., 2009; Wang et al., 2018a). Currently, commercial production of Ast is dominated by synthetic Ast because of its relatively lower production costs compared with the other alternatives (Saini and Keum, 2018). Over the years, an increasing number of reports have revealed the positive correlations between dietary synthetic Ast supplementation and growth performance and survival, or either of them in different species of aquatic animals (Wade et al., 2017; Wang et al., 2019). A few studies have been conducted to evaluate the *P. rhodozyma* Ast on growth performance due to its production capacity limitation. Recently, the increasing demand of consumers for biotechnological production makes synthetic pigment less desirable, and Ast obtained from biological sources perform a long-term gain potential in the global market. Furthermore, the Ast form (3R, 3′R optical isomer) in *P. rhodozyma* is supposed to own greater bioavailability (Bjerkeng et al., 2007). Previous studies have demonstrated the beneficial effects of dietary synthetic and algal Ast in a variety of shrimp species with evidence that Ast supplementation could boost weight gain and improve survival in *P. monodon* (Niu et al., 2012), *Litopenaeus vannamei* (Flores et al., 2007; Niu et al., 2009), *Macrobrachium rosenbergii* (Kumar et al., 2009), *Paralithodes camtschaticus* (Daly et al., 2013), and *Marsupenaeus japonicus* (Wang et al., 2018b). The current study supported the positive effect of yeasty Ast supplementation on the growth and survival performance in *P. monodon*. Combined, these data consistently suggest that dietary Ast as a nutritional factor is important in stimulating aquatic animals' growth and survival. However, some controversies were found among studies on *L. vannamei* (Ju et al., 2011), *M. japonicus* (Yamada et al., 1990; Chien and Jeng, 1992), and *Eriocheir sinensis* (Long et al., 2017; Jiang et al., 2020), which demonstrated that growth and survival of juveniles were similar regardless of whether including Ast in the diet or not. These inconsistent conclusions may be explained by different carotenoid requirements among aquatic animal species, culture condition (indoor or not, exogenous carotenoids intake or not, culture period, temperature, and density), the composition of feed (basal carotenoid content in the diet), and state of animal health.

Likewise, dietary Ast supplementation between 25 and 100 mg/kg diet was found to remarkably boost weight gain of *P. monodon* but without affecting survival rate (Wade et al., 2015). In another study, *L. vannamei* performed considerable growth increasing on 125 and 150 mg/kg levels of Ast intake than those fed with comparatively lower levels of Ast (25, 50, 75, and 100 mg/kg diet), but survival was not affected (Zhang et al., 2013). Significant correlations have been observed between tissue carotenoid concentration and survival (Chien and Jeng, 1992). Wade et al. (2017) suggested that survival would not be affected when body carotenoid contents are above a certain level, otherwise, they would be compromised below that level without carotenoid supplementation. Thus, when initial tissue carotenoid levels are high enough during the feeding trial, further carotenoids supplementation allows improved growth rather than survival improvement (Niu et al., 2014). Growth parameters, including final body weight (FBW), body weight gain (BWG), and specific growth rate (SGR), mainly reflect the retention or deposition of nutrients from feed into the body but do not precisely equate to the health status of the aquatic animal (Du and Turchini, 2021). Moreover, the positive effect on survivability by dietary Ast appears to be closely linked to its proposed antioxidant capacity, immune response regulation, and

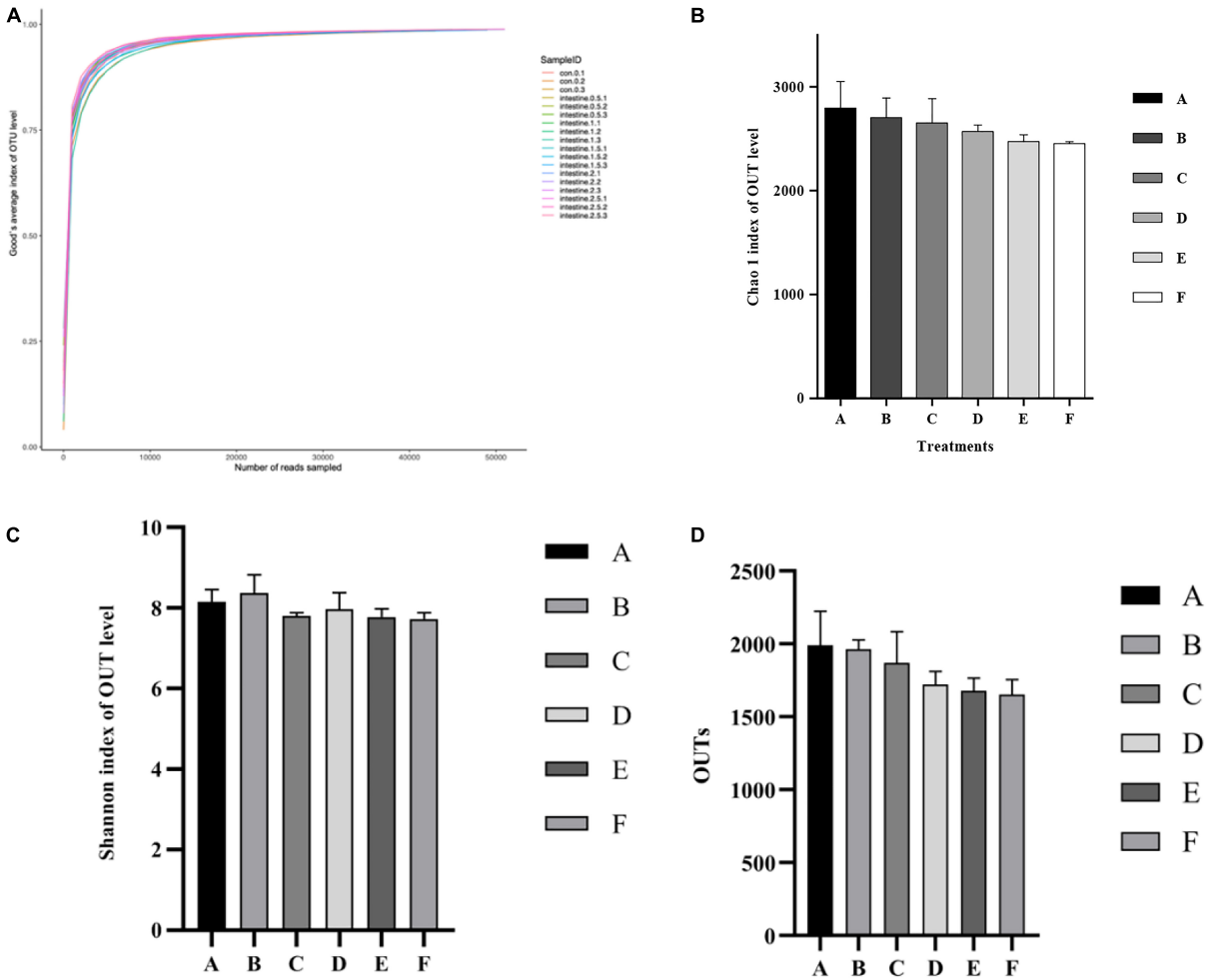

FIGURE 3 | Analysis of alpha diversity comparisons with the microbial communities in intestine of shrimp fed with different astaxanthin levels for 56 days. **(A)** Good's coverage curve; **(B)** Chao species richness index; **(C)** Shannon's diversity index; **(D)** OTUs richness comparison index for A, B, C, D, E, and F intestinal samples. Data are expressed as mean ± SEM from triplicate groups. Different letters indicate significant ($p < 0.05$) differences among various bars. OTUs, operational taxonomic units.

stress alleviative property (Niu et al., 2012; Wade et al., 2017). Thus, non-specific immune response and disease resistance against *V. parahaemolyticus* parameters were complemented in the current study to achieve a more reliable assessment of healthy growth of juveniles fed with *P. rhodozyma* Ast.

Whole-Body Composition and Total Carotenoid Contents of Shrimp

The whole-body composition results are consistent with the findings of Niu et al. (2009) and Zhang et al. (2013) where the carotenoid supplementation seemed to not affect the proximate composition of shrimp whole-body.

Aquatic animals, including crustaceans, cannot synthesize carotenoids *de novo*, must obtain carotenoids through their diets (Matsuno, 2001). Numerous studies have demonstrated that dietary carotenoids could increase the deposition of carotenoids in the tissues (Ju et al., 2011; Wang et al., 2018b). In the current study, total carotenoid content in various tissues (**Figure 1**) significantly increased with the increasing Ast supplemented levels, which showed similar trends on growth, antioxidant capacity, and immune response performance. This phenomenon implied that crustaceans generally accumulate carotenoids in tissues, including hepatopancreas, shell, muscle, and ovaries, that would be metabolized when dietary supply is low to optimize health status during developmental processes or in response to environmental circumstances (Wade et al., 2017; Babin et al., 2019).

As the best-established function, there is no doubt that shrimp dietary with Ast supplementation would achieve desired red color due to increased Ast concentration in shell (Shahidi and Brown, 1998). Jiang et al. (2020) reported that exoskeleton Ast contents are correlated with the redness (a^*) value of crustaceans on cooking, which reflects the Ast concentrations in tissues. The current study detected increased Ast concentration in shell with the increasing dietary Ast levels as expected. Moreover, dietary Ast significantly affected the zeaxanthin, canthaxanthin,

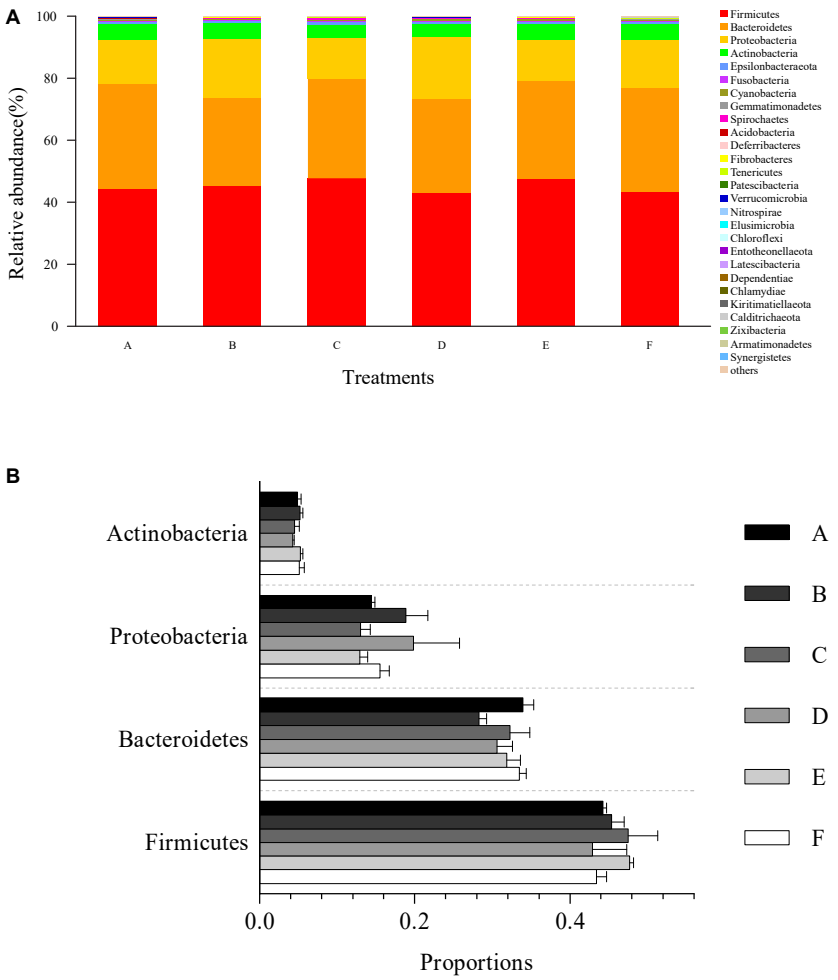

FIGURE 4 | Relative abundances of dominant phyla and comparison with bacterial abundances in the intestine at the phylum level. **(A)** Relative abundances of dominant phyla (top 30) from all classifiable sequencing data. Unclassified phyla with relative abundances lower than 1% were assigned as "others." **(B)** The abundance comparison with four dominant microbial community members at the phylum level, including Firmicutes, Bacteroidetes, Proteobacteria, and Actinobacteria. Data are expressed as mean ± SEM from triplicate groups.

and β-carotene levels in tissues. Yamada et al. (1990) stated that decapod crustaceans have carotenoid metabolic conversion capacity in their internal organs. The accumulation of specific carotenoids also implies their corresponding particular function in different tissues. Moreover, an increased presence of Ast in shrimp muscle (**Table 5**) could confer many benefits for human health due to its potent antioxidant activity, such as anti-inflammatory, anti-aging, immune system boosting, anti-cancer, and sun proofing (Lim et al., 2017).

Antioxidant Capacity and Non-specific Immune Response

High-density shrimp aquaculture operations are frequently subject to various physical and surrounding environment stressors involving grading, transport, crowding, hypoxia, temperature fluctuation, and high ammonia nitrogen loading, ultimately leading to bodily physiological dysfunction and immune suppression that are susceptible toward pathogenic invasions (Liu et al., 2016). Invertebrates lack an adaptive immune system, mainly relying on innate immune responses as the first line to defend against invaders (Yan et al., 2020). AKP is a crucial phosphatase that regulates phosphorylation and dephosphorylation processes involving animal growth, nutrient transport, and pathogen storage in the lysosome (Zhu et al., 2021). In the current study, the AKP activities in hemolymph significantly increased with the increase in dietary Ast levels, indicating a positive effect of dietary Ast on the immunity of *P. monodon*. This finding agreed with previous studies on *Eriocheir sinensis* (Jiang et al., 2020). Changes in the ALT and AST enzymes levels in hemolymph always indicate the physiological state of hepatopancreas cells (Ettefaghdoost and Haghighi, 2021). Generally, kept at a low level, they are significantly increased in the hemolymph when the hepatopancreas are severely damaged. There is a similarity in the mentioned studies (Niu et al., 2012) with the current one on the significant reduction of ALT and AST activities in Ast-supplemented treatments

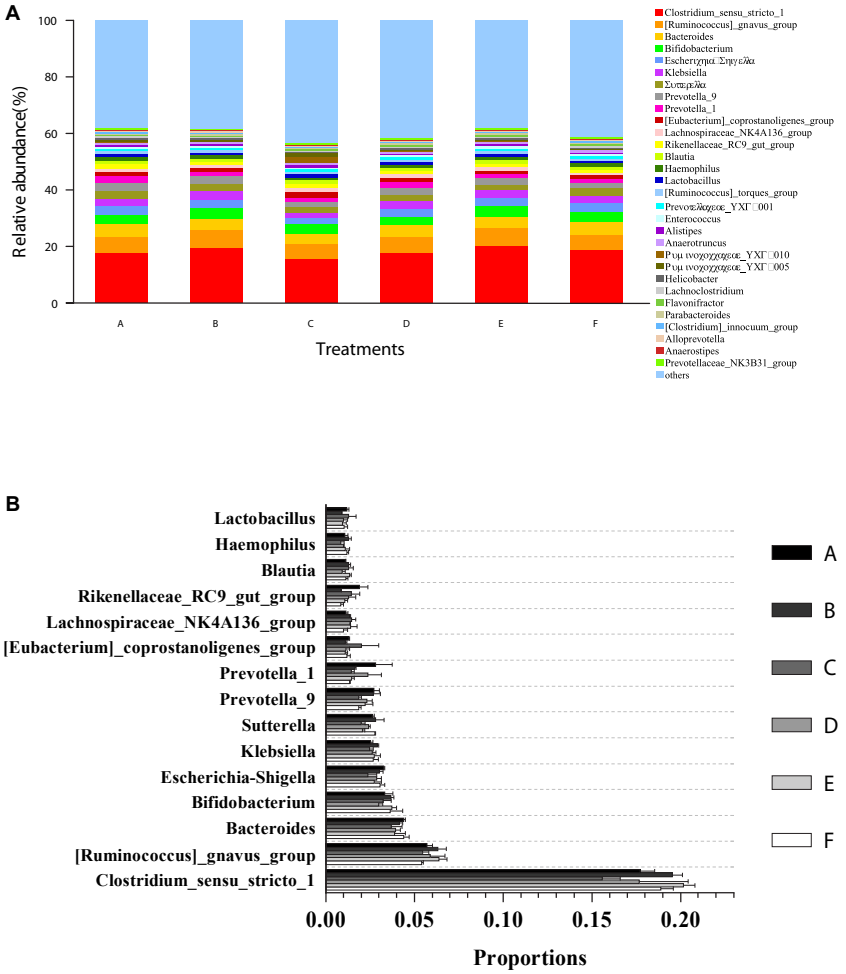

FIGURE 5 | Relative abundances of dominant genera and comparison with bacterial abundances in the intestine at the genus level. **(A)** Relative abundances of dominant genera (top 30) from all classifiable sequencing data. Unclassified genera with relative abundances lower than 1% were assigned as "others." **(B)** The abundance comparison with 15 most abundant genera in shrimp intestine among all the treatments. Data are expressed as mean ± SEM from triplicate groups.

(**Table 7**). Furthermore, a study on *Oncorhynchus mykiss* indicated decreased serum ALT and AST fed with *P. rhodozyma* (Nakano et al., 1999). Combined results indicated the significant role of Ast on the status improvements of hepatopancreatic cells in *P. monodon*.

As a vital and multifunctional organ, the hepatopancreas of crustaceans performed critical functions, including metabolism, detoxification, and secretion (Vogt, 2019). The hepatopancreatic antioxidant enzymes were used as biomarkers to display the effect of dietary Ast on the antioxidant status of *P. monodon*. The immune and antioxidant systems in crustaceans are two crucial physiological mechanisms that modulate immunological function, ensuring optimal cellular functions and confer physiological improvements (Zhu et al., 2021). SOD is a major antioxidant enzyme that acts as a scavenger for superoxide radicals that result from oxidative stress (Chien et al., 2003). CAT is widely distributed in several tissues to consume the peroxides as an intracellular H_2O_2 scavenger (Hugo, 1984). In general, the activities of SOD and CAT would be upregulated to quench reactive oxygen species (ROS) produced during stress (Duan et al., 2015). Studies on *Macrobrachium nipponense* (Ettefaghdoost and Haghighi, 2021), *P. monodon* (Niu et al., 2014), and *E. sinensis* (Jiang et al., 2020) showed a significant reduction of these two enzymes in treatments containing Ast compared with control, which were consistent with the present study. T-AOC represents a comprehensive indicator of the antioxidant status of an individual (Zhang et al., 2013). MDA is the primary product of lipid peroxidation and can destroy the structure and function of cells. Assaying the activity of this enzyme indicates lipid peroxidation (Esterbauer and Cheeseman, 1990). In the current study, dietary Ast significantly increased T-AOC and reduced the MDA in hepatopancreas, which supports the result on SOD and CAT, indicating a lower oxidative stress level in shrimp dietary Ast supplementation. The positive performance on antioxidant parameters of Ast could attribute to its extreme capacity to scavenge oxygen free radicals and prevention of peroxidation of PUFAs in tissues (Wade et al., 2017).

Susceptibility of Shrimp to *Vibrio parahaemolyticus*

Various disease outbreaks caused by vibriosis due to environmental deterioration have occurred within booming *P. monodon* aquaculture, leading to significant economic impacts worldwide (Duan et al., 2015). Several studies have reported that *V. parahaemolyticus* could induce acute hepatopancreatic necrosis (AHPND) by causing a compromised immunity and hepatopancreatic damage of shrimp (Zhu et al., 2021). Dietary yeasty Ast significantly increased resistance to *V. parahaemolyticus* according to the LT_{50} results in the current study, which may be contributing to the anti-bacterial effects, which indicated that dietary Ast could suppress *V. parahaemolyticus* infection. However, *V. parahaemolyticus* is a conditional pathogen: the pathogenicity is triggered by physical stressors that disrupt the delicate balance between aquatic animals and surrounding environments (Pang et al., 2019). Thus, improved immune status by inducing AST, ALT, AKP, and SOD in the shrimp by dietary Ast is also one of the primary reasons to defend against pathogenic infections in the current study.

Intestinal Microbiota Analysis

Bacterial microbiota analysis in the intestines of farmed aquatic animals has been paid attention to reveal its relationships and shrimp health (Zhu et al., 2021). Intestinal bacteria and bacterial metabolites directly affect the nutrient absorption and immunity of the host (Ayiku et al., 2020). The current study is the first time to discuss the effect of dietary Ast supplementation on the microbial community in the intestine of *P. monodon*. No significant differences were observed in the intestinal bacterial richness and diversities among all the treatments. Consistent with the research on *L. vannamei* (Ayiku et al., 2020; Wang et al., 2021), Firmicutes, Bacteroidetes, Proteobacteria, and Actinobacteria performed the predominant phyla in the intestine of shrimp. These bacteria have been well known to play a significant role in the physiological metabolism of the host (Sun et al., 2020). While the relative abundances of these four significant phyla could be influenced by the rearing environment and the basal nutrient composition of the diet, compositions of the intestinal bacteria at the phylum levels were quite similar among different studies. The predominant genera in the current study differ from the results obtained in other organisms: for example, Wang et al. (2021) revealed that *Candidatus Bacilloplasma, Vibrio, Lactobacillus*, *Spongiimonas*, and *Flavirhabdus* were the predominant genera in the intestine of *L. vannamei*. In the intestines of *P. monodon*, Chaiyapechara et al. (2012) found the dominant bacterial genera were *Vibrio*, *Photobacterium*, *Aeromonas*, or *Propionigenium*, which conclude that the intestinal bacteria in genus levels varied significantly and were distinct from their rearing environment. No significant differences were detected on the dominant phyla and genera among all treatments in the current. Combined results indicated that dietary Ast supplementation did not significantly affect bacterial diversity, dominant bacterial communities, or bacterial community similarities in the intestine of *P. monodon*.

CONCLUSION

Dietary Ast from *P. rhodozyma* could provide desired growth performance, antioxidant status, non-specific immune response, resistance to disease, and carotenoid contents of *P. monodon.* Moreover, the promising performance of *P. rhodozyma* Ast as the natural source could provide an alternative to synthetic Ast in the *Penaeus monodon* culture industry.

DATA AVAILABILITY STATEMENT

The datasets presented in this study can be found in online repositories. The names of the repository/repositories and accession number(s) can be found below: BioProject accession number: PRJNA761235.

AUTHOR CONTRIBUTIONS

WW drafted the manuscript. ML finished the feeding trial and chemical analysis. SF helped to analyze the data. YX made the figures. MW put forward relevant experimental guidance. GY and XH designed the research. QL worked on manuscript revision. All authors read and gave final approval of the manuscript.

ACKNOWLEDGMENTS

The work was supported by the National Natural Science Foundation of China (31902385), Chinese Postdoctoral Science Foundation (219724), Shanghai Agriculture Applied Technology Development Program, China (No. 202102080012F00761), Shanghai Collaborative Innovation for Aquatic Animal Genetics and Breeding Foundation, Shanghai Ocean University, Key Laboratory of Aquatic Functional Feed, and Environmental Regulation of Fujian Province Open Project (FACE20200001).

REFERENCES

Akiba, Y., Kan, S., Takahashi, K., Toyomizu, M., and Nagao, H. (2008). Improved pigmentation of egg yolk by feeding of yeast *Phaffia rhodozyma* containing high concentration of astaxanthin in laying hens. *Jpn. Poult. Sci.* 37, 162–170. doi: 10.2141/jpsa.37.162

Andrewes, A. G., Phaff, H. J., and Starr, M. P. (1976). Carotenoids of *Phaffia rhodozyma*, a red-pigmented fermenting yeast. *Phytochemistry* 15, 1003–1007. doi: 10.1016/s0031-9422(00)84390-3

AOAC (2006). *Official Methods of Analysis of Official Analytical Chemists International*, 18th Edn. Arlington, VA: Association of Official Analytical Chemists.

Ayiku, S., Shen, J. F., Tan, B. P., Dong, X. H., and Liu, H. Y. (2020). Effects of dietary yeast culture on shrimp growth, immune response, intesinal health and disease resistance against *Vibrio harveyi*. *Fish Shellfish Immunol.* 102, 286–295. doi: 10.1016/j.fsi.2020.04.036

Babin, A., Moreau, J., and Moret, Y. (2019). Storage of carotenoids in crustaceans as an adaptation to modulate immunopathology and optimize immunological and life−history strategies. *BioEssays* 41:1800254. doi: 10.1002/bies.201800254

Biao, X., and Yu, K. J. (2007). Shrimp farming in China: operating characteristics, environmental impact and perspectives. *Ocean Coast. Manag.* 50, 538–550. doi: 10.1016/j.ocecoaman.2007.02.006

Bjerkeng, B., Peisker, M., Schwartzenberg, K. V., Ytrestoyl, T., and Asgard, T. (2007). Digestibility and muscle retention of astaxanthin in Atlantic salmon, *Salmo salar*, fed diets with the red yeast *Phaffia rhodozyma* in comparison with synthetic formulated astaxanthin. *Aquaculture* 269, 476–489. doi: 10.1016/j.aquaculture.2007.04.070

Bolger, A. M., Lohse, M., and Usadel, B. (2014). Trimmomatic: a flexible trimmer for Illumina sequence data. *Bioinformatics* 30, 2114–2120. doi: 10.1093/bioinformatics/btu170

Bossier, P., and Ekasari, J. (2017). Biofloc technology application in aquaculture to support sustainable development goals. *Microb. Biotechnol.* 10, 1012–1016.

Brun, H., and Vidal, F. (2006). Shrimp pigmentation with natural carotenoids. *Feed Technol. Aquac. Asia Pac. Mag.* 2, 34–35.

Chaiyapechara, S., Rungrassamee, W., Suriyachay, I., Kuncharin, Y., Klanchui, A., Karoonuthaisiri, N., et al. (2012). Bacterial community associated with the intestinal tract of P. monodon in commercial farms. *Microbiol. Ecol.* 63, 938–953. doi: 10.1007/s00248-011-9936-2

Chien, Y. H., and Jeng, S. C. (1992). Pigmentation of kuruma prawn, *Penaeus japonicus* Bate, by various pigment sources and levels and feeding regimes. *Aquaculture* 102, 333–346. doi: 10.1016/0044-8486(92)90186-o

Chien, Y. H., and Shiau, W. C. (2005). The effects of dietary supplementation of algae and synthetic astaxanthin on body astaxanthin, survival, growth, and low dissolved oxygen stress resistance of kuruma prawn, *Marsupenaeus japonicus* Bate. *J. Exp. Mar. Biol. Ecol.* 318, 201–211. doi: 10.1016/j.jembe.2004.12.016

Chien, Y. H., Pan, C. H., and Hunter, B. (2003). The resistance to physical stresses by Penaeus monodon juveniles fed diets supplemented with astaxanthin. *Aquaculture* 216, 177–191. doi: 10.1016/s0044-8486(02)00056-x

Daly, B., Swingle, J. S., and Eckert, G. L. (2013). Dietary astaxanthin supplementation for hatchery-cultured red king crab, *Paralithodes camtschaticus*, juveniles. *Aquac. Nutr.* 19, 312–320. doi: 10.1111/j.1365-2095.2012.00963.x

Dauda, A. B. (2020). Biofloc technology: a review on the microbial interactions, operational parameters and implications to disease and health management of cultured aquatic animals. *Rev. Aquac.* 12, 1193–1210. doi: 10.1111/raq.12379

Du, Z. Y., and Turchini, G. M. (2021). Are we actually measuring growth?-An appeal to use a more comprehensive growth index system for advancing aquaculture research. *Rev. Aquac.* 1–3.

Duan, Y., Zhang, J. S., Dong, H. B., Wang, Y., Liu, Q. S., and Li, H. (2015). Oxidative stress response of the black tiger shrimp *Penaeus monodon* to *Vibrio parahaemolyticus* challenge. *Fish Shellfish Immunol.* 46, 354–365. doi: 10.1016/j.fsi.2015.06.032

Edgar, R. C., Haas, B. J., Clemente, J. C., Quince, C., and Knight, R. (2011). UCHIME improves sensitivity and speed of chimera detection. *Bioinformatics* 27, 2194–2200. doi: 10.1093/bioinformatics/btr381

Esterbauer, H., and Cheeseman, K. H. (1990). Determination of aldehydic lipid peroxidation products: malonaldehyde and 4-hydroxynonenal. *Methods Enzymol.* 186, 407–421. doi: 10.1016/0076-6879(90)86134-h

Ettefaghdoost, M., and Haghighi, H. (2021). Impact of different dietary lutein levels on growth performance, biochemical and immuno-physiological parameters of oriental river prawn (*Macrobrachium nipponense*). *Fish Shellfish Immunol.* 115, 86–94. doi: 10.1016/j.fsi.2021.05.024

Flores, M., Díaz, F., Medina, R., Re, A. D., and Licea, A. (2007). Physiological, metabolic and haematological responses in white shrimp *Litopenaeus vannamei* (Boone) juveniles fed diets supplemented with astaxanthin acclimated to low−salinity water. *Aquac. Res.* 38, 740–747. doi: 10.1111/j.1365-2109.2007.01720.x

Han, J. E., Mohney, L. L., Tang, K., Pantoja, C. R., and Lightner, D. V. (2015). Plasmid mediated tetracycline resistance of *Vibrio parahaemolyticus* associated with acute hepatopancreatic necrosis disease (AHPND) in shrimps. *Aquac. Rep.* 2, 17–21. doi: 10.1016/j.aqrep.2015.04.003

Han, T., Li, X., Wang, J., Wang, C., Yang, M., and Zheng, P. (2018). Effects of dietary astaxanthin (AX) supplementation on pigmentation, antioxidant capacity and nutritional value of swimming crab, *Portunus trituberculatus*. *Aquaculture* 490, 169–177. doi: 10.1016/j.aquaculture.2018.02.030

Ho, Y. H., Man, L. H., Yuen, S. Y., Ng, K. S., and Wong, Y. K. (2018). Maximization of astaxanthin production from green microalga *Haematococcus pluvialis* using internally-Illuminated photobioreactor. *Adv. Biosci. Bioeng.* 6, 10–22. doi: 10.11648/j.abb.20180602.11

Hugo, A. (1984). Catalase *in vitro*. *Methods Enzymol.* 105, 121–126.

Jiang, X., Zu, L., Wang, Z., Cheng, Y., Yang, Y., and Wu, X. (2020). Micro-algal astaxanthin could improve the antioxidant capability, immunity and ammonia resistance of juvenile Chinese mitten crab, Eriocheir sinensis. *Fish Shellfish Immunol.* 102, 499–510. doi: 10.1016/j.fsi.2020.05.021

Jin, J., Ying, W., Yao, M., Gu, X., Bo, L., Hong, L., et al. (2018). Astaxanthin overproduction in yeast by strain engineering and new gene target uncovering. *Biotechnol. Biofuels* 11:230.

Johnston, I. A., Alderson, R., Sandham, C., Dingwall, A., Mitchell, D., Selkirk, C., et al. (2000). Muscle fibre density in relation to the colour and texure of smoked Atlantic salmon (*Salmo salar* L.). *Aquaculture* 189, 335–349. doi: 10.1016/s0044-8486(00)00373-2

Ju, Z. Y., Deng, D. F., Dominy, W. G., and Forster, I. P. (2011). Pigmentation of Pacific white shrimp, *Litopenaeus vannamei*, by dietary astaxanthin extracted from *Haematococcus pluvialis*. *J. World Aquac. Soc.* 42, 633–644. doi: 10.1111/j.1749-7345.2011.00511.x

Kumar, V., Pillai, B. R., Sahoo, P. K., Mohanty, J., and Mohanty, S. (2009). Effect of dietary astaxanthin on growth and immune response of Giant freshwater prawn *Macrobrachium rosenberigii* (de man). *Asian Fish. Sci.* 22, 61–69. doi: 10.33997/j.afs.2009.22.1.007

Li, F., Huang, S. Y., Lu, X. X., Wang, J., Lin, M. W., An, Y., et al. (2018). Effects of dietary supplementation with algal astaxanthin on growth, pigmentation, and antioxidant capacity of the blood parrot (*Cichlasoma citrinellum* × *Cichlasoma synspilum*). *J. Oceanol. Limnol.* 36, 1851–1859. doi: 10.1007/s00343-019-7172-7

Lim, K. C., Yusoff, F. M., Shariff, M., and Kamarudin, M. S. (2017). Astaxanthin as feed supplement in aquatic animals. *Rev. Aquac.* 10-3, 738–773. doi: 10.1111/raq.12200

Liu, F., Shi, H., Guo, Q., Yu, Y., Wang, A., Lv, F., et al. (2016). Effects of astaxanthin and emodin on the growth, stress resistance and disease resistance of yellow catfish (*Pelteobagrus fulvidraco*). *Fish Shellfish Immunol.* 51, 125–135. doi: 10.1016/j.fsi.2016.02.020

Long, X., Wu, X., Zhao, L., Liu, J., and Cheng, Y. (2017). Effects of dietary supplementation of *Haematococcus pluvialis* powder on gonadal development, coloration and antioxidant capacity of adult male Chinese mitten crab (*Eriocheir sinensis*). *Aquac. Res.* 48, 5214–5223. doi: 10.1111/are.13333

Lorenz, R. T., and Cysewski, G. R. (2000). Commercial potential for Haematococcus microalgae as a natural source of astaxanthin. *Trends Biotechnol.* 18, 160–167. doi: 10.1016/s0167-7799(00)01433-5

Mata-Gomez, L. C., Montanez, J. C., Mendez-Zavala, A., and Aguilar, C. N. (2014). Biotechnological production of carotenoids by yeasts: an overview. *Microb. Cell Fact.* 13:12.

Matsuno, T. (2001). Aquatic animal carotenoids. *Fish. Sci.* 67, 771–783. doi: 10.1046/j.1444-2906.2001.00323.x

Mora, G., Arredondo-Figueroa, J. L., Ponce-Palafox, J. T., Barriga-Soca, I., and Vernon-Carter, J. E. (2006). Comparison of red chilli (*Capsicum annuum*) oleoresin and astaxanthin on rainbow trout (*Oncorhyncus mykiss*) fillet pigmentation. *Aquaculture* 258, 487–495. doi: 10.1016/j.aquaculture.2006.04.005

Nakano, T., Kanmuri, T., Sato, M., and Takeuchi, M. (1999). Effect of astaxanthin rich red yeast (*Phaffia rhodozyma*) on oxidative stress in rainbow trout. *Biochim. Biophys. Acta Gen. Subj.* 1426, 119–125. doi: 10.1016/s0304-4165(98)00145-7

Niu, J., Li, C. H., Liu, Y. J., Tian, L. X., Chen, X., Huang, Z., et al. (2012). Dietary values of astaxanthin and canthaxanthin in Penaeus monodon in the presence and absence of cholesterol supplementation: effect on growth, nutrient digestibility and tissue carotenoid composition. *Br. J. Nutr.* 108, 80–91. doi: 10.1017/S0007114511005423

Niu, J., Tian, L. X., Liu, Y. J., Yang, H. J., Ye, C. X., Gao, W., et al. (2009). Effect of dietary astaxanthin on growth, survival, and stress tolerance of postlarval shrimp, *Litopenaeus vannamei*. *J. World Aquac. Soc.* 40, 795–802. doi: 10.1111/j.1749-7345.2009.00300.x

Niu, J., Wen, H., Li, C. H., Liu, Y. J., Tian, L. X., Chen, X., et al. (2014). Comparison effect of dietary astaxanthin and β-carotene in the presence and absence of cholesterol supplementation on growth performance, antioxidant capacity and

gene expression of Penaeus monodon under normoxia and hypoxia condition. *Aquaculture* 422, 8–17. doi: 10.1016/j.aquaculture.2013.11.013

Pan, C. H., Chien, Y. H., and Hunter, B. (2003). The resistance to ammonia stress of *Penaeus monodon Fabricius juvenile* fed diets supplemented with astaxanthin. *J. Exp. Mar. Biol. Ecol.* 297, 107–118. doi: 10.1016/j.jembe.2003.07.002

Pang, H. Y., Wang, G., Zhou, S. H., Wang, J. L., Zhao, J. C., Hoare, R., et al. (2019). Survival and immune response of white shrimp *Litopenaeus vannamei* following single and concurrent infections with WSSV and Vibrio parahaemolyticus. *Fish Shellfish Immunol.* 92, 712–718. doi: 10.1016/j.fsi.2019.06.039

Pashkow, F. J., Watumull, D. G., and Campbell, C. L. (2008). Astaxanthin: a novel potential treatment for oxidative stress and inflammation in cardiovascular disease. *Am. J. Cardiol.* 101, 58d–68d.

Perenlei, G., Tojo, H., Okada, T., Kubota, M., Kadowaki, M., and Fujimura, S. (2015). Effect of dietary astaxanthin rich yeast, *Phaffia rhodozyma*, on meat quality of broiler chickens. *Anim. Sci. J.* 85, 895–903. doi: 10.1111/asj.12221

Rognes, T., Flouri, T., Nichols, B., Quince, C., and Mahe, F. (2016). VSEARCH: a versatile open source tool for metagenomics. *Peerj* 4:e2584. doi: 10.7717/peerj.2584

Saini, R. K., and Keum, Y. S. (2018). Carotenoid extration methods: a review of recent developments. *Food Chem.* 240, 90–103. doi: 10.1016/j.foodchem.2017.07.099

Shahidi, F., and Brown, J. A. (1998). Carotenoid pigments in seafoods and aquaculture. *Crit. Rev. Food Sci.* 38, 1–67. doi: 10.1080/10408699891274165

Soonthornchai, W., Rungrassamee, W., Karoonuthaisiri, N., Jarayabhand, P., and Jiravanichpaisal, P. (2009). Expression of immune-related genes in the digestive organ of shrimp, *Penaeus monodon*, after an oral infection by *Vibrio harveyi*. *Dev. Comp. Immunol.* 34, 19–28. doi: 10.1016/j.dci.2009.07.007

Sun, Y. F., Han, W. F., Liu, J., Liu, F., and Cheng, Y. X. (2020). Microbiota comparison in the intestine of juvenile Chinese mitten crab *Eriocheir sinensis* fed different diets. *Aquaculture* 515:734518. doi: 10.1016/j.aquaculture.2019.734518

Takahashi, K., Takimoto, T., Sato, K., and Akiba, Y. (2011). Effect of dietary supplementation of astaxanthin from *Phaffia rhodozyma* on lipopolysaccharide-induced early inflammatory responses in male broiler chickens (*Gallus gallus*) fed a corn-enriched diet. *Anim. Sci. J.* 82, 753–758. doi: 10.1111/j.1740-0929.2011.00898.x

Torrissen, O. J. (1995). "Effect of dietary astaxanthin supplementation on accumulation, survival and growth in postlarvae of *Penaeus* monodon *Fabricius*," in *Proceedings of the Larvi '95-fish and Shellfish Larviculture Symposium:* Special Publication No. 24 eds P. Lavens, E. Jaspers, and I. Roelants, (Ghent: EAS Special Publication), 251–254.

Verdegem, M. C. J. (2013). Nutrient discharge from aquaculture operations in function of system design and production environment. *Rev. Aquac.* 5, 158–171. doi: 10.1111/raq.12011

Vogt, G. (2019). Functional cytology of the hepatopancreas of decapod crustaceans. *J. Morphol.* 280, 1405–1444.

Wade, N. M., Cheers, S., Bourne, N., Irvin, S., Blyth, D., and Glencross, B. D. (2015). Dietary astaxanthin levels affect color, growth, carotenoid digestibility and the accumulation of specific carotenoid esters in the Giant Tiger Shrimp, *Penaeus* monodon. *Aquac. Res.* 48, 395–406. doi: 10.1111/are.12888

Wade, N. M., Gabaudan, J., and Glencross, B. D. (2017). A review of carotenoid utilisation and function in crustacean aquaculture. *Rev. Aquac.* 9, 141–156. doi: 10.1111/raq.12109

Wang, P., Chen, S. Q., Wei, C. Y., Yan, Q. P., Sun, Y. Z., Yi, G. F., et al. (2021). Monasus purpureus M-32 improves growth performance, immune response, intestinal morphology, microbiota and disease resistance in *Litopenaeus vannamei*. *Aquaculture* 530:735947. doi: 10.1016/j.aquaculture.2020.735947

Wang, W., Ishikawa, M., Koshio, S., Yokoyama, S., Hossain, M. S., and Moss, A. S. (2018b). Effects of dietary astaxanthin supplementation on juvenile kuruma shrimp, *Marsupenaeus japonicus*. *Aquaculture* 491, 197–204. doi: 10.1016/j.aquaculture.2018.03.025

Wang, W., Ishikawa, M., Koshio, S., Yokoyama, S., Dawood, M. A., and Zhang, Y. (2018a). Effects of dietary astaxanthin supplementation on survival, growth and stress resistance in larval and post−larval kuruma shrimp, *Marsupenaeus japonicus*. *Aquac. Res.* 49, 2225–2232. doi: 10.1111/are.13679

Wang, W., Ishikawa, M., Koshio, S., Yokoyama, S., Dawood, M. A., Hossain, M. S., et al. (2019). Interactive effects of dietary astaxanthin and cholesterol on the growth, pigmentation, fatty acid analysis, immune response and stress resistance of kuruma shrimp (*Marsupenaeus japonicus*). *Aquac. Nutr.* 25, 946–958. doi: 10.1111/anu.12913

Yamada, S., Tanaka, Y., Sameshima, M., and Ito, Y. (1990). Pigmentation of prawn (*Penaeus japonicus*) with carotenoids: I. Effect of dietary astaxanthin, β-carotene and canthaxanthin on pigmentation. *Aquaculture* 87, 323–330. doi: 10.1016/0044-8486(90)90069-Y

Yan, M. L., Wang, W. L., Huang, X. X., Wang, X. L., and Wang, Y. (2020). Interactive effects of dietary cholesterol and phospholipids on the growth perfromance, expression of immune-related genes and resistance against *Vibrio alginolyticus* in white shrimp (*Litopenaeus vannamei*). *Fish Shellfish Immunol.* 97, 100–107. doi: 10.1016/j.fsi.2019.11.048

Yang, Y. (2006). Effects of dietary supplementation of astaxanthin on production performance, egg quality in layers and meat quality in finishing pigs. *Asian Aust. J. Anim. Sci.* 19, 1019–1025.

Zhang, J., Liu, Y. J., Tian, L. X., Yang, H. J., Liang, G. Y., Yue, Y. R., et al. (2013). Effects of dietary astaxanthin on growth, antioxidant capacity and gene expression in Pacific white shrimp *Litopenaeus vannamei*. *Aquac. Nutr.* 19, 917–927. doi: 10.1111/anu.12037

Zhang, W. B., Murray, F. J., Liu, L. P., and Little, D. C. (2017). A comparative analysis of four internationally traded farmed seafood commodities in China: domestic and international markets as key drivers. *Rev. Aquac.* 9, 157–178. doi: 10.1111/raq.12110

Zhu, X. F., Guo, H., Li, G. L., and Zhu, C. H. (2021). Effect of dietary hydrolysable tannins on growth performance, antioxidant capacity, intestinal microflora and resistance against *Vibrio parahaemolyticus* of juvenile Pacific white shrimp, *Litopenaeus vannamei* (Boone, 1931). *Aquac. Rep.* 19:100601. doi: 10.1016/j.aqrep.2021.100601

Conflict of Interest: GY was employed by the company Beijing Dabeinong Technology Group Co., Ltd.

The remaining authors declare that the research was conducted in the absence of any commercial or financial relationships that could be construed as a potential conflict of interest.

Publisher's Note: All claims expressed in this article are solely those of the authors and do not necessarily represent those of their affiliated organizations, or those of the publisher, the editors and the reviewers. Any product that may be evaluated in this article, or claim that may be made by its manufacturer, is not guaranteed or endorsed by the publisher.

frontiers in Microbiology

ORIGINAL RESEARCH
published: 16 November 2021
doi: 10.3389/fmicb.2021.784211

Caffeic Acid Supplement Alleviates Colonic Inflammation and Oxidative Stress Potentially Through Improved Gut Microbiota Community in Mice

Fan Wan[1,2†], Ruqing Zhong[1†], Mengyu Wang[1], Yexun Zhou[1], Yuxia Chen[1], Bao Yi[1], Fujiang Hou[2], Lei Liu[1], Yong Zhao[1], Liang Chen[1] and Hongfu Zhang[1]**

[1] State Key Laboratory of Animal Nutrition, Institute of Animal Science, Chinese Academy of Agricultural Sciences, Beijing, China, [2] State Key Laboratory of Grassland Agro-Ecosystem, Key Laboratory of Grassland Livestock Industry Innovation, Ministry of Agriculture and Rural Affairs, College of Pastoral Agriculture Science and Technology, Lanzhou University, Lanzhou, China

OPEN ACCESS

Edited by:
Tingtao Chen,
Nanchang University, China

Reviewed by:
Hu Liu,
China Agricultural University, China
Tongxing Song,
Huazhong Agricultural University, China

***Correspondence:**
Liang Chen
chenliang01@caas.cn
Hongfu Zhang
zhanghongfu@caas.cn

[†]These authors have contributed equally to this work

Specialty section:
This article was submitted to Microbial Symbioses, a section of the journal Frontiers in Microbiology

Received: 27 September 2021
Accepted: 20 October 2021
Published: 16 November 2021

Citation:
Wan F, Zhong R, Wang M, Zhou Y, Chen Y, Yi B, Hou F, Liu L, Zhao Y, Chen L and Zhang H (2021) Caffeic Acid Supplement Alleviates Colonic Inflammation and Oxidative Stress Potentially Through Improved Gut Microbiota Community in Mice. Front. Microbiol. 12:784211. doi: 10.3389/fmicb.2021.784211

Caffeic acid (CA) is one of the major phenolic acids of coffee with multiple biological activities. Our previous study found that 500 mg/kg of chlorogenic acid (CGA) had the potential capacity of alleviating colonic inflammation. Moreover, CGA can be degraded into caffeic acid (CA) by the gut microbiota in the colon. Therefore, we hypothesize that CA can exert protective effects on colonic inflammation. To test the hypothesis, 251 mg/kg CA was supplemented to DSS-induced colitis mice. The results showed that CA treatment recovered DSS-induced disease activity index (DAI), colon length, and histopathology scores of colon tissue. Additionally, CA treatment significantly decreased pro-inflammatory cytokines and malondialdehyde (MDA) levels and increased the level of IL-10, total antioxidant capacity (T-AOC), superoxide dismutase (SOD), glutathione peroxidase (GSH-Px), and catalase (CAT) in serum. qPCR results indicated that CA treatment dramatically downregulated mRNA expression of *IL-1β*, *IL-6*, and *TNF-α* as well as upregulated *SOD1*, *GPX1*, *GPX2*, *CAT*, and *IL-10*. In addition, CA supplementation significantly increased mRNA expression of *Nrf-2*, *HO-1*, and *NQO1*, which showed its antioxidant and anti-inflammatory capacities potentially by activating the Nrf-2/HO-1 pathway. Moreover, CA supplementation prevented gut barrier damage by enhancing *Occludin* gene expression. Furthermore, CA supplementation altered the gut microbiome composition by decreasing the relative abundance of *Bacteroides* and *Turicibacter*, and enhancing the relative abundance of *Alistipes* and *Dubosiella*. Meanwhile, CA supplementation increases the abundance of *Dubosiella* and *Akkermansia*. In conclusion, CA supplementation could effectively alleviate DSS-induced colitis by improving the defense against oxidative stress and inflammatory response.

Keywords: caffeic acid, colitis, gut microbiota, oxidative stress, inflammatory responses

INTRODUCTION

Intestinal bowel disease (IBD) is a chronic and recurrent inflammatory disease (Maloy and Powrie, 2011). There are two main clinical forms of IBD including Crohn's disease (CD) and ulcerative colitis (UC), which can affect the gastrointestinal tract inflammation (Kaplan, 2015). It is a many-sided and recurrent immunologic dysfunction that requires long-term potent medication (Danese et al., 2016). The genetic and environmental factors are the major causes of UC, but the explicit mechanism is still not clear at the moment (Chow et al., 2009). The main symptom changes of UC are located in the colon mucosa, recurring inflammatory conditions, and gradually spreading to the entire colon (Zhang et al., 2015). The inflammatory responses and oxidative stress often occur in the pathogenesis and development of UC, which explains that inflammatory infiltration and oxidative damage lead to the occurrence and aggravation of UC (Roessner et al., 2008). Recent researches suggested that the possible mechanisms of UC were involved in inflammatory response, oxidative stress, gut barrier dysfunction, and gut microbiota dysbiosis, etc. (Martens et al., 2018; Zhai et al., 2019; Yang et al., 2020).

In the recent reports, the possible regulation measures of UC included decreasing intestinal inflammation, alleviating oxidative stress, enhancing gut barrier function, and improving gut microbiota, etc. (Almousa et al., 2018; Bai et al., 2019; Xiao et al., 2019). The mucosal immune system is activated during colitis, which is accompanied by increasing mRNA expression of pro-inflammatory cytokines, including tumor necrosis factor (*TNF*)-α, interleukin (*IL*)-1β, and *IL-6* (Akanda et al., 2018). Meanwhile, inflammatory infiltration and an uncontrolled immune system could increase the oxidative burden, which is attributed to the continuous overproduction of ROS by activating macrophages and neutrophils (Roessner et al., 2008). It has been found that mice with colitis were often accompanied by increasing oxidative stress and inflammatory responses, and it is related to the Nrf-2 pathway closely (Zhang et al., 2020). In addition, the Toll-like receptor 4 (TLR4) was activated, which caused the elevation in the level of its ligand LPS on DSS-induced colitis (Mahmoud et al., 2020). Besides, as the first protection of the intestine, the intestinal epithelial barrier consists of the mucous layer, intercellular tight junction (TJ) proteins, and epithelial cells (Martens et al., 2018), which are responsible for regulating the mucosal barrier permeability (Mahmoud et al., 2020). When the barrier is damaged, the toxins and inflammatory cytokines penetrate the intestinal mucosa, thus, aggravating the development of UC (Hu et al., 2015). Importantly, UC often causes gut barrier damage by reducing the mRNA expression of TJ proteins including *ZO-1*, *Occludin*, and *claudin-1* (Zhao et al., 2020). Besides, gut microbiota plays a vital role in colitis. A previous study showed that the relative abundance of *Bacteroidetes* and *Turicibacter* significantly increased in patients with UC and mice with colitis, and the relative abundance of *Firmicutes* markedly decreased in colitis mice (Gophna et al., 2006; Liu A. et al., 2020; Li et al., 2021). Moreover, as the microbial metabolites, the levels of short-chain fatty acids (SCFAs) were significantly decreased in colitis mice (Wang R. X. et al., 2020). Numerous studies have also confirmed that enhancing SCFAs levels could attenuate colitis by reducing pro-inflammatory cytokines (Parada Venegas et al., 2019; Zhao et al., 2020). Therefore, targeting the inhibiting inflammatory response, improving gut barrier, and regulating gut microbiota structure are considered as wise strategies for the discovery of UC prevention and treatment drugs.

CA is the major component of coffee, argan, oil, oats, wheat, rice, and olive oil (Zhang et al., 2016). It has been reported that there are several pharmacological activities such as anti-oxidant, anti-inflammatory, and free radical scavenging effects (Ruan et al., 2016; Rui et al., 2017; Lee and Lee, 2018; Li et al., 2018). Our previous study found that 500 mg/kg of chlorogenic acid (CGA) had the potential capacity of alleviating colonic inflammation by inhibiting oxidative stress and inflammation. When CGA was absorbed completely after entering into the body, not only its original form but also its hydrolytic form occurred mostly, namely, caffeic acid (CA) and quinic acid (QA) before being absorbed in the gastrointestinal tract (Shin et al., 2015; Clifford et al., 2017). However, whether metabolite CA plays a significant role in performing anti-inflammatory and antioxidant capacity on colitis mice, there is still a need for more clear information to study it. In the present study, we hypothesized that metabolites CA may exert anti-inflammatory and antioxidant capacity to alleviate DSS-induced colitis. Therefore, equimolar CA was pretreated to explore whether it plays an anti-inflammatory and antioxidant ability by regulating oxidative stress and inflammatory response in DSS-induced colitis mice.

MATERIALS AND METHODS

All animal procedures were performed in accordance with the Guidelines for Care and Use of Laboratory Animals of the Chinese Academy of Agriculture Sciences and Experiments and were approved by the Animal Ethics Committee of Experimental Animal Welfare and Ethical of Institute of Animal Science, Chinese Academy of Agriculture Sciences (IAS2020-88).

Chemicals and Reagents

CA (≥95%) and fluorescein isothiocyanate (FITC)-dextran (70 kDa) were purchased from Sigma-Aldrich (St. Louis, MO, United States). DSS (36–50 kDa) was purchased from MP Biomedicals (Irvine, CA, United States). Assay kits, including tumor necrosis factor (TNF)-α, interleukin (IL)-6, IL-1β, IL-10, total antioxidant capacity (T-AOC), glutathione peroxidase (GSH-Px), superoxide dismutase (SOD), catalase (CAT), malondialdehyde (MDA), lipopolysaccharide (LPS), and reactive oxygen species (ROS) were purchased from Nanjing Jian Cheng Bioengineering Institute (Nanjing, China). Trizol reagent was purchased from Invitrogen (Carlsbad, CA, United States). Quantitative real-time polymerase chain reaction (qRT-PCR) was performed using TB Green Premix Ex Taq (TaKaRa, Kusatsu, Japan). The primers used for qPCR were purchased from Sangon Biotech Co., Ltd. (Shanghai, China).

Animal Care and Experimental Design

Female ICR mice (3-week-old) were obtained from the Vital River Laboratory Animal Technology (Beijing, China). All mice (four per house) were placed under a controlled temperature of 21 ± 2°C, a 12-h light/dark cycle, and were free to access food and water during the whole experiment. After acclimation for 1 week, the mice (body weight 22.23 ± 1.65 g) were randomly divided into three groups (n = 16): (1) control group (CON group), mice were fed a basal diet; (2) DSS-administered group (DSS group), mice received a basal diet; (3) caffeic acid group (CA group), mice were fed a basal diet supplementation with 251 mg/kg (W/W) CA for 23 days. Mice in the CON group received normal drinking water for 23 days. Mice in DSS and CA groups received normal drinking water for 14 days, and then both DSS and CA groups were given 3% DSS in drinking water in days 15–21, followed by 2 days of drinking water without DSS. The experimental design is shown in **Figure 1A**. At the end of the experiment, colonic barrier integrity was evaluated by the method of gavage with 70-kDa FITC-dextran in sterile water. Blood samples were collected, and then serum was stored at −80°C after centrifugation at 3,000 rpm for 10 min. The mice were sacrificed by cervical dislocation under anesthesia. The colon length of the mice was recorded. The colon tissues were taken out as soon as possible. The proximal colon (2 mm × 6 mm) was stored in 4% paraformaldehyde for histopathology examinations. Colonic contents and remnant colon tissue were frozen in liquid nitrogen for further analysis.

Evaluation of the Disease Activity Index

To assess colitis statuses, comprehensive DAI scores for each of weight loss, stool consistency, and rectal hemorrhage were checked daily for assessing the DAI score of each mice to assess the status of the disease based on the previous literature research (Wang R. X. et al., 2020). Scores were defined as (i) percentage of weight loss: 0 (0%), 1 (1–5%), 2 (5–10%), 3 (11–20%), and 4 (>20%); (ii) stool consistency: 0 (well-formed pellets), 2 (pasty, semi-formed pellets), and 4 (liquid stools), and rectal bleeding: 0 (no blood), 2 (hemoccult positive), and 4 (gross bleeding) (Wang R. X. et al., 2020).

Hematoxylin and Eosin Staining and Histopathological Examination

Colon tissues (4 μm) were embedded in paraffin and sectioned, and then histological changes were observed with H&E staining. The histological changes were observed by an optical microscope (Olympus, Tokyo, Japan). Histopathological examination was evaluated based on the infiltration of inflammatory cells and epithelial damage (Yang et al., 2017).

Serum Inflammatory Cytokines and Antioxidant Analysis

The levels of pro-inflammatory cytokines (TNF-α, IL-1β, IL-6, and IL-12), anti-inflammatory cytokine (IL-10), antioxidant-related parameters (T-AOC, SOD, GSH-Px, CAT, ROS, and MDA), and LPS in serum were tested by ELISA kits (Nanjing Jiancheng Bioengineering Institute, Nanjing, China) following the instructions of the manufacturer.

Colon Permeability

Mice were administered with 100 μl of 100 mg/ml of 70-kDa FITC-dextran (Sigma-Aldrich) in sterile water by oral gavage, and blood was collected by orbital blooding after 4 h before sacrifice (Wang R. X. et al., 2020). Serum was obtained by centrifugation (3,000 rpm, 10 min, 4°C). The concentration of FITC in serum was determined by SynergyH1 automatic microplate reader (Biotek) with excitation wavelength of 485 nm and an emission wavelength of 528 nm (Pu et al., 2021).

Quantitative Real-Time Polymerase Chain Reaction Assay

Total RNA from the colon samples were extracted using Trizol reagent (Invitrogen, United States), chloroform, isopropanol, and 75% ethanol solution, and then treated with DNase I (TaKaRa, China) for possible DNA contamination. The concentration of each RNA sample was quantified using the NanoDrop 2000 (NanoDrop Technologies, United States). The HiFiScript cDNA was generated using the Prime Script RT Master Mix (TaKaRa, China) according to the instructions of the manufacturer. The reverse transcription was conducted at 37°C for 15 min and 85°C for 5 s. qPCR was conducted using the KAPA SYBR FAST qPCR Master Mix kit according to the instructions of the manufacturer. Briefly, 1 μl of cDNA template was added to a total volume of 10 μl containing 5 μl of KAPA SYBR FAST qPCR Master Mix Universal, 0.4 μl of PCR forward primer, 0.4 μl of PCR reverse primer, 0.2 μl of ROX low, and 3 μl of PCR-grade water (KAPA Biosystems, United States). All samples were run in an Applied Biosystems 7,500 RT-PCR System (Thermo Fisher Scientific, China). Relative gene expression was normalized to the housekeeping gene GADPH and calculated using the $2^{-\Delta\Delta Ct}$ method, where $\Delta C_t = C_t$ (Target) – C_t (GAPDH). Primer sequences were designed using Primer 5.0 software and synthesized by Sangon Biotech Co., Ltd. (Shanghai, China). The primers used in this study are listed in **Table 1**.

Gut Microbiota Analysis

Total genome DNA from colonic digesta was extracted using the Fast DNA® SPIN for soil kit (MP Biomedicals, Solon, OH, United States). The quality of the DNA was detected by 1% agarose gel, and DNA was quantified by a NanoDrop 2000 UV-vis spectrophotometer (Thermo Fisher Scientific, Wilmington, DE, United States). The V3–V4 hypervariable region of the bacterial 16S rRNA gene was amplified with PCR using primer pairs 338F (5′-ACTCCTACGGGAGGCAGCAG-3′) and 806R (5′-GGACTACHVGGGTWTCT AAT-3′). The PCR system and amplification conditions are referred to in previous reports (Wang L. et al., 2020). PCR amplified products were extracted from 2% agarose gel and purified using the AxyPrep DNA Gel Extraction Kit (AXYGEN, New York, NY, United States) according to the instructions of the manufacturer. After being quantified and purified, amplicons were sequenced. The sequences were analyzed and assigned to operational taxonomic units (OTUs; 97% identity). The products were directly sequenced by an Illumina MiSeq platform (Illumina, SD, United States) (2 × 300, pair-end). After being quantified

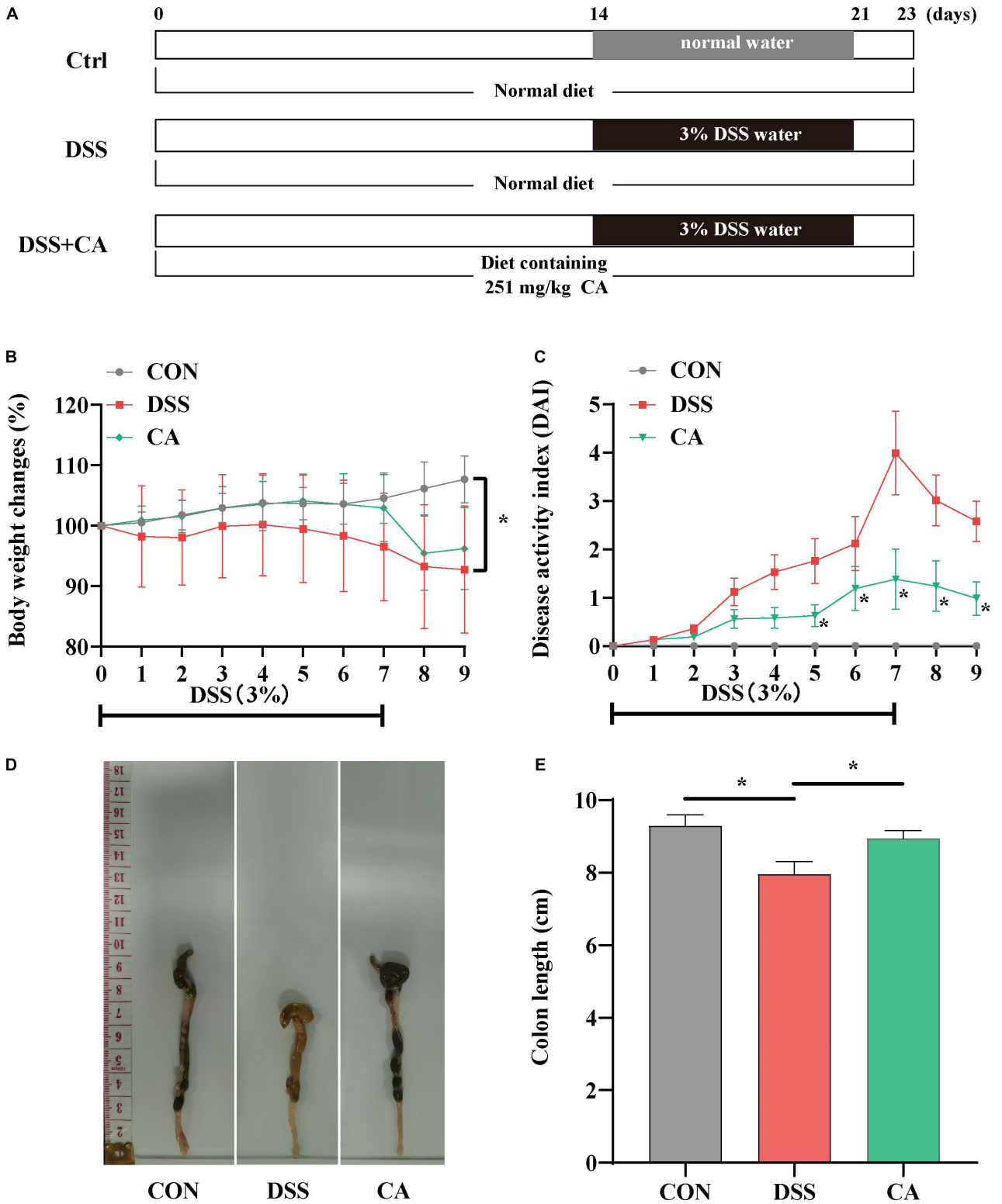

FIGURE 1 | Experimental schedule and basic indicators of caffeic acid (CA) on DSS-induced colitis mice. **(A)** Animal treatments schedule. **(B)** Body weight changes. **(C)** Disease activity index (DAI) score during experimental colitis. **(D)** Images of the colon length. **(E)** The colon length in the different treatment groups. Data are presented as means ± SEM (n = 16 per group). *$p < 0.05$ vs. the DSS-treated group on the same day. CON, control group; DSS, DSS group; CA, caffeic acid group. The same as below.

TABLE 1 | Primers used for qPCR assay.

Genes	Forward primer (5′–3′)	Reverse primer (5′–3′)
IL-1β	TCCTCCTTGCCTCTGATGG	GAGTGCTGCCTAATGTCCC
IL-6	GCTGGAGTCACAGAAGGAG	GGCATAACGCACTAGGTTT
TNF-α	ACCACCATCAAGGACTCAA	CAGGGAAGAATCTGGAAAG
IL-10	GCCATGAATGAATTTGACA	CAAGGAGTTGTTTCCGTTA
SOD1	GTGAACCAGTTGTGTTGTC	ATCACACGATCTTCAATGGA
CAT	TCAGGTGCGGACATTCTA	ATTGCGTTCTTAGGCTTCT
GPX1	ATCAGTTCGGACACCAGA	TTCACTTCGCACTTCTCAA
GPX2	GTGGCGTCACTCTGAGGAACA	CAGTTCTCCTGATGTCCGAACTG
Nrf2	CAGTGCTCCTATGCGTGAA	GCGGCTTGAATGTTTGTCT
HO-1	CACAGATGGCGTCACTTCG	GTGAGGACCCACTGGAGGA
NQO1	AGCTTTAGGGTCGTCTTGG	TGGCGTAGTTGAATGATGTCT
ZO-1	GAAGAACTGTCAGGCATTG	CATTTACTGGCTGGTATTTT
Occludin	ACCGTCTAATCAATCTTTG	AACTCCTGAACCAGCACTC
GAPDH	GGTCCCAGCTTAGGTTCAT	CAATCTCCACTTTGCCACT

and purified, amplicons were sequenced using Illumina MiSeq platform (Illumina, San Diego, CA, United States) at the Majorbio Bio-Pharm Technology Co., Ltd. (Shanghai, China) according to standard protocols.

Short-Chain Fatty Acids Analysis

Concentrations of SCFAs in colonic contents were measured using GC-MS. Briefly, colonic contents samples were weighed into 1.5-ml centrifuge tubes and mixed with 1 ml of ddH_2O, homogenized, and centrifuged (10,000 rpm, 10 min, 4°C). A mixture of the supernatant fluid and 25% metaphosphoric acid solution (0.9 and 0.1 ml, respectively) were vortexed for 1 min and centrifuged (1,000 rpm, 10 min, 4°C) after standing in a 1.5-ml centrifuge tube at 4°C for over 2 h. The supernatant portion was then filtered through a 0.45-μm polysulfone filter and analyzed using Agilent 6890 gas chromatography (Agilent Technologies, Inc., Palo Alto, CA, United States).

Statistical Analysis

Data were presented as the mean ± standard error of the mean (SEM). All data were compared by one-way analysis of variance (ANOVA) with Tukey's test (SPSS 21.0 software, Chicago, IL, United States). Spearman's correlation analysis was performed using RStudio (version 4.0.3) platform. A value of $p < 0.05$ was considered significant. $^{*}p < 0.05$ indicates a significant difference, and $^{**}p < 0.01$ indicates an extremely significant difference. Plots were performed using GraphPad Prism 8.0.2.

RESULTS

Caffeic Acid Supplementation Improved Clinical Signs, Colonic Histopathological Score, and Colon Permeability

The body weight in the DSS group was significantly decreased compared with the CON group, while supplement with CA reversed the decreased body weight ($p < 0.05$) (**Figure 1B**). In **Figure 1C**, the DAI score was dramatically increased owing to the DSS treatment, but the CA treatment notably suppressed the increased DAI score ($p < 0.05$). As shown in **Figures 1D,E**, the colon length was shortened in the DSS group. However, CA supplementation significantly inhibited the shortened colon induced by DSS ($p < 0.05$). These results implied that supplementation of CA alleviated DSS-induced colitis symptoms.

H&E staining results indicated that the permeability of intestinal epithelium was increased, and the number of goblet cells was significantly decreased in the mucosa and submucosa when treated with DSS ($p < 0.05$). Meantime, CA supplementation improved the severely damaged histology of the colon (**Figures 2A,B**). In addition, colonic barrier integrity was examined by gavage with 70-kDa FITC-dextran in sterile water, and the results showed that the permeability of the gut barrier was increased in the DSS group, however, CA supplementation enhanced gut barrier function as shown by the decreased FITC-dextran concentration in serum ($p < 0.05$) (**Figure 2C**).

Caffeic Acid Supplementation Altered Levels of Serum Inflammatory Cytokines

To investigate the effect of CA supplementation on cytokine contents in the serum of colitis mice, the inflammatory cytokines IL-6, TNF-α, IL-1β, IL-12, and anti-inflammatory cytokine IL-10 were detected. The results indicated that DSS treatment dramatically increased IL-6, TNF-α, IL-1β, and IL-12 levels compared with the CON group, while CA treatments reduced levels of pro-inflammatory cytokines IL-6, TNF-α, IL-1β, and IL-12 ($p < 0.05$) (**Figures 3A–D**). In addition, mice with DSS-induced colitis exhibited a significant decrease in IL-10 in the serum. In the meantime, CA treatment significantly relieved inflammatory responses by increasing the IL-10 level ($p < 0.05$) (**Figure 3E**). In this study, we also found increased level of LPS in the DSS group. As expected, CA supplementation dramatically decreased the production of LPS ($p < 0.05$) (**Figure 3L**).

Caffeic Acid Supplementation Alleviated Oxidative Stress in the Serum

It is well known that T-AOC and antioxidative enzyme activities of GSH-Px, SOD, and CAT index are important factors to oxidative stress in colitis (Dudzinska et al., 2018). Compared with the CON group, the serum level of T-AOC, enzyme activities of GSH-Px, SOD, and CAT significantly decreased in the DSS group, which were enhanced by CA administration ($p < 0.05$) (**Figures 3F–I**). Meanwhile, the level of MDA in the serum significantly increased in the DSS group; in the CA supplementation group, it was decreased instead ($p < 0.05$) (**Figure 3J**).

ROS played an important role in colitis because overproduction of ROS led to severe oxidative stress (Piechota-Polanczyk and Fichna, 2014). In this study, we also found that the level of ROS increased in the serum during DSS-treated immune epithelial injury. However, CA supplementation significantly decreased the production of ROS ($p < 0.05$) (**Figure 3K**).

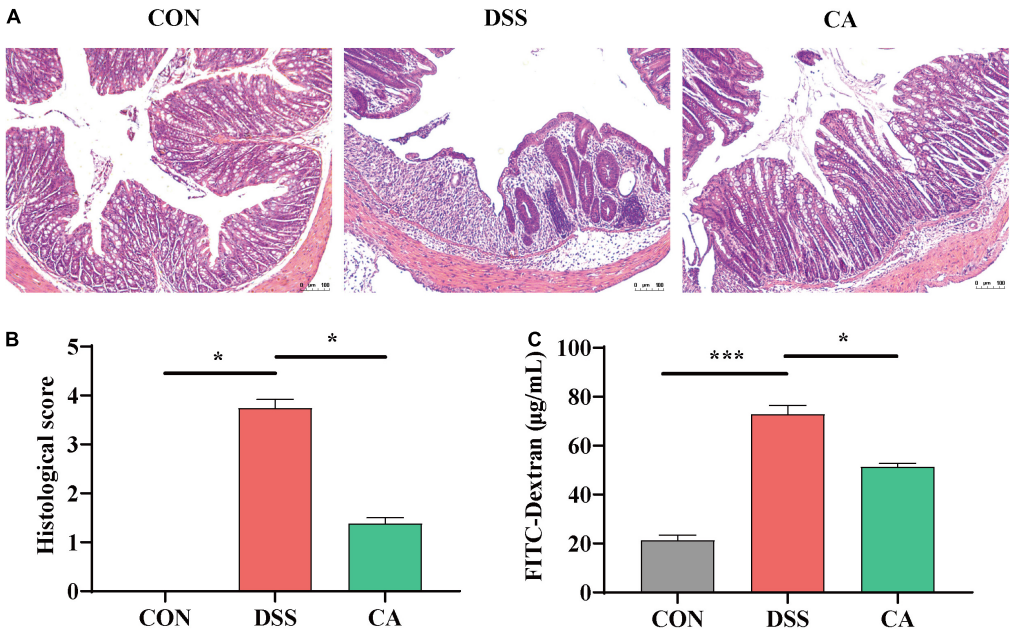

FIGURE 2 | Effects of CA supplementation on histopathological changes in DSS-induced mice colon. **(A)** Hematoxylin and Eosin (H&E) staining images of each group. **(B)** Histological score of each group. **(C)** Serum fluorescein isothiocyanate (FITC)-dextran levels of each group. Data are presented as mean ± SEM; $n = 4$. $^{*}p < 0.05$ and $^{***}p < 0.001$ vs. the DSS-treated group on the same day.

Caffeic Acid Altered Gene Expression of Inflammatory Cytokines in the Colon

To confirm the anti-inflammatory effect of CA, the colonic mRNA expressions of inflammatory cytokines IL-1β, IL-6, TNF-α, and IL-10 were investigated. Results showed that mice in the DSS group had significantly higher relative mRNA levels of IL-1β, IL-6, and TNF-α compared with both the CON and the CA groups ($p < 0.05$) (**Figures 4A–C**). Furthermore, the CA group showed higher mRNA level of anti-inflammatory cytokine IL-10 than the DSS group ($p < 0.05$) (**Figure 4D**).

Caffeic Acid Altered Antioxidant Gene Expression and Modulation of Nrf-2 Activation in the Colon

To explore the antioxidant effect of CA, we further tested the colonic mRNA expression levels of *CAT*, *GPX1*, *GPX2*, and *SOD1*. As shown in **Figures 4E–H**, CA supplementation significantly increased the transcript levels of *CAT*, *GPX1*, *GPX2*, and *SOD1* compared with the DSS group ($p < 0.05$). Additionally, the mRNA expression of *Nrf-2*, *HO-1*, and *NQO1* were significantly higher in the CA group compared with the DSS group ($p < 0.05$) (**Figures 4I–K**). Therefore, CA treatments were potential activated Nrf-2 pathway to ameliorate DSS-induced colitis mice.

Caffeic Acid Enhanced the Gene Expression of Tight Junction Proteins

To further confirm the protective effects of CA supplementation in the colon, tight junction proteins were tested. The mRNA expressions of *ZO-1* and *Occludin* were significantly lower in the DSS group compared with the CON group ($p < 0.05$) (**Figures 4L,M**). The mRNA expression of *Occludin* was markedly higher in the CA group than the DSS group ($p < 0.01$) (**Figure 4M**).

Caffeic Acid Supplementation Modulated Composition of Colonic Microbiota

Using 16S rRNA amplicon sequencing, the microbiota in the colonic content was analyzed. Each sequence length was 401–440 base pairs. The Venn diagram shows that mice in the CON, DSS, and CA groups contained 360 common OTUs, and 105, 28, and 51 unique OTUs, respectively (**Figure 5A**). β-diversity was conducted by principal coordinate analysis (PCoA) based on weighted unifrac metrics. The results showed that the gut microbiota in the DSS group was significantly different from the mice in the CON group ($p < 0.01$), and was of a different trend from the mice in the CA group (**Figure 5B**). α-Diversity results showed that there was significant difference in the indexes of ACE among the three groups ($p < 0.05$) (**Figure 5C**).

At the genus levels, *Bacteroides*, *Turicibacter*, *Alistipes*, *Dubosiella*, and *Akkermansia* were bacteria with different contents. *Lactobacillus* is an important bacterial genus, but there was no significant difference among all groups (**Figures 6A,B**). *Bacteroides* (7.9%) and *Turicibacter* (3.9%) were important bacterial genus in the DSS group, while it showed significantly decreased relative abundance of *Bacteroides* ($p < 0.01$) in the CON group (**Figure 6C**). In addition, the relative abundance of *Turicibacter* in the CON group ($p < 0.001$) and the CA

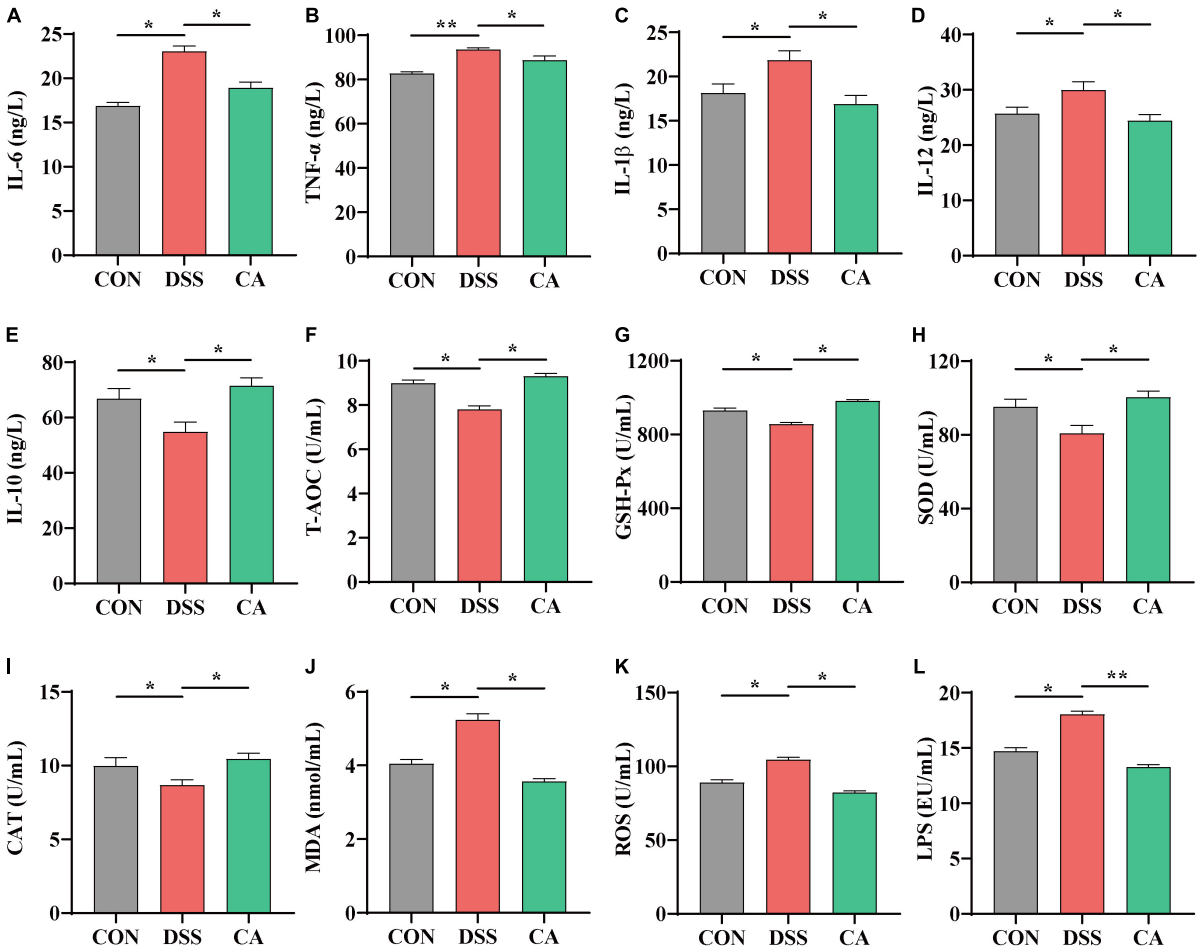

FIGURE 3 | Effects of CA supplementation on the serum inflammation cytokine and antioxidant parameters in DSS-induced colitis mice. **(A)** IL-6. **(B)** TNF-α. **(C)** IL-1β. **(D)** IL-12. **(E)** IL-10. **(F)** T-AOC. **(G)** GSH-Px. **(H)** SOD. **(I)** CAT. **(J)** MDA. **(K)** ROS. **(L)** LPS. Data are presented as mean ± SEM; $n = 10$. *$p < 0.05$ and **$p < 0.01$ vs. the DSS-treated group.

group ($p < 0.01$) were significantly decreased compared with the DSS group (**Figure 6D**). In addition, *Alistipes* (3.2%) is an important bacterial genus in the CON group, while the DSS group showed significantly decreased relative abundance of *Alistipes* (0.4%) ($p < 0.01$); however, the CA group showed the enhanced trend of relative abundance of *Alistipes* (0.9%) ($p < 0.05$) (**Figure 6E**). *Dubosiella* (4.7%) and *Akkermansia* (3.09%) were important bacterial genera in the CA group, but the CON and DSS groups showed significantly lower relative abundance of *Dubosiella* ($p < 0.05$) and *Ruminococcus* ($p < 0.05$) (**Figures 6F,G**).

The overall microbial composition in the CON, DSS, and CA groups differed at the phylum and genus levels. Linear discriminant analysis effect size (LEfSe) analysis was performed to evaluate the differentially expressed bacteria. The yellow dots inserted in the circle suggest no significant difference in bacteria among different treatments. LEfSe results showed that 19 bacterial clades at all taxonomic levels were differentially abundant (LDA > 4.0) in the colon microbiota (**Supplementary Figures 1A,B**).

Caffeic Acid Supplementation Influenced Short-Chain Fatty Acids

SCFAs in the colonic content as metabolites of gut microbiota, which can protect the intestine by alleviating inflammation and maintaining the integrity of the intestinal epithelial cells, were examined. The results showed that there was a significantly decreased butyric acid in the DSS group compared with the CON group ($p < 0.05$). However, the levels of butyric acid in the CA group were significantly improved compared with the DSS group ($p < 0.05$) (**Figure 7**).

Correlation Analysis Among the Microorganisms, Short-Chain Fatty Acids and Biochemical Parameters in DSS-Induced Colitis Mice

In order to find the correlation among the colonic microbiota, colonic SCFAs and other biochemical parameters in DSS-induced colitis mice, the Spearman's correlation analysis was carried

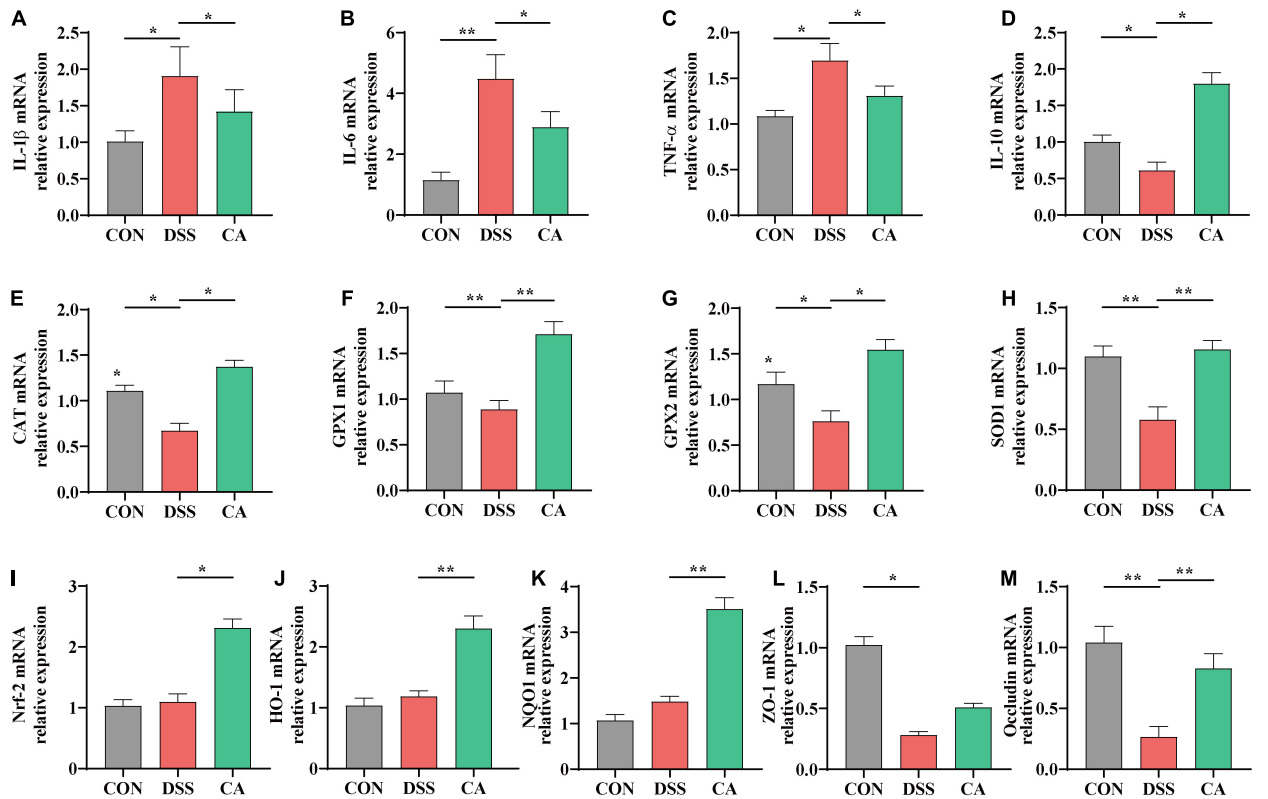

FIGURE 4 | Effects of CA supplementation on colon inflammation cytokine, antioxidant parameters, and expression of Nrf2 target gene mRNAs in the colon in DSS-induced colitis mice. **(A)** IL-1β. **(B)** IL-6. **(C)** TNF-α. **(D)** IL-10. **(E)** CAT. **(F)** GPX1. **(G)** GPX2. **(H)** SOD1. **(I)** Nrf-2. **(J)** HO-1. **(K)** NQO1 **(L)** ZO-1. **(M)** Occludin. Data are presented as mean ± SEM; $n = 10$. *$p < 0.05$ and **$p < 0.01$ vs. the DSS-treated group.

out based on experimental parameters. The correlation result is shown in **Figure 8**. It shows that there was a significant correlation among *Bacteroides*, inflammatory cytokines, SCFAs, and tight junctions (TJs). More precisely, the increased abundance of *Bacteroides* had been discovered to have a significant positive correlation with mRNA expression of *IL-6* ($r = 0.532$, $p = 0.034$) and *IL-1*β ($r = 0.493$, $p = 0.032$), Meanwhile, the increased abundance of *Bacteroides* was negatively correlated with the mRNA expression of *ZO-1* ($r = -0.576$, $p = 0.019$) and *Occludin* ($r = 0.554$, $p = 0.014$), and similar results were found in *Turicibacter*. In addition, the increased abundance of *Turicibacter* had a negative correlation with propionic acid ($r = -0.392$, $p = 0.027$) and butyric acid ($r = -0.507$, $p = 0.005$). However, the increased abundance of *Dubosiella* had been discovered to have a significantly positive correlation with the mRNA expression of *IL-10* ($r = 0.665$, $p = 0.0001$). A similar result was found in *Akkermansia*. More importantly, the increased abundance of *Akkermansia* has a significantly positive correlation with the butyric acid level ($r = 0.457$, $p = 0.009$).

DISCUSSION

IBD, which is a complex and recurrent colonic inflammatory disease, is still increasing in incidence from all over the world, thereby more and more novel medicines need to be developed in order to treat it. CGA is a polyphenol source of health benefit, and CA is one of the metabolites of CGA in the colonic lumen by gut microbiota (Clifford et al., 2017). However, the certain metabolite of CGA that can alleviate colitis has not been sufficiently elucidated. Based on the molecular structure of CA, it was contained in the catechol group, and we assumed that CA may be a major functional metabolite of CGA, which could exert therapeutic effects by improving the regulation of oxidative stress and inflammatory response to alleviate DSS-induced colitis. In the present study, we found that CA supplementation could significantly improve the pathological symptoms of DSS-induced colitis, colonic inflammation and oxidative stress, and intestinal-barrier disruption through the regulation of the gut microbiota. The CA supplementation reversed the dysbiosis of colitis-related gut microbiota and restored the gut barrier, which further relieves inflammatory infiltration in the colonic tissues. More specially, CA supplementation enhanced specific beneficial bacteria to maintain gut microecology.

DSS-induced colitis is a classic UC model in mice because the symptoms are similar to the patients who suffered from UC (Kaplan, 2015). The major indicators of DAI, colon length, and the ratio of colon length/body weight have shown that DSS exposure can induce classic symptoms of colitis in mice (Ma et al., 2018; Zhao et al., 2019, 2020; Dong et al., 2020). In the present

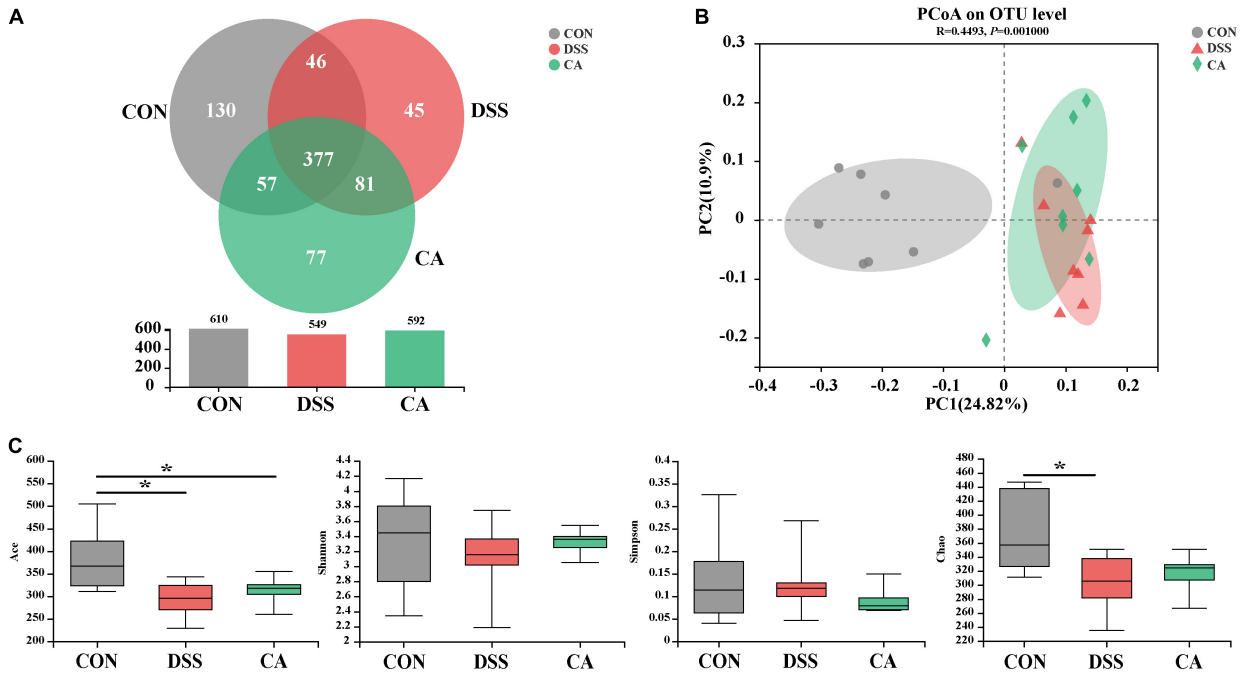

FIGURE 5 | Effects of CA administration on intestinal microbiota inflammation in DSS-induced colitis mice. **(A)** A Venn diagram showing the overlap of the operational taxonomic units (OTUs) identified in the intestinal microbiota among three groups; **(B)** principal coordinate analysis (PCoA) plot of the gut microbiota based on weighted Unifrac distance; **(C)** α-diversity of each group. Data are presented as mean ± SEM. (n = 8 mice). *$p < 0.05$.

study, we established a murine colitis model using drinking water administration of 3% DSS for 7 days. We also found similar results in colitis symptoms with DSS induction. However, the present study demonstrated that many symptoms were effectively alleviated by the supplementation of CA. CGA, as a kind of polyphenol, has been shown to have a protective effect against DSS-induced colitis during the disease active stage and recovery period in a previous study (Zhang et al., 2019). Interestingly, in our study, CA also significantly ameliorated DSS-induced colitis mice. Hence, the effect of CA alleviating DSS-induced colitis was also investigated.

The gut barrier function consists of TJs and adherens junction, which form a physical barrier to inhibit inflammatory infiltration and protect gut health (Turner, 2009). The barrier is broken when the intestinal TJs (ZO-1, Occludin, and claudin-1) of the epithelium cells are disrupted (Grosheva et al., 2020). Recent researches reported that colon disruption of the intestinal epithelial and inflammatory infiltration was deepened in UC patients and colitis mice (Marafini et al., 2019; Grosheva et al., 2020; Zhao et al., 2020). As reported, mice showed mucosal damage and increased intestinal permeability by DSS via drinking water for a week (Llewellyn et al., 2018). In this study, we also found the decrease in histological score after DSS treatment, while CA supplementation reversed this change. Especially, the (FITC)-dextran concentration of serum was notably lower with CA supplementation compared with DSS treatment. A previous study showed that supplementation of CA could increase expression of *Occludin* and *claudin* in TGF-β1-stimulated/unstimulated human cervical cancer cell lines (C-4I) (Tyszka-Czochara et al., 2018). Meanwhile, oral CGA (60 mg/kg body weight) also could increase the expression of ZO-1 and Occludin against high-fat diet (HFD)-induced hepatic steatosis and inflammation (Shi et al., 2021). In this study, we found that the loss of intestinal epithelial ZO-1 and Occludin caused triggered inflammatory infiltration in the DSS group, while CA supplementation in the diet reversed these changes. Combined with the above analysis results, this study indicated that CA supplementation indicates a protective effect to the gut integrity and effectively alleviates elevation of gut permeability. This new information in our study contributed to understanding the potential effect of CA as a protection to maintain gut barrier integrity.

Inflammatory response plays a key role in activating the production of mature IL-6, IL-1β, and TNF-α in UC patients and colitis mice (Marafini et al., 2019). Numerous phenolic acids can inhibit the inflammatory responses to improve colitis (Sandoval-Ramirez et al., 2021). For example, caffeic acid, tea polyphenols, salvianolic acid, and sesamol could ameliorate colitis by reducing the levels of IL-1β, IL-6, TNF-α, and other pro-inflammatory cytokines in DSS-induced colitis mice (Ye et al., 2009; Wang et al., 2018; Liu Y. et al., 2020; Zhao et al., 2020). In our study, we also found that the levels of IL-1β, IL-6, and TNF-α in the serum were increased in DSS-induced colitis, while CA supplementation could decrease the above inflammatory cytokines. In addition, IL-10 is necessary for induction and maintenance of Treg cells against colitis mice (Sivaprakasam et al., 2016). In humans, inhibition of IL-10 could cause the early IBD and more severe colitis (Galatola et al., 2013).

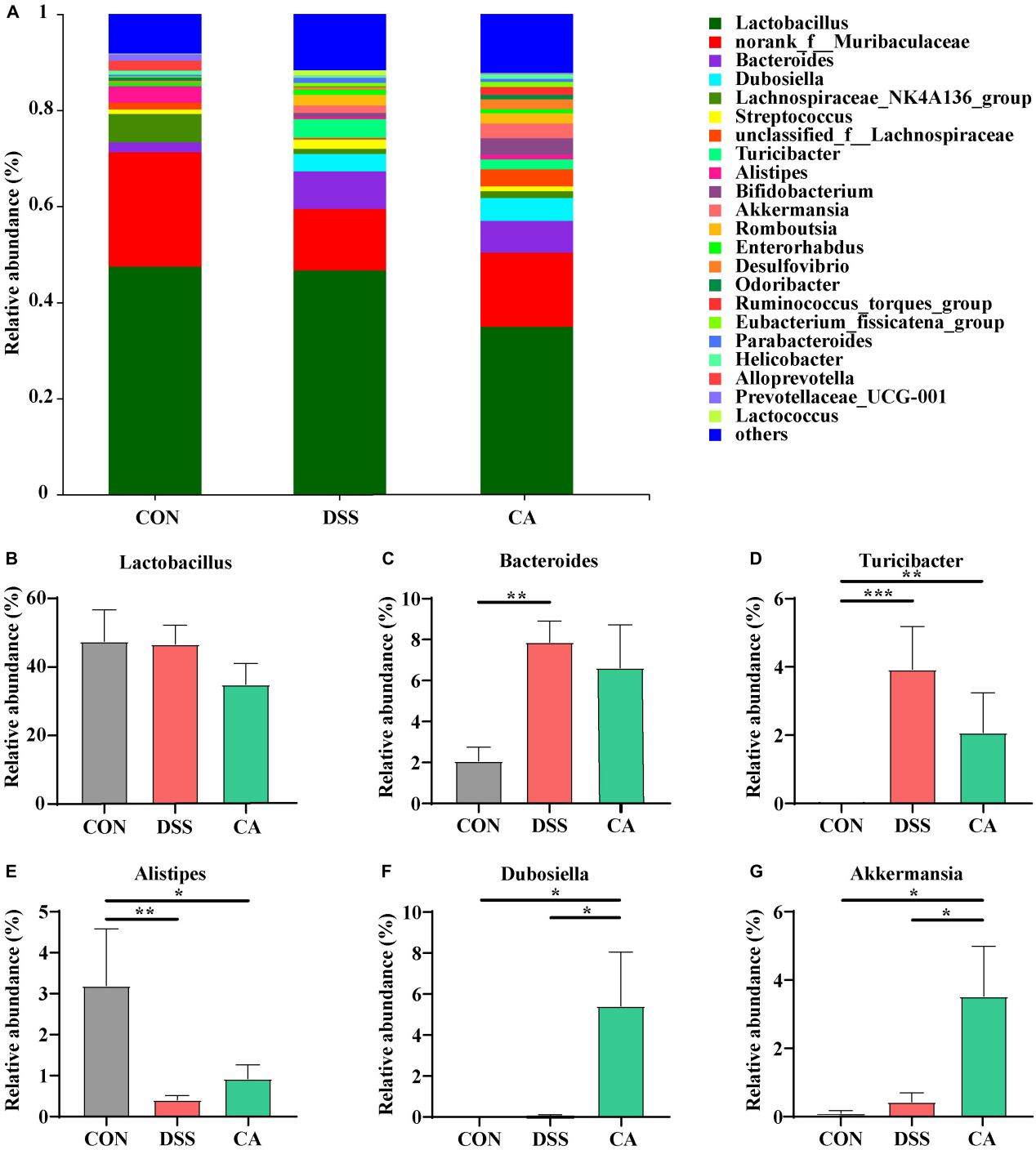

FIGURE 6 | Effects of CA administration on intestinal microbiota inflammatory in DSS-induced colitis mice. **(A)** Structural comparison of intestinal microbiota between the CON, DSS, and CA groups at genus levels. **(B)** Relative abundance of *Lactobacillus* **(C)** relative abundance of *Bacteroides*. **(D)** Relative abundance of *Turicibacter*. **(E)** Relative abundance of *Alistipes*. **(F)** Relative abundance of *Dubosiella*. **(G)** Relative abundance of *Akkermansia*. Data are presented as mean ± SEM. (n = 8 mice). Groups with different letters statistically differ. *$p < 0.05$, **$p < 0.01$, and ***$p < 0.001$.

A previous study showed that CGA supplementation could remedy 1-methyl-4-phenyl-1,2,3,6-tetrahydropyridine (MPTP) intoxicated mice by enhancing gene expression of *IL-10* and reducing oxidative stress (Singh et al., 2018). In addition, major bioactive phenolics of Berberis Lycium Royle fruit extract (BLFE) including CGA also could enhance IL-10 level in the attenuation of LPS-induced inflammatory responses (Sharma et al., 2020). It was proposed that CGA supplementation

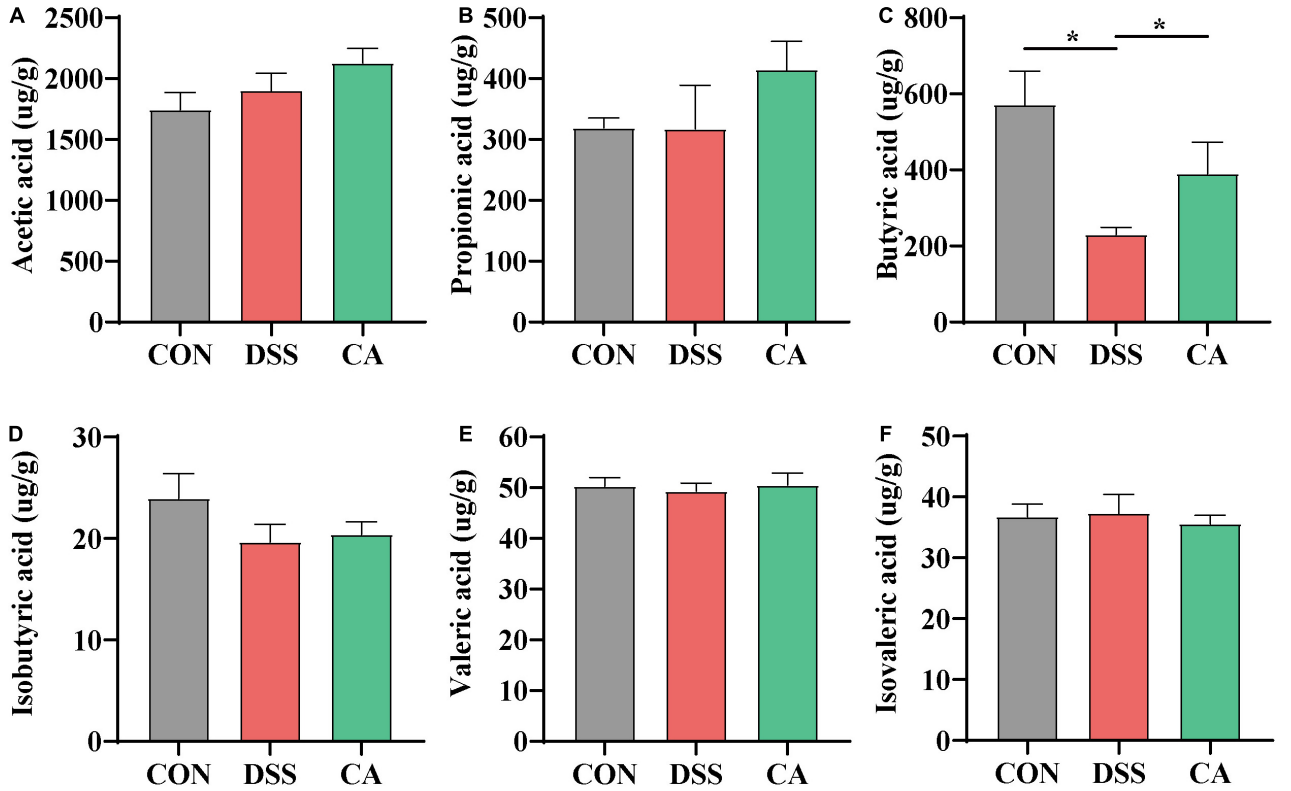

FIGURE 7 | Effect of CA administration on short-chain fatty acid (SCFA) production in DSS-induced colitis. **(A)** Acetic acid. **(B)** Propionic acid. **(C)** Butyric acid. **(D)** Isobutyric acid. **(E)** Valeric acid. **(F)** Isovaleric acid. The values are expressed as mean ± SEM. (n = 16 mice). *$p < 0.05$.

improved the anti-inflammatory ability and upregulated IL-10 level. We found CA could enhance anti-inflammatory cytokine IL-10 level to inhibit inflammatory response, which indicates that CA treatment not only inhibits inflammatory response but also enhances anti-inflammatory capacity in DSS-induced colitis mice. Hence, the metabolite CA may play anti-inflammatory response after CGA entering into the body.

Previous studies demonstrated that histological injury was related to the increase in the production of ROS and LPS in the serum obviously (Tian et al., 2017; Mahmoud et al., 2020). In addition, it was verified that UC causes the overproduction of ROS, which results in serious UC (Zhu and Li, 2012). However, polyphenols could decrease the production of ROS and LPS in serum (Liu Y. et al., 2020; Mahmoud et al., 2020). As an example, coffee phenolic metabolite mixes could ameliorate some adverse health effects of daily exposure to air pollution by depleting intracellular ROS (Tyszka-Czochara et al., 2018). The reason may be that the mixes consisted of CA (Tyszka-Czochara et al., 2018). Correspondingly, CA also could prevent the production of ROS in DNA oxidation of cancer cells (Espíndola et al., 2019). Orally administered polyphenols such as *Canna* × *generalis* rhizome ethanol extract (CGE) alleviated DSS-induced colitis mice by reducing the activity of LPS in serum (Mahmoud et al., 2020). In addition, CA plays a role in anti-inflammatory property in LPS-challenged macrophages (RAW 264.7) (Schröter et al., 2019). In our study, compared with DSS treatment, CA supplementation in the diet could decrease the production of ROS and LPS in serum. Consequently, CA treatment successfully inhibited the secretion of inflammatory cytokines, decreased oxidative stress, and cytotoxicity.

Nrf-2 signaling pathway has been considered as a classical antioxidative stress pathway. A large number of studies indicated that oxidative stress was also associated with IBD (Bourgonje et al., 2020; Hossen et al., 2020). Inhibiting the oxidative stress index expression is an effective way to activate Nrf-2 signaling pathway, which possibly explains the antioxidative mechanism by the polyphenols to mitigate colitis (Guvenc et al., 2019; Yang et al., 2020). Recent research manifested that Divya–Swasari–Kwath could inhibit asthma in mice by increasing the mRNA expression of antioxidant defense gene *Nrf-2* and upregulating downstream target genes *HO-1* and *NQO-1* (Balkrishna et al., 2020). The reason may be that Divya–Swasari–Kwath contains CGA, which may be a functional constituent for antioxidation (Balkrishna et al., 2020). In addition, CGA had been indicated to prevent diabetic nephropathy by regulating the Nrf2/HO-1 pathway to inhibit oxidative stress (Kanzaki et al., 2016). As a metabolite of CGA, CA could effectively ameliorate DSS-induced colitis mice by increasing mRNA expression levels of *HO-1*, *NQO1*, and *Nrf-2* potentially associated with Nrf-2 pathway in this study. This result indicated that the metabolite CA may be a major activate content after CGA entering into the body to activate Nrf-2 signaling pathway. In addition, decreased expression levels of

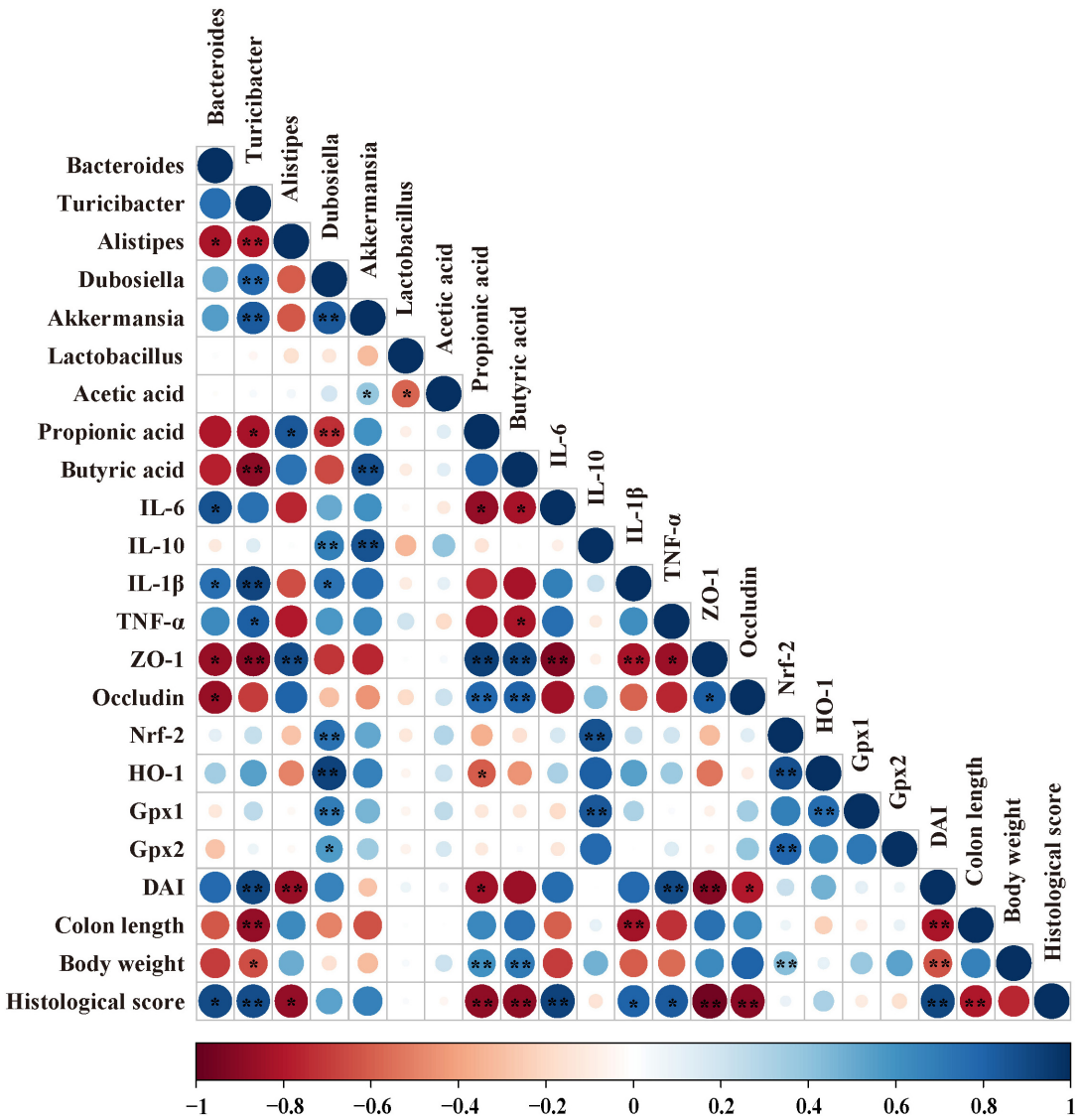

FIGURE 8 | Correlation analysis among biochemical indexes in DSS-induced colitis mice. The color of the circle represents positive or negative correlation, and the size of the circle represents the strength of the correlation. $^{*}p < 0.05$, $^{**}p < 0.01$ (large circle = stronger correlation).

colonic oxidative stress index, such as *CAT*, *GPX*, and *SOD*, are treated as notable features of IBD patients (Mrowicki et al., 2016). In this study, CA supplementation improved DSS-induced colitis mice by enhancing anti-oxidative ability. These results indicated that the protective effects of CA supplementation on colitis development could be partly explained potentially by activating the Nrf-2 pathway and enhancing antioxidant ability.

In the procedure of colitis development, the intestinal microbes play a vital role. A recent study has shown that the gut microbiota is highly dysregulated in patients with IBD and experimental animal models, and the most commonly affected genera include *Lactobacillus*, *Akkermansia*, *Alistipes*, *Turicibacter*, and *Bacteroides* (Caenepeel et al., 2020; Thomann et al., 2020; Li et al., 2021; Zhang et al., 2021). Especially, the development of UC is usually accompanied by the decrease in beneficial microbiota, such as *Alistipes*, and the increase in abundance of harmful microbiota such as *Turicibacter* and *Bacteroides* (Li et al., 2021; Zhang et al., 2021). In our present research, we also found that *Turicibacter* and *Bacteroides* were the dominant microbiota in DSS-induced colitis mice, while CA supplementation could reduce its abundance. These deleterious effects were also reversed by CA supplementation, indicating the potential of CA for restoring the intestinal microbial community. In addition, the abundance of *Alistipes* was enhanced with CA supplementation in DSS-induced colitis mice. Therefore, CA supplementation not only decreases the abundance of harmful microbiota but also enhances the abundance of beneficial microbiota. In the previous research, *Akkermansia* has already been proven to mostly exist to ameliorate colitis with CA supplementation (Zhang et al., 2016). In the present study, the

relative abundance of *Akkermansia* was significantly increased with CA supplementation, which is similar to the previous study. In addition, compared with the DSS-induced colitis mice, the control group had more *Dubosiella*, showing that *Dubosiella* may be a potentially beneficial bacteria to fight against UC mice in a previous report (Zhai et al., 2019). In the current study, we found that the proportions of *Dubosiella* were increased by CA supplementation. But the mechanism is not distinct. Therefore, more researches are needed be done to explore the mechanism of *Dubosiella*, which could affect the colitis or not. In total, we proved that the relative abundance of *Turicibacter* and *Bacteroide* was decreased, and the relative abundance of *Alistipes* was increased by CA supplementation in colitis mice. We also found that the relative abundance of some specific bacteria, such as *Akkermansia* and *Dubosiella*, was increased after CA supplementation in DSS-induced colitis mice, which provided us with a promising approach for the future development of probiotics in the gut.

SCFAs, as gut microbiota-derived metabolites, can promote the activation of T cells in the intestinal mucosal tissue to form immune regulatory cells (Park et al., 2015). The specific mechanism of butyric acid was to inhibit G protein-coupled receptor 43 to inhibit histone deacetylase in regulatory T cells, so that the anti-inflammatory effectiveness can be achieved (Sivaprakasam et al., 2016). A previous study showed that butyric acid was reduced in the feces of UC patients (Machiels et al., 2014). Conversely, oral butyrate could alleviate DSS-induced colitis in mice (Wang R. X. et al., 2020). In addition, another previous study has demonstrated that supplementation of CGA could increase the production of butyric acid subsequently to alleviate HFD-induced intestinal inflammation in rats (Xie et al., 2021). In parallel, dietary CGA supplementation increased butyric acid concentration in the colon, which means that CGA supplementation could improve the gut health of weaned pigs (Zhang et al., 2018). In the present study, we also found that CA supplementation can markedly enhance butyric acid level. This new information in our study contributed to understanding the potential effect of CGA, at least in part, due to metabolite CA as a protection to keep gut healthy by enhancing the butyric acid level.

Based on all the results, we found that CA supplementation could alter microbial composition, inhibit inflammatory response and oxidative stress, and enhance butyric acid level. To confirm whether the CA supplementation modified microbial composition was associated with alleviated inflammation response and oxidative stress, Spearman's correlation analysis was conducted between the microbial flora, SCFAs, and biochemical parameters. In a previous study, *Bacteroides* was positively correlated with pro-inflammatory cytokine IL-6 in DSS-induced colitis mice (Wan et al., 2019). However, a decreased proportion of *Bacteroides* may be associated with lower pro-inflammatory cytokines, which is identical with our results. In addition, CA supplementation could alleviate DSS-induced colitis mice by improving the abundance of *Akkermansia* in a previous study (Zhang et al., 2016). Meanwhile, a previous reported oral 0.2 ml/day of *A. muciniphila* (3×10^9 CFU) could alleviate DSS-induced colitis mice by enhancing the mRNA expression of *IL-10* (Bian et al., 2019). In the present study, we further found *Akkermansia* was highly correlated with the mRNA expression of *IL-10* in the colon tissue, suggesting that *Akkermansia* may play a role in enhancing anti-inflammatory capacity. In addition, a previous study found that *Dubosiella* may be potentially beneficial bacteria (Zhai et al., 2019). We further found that *Dubosiella* was highly correlated with the mRNA expression of *Nrf-2*, *HO-1*, *Gpx1*, *Gpx2*, and *IL-10* in the colon tissue, suggesting that *Dubosiella* may play a role in enhancing antioxidative and anti-inflammatory capacity. This new information in our study contributed to understanding the increased anti-inflammatory and antioxidative ability, which was effected by supplementing CA; a part of the reason may be due to the gut microbiota that had been altered. Moreover, oral butyrate could alleviate DSS-induced colitis by improving the gut barrier in previous study (Wang R. X. et al., 2020). We further found that *Akkermansia* had a direct correlation with butyric acid. As whether there exists an interactive action between *Akkermansia* and butyric acid, more efforts are needed to explore their relationship.

CONCLUSION

In conclusion, our data provides evidence that CA supplementation in diet can increase the anti-inflammatory and antioxidative capacity by modulating the gut microbiota community and enhancing gut barrier in DSS-induced colitis mice, which is also confirmed in our correlation analysis. CA, one of the gut microbiota metabolite of CGA, may be potentially used as a safe and effective dietary strategy in preventing ulcerative colitis.

DATA AVAILABILITY STATEMENT

The datasets presented in this study can be found in online repositories. The names of the repository/repositories and accession number(s) can be found in the article/**Supplementary Material**.

ETHICS STATEMENT

The animal study was reviewed and approved by the Animal Care and Use Committee of the Chinese Academy of Agriculture Sciences.

AUTHOR CONTRIBUTIONS

FW, RZ, FH, BY, YZ, LC, and HZ conceived and designed the experiments. FW and MW performed the experiments. FW analyzed the data and wrote the manuscript. FW, YxZ, YC, and

LL contributed to the reagents, materials, and analysis tools. All authors read and approved the final manuscript.

FUNDING

This work was supported by the Central Public-Interest Scientific Institution Basal Research Fund (Y2021GH01-4), the Major Scientific Research Tasks for Scientific and Technological Innovation Projects of the Chinese Academy of Agricultural Sciences (CAAS-ZDRW202006-02), and the State Key Laboratory of Animal Nutrition (2004DA125184G2102).

SUPPLEMENTARY MATERIAL

The Supplementary Material for this article can be found online at: https://www.frontiersin.org/articles/10.3389/fmicb.2021.784211/full#supplementary-material

REFERENCES

Akanda, M. R., Nam, H. H., Tian, W., Islam, A., Choo, B. K., and Park, B. Y. (2018). Regulation of JAK2/STAT3 and NF-kappaB signal transduction pathways; veronica polita alleviates dextran sulfate sodium-induced murine colitis. *Bio. Pharm.* 100, 296–303. doi: 10.1016/j.biopha.2018.01.168

Almousa, A. A., Meurens, F., Krol, E. S., and Alcorn, J. (2018). Linoorbitides and enterolactone mitigate inflammation-induced oxidative stress and loss of intestinal epithelial barrier integrity. *Int. Immunopharmacol.* 64, 42–51. doi: 10.1016/j.intimp.2018.08.012

Bai, X., Gou, X., Cai, P., Xu, C., Cao, L., Zhao, Z., et al. (2019). Sesamin enhances Nrf2-mediated protective defense against oxidative stress and inflammation in colitis via AKT and ERK activation. *Oxid Med. Cell. Longev.* 2019, 1–20. doi: 10.1155/2019/2432416

Balkrishna, A., Solleti, S. K., Singh, H., Verma, S., Sharma, N., Nain, P., et al. (2020). Herbal decoction divya-swasari-kwath attenuates airway inflammation and remodeling through Nrf-2 mediated antioxidant lung defence in mouse model of allergic asthma. *Phytomedicine* 78:153295. doi: 10.1016/j.phymed.2020.153295

Bian, X., Wu, W., Yang, L., Lv, L., Wang, Q., Li, Y., et al. (2019). Administration of akkermansia muciniphila ameliorates dextran sulfate sodium-induced ulcerative colitis in mice. *Front. Microbiol.* 10:2259. doi: 10.3389/fmicb.2019.02259

Bourgonje, A. R., Feelisch, M., Faber, K. N., Pasch, A., Dijkstra, G., and van Goor, H. (2020). Oxidative stress and redox-modulating therapeutics in inflammatory bowel disease. *Trends Mol. Med.* 26, 1034–1046. doi: 10.1016/j.molmed.2020.06.006

Caenepeel, C., Tabib, N. S. S., Vieira-Silva, S., and Vermeire, S. (2020). Review article: how the intestinal microbiota may reflect disease activity and influence therapeutic outcome in inflammatory bowel disease. *Aliment. Pharmacol. Ther.* 52, 1453–1468. doi: 10.1111/apt.16096

Chow, D. K., Leong, R. W., Tsoi, K. K., Ng, S. S., Leung, W. K., Wu, J. C., et al. (2009). Long-term follow-up of ulcerative colitis in the Chinese population. *Am. J. Gastroenterol.* 104, 647–654. doi: 10.1038/ajg.2008.74

Clifford, M. N., Jaganath, I. B., Ludwig, I. A., and Crozier, A. (2017). Chlorogenic acids and the acyl-quinic acids: discovery, biosynthesis, bioavailability and bioactivity. *Nat. Prod. Rep.* 34, 1391–1421. doi: 10.1039/c7np00030h

Danese, S., Fiocchi, C., and Panés, J. (2016). Drug development in IBD from novel target identification to early clinical trials. *Gut* 65, 1233–1239. doi: 10.1136/gutjnl-2016-311717

Dong, Y., Lei, J., and Zhang, B. (2020). Dietary quercetin alleviated DSS-induced colitis in mice through several possible pathways by transcriptome analysis. *Curr. Pharm. Biotechnol.* 21, 1666–1673. doi: 10.2174/1389201021666200711152726

Dudzinska, E., Gryzinska, M., Ognik, K., Gil-Kulik, P., and Kocki, J. (2018). Oxidative stress and effect of treatment on the oxidation product decomposition processes in IBD. *Oxid Med. Cell. Longev.* 2018:7918261. doi: 10.1155/2018/7918261

Espíndola, K. M. M., Ferreira, R. G., Narvaez, L. E. M., Silva Rosario, A. C. R., da Silva, A. H. M., Silva, A. G. B., et al. (2019). Chemical and pharmacological aspects of caffeic acid and its activity in hepatocarcinoma. *Front. Oncol.* 9:541. doi: 10.3389/fonc.2019.00541

Galatola, M., Miele, E., Strisciuglio, C., Paparo, L., Rega, D., Delrio, P., et al. (2013). Synergistic effect of interleukin-10-receptor variants in a case of early-onset ulcerative colitis. *World J. Gastroenterol.* 19, 8659–8670. doi: 10.3748/wjg.v19.i46.8659

Gophna, U., Sommerfeld, K., Gophna, S., Doolittle, W. F., and Veldhuyzen van Zanten, S. J. (2006). Differences between tissue-associated intestinal microfloras of patients with Crohn's disease and ulcerative colitis. *J. Clin. Microbiol.* 44, 4136–4141. doi: 10.1128/JCM.01004-06

Grosheva, I., Zheng, D., Levy, M., Polansky, O., Lichtenstein, A., Golani, O., et al. (2020). High-throughput screen identifies host and microbiota regulators of intestinal barrier function. *Gastroenterology* 159, 1807–1823. doi: 10.1053/j.gastro.2020.07.003

Guvenc, M., Cellat, M., Ozkan, H., Tekeli, I. O., Uyar, A., Gokcek, I., et al. (2019). Protective effects of tyrosol against DSS-induced ulcerative colitis in rats. *Inflammation* 42, 1680–1691. doi: 10.1007/s10753-019-01028-8

Hossen, I., Hua, W., Ting, L., Mehmood, A., Jingyi, S., Duoxia, X., et al. (2020). Phytochemicals and inflammatory bowel disease: a review. *Crit. Rev. Food Sci. Nutr.* 60, 1321–1345. doi: 10.1080/10408398.2019.1570913

Hu, C. A., Hou, Y., Yi, D., Qiu, Y., Wu, G., Kong, X., et al. (2015). Autophagy and tight junction proteins in the intestine and intestinal diseases. *Anim Nutr.* 1, 123–127. doi: 10.1016/j.aninu.2015.08.014

Kanzaki, H., Shinohara, F., Kanako, I., Yamaguchi, Y., Fukaya, S., Miyamoto, Y., et al. (2016). Molecular regulatory mechanisms of osteoclastogenesis through cytoprotective enzymes. *Redox Biol.* 8, 186–191. doi: 10.1016/j.redox.2016.01.006

Kaplan, G. G. (2015). The global burden of IBD: from 2015 to 2025. *Nat. Rev. Gastroenterol. Hepatol.* 12, 720–727. doi: 10.1038/nrgastro.2015.150

Lee, B., and Lee, D. G. (2018). Depletion of reactive oxygen species induced by chlorogenic acid triggers apoptosis-like death in *Escherichia coli*. *Free Radic Res.* 52, 605–615. doi: 10.1080/10715762.2018.1456658

Li, Q., Cui, Y., Xu, B., Wang, Y., Lv, F., Li, Z., et al. (2021). Main active components of jiawei gegen qinlian decoction protects against ulcerative colitis under different dietary environments in a gut microbiota-dependent manner. *Pharmacol. Res.* 170:105694. doi: 10.1016/j.phrs.2021.105694

Li, Y., Ren, X., Lio, C., Sun, W., Lai, K., Liu, Y., et al. (2018). A chlorogenic acid-phospholipid complex ameliorates post-myocardial infarction inflammatory response mediated by mitochondrial reactive oxygen species in SAMP8 mice. *Pharmacol. Res.* 130, 110–122. doi: 10.1016/j.phrs.2018.01.006

Liu, A., Lv, H., Wang, H., Yang, H., Li, Y., and Qian, J. (2020). Aging increases the severity of colitis and the related changes to the gut barrier and gut microbiota in humans and mice. *J. Gerontol. A Biol. Sci. Med. Sci.* 75, 1284–1292. doi: 10.1093/gerona/glz263

Liu, Y., Wang, X., Chen, Q., Luo, L., Ma, M., Xiao, B., et al. (2020). Camellia sinensis and litsea coreana ameliorate intestinal inflammation and modulate gut microbiota in dextran sulfate sodium-induced colitis mice. *Mol Nutr Food Res.* 64, e1900943. doi: 10.1002/mnfr.201900943

Llewellyn, S. R., Britton, G. J., Contijoch, E. J., Vennaro, O. H., Mortha, A., Colombel, J.-F., et al. (2018). Interactions between diet and the intestinal microbiota alter intestinal permeability and colitis severity in mice. *Gastroenterology* 154, 1037–1046.e1032. doi: 10.1053/j.gastro.2017.11.030

Ma, J., Yin, G., Lu, Z., Xie, P., Zhou, H., Liu, J., et al. (2018). Casticin prevents DSS induced ulcerative colitis in mice through inhibitions of NF-kappaB pathway and ROS signaling. *Phytother Res.* 32, 1770–1783. doi: 10.1002/ptr.6108

Machiels, K., Joossens, M., Sabino, J., De Preter, V., Arijs, I., Eeckhaut, V., et al. (2014). A decrease of the butyrate-producing species roseburia hominis and

Faecalibacterium prausnitzii defines dysbiosis in patients with ulcerative colitis. *Gut* 63, 1275–1283. doi: 10.1136/gutjnl-2013-304833

Mahmoud, T. N., El-Maadawy, W. H., Kandil, Z. A., Khalil, H., El-Fiky, N. M., and El Alfy, T. (2020). Canna x generalis L.H. bailey rhizome extract ameliorates dextran sulphate sodium-induced colitis via modulating intestinal mucosal dysfunction, oxidative stress, inflammation, and TLR4/ NF-B and NLRP3 inflammasome pathways. *J. Ethnopharmacol.* 269:113670. doi: 10.1016/j.jep.2020.113670

Maloy, K. J., and Powrie, F. (2011). Intestinal homeostasis and its breakdown in inflammatory bowel disease. *Nature* 474, 298–306. doi: 10.1038/nature10208

Marafini, I., Sedda, S., Dinallo, V., and Monteleone, G. (2019). Inflammatory cytokines: from discoveries to therapies in IBD. *Expert Opin. Biol. Ther.* 19, 1207–1217. doi: 10.1080/14712598.2019.1652267

Martens, E. C., Neumann, M., and Desai, M. S. (2018). Interactions of commensal and pathogenic microorganisms with the intestinal mucosal barrier. *Nat. Rev. Microbiol.* 16, 457–470. doi: 10.1038/s41579-018-0036-x

Mrowicki, J., Mrowicka, M., Majsterek, I., Mik, M., Dziki, A., and Dziki, L. (2016). Evaluation of effect CAT –262C/T, SOD + 35A/C, GPx1 Pro197 leu polymorphisms in patients with IBD in the polish population. *Pol. Przegl. Chir.* 88, 321–327. doi: 10.1515/pjs-2016-0071

Parada Venegas, D., De la Fuente, M. K., Landskron, G., Gonzalez, M. J., Quera, R., Dijkstra, G., et al. (2019). Short chain fatty acids (SCFAs)-mediated gut epithelial and immune regulation and its relevance for inflammatory bowel diseases. *Front. Immunol.* 10:277. doi: 10.3389/fimmu.2019.00277

Park, J., Kim, M., Kang, S. G., Jannasch, A. H., Cooper, B., Patterson, J., et al. (2015). Short-chain fatty acids induce both effector and regulatory T cells by suppression of histone deacetylases and regulation of the mTOR-S6K pathway. *Mucosal. Immunol.* 8, 80–93. doi: 10.1038/mi.2014.44

Piechota-Polanczyk, A., and Fichna, J. (2014). Review article: the role of oxidative stress in pathogenesis and treatment of inflammatory bowel diseases. *Naunyn Schmiedebergs Arch. Pharmacol.* 387, 605–620. doi: 10.1007/s00210-014-0985-1

Pu, Y., Song, Y., Zhang, M., Long, C., Li, J., Wang, Y., et al. (2021). GOLM1 restricts colitis and colon tumorigenesis by ensuring notch signaling equilibrium in intestinal homeostasis. *Signal Trans. Target Ther.* 6:148. doi: 10.1038/s41392-021-00535-1

Roessner, A., Kuester, D., Malfertheiner, P., and Schneider-Stock, R. (2008). Oxidative stress in ulcerative colitis-associated carcinogenesis. *Pathol. Res. Pract.* 204, 511–524. doi: 10.1016/j.prp.2008.04.011

Ruan, Z., Mi, S., Zhou, L., Zhou, Y., Li, J., Liu, W., et al. (2016). Chlorogenic acid enhances intestinal barrier by decreasing MLCK expression and promoting dynamic distribution of tight junction proteins in colitic rats. *J. Funct. Foods* 26, 698–708. doi: 10.1016/j.jff.2016.08.038

Rui, L., Xie, M., Hu, B., Zhou, L., Saeeduddin, M., and Zeng, X. (2017). Enhanced solubility and antioxidant activity of chlorogenic acid-chitosan conjugates due to the conjugation of chitosan with chlorogenic acid. *Carbohydr Polym.* 170, 206–216. doi: 10.1016/j.carbpol.2017.04.076

Sandoval-Ramirez, B. A., Catalan, U., Pedret, A., Valls, R. M., Motilva, M. J., Rubio, L., et al. (2021). Exploring the effects of phenolic compounds to reduce intestinal damage and improve the intestinal barrier integrity: a systematic review of *in vivo* animal studies. *Clin. Nut.* 40, 1719–1732. doi: 10.1016/j.clnu.2020.09.027

Schröter, D., Neugart, S., Schreiner, M., Grune, T., Rohn, S., and Ott, C. (2019). Amaranth's 2-caffeoylisocitric acid-an anti-inflammatory caffeic acid derivative that impairs NF-κB signaling in LPS-challenged RAW 264.7 macrophages. *Nutrients* 11:571. doi: 10.3390/nu11030571

Sharma, A., Sharma, R., Kumar, D., and Padwad, Y. (2020). Berberis lycium royle fruit extract mitigates oxi-inflammatory stress by suppressing NF-kappaB/MAPK signalling cascade in activated macrophages and treg proliferation in splenic lymphocytes. *Inflammopharmacology* 28, 1053–1072. doi: 10.1007/s10787-018-0548-z

Shi, A., Li, T., Zheng, Y., Song, Y., Wang, H., Wang, N., et al. (2021). Chlorogenic acid improves NAFLD by regulating gut microbiota and GLP-1. *Front. Pharmacol.* 12:693048. doi: 10.3389/fphar.2021.693048

Shin, H. S., Satsu, H., Bae, M. J., Zhao, Z., Ogiwara, H., Totsuka, M., et al. (2015). Anti-inflammatory effect of chlorogenic acid on the IL-8 production in caco-2 cells and the dextran sulphate sodium-induced colitis symptoms in C57BL/6 mice. *Food Chem.* 168, 167–175. doi: 10.1016/j.foodchem.2014.06.100

Singh, S. S., Rai, S. N., Birla, H., Zahra, W., Kumar, G., Gedda, M. R., et al. (2018). Effect of chlorogenic acid supplementation in MPTP-intoxicated mouse. *Front. Pharmacol.* 9:757. doi: 10.3389/fphar.2018.00757

Sivaprakasam, S., Prasad, P. D., and Singh, N. (2016). Benefits of short-chain fatty acids and their receptors in inflammation and carcinogenesis. *Pharmacol. Ther.* 164, 144–151. doi: 10.1016/j.pharmthera.2016.04.007

Thomann, A. K., Mak, J. W. Y., Zhang, J. W., Wuestenberg, T., Ebert, M. P., Sung, J. J. Y., et al. (2020). Review article: bugs, inflammation and mood-a microbiota-based approach to psychiatric symptoms in inflammatory bowel diseases. *Aliment Pharmacol. Ther.* 52, 247–266. doi: 10.1111/apt.15787

Tian, T., Wang, Z., and Zhang, J. (2017). Pathomechanisms of oxidative stress in inflammatory bowel disease and potential antioxidant therapies. *Oxid Med. Cell. Longev.* 2017:4535194. doi: 10.1155/2017/4535194

Turner, J. R. (2009). Intestinal mucosal barrier function in health and disease. *Nat. Rev. Immunol.* 9, 799–809. doi: 10.1038/nri2653

Tyszka-Czochara, M., Lasota, M., and Majka, M. (2018). Caffeic acid and metformin inhibit invasive phenotype induced by TGF-beta1 in C-4I and HTB-35/SiHa human cervical squamous carcinoma cells by acting on different molecular targets. *Int. J. Mol. Sci.* 19:266. doi: 10.3390/ijms19010266

Wan, P., Peng, Y., Chen, G., Xie, M., Dai, Z., Huang, K., et al. (2019). Modulation of gut microbiota by Ilex kudingcha improves dextran sulfate sodium-induced colitis. *Food Res. Int.* 126:108595. doi: 10.1016/j.foodres.2019.108595

Wang, K., Yang, Q., Ma, Q., Wang, B., Wan, Z., Chen, M., et al. (2018). Protective effects of salvianolic acid a against dextran sodium sulfate-induced acute colitis in rats. *Nutrients* 10:791. doi: 10.3390/nu10060791

Wang, L., Tang, L., Feng, Y., Zhao, S., Han, M., Zhang, C., et al. (2020). A purified membrane protein from akkermansia muciniphila or the pasteurised bacterium blunts colitis associated tumourigenesis by modulation of CD8(+) T cells in mice. *Gut* 69, 1988–1997. doi: 10.1136/gutjnl-2019-320105

Wang, R. X., Lee, J. S., Campbell, E. L., and Colgan, S. P. (2020). Microbiota-derived butyrate dynamically regulates intestinal homeostasis through regulation of actin-associated protein synaptopodin. *Proc. Natl. Acad. Sci. U.S.A.* 117, 11648–11657. doi: 10.1073/pnas.1917597117

Xiao, H. T., Peng, J., Wen, B., Hu, D. D., Hu, X. P., Shen, X. C., et al. (2019). Indigo naturalis suppresses colonic oxidative stress and Th1/Th17 responses of DSS-induced colitis in mice. *Oxid Med. Cell. Longev.* 2019:9480945. doi: 10.1155/2019/9480945

Xie, M. G., Fei, Y. Q., Wang, Y., Wang, W. Y., and Wang, Z. (2021). Chlorogenic acid alleviates colon mucosal damage induced by a high-fat diet via gut microflora adjustment to increase short-chain fatty acid accumulation in rats. *Oxid Med. Cell. Longev.* 2021:3456542. doi: 10.1155/2021/3456542

Yang, H., Yue, Y., Li, Y., Su, L., and Yan, S. (2020). Geniposide attenuates dextran sulfate sodium-induced colitis in mice via Nrf-2/HO-1/NF-kappaB pathway. *Ann. Palliat. Med.* 9, 2826–2836. doi: 10.21037/apm-20-279

Yang, Y., Chen, G., Yang, Q., Ye, J., Cai, X., Tsering, P., et al. (2017). Gut microbiota drives the attenuation of dextran sulphate sodium-induced colitis by *Huangqin decoction*. *Oncotarget* 8, 48863–48874. doi: 10.18632/oncotarget.16458

Ye, Z., Liu, Z., Henderson, A., Lee, K., Hostetter, J., Wannemuehler, M., et al. (2009). Increased CYP4B1 mRNA is associated with the inhibition of dextran sulfate sodium–induced colitis by caffeic acid in mice. *Exp. Biol. Med.* 234, 605–616. doi: 10.3181/0901-rm-1

Zhai, Z., Zhang, F., Cao, R., Ni, X., Xin, Z., Deng, J., et al. (2019). Cecropin a alleviates inflammation through modulating the gut microbiota of C57BL/6 mice with DSS-induced IBD. *Front. Microbiol.* 10:1595. doi: 10.3389/fmicb.2019.01595

Zhang, P., Jiao, H., Wang, C., Lin, Y., and You, S. (2019). Chlorogenic acid ameliorates colitis and alters colonic microbiota in a mouse model of dextran sulfate sodium-induced colitis. *Front. Physiol.* 10:325. doi: 10.3389/fphys.2019.00325

Zhang, Y., Brenner, M., Yang, W. L., and Wang, P. (2015). Recombinant human MFG-E8 ameliorates colon damage in DSS- and TNBS-induced colitis in mice. *Lab. Invest.* 95, 480–490. doi: 10.1038/labinvest.2015.32

Zhang, Y., Jiang, D., Jin, Y., Jia, H., Yang, Y., Kim, I. H., et al. (2021). Glycine attenuates citrobacter rodentium-induced colitis by regulating ATF6-mediated endoplasmic reticulum stress in mice. *Mol. Nut. Food Res.* 65:e2001065. doi: 10.1002/mnfr.202001065

Zhang, Y., Wang, Y., Chen, D., Yu, B., Zheng, P., Mao, X., et al. (2018). Dietary chlorogenic acid supplementation affects gut morphology, antioxidant capacity

and intestinal selected bacterial populations in weaned piglets. *Food Funct.* 9, 4968–4978. doi: 10.1039/c8fo01126e

Zhang, Y., Yan, T., Sun, D., Xie, C., Wang, T., Liu, X., et al. (2020). Rutaecarpine inhibits KEAP1-NRF2 interaction to activate NRF2 and ameliorate dextran sulfate sodium-induced colitis. *Free Radic Biol. Med.* 148, 33–41. doi: 10.1016/j.freeradbiomed.2019.12.012

Zhang, Z., Wu, X., Cao, S., Wang, L., Wang, D., Yang, H., et al. (2016). Caffeic acid ameliorates colitis in association with increased akkermansia population in the gut microbiota of mice. *Oncotarget* 7, 31790–31799. doi: 10.18632/oncotarget.9306

Zhao, B., Xia, B., Li, X., Zhang, L., Liu, X., Shi, R., et al. (2020). Sesamol supplementation attenuates DSS-induced colitis via mediating gut barrier integrity, inflammatory responses, and reshaping gut microbiome. *J. Agric. Food Chem.* 68, 10697–10708. doi: 10.1021/acs.jafc.0c04370

Zhao, H., Cheng, N., Zhou, W., Chen, S., Wang, Q., Gao, H., et al. (2019). Honey polyphenols ameliorate DSS-induced ulcerative colitis via modulating gut microbiota in rats. *Mol. Nut. Food Res.* 63:e1900638. doi: 10.1002/mnfr.201900638

Zhu, H., and Li, Y. R. (2012). Oxidative stress and redox signaling mechanisms of inflammatory bowel disease: updated experimental and clinical evidence. *Exp. Biol. Med.* 237, 474–480. doi: 10.1258/ebm.2011.011358

Conflict of Interest: The authors declare that the research was conducted in the absence of any commercial or financial relationships that could be construed as a potential conflict of interest.

Publisher's Note: All claims expressed in this article are solely those of the authors and do not necessarily represent those of their affiliated organizations, or those of the publisher, the editors and the reviewers. Any product that may be evaluated in this article, or claim that may be made by its manufacturer, is not guaranteed or endorsed by the publisher.

frontiers in Microbiology

ORIGINAL RESEARCH
published: 22 November 2021
doi: 10.3389/fmicb.2021.753195

Effects of Phytic Acid-Degrading Bacteria on Mineral Element Content in Mice

Diao Zhou[1†], Ying Zhao[1†], Jing Li[2], Vinothkannan Ravichandran[3], Leli Wang[1], Qiuyun Huang[1], Cang Chen[1], Hengjia Ni[2] and Jia Yin[1*]*

[1] Key Laboratory of Protein Chemistry and Developmental Biology of Fish of Ministry of Education, Hunan Provincial Key Laboratory of Animal Intestinal Function and Regulation, Hunan International Joint Laboratory of Animal Intestinal Ecology and Health, Hunan Normal University, Changsha, China, [2] Key Laboratory of Agro-Ecological Processes in Subtropical Region, Hunan Provincial Key Laboratory of Animal Nutritional Physiology and Metabolic Process, Hunan Research Center of Livestock and Poultry Sciences, South Central Experimental Station of Animal Nutrition and Feed Science in the Ministry of Agriculture, Institute of Subtropical Agriculture, Chinese Academy of Sciences, Changsha, China, [3] State Key Laboratory of Microbial Technology, Shandong University-Helmholtz Institute of Biotechnology, Shandong University, Qingdao, China

OPEN ACCESS

Edited by:
Norhaizan Mohd Esa,
University of Putra Malaysia, Malaysia

Reviewed by:
Mohammad Affan Baig,
United Arab Emirates University, United Arab Emirates
Pradip Behare,
National Dairy Research Institute (ICAR), India

***Correspondence:**
Hengjia Ni
nihengjia@isa.ac.cn
Jia Yin
jiayin@hunnu.edu.cn

[†] These authors have contributed equally to this work

Specialty section:
This article was submitted to Microbial Symbioses, a section of the journal Frontiers in Microbiology

Received: 04 August 2021
Accepted: 18 October 2021
Published: 22 November 2021

Citation:
Zhou D, Zhao Y, Li J, Ravichandran V, Wang L, Huang Q, Chen C, Ni H and Yin J (2021) Effects of Phytic Acid-Degrading Bacteria on Mineral Element Content in Mice. Front. Microbiol. 12:753195. doi: 10.3389/fmicb.2021.753195

Trace minerals are extremely important for balanced nutrition, growth, and development in animals and humans. Phytic acid chelation promotes the use of probiotics in nutrition. The phytic acid-degrading strain *Lactococcus lactis* psm16 was obtained from swine milk by enrichment culture and direct plate methods. In this study, we evaluated the effect of the strain psm16 on mineral element content in a mouse model. Mice were divided into four groups: basal diet, 1% phytic acid, 1% phytic acid + psm16, 1% phytic acid + 500 U/kg commercial phytase. Concentrations of acetic acid, propionic acid, butyric acid, and total short-chain fatty acids were significantly increased in the strain psm16 group compared to the phytic acid group. The concentrations of copper ($p = 0.021$) and zinc ($p = 0.017$) in liver, calcium ($p = 0.000$), manganese ($p = 0.000$), and zinc ($p = 0.000$) in plasma and manganese ($p = 0.010$) and zinc ($p = 0.022$) in kidney were significantly increased in psm16 group, while copper ($p = 0.007$) and magnesium ($p = 0.001$) were significantly reduced. In conclusion, the addition of phytic acid-degrading bacteria psm16 into a diet including phytic acid can affect the content of trace elements in the liver, kidney, and plasma of mice, counteracting the harmful effects of phytic acid.

Keywords: ***Lactococcus lactis*** **psm16 strain, phytic acid, phytase, short-chain fatty acid, trace minerals**

INTRODUCTION

Trace elements play an important role in the growth, development, and metabolism of animals and humans. Significant fluctuations in their levels can lead to metabolic disorders and immune dysfunction (Cannas et al., 2020). Phytic acid is present in many plant organs, accounting for 1–5% of most seeds, roots, and stems of grains and vegetables (Wang et al., 2013). Numerous animals feed on fiber-rich grains while the daily intake of humans is influenced by culture and society (Wang and Guo, 2021). Grains and vegetables are an important source of all nutrients, including minerals (Olza et al., 2017). Phytic acid is a sugar phosphate with six strong negative charges and has commonly been reported as an anti-nutritional factor in humans and animals due to its strong

chelating ability (Kumar et al., 2021). Phytic acid inhibits the absorption of calcium, magnesium, zinc, iron, and other trace elements in humans and animals (Shi et al., 2018). Furthermore, phytic acid can also combine with cationic groups on food proteins, digestive enzymes, and lipids to form insoluble complexes in the gastrointestinal tract (Kumar et al., 2010). Endogenously secreted minerals cannot be absorbed and reabsorbed due to the lack of intestinal phytase, causing potential digestion problems in monogastric animals and humans (Hui et al., 2016).

Many animals feed on fiber-rich grains, while the daily human diet is influenced by culture and society (Wang and Guo, 2021). In recent years, phytate hydrolysis has attracted great attention as a mechanism to further improve the bioavailability of minerals and proteins. Phytases are enzymes capable of hydrolyzing phytic acid into phosphate and inositol with penta- to mono-phosphate intermediates and are widely distributed in nature in plants, animal tissues, and microorganisms (Rosa-Sibakov et al., 2018). Phytases in plant and animal tissues have minimal activity and weak stability, but microorganisms with phytase activity are highly effective in the promotion of mineral absorption in animals (Haros et al., 2001). Previous studies have indicated that the microorganisms *Aspergillus ficuum* (Zhang et al., 2010), *Aspergillus niger* (Corrêa and de Araújo, 2020), yeast (Greppi et al., 2015), and *Escherichia coli* are primary producers of phytase (Mezeli et al., 2017).

The beneficial properties of microorganisms depend mainly on the source of the bacterial strain (Lyons et al., 2020; Ren et al., 2021). Most microorganisms that produce phytase are isolated from the soil, rarely from breast milk. The latter provides nutrition and contains biologically active ingredients that guide the development of a newborn's intestinal immune system (Cheng et al., 2021). Moreover, the maternal intake of phytic acid-rich foods may affect the bioavailability of mineral elements in breast milk. An iron, zinc, or calcium deficiency could lead to a profound adverse impact on the growth, health, and cognitive development of an infant (Gibson et al., 2010). Breast milk is the best nutrition for infant growth and development, and the microbiota of breast milk is a factor that significantly influences infant health (Quigley et al., 2013). Probiotics are an important concept for healthcare in the 21st century, and lactic acid bacteria (LAB) are the main source of probiotics (Zielińska and Kołożyn-Krajewska, 2018). LAB are considered to be safe strains and can be used directly. They can regulate the intestinal microbiota, improve the intestinal barrier (Yang et al., 2015), enhance immunity, slow the progression of cancer (Riaz Rajoka et al., 2017), prevent diarrhea (Sirichokchatchawan et al., 2018), and produce bioactive compounds with desirable biological effects (Yerlikaya, 2019).

This study aimed to investigate the effect of phytic acid-degrading bacteria isolated from sow milk on the mineral elements content in mice. Based on a control group with and without 1% phytic acid, the minerals in the liver, kidney, and plasma of mice were determined using an inductively coupled plasma emission spectrometer. The results showed that higher levels of trace element were found in the organs of mice fed with *Lactobacillus lactis* psm16 or commercial phytase in the presence of anti-nutritional factor phytic acid.

MATERIALS AND METHODS

Isolation and Genotypic Identification of Lactic Acid Bacteria Strains

All sow milk samples were serially diluted in sterile phosphate-buffered saline (PBS) and inoculated anaerobically in De Man, Rogosa, and Sharpe (MRS) agar (Hopebio, Qingdao, China) at 37°C for 48–72 h (Xu and Kim, 2014). White colonies were picked and cultured in MRS broth at 37°C for 24 h (Ji et al., 2015). The crystal violet-stained colonies were observed under a microscope using the ×100 oil immersion objective lens. Gram-positive bacteria retained the color of crystalline violet staining, while Gram-negative bacteria lost the initial staining color of neutral red. Subsequently, strains were frozen at −80°C and stored in MRS broth with 50% glycerol until use.

The isolated strains were cultured in MRS broth at 37°C for 18 h under anaerobic conditions and identified *via* the analysis of their 16S rRNA gene sequences. Bacterial DNA was extracted using QIAamp DNA Stool Kit (Qiagen, Gaithersburg, MD, United States) according to the manufacturer's protocols. The partial 16S rRNA genes was amplified by polymerase chain reaction (PCR) using universal primers 27F (5′-AGAGTTTGATCMTGGCTCAG-3′) and 1492R (5′-GGTTACCTTGTTACGACTT-3′). Reaction was carried out in a reaction volume of 50 μl, containing 25 μl of PrimeSTAR Max Premix 2× (TaKaRa, Shiga, Japan), 16.5 μl of ddH_2O, 0.5 μmol/l of each primer, and 50–100 ng of DNA template (Rahmdel et al., 2019). PCR was performed under the following conditions: initial denaturation at 96°C for 2 min, followed by 35 cycles of denaturation at 96°C for 10 s, annealing at 56°C for 15 s, and polymerization at 72°C for 1 min. Subsequently, the final polymerization was performed at 72°C for 10 min. PCR products obtained were sequenced by Sanger company (Sangon Biotechnology Co., Ltd., Shanghai, China).

The obtained 16S rRNA sequences were manually corrected and then subjected to Basic Local Alignment Search Tool Nucleotide (BLASTN) analysis to check the similarity with those already deposited sequences in the National Center for Biotechnology Information (NCBI). The retrieved 16S rRNA sequences were aligned using the ClustalW program. The phylogenetic tree of the aligned sequences was performed using the neighbor-joining (NJ) method in MEGA 7 software (Xu et al., 2019).

Screening of Phytic Acid-Degrading Bacteria

The isolated LAB strains were cultured for 24 h in modified MRS (MRS-MOPS) broth, in which inorganic phosphate (KH_2PO_4) was replaced by 0.65 g/l sodium phytate and 0.1 M3-[N-morpholino]propane sulfonic acid (Sangon Biotechnology Co., Ltd., Shanghai, China) (Raghavendra and Halami, 2009). The growth of bacteria in liquid culture media is commonly

evaluated by measuring the optical density at 600 nm (OD600) by UV spectrophotometry. Colony-forming units (CFU) were determined by plate counting after gradient dilution (Simova et al., 2008). The bacterial suspension (8 μl of 10^7–10^8 CFU/ml) was spotted on a modified MRS (mMRS) agar surface and incubated at 37°C for 24–72 h. Inorganic phosphate (KH_2PO_4) in MRS agar medium was replaced by 20 g/l MOPS, 2 g/l calcium chloride, and 2.5 g/l sodium phytate (Fischer et al., 2014). Anhydrous calcium chloride and sodium phytate were filtered through a 0.2-micron filter and added to the autoclaved medium at 55°C. Since the medium was opaque after phytic acid precipitation, the formation of a transparent zone was an indicator of phytic acid hydrolysis.

To avoid false-positive results due to hyaline circles caused by acid solubilization, the colonies on the plates were washed from the agar surface with double-distilled water after incubation and then soaked in 2% (w/v) aqueous cobalt chloride solution for 5 min. Furthermore, an equal volume of 6.25% (w/v) ammonium molybdate solution and 0.42% (w/v) ammonium metavanadate solution was used to replace cobalt chloride hexahydrate for 5 min incubation at room temperature and then removed to check the hydrolysis plate (Bhagat et al., 2020).

Phytase Enzyme Assay

To further identify the phytase activity of the LAB, preliminarily screened strains were cultured in different centrifuge tubes containing 1 ml MRS broth at 37°C and 900 rpm for 24 h. Then, 50 μl of culture was transferred to 10 ml MRS broth and incubated at 37°C and 200 rpm for 72 h. The culture broth was frozen overnight at −80°C, then concentrated three times in an Ultra-Low Temperature Freezer and centrifuged at 4°C and 8,000 rpm for 10 min. The supernatant was taken and tested for phytase activity analysis with a phytase assay kit (Suzhou Comin Biotechnology Co., Ltd., Suzhou, China). Commercial phytase was directly added to MRS broth as a control. Strains with the highest phytase activity were selected for further study.

Animals and Experimental Treatments

Four-week-old male Kunming mice (initial body weight 18–21 g) were purchased from Hunan SJA Laboratory Animal Co., Ltd. (Changsha, Hunan, China). The mice were placed under controlled environmental conditions (temperature 22 ± 2°C, relative humidity 55 ± 2%) with light/dark cycles of 12 h. All animals were acclimatized for 3 days prior to an experiment and had free access to food and water. Standard commercially available mouse food (Jiangsu Xietong Pharmaceutical Bioengineering Co., Ltd., Jiangsu, China) was fed separately, and its specific nutritional index is shown (**Supplementary Table 1**). The experimental protocol was reviewed and approved by the Animal Care and Use Committee (SYXK 2014-0007) of Hunan Normal University. All experiments were performed in accordance with relevant guidelines and regulations.

Thirty-two mice were randomly divided into four groups (**Supplementary Table 2**), with eight mice per group, and fed different diets for 28 days: (1) control, (2) PA, (3) PA + psm16, and (4) PA + phytase. Group 1 mice were fed the basal diet. Group 2–3 mice received 1% phytic acid supplementation in the basal diet. Group 4 mice were fed a basal diet with 1% phytate and 500 U/kg commercial phytase. Group 1, 2, and 4 mice were gavaged with 200 μl PBS, and group 3 mice were gavaged with strain psm16 (1×10^9 CFU in 200 μl PBS). All groups of mice were gavaged once a day for the first 18 days and then once every 3 days for a total of 21 times. Animals were fasted for 12 h and sacrificed prior to sampling.

Blood samples were placed in plastic tubes containing heparin for at least 3 h and then centrifuged at 4,000 rpm for 15 min at 4°C. The serum was recovered and stored at −80°C to be used for mineral content determination. After blood sampling, the livers, kidneys, and ceca were taken and weighed and stored at −80°C until use. The cecum wall was flushed and weighed, and the cecum contents were used in a short-chain fatty acid (SCFA) assay and pH determination. Feces were collected for an SCFA assay during the last 3 days of the experiment.

Short-Chain Fatty Acid and pH Analysis

The SCFA of concentration was measured using the method of gas chromatography, as reported earlier with minor modifications (Zhou et al., 2019). Stool and cecum content samples were homogenized and diluted with distilled water. After mechanical vibration and centrifugation at 15,000 rpm for 15 min at 4°C, a mixture of supernatant fluid and 25% metaphosphoric acid solution (9:1) was allowed to stand for 3 h. Then, the mixed solution was centrifuged at 15,000 rpm for 10 min and filtered through a membrane filter (pore size 0.45 μm). SCFAs were measured with a gas chromatography (Agilent Technologies 7890B System) equipped with a DB-FFAP column (30 m × 250 μm × 0.25 μm). The carrier gas was nitrogen (flow 0.8 ml/min, split ratio 50:1, volume of sampling 1 μl). The oven, detector, and injector temperatures were 220, 280, and 250°C, respectively. The SCFA content was quantified using an external standard curve method with standard solutions of acetate, propionate, butyrate, isobutyrate, isovalerate, and valerate (Wang et al., 2017).

The pH of the cecum contents was measured by centrifugation at 8,000 rpm for 1 min at 4°C, then testing 0.8 μl of supernatant with pH paper (pH 5–9) and observing the color change.

Measurement of Minerals

The levels of copper, iron, zinc, manganese, magnesium, phosphorus, and calcium in mouse liver, kidney, and plasma were determined using an inductively coupled plasma emission spectrometer (ICP-OES 5110, Agilent, Santa Clara, CA, United States) (Wan et al., 2018). The samples were completely dried at 60°C and ground into powder before pretreatment, and approximately 0.2 g frozen tissue and approximately 0.2 ml plasma sample were used in each experiment. Livers and kidneys were decolorized with 1 ml hydrogen peroxide, digested with nitric acid and perchloric acid at 180°C for 100 min, then dried at 260°C, redissolved in 1% HNO_3, filtered, and subjected to an ICP analysis. The detection wavelengths were Ca (λ = 317.933 nm), Cu (λ = 324.754 nm), Fe (λ = 238.204 nm), Mg (λ = 279.553 nm), Mn (λ = 257.610 nm), P (λ = 213.618 nm), and Zn (λ = 206.200 nm). The metal and trace element content data in the liver, serum, and kidney were expressed as ppm. The

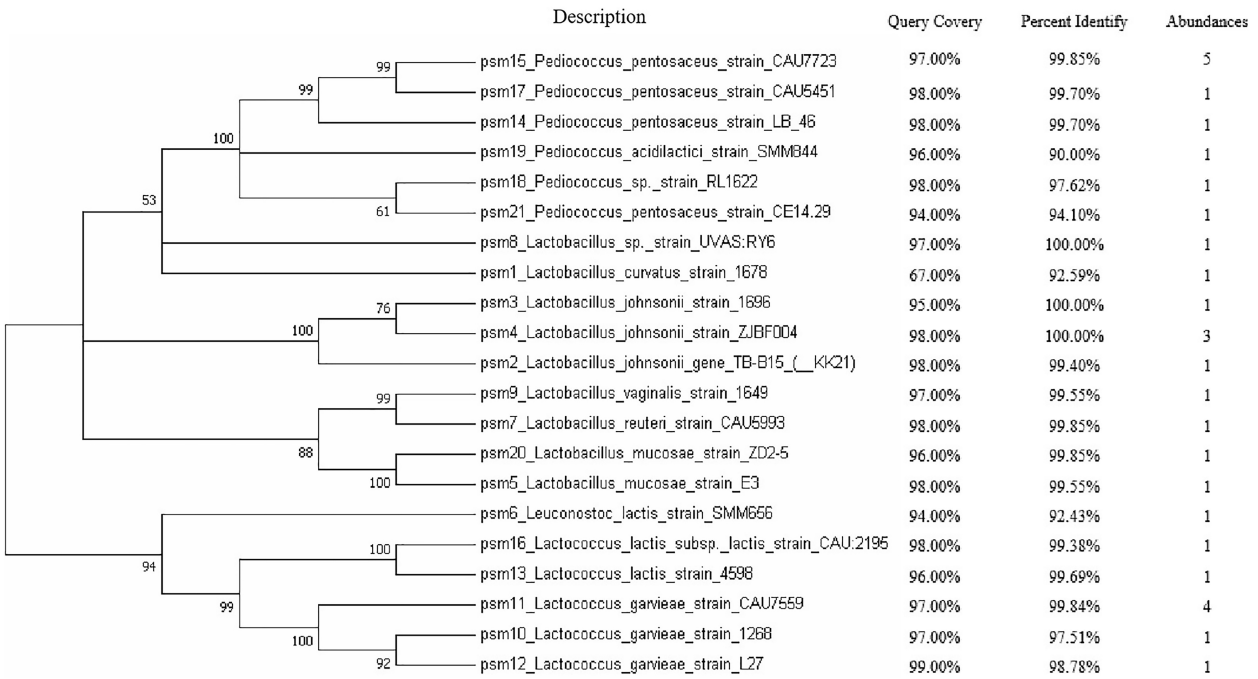

FIGURE 1 | The evolutionary history was inferred using the neighbor-joining method. A bootstrap consensus tree inferred from 1,000 replicates was used to represent the evolutionary history of the taxa analyzed. Branches corresponding to partitions reproduced in less than 50% bootstrap replicates are collapsed. The percentage of replicate trees in which the associated taxa clustered together in the bootstrap test (1,000 replicates) are shown next to the branches whereas the BLAST alignment results are shown. The abundances of the isolated bacterial are shown in the last column.

content of trace elements in different dietary groups was assayed by the company SGS-CSTC Standards Technical Services Co., Ltd. (Shanghai, China) (**Supplementary Table 3**).

Statistical Analysis

Experimental data were initially compiled using the WPS Education Test Edition and then analyzed using IBM SPSS Statistics 20.0. The normality and homoscedasticity of the data were tested before performing a one-way ANOVA. Non-parametric tests were used to ensure the accuracy of the analysis for data that did not meet the assumption of normality and homogeneity of variance, and the Duncan and LSD methods were used to meet the requirements. Phytase data were processed with GraphPad Prism 8 (GraphPad Software, San Diego, CA, United States). The results were expressed as the mean ± standard error, and significance was defined as a p-value < 0.05.

RESULTS

Screening and Identification of Phytic Acid-Degrading Lactic Acid Bacteria

After cultivation of microbes from sow milk samples, a total of 30 strains were isolated based on colony morphology and 16Sr RNA gene sequence to include as much diversity as possible at the species level. A phylogenetic tree was constructed using an NJ analysis with MEGA 7, which indicated the relative phylogeny of the isolates in comparison to reference strains. *Lactobacillus* (11/30), *Pediococcus pentosaceus* (9/30), and *Lactococcus* (8/30) were the most abundant species in the isolated microbial flora. Minor populations of other species such as *Pediococcus acidilactici* (1/30) and *Leuconostoc lactis* are (1/30) were also seen in the phylogenetic tree (**Figure 1**).

The isolates were screened for extracellular phytase production with a plate screening method. Psm6, psm15, psm16, and psm17 showed the ability to degrade phytic acid. Psm15 and psm17 are *P. pentosaceus* strains, psm16 is a *Lactococcus lactis* subsp. *lactis* strain, and psm6 is a *L. lactis* strain. Of the four isolates, strain psm16 showed the largest degradation transparent circle on the plate (**Supplementary Figure 1**) and had the strongest phytase activity (**Figure 2**). For further verification, microscopic observation indicated that isolated strain psm16 was cocci (**Supplementary Figure 2**). Strain psm16 was deposited in the China General Microbiological Culture Collection Center (CGMCC 22933).

Effects of Dietary Conditions on Physiological Variables

The weights of liver, kidney, cecum, and cecum contents and the lengths of large intestine (LIL) and small intestine (SIL) in mice were measured and compared with the animal's final weight (**Table 1**). The addition of phytic acid to the diet as well as the gavaged strain had no effect on the final weight of the mice. There were no significant differences in LIL, SIL, liver weight, kidney

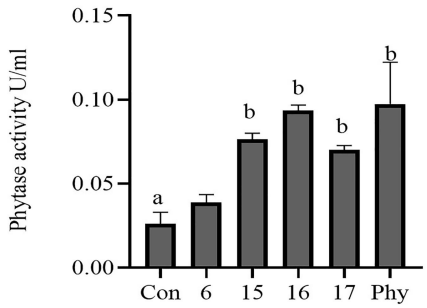

FIGURE 2 | Phytase activity in four selected phytate-degrading strains was assayed. The supernatant of the cultured strains was assayed for phytase activity using a phytase assay kit. Con, MRS; 6, psm 6; 15, psm 15; 16, psm16; 17, psm17; Phy, Phytase. Differences in the bar are not significant without marked letters ($p > 0.05$). a, b values that do not share a common letter in the bar graph above differ significantly ($p < 0.05$).

weight, and cecum weight due to the dietary treatments in mice. In contrast, the addition of strain psm16 significantly increased the weight of the cecum contents ($p < 0.045$), and the addition of commercial phytase had a profound effect on the cecum wall weight ($p < 0.010$). Compared with the basic group, the pH value in the cecum was relatively lower in the phytic acid group and the addition of psm16 restored the pH to the value of the control group and was acidic, but the pH value became slightly alkaline after the addition of phytase (**Supplementary Figure 3**).

Effects of Dietary Treatments on Cecal and Fecal Short-Chain Fatty Acid

We investigated whether the various diets influenced SCFA concentrations in mice. Compared to the control, there were changes in the cecal and fecal SCFA levels in mice fed with phytic acid (**Table 2**). Propionate, butyrate, isovalerate, valerate, and total SCFA were lower in the ceca of mice on phytic acid diets than on basal diet. In addition, acetic acid was significantly reduced. When mice were orally gavaged with strain psm16, the concentrations of acetate ($p < 0.015$), propionate ($p < 0.014$), butyrate ($p < 0.036$), and total SCFA ($p < 0.009$) in the ceca of mice were significantly increased. Compared with the group fed phytic acid alone, the groups fed phytic acid and treated with strain psm16 had higher fecal acetate ($p < 0.034$), propionate ($p < 0.000$), butyrate ($p < 0.000$), and total SCFA ($p < 0.009$) levels. Additionally, significant increases in the acetate and total SCFA levels were observed in the phytase group.

Effects of Dietary Condition on Trace Elements Status

To verify whether strain psm16 affects the content of mineral elements in mice, we studied the calcium, magnesium, copper, zinc, iron, phosphorus, and manganese levels in the liver, kidney, and plasma. Mineral elements in the various diets were determined, and no differences were evident (**Supplementary Table 3**). In mice fed with phytic acid, the levels of Fe ($p < 0.048$) and Zn in the liver were lower than in the basal diet group, whereas Cu ($p < 0.021$) and Zn ($p < 0.017$) were significantly higher when strain psm16 was given orally, and Fe was increased in the phytase group (**Table 3**). In kidney tissue, phytic acid significantly decreased the levels of Fe ($p < 0.002$) and Mn ($p < 0.010$). Gavage with strain psm16 also changed the mineral level in the kidney: a significant increase of Mn and Zn ($p < 0.022$) was seen, whereas the levels of Cu ($p < 0.007$) and Mg ($p < 0.001$) were significantly decreased. Addition of phytase together with a phytic acid diet increased the content of Mn ($p < 0.010$) and decreased the contents of Cu ($p < 0.007$) and Mg ($p < 0.001$) in the kidney (**Table 3**). The levels of Ca ($p < 0.000$), Mn ($p < 0.000$), and Zn ($p < 0.000$) in plasma were significantly increased by gavage with strain psm16. Cu ($p < 0.040$) was significantly increased in the phytase group compared with the basal diet group (**Table 3**). In addition, the content of P in the kidney and the plasma was lower after adding phytic acid, but it returned to normal levels after treatment with strain psm16 or phytase, although the differences were not statistically significant.

DISCUSSION

Phytic acid is known for its anti-nutritive effects, such as the inhibition of mineral uptake, especially of Cu, Zn, or Fe absorption in the gastrointestinal tract (Lopez et al., 2000). Phytic acid also reduces the activity of enzymes such as trypsin, pepsin, and β-galactosidase (Mohammadi-Kouchesfahani et al., 2019). Moreover, it has been shown that diets high in phytic acid reduce the expression of some genes responsible for appetite and glucose or sodium absorption in fish and piglets, respectively (Woyengo et al., 2012; Liu et al., 2014). Here, in this study we isolated a strain of *L. lactis* psm16 from porcine milk that exhibited better phytate degrading activity. In mice gavaged with strain psm16, a higher content of mineral elements was found in the organs of mice. It is possible that phytase production facilitates phytic acid hydrolysis, thus altering the absorption of host minerals. This is something we need to explore further in the future.

Humans and mice rely on bacteria to break down indigestible dietary ingredients such as phytic acid (Raghavendra and Halami, 2009). Previous studies have shown that SCFAs are bacterial fermentation products, which can promote the digestion and absorption of nutrients, improve intestinal health and immunity, maintain intestinal function, promote mineral absorption and utilization, and improve the structure of the intestinal flora (Scholz-Ahrens et al., 2007). An SCFA assay showed that when compared with the phytic acid group, acetic acid, propionic acid, butyric acid, and total SCFA in the cecum contents and feces increased significantly in the strain psm16 group. SCFAs produced by bacteria are associated with host health, whereas butyrate in feces is significantly associated with an improved insulin response (Serino, 2019).

Zinc is an essential trace element for normal cell function. It is involved in the regulation of enzyme formation, cell signaling, antioxidant defenses, insulin biosynthesis, secretion, and mRNA expression (Maret, 2013). The present study revealed that the Zn content in the phytic acid group was significantly lower than that in the control group in the liver and significantly lower in the plasma than that in the phytase group. In mice gavaged with

TABLE 1 | The effects of dietary supplementation with phytic acid and bacterial strains on growth parameters in mice (mean ± SEM).

	Dietary treatment				
Items	**BD (*n* = 8)**	**PA (*n* = 8)**	**PA + psm16 (*n* = 7)**	**Phy (*n* = 8)**	***p*-value**
BW (g)	39.585 ± 0.924	39.740 ± 0.856	38.523 ± 1.301	40.693 ± 1.003	0.54
LW/BW (g/g)	0.036 ± 0.003	0.039 ± 0.003	0.042 ± 0.001	0.038 ± 0.001	0.478
KW/BW (g/g)	0.016 ± 0.000	0.017 ± 0.000	0.017 ± 0.001	0.016 ± 0.001	0.153
LIL/BW (cm/g)	0.216 ± 0.011	0.235 ± 0.016	0.223 ± 0.021	0.229 ± 0.011	0.83
SIL/BW (cm/g)	1.276 ± 0.025	1.293 ± 0.035	1.353 ± 0.039	1.333 ± 0.028	0.321
CW/BW (mg/g)	8.300 ± 0.370	7.700 ± 0.470	8.700 ± 0.450	7.500 ± 0.580	0.346
CWW/BW (mg/g)	5.350 ± 0.326^{a}	5.180 ± 0.222^{ab}	4.300 ± 0.244^{bc}	4.010 ± 0.388^{c}	0.010
CCW/BW (mg/g)	2.960 ± 0.459^{b}	2.530 ± 0.415^{b}	4.360 ± 0.354^{a}	3.540 ± 0.509^{ab}	0.045

BD, basal diet; PA, basal diet added with 1% phytic acid; PA + psm16, 1% phytic acid group was treated with Lactococcus lactis psm16; Phy, phytase; BW, body weight; KW, kidney weight; LIL, large intestine length; SIL, small intestine length; CW, cecum weight; CWW, cecal wall weight; CCW, cecal content weight.
Differences in the same row are not significant without marked letters ($p > 0.05$).
$^{a–c}$Values in the same row not sharing a common superscript differ significantly ($p < 0.05$).

TABLE 2 | Effects of strains and PA on the levels of SCFA in the cecum and feces (mean ± SEM, *n* = 7).

Items	Dietary treatment				
	BD	**PA**	**PA + psm16**	**Phy**	***p*-value**
Acetate (mg/g)					
Cecal contents	3.52 ± 0.29^{ab}	2.81 ± 0.17^{b}	4.30 ± 0.34^{a}	3.78 ± 0.36^{a}	0.015
Late fecal	2.9 ± 0.24^{a}	3.02 ± 0.15^{a}	3.6 ± 0.18^{b}	3.58 ± 0.14^{b}	0.034
Propionate (mg/g)					
Cecal contents	0.72 ± 0.07^{b}	0.62 ± 0.02^{b}	0.90 ± 0.06^{a}	0.78 ± 0.06^{ab}	0.014
Late fecal	0.52 ± 0.04^{a}	0.62 ± 0.03^{b}	0.73 ± 0.03^{c}	0.75 ± 0.03^{c}	0
Isobutyrate (mg/g)					
Cecal contents	0.15 ± 0.02	0.12 ± 0.01	0.16 ± 0.01	0.14 ± 0.01	0.08
Late fecal	0.06 ± 0.01^{a}	0.08 ± 0.00^{ab}	0.08 ± 0.00^{ab}	0.09 ± 0.00^{b}	0.025
Butyrate (mg/g)					
Cecal contents	0.72 ± 0.12^{a}	0.40 ± 0.04^{b}	0.62 ± 0.06^{a}	0.46 ± 0.06^{ab}	0.036
Late fecal	0.35 ± 0.05^{a}	0.47 ± 0.03^{b}	0.63 ± 0.04^{c}	0.58 ± 0.03^{bc}	0
Isovalerate (mg/g)					
Cecal contents	0.16 ± 0.01	0.14 ± 0.01	0.18 ± 0.01	0.16 ± 0.01	0.14
Late fecal	0.09 ± 0.01^{a}	0.10 ± 0.01^{ab}	0.12 ± 0.01^{bc}	0.13 ± 0.00^{c}	0.003
Valerate (mg/g)					
Cecal contents	0.19 ± 0.02	0.14 ± 0.01	0.19 ± 0.02	0.16 ± 0.02	0.103
Late fecal	0.09 ± 0.01^{a}	0.09 ± 0.00^{a}	0.11 ± 0.00^{ab}	0.12 ± 0.00^{b}	0.003
Total SCFA (mg/g)					
Cecal contents	5.18 ± 0.47^{ab}	4.22 ± 0.18^{b}	6.35 ± 0.45^{a}	5.49 ± 0.49^{a}	0.009
Late fecal	4.01 ± 0.34^{a}	4.38 ± 0.22^{a}	5.26 ± 0.26^{b}	5.24 ± 0.20^{b}	0.009

BD, basal diet; PA, basal diet added with 1% phytic acid; PA + psm16, 1% phytic acid group was treated with Lactococcus lactis psm16; Phy, phytase; SCFA, short chain fatty acids.
Differences in the same row are not significant without marked letters ($p > 0.05$).
$^{a–c}$Values in the same row not sharing a common superscript differ significantly ($p < 0.05$).

strain psm16, the Zn content in the liver, kidney, and serum increased significantly. The beneficial effect of strain psm16 on zinc absorption can be explained by at least two possible mechanisms: phytic acid hydrolysis induced by microbial phytase produced by strain psm16 or the existence of organic acids such as lactic acid and SCFA that form soluble ligands with zinc, which prevents the formation of insoluble zinc phytate (Lopez et al., 2000).

Iron is an important element in hemoglobin and myoglobin and plays a vital role in the metabolism of humans and animals. It is also a metal contained in many important enzyme active sites, such as catalase, peroxidase, and cytochrome (Silva and Faustino, 2015). During human life, the iron demand in infants during weaning is the highest per unit weight, and diet is insufficient to meet the iron needs. The absorption of non-heme and heme iron in typical weaning porridge, whether ascorbic acid is present or

TABLE 3 | Effects of strains and phytic acid on the levels of trace elements in the liver, kidney, and plasma (mean ± SEM).

	Dietary treatment				
Items	**BD (*n* = 8)**	**PA (*n* = 8)**	**PA + psm16 (*n* = 7)**	**Phy (*n* = 8)**	***p*-value**
Liver					
Ca (ppm)	391.75 ± 28.69	363.91 ± 22.42	360.73 ± 66.06	417.31 ± 57.25	0.469
Cu (ppm)	17.81 ± 0.76^{b}	18.27 ± 0.57^{b}	21.34 ± 0.51^{a}	20.69 ± 1.22^{ab}	0.021
Fe (ppm)	316.21 ± 19.05^{b}	229.04 ± 13.21^{a}	270.25 ± 25.02^{ab}	297.10 ± 25.75^{b}	0.048
Mg (ppm)	702.84 ± 22.3	724.49 ± 15.86	746.62 ± 19.63	692.44 ± 17.49	0.224
Mn (ppm)	3.31 ± 0.15	3.18 ± 0.16	3.43 ± 0.18	3.34 ± 0.14	0.743
P (ppm)	10689.51 ± 397.21	11050.66 ± 241.84	11465.32 ± 244.71	10752.23 ± 319.96	0.319
Zn (ppm)	133.41 ± 12.90^{b}	103.18 ± 3.21^{a}	117.11 ± 2.46^{b}	111.32 ± 2.57^{ab}	0.017
Kidney					
Ca (ppm)	736.84 ± 102.78	749.42 ± 37.43	576.76 ± 86.23	684.66 ± 26.38	0.33
Cu (ppm)	27.11 ± 1.94^{ab}	27.01 ± 0.66^{a}	22.41 ± 2.18^{b}	18.88 ± 0.35^{b}	0.007
Fe (ppm)	284.98 ± 10.19^{a}	237.55 ± 7.08^{b}	253.12 ± 4.94^{b}	247.08 ± 8.37^{b}	0.002
Mg (ppm)	823.86 ± 9.33^{a}	829.73 ± 7.15^{a}	783.40 ± 8.01^{b}	791.47 ± 7.19^{b}	0.001
Mn (ppm)	6.14 ± 0.26^{b}	4.98 ± 0.22^{a}	5.85 ± 0.26^{b}	6.09 ± 0.27^{b}	0.010
P (ppm)	13702.29 ± 129.12	13458.39 ± 82.07	13780.06 ± 86.35	13785.03 ± 84.47	0.083
Zn (ppm)	88.62 ± 1.26^{c}	90.18 ± 2.22^{ac}	97.13 ± 4.08^{b}	93.39 ± 0.63^{ab}	0.022
Plasma					
Ca (ppm)	65.28 ± 16.40^{a}	61.83 ± 12.29^{a}	486.34 ± 177.17^{b}	818.32 ± 238.63^{b}	0.00
Cu (ppm)	0.62 ± 0.02^{a}	0.68 ± 0.03^{ab}	0.67 ± 0.06^{ab}	0.74 ± 0.02^{b}	0.04
Fe (ppm)	3.64 ± 0.35	4.06 ± 0.52	4.84 ± 0.47	3.54 ± 0.35	0.13
Mg (ppm)	22.19 ± 0.61	20.98 ± 0.47	24.55 ± 1.65	23.43 ± 1.39	0.29
Mn (ppm)	37.19 ± 6.27^{b}	45.66 ± 4.11^{b}	176.34 ± 51.65^{a}	283.52 ± 69.37^{a}	0.00
P (ppm)	161.45 ± 4.70	156.40 ± 4.03	166.55 ± 9.34	165.30 ± 6.62	0.67
Zn (ppm)	1.57 ± 0.82^{a}	1.27 ± 0.71^{a}	28.94 ± 11.10^{b}	48.70 ± 14.75^{bc}	0.00

BD, basal diet; PA, basal diet added with 1% phytic acid; PA + psm16, 1% phytic acid group was treated with Lactococcus lactis psm16; PHY, phytase. Differences in the same row are not significant without marked letters ($p > 0.05$).
$^{a-c}$Values in the same row not sharing a common superscript differ significantly ($p < 0.05$).

not, improves iron bioavailability (Hallberg et al., 2003). Evidence also indicates that phytic acid inhibits non-heme Fe absorption in humans (Gillooly et al., 1983). Interestingly, only small amounts of phytic acid (5–10 mg phytates) in a meal are sufficient to reduce Fe absorption (Hallberg et al., 1989). In our study, the presence of 1% phytic acid in the diet altered the Fe levels in the liver and kidney. In mice gavaged with strain psm16 or fed commercial phytase, the Fe content approached control levels. LAB themselves may metabolize trace elements in the chyme and indirectly change host mineral elements. It has been reported that mineral elements were increased in colostrum when fermented with LAB (Bartkiene et al., 2018). Studies on the role of iron in a microbial context are scarce. Although Fe absorption and assimilation *in vivo* have been well established, the mechanism of intestinal flora regulation is not completely clear yet.

Manganese can be released by adding xylanase and phytase from wheat, barley, soybean meal, corn, and wheat bran (Yu et al., 2018). Low levels of manganese support growth and reproduction in pigs, while a lack of manganese causes multiple skeletal abnormalities in poultry and cattle (Spears, 2019). Manganese may also delay pork decomposition and improve pork quality by reducing oxidative damage (Sawyer et al., 2007). In our study, the manganese content in the kidney and plasma increased significantly after adding strain psm16 strain or commercial phytase. The addition of strain psm16 may produce phytase, which degrades phytic acid and improves Mn levels, even if a strong anti-correlation between Mn uptake and phytic acid content in food existed.

Copper is an essential element for several enzymes involved in antioxidant responses, such as superoxide dismutase and for ATP production (Dalecki et al., 2017). Over the years, copper has been widely used as a feed additive in pig production in the United States and China. It promotes pig growth and survival after weaning by increasing feed intake and metabolic activity (Shelton et al., 2011; Carpenter et al., 2019). The current results showed that copper is significantly increased in the liver after the addition of strain psm16, while in the kidney, after the addition of psm16 strain or commercial phytase, the level of copper is still in the normal range, but lower than in phytic acid group alone, and magnesium also shows the same change. In contrast to previous studies, the addition of phytic acid in white wheat bread can inhibit partial apparent magnesium absorption in the human body (Bohn et al., 2004). Various reports document the effect of phytase supplementation on copper metabolism in corn-soybean meal diets. It has been reported that vegetable protein with a high phytic acid level in adults inhibited the absorption of iron, zinc,

calcium, and manganese but did not inhibit the absorption of copper (Hurrell, 2003). However, it was also found that phytase supplementation in low phosphorus corn-soybean meal diets increased copper retention in chickens (Banks et al., 2004). The above studies indicated that the element absorption was not changed, while others observed an increase in the bioavailability of elements. These apparent inconsistencies can be attributed to two different circumstances: the different supplied doses of phytate and the nature and the amount of the other dietary components (Grases et al., 2001). The antagonistic relationship between zinc and copper in absorption and utilization may also be related to the higher basal level of copper in the diets. The effect of phytase on copper has not been shown, and the exact mechanism should be further studied.

Milk and dairy products are the most important sources of calcium for people living in developed countries, and plant foods are the main sources of calcium in China. It has been reported that only the highest phytic acid supplementation can significantly reduce serum iron concentration, while calcium and magnesium were not changed (Szkudelski, 2005). In this study, the calcium contents in the liver and kidney were not affected. However, after phytic acid was added to the diet, the calcium content decreased compared with that in the basal diet group, and the calcium concentration increased significantly after adding strain psm16 in the plasma. The lactic acid fermentation products produced by the psm16 strain makes the cecum acidic, which provides good conditions for endogenous phytase to have a role in reducing phytic acid, thereby increasing the concentration of soluble Ca (Rosa-Sibakov et al., 2018).

In conclusion, we isolated a strain of *L. lactis* psm16 from porcine milk that exhibited better phytate-degrading activity. In the presence of the anti-nutritional factor phytic acid, high levels of trace elements were found in the plasma, liver, and kidney of mice orally gavaged with strain psm16. Further studies are essential to revealing the mechanism of phytase production and phytic acid degradation by *L. lactis* psm16 *in vivo* and to optimizing the conditions for phytase production by psm16.

DATA AVAILABILITY STATEMENT

The original contributions presented in the study are included in the article/**Supplementary Material**, further inquiries can be directed to the corresponding author/s.

ETHICS STATEMENT

The animal study was reviewed and approved by the Institutional Animal Care and Use Committee at Hunan Normal University.

AUTHOR CONTRIBUTIONS

JY and HN contributed to conceiving and designing the experiments. DZ wrote the original draft of the manuscript. DZ, YZ, JL, LW, CC, and QH performed the mouse-feeding trial and sample collection. DZ and LW conducted the strain screening and short-chain fatty acid assay. JL, DZ, and YZ contributed to the trace element analysis experiment. JY, HN, and VR reviewed and revised the manuscript. JY obtained the funding and supervised the project. All authors contributed to the article and approved the submitted version.

FUNDING

This work was supported by the National Natural Science Foundation of China (31700004), Construction of Innovative Provinces in Hunan Province (2019RS3022), the National Students Platform for Innovation and Entrepreneurship Training Program (2020056), and Shandong Key Research and Development Program (2019QYTPY002 and 2019JZZY010724). The funding bodies had no contribution in the study design, data collection, interpretation, or preparation of the manuscript.

SUPPLEMENTARY MATERIAL

The Supplementary Material for this article can be found online at: https://www.frontiersin.org/articles/10.3389/fmicb.2021.753195/full#supplementary-material

Supplementary Figure 1 | Application of four phytic acid-degrading bacteria in psm. Application of four acid-degrading bacteria in modified MRS plate.

Supplementary Figure 2 | The microscope micrographs of psm16 strain.

Supplementary Figure 3 | The pH values detection of the cecum contents in mice. Samples were centrifuged at 4°C for 8000 rpm for 1 min, and the further 0.8 μL of the supernatant tested with pH indicator paper (pH 5–9) and the color change was observed.

REFERENCES

Banks, K. M., Thompson, K. L., Jaynes, P., and Applegate, T. J. (2004). The effects of copper on the efficacy of phytase, growth, and phosphorus retention in broiler chicks. *Poult. Sci.* 83, 1335–1341.

Bartkiene, E., Bartkevics, V., Ikkere, L. E., Pugajeva, I., Zavistanaviciute, P., Lele, V., et al. (2018). The effects of ultrasonication, fermentation with *Lactobacillus* sp., and dehydration on the chemical composition and microbial contamination of bovine colostrum. *J. Dairy Sci.* 101, 6787–6798. doi: 10.3168/jds.2018-14692

Bhagat, D., Raina, N., Kumar, A., Katoch, M., Khajuria, Y., Slathia, P. S., et al. (2020). Probiotic properties of a phytase producing Pediococcus acidilactici strain SMVDUDB2 isolated from traditional fermented cheese product, Kalarei. *Sci. Rep.* 10:1926. doi: 10.1038/s41598-020-58676-2

Bohn, T., Davidsson, L., Walczyk, T., and Hurrell, R. F. (2004). Phytic acid added to white-wheat bread inhibits fractional apparent magnesium absorption in humans. *Am. J. Clin. Nutr.* 79, 418–423.

Cannas, D., Loi, E., Serra, M., Firinu, D., Valera, P., and Zavattari, P. (2020). Relevance of essential trace elements in nutrition and drinking water for human health and autoimmune disease risk. *Nutrients* 12:2074. doi: 10.3390/nu12072074

Carpenter, C. B., Woodworth, J. C., Derouchey, J. M., Tokach, M. D., Goodband, R. D., Dritz, S. S., et al. (2019). Effects of increasing copper from either copper sulfate or combinations of copper sulfate and a copper-amino acid complex on finishing pig growth performance and carcass characteristics. *Transl. Anim. Sci.* 3, 1263–1269. doi: 10.1093/tas/txz112

Cheng, L., Akkerman, R., Kong, C., Walvoort, M. T. C., and de Vos, P. (2021). More than sugar in the milk: human milk oligosaccharides as essential bioactive

molecules in breast milk and current insight in beneficial effects. *Crit. Rev. Food Sci. Nutr.* 61, 1184–1200. doi: 10.1080/10408398.2020.1754756

Corrêa, T. L. R., and de Araújo, E. F. (2020). Fungal phytases: from genes to applications. *Braz. J. Microbiol.* 51, 1009–1020. doi: 10.1007/s42770-020-00289-y

Dalecki, A. G., Crawford, C. L., and Wolschendorf, F. (2017). Copper and antibiotics: discovery, modes of action, and opportunities for medicinal applications. *Adv. Microb. Physiol.* 70, 193–260. doi: 10.1016/bs.ampbs.2017.01.007

Fischer, M. M., Egli, I. M., Aeberli, I., Hurrell, R. F., and Meile, L. (2014). Phytic acid degrading lactic acid bacteria in tef-injera fermentation. *Int. J. Food Microbiol.* 190, 54–60. doi: 10.1016/j.ijfoodmicro.2014.08.018

Gibson, R. S., Bailey, K. B., Gibbs, M., and Ferguson, E. L. (2010). A review of phytate, iron, zinc, and calcium concentrations in plant-based complementary foods used in low-income countries and implications for bioavailability. *Food Nutr. Bull.* 31(2 Suppl), S134–S146.

Gillooly, M., Bothwell, T. H., Torrance, J. D., MacPhail, A. P., Derman, D. P., Bezwoda, W. R., et al. (1983). The effects of organic acids, phytates and polyphenols on the absorption of iron from vegetables. *Br. J. Nutr.* 49, 331–342.

Grases, F., Simonet, B. M., Prieto, R. M., and March, J. G. (2001). Dietary phytate and mineral bioavailability. *J. Trace Elem. Med. Biol.* 15, 221–228.

Greppi, A., Krych, Ł, Costantini, A., Rantsiou, K., Hounhouigan, D. J., Arneborg, N., et al. (2015). Phytase-producing capacity of yeasts isolated from traditional African fermented food products and PHYPk gene expression of *Pichia kudriavzevii* strains. *Int. J. Food microbiol.* 205, 81–89. doi: 10.1016/j.ijfoodmicro.2015.04.011

Hallberg, L., Brune, M., and Rossander, L. (1989). Iron absorption in man: ascorbic acid and dose-dependent inhibition by phytate. *Am. J. clin. Nutr.* 49, 140–144.

Hallberg, L., Hoppe, M., Andersson, M., and Hulthén, L. (2003). The role of meat to improve the critical iron balance during weaning. *Pediatrics* 111(4 Pt 1), 864–870.

Haros, M., Rosell, C. M., and Benedito, C. (2001). Use of fungal phytase to improve breadmaking performance of whole wheat bread. *J. Agric. Food Chem.* 49, 5450–5454.

Hui, Q., Yang, R., Shen, C., Zhou, Y., and Gu, Z. (2016). Mechanism of calcium lactate facilitating phytic acid degradation in soybean during germination. *J. Agric. Food Chem.* 64, 5564–5573. doi: 10.1021/acs.jafc.6b01598

Hurrell, R. F. (2003). Influence of vegetable protein sources on trace element and mineral bioavailability. *J. Nutr.* 133, 2973S–2977S.

Ji, K., Jang, N. Y., and Kim, Y. T. (2015). Isolation of lactic acid bacteria showing antioxidative and probiotic activities from kimchi and infant feces. *J. Microbiol. Biotechnol.* 25, 1568–1577. doi: 10.4014/jmb.1501.01077

Kumar, A., Singh, B., Raigond, P., Sahu, C., Mishra, U. N., Sharma, S., et al. (2021). Phytic acid: blessing in disguise, a prime compound required for both plant and human nutrition. *Food Res. Int.* 142:110193. doi: 10.1016/j.foodres.2021.110193

Kumar, V., Sinha, A. K., Makkar, H. P. S., and Becker, K. (2010). Dietary roles of phytate and phytase in human nutrition: a review. *Food Chem.* 120, 945–959. doi: 10.1016/j.foodchem.2009.11.052

Liu, L., Liang, X.-F., Li, J., Yuan, X., Zhou, Y., and He, Y. (2014). Feed intake, feed utilization and feeding-related gene expression response to dietary phytic acid for juvenile grass carp (*Ctenopharyngodon idellus*). *Aquaculture* 424–425, 201–206. doi: 10.1016/j.aquaculture.2013.12.044

Lopez, H. W., Coudray, C., Levrat-Verny, M. A., Feillet-Coudray, C., Demigné, C., and Rémésy, C. (2000). Fructooligosaccharides enhance mineral apparent absorption and counteract the deleterious effects of phytic acid on mineral homeostasis in rats. *J. Nutr. Biochem.* 11, 500–508.

Lyons, K. E., Ryan, C. A., Dempsey, E. M., Ross, R. P., and Stanton, C. (2020). Breast milk, a source of beneficial microbes and associated benefits for infant health. *Nutrients* 12:1039. doi: 10.3390/nu12041039

Maret, W. (2013). Zinc biochemistry: from a single zinc enzyme to a key element of life. *Adv. Nutr.* 4, 82–91. doi: 10.3945/an.112.003038

Mezeli, M. M., Menezes-Blackburn, D., George, T. S., Giles, C. D., Neilson, R., and Haygarth, P. M. (2017). Effect of citrate on *Aspergillus niger* phytase adsorption and catalytic activity in soil. *Geoderma* 305, 346–353. doi: 10.1016/j.geoderma.2017.06.015

Mohammadi-Kouchesfahani, M., Hamidi-Esfahani, Z., and Azizi, M. H. (2019). Isolation and identification of lactic acid bacteria with phytase activity from sourdough. *Food Sci. Nutr.* 7, 3700–3708. doi: 10.1002/fsn3.1229

Olza, J., Aranceta-Bartrina, J., González-Gross, M., Ortega, R. M., Serra-Majem, L., Varela-Moreiras, G., et al. (2017). Reported dietary intake and food sources of zinc, selenium, and vitamins A, E and C in the Spanish population: findings from the ANIBES study. *Nutrients* 9:697. doi: 10.3390/nu9070697

Quigley, L., O'Sullivan, O., Stanton, C., Beresford, T. P., Ross, R. P., Fitzgerald, G. F., et al. (2013). The complex microbiota of raw milk. *FEMS Microbiol. Rev.* 37, 664–698. doi: 10.1111/1574-6976.12030

Raghavendra, P., and Halami, P. M. (2009). Screening, selection and characterization of phytic acid degrading lactic acid bacteria from chicken intestine. *Int. J. Food Microbiol.* 133, 129–134. doi: 10.1016/j.ijfoodmicro.2009.05.006

Rahmdel, S., Shekarforoush, S. S., Hosseinzadeh, S., Torriani, S., and Gatto, V. (2019). Antimicrobial spectrum activity of bacteriocinogenic *Staphylococcus* strains isolated from goat and sheep milk. *J. Dairy Sci.* 102, 2928–2940. doi: 10.3168/jds.2018-15414

Ren, C., Faas, M. M., and de Vos, P. (2021). Disease managing capacities and mechanisms of host effects of lactic acid bacteria. *Crit. Rev. Food Sci. Nutr.* 61, 1365–1393. doi: 10.1080/10408398.2020.1758625

Riaz Rajoka, M. S., Shi, J., Zhu, J., Shao, D., Huang, Q., Yang, H., et al. (2017). Capacity of lactic acid bacteria in immunity enhancement and cancer prevention. *Appl. Microbiol. Biotechnol.* 101, 35–45. doi: 10.1007/s00253-016-8005-7

Rosa-Sibakov, N., Re, M., Karsma, A., Laitila, A., and Nordlund, E. (2018). Phytic acid reduction by bioprocessing as a tool to improve the in vitro digestibility of faba bean protein. *J. Agric. Food Chem.* 66, 10394–10399. doi: 10.1021/acs.jafc.8b02948

Sawyer, J. T., Tittor, A. W., Apple, J. K., Morgan, J. B., Maxwell, C. V., Rakes, L. K., et al. (2007). Effects of supplemental manganese on performance of growing-finishing pigs and pork quality during retail display. *J. Anim. Sci.* 85, 1046–1053.

Scholz-Ahrens, K. E., Ade, P., Marten, B., Weber, P., Timm, W., Açil, Y., et al. (2007). Prebiotics, probiotics, and synbiotics affect mineral absorption, bone mineral content, and bone structure. *J. Nutr.* 137(3 Suppl. 2), 838S–846S. doi: 10.1093/jn/137.3.838S

Serino, M. (2019). SCFAs - the thin microbial metabolic line between good and bad. *Nat. Rev. Endocrinol.* 15, 318–319. doi: 10.1038/s41574-019-0205-7

Shelton, N. W., Tokach, M. D., Nelssen, J. L., Goodband, R. D., Dritz, S. S., DeRouchey, J. M., et al. (2011). Effects of copper sulfate, tri-basic copper chloride, and zinc oxide on weanling pig performance. *J. Anim. Sci.* 89, 2440–2451. doi: 10.2527/jas.2010-3432

Shi, L., Arntfield, S. D., and Nickerson, M. (2018). Changes in levels of phytic acid, lectins and oxalates during soaking and cooking of Canadian pulses. *Food Res. Int.* 107, 660–668. doi: 10.1016/j.foodres.2018.02.056

Silva, B., and Faustino, P. (2015). An overview of molecular basis of iron metabolism regulation and the associated pathologies. *Biochim. Biophys. Acta* 1852, 1347–1359. doi: 10.1016/j.bbadis.2015.03.011

Simova, E. D., Beshkova, D. M., Angelov, M. P., and Dimitrov, Z. P. (2008). Bacteriocin production by strain *Lactobacillus delbrueckii* ssp. bulgaricus BB18 during continuous prefermentation of yogurt starter culture and subsequent batch coagulation of milk. *J. Ind. Microbiol. Biotechnol.* 35, 559–567. doi: 10.1007/s10295-008-0317-x

Sirichokchatchawan, W., Temeeyasen, G., Nilubol, D., and Prapasarakul, N. (2018). Protective effects of cell-free supernatant and live lactic acid bacteria isolated from Thai pigs against a pandemic strain of porcine epidemic diarrhea virus. *Probiotics Antimicrob. Proteins* 10, 383–390. doi: 10.1007/s12602-017-9281-y

Spears, J. W. (2019). Boron, chromium, manganese, and nickel in agricultural animal production. *Biol. Trace Elem. Res.* 188, 35–44. doi: 10.1007/s12011-018-1529-1

Szkudelski, T. (2005). Phytic acid-induced metabolic changes in the rat. *J. Anim. Physiol. Anim. Nutr.* 89, 397–402.

Wan, D., Zhang, Y. M., Wu, X., Lin, X., Shu, X. G., Zhou, X. H., et al. (2018). Maternal dietary supplementation with ferrous N-carbamylglycinate chelate affects sow reproductive performance and iron status of neonatal piglets. *Animal* 12, 1372–1379. doi: 10.1017/S1751731117003172

Wang, H., Zhou, Y., Ma, J., Zhou, Y., and Jiang, H. (2013). The effects of phytic acid on the Maillard reaction and the formation of acrylamide. *Food Chem.* 141, 18–22. doi: 10.1016/j.foodchem.2013.02.107

Wang, L., Hu, L., Yan, S., Jiang, T., Fang, S., Wang, G., et al. (2017). Effects of different oligosaccharides at various dosages on the composition of gut microbiota and short-chain fatty acids in mice with constipation. *Food Funct.* 8, 1966–1978. doi: 10.1039/c7fo00031f

Wang, R., and Guo, S. (2021). Phytic acid and its interactions: contributions to protein functionality, food processing, and safety. *Compr. Rev. Food Sci. Food Saf.* 20, 2081–2105. doi: 10.1111/1541-4337.12714

Woyengo, T. A., Weihrauch, D., and Nyachoti, C. M. (2012). Effect of dietary phytic acid on performance and nutrient uptake in the small intestine of piglets. *J. Anim. Sci.* 90, 543–549. doi: 10.2527/jas.2011-4001

Xu, R. H., Xiu, L., Zhang, Y. L., Du, R. P., and Wang, X. (2019). Probiotic and hepatoprotective activity of *Lactobacillus* isolated from Mongolian camel milk products. *Benef. Microbes* 10, 699–710. doi: 10.3920/BM2018.0131

Xu, S. J., and Kim, B. S. (2014). Biocontrol of fusarium crown and root rot and promotion of growth of tomato by *Paenibacillus* strains isolated from soil. *Mycobiology* 42, 158–166. doi: 10.5941/MYCO.2014.42.2.158

Yang, F., Hou, C., Zeng, X., and Qiao, S. (2015). The use of lactic acid bacteria as a probiotic in swine diets. *Pathogens* 4, 34–45. doi: 10.3390/pathogens4010034

Yerlikaya, O. (2019). Probiotic potential and biochemical and technological properties of *Lactococcus lactis* ssp. lactis strains isolated from raw milk and kefir grains. *J. Dairy Sci.* 102, 124–134. doi: 10.3168/jds.2018-14983

Yu, X., Han, J., Li, H., Zhang, Y., and Feng, J. (2018). The effect of enzymes on release of trace elements in feedstuffs based on in vitro digestion model for monogastric livestock. *J. Anim. Sci. Biotechnol.* 9:73. doi: 10.1186/s40104-018-0289-2

Zhang, G. Q., Dong, X. F., Wang, Z. H., Zhang, Q., Wang, H. X., and Tong, J. M. (2010). Purification, characterization, and cloning of a novel phytase with low pH optimum and strong proteolysis resistance from *Aspergillus ficuum* NTG-23. *Bioresour. Technol.* 101, 4125–4131. doi: 10.1016/j.biortech.2010.01.001

Zhou, Z., Zhang, J., Zhang, X., Mo, S., Tan, X., Wang, L., et al. (2019). The production of short chain fatty acid and colonic development in weaning piglets. *J. Anim. Physiol. Anim. Nutr.* 103, 1530–1537. doi: 10.1111/jpn.13164

Zielińska, D., and Kołożyn-Krajewska, D. (2018). Food-origin lactic acid bacteria may exhibit probiotic properties: review. *Biomed Res. Int.* 2018:5063185. doi: 10.1155/2018/5063185

Conflict of Interest: The authors declare that the research was conducted in the absence of any commercial or financial relationships that could be construed as a potential conflict of interest.

Publisher's Note: All claims expressed in this article are solely those of the authors and do not necessarily represent those of their affiliated organizations, or those of the publisher, the editors and the reviewers. Any product that may be evaluated in this article, or claim that may be made by its manufacturer, is not guaranteed or endorsed by the publisher.

frontiers in Microbiology

ORIGINAL RESEARCH
published: 08 December 2021
doi: 10.3389/fmicb.2021.786121

OPEN ACCESS

Edited by:
Jia Yin,
Hunan Normal University, China

Reviewed by:
Zeying Huang,
Institute of Food and Nutrition Development, Chinese Academy of Agricultural Sciences (CAAS), China
Faizul Hassan,
University of Agriculture, Faisalabad, Pakistan
Dunxue Chen,
Guizhou University, China
Lu Ma,
Institute of Animal Sciences, Chinese Academy of Agricultural Sciences (CAAS), China

***Correspondence:**
Jianguo Zeng
zengjianguo@hunau.edu.cn
Qiuzhong Dai
daiqiuzhong@163.com
Qian Lin
linqian@caas.cn

† These authors have contributed equally to this work and share first authorship

Specialty section:
This article was submitted to Microbial Symbioses, a section of the journal Frontiers in Microbiology

Received: *29 September 2021*
Accepted: *10 November 2021*
Published: *08 December 2021*

Citation:
Peng S, Wang X, Wang Y, Lv T, Zhao H, Wang Y, Zhu S, Qiu H, Zeng J, Dai Q and Lin Q (2021) Effects of Dietary Bacillus and Non-starch Polysaccharase on the Intestinal Microbiota and the Associated Changes on the Growth Performance, Intestinal Morphology, and Serum Antioxidant Profiles in Ducks. Front. Microbiol. 12:786121. doi: 10.3389/fmicb.2021.786121

Effects of Dietary *Bacillus* and Non-starch Polysaccharase on the Intestinal Microbiota and the Associated Changes on the Growth Performance, Intestinal Morphology, and Serum Antioxidant Profiles in Ducks

Simin Peng[1,2†], Xin Wang[1†], Yuyu Wang[3†], Tuo Lv[1], Haohan Zhao[1], Yanzhou Wang[1], Siyuan Zhu[1], Huajiao Qiu[1], Jianguo Zeng[1,3*], Qiuzhong Dai[1,2*] and Qian Lin[1,3*]

[1] Institute of Bast Fiber Crops, Chinese Academy of Agricultural Sciences, Changsha, China, [2] Hunan Institute of Animal and Veterinary Science, Changsha, China, [3] College of Veterinary Medicine, Hunan Agricultural University, Changsha, China

Given the desirable results of using probiotics and enzyme preparations as feed supplements in poultry health, here, the effects of *Bacillus* and Non-starch Polysaccharase (NSPase) on the growth performance, serum antioxidant profiles, and gut microbial communities of early stage ducks is investigated. A total of 400 *Zhijiang* ducks (of similar body weight and 1 day age) was selected and randomly divided into four groups. The feeding period was 28 days. Each group contained 10 replicates of 10 birds. Control group (I) was fed with basal diet, while treatment groups II to IV were fed, respectively, with 150 mg/kg NSPases, 25 mg/kg *Bacillus* probiotics, and 150 mg/kg NSPases + 25 mg/kg *Bacillus* probiotics in their basal diet. The results demonstrated that dietary *Bacillus* (25 mg/kg) increased average final weight, average daily gain (ADG), and decreased the malonaldehyde (MDA) in birds ($P < 0.05$). Dietary *Bacillus* (25 mg/kg) and NSPases + *Bacillus* (150 mg/kg + 25 mg/kg) presented much higher glutathione (GSH) and activities of superoxide dismutase (SOD) in birds ($P < 0.05$). Additionally, as revealed by β-diversity indices and analysis of similarities, dietary NSPases + *Bacillus* could affect the ileum microbial abundances and diversities at the genera level ($P < 0.05$), but it had no effect on the caecal microbiota. Also, 16S rRNA sequencing revealed that dietary *Bacillus* and NSPases + *Bacillus* increased the populations of *Ruminococcaceae* genera in the cecum ($P < 0.05$), and *S24-7_group* and *Lactobacillus* genera in the ileum ($P < 0.05$). However, dietary NSPases and *Bacillus* alone and in combination could significantly decrease the content of *Bacteroides* in the ileum ($P < 0.05$). According to Spearman correlation analysis, 7 ilea bacterial microbiomes (*S24-7 group, Lactobacillus, Subgroup 2, Subgroup 1, Kitasatospora,*

Candidatus Solibacter, and Akkermansia) were positively correlated with SOD ($P < 0.05$). In conclusion, *Bacillus* (25 mg/kg) and NSPases (150 mg/kg) included in the diet could efficiently enhance the growth performance by altered gut microbiota composition at the genera level and antioxidant indices of ducks.

Keywords: gut microbiota, *Bacillus*, non-starch polysaccharidase, growth performance, serum antioxidant profiles, intestinal morphology, duck

INTRODUCTION

Due to the antibiotic resistance of bacteria being on the rise (Guo et al., 2016) and the increasing consumer concern regarding poultry products, antibiotic-free flocks (Gadde et al., 2017), and environmental sustainability (Xing et al., 2015), a prohibition on antibiotics had been imposed in Europe (Stolker et al., 2007), South Korea (Kumar et al., 2012), and China (Hu and Cowling, 2020) since 2006, 2012, and 2020, respectively. Hence, replacing antibiotics with alternative products (Han et al., 2017) has become a hot research topic in recent years. Probiotics and enzymes are attracting much attention as important alternatives to antibiotics.

Bacillus is widely used in poultry diets as a type of probiotic, which improves the productive performance of poultry (Naumova et al., 2021) by producing naturally synthesized antimicrobial peptides, maintaining microbial flora balance in the intestie, accelerating the increase of beneficial microbiota along the gastrointestinal tract, and adjusting the immunological function and gut morphology (Sen et al., 2012; Grant et al., 2018). Many findings confirmed the significant improvement of growth performance, immune response, cecal microbial population, and intestinal morphology of weanling pig (Lee et al., 2014), Cherry Valley ducks (Guo et al., 2016), and Ross broiler chicks (Sen et al., 2012) with Bacillus-based diets. In addition, lacking enough enzymes to fully digest fiber, birds rely on exogenous enzymes in their diets to improve the fiber digestion process (Alagawany et al., 2018). As one of the most important exogenous enzymes, non-starch polysaccharidase (NSPase) is commonly used in poultry diets and plays many essential roles such as breaking down the non-starch polysaccharides, releasing nutrients encapsulated by the cell wall, reducing intestinal viscosity, improving animals' utilization of nutrients, and affecting the composition and metabolic potential of bacterial populations (Kiarie et al., 2013; Ravindran, 2013; Amerah, 2015). Ao et al. (2010) and Coppedge et al. (2012) reported the supplementation of NSPase could improve the growth performance of market broilers and pigs and be used as a strategy to degrade antinutritional compounds so as to reduce dietary energy levels and costs.

Both *Bacillus* and NSPase can improve the productive performance of poultry, and are able to directly or indirectly affect the intestinal flora. However, it is not clear whether there is a synergistic effect between them. A few studies demonstrated that there was a certain synergistic effect on improving intestinal health, promoting nutrient digestion and growth in broiler chickens, when both *Bacillus* and NSPase were used as a supplement in the feed (Lin Q. et al., 2012; Wealleans et al., 2017). However, no such study has been conducted in ducks. In the present study, we aimed to study the effects of *Bacillus* and NSPase on the growth performance, serum antioxidant profiles, intestine morphology, and intestinal microbiota composition in ducks.

MATERIALS AND METHODS

All the experimental procedures of this study were approved by the Animal Care and Use Committee of the Institute of Bast Fiber Crops, Chinese Academy of Agricultural Sciences.

Experimental Design, Diets, and Birds

Zhijiang duck, an important indigenous bird breed in Southern China, is characterized by rapid growth, strong disease resistance, unique flavor, and delicious meat. Usually, they are sold as products in the marketplace at the age of 56 days, often with an average body weight of around 2,650 g for a single duck. From the age of 1–28 days, *Zhijiang* duck are at the critical stage of intestinal development and maximum growth. Therefore, a total of 400 female *Zhijiang* ducks (aged 1 day and free of infectious disease) were obtained from Hunan Hexiang Duck Industrial Co., Ltd. They were then transferred into the laboratory of the Bast Fiber Crops Institute, Chinese Academy of Agricultural Sciences for a feeding period of 28 days. Feed and water were provided *ad libitum* during the whole trial period. Each *Zhijiang* duck was weighed at the beginning to obtain the average initial weight, in order to divide them into four groups without significant difference among groups. Each group (100 *Zhijiang* ducks) was further subdivided into 10 cages (10 ducks/cage), and the dimension of each cage was 150 cm × 150 cm. Group I received a basal diet (BD), Group II received BD supplemented with 150 mg/kg NSPases (Manufactured by Shanghai CJYOUTELL Biotechnology Co., Ltd., China); the main components of this NSPases are cellulase (≥ 2,000 IU/g) and xylanase (≥ 30,000 IU/g). Group II received BD supplemented with 25 mg/kg *Bacillus* probiotics; the main components being *Bacillus subtilis* and *Bacillus lichenif or mi s*, 5×10^{12} CFU/g, manufactured by Wuhan Xiongfeng Technology Co., Ltd., China. Group IV received BD supplemented with 150 mg/kg NSPases + 25 mg/kg *Bacillus* probiotics. The BD was prepared in accordance with the Nutrient Requirements of Ducks (National Research Council, 1994) and the Nutrient Requirements of Meat-type Duck (China,

NY/T 2122-2012) (Ministry of Agriculture of the People's Republic of China, 2012; **Table 1**).

Growth Performance

Birds were weighed at the beginning (day 1) and the end (day 28) of the trial for calculation of growth performance. Average daily weight gain (ADG), average daily feed intake (ADFI), and feed/gain ratio (F/G) were calculated according to the data from each cage for the whole experimental period. The birds were fasted for 12 h before weighting and sampling.

Sample Collection

At the end of the trail, one bird per cage with a live weight close to the mean (10 birds per group) were selected for sampling. Blood samples from the wing vein were collected into vacuum blood collection tubes and were centrifuged at 3,000 × g for 10 min to collect the serums. Birds were slaughtered by exsanguination from the jugular vein. Samples of the small intestine were immediately removed and then divided into three parts: Duodenum, jejunum, and ileum. Intestinal tissue samples were cut from the medial of the duodenum, jejunum, and ileum with a segment of 1.5 cm, and lightly flushed using physiological saline (154 mmol/L) and drained on filter paper. Then these fresh samples were fixed into 10% neutral buffered formalin for further analysis of intestinal mucosal morphology (Watkins et al., 2004; Applegate et al., 2005). Samples of chyme in each duck's ileum and cecum were collected separately into 2 mL EP tubes and flash-frozen using liquid N_2 and stored at −80℃ until analysis.

Serum Antioxidant Capacity

Samples of serum were analyzed for malonaldehyde (MDA), antioxidant biomarkers including glutathione (GSH), activities of superoxide dismutase (SOD),glutathione peroxidase (GSH-Px), total antioxidant capacity (T-AOC), and Catalase (CAT) were determined by the commercial assay kits (Nanjing Jiancheng Bioengineering Institute, China) with an automated fluorescence instrument (MultiskanM^{TM} SkyHigh, Thermo Fisher Scientific, Waltham, MA, United States).

TABLE 1 | Composition and nutrient levels of basal diets (air-dry basis,%).

Item	Ingredients	Item	Nutrient levels[b]
Corn	46.95	ME/(Mcal/kg)	2.83
Soybean meal	25.30	CP	17.37
Rice bran	9.00	Calcium	0.90
Barley	14.52	Total P	0.68
Limestone	1.53	Available P	0.36
$CaHPO_4{\cdot}2H_2O$	1.20	NaCl	0.34
NaCl	0.30	Lys	1.00
98.5% *DL*- Met	0.11	Met	0.39
78% *L*- Lys	0.09	Met + Cys	0.68
1% Premix[a]	1.00	CF	3.34
Total	100.00		

[a] *The premix provided the following (per kilogram of complete diet) micronutrients: VA 12 000 IU, VD_3 2 500 IU, VE 20 mg, VK_3 3 mg, VB_1 3 mg, VB_2 8 mg, VB_6 7 mg, VB_{12} 0.03 mg, D-pantothenic acid 20 mg, nicotinic acid 50 mg, biotin 0.1 mg, folic acid 1.5 mg, Cu (as copper sulfate) 9 mg, Zn (as zinc sulfate) 110 mg, Fe (as ferrous sulfate) 100 mg, Mn (as manganese sulfate) 100 mg, Se (as sodium selenite) 0.16 mg, I (as potassium iodide) 0.6 mg.* [b] *Nutrient levels are calculated values.*

Measurement of Intestinal Mucosal Morphology

The intestinal morphological measurement of the duodenum, jejunum, and ileum was based on the method reported in our previous research (Lin Q. et al., 2017). Briefly, 1.5 cm-intestinal tissue samples of the duodenum, jejunum, and ileum were fixed and embedded in paraffin, sectioned at a thickness of 5 or 6 μm using a microtome (RM-2235, Leica microsystems AG., Hessen, Germany), then mounted on glass slides and subsequently stained with hematoxylin and eosin (HE staining). We observed the finished slides and chose the typical microscopic fields to take photos of under an Olympus Van-Ox S microscope (Opelco, Washington, DC). Visual measurements of the villus height, crypt depth, and intestinal wall thickness from each slide were made on 10 readings at 40 × and 100 × magnifications using an image analysis system (Image-Pro, Media Cybernetics, Inc., Silver Springs, MD, United States). Then the ratios of villus height to crypt depth (V/C) can be calculated.

Gut Microbiota Composition by 16S rRNA Gene Sequencing

The genomic DNA of the ileum and cecum microbial community were extracted according to the manufacturer's instructions by the E.Z.N.A. DNA kits (Omega Bio-tech, Norcross, GA, United States). Ten ileum/cecum digesta samples were mixed in pairs for the 16S rDNA sequence determination. The 16S rRNA gene V3 + V4 regions of the bacteria were amplified with the primer pairs 806R (5′-GGACTACHVGGGTWTCTAAT-3′) and 338F (5′-ACTCCTACGGGAGGCAGCAG-3′) combined with adapter sequences and barcode sequences. Next, the DNA was purified by AxyPrep DNA Gel Extraction Kits (Axygen Bioscience, Union City, CA, United States). Finally, the sequencing of 16S rRNA gene was performed on an Illumina HiSeq 2500 platform (Illumina, San Diego, CA, United States) with purified amplicons were paired.

Reads with complete (length > 300 bp) sequence barcodes were screened for the following analysis. Obtained sequences of samples were filtered by using QIIME (version 1.17) software and the number of operational taxonomic units (OTUs) with a cut of 97% sequence similarity were determined by using UPARSE (version 7.1). Each OTU represented sequence was analyzed by Ramer-Douglas-Peucker (RDP) Classifier version 2.2 via the 16S rRNA database.

The alpha diversities of the ileal and cecal microbiota, including abundance-based coverage estimator (ACE), Chao1 estimator, Simpson and Shannon diversity index were calculated to investigate the richness and diversity of the community, respectively. Principal coordinate analysis (PCoA), and Non-MetricMulti- Dimensional Scaling (NMDS) were calculated to evaluate the difference of the microbial community based on the Bray-Curtis dissimilarity matrix. The analysis procedures of ileal and cecal microbiota were processed on the free online

platform of BMK Cloud Platform (BioMarker Technologies Co., Ltd., Beijing, China).

Statistical Analysis

One-way ANOVA model was performed to identify significant differences in growth performance, serum antioxidant profiles, intestinal mucosal morphology, and richness and community diversity of bacteria. All the results were presented as means plus standard errors of the means (SEM). Differences between means of all groups were considered significant at *P*-value less than 0.05. The analysis of statistical comparison was conducted on the basis of Student's *t*-test to declare the difference of the relative abundance of the ileal and cecal microbiota between two groups. Spearman correlation analysis was performed to identify the relationship between ileum and cecum microbial community and measured parameters. Heatmap was constructed using Prism 9.0 (GraphPad Software, San Diego, CA). All the statistical analysis was done with SPSS 19.0 (IBM, Armonk, New York).

RESULTS

Growth Performance

Growth performances are shown in **Table 2**. Compared to the control group I, the values of average final weight and ADG showed a significant increase in Group III, whereas Group II and Group IV exhibited an increasing trend with no significant difference ($P > 0.05$). The ADFI and F/G of ducks among any groups did not change significantly ($P > 0.05$) during the entire experimental period.

Serum Antioxidant Profiles

Six serum antioxidant indicators were presented in **Table 3**. GSH-Px ($P = 0.878$), T-AOC ($P = 0.411$) and CAT ($P = 0.282$) in different treatment group showed similar levels. But significant differences were told among groups in the serum levels of GSH, SOD, and MDA ($P < 0.01$). Compared to Group I, Groups III, and IV showed a significant increase in the serum level of SOD and GSH ($P < 0.01$). In contrast, the level of MDA showed a significant decrease in Groups II, III, and IV compared to that of Group I.

TABLE 2 | Effects of each treatment[1] on growth performance of Zhijiang ducks[2] (1 28 days).

Item	Group I	Group II	Group III	Group IV	SEM	*P*-value
Average initial weight, g	45.72	45.82	45.84	45.80	0.048	0.835
Average final weight, g	1323.00^{b}	1343.19^{a,b}	1369.58^{a}	1355.28^{a,b}	6.161	0.046
ADG, g	47.31^{b}	48.05^{a,b}	49.03^{a}	48.50^{a,b}	0.228	0.046
ADFI, g	99.87	99.95	98.62	100.31	0.918	0.929
F/G	2.11	2.08	2.01	2.07	0.020	0.344

ADG, average daily weight gain; ADFI, average daily feed intake; F/G, feed to gain ratio.
[1]Group I (control group), Group II (150 mg/kg NSPases in basal diet), Group III (25 mg/kg Bacillus probiotics in basal diet), Group IV (150 mg/kg NSPases + 25 mg/kg Bacillus probiotics in basal diet).
[2]Data is the mean of 10 replicates per treatment.
$^{a-b}$Different superscript letters in the same row indicate significant differences at $P < 0.05$.

TABLE 3 | Effects of each treatment[1] on antioxidative parameters of Zhijiang ducks[2] (1 28 days).

Item	Group I	Group II	Group III	Group IV	SEM	*P*-value
MDA, nmol/mL	7.00^{a}	5.39^{b}	3.65^{c}	5.76^{b}	0.306	<0.01
GSH, μmol/L	16.46^{b}	17.12^{b}	21.08^{a}	19.81^{a}	0.494	<0.01
SOD, U/mL	65.32^{b}	68.83^{b}	74.31^{a}	76.31^{a}	1.164	<0.01
GSH-Px, U/mL	193.97	189.16	187.39	188.28	2.908	0.878
T-AOC, mmol/mL	0.86	0.97	0.93	1.01	0.032	0.411
CAT, U/mL	1.03	0.92	0.96	0.87	0.029	0.282

MDA, malonaldehyde; GSH, glutathione; SOD, superoxide dismutase; GSH-Px, glutathione peroxidase; T-AOC, total antioxidant capacity; CAT, Catalase.
[1]Group I (control group), Group II (150 mg/kg NSPases in basal diet), Group III (25 mg/kg Bacillus probiotics in basal diet), Group IV (150 mg/kg NSPases + 25 mg/kg Bacillus probiotics in basal diet).
[2]Data is the mean of 10 replicates per treatment.
$^{a-c}$Different superscript letters in the same row indicate significant differences at $P < 0.05$.

Intestinal Mucosal Morphology

According to **Table 4**, no significant difference ($P > 0.05$) was observed on any intestinal morphology parameters of all groups. But for the duodenum, jejunum, and ileum, an increasing trend in villus height and V/C, and a decreasing trend in Crypt depth has been shown in Groups II, III, or IV when compared to Group I.

Modulation of Intestinal Microbiota

Shannon, Simpson, ACE, and Chao, are important indexes of the α diversity of a bacterial community. The results (as shown in **Table 5**) were obtained through the 16S rRNA sequencing. For ileum, the values of ACE ($P = 0.007$) and Chao ($P = 0.006$) showed a significant increasing trend in Group IV, and they also increased in Group II and Group III. But instead, the α diversity parameters of the cecum showed no change ($P > 0.05$) among groups. PCoA and NMDS revealed the variation between microbiome profiles based upon Bray-Curtis dissimilarity. For cecum, PCoA plot (**Figure 1A**) and NMDS plot (**Figure 1B**) revealed no differences in microorganism distributions between the four groups at the genera level. However, in the ileum, samples from Group I and Group II were clearly distributed in both clusters, on the left and right parts of both PC1 (**Figure 1C**) and NMDS1 (**Figure 1D**), respectively.

In cecum, microbial communities among different groups at the genus level are shown in **Figure 2A**. *Faecalibacterium*, *Ruminococcaceae*, *Lachnospiraceae*, *Torques group*, and *UCG-014* were the dominant microbes and occupied approximately 50% of the total genera. *Faecalibacterium* was detected in the highest abundance in Group I, whereas the *Ruminococcaceae* and *Torques group* showed lower abundance than other groups. As for *Lachnospiraceae*, higher abundance was observed in Group II and IV. For the microbial composition analysis, pair-wise comparisons with Student's T approach were used between

experimental groups and the control group. Significant differences were found in *Ruminococcaceae* ($P < 0.01$) (**Figure 2B**) and *vadinBB60 group* ($P < 0.05$) (**Figure 2C**) between Group I and IV, *Ruminococcaceae* ($P < 0.05$) (**Figure 2B**) between Group I and IV.

In the ileum (**Figure 3A**), *Candidatus Arthromitus* and *Bacteroides* were dominant genera in Groups I, II, and III which represented more than 30% of the genus type. However, they were detected in Group IV with low abundance. As for *Barnesiella*, *Intestinibacter,* and *Faecalibacterium*, higher abundance was observed in Group I. Additionally, the relative abundance of *S24-7 group*, *Lactobacillus,* and *Subgroup 2* in Group IV were higher compared with other groups. Through the Student's *T*-test, there were significant differences of *Bacteroides*, *S24-7 group*, *Lactobacillus,* and *Subgroup 2* ($P < 0.05$) (**Figures 3B–E**) between Group I and test groups.

Furthermore, the correlation between the microbiota composition of ceacum/ileum and the indices of growth performance and antioxidative capacity were shown in **Figure 4**. After Spearman's correlation analysis in ceacum, ADFI and F/G were found to have significant positive correlations with *Faecalibacterium* ($P = 0.018$ and $P = 0.031$), while negative correlations were examined between GSH and the *Bacteroides* ($P = 0.039$), and ADFI and the *Eisenbergiella* ($P = 0.027$). In ileum (**Figure 4B**), significantly positive results were observed between SOD and *S24-7 group* ($P = 0.013$), *Lactobacillus* ($P = 0.024$), *Subgroup 2* ($P = 0.013$), *Subgroup 1* ($P = 0.010$), *Kitasatospora* ($P = 0.002$), *Candidatus Solibacter* ($P = 0.009$), and *Akkermansia* ($P = 0.040$). Meanwhile, SOD was significantly negative in the *Bacteroides* ($P = 0.024$) and *Alistipes* ($P = 0.009$). In addition, significant positive correlations were existed between T-AOC and *Akkermansia* ($P = 0.015$),GSH

TABLE 4 | Effect of each treatment[a] on intestinal morphology of *Zhijiang* ducks[b] (1 28 days).

Item	Group I	Group II	Group III	Group IV	SEM	*P*-value
Duodenum						
Villus height, μm	577.45	590.31	598.00	610.14	12.455	0.835
Crypt depth, μm	130.20	122.07	121.67	129.11	2.376	0.452
V/C	4.45	4.86	4.98	4.77	0.113	0.394
Intestinal wall thickness, μm	193.62	185.93	188.24	196.25	3.886	0.785
Jejunum						
Villus height, μm	582.71	586.32	606.55	602.88	11.677	0.866
Crypt depth, μm	129.62	122.12	117.19	125.40	2.392	0.314
V/C	4.53	4.88	5.23	4.85	0.124	0.256
Intestinal wall thickness, μm	192.18	190.62	176.98	184.00	3.161	0.313
Ileum						
Villus height, μm	544.05	554.70	562.82	537.81	8.685	0.761
Crypt depth, μm	123.71	117.50	121.86	120.09	2.201	0.794
V/C	4.42	4.76	4.65	4.51	0.073	0.356
Intestinal wall thickness, μm	192.30	182.38	183.14	182.94	3.292	0.684

V/C, the ratios of villus height to crypt depth.
[a]Group I (control group), Group II (150 mg/kg NSPases in basal diet), Group III (25 mg/kg Bacillus probiotics in basal diet), Group IV (150 mg/kg NSPases + 25 mg/kg Bacillus probiotics in basal diet).
[b]Data is the mean of 10 replicates per treatment.

TABLE 5 | α diversity of cecum and ileum microbial community in different groups[1,2].

Item	Group I	Group II	Group III	Group IV	SEM	*P*-value
Cecum						
Shannon	3.00	3.61	3.47	3.19	0.135	0.404
Simpson	0.208	0.089	0.114	0.147	0.023	0.319
ACE	294.40	311.18	304.62	305.61	4.449	0.639
Chao	299.04	313.05	304.77	309.10	4.604	0.766
Ileum						
Shannon	3.15926	4.22804	3.84302	5.84306	0.391	0.081
Simpson	0.13528	0.1852	0.16514	0.01094	0.043	0.508
ACE	460.473[b]	667.262[b]	735.252[a,b]	975.853[a]	58.653	0.007
Chao	441.658[c]	674.64[b,c]	740.653[a,b]	982.825[a]	60.437	0.006

[1]Group I (control group), Group II (150 mg/kg NSPases in basal diet), Group III (25 mg/kg Bacillus probiotics in basal diet), Group IV (150 mg/kg NSPases + 25 mg/kg Bacillus probiotics in basal diet).
[2]Data is the mean of 5 replicates per treatment.
[a−c]Different superscript letters in the same row indicate significant differences at $P < 0.05$.

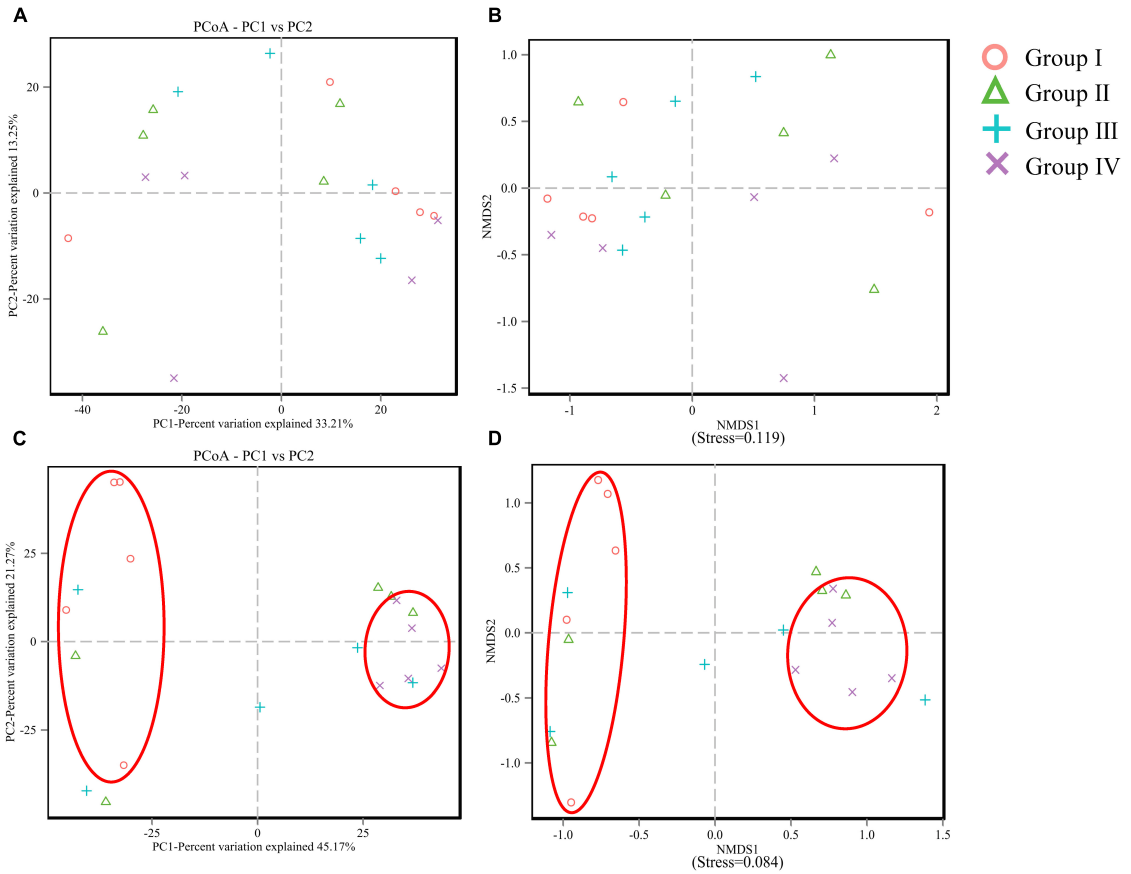

FIGURE 1 | PCoA and NMDS analysis of cecum **(A,B)** and ileum **(C,D)** microbial community compositions based on information of operational taxonomic units (OTU).

and *Subgroup 1* (P = 0.042),and GSH and *Kitasatospora* (P = 0.042).

DISCUSSION

Several lines of studies demonstrated that *Bacillus* Probiotics could improve the growth performance of poultry (Jeong and Kim, 2014; Lee et al., 2015; Lin Y. et al., 2017). In the current study, we found that *Bacillus* probiotics supplementation could increase the average final weight and ADG by modulating antioxidative status and intestinal microflora. In fact, the antioxidant effect of *Bacillus* Probiotics has been verified in rats before (Paik et al., 2005). In our study, we found *Bacillus* probiotics have the efficacy of significantly decreasing the serum level of MDA and increasing the level of SOD and GSH. These results revealed that feeding ducks with *Bacillus* Probiotics can also improve the antioxidant status. Meanwhile, there were a higher relative proportion of the genera *Ruminococcaceae*, *vadinBB60 group, and S24-7 group* in the *Bacillus*-fed group in the cecal or ileal microbial community. Many species belonging to these genera are able to produce short-chain fatty acid (SCFA), especially butyrate (Hooda et al., 2012; Ridlon et al., 2015), which serves as a preferred energy source for enterocytes and a known regulator of cellular differentiation and proliferation within the intestinal mucosa (Sikandar et al., 2017; Bedford and Gong, 2018). This can contribute to improving the morphological development of the intestines and to reinforce the intestinal defense barrier, for instance, strengthening tight junctions, thereby promoting animal growth (Le Blay et al., 2000; Fukunaga et al., 2003; Bordin et al., 2004; Peng et al., 2007). Additionally, a significant increasing trend was also observed for *Lactobacillus* of the ileum in the *Bacillus*-treated group. This point deserves further investigation as it might be of interest, as *Lactobacillus* may provide nutrients to the host and help defend against opportunistic pathogens (Cross, 2002; LeBlanc et al., 2013). Interestingly, the *Bacteroides* genus was largely decreased with the presence of *Bacillus*, which conflicts with the findings of a very recent broiler study (Wang et al., 2017). However, studies using other species, such as swine, have shown that *Bacillus subtilis* supplementation decreased the copy numbers and percentage of *Bacteroidetes* while it increased the percentage of *Firmicutes* in the cecal contents (Cui et al., 2013). Similarly, a significant decrease trend was also revealed in *Bacteroidetes* of the ileum in our study. Given the fact that the decrease in *Bacteroidetes* and the increase in the *Firmicutes*/*Bacteroidetes* ratio are positively correlated with

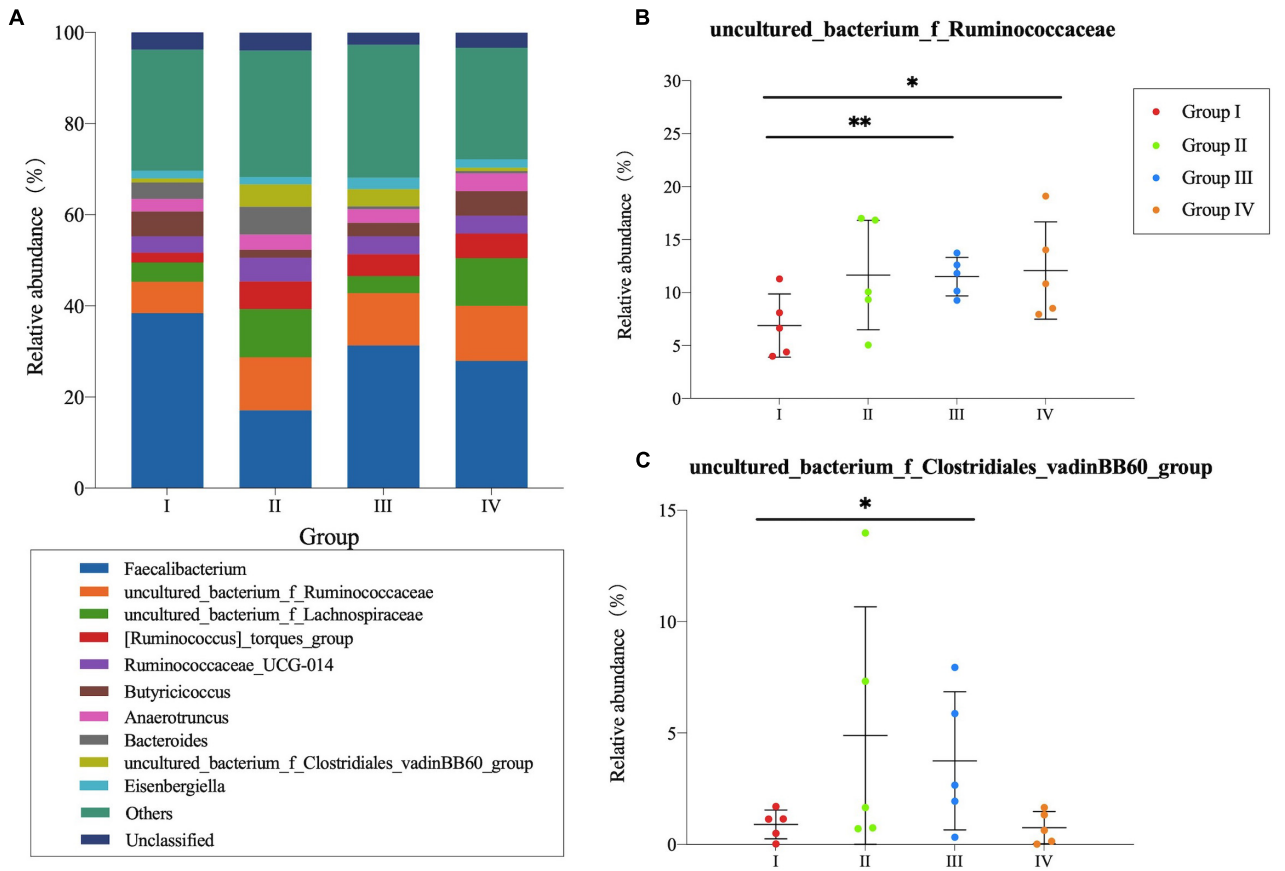

FIGURE 2 | Community structure of bacteria at genus level in the cecum of *Zhijiang* ducks. Histogram **(A)** of the top 10 genera in each group. Significant difference relative abundance of *Ruminococcaceae* **(B)** and *vadinBB60_group* **(C)** at the genera level. (*$P < 0.05$ and **$P < 0.01$ compared with control group).

body mass index in humans (Koliada et al., 2017) and associated with an increase in ADG (Salaheen et al., 2017), our data revealed that *Bacillus* Probiotics promotes duck growth by improving the intestinal flora.

Nowadays, poultry feed with higher levels of NSP may reduce the digestibility of nutrients in their diets (Salim et al., 2010), which can lead to poorer growth and performance of birds (Annison and Choct, 1991). One solution to this issue accounting for feed cost and variability is to use exogenous enzymes (Woyengo et al., 2019), including NSPases. In our study, the addition of NSPases increased the average final weight and ADG of ducks, but insignificantly. A similar result was also obtained by Uthai et al. (2004). They found NSPase type mixture supplementation could improve the growth performances (average total weight gained, average daily gain, and average feed intake) of pigs also with non-statistically significant differences. Besides, Ao et al. (2010) reported that 2% NSPase supplementation to based diets for weaned piglets did not significantly improve performance. But interestingly, the average daily gain and gain/feed were increased 4.40 and 6.26% when fed with 1% NSPase supplementation. Variation in the results is likely associated with the content of substrates (Ao et al., 2010). However, a significant increase was found in the proportions of the *S24-7 group*, *Lactobacillus*, and *Subgroup 2,* while a significant decrease was found in the proportion of *Bacteroides* in the NSPase-treated group at the ileal level. Considering the results that the decrease in *Bacteroidetes* and the increase in *S24-7 group*, *Lactobacillus,* and *Subgroup 2* are positively correlated with SOD activity. Thus, ducks fed with NSPases showed improved growth performance, and increased antioxidant capacity might be linked to the microbial changes. In many studies, the change of intestinal microflora was beneficial for the health and welfare of poultry. Naumova et al. (2021) found that the beneficial effect on the production of ducks was associated with the changes in gut microbiota due to *Bacillus*-feed probiotic supplementation. Dietary probiotics can enhance growth performance by the regulation of intestinal microbial composition, the immune system, and maintenance of intestinal integrity and barrier function, as described by Tuohy et al. (2003). In our study, the major changes were found within the foregut area and the predominant role of *Lactobacillus* was enhanced. Lactobacillus consists of gram-positive and facultative anaerobes that produce lactic acid, which can create a low pH environment and inhibit the growth of pathogens (Rodriguez-Cabezas et al., 2010). In addition, Lactobacillus was proven to be of antioxidant activity (Lin and Chang, 2000), and having the capacity of

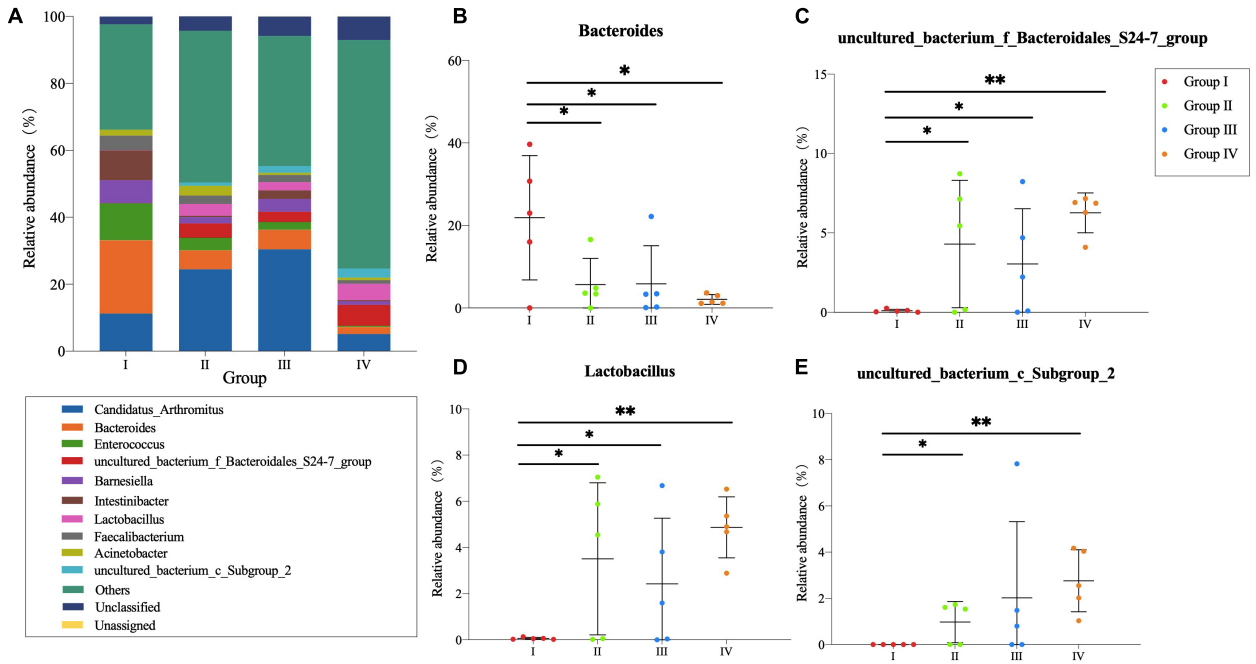

FIGURE 3 | Community structure of bacteria at genus level in the ileum of *Zhijiang* ducks. Histogram **(A)** of the top 10 genera in each group. Significant difference relative abundance of *Bacteroides* **(B)**, *S24-7_group* **(C)**, *Lactobacillus* **(D)**, and *Subgroup_2* **(E)** at the genera level. (*$P < 0.05$ and **$P < 0.01$ compared with the control group).

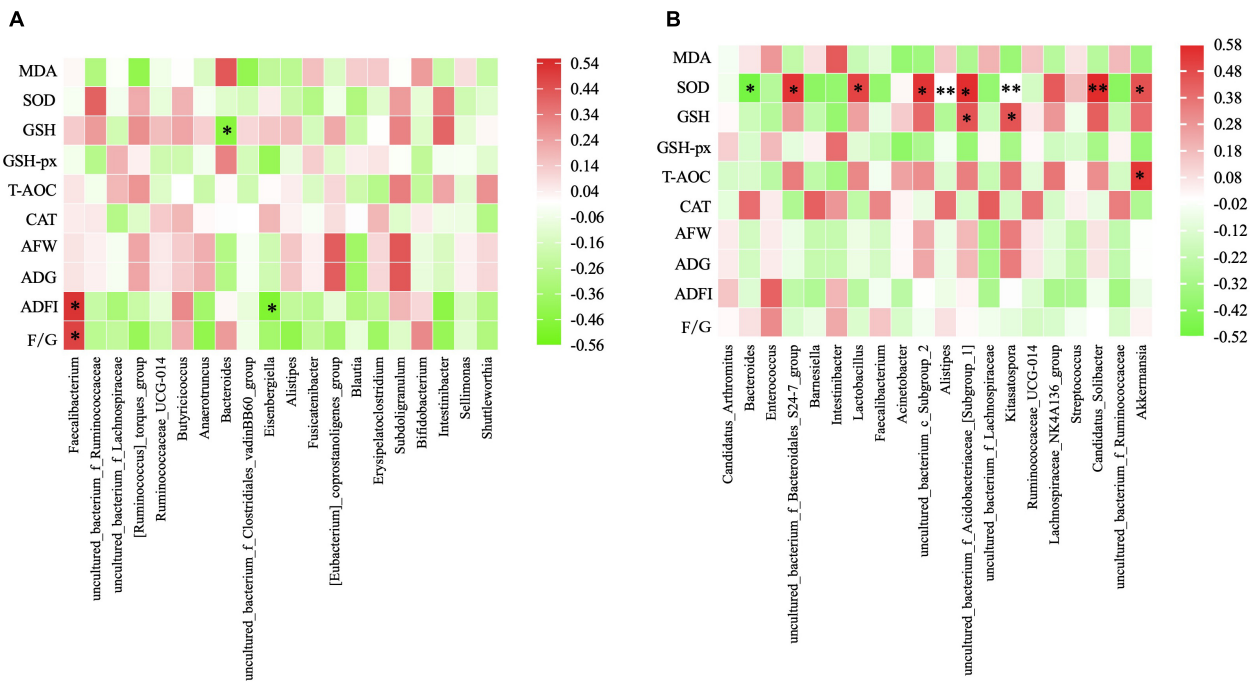

FIGURE 4 | Heatmap of Spearman rank correlation between the cecal microbiota. **(A)** /ileum microbiota **(B)** and the measured parameters under different treatment. The genus with relative abundance in the top 10 are presented and the intensity of the colors performed the degree of association. Green, negative correlation; Red, positive correlation. AFW, average final weight; ADG, average daily weight gain; ADFI, average daily feed intake; F/G, feed to gain ratio. MDA, malonaldehyde; GSH, glutathione; SOD, activities of superoxide dismutase; GSH-Px, glutathione peroxidase; T-AOC, total antioxidant capacity; CAT, catalase. *$P \leq 0.05$, **$P \leq 0.01$.

scavenging free radicals to alleviate damages induced by oxidative stress (Xin et al., 2014). It indicated that the increase of the genus Lactobacillus probably enhances the antioxidant activity of duck. However, other bacterial species and their interaction (significantly positively associated with SOD) were still unclear.

In the present study, *Bacillus* probiotics and *NSPases* supplementation have been proven to be a potential method to improve the average final weight and ADG of ducks. Our findings are consistent with the result reported by Lin Q. et al. (2012), who demonstrated that *Bacillus* probiotics and NSPases showed obvious synergistic growth-promoting effects on yellow-feathered broilers. Most noteworthily, compared to the basal diet group, the diversity index of ACE and Chao increased when the treatment of NSPase or *Bacillus* Probiotics alone or combined, especially, the significantly increased ($P < 0.05$) of ACE and Chao revealed in group IV. The PCoA and NMDS results further indicated that the group of diet NSPases + *Bacillus* was far from the control group, which was consistent with the above ACE and Chao analysis results. Our results were consistent with Klein et al. (2015) and Liu et al. (2018). They reported that the beneficial effects may be observed from the use of multiple enzymes or mixed-use of Bacillus subtilis and photosynthetic bacteria. Moreover, a significant increase was found in proportions of *Ruminococcaceae*, *S24-7 group*, *Lactobacillus*, and *Subgroup 2,* and a significant decrease was found in the proportion of *Bacteroides* in NSPase + *Bacillus* Probiotics-treated group at the cecal or ileal level. An obvious change in ACE or Chao index would suggest the deep changes in microbial diversity. On one hand, NSPase might affect the intestinal microbiota by reducing the undigested substrates and some short-chain oligosaccharides with potential prebiotic effects were created (*in situ*) from cell wall NSP (Kiarie et al., 2013). On the other hand, *Bacillus* probiotics could influence the distribution and colonization of the innate microflora along the gastrointestinal tract, reduce the competition for nutrients between microbes and the host, promote the growth and proliferation of other good symbiotic bacteria (Grant et al., 2018). To summarize, it has been suggested that *Bacillus* Probiotics and NSPases have a significant synergistic effect on improving the intestinal microflora of ducks.

CONCLUSION

Including *Bacillus* (25 mg/kg) and NSPases (150 mg/kg) in the diet could efficiently enhance growth performance via altering gut microbiota composition at the genera level and antioxidant indices of ducks. By comparison, the supplementation combining both *Bacillus* and NSPases showed the best effect for microbial abundances and diversities. Thus, using an additive of both *Bacillus* and NSPases could be recommended in diets during the early stage of *Zhijiang* ducks.

DATA AVAILABILITY STATEMENT

The data analyzed in this study is subject to the following licenses/restrictions: The data used to support the findings of this study are available from the corresponding author upon request. Requests to access these datasets should be directed to QL, linqian@caas.cn.

ETHICS STATEMENT

The animal study was reviewed and approved by the experimental procedures of this study were approved by the Institutional Animal Care and Use Committee of Institute of Bast Fiber Crops, Chinese Academy of Agricultural Sciences.

AUTHOR CONTRIBUTIONS

HQ, QL, and QD conceived and designed the experiments. XW, YZW, TL, SP, and HZ prepared the samples. XW completed the serum indices measurement. YYW detected the growth performance index. YYW and QL performed the sequencing of the 16S rRNA gene. SP and SZ completed the data analysis. SP and QL wrote the manuscript. QL and JZ refined the article. All authors contributed to the article and approved the submitted version.

FUNDING

The authors gratefully acknowledge the support from the Key R&D Program of Hunan Province (Grants: 2020NK2061 and 2020NK2031), Hunan Natural Science Foundation (Grant: 2019JJ50710), Agricultural Science and Technology Innovation Program (ASTIP-IBFC), Central Public-interest Scientific Institution Basal Research Fund (Grants: 1610242021005 and 1610242021006), and Modern Agricultural Technical System Foundation of China (CARS-42).

REFERENCES

Alagawany, M., Elnesr, S. S., and Farag, M. R. (2018). The role of exogenous enzymes in promoting growth and improving nutrient digestibility in poultry. *Iranian J. Vet. Res.* 19:157.

Amerah, A. M. (2015). Interactions between wheat characteristics and feed enzyme supplementation in broiler diets. *Anim. Feed Sci. Technol.* 199, 1–9. doi: 10.1016/j.anifeedsci.2014.09.012

Annison, G., and Choct, M. (1991). Anti-nutritive activities of cereal non-starch polysaccharides in broiler diets and strategies minimizing their effects. *World's Poultry Sci. J.* 47, 232–242. doi: 10.1079/wps19910019

Ao, X., Meng, Q. W., Yan, L., Kim, H. J., Hong, S. M., Cho, J. H., et al. (2010). Effects of non-starch polysaccharide-degrading enzymes on nutrient digestibility, growth performance and blood profiles of growing pigs fed a diet based on corn and soybean meal. *Asian Austral. J. Anim. Sci.* 23, 1632–1638. doi: 10.5713/ajas.2010.10123

Applegate, T. J., Karcher, D. M., and Lilburn, M. S. (2005). Comparative development of the small intestine in the turkey poult and Pekin duckling. *Poult. Sci.* 84, 426–431. doi: 10.1093/ps/84.3.426

Bedford, A., and Gong, J. (2018). Implications of butyrate and its derivatives for gut health and animal production. *Anim. Nutr.* 4, 151–159. doi: 10.1016/j.aninu.2017.08.010

Bordin, M., D'Atri, F., Guillemot, L., and Citi, S. (2004). Histone deacetylase inhibitors up-regulate the expression of tight junction proteins11swiss cancer league, swiss national science foundation, Ministry for Italian University and Research, ERASMUS Program (M. Bordin), and Roche Research Foundation fellowship (L. Guillemot). *Mol. Cancer Res.* 2, 692–701.

Coppedge, J. R., Oden, L. A., Ratliff, B., Brown, B., Ruch, F., and Lee, J. T. (2012). Evaluation of nonstarch polysaccharide-degrading enzymes in broiler diets varying in nutrient and energy levels as measured by broiler performance and processing parameters. *J. Appl. Poult. Res.* 21, 226–234. doi: 10.3382/japr.2011-00329

Cross, M. L. (2002). Microbes versus microbes: immune signals generated by probiotic lactobacilli and their role in protection against microbial pathogens. *FEMS Immunol. Med. Microbiol.* 34, 245–253. doi: 10.1111/j.1574-695X.2002.tb00632.x

Cui, C., Shen, C. J., Jia, G., and Wang, K. N. (2013). Effect of dietary *Bacillus subtilis* on proportion of Bacteroidetes and Firmicutes in swine intestine and lipid metabolism. *Genet. Mol. Res.* 12, 1766–1776. doi: 10.4238/2013.May.23.1

Fukunaga, T., Sasaki, M., Araki, Y., Okamoto, T., Yasuoka, T., Tsujikawa, T., et al. (2003). Effects of the soluble fibre pectin on intestinal cell proliferation, fecal short chain fatty acid production and microbial population. *Digestion* 67, 42–49. doi: 10.1159/000069705

Gadde, U., Kim, W. H., Oh, S. T., and Lillehoj, H. S. (2017). Alternatives to antibiotics for maximizing growth performance and feed efficiency in poultry: a review. *Anim. Health Res. Rev.* 18, 26–45. doi: 10.1017/S1466252316000207

Grant, A. Q., Gay, C. G., and Lillehoj, H. S. (2018). *Bacillus* spp. as direct-fed microbial antibiotic alternatives to enhance growth, immunity, and gut health in poultry. *Avian Pathol.* 47, 339–351. doi: 10.1080/03079457.2018.1464117

Guo, M., Hao, G., Wang, B., Li, N., Li, R., Wei, L., et al. (2016). Dietary administration of *Bacillus subtilis* enhances growth performance, immune response and disease resistance in Cherry Valley ducks. *Front. Microbiol.* 7:1975. doi: 10.3389/fmicb.2016.01975

Han, X. Y., Yan, F. Y., Nie, X. Z., Wei, X. I. A., Sha, C. H. E. N., Zhang, X. X., et al. (2017). Effect of replacing antibiotics using multi-enzyme preparations on production performance and antioxidant activity in piglets. *J. Integr. Agric.* 16, 640–647. doi: 10.1016/s2095-3119(16)61425-9

Hooda, S., Boler, B. M. V., Serao, M. C. R., Brulc, J. M., Staeger, M. A., Boileau, T. W., et al. (2012). 454 pyrosequencing reveals a shift in fecal microbiota of healthy adult men consuming polydextrose or soluble corn fiber. *J. Nutr.* 142, 1259–1265. doi: 10.3945/jn.112.158766

Hu, Y. J., and Cowling, B. J. (2020). Reducing antibiotic use in livestock, China. *Bull. World Health Organ.* 98:360. doi: 10.2471/blt.19.243501

Jeong, J. S., and Kim, I. H. (2014). Effect of *Bacillus subtilis* C-3102 spores as a probiotic feed supplement on growth performance, noxious gas emission, and intestinal microflora in broilers. *Poult. Sci.* 93, 3097–3103. doi: 10.3382/ps.2014-04086

Kiarie, E., Romero, L. F., and Nyachoti, C. M. (2013). The role of added feed enzymes in promoting gut health in swine and poultry. *Nutr. Res. Rev.* 26, 71–88. doi: 10.1017/S0954422413000048

Klein, J., Williams, M., Brown, B., Rao, S., and Lee, J. T. (2015). Effects of dietary inclusion of a cocktail NSPase and β-mannanase separately and in combination in low energy diets on broiler performance and processing parameters. *J. Appl. Poult. Res.* 24, 489–501. doi: 10.3382/japr/pfv055

Koliada, A., Syzenko, G., Moseiko, V., Budovska, L., Puchkov, K., Perederiy, V., et al. (2017). Association between body mass index and Firmicutes/Bacteroidetes ratio in an adult Ukrainian population. *BMC Microbiol.* 17:120. doi: 10.1186/s12866-017-1027-1

Kumar, R. R., Lee, J. T., and Cho, J. Y. (2012). Fate, occurrence, and toxicity of veterinary antibiotics in environment. *J. Korean Soc. Appl. Biol. Chem.* 55, 701–709. doi: 10.1007/s13765-012-2220-4

Le Blay, G., Blottière, H. M., Ferrier, L., Le Foll, E., Bonnet, C., Galmiche, J. P., et al. (2000). Short-chain fatty acids induce cytoskeletal and extracellular protein modifications associated with modulation of proliferation on primary culture of rat intestinal smooth muscle cells. *Dig. Dis. Sci.* 45, 1623–1630. doi: 10.1023/a:1005529414765

LeBlanc, J. G., Milani, C., De Giori, G. S., Sesma, F., Van Sinderen, D., and Ventura, M. (2013). Bacteria as vitamin suppliers to their host: a gut microbiota perspective. *Curr. Opin. Biotechnol.* 24, 160–168. doi: 10.1016/j.copbio.2012.08.005

Lee, K. W., Kim, D. K., Lillehoj, H. S., Jang, S. I., and Lee, S. H. (2015). Immune modulation by *Bacillus subtilis*-based direct-fed microbials in commercial broiler chickens. *Anim. Feed Sci. Technol.* 200, 76–85. doi: 10.1016/j.anifeedsci.2014.12.006

Lee, S. H., Ingale, S. L., Kim, J. S., Kim, K. H., Lokhande, A., Kim, E. K., et al. (2014). Effects of dietary supplementation with *Bacillus subtilis* LS 1–2 fermentation biomass on growth performance, nutrient digestibility, cecal microbiota and intestinal morphology of weanling pig. *Anim. Feed Sci. Technol.* 188, 102–110. doi: 10.1016/j.anifeedsci.2013.12.001

Lin, M. Y., and Chang, F. J. (2000). Antioxidative effect of intestinal bacteria *Bifidobacterium longum* ATCC 15708 and *Lactobacillus acidophilus* ATCC 4356. *Dig. Dis. Sci.* 45, 1617–1622. doi: 10.1023/A:1005577330695

Lin, Q., Dai, Q., Bin, S., Jiang, G. T., and Zhang, J. H. (2012). Probiotics and enzyme preparation: effects on growth performance of yellow-feathered broilers and its mechanism. *Chinese J. Anim. Nutr.* 24, 1955–1965.

Lin, Q., Zhao, J., Xie, K., Wang, Y., Hu, G., Jiang, G., et al. (2017). Magnolol additive as a replacer of antibiotic enhances the growth performance of Linwu ducks. *Anim. Nutr.* 3, 132–138. doi: 10.1016/j.aninu.2017.03.004

Lin, Y., Xu, S., Zeng, D., Ni, X., Zhou, M., Zeng, Y., et al. (2017). Disruption in the cecal microbiota of chickens challenged with *Clostridium perfringens* and other factors was alleviated by *Bacillus licheniformis* supplementation. *PLoS One* 12:e0182426. doi: 10.1371/journal.pone.0182426

Liu, J., Xia, B., Du, X., Zeng, T., Liu, Y., Chen, L., et al. (2018). Effects of water supplemented with *Bacillus subtilis* and photosynthetic bacteria on egg production, egg quality, serum immunoglobulins and digestive enzyme activity of ducks. *J. Appl. Anim. Res.* 46, 322–326. doi: 10.1080/09712119.2017.1299741

Ministry of Agriculture of the People's Republic of China (2012). *Nutrient requirements of Meat-Type Duck*. NY/T 2122–2012. Beijing: China Agriculture Press.

National Research Council (1994). *Nutrient Requirements of Poultry: 1994*. Washington, DC: National Academies Press.

Naumova, N. B., Alikina, T. Y., Zolotova, N. S., Konev, A. V., Pleshakova, V. I., Lescheva, N. A., et al. (2021). *Bacillus*-based probiotic treatment modified bacteriobiome diversity in duck feces. *Agriculture* 11:406. doi: 10.3390/agriculture11050406

Paik, H. D., Park, J. S., and Park, E. (2005). Effects of *Bacillus polyfermenticus* SCD on lipid and antioxidant metabolisms in rats fed a high-fat and high-cholesterol diet. *Biol. Pharm. Bull.* 28, 1270–1274. doi: 10.1248/bpb.28.1270

Peng, L., He, Z., Chen, W., Holzman, I. R., and Lin, J. (2007). Effects of butyrate on intestinal barrier function in a Caco-2 cell monolayer model of intestinal barrier. *Pediatr. Res.* 61, 37–41. doi: 10.1203/01.pdr.0000250014.92242.f3

Ravindran, V. (2013). Feed enzymes: the science, practice, and metabolic realities. *J. Appl. Poult. Res.* 22, 628–636. doi: 10.3382/japr.2013-00739

Ridlon, J. M., Kang, D. J., Hylemon, P. B., and Bajaj, J. S. (2015). Gut microbiota, cirrhosis, and alcohol regulate bile acid metabolism in the gut. *Dig. Dis.* 33, 338–345. doi: 10.1159/000371678

Rodriguez-Cabezas, M. E., Camuesco, D., Arribas, B., Garrido-Mesa, N., Comalada, M., Bailon, E., et al. (2010). The combination of fructooligosaccharides and resistant starch shows prebiotic additive effects in rats. *Clin. Nutr.* 29, 832–839. doi: 10.1016/j.clnu.2010.05.005

Salaheen, S., Kim, S. W., Haley, B. J., Van Kessel, J. A. S., and Biswas, D. (2017). Alternative growth promoters modulate broiler gut microbiome and enhance body weight gain. *Front. Microbiol.* 8:2088. doi: 10.3389/fmicb.2017.02088

Salim, H. M., Kruk, Z. A., and Lee, B. D. (2010). Nutritive value of corn distillers dried grains with solubles as an ingredient of poultry diets: a review. *World's Poult. Sci. J.* 66, 411–432. doi: 10.1017/s0043933910000504

Sen, S., Ingale, S. L., Kim, Y. W., Kim, J. S., Kim, K. H., Lohakare, J. D., et al. (2012). Effect of supplementation of *Bacillus subtilis* LS 1-2 to broiler diets on growth performance, nutrient retention, caecal microbiology and small intestinal morphology. *Res. Vet. Sci.* 93, 264–268. doi: 10.1016/j.rvsc.2011.05.021

Sikandar, A., Zaneb, H., Younus, M., Masood, S., Aslam, A., Khattak, F., et al. (2017). Effect of sodium butyrate on performance, immune status, microarchitecture of small intestinal mucosa and lymphoid organs in broiler chickens. *Asian Austral. J. Anim. Sci.* 30:690. doi: 10.5713/ajas.16.0824

Stolker, A. A. M., Zuidema, T., and Nielen, M. W. F. (2007). Residue analysis of veterinary drugs and growth-promoting agents. *TrAC Trends Anal. Chem.* 26, 967–979. doi: 10.1016/j.trac.2007.09.008

Tuohy, K. M., Probert, H. M., Smejkal, C. W., and Gibson, G. R. (2003). Using probiotics and prebiotics to improve gut health. *Drug Discov. Today* 8, 692–700. doi: 10.1016/S1359-6446(03)02746-6

Uthai, K., Jattupornpong, S., Vandepitte, W., and Vanderbeke, E. (2004). Effects of dietary supplementation of enzymes in soybean meal rich diet on performance of growing-finishing (20-100 kg) pigs. *Agric. Nat. Resour.* 38, 125–131.

Wang, H., Wang, Y., and Yang, R. (2017). Recent progress in *Bacillus subtilis* spore-surface display: concept, progress, and future. *Appl. Microbiol. Biotechnol.* 101, 933–949. doi: 10.1007/s00253-016-8080-9

Watkins, E. J., Butler, P. J., and Kenyon, B. P. (2004). Posthatch growth of the digestive system in wild and domesticated ducks. *Br. Poult. Sci.* 45, 331–341. doi: 10.1080/00071660410001730824

Wealleans, A. L., Walsh, M. C., Romero, L. F., and Ravindran, V. (2017). Comparative effects of two multi-enzyme combinations and a *Bacillus* probiotic on growth performance, digestibility of energy and nutrients, disappearance of non-starch polysaccharides, and gut microflora in broiler chickens. *Poult. Sci.* 96, 4287–4429. doi: 10.3382/ps/pex226

Woyengo, T. A., Bogota, K. J., Noll, S. L., and Wilson, J. (2019). Enhancing nutrient utilization of broiler chickens through supplemental enzymes. *Poult. Sci.* 98, 1302–1309. doi: 10.3382/ps/pey452

Xin, J., Zeng, D., Wang, H., Ni, X., Yi, D., Pan, K., et al. (2014). Preventing nonalcoholic fatty liver disease through *Lactobacillus johnsonii* BS15 by attenuating inflammation and mitochondrial injury and improving gut environment in obese mice. *Appl. Microbiol. Biotechnol.* 98, 1–13. doi: 10.1007/s00253-014-5752-1

Xing, Y., Wang, S., Fan, J., Oso, A. O., Kim, S. W., Xiao, D., et al. (2015). Effects of dietary supplementation with lysine-yielding *Bacillus subtilis* on gut morphology, cecal microflora, and intestinal immune response of Linwu ducks. *J. Anim. Sci.* 93, 3449–3457. doi: 10.2527/jas.2014-8090

Conflict of Interest: The authors declare that the research was conducted in the absence of any commercial or financial relationships that could be construed as a potential conflict of interest.

Publisher's Note: All claims expressed in this article are solely those of the authors and do not necessarily represent those of their affiliated organizations, or those of the publisher, the editors and the reviewers. Any product that may be evaluated in this article, or claim that may be made by its manufacturer, is not guaranteed or endorsed by the publisher.

frontiers in Microbiology

REVIEW
published: 13 December 2021
doi: 10.3389/fmicb.2021.785634

Prophage Activation in the Intestine: Insights Into Functions and Possible Applications

*Jie Hu, Hao Ye, Shilan Wang, Junjun Wang and Dandan Han**

State Key Laboratory of Animal Nutrition, College of Animal Science and Technology, China Agricultural University, Beijing, China

Prophage activation in intestinal environments has been frequently reported to affect host adaptability, pathogen virulence, gut bacterial community composition, and intestinal health. Prophage activation is mostly caused by various stimulators, such as diet, antibiotics, some bacterial metabolites, gastrointestinal transit, inflammatory environment, oxidative stress, and quorum sensing. Moreover, with advancements in biotechnology and the deepening cognition of prophages, prophage activation regulation therapy is currently applied to the treatment of some bacterial intestinal diseases such as Shiga toxin-producing *Escherichia coli* infection. This review aims to make headway on prophage induction in the intestine, in order to make a better understanding of dynamic changes of prophages, effects of prophage activation on physiological characteristics of bacteria and intestinal health, and subsequently provide guidance on prophage activation regulation therapy.

Keywords: gut microbes, prophage activation, intestinal health, microbial regulation, phage therapy

OPEN ACCESS

Edited by:
Jia Yin,
Hunan Normal University, China

Reviewed by:
Bozena Nejman-Falenczyk,
University of Gdańsk, Poland
Xiaolong Xu,
Capital Medical University, China

***Correspondence:**
Dandan Han
handandan@cau.edu.cn

Specialty section:
This article was submitted to Microbial Symbioses, a section of the journal Frontiers in Microbiology

Received: *29 September 2021*
Accepted: *25 November 2021*
Published: *13 December 2021*

Citation:
Hu J, Ye H, Wang S, Wang J and Han D (2021) Prophage Activation in the Intestine: Insights Into Functions and Possible Applications. Front. Microbiol. 12:785634. doi: 10.3389/fmicb.2021.785634

INTRODUCTION

Bacteriophages represent the majority of intestinal microorganisms, which have been intimately associated with gut health, since they play crucial roles in maintaining intestinal homeostasis, bacterial concentrations, and microbiota diversity, etc. (Hatfull and Hendrix, 2011; Vitetta et al., 2018; Gogokhia et al., 2019). Temperate phages are defined by their life characteristics to switch between the lysogenic and lytic life states, and ultimately affect fitness benefits of the hosts and the function of the entire gut ecosystem (Jover et al., 2013; Obeng et al., 2016; Cornuault et al., 2018). Prophages, viral DNA that originates from temperate phages, have been identified in the genome of approximately 40–50% of microbe (Howard-Varona et al., 2017). A large amount of commensal bacteria in the intestinal tract of C57BL/6J mice are lysogens, of which there are more prophages in Firmicutes and Proteobacteria than in Bacteroidetes and Actinobacteria (Kim and Bae, 2018). Most prophage sequences are integrated into bacterial chromosome, accounting for as much as 20% of host genome (Khan and Wahl, 2019). Particularly, *Escherichia coli* phage P1 and lambda-related phage N15 exists extrachromosomally as a plasmid in a circular form and with hairpin telomeres in a linear form, respectively (Łobocka et al., 2004; Ravin, 2015). Prophages and their hosts coexist and coevolve in intestinal environments (Cornuault et al., 2020).

While most prophages are highly stable, prophages can be specifically activated, leading to the excision of DNA and release of active phages (Oh et al., 2019). There are evidences suggesting that a

large number of virus-like particles contained in human gut are derived from prophages instead of lytic phages (Breitbart et al., 2003; Reyes et al., 2012; Howe et al., 2016). Various factors (for example, diet and some commonly used drinks) may activate prophages in the intestine (Pierzynowska et al., 2018; Boling et al., 2020). Both bacteria characteristic and intestinal health have been clarified to be influenced by the activity of prophages, which is of particularly important to understand prophage activation that occurs frequently in the gut (Balasubramanian et al., 2016; Vitetta et al., 2018).

Phage therapy has been used as a medical alternative in certain countries considering its advantage on host specificity, micro-ecological balance, cost, biofilm penetration, wide distribution, and low inherent toxicity over antibiotic treatment. With the in-depth understanding of phages and the development of biotechnology, phage types used in phage therapy are not limited to the lytic phages, but also expanded into the prophages (i.e., prophage activation) (Sheng et al., 2016; Alexander et al., 2019). In the present review, we discuss the current knowledge on the impact factors and mechanisms of prophage activation in the intestine, the spreading of induced active phages in the intestine, effects of prophage activation on physiological characteristics of bacteria and intestinal health, and phage therapy by regulating prophage activation.

IMPACT FACTORS AND MECHANISMS OF PROPHAGE ACTIVATION IN GUT

Factors Mediated Prophage Activation in Intestinal Environments

Many studies indicated that diet could alter the composition of gut microbial community (Turnbaugh et al., 2009; Muegge et al., 2011; Boling et al., 2020). The response of gut microbiome to short-term macronutrient intake is rapid, diet-specific, and reproducible. However, this effect can only last in a short period, and as a consequence, bacterial composition will revert to the initial state after the dietary interference (Martínez et al., 2010; David et al., 2014; Howe et al., 2016). The effect of dietary intervention on bacteriophages was found to be more lasting and significant than it on the bacterial communities (Minot et al., 2011). Specifically, the dynamic changes in phage community compositions induced by diet retained long-term consequences (Howe et al., 2016). The prophage metagenome in the murine intestine had high sequence similarity with the free phage genome at the end of consecutive dietary shifts, indicating that most lysogens are active (Kim and Bae, 2018). As described by Boling et al. (2020), clove, artificial sweeteners, grapefruit seed extract, and propolis glycerite etc. were able to manipulate the gut microbiome by activating prophages. Dietary sugar (fructose, galactose, and xylose) promoted phage production in *Lactobacillus reuteri* (*L. reuteri*) (Oh et al., 2019). Although numerous evidences for diet modulation on intestinal phages have been reported, the biological meaning is rarely known. Only one study found that some commonly used drinks enhanced Stx prophage activation in enterohemorrhagic *Escherichia coli* (EHEC), potentially enhancing pathogenicity of the pathogen (Pierzynowska et al., 2018). Further studies are needed to clarify diet-mediated effects.

Most antibiotics cause disruption of prophage maintenance. Prophage activation was observed in *Staphylococcus aureus* treated with β-lactam antibiotics (Maiques et al., 2006). Quinolone antibiotics that caused DNA double-strand breaks were typical prophage inducers (Zhang et al., 2000). Antibiotic-mediated prophage induction is usually intimately associated with dissemination of virulence factors (for example, Shiga toxin) and antibiotic resistant genes in bacteria. Some metabolites of bacteria are also confirmed to be efficient inducers of prophages. Bile acid has been reported to induce prophages in *Salmonella* (Hernández et al., 2012). Short-chain fatty acids (SCFAs) produced by bacterial metabolism or administrated exogenously resulted in increased active phage production in *L. reuteri* 6475, *L. reuteri* ATCC 55730, and *Lactococcus lactis* NZ9000 (Oh et al., 2019). These facts indicate that metabolic status of intestinal microorganisms contributes to reconstruction of microbial community structure (bacteria and viruses).

Furthermore, intestinal environment (i.e., temperature, gastrointestinal transit, intestinal disease, and oxidative stress) has been recognized as a crucial factor in regulating prophage induction. Previous studies indicated that prophage induction could mainly be associated with high temperature (Horiuchi and Inokuchi, 1967). Notably, the dynamic changes in prophages were also observed during bacterial cold stress (Zeng et al., 2016). Oh et al. (2019) demonstrated that the ecological conditions in gut environment affected the phageome. Prophages LRΦ1 and LRΦ2 were identified in strain *L. reuteri* 6475 (Oh et al., 2019). The survival rate of wild-type *L. reuteri* was at least 3.7-fold lower than the level of mutant bacteria without prophages in the cecum, colon, and feces of mice after oral administration of *L. reuteri*. Phage LRΦ1 was predominantly produced in the gut. Thus, prophages could be activated during gastrointestinal transit. Similar results were observed in *L. reuteri* VPL1014 (Alexander et al., 2019). Inflammatory bowel disease (IBD) led to elevated phage number in the intestine (Duerkop et al., 2018). Prophage activation of four *Myoviridae* phages were identified in patients suffering from *Clostridium difficile* infection (CDI) (Meessen-Pinard et al., 2012). Intestinal oxidative stress (for example, hydrogen peroxide) provoked induction of Shiga toxin-carrying lambdoid prophages (Licznerska et al., 2015). Collectively, under the threat of changes in intestinal environments, prophages are generally activated, which possibly alter the gut microbial communities and affect survival of the hosts.

What's more, free Pf1-like phages were highly abundant when *Pseudomonas aeruginosa* was infected with N4-like lytic podovirus Ab09, suggesting that Pf1-like prophages were largely excised (Latino et al., 2019). Prophage activation occurred in intestinal pioneer bacteria in early infants (1 month old) and led to formation of active phages that occupied a dominant part of viral-like particles (Liang et al., 2020). So far, several pieces of evidences suggest that quorum sensing caused the modification of prophages induction rate, and ultimately affected ecological networks in gut bacterial communities and functional gene distribution (for example, virulence genes)

(Rossmann et al., 2015; Liang et al., 2019; Tan et al., 2020). It is also well known that prophage spontaneous activation is universal among lysogenic bacteria, though at low frequency (Bertani, 1951). Additionally, intestinal cells may contribute to the change of phageome structure. For example, cells (such as macrophages)-producing nitric oxide, an antimicrobial defense molecule, was shown to increase Shiga toxin-converting phage production in EHEC (Ichimura et al., 2017).

Altogether, these findings indicate instability of intestinal prophages (**Table 1**) and a great potential impact of prophage activation on altering the gut microflora. Indeed, almost all tested gut bacteria have been experimentally confirmed to contain active prophages (reviewed in Sausset et al., 2020).

The Mechanisms of Prophage Activation

The induction of prophages by various factors are mostly related to the RecA protein and SOS response of bacteria (Diard et al., 2017; Oh et al., 2019). The commensal relationship between prophages and hosts is mainly supported by the silence of the SOS system, which is a pathway mainly responsible for bacterial DNA damage response (Au et al., 2005; Kreuzer, 2013). The SOS system in bacteria coordinates cellular response to DNA damage via linkage action between RecA protein and LexA repressor (Friedberg et al., 2005). Naturally, the expression level of SOS regulon genes are limited by inactive promoter regions that are occupied by LexA. Upon DNA damaged, RecA protein forms active RecA filament termed activated RecA, on single-stranded DNA, and acts as a coprotease which catalyzes the self-cleavage reaction of LexA in DNA-free form, probably through reducing the pK_a of a key lysine residue (Little, 1991; Luo et al., 2001; Matej et al., 2011). Consequently, SOS genes expression are up-regulated. By using single-molecule imaging techniques for live cells, it was proved that the RecA protein was sequestered in storage structures until DNA damage happened, and early SOS-signaling complexes were formed subsequently (Ghodke et al., 2019). The polymerases ImuB and ImuC acting as factors involved in the regulation of SOS system were co-transcribed under the control of LexA in *Pseudomonas aeruginosa* (Luján et al., 2019). The *exo-xis* region of lambdoid bacteriophages and OxyR regulator influenced prophage maintenance and induction (Bloch et al., 2013; Licznerska et al., 2015). Importantly, production of viral progeny was dependent on inactivation of phage repressor, expression of phage antirepressor, or activation of specific mutagenesis proteins (for example, Umud protein) (Carrasco et al., 2016; Diard et al., 2017; Ichimura et al., 2017; Silpe and Bassler, 2019). Various phages replicated either by transposition or episomally once induced, and virion particles were then assembled and packaged with phage DNA by endonucleolytic enzymes (reviewed in Howard-Varona et al., 2017).

Spontaneous DNA damage and low levels of SOS genes expression were observed in wild-type bacterial cells, which might be associated with mismatches during DNA replication and the DNA "damage-up" proteins (DDPs) (Mccool et al., 2004; Xia et al., 2019). Moreover, low-fidelity polymerase pol VICE391 (RumA'2B) encoded by conjugative transposone R391 could further promote higher levels of spontaneous SOS mutagenesis, partly because of the longer binding time of RumB to genomic DNA (Walsh et al., 2019). While the mechanisms of some prophage inducers (for example, diet, clove, stevia, grapefruit seed extract, and aspartame)-mediated prophage activation have remained poorly understood, inflammation (e.g., reactive nitrogen species, reactive oxygen species, and hypochlorite), dietary fructose, nitric oxide, SCFAs, β-lactam

TABLE 1 | Factors influencing prophage induction in the gut.

Factors	Prophage	Host	References
High and low fat diets	Gut prophages	Gut bacterial communities	Howe et al., 2016
Stevia, clove, and propolis	Unspecified	*Bacteroides thetaiotaomicron* VPI-5482	Boling et al., 2020
Uva ursi, propolis, and aspartame	Unspecified	*Enterococcus faecalis*	Boling et al., 2020
Grapefruit seed extract, stevia, and toothpaste	Unspecified	*Staphylococcus aureus* CA15	Boling et al., 2020
Fructose, galactose, and xylose	LRΦ1 and LRΦ2	*Lactobacillus reuteri* 6475	Oh et al., 2019
Fructose	Unspecified	*Lactobacillus reuteri* 55730	Oh et al., 2019
Nestea	933W Stx	*Escherichia coli* MG1655	Pierzynowska et al., 2018
β-Lactam antibiotics	80α and φ11	*Staphylococcus aureus* RN27 and RN451	Maiques et al., 2006
Quinolone antibiotics	Stx2	*Escherichia coli* O157:H7	Zhang et al., 2000
Ciprofloxacin	Unspecified	*Enterococcus faecalis* V583ΔABC	Rossmann et al., 2015
Short-chain fatty acids	LRΦ1 and LRΦ2	*Lactobacillus reuteri* 6475	Oh et al., 2019
Short-chain fatty acids	Unspecified	*Lactobacillus reuteri* ATCC 55730	Oh et al., 2019
Short-chain fatty acids	ΦTP901	*Lactococcus lactis* NZ9000	Oh et al., 2019
Gastrointestinal transit	LRΦ1	*Lactobacillus reuteri* 6475	Oh et al., 2019
Quorum sensing	Unspecified	*Enterococcus faecalis* V583ΔABC	Rossmann et al., 2015
High temperature	λts type II	*Escherichia coli*	Horiuchi and Inokuchi, 1967
Hydrogen peroxide	Lambdoid	*Escherichia coli* MG1655	Łoś et al., 2009
Inflammation	SopEΦ	*Salmonella enterica* Typhimurium SL1344	Diard et al., 2017
Nitric oxide	Stx2	*Escherichia coli* O157:H7	Ichimura et al., 2017
Acyl-homoserine lactones	Lambda	*Escherichia coli* BW25113	Ghosh et al., 2009

antibiotics, and hydrogen peroxide have been shown to induce phage production by activating the SOS response in *Salmonella enterica* Typhimurium (*S*.Tm) SL1344, *L. reuteri* 6475, EHEC O157, *Lactococcus lactis* NZ9000, *Staphylococcus aureus*, and *Escherichia coli* MG1655, respectively (Maiques et al., 2006; Howe et al., 2016; Diard et al., 2017; Ichimura et al., 2017; Bloch et al., 2018; Kim and Bae, 2018; Oh et al., 2019; Boling et al., 2020).

In general, high-level expression of SOS genes has been considered as a consequence of the decrease in LexA repressor levels, whereas the decreasing signal from RecA protein or LexA allows the SOS system to be shut off. The activation of SOS system induces production of active phages.

However, it is worth noting that in addition to the SOS response, some alternative pathways can induce the activation of prophages. In some lysogenic cells (for example, *Staphylococcus aureus* and *Escherichia coli*), spontaneous prophage induction does not require SOS response, but depend on phage repressor cleavage or cell density (Ghosh et al., 2009; Haaber et al., 2016). Prophages encoding Shiga toxin 2 were still inducible in Δ*recA* mutants, indicating that there may be multiple causes for prophage induction (Colon et al., 2016). The SOS-independent prophage induction was well demonstrated in a co-culture system, in which acyl-homoserine lactones (AHL) produced from *Pseudomonas aeruginosa* triggered lambda phage production in *recA*-deficient *Escherichia coli* (Ghosh et al., 2009). The specific counteraction of xenogeneic silencers (XS) including H-NS etc. can also modulate prophage activity. For example, double depletion of the MvaT and MvaU proteins, belonging to the H-NS family, activated prophage Pf4 in *Pseudomonas aeruginosa* PAO1 (Li et al., 2009). Moreover, inhibition of the transcription termination factor Rho led to induction of lytic cycle of prophages in *Escherichia coli* (Menouni et al., 2013). These examples highlight the diversity mechanisms of prophage activation.

The Spreading of Induced Active Phages in the Intestine

Temperate phages exhibit lysogenic conversion or transduction in specific environments (**Figure 1**). Transduction typically occurs at low frequency and comes in two varieties: specialized transduction (flanking bacterial DNA of prophages is excised and packaged into the capsid) and generalized transduction (random bacterial or plasmid DNA fragments are accidently packaged into the capsid) (Touchon et al., 2017). Whereas all phages have the potential for transduction, transduction rates vary significantly between phages (Kenzaka et al., 2007). Phages utilizing the headful packing strategy showed relatively high transduction rates (Wu et al., 2002). In addition, the ratio of phage particles to potential bacterial hosts (phage: bacteria ratio/multiplicity of infection) may change transduction frequency. For example, as the phage: bacteria ratio increased from 0.01 to 1, the frequency of plasmid pNZ8048 transduction by bacteriophage 5171F increased first and then decreased (Marcelli et al., 2020). It is commonly assumed that most transducing phages are incomplete/defective and thus transduction can be regarded as one-shot event (Touchon et al., 2017). Lysogenic conversion can be associated with specialized transduction in certain cases if the prophage excision from a donor cell is not precise. Inflammatory factors reactive oxygen species and reactive nitrogen species etc. could induce the SOS response of *S*.Tm and enhance the expression of phage (SopEΦ) anti-repressor Tum, and as a result, free phages were produced (Diard et al., 2017). SopEΦ, the temperate phage belonging to P2 family, was observed with a low degree of lysogenic conversion from *S*.Tm SL1344 to *S*.Tm ATCC14028S in the gut lumen of mice without inflammation (Diard et al., 2017). However, intestinal inflammation and disease triggered 10^5-fold SopEΦ transfer within 3 days in that study. During an epidemic, the bacteriophage *sopE* gene spread extensively in monophasic *S*.Tm (Petrovska et al., 2016). Therefore, prophage activation drives lysogenic conversion. Furthermore, β-lactam antibiotics facilitated horizontal transfer of phages in *Staphylococcus aureus* (Maiques et al., 2006). As a matter of fact, use of antibiotics is tightly linked to efficient phage transfer in a few pathogenic bacteria (for example, Shiga toxin-producing *Escherichia coli*, *Clostridium botulinum*, and *Salmonella*) (reviewed in Tamang et al., 2017).

A study indicates that phages released from a subpopulation of lysogenic *Staphylococcus aureus* were able to capture DNA from competitor cells, and subsequently transferred to remaining population, the process which termed "auto-transduction" (**Figure 1**; Haaber et al., 2016). Nevertheless, it remains unclear whether auto-transduction is restricted to *Staphylococcus aureus.* Both transduction and auto-transduction facilitate the transfer of bacterial DNA to sensitive population.

Certain bacteriophages possess a dual strategy for perpetuation (Wadhwa, 2017; Laganenka et al., 2019). Induced active phages can reproduce in a short-time lytic life (**Figure 1**). It should be also mentioned that the filamentous single-stranded deoxyribonucleic acid (ssDNA) phages of the subclass *Inoviridae* uniquely follow a productive chronic life cycle in which the maturing phage progeny is secreted through the cell envelop without killing the host (reviewed in Sausset et al., 2020). The small-molecule communication system termed "arbitrium" system, quorum sensing, metabolic state of bacteria, and multiplicity of infection etc. controlled lysis–lysogeny decision of bacteriophages (Erez et al., 2017; Wadhwa, 2017; Laganenka et al., 2019). Depending on specific phage receptors present on the cell surface of target bacteria, some of the phages were only capable of infecting a single strain, while others could infect bacteria belonging to different genera. Phage receptors on the bacterial surface include lipopolysaccharide, pili, flagella, membrane proteins (for example, porins) and so on (reviewed in Dy et al., 2014).

Since one bacterium is capable of releasing hundreds of phage particles, prophage induction may increase the struggle between bacteriophage and bacteria, and drive bacterial anti-phage system evolution. Indeed, at each stage of phage infection process, bacteria have evolved anti-phage approaches, such as adsorption and DNA injection inhibition, abortive infection, toxin-antitoxin, and CRISPR-Cas systems (reviewed in Dy et al., 2014). In recent years, some novel anti-phage defenses were reported, such as defense island system associated with restriction-modification, the chemical anti-phage defense system, and prophage defense

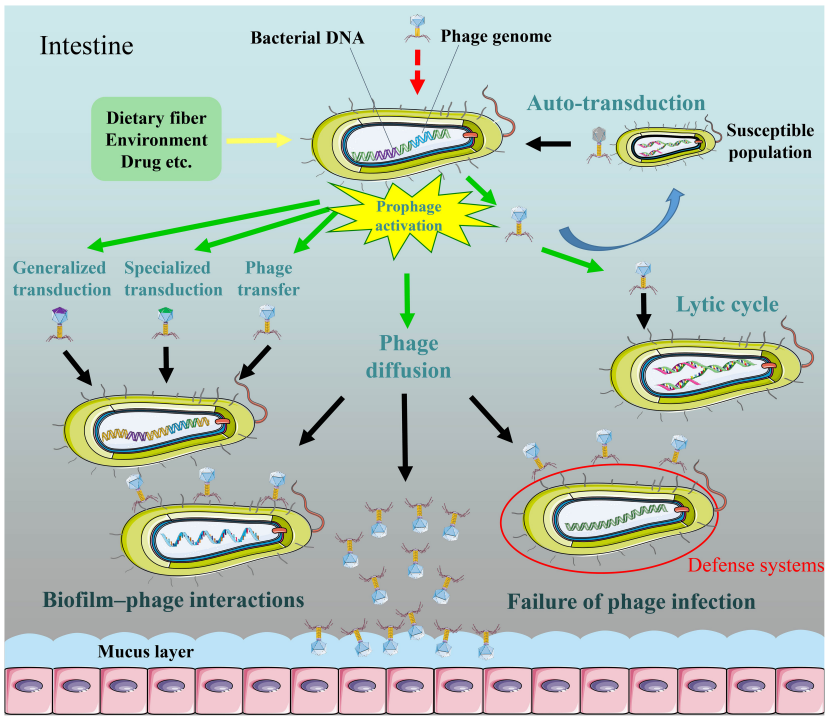

FIGURE 1 | The diffusion of induced active bacteriophages in the intestine. Activators may activate SOS system in lysogenic bacteria and then induce production of active phages. Phages released from a subpopulation of lysogenic bacteria are able to capture DNA from competitor cells, and subsequently transfer to remaining population, the process which termed "auto-transduction." Some temperate phages exhibit lysogenic conversion or transduction (generalized transduction or specialized transduction) in specific environments. Temperate phages can infect specific bacteria for lytic cycles. Phages are adapted for attaching to bacteria and forming multicellular communities in a biofilm environment. Bacterial defense systems are able to restrict temperate phage acquisition and lytic phage predation. Phages have more potential to enrich in mucus layer relative to the adjacent environment.

strategy (**Figure 1**; Kronheim et al., 2018; Ofir et al., 2018; Ragunathan and Vanderpool, 2019). Evolutional arm race also promotes phages to develop evasion mechanisms to escape bacterial resistance strategies (reviewed in Dy et al., 2014). Overall, prophage induction in the intestine may greatly enhance phage-bacterium interactions.

Despite it is known that intestine contains vast numbers of free phages and microorganisms, the mechanisms of long-term coexistence of phages and bacterial population remain largely unexplored. The study of Chaudhry et al. (2019) illustrated that mucoidy was related to this biological phenomenon, thereby ensuring a stable bacterial density in intestine. A recent study demonstrated that phage-inaccessible sites in the mucosal layer protected bacteria against phage predation, suggesting that coexistence of phages with phage-susceptible bacteria benefits from the heterogeneous biogeography of microbe (Lourenço et al., 2020). Active phages were adapted for attaching to bacteria and forming multicellular communities in a biofilm environment (Simmons et al., 2018). Biofilm–phage interaction life is likely to be ubiquitous as a natural feature of bacteriophages (**Figure 1**). It should be noted that phages have more potential to enrich in mucus layer relative to the adjacent environment (**Figure 1**; Barr et al., 2013). This bacteriophage adherence to mucus model occurs via binding interactions between phage Ig-like protein domains (for example, Hoc) and glycan residues of mucin glycoproteins. In addition, the intrusion of intestinal phages to other body tissues (for example, the kidney and liver) by bloodstream was not only caused by impaired integrity of the intestinal epithelium due to intestinal inflammation, but also occurred in some normal physiological conditions (reviewed in Chatterjee and Duerkop, 2018). Beyond these examples, induced active phages may have more extensive diffusion pathways.

EFFECTS OF PROPHAGE ACTIVATION ON PHYSIOLOGICAL CHARACTERISTICS OF BACTERIA AND INTESTINAL HEALTH

Effects of Prophage Activation on Physiological Characteristics of Bacteria

In recent years, prophage induction (or excision) in the intestine have attracted great attention for its potentially important functions. In a phenomenon called reversible active lysogeny, the excision of prophage of the *Listeria monocytogenes* genome during infection would reactivate the host *comK* gene for immune evasion, avoiding phagosomes in macrophage cells, but this process didn't produce progeny virions (Rabinovich et al., 2012). Excision of cryptic prophages that affected the

expression of transfer-messenger RNA and biofilm formation improved *Shewanella oneidensis*'s adaptability to low temperature (Zeng et al., 2016). The results of Nedialkova et al. (2016)'s study indicated that activation of lambdoid prophages in *S*.Tm was necessary to release the bacteriocin Colicin Ib that conferred a competitive advantage for bacterial hosts in the competition against Colicin Ib-susceptible competitors. Previous reports showed that spontaneously induced prophages could affect the living strategy of bacteria, deliver fitness benefits to the host, and increase virulence of specific pathogens (Nanda et al., 2015; Chakraborty et al., 2018; Balasubramanian et al., 2019). Given the ability of bacteriophages to switch their infection modes, prophage activation is a strategy to kill competitors once the prophages are induced and released, assuming that not all the lysogenic cells will die (Haaber et al., 2016). With the above mentioned results, it can be seen that prophage activation (or excision) is crucial for bacterial survival and adaptability in response to complex and unfavorable living environment.

Lysogenic conversion and horizontal gene transfer by transduction mediated by prophage activation promote bacterial virulence and pathogen evolution as well as antibiotic resistance encoded by accessory loci, which allow bacteria to rapidly adapt to new hosts. Livestock-associated *Staphylococcus aureus* CC398 strains gained the ability to produce staphylokinase, enterotoxin A, and Panton-Valentine leucocidin (PVL) toxin by lysogeny with immune evasion cluster (IEC)/PVL-converting bacteriophages, utilizing the temperate phages P240, P282, P630, and P1105 (Kraushaar et al., 2017). *Streptococcus thermophilus* phage DLP4 had lysogenic transformation ability which could help host strains acquire antibiotic resistance (Peters et al., 2019). The transfer of prophage Φ3538 Δstx2:cat contributed to converting atypical enteropathogenic *Escherichia coli* (aEPEC) to EHEC (Eichhorn et al., 2018). A study showed that lysogenic conversion by filamentous prophage CTXΦ in *Vibrio cholerae* caused the spread of virulence genes (i.e., cholera toxin gene *ctxAB*) in non-pathogenic bacteria, which made these strains become toxic (Waldor and Mekalanos, 1996). Prophages can transfer not only their own genomes, but also bacterial DNA. Transducing phages may lost part or all of own genome and phage capsid allows to package appropriate length of hosts DNA that is even longer than phage genome (reviewed in Touchon et al., 2017). Prophage-mediated lateral transduction was capable of transferring large metameric spans of the *Staphylococcus aureus* genome (Chen et al., 2018). The spread of virulence genes can be strongly facilitated by Viunalikevirus-relevant generalized transduction (Matilla et al., 2014). Transduction bias in transferred DNA may be present. This is because some mobile genetic elements such as phage-inducible chromosomal islands (PICI) tend to hijack transduction for their priority transmission (Fillol-Salom et al., 2019). The PICI-encoded RppC (for redirecting phage packaging) protein bound to the phage terminase TerS to form a heterocomplex that only recognized PICI genome while excluding phage DNA, thus packaging PICI into a newly formed phage head and furthering the dissemination of pathogenic features among Gram-negative bacteria. In particular, auto-transduction of *Staphylococcus aureus* helped to obtain DNA from competitors through phage transducing particles, which conferred potentially beneficial traits (i.e., antibiotic resistance) to remaining, prophage-containing population (Haaber et al., 2016). Overall, a set of data suggests that temperate bacteriophages play important roles in bacterial adaption and evolution (via lysogenic conversion, transduction, or auto-transduction).

However, prophage induction exerts negative effects on their bacterial host in most cases. Prophage induction triggered by stochastic fluctuations or environmental stressors tend to resume the lytic cycle and subsequent lysis of the lysogen. During the gastrointestinal transit, phage production was found to negatively impact on the survival of *L. reuteri* (Alexander et al., 2019; Oh et al., 2019). Furthermore, in IBD patients, prophage activation had been associated with the depletion of *Faecalibacterium prausnitzii* (*F. prausnitzii*), a main commensal bacteria in the human gut (Cornuault et al., 2018). Collectively, the survival of intestinal bacteria is challenged by unstable prophages that can kill the hosts at any time.

On balance, host's fitness, metabolic repertoire, and ecological evolution can be changed with prophage induction.

Effects of Prophage Activation on Intestinal Health

The effects of prophage activation on intestinal health are reflected in two aspects. In terms of direct microbial-related effects, prophage activation in an inflammatory environment could aggravate *Salmonella*-induced diarrhea and intestinal microbiota dysbiosis (Diard et al., 2017; Cornuault et al., 2018). In mouse infected by EHEC, prophage induction that didn't produce active virus particles was essential for the production of Shiga toxin and lethal disease (Balasubramanian et al., 2019). Several studies have investigated the relationship between gut viriome composition and pathological state of individuals. During inflammatory disease, increased intestinal phage population was found, especially the phages specific to pathobiotic hosts, suggesting enhanced mortality of lysogens (Duerkop et al., 2018). A study reported more abundant *F. prausnitzii* phages in IBD than in those of healthy mice (Cornuault et al., 2018). Notably, it is well known that the lack of gut microbiota homeostasis is highly correlated with several diseases (for example, Crohn's disease and ulcerative colitis). Taken together, one may speculate that the prevalence of prophage activation during IBD results in lysis of the normal intestinal flora or bacterial symbionts, thereby aggravating dysbiosis. Prophages are potentially as natural modulators of the bacterial dynamics in the human intestine and thus in preventing/establishing gut microbiota dysbiosis. Moreover, liberating cellular contents can be supplied as nutrients to neighboring bacteria (Nanda et al., 2015). On the other hand, due to the activation of prophages, a large number of progeny phage particles are produced in the intestine. Gut bacteriophages were able to pass through the epithelial cell layer of the intestine. This fact was evidenced by either *in vitro* transwell system or *in vivo* orally administered experiments (Reynauda et al., 1992; Nguyen et al., 2017). Since bacteriophages share some common features with viruses that target mammalian cells, they can be recognized by innate host receptors (for

example, members of the Toll-like receptor family). There is ample evidence about direct interactions between intestinal phages and host immune cells (dendritic cells, B cells, and monocytes) recently reviewed by Seo and Kweon (2019) and Federici et al. (2020), which are shown to increase the production of antiviral cytokines (for example, chemokines, interferon-γ, and interleukin-12) and potential contamination of endotoxin (for example, lipopolysaccharide). Consistently, according to results of Gogokhia et al. (2019), expansion of bacteriophages might induce expression of cytokines, aggravate intestinal inflammation, heighten immune response, and exacerbate murine colitis. The important point is that not all phages stimulate such immune response (for example, T4 phage) (Miernikiewicz et al., 2013). Indeed, phages from the ulcerative colitis patients induced secretion of higher amount of interferon-γ than those from health controls, suggesting the critical role of specific bacteriophages in immunomodulation (Gogokhia et al., 2019). By contrast, Vitetta et al. (2018) noted that bacteriophages displayed effects in protecting against commensal pathobionts, maintaining intestinal homeostasis, and controlling bacterial concentrations in gut. Mucus-adherent phages could form an antibacterial barrier that actively protect the mucosal surfaces of the intestinal epithelium from bacterial infection (Barr et al., 2013). Released temperate phages may modify gut bacterial communities by multiple life cycles including lysing competitive or sensitive cells, lysogenizing other bacteria as well as continuous and complex phage-bacterium interactions (reviewed in Sausset et al., 2020). Prophage activation induced by antibiotics (for example, ciprofloxacin) promoted transfer of Stx2 prophage and thus non-pathogenic bacteria may produce toxin in the gut and stimulate the host immune response, an example of lysogenic conversion demonstrating the indirect modulation of host immunity by phages (Zhang et al., 2000). This observation suggests that phage transfer could have an ultimately downstream influence on bacterial-mammalian interactions. Beyond that, cascading effects were observed in non-susceptible bacteria via interbacterial interactions when specific phage predation occurred (Hsu et al., 2019). Hence one can see that prophage activation may have a systemic effects. Currently, the effects of bacteriophages on gut health did not show a consistent pattern in previous studies and phages may play dual roles (positive and negative aspects) in gut health. Impact of prophage activation may dependent on the activation response amplitude, prophage types, specific intestinal environments (healthy intestinal inter-environment and IBD, etc.), and bacterial community composition.

Phage Therapy by Regulating Prophage Activation

Lytic phages have become the unanimous first choice for phage therapy, avoiding increased bacterial virulence mediated by lysogenic conversion. Even so, people have never stopped looking for novel approaches to phage therapy, such as the use of temperate phages against bacterial infection (Monteiro et al., 2019). Since prophage activation and subsequently potential phage transfer are common and important physiological phenomenon in bacteria (as mentioned earlier), we can expand our arsenal against the persistent threat of drug resistance of bacteria by utilizing advanced biotechnologies and regulating prophage activation properly. Below we discuss phage therapy strategies that rely on the process of prophage activation.

The property of induction of prophage genomes provides new avenues for clinical treatment. By using gene editing technology to insert the leptin gene into native phage genome of *L. reuteri* VPL1014, the leptin protein was released with prophage activation, implying that prophages can serve as a microbial therapeutic delivery target (**Figure 2A**; Alexander et al., 2019). The application of dietary prophage inducers opens a new path for altering the gut microbiome (Boling et al., 2020). It is also possible to genetically modify the phage genome involved in prophage maintenance, and then start lytic cycles in pathogens (Zhang et al., 2013). In contrast, cinnamon oil eliminated RecA protein, polynucleotide phosphorylase, and poly(A) polymerase in *Escherichia coli* O157:H7, thereby inhibiting prophage activation and Shiga toxin production (**Figure 2B**; Sheng et al., 2016). Under oxidative stress conditions, suppressing induction of the prophage in Shiga toxin-producing *Escherichia coli* using some derivatives (for example, CM092, CM032D, and CM3186B) of quinolone, indazole, indenoindole, triazole, carbazole, and ninhydrine reduced bacterial virulence (Bloch et al., 2018). This inhibitory effect on prophage induction was achieved by increasing the expression of genes responsible for encoding *c*I repressor and reducing the expression of oxidative stress genes as well as phage lysis genes. One mechanistically particular example is suppressing Shiga toxin production in EHEC via activation of guanosine tetraphosphate (ppGpp) synthesis (Nowicki et al., 2014). These facts provide the guidance for the proper use of prophage activation regulation therapy during treatment for bacterial intestinal disease.

Increased bacterial virulence and antibiotic resistance that may be caused by phage lysogenic conversion pose great threats to the human's health, and therefore, prevention of bacterial lysogenic conversion is necessary for disease prevention and medical treatment. It can be approached from the following five aspects: (1) Block bacterial SOS response pathway; (2) Interrupt SOS-to-prophage activation signal; (3) Reduce bacterial inflammatory properties or relieve intestinal inflammation with external intervention; (4) Vaccination against gut disease; (5) Avoid the abuse of antibiotics (**Figure 2C**). In recent years, the short first in class α-helical peptide, phenolic compound N-acetylcysteine, 5-amino-1-(carbamoylmethyl)-1H-1, 2, 3-triazole-4-carboxamide scaffold, zinc, phthalocyanine tetrasulfonic acid, fermentates from probiotic strains, and p-Coumaric acid were found to inhibit RecA protein activities, thereby blocking the SOS system (Alam et al., 2016; Bunnell et al., 2017; Yakimov et al., 2017; Selwood et al., 2018; Ojha and Patil, 2019; Prazdnova et al., 2019; Rodríguez-Rosado et al., 2019). RecA protein inhibitor bind to the L2 loop through the ssDNA site on the epithelium (Bellio et al., 2017). Diard et al. (2017) found that during inflammation, phage transfer was blocked when the *tum* gene encoding phage antirepressor was deleted (signal interruption from bacterial SOS response to prophage induction). Their results also showed that avirulent *S*.Tm

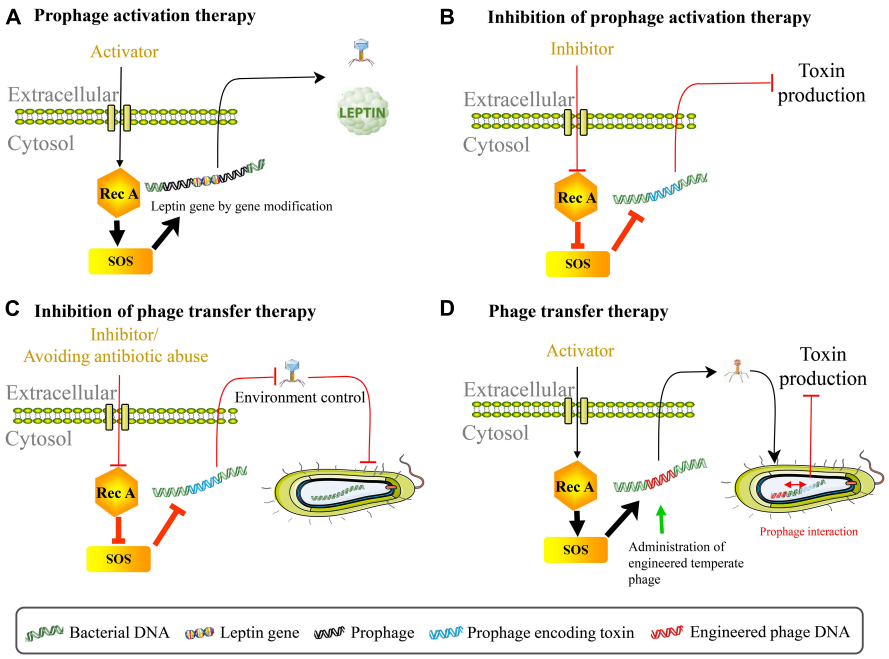

FIGURE 2 | Phage therapy by regulating prophage activation. **(A)** Prophage activation therapy. The leptin protein can be released with prophage activation using gene editing technology to insert the leptin gene into native phage genome in *Lactobacillus reuteri* VPL1014. **(B)** Inhibition of prophage activation therapy. Suppressing the spontaneous induction of virulence-carrying prophage in *Escherichia coli* O157:H7 can reduce the production of toxin. **(C)** Inhibition of phage transfer therapy. Preventing lysogenic conversion among pathogens includes following aspects: block bacterial SOS response pathway through using RecA protein inhibitor, avoid antibiotic abuse, interrupt SOS-to-prophage activation signal, and regulate intestinal environment etc. **(D)** Phage transfer therapy. The administration of temperate engineered phages inhibits toxin production caused by virulence-carrying prophages in EHEC through phage transfer and prophage interaction.

variants constructed by destroying type III secretion system 1 and 2 couldn't trigger inflammation and therefore reduced rates of phage transfer. More studies are expected to explore whether functional compounds such as *Pteris multifida*, *Cortex phellodendri*, and astragalus polysaccharide which could attenuate *Salmonella*-induced intestinal inflammation can inhibit phage-mediated horizontal gene transfer (Yin et al., 2018; Dong et al., 2019). Importantly, mucosal vaccination prevented inflammation disease and limited inflammation-dependent lysogenic conversion by phages, indicating that vaccination may be one of an effective strategy for blocking pathogen evolution (Diard et al., 2017). Since antibiotics may not only exacerbate virulence via inducing toxin-encoded prophages but also promote horizontal dissemination of virulence factors, it is critical to control the abuse of antibiotics and explore novel therapeutic strategies in the treatment of bacterial infection (for example, phage therapy) (Zhang et al., 2000; Maiques et al., 2006; Monteiro et al., 2019). Intriguingly, bacterial dormancy might curb phage epidemics (Jackson and Fineran, 2019). These approaches may also provide reference to the inhibition of phage transduction/auto-transduction that potentially accelerate pathogen evolution. Contrarily, it has to be mentioned that recent discovery of bacteriophage transfer therapy that used engineered λ phages overcame resistance and reduced the production of Shiga toxin encoded by the virulence-expressing prophages in EHEC through transcriptional repression strategy (**Figure 2D**; Hsu et al., 2020). In this case, lysogenic conversion of engineered λ phages in bacterial communities rather than anti-bacterial action enhanced the curative effect of stable neutralization of virulent *Escherichia coli*. Therefore, phage transfer may act as a double-edged sword for gut health.

Despite prophage as a novel potential therapeutic agent is important and promising, it still remains largely unexplored. Scientific evidence for prophage activation regulation therapy is relatively scarce. There are several major concerns about the application of prophage genome as targets for phage therapy. First, compared with phage therapy using strictly lytic phages, prophage activation regulation therapy is limited to functional prophage genome (i.e., prophage encoding specific function or easily genetically modified and activated). Second, considering complex internal environment of the intestine, therapeutic effects of prophage activation regulation therapy may be affected by unknown factors. Third, much less is known about specialized transduction, generalized transduction, and auto-transduction that may transfer resistance and virulence determinants to intestinal beneficial bacteria. Finally, due to lack of understanding of the most phage genes, unexpected and undesirable events may happen after gene modification. A better understanding of basic gene function of phages is urgently needed.

Research Prospects

Over the last years, a large number of studies have shown the effects of multiple factors (e.g., exercise, physiological changes, diets) on the alteration of gut microbiome (Muegge et al., 2011;

Jensen et al., 2020; Mahizir et al., 2020). However, the research on enteroviruses is still relatively backward. Although the effect of certain drugs or bacterial activities on prophages have not been comprehensively clarified, it has been proven that they can trigger SOS response in bacteria. For example, continued exposure to sublethal doses of ciprofloxacin increased competitive fitness of *Pseudomonas aeruginosa* through SOS pathway (Torres-Barceló et al., 2015). The uptake of DNA from prey cells by *Acinetobacter baylyi* using type VI secretion system resulted in the upregulation of the SOS response and extensive filamentation (Lin et al., 2019). Antimicrobial peptide (AMP) including periplanetasin-2 and bac8c induced *Escherichia coli* apoptosis-like death via reactive oxygen species (ROS) relating to the participation of RecA protein and the SOS system (Lee and Lee, 2019; Lee et al., 2019). Bacterial ROS production and SOS response could increase bacterial mutagenesis and resistance (for example, fluoroquinolones) (Rodríguez-Rosado et al., 2019). The deleterious effects such as mutagenesis and cell death in *Bacillus subtilis* caused by hexavalent chromium were counteracted by SOS response system in a RecA protein-dependent manner (Santos-Escobar et al., 2019). DNA gyrase depletion in *Mycobacterium tuberculosis* could activate RecA/LexA-mediated SOS response by inducing persistent subpopulations (Choudhary et al., 2019). Based on the phage production mechanisms discussed above, it can be speculated that these drugs or bacterial activities may induce more active phages in the intestine due to the activation of bacterial SOS system. The work of Oh et al. (2019) confirmed that SCFAs served as an activator of RecA protein in *L. reuteri*. Small molecules together with other metabolites produced in bacteria in relationship to the activation of prophages deserve in-depth and extensive research. It is a remarkable fact that some strains, such as *Acinetobacter baumannii* and *Acinetobacter baylyi*, do not have a homolog of LexA, suggesting that we should pay particular attention to prophage activation of these strains (Hare et al., 2014; Nguyen et al., 2019). The distribution of released phages is specific in the medium containing different inducers or cultivating in different stimulative environment, which implies the particularity of phage production dynamics (Fang et al., 2017; Oh et al., 2019). The types of temperate phages, prophage gene length, the interaction with bacterial genome, the interaction with other prophages, the SOS response intensity, special regulatory factors, integration site, and physiological characteristics of bacterial phages may play important roles in regulating of the prophage response during bacterial global stress (Tang et al., 2017). Currently, the knowledge of coexistence of free phages and bacterial community in gut is limited. It needs to be further studied whether or not there is an ecological niche competition between active phages and bacteria. Few studies comprehensively and systematically investigated how prophage activation induced by exogenous interference affect intestinal health. The roles of gut temperate phages and the potential biological significance of the increased number of bacteriophages in the intestines of patients such as IBD and CDI remain largely to be explored. Classification and susceptible hosts of intestinal temperate phages are weakly unknown, which are crucial problems for the further understanding of intestinal phages. Although understanding prophage activation of pathogenic bacteria may be of greater significance, we have little knowledge about the activation and transfer of prophages in non-pathogenic gut bacteria.

With the in-depth understanding of phages and the development of biotechnology, temperate phages are introduced into phage therapy. Prophage activation regulation therapy has broad application prospects in terms of the bacterial disease treatment. It inspires us that dietary intervention, medicine use, genome editing, genetically engineered bacteriophages, and environmental control which can potentially regulate the dynamic changes of prophages can be used to maintain the intestinal health. In addition, cryptic (defective) prophage excision that cannot lyse their hosts and produce active phages is a potentially promising target for the phage therapy development (Wang and Wood, 2016). Many studies have investigated roles of prophages in their bacterial hosts, wherein, some (cryptic) prophages were considered as being mutualistic (Obeng et al., 2016). A wealth of evidence has revealed that cryptic prophages make contributions in some beneficial phenotypes (for example, virulence, antibiotic resistance, and antibiotic tolerance) in bacteria and has been thoroughly reviewed by Wang and Wood (2016). Therefore, once the beneficial cryptic prophages are excised by using inducers or genetically modified methods, the adaptive advantage of host obtained from prophages is likely to be lost. Cryptic prophage excision may also reduce the cell viability via enhancing the expression of cell lysis genes (for example, *alpA and intD*) (Wang et al., 2009). However, it should be noted that cryptic prophage excision has a low probability of occurrence under various environments, which may hinder its application in bacterial disease (Sozhamannan et al., 2006). In short, we are looking forward to making a breakthrough in prophage activation/excision regulation therapy in the future.

CONCLUSION

Intestinal prophages can be activated by a variety of factors, including diet, antibiotics, certain bacterial metabolites, gastrointestinal transit, inflammatory environment, intestinal temperature change, oxidative stress, and quorum sensing, etc. Released active phages may experience several different life status, including lysogenic conversion, transduction, auto-transduction, lytic cycles, mucoidy, biofilm–phage interaction, and bacteriophage adherent to mucus model etc. Effects of prophage induction on bacterial host and gut health have both positive and negative sides. Thus, as part of the multidimensional strategies for bacterial disease, prophage activation regulation therapy is flexible. Nevertheless, efforts should been made to know more mechanisms about how prophage induction happened, dynamic transformation of prophages, and the role of prophage activation in gut health. While lytic phages are likely to remain the main choice for phage therapy, considering the importance of prophages in bacterial function and evolution, prophage activation regulation therapy is worthy of thorough study by researchers.

AUTHOR CONTRIBUTIONS

JH: writing–original draft preparation, visualization, and conceptualization. HY: writing–review and editing. SW: conceptualization. JW: conceptualization, funding acquisition, and project administration. DH: supervision, project administration, writing–review and editing, and funding acquisition. All authors have approved this work for publication.

FUNDING

This work was supported by the National Natural Science Foundation of China (grant nos. 31902170 and 31630074), the Beijing Municipal Natural Science Foundation (grant no. S170001), and the Fundamental Research Funds for the Central Universities (grant no. 2020TC067).

REFERENCES

Alam, M. K., Alhhazmi, A., DeCoteau, J. F., Luo, Y., and Geyer, C. R. (2016). RecA inhibitors potentiate antibiotic activity and block evolution of antibiotic resistance. *Cell Chem. Biol.* 23, 381–391. doi: 10.1016/j.chembiol.2016.02.010

Alexander, L. M., Oh, J.-H., Stapleton, D. S., Schueler, K. L., Keller, M. P., Attie, A. D., et al. (2019). Exploiting prophage-mediated lysis for biotherapeutic release by *Lactobacillus reuteri*. *Appl. Environ. Microbiol.* 85:e02335-18. doi: 10.1128/aem.02335-18

Au, N., Kuester-Schoeck, E., Mandava, V., Bothwell, L. E., Canny, S. P., Chachu, K., et al. (2005). Genetic composition of the *Bacillus subtilis* SOS system. *J. Bacteriol.* 187, 7655–7666. doi: 10.1128/JB.187.22.7655-7666.2005

Balasubramanian, D., Ragunathan, P. T., Fei, J., and Vanderpool, C. K. (2016). A prophage-encoded small RNA controls metabolism and cell division in *Escherichia coli*. *mSystems* 1:e00021-15. doi: 10.1128/msystems.00021-15

Balasubramanian, S., Osburne, M. S., Brinjones, H., Tai, A. K., and Leong, J. M. (2019). Prophage induction, but not production of phage particles, is required for lethal disease in a microbiome-replete murine model of enterohemorrhagic *E. coli* infection. *PLoS Pathog.* 15:e1007494. doi: 10.1371/journal.ppat.1007494

Barr, J. J., Auro, R., Furlan, M., Whiteson, K. L., Erb, M. L., Pogliano, J., et al. (2013). Bacteriophage adhering to mucus provide a non-host-derived immunity. *Proc. Natl. Acad. Sci. U.S.A.* 110, 10771–10776. doi: 10.1073/pnas.1305923110

Bellio, P., Di Pietro, L., Mancini, A., Piovano, M., Nicoletti, M., Brisdelli, F., et al. (2017). SOS response in bacteria: inhibitory activity of lichen secondary metabolites against *Escherichia coli* RecA protein. *Phytomedicine* 29, 11–18. doi: 10.1016/j.phymed.2017.04.001

Bertani, G. (1951). Studies on lysogenesis . I. The mode of phage liberation by lysogenic *Escherichia coli*. *J. Bacteriol.* 62, 293–300. doi: 10.1128/jb.62.3.293-300.1951

Bloch, S., Nejman-Faleńczyk, B., Łoś, J. M., Barańska, S., Łepek, K., Felczykowska, A., et al. (2013). Genes from the exo-xis region of lambda and Shiga toxin-converting bacteriophages influence lysogenization and prophage induction. *Arch. Microbiol.* 195, 693–703. doi: 10.1007/s00203-013-0920-8

Bloch, S., Nejman-Faleńczyk, B., Pierzynowska, K., Piotrowska, E., Wêgrzyn, A., Marminon, C., et al. (2018). Inhibition of Shiga toxin-converting bacteriophage development by novel antioxidant compounds. *J. Enzyme. Inhib. Med. Chem.* 33, 639–650. doi: 10.1080/14756366.2018.1444610

Boling, L., Cuevas, D. A., Grasis, J. A., Kang, H. S., Knowles, B., Levi, K., et al. (2020). Dietary prophage inducers and antimicrobials: toward landscaping the human gut microbiome. *Gut Microb.* 11, 721–734. doi: 10.1080/19490976.2019.1701353

Breitbart, M., Hewson, I., Felts, B., Mahaffy, J. M., Nulton, J., Salamon, P., et al. (2003). Metagenomic analyses of an uncultured viral community from human feces. *J. Bacteriol.* 185, 6220–6223. doi: 10.1128/jb.185.20.6220-6223.2003

Bunnell, B. E., Escobar, J. F., Bair, K. L., Sutton, M. D., and Crane, J. K. (2017). Zinc blocks SOS-induced antibiotic resistance via inhibition of RecA in *Escherichia coli*. *PLoS One* 12:e0178303. doi: 10.1371/journal.pone.0178303

Carrasco, B., Escobedo, S., Alonso, J. C., and Suárez, J. E. (2016). Modulation of *Lactobacillus casei* bacteriophage A2 lytic/lysogenic cycles by binding of Gp25 to the early lytic mRNA. *Mol. Microbiol.* 99, 328–337. doi: 10.1111/mmi.13234

Chakraborty, D., Clark, E., Mauro, S. A., and Koudelka, G. B. (2018). Molecular mechanisms governing "hair-trigger" induction of Shiga toxin-encoding prophages. *Viruses* 10:228. doi: 10.3390/v10050228

Chatterjee, A., and Duerkop, B. A. (2018). Beyond bacteria: bacteriophage-eukaryotic host interactions reveal emerging paradigms of health and disease. *Front. Microbiol.* 9:1394. doi: 10.3389/fmicb.2018.01394

Chaudhry, W., Lee, E., Worthy, A., Weiss, Z., Grabowicz, M., Vega, N., et al. (2019). Mucoidy, a general mechanism for maintaining lytic phage in populations of bacteria. *BioRxiv* [Preprint]. doi: 10.1101/775056

Chen, J., Quiles-Puchalt, N., Chiang, Y. N., Bacigalupe, R., Fillol-Salom, A., Chee, M. S. J., et al. (2018). Genome hypermobility by lateral transduction. *Science* 362, 207–212. doi: 10.1126/science.aat5867

Choudhary, E., Sharma, R., Kumar, Y., and Agarwal, N. (2019). Conditional silencing by CRISPRi reveals the role of DNA gyrase in formation of drug-tolerant persister population in *Mycobacterium tuberculosis*. *Front. Cell Infect. Microbiol.* 9:70. doi: 10.3389/fcimb.2019.00070

Colon, M. P., Chakraborty, D., Pevzner, Y., and Koudelka, G. B. (2016). Mechanisms that determine the differential stability of Stx^{+} and Stx(−) lysogens. *Toxins* 8:96. doi: 10.3390/toxins8040096

Cornuault, J. F., Petit, M.-A., Mariadassou, M., Benevides, L., Moncaut, E., Langella, P., et al. (2018). Phages infecting *Faecalibacterium prausnitzii* belong to novel viral genera that help to decipher intestinal viromes. *Microbiome* 6:65. doi: 10.1186/s40168-018-0452-1

Cornuault, J. K., Moncaut, E., Loux, V., Mathieu, A., Sokol, H., Petit, M., et al. (2020). The enemy from within: a prophage of *Roseburia intestinalis* systematically turns lytic in the mouse gut, driving bacterial adaptation by CRISPR spacer acquisition. *ISME J.* 14, 771–787. doi: 10.1038/s41396-019-0566-x

David, L. A., Maurice, C. F., Carmody, R. N., Gootenberg, D. B., Button, J. E., Wolfe, B. E., et al. (2014). Diet rapidly and reproducibly alters the human gut microbiome. *Nature* 505, 559–563. doi: 10.1038/nature12820

Diard, M., Bakkeren, E., Cornuault, J. K., Moor, K., Hausmann, A., Sellin, M. E., et al. (2017). Inflammation boosts bacteriophage transfer between *Salmonella* spp. *Science* 355, 1211–1215. doi: 10.1126/science.aaf8451

Dong, N., Li, X., Xue, C., Wang, C., Xu, X., Bi, C., et al. (2019). Astragalus polysaccharides attenuated inflammation and balanced the gut microflora in mice challenged with *Salmonella* Typhimurium. *Int. Immunopharmacol.* 74:105681. doi: 10.1016/j.intimp.2019.105681

Duerkop, B. A., Kleiner, M., Paez-Espino, D., Zhu, W., Bushnell, B., Hassell, B., et al. (2018). Murine colitis reveals a disease-associated bacteriophage community. *Nat. Microbiol.* 3, 1023–1031. doi: 10.1038/s41564-018-0210-y

Dy, R. L., Richter, C., Salmond, G. P. C., and Fineran, P. C. (2014). Remarkable mechanisms in microbes to resist phage infections. *Annu. Rev. Virol.* 1, 307–331. doi: 10.1146/annurev-virology-031413-085500

Eichhorn, I., Heidemanns, K., Ulrich, R. G., Schmidt, H., Semmler, T., Fruth, A., et al. (2018). Lysogenic conversion of atypical enteropathogenic *Escherichia coli* (aEPEC) from human, murine, and bovine origin with bacteriophage Φ3538 Δstx2:: cat proves their enterohemorrhagic *E. coli* (EHEC) progeny. *Int. J. Med. Microbiol.* 308, 890–898. doi: 10.1016/j.ijmm.2018.06.005

Erez, Z., Steinberger-Levy, I., Shamir, M., Doron, S., Stokar-Avihail, A., Peleg, Y., et al. (2017). Communication between viruses guides lysis–lysogeny decisions. *Nature* 541, 488–493. doi: 10.1038/nature21049

Fang, Y., Mercer, R. G., Mcmullen, L. M., and Gänzle, M. G. (2017). Induction of Shiga toxin-encoding prophage by abiotic environmental stress in food. *Appl. Environ. Microbiol.* 83:e01378-17. doi: 10.1128/aem.01378-17

Federici, S., Nobs, S. P., and Elinav, E. (2020). Phages and their potential to modulate the microbiome and immunity. *Cell Mol. Immunol.* 18, 889–904. doi: 10.1038/s41423-020-00532-4

Fillol-Salom, A., Bacarizo, J., Alqasmi, M., Ciges-Tomas, J. R., Martínez-Rubio, R., Roszak, A. W., et al. (2019). Hijacking the hijackers: *Escherichia coli* pathogenicity islands redirect helper phage packaging for their own benefit. *Mol. Cell.* 75, 1020–1030. doi: 10.1016/j.molcel.2019.06.017

Friedberg, E. C., Walker, G. C., Siede, W., Wood, R. D., Schultz, R. A., and Ellenberger, T. (2005). *DNA Repair and Mutagenesis*. Washington, DC: American Society for Microbiology Press.

Ghodke, H., Paudel, B. P., Lewis, J. S., Jergic, S., Gopal, K., Romero, Z. J., et al. (2019). Spatial and temporal organization of RecA in the *Escherichia coli* DNA-damage response. *eLife* 8:e42761. doi: 10.7554/elife.42761

Ghosh, D., Roy, K., Williamson, K. E., Srinivasiah, S., Wommack, K. E., and Radosevich, M. (2009). Acyl-homoserine lactones can induce virus production in lysogenic bacteria: an alternative paradigm for prophage induction. *Appl. Environ. Microbiol.* 75, 7142–7152. doi: 10.1128/AEM.00950-09

Gogokhia, L., Buhrke, K., Bell, R., Hoffman, B., Brown, D. G., Hanke-Gogokhia, C., et al. (2019). Expansion of bacteriophages is linked to aggravated intestinal inflammation and colitis. *Cell Host Microbe* 25, 285.e8–299.e8. doi: 10.1016/j.chom.2019.01.008

Haaber, J., Leisner, J. J., Cohn, M. T., Catalan-Moreno, A., Nielsen, J. B., Westh, H., et al. (2016). Bacterial viruses enable their host to acquire antibiotic resistance genes from neighbouring cells. *Nat. Commun.* 7:13333. doi: 10.1038/ncomms13333

Hare, J. M., Ferrell, J. C., Witkowski, T. A., and Grice, A. N. (2014). Prophage induction and differential RecA and UmuDAb transcriptome regulation in the DNA damage responses of *Acinetobacter baumannii* and *Acinetobacter baylyi*. *PLoS One* 9:e93861. doi: 10.1371/journal.pone.0093861

Hatfull, G. F., and Hendrix, R. W. (2011). Bacteriophages and their genomes. *Curr. Opin. Virol.* 1, 298–303. doi: 10.1016/j.coviro.2011.06.009

Hernández, S. B., Cota, I., Ducret, A., Aussel, L., and Casadesús, J. (2012). Adaptation and preadaptation of *Salmonella enterica* to bile. *PLoS Genet.* 8:e1002459. doi: 10.1371/journal.pgen.1002459

Horiuchi, T., and Inokuchi, H. (1967). Temperature-sensitive regulation system of prophage lambda induction. *J. Mol. Biol.* 23, 217–224. doi: 10.1016/s0022-2836(67)80029-9

Howard-Varona, C., Hargreaves, K. R., Abedon, S. T., and Sullivan, M. B. (2017). Lysogeny in nature: mechanisms, impact and ecology of temperate phages. *ISME J.* 11, 1511–1520. doi: 10.1038/ismej.2017.16

Howe, A., Ringus, D. L., Williams, R. J., Choo, Z.-N., Greenwald, S. M., Owens, S. M., et al. (2016). Divergent responses of viral and bacterial communities in the gut microbiome to dietary disturbances in mice. *ISME J.* 10, 1217–1227. doi: 10.1038/ismej.2015.183

Hsu, B. B., Gibson, T. E., Yeliseyev, V., Liu, Q., Lyon, L., Bry, L., et al. (2019). Dynamic modulation of the gut microbiota and metabolome by bacteriophages in a mouse model. *Cell Host Microbe* 25, 803.e5–814.e5. doi: 10.1016/j.chom.2019.05.001

Hsu, B. B., Way, J. C., and Silver, P. A. (2020). Stable neutralization of virulent bacteria using temperate phage in the mammalian gut. *mSystems* 5:e00013-20. doi: 10.1128/mSystems.00013-20

Ichimura, K., Shimizu, T., Matsumoto, A., Hirai, S., Yokoyama, E., Takeuchi, H., et al. (2017). Nitric oxide-enhanced Shiga toxin production was regulated by Fur and RecA in enterohemorrhagic *Escherichia coli* O157. *MicrobiologyOpen* 6:e00461. doi: 10.1002/mbo3.461

Jackson, S. A., and Fineran, P. C. (2019). Bacterial dormancy curbs phage epidemics. *Nature* 570, 173–174. doi: 10.1038/d41586-019-01595-8

Jensen, E. A., Young, J. A., Jackson, Z., Busken, J., List, E. O., Carroll, R. K., et al. (2020). Growth hormone deficiency and excess alter the gut microbiome in adult male mice. *Endocrinology* 161, 1–18. doi: 10.1210/endocr/bqaa026

Jover, L. F., Cortez, M. H., and Weitz, J. S. (2013). Mechanisms of multi-strain coexistence in host–phage systems with nested infection networks. *J. Theor. Biol.* 332, 65–77. doi: 10.1016/j.jtbi.2013.04.011

Kenzaka, T., Tani, K., Sakotani, A., Yamaguchi, N., and Nasu, M. (2007). High-frequency phage-mediated gene transfer among *Escherichia coli* cells, determined at the single-cell level. *Appl. Environ. Microbiol.* 73, 3291–3299. doi: 10.1128/AEM.02890-06

Khan, A., and Wahl, L. M. (2019). Quantifying the forces that maintain prophages in bacterial genomes. *Theor. Popul. Biol.* 133, 168–179. doi: 10.1016/j.tpb.2019.11.003

Kim, M.-S., and Bae, J.-W. (2018). Lysogeny is prevalent and widely distributed in the murine gut microbiota. *ISME J.* 12, 1127–1141. doi: 10.1038/s41396-018-0061-9

Kraushaar, B., Hammerl, J. A., Kienöl, M., Heinig, M. L., Sperling, N., Thanh, M. D., et al. (2017). Acquisition of virulence factors in livestock-associated MRSA: lysogenic conversion of CC398 strains by virulence gene-containing phages. *Sci. Rep.* 7:2004. doi: 10.1038/s41598-017-02175-4

Kreuzer, K. N. (2013). DNA damage responses in prokaryotes: regulating gene expression, modulating growth patterns, and manipulating replication forks. *Cold Spring Harb. Perspect. Biol.* 5:a012674. doi: 10.1101/cshperspect.a012674

Kronheim, S., Daniel-Ivad, M., Duan, Z., Hwang, S., Wong, A. I., Mantel, I., et al. (2018). A chemical defence against phage infection. *Nature* 564, 283–286. doi: 10.1038/s41586-018-0767-x

Laganenka, L., Sander, T., Lagonenko, A., Chen, Y., Link, H., and Sourjik, V. (2019). Quorum sensing and metabolic state of the host control lysogeny-lysis switch of bacteriophage T1. *mBio* 10:e01884-19. doi: 10.1128/mbio.01884-19

Latino, L., Midoux, C., Vergnaud, G., and Pourcel, C. (2019). Investigation of *Pseudomonas aeruginosa* strain PcyII-10 variants resisting infection by N4-like phage Ab09 in search for genes involved in phage adsorption. *PLoS One* 14:e0215456. doi: 10.1371/journal.pone.0215456

Lee, B., Hwang, J. S., and Lee, D. G. (2019). Induction of apoptosis-like death by periplanetasin-2 in *Escherichia coli* and contribution of SOS genes. *Appl. Microbiol. Biotechnol.* 103, 1417–1427. doi: 10.1007/s00253-018-9561-9

Lee, H., and Lee, D. G. (2019). SOS genes contribute to Bac8c induced apoptosis-like death in *Escherichia coli*. *Biochimie* 157, 195–203. doi: 10.1016/j.biochi.2018.12.001

Li, C., Wally, H., Miller, S. J., and Lu, C. D. (2009). The multifaceted proteins MvaT and MvaU, members of the H-NS family, control arginine metabolism, pyocyanin synthesis, and prophage activation in *Pseudomonas aeruginosa* PAO1. *J. Bacteriol.* 191, 6211–6218. doi: 10.1128/jb.00888-09

Liang, G., Zhao, C., Zhang, H., Mattei, L., Sherrill-Mix, S., Bittinger, K., et al. (2020). The stepwise assembly of the neonatal virome is modulated by breastfeeding. *Nature* 581, 470–474. doi: 10.1038/s41586-020-2192-1

Liang, X., Wagner, R. E., Li, B., Zhang, N., and Radosevich, M. (2019). Prophage induction mediated by quorum sensing signals alters soil bacterial community structure. *bioRxiv* [Preprint]. doi: 10.1101/805069

Licznerska, K., Nejman-Faleńczyk, B., Bloch, S., Dydecka, A., Topka, G., Gąsior, T., et al. (2015). Oxidative stress in Shiga toxin production by enterohemorrhagic *Escherichia coli*. *Oxid. Med. Cell Longev.* 2016:3578368. doi: 10.1155/2016/3578368

Lin, L., Ringel, P. D., Vettiger, A., Dürr, L., and Basler, M. (2019). DNA uptake upon T6SS-dependent prey cell lysis induces SOS response and reduces fitness of *Acinetobacter baylyi*. *Cell Rep.* 29, 1633–1644. doi: 10.1016/j.celrep.2019.09.083

Little, J. W. (1991). Mechanism of specific LexA cleavage: autodigestion and the role of RecA coprotease. *Biochimie* 73, 411–421. doi: 10.1016/0300-9084(91)90108-d

Łobocka, M. B., Rose, D. J., Plunkett, G., Rusin, M., Samojedny, A., Lehnherr, H., et al. (2004). Genome of bacteriophage P1. *J. Bacteriol.* 186, 7032–7068. doi: 10.32388/ieb39m

Łoś, J. M., Łoś, M., Wêgrzyn, G., and Wêgrzyn, A. (2009). Differential efficiency of induction of various lambdoid prophages responsible for production of Shiga toxins in response to different induction agents. *Microb. Pathog.* 47, 289–298. doi: 10.1016/j.micpath.2009.09.006

Lourenço, M., Chaffringeon, L., Lamy-Besnier, Q., Pédron, T., Campagne, P., Eberl, C., et al. (2020). The spatial heterogeneity of the gut limits predation and fosters coexistence of bacteria and bacteriophages. *Cell Host Microbe* 28, 390.e5–401.e5. doi: 10.1016/j.chom.2020.06.002

Luján, A. M., Moyano, A. J., Martino, R. A., Feliziani, S., Urretavizcaya, M., and Smania, A. M. (2019). ImuB and ImuC contribute to UV-induced mutagenesis as part of the SOS regulon in *Pseudomonas aeruginosa*. *Environ. Mol. Mutagen.* 60, 594–601. doi: 10.1002/em.22290

Luo, Y., Pfuetzner, R. A., Mosimann, S., Paetzel, M., Frey, E. A., Cherney, M., et al. (2001). Crystal structure of LexA: a conformational switch for regulation of self-cleavage. *Cell* 106, 585–594. doi: 10.1016/s0092-8674(01)00479-2

Mahizir, D., Briffa, J. F., Wood, J. L., Anevska, K., Hill-Yardin, E. L., Jefferies, A. J., et al. (2020). Exercise improves metabolic function and alters the microbiome in rats with gestational diabetes. *FASEB J.* 34, 1728–1744. doi: 10.1096/fj.201901424R

Maiques, E., Ubeda, C., Campoy, S., Salvador, N., Lasa, I., Novick, R. P., et al. (2006). β-Lactam antibiotics induce the SOS response and horizontal transfer of virulence factors in *Staphylococcus aureus*. *J. Bacteriol.* 188, 2726–2729. doi: 10.1128/jb.188.7.2726-2729.2006

Marcelli, B., Karsens, H., Nijland, M., Oudshoorn, R., Kuipers, O. P., and Kok, J. (2020). Employing lytic phage-mediated horizontal gene transfer in *Lactococcus lactis*. *PLoS One* 15:e0238988. doi: 10.1371/journal.pone.0238988

Martínez, I., Kim, J., Duffy, P. R., Schlegel, V. L., and Walter, J. (2010). Resistant starches types 2 and 4 have differential effects on the composition of the fecal microbiota in human subjects. *PLoS One* 5:e15046. doi: 10.1371/journal.pone.0015046

Matej, B., Daniel, K., Vesna, H., Ana, R., Zdravko, P., Klare, J. P., et al. (2011). Interconversion between bound and free conformations of LexA orchestrates the bacterial SOS response. *Nucleic Acids Res.* 39, 6546–6557. doi: 10.1093/nar/gkr265

Matilla, M. A., Fang, X., and Salmond, G. P. C. (2014). Viunalikeviruses are environmentally common agents of horizontal gene transfer in pathogens and biocontrol bacteria. *ISME J.* 8, 2143–2147. doi: 10.1038/ismej.2014.150

Mccool, J. D., Long, E., Petrosino, J. F., Sandler, H. A., Rosenberg, S. M., and Sandler, S. J. (2004). Measurement of SOS expression in individual *Escherichia coli* K-12 cells using fluorescence microscopy. *Mol. Microbiol.* 53, 1343–1357. doi: 10.1111/j.1365-2958.2004.04225.x

Meessen-Pinard, M., Sekulovic, O., and Fortier, L. C. (2012). Evidence of in vivo prophage induction during *Clostridium difficile* infection. *Appl. Environ. Microbiol.* 78, 7662–7670. doi: 10.1128/aem.02275-12

Menouni, R., Champ, S., Espinosa, L., Boudvillain, M., and Ansaldi, M. (2013). Transcription termination controls prophage maintenance in *Escherichia coli* genomes. *Proc. Natl. Acad. Sci. U.S.A.* 110, 14414–14419. doi: 10.1073/pnas.1303400110

Miernikiewicz, P., Dąbrowska, K., Piotrowicz, A., Owczarek, B., Wojas-Turek, J., Kicielińska, J., et al. (2013). T4 phage and its head surface proteins do not stimulate inflammatory mediator production. *PLoS One* 8:e71036. doi: 10.1371/journal.pone.0071036

Minot, S., Sinha, R., Chen, J., Li, H., Keilbaugh, S. A., Wu, G. D., et al. (2011). The human gut virome: inter-individual variation and dynamic response to diet. *Genome Res.* 21, 1616–1625. doi: 10.1101/gr.122705.111

Monteiro, R., Pires, D. P., Costa, A. R., and Azeredo, J. (2019). Phage therapy: going temperate? *Trends Microbiol.* 27, 368–378. doi: 10.1016/j.tim.2018.10.008

Muegge, B. D., Kuczynski, J., Knights, D., Clemente, J. C., González, A., Fontana, L., et al. (2011). Diet drives convergence in gut microbiome functions across mammalian phylogeny and within humans. *Science* 332, 970–974. doi: 10.1126/science.1198719

Nanda, A., Thormann, K., and Frunzke, J. (2015). Impact of spontaneous prophage induction on the fitness of bacterial populations and host-mcrobe interactions. *J. Bacteriol.* 197, 410–419. doi: 10.1128/jb.02230-14

Nedialkova, L. P., Sidstedt, M., Koeppel, M. B., Spriewald, S., Ring, D., Gerlach, R. G., et al. (2016). Temperate phages promote colicin-dependent fitness of *Salmonella enterica* serovar Typhimurium. *Environ. Microbiol.* 18, 1591–1603. doi: 10.1111/1462-2920.13077

Nguyen, B. H., Macguire, A. E., Ching, C., and Godoy, V. H. (2019). Identification of a TetR-like repressor involved in the regulation of error-prone DNA polymerases in *Acinetobacter baumannii*. *FASEB J.* 33:458.

Nguyen, S., Baker, K., Padman, B. S., Patwa, R., Dunstan, R. A., Weston, T. A., et al. (2017). Bacteriophage transcytosis provides a mechanism to cross epithelial cell layers. *mBio* 8:e01874-17. doi: 10.1128/mbio.01874-17

Nowicki, D., Maciąg-Dorszyńska, M., Kobiela, W., Herman-Antosiewicz, A., Węgrzyn, A., Szalewska-Pałasz, A., et al. (2014). Phenethyl isothiocyanate inhibits Shiga toxin production in enterohemorrhagic *Escherichia coli* by stringent response induction. *Antimicrob. Agents Chem.* 58, 2304–2315. doi: 10.1128/AAC.02515-13

Obeng, N., Pratama, A. A., and Elsas, J. D. V. (2016). The significance of mutualistic phages for bacterial ecology and evolution. *Trends Microbiol.* 24, 440–449. doi: 10.1016/j.tim.2015.12.009

Ofir, G., Melamed, S., Sberro, H., Mukamel, Z., Silverman, S., Yaakov, G., et al. (2018). DISARM is a widespread bacterial defence system with broad anti-phage activities. *Nat. Microbiol.* 3, 90–98. doi: 10.1038/s41564-017-0051-0

Oh, J.-H., Alexander, L. M., Pan, M., Schueler, K. L., Keller, M. P., Attie, A. D., et al. (2019). Dietary fructose and microbiota-derived short-chain fatty acids promote bacteriophage production in the gut symbiont *Lactobacillus reuteri*. *Cell Host Microbe* 25, 273.e6–284.e6. doi: 10.1016/j.chom.2018.11.016

Ojha, D., and Patil, K. N. (2019). p-Coumaric acid inhibits the *Listeria monocytogenes* RecA protein functions and SOS response: an antimicrobial target. *Biochem. Biophys. Res. Commun.* 517, 655–661. doi: 10.1016/j.bbrc.2019.07.093

Peters, D. L., Mccutcheon, J. G., Stothard, P., and Dennis, J. J. (2019). Novel *Stenotrophomonas* maltophilia temperate phage DLP4 is capable of lysogenic conversion. *BMC Genom.* 20:300. doi: 10.1186/s12864-019-5674-5

Petrovska, L., Mather, A. E., AbuOun, M., Branchu, P., Harris, S. R., Connor, T., et al. (2016). Microevolution of monophasic *Salmonella* Typhimurium during epidemic, United Kingdom, 2005–2010. *Emerg. Infect. Dis.* 22, 617–624. doi: 10.3201/eid2204.150531

Pierzynowska, K., Jasińska, W., Cyske, Z., Bunikowska, M., Droczek, R., and Wêgrzyn, G. (2018). Effects of some commonly used drinks on induction of Shiga toxin-converting prophage in *Escherichia coli*. *J. Verbrauch. Lebensm.* 13, 125–129. doi: 10.1007/s00003-018-1155-z

Prazdnova, E. V., Mazanko, M. S., Bren, A. B., Chistyakov, V. A., Weeks, R., and Chikindas, M. L. (2019). SOS response inhibitory properties by potential probiotic formulations of *Bacillus amyloliquefaciens* B-1895 and *Bacillus subtilis* KATMIRA1933 obtained by solid-state fermentation. *Curr. Microbiol.* 76, 312–319. doi: 10.1007/s00284-018-01623-2

Rabinovich, L., Sigal, N., Borovok, I., Nir-Paz, R., and Herskovits, A. A. (2012). Prophage excision activates Listeria competence genes that promote phagosomal escape and virulence. *Cell* 150, 792–802. doi: 10.1016/j.cell.2012.06.036

Ragunathan, P. T., and Vanderpool, C. K. (2019). Cryptic-prophage-encoded small protein DicB protects *Escherichia coli* from phage infection by inhibiting inner membrane receptor proteins. *J. Bacteriol.* 201:e00475-19. doi: 10.1128/JB.00475-19

Ravin, N. V. (2015). Replication and maintenance of linear phage-plasmid N15. *Microbiol. Spectr.* 3:PLAS-0032-2014. doi: 10.1128/microbiolspec.plas-0032-2014

Reyes, A., Semenkovich, N. P., Whiteson, K., Rohwer, F., and Gordon, J. I. (2012). Going viral: next-generation sequencing applied to phage populations in the human gut. *Nat. Rev. Microbiol.* 10, 607–617. doi: 10.1038/nrmicro2853

Reynauda, A., Cloastrea, L., Bernarda, J., Laveranb, H., Ackermannc, H.-W., Licoisd, D., et al. (1992). Characteristics and diffusion in the rabbit of a phage for *Escherichia coli* 0103. Attempts to use this phage for therapy. *Vet. Microbiol.* 30, 203–212. doi: 10.1016/0378-1135(92)90114-9

Rodríguez-Rosado, A. I., Valencia, E. Y., Rodríguez-Rojas, A., Costas, C., Galhardo, R. S., Rodríguez-Beltrán, J., et al. (2019). N-acetylcysteine blocks SOS induction and mutagenesis produced by fluoroquinolones in *Escherichia coli*. *J. Antimicrob. Chemother.* 74, 2188–2196. doi: 10.1093/jac/dkz210

Rossmann, F. S., Racek, T., Wobser, D., Puchalka, J., Rabener, E. M., Reiger, M., et al. (2015). Phage-mediated dispersal of biofilm and distribution of bacterial virulence genes is induced by quorum sensing. *PLoS Pathog.* 11:e1004653. doi: 10.1371/journal.ppat.1004653

Santos-Escobar, F., Leyva-Sánchez, H. C., Ramírez-Ramírez, N., Obregón-Herrera, A., and Pedraza-Reyes, M. (2019). Roles of *Bacillus subtilis* RecA, nucleotide excision repair, and translesion synthesis polymerases in counteracting Cr (VI)-promoted DNA damage. *J. Bacteriol.* 201:e00073-19. doi: 10.1128/jb.00073-19

Sausset, R., Petit, M. A., Gaboriau-Routhiau, V., and De Paepe, M. (2020). New insights into intestinal phages. *Mucosal Immunol.* 13, 205–215. doi: 10.1038/s41385-019-0250-5

Selwood, T., Larsen, B. J., Mo, C. Y., Culyba, M. J., Hostetler, Z. M., Kohli, R. M., et al. (2018). Advancement of the 5-amino-1-(carbamoylmethyl)-1H-1, 2, 3-triazole-4-carboxamide scaffold to disarm the bacterial SOS response. *Front. Microbiol.* 9:2961. doi: 10.3389/fmicb.2018.02961

Seo, S.-U., and Kweon, M.-N. (2019). Virome-host interactions in intestinal health and disease. *Curr. Opin. Virol.* 37, 63–71. doi: 10.1016/j.coviro.2019.06.003

Sheng, L., Rasco, B., and Zhu, M.-J. (2016). Cinnamon oil inhibits Shiga toxin type 2 phage induction and Shiga toxin type 2 production in *Escherichia coli* O157:H7. *Appl. Environ. Microbiol.* 82, 6531–6540. doi: 10.1128/aem.01702-16

Silpe, J. E., and Bassler, B. L. (2019). A host-produced quorum-sensing autoinducer controls a phage lysis-lysogeny decision. *Cell* 176, 268.e13–280.e13. doi: 10.1016/j.cell.2018.10.059

Simmons, M., Drescher, K., Nadell, C. D., and Bucci, V. (2018). Phage mobility is a core determinant of phage–bacteria coexistence in biofilms. *ISME J.* 12, 531–543. doi: 10.1038/ismej.2017.190

Sozhamannan, S., Chute, M. D., McAfee, F. D., Fouts, D. E., Akmal, A., Galloway, D. R., et al. (2006). The *Bacillus anthracis* chromosome contains four conserved, excision-proficient, putative prophages. *BMC Microbial* 6:34. doi: 10.1186/1471-2180-6-34

Tamang, M. D., Sunwoo, H., and Jeon, B. (2017). Phage-mediated dissemination of virulence factors in pathogenic bacteria facilitated by antibiotic growth promoters in animals: a perspective. *Anim. Health Res. Rev.* 18, 160–166. doi: 10.1017/s1466252317000147

Tan, D., Hansen, M. F., de Carvalho, L. N., Røder, H. L., Burmølle, M., Middelboe, M., et al. (2020). High cell densities favor lysogeny: induction of an H20 prophage is repressed by quorum sensing and enhances biofilm formation in *Vibrio anguillarum*. *ISME J.* 14, 1731–1742. doi: 10.1038/s41396-020-0641-3

Tang, Y., Nielsen, L. N., Hvitved, A., Haaber, J. K., Wirtz, C., Andersen, P. S., et al. (2017). Commercial biocides induce transfer of prophage Φ13 from human strains of *Staphylococcus aureus* to livestock CC398. *Front. Microbiol.* 8:2418. doi: 10.3389/fmicb.2017.02418

Torres-Barceló, C., Kojadinovic, M., Moxon, R., and Maclean, R. C. (2015). The SOS response increases bacterial fitness, but not evolvability, under a sublethal dose of antibiotic. *Proc. Biol. Sci.* 282:20150885. doi: 10.1098/rspb.2015.0885

Touchon, M., de Sousa, J. A. M., and Rocha, E. (2017). Embracing the enemy: the diversification of microbial gene repertoires by phage-mediated horizontal. *Curr. Opin. Microbiol.* 38, 66–73. doi: 10.1016/j.mib.2017.04.010

Turnbaugh, P. J., Ridaura, V. K., Faith, J. J., Rey, F. E., Knight, R., and Gordon, J. I. (2009). The effect of diet on the human gut microbiome: a metagenomic analysis in humanized gnotobiotic mice. *Sci. Transl. Med.* 1:6ra14. doi: 10.1126/scitranslmed.3000322

Vitetta, L., Vitetta, G., and Hall, S. (2018). Immunological tolerance and function: associations between intestinal bacteria, probiotics, prebiotics, and phages. *Front. Immunol.* 9:2240. doi: 10.3389/fimmu.2018.02240

Wadhwa, D. (2017). Design principle of Lambda's lysis/lysogeny decision vis-a-vis multiplicity of infection. *BioRxiv* [Preprint]. doi: 10.1101/146308

Waldor, M. K., and Mekalanos, J. J. (1996). Lysogenic conversion by a filamentous phage encoding cholera toxin. *Science* 272, 1910–1914. doi: 10.1126/science.272.5270.1910

Walsh, E., Henrikus, S. S., Vaisman, A., Makiela-Dzbenska, K., Armstrong, T. J., Łazowski, K., et al. (2019). Role of RNase H enzymes in maintaining genome stability in *Escherichia coli* expressing a steric-gate mutant of pol VICE391. *DNA Repair* 84:102685. doi: 10.1016/j.dnarep.2019.102685

Wang, X., Kim, Y., and Wood, T. K. (2009). Control and benefits of CP4-57 prophage excision in *Escherichia coli* biofilms. *ISME J.* 3, 1164–1179. doi: 10.1038/ismej.2009.59

Wang, X., and Wood, T. K. (2016). Cryptic prophages as targets for drug development. *Drug Resist. Update* 27, 30–38. doi: 10.1016/j.drup.2016.06.001

Wu, H., Sampson, L., Parr, R., and Casjens, S. (2002). The DNA site utilized by bacteriophage P22 for initiation of DNA packaging. *Mol. Microbiol.* 45, 1631–1646. doi: 10.1046/j.1365-2958.2002.03114.x

Xia, J., Chiu, L. Y., Nehring, R. B., Núñez, M. A. B., Mei, Q., Perez, M., et al. (2019). Bacteria-to-human protein networks reveal origins of endogenous DNA damage. *Cell* 176, 127.e24–143.e24. doi: 10.1016/j.cell.2018.12.008

Yakimov, A., Pobegalov, G., Bakhlanova, I., Khodorkovskii, M., Petukhov, M., and Baitin, D. (2017). Blocking the RecA activity and SOS-response in bacteria with a short α-helical peptide. *Nucleic Acids Res.* 45, 9788–9796. doi: 10.1093/nar/gkx687

Yin, M.-C., Chang, C.-H., Su, C.-H., Yu, B., and Hsu, Y.-M. (2018). Pteris multifida, Cortex phellodendri, and probiotics attenuated inflammatory status and immunity in mice with a *Salmonella enterica* serovar Typhimurium infection. *Biosci. Biotechnol. Biochem.* 82, 836–847. doi: 10.1080/09168451.2018.1447356

Zeng, Z., Liu, X., Yao, J., Guo, Y., Li, B., Li, Y., et al. (2016). Cold adaptation regulated by cryptic prophage excision in *Shewanella oneidensis*. *ISME J.* 10, 2787–2800. doi: 10.1038/ismej.2016.85

Zhang, H., Fouts, D. E., DePew, J., and Stevens, R. H. (2013). Genetic modifications to temperate *Enterococcus faecalis* phage Ef11 that abolish the establishment of lysogeny and sensitivity to repressor, and increase host range and productivity of lytic infection. *Microbiology* 159, 1023–1035. doi: 10.1099/mic.0.067116-0

Zhang, X., Mcdaniel, A. D., Wolf, L. E., Keusch, G. T., Waldor, M. K., and Acheson, D. W. K. (2000). Quinolone antibiotics induce Shiga toxin-encoding bacteriophages, toxin production, and death in mice. *J. Infect. Dis.* 181, 664–670. doi: 10.1086/315239

Conflict of Interest: The authors declare that the research was conducted in the absence of any commercial or financial relationships that could be construed as a potential conflict of interest.

Publisher's Note: All claims expressed in this article are solely those of the authors and do not necessarily represent those of their affiliated organizations, or those of the publisher, the editors and the reviewers. Any product that may be evaluated in this article, or claim that may be made by its manufacturer, is not guaranteed or endorsed by the publisher.

frontiers in Microbiology

ORIGINAL RESEARCH
published: 04 January 2022
doi: 10.3389/fmicb.2021.795081

Supplementing Mannan Oligosaccharide Reduces the Passive Transfer of Immunoglobulin G and Improves Antioxidative Capacity, Immunity, and Intestinal Microbiota in Neonatal Goats

*Chao Yang[1,2], Tianxi Zhang[1,2], Quanhua Tian[1,3], Yan Cheng[1,2], Kefyalew Gebeyew[1,2], Guowei Liu[1,4], Zhiliang Tan[1,2] and Zhixiong He[1,2]**

[1]CAS Key Laboratory for Agro-Ecological Processes in Subtropical Region, National Engineering Laboratory for Pollution Control and Waste Utilization in Livestock and Poultry Production, South-Central Experimental Station of Animal Nutrition and Feed Science in Ministry of Agriculture, Hunan Provincial Engineering Research Center for Healthy Livestock and Poultry Production, Institute of Subtropical Agriculture, The Chinese Academy of Sciences, Changsha, China, [2]University of Chinese Academy of Sciences, Beijing, China, [3]School of Environmental Ecology and Biological Engineering, Wuhan Institute of Technology, Wuhan, China, [4]College of Animal Science and Technology, Southwest University, Chongqing, China

OPEN ACCESS

Edited by:
Jia Yin,
Hunan Normal University, China

Reviewed by:
Li Fei,
Lanzhou University, China
Yordan Martinez Aguilar,
Zamorano, Honduras
Chen Zheng,
Gansu Agricultural University, China

***Correspondence:**
Zhixiong He
zxhe@isa.ac.cn

Specialty section:
This article was submitted to Microbial Symbioses, a section of the journal Frontiers in Microbiology

Received: 14 October 2021
Accepted: 15 November 2021
Published: 04 January 2022

Citation:
Yang C, Zhang T, Tian Q, Cheng Y, Gebeyew K, Liu G, Tan Z and He Z (2022) Supplementing Mannan Oligosaccharide Reduces the Passive Transfer of Immunoglobulin G and Improves Antioxidative Capacity, Immunity, and Intestinal Microbiota in Neonatal Goats. Front. Microbiol. 12:795081. doi: 10.3389/fmicb.2021.795081

Successful establishment of passive immunity (PIT) and regulation of intestinal microbiota are crucial for ruminants to maintain body health and reduce the risk of disease during the neonatal period. Thus, the objective of this study was to investigate the effects of mannan oligosaccharide (MOS) supplementation on passive transfer of immunoglobulin G (IgG), serum inflammatory cytokines and antioxidant levels as well as bacteria composition in the ileal digesta. A total of 14 healthy neonatal Ganxi black goats with similar birth weight (BW: 2.35 ± 0.55 kg) were selected and allocated into two groups, only fed colostrum and milk replacer (CON, $n = 7$) and supplemented MOS (0.06% of birth BW) in the colostrum and milk replacer (MOS, $n = 7$). The results indicated that MOS supplementation significantly reduced ($p < 0.05$) serum IgG level at 3 and 6 h after colostrum feeding. Serum GLP-1 level of goats in the MOS group was significantly lower ($p = 0.001$) than that in the CON group. Goats in the MOS group had higher serum CAT and lower MDA level than those in the CON group ($p < 0.05$). Serum anti-inflammatory cytokine level of interleukin 4 (IL-4) was increased ($p < 0.05$), while pro-inflammatory cytokine IL-6 level was reduced ($p < 0.05$) in the MOS group when compared with the CON group. In addition, MOS supplementation remarkably increased ($p < 0.05$) the level of secretory IgA (sIgA) in the ileal digesta. Principal coordinate analysis of 16S rRNA sequence based on Brinary jaccard, Bray curtis, and weighted UniFrac distance of ileal microbiota showed a distinct microbial differentiation between the CON and MOS groups ($p < 0.05$). The relative abundance of *Firmicutes* in the MOS group was higher than that in the CON group, while

the abundance of *Verrucomicrobia* was lower in the MOS group than that in the CON group at the phylum level ($p < 0.05$). The relative abundance of *Proteobacteria* tended to decrease ($p = 0.078$) in the MOS group at the phylum level. The results of LEfSe analysis showed that MOS group was characterized by a higher relative abundance of *Lactobacillus*, while the CON group was represented by a higher relative abundance of *Akkermansia* and *Ruminiclostridium_5*. Our findings demonstrated that MOS supplementation during the neonatal period increases antioxidant capacity and reduces the inflammatory response, and promotes IgA secretion and *Lactobacillus* colonization in the ileum. Thus, MOS induced positive effects are more pronounced in neonatal goats that might be an effective approach to maintain intestinal health and improve the surviving rate of neonatal ruminants.

Keywords: neonatal goat, mannan oligosaccharides, passive immunity, IgG, intestinal microbiota

INTRODUCTION

The morbidity and mortality of newborn ruminants is the main factor that largely restricts the development of animal husbandry and farm profitability (Dwyer et al., 2016). In the last decades, the mortality is up to 50% in sheep and goats during the pre-weaning period (Thiruvenkadan and Karunanithi, 2007), and the mortality in kid goat ranges from 11.5 to 37% (Thiruvenkadan and Karunanithi, 2007; Singh et al., 2011). Neonatal animals are susceptible to infectious diseases, including respiratory disorders and gastrointestinal diseases, because their imperfect immune system exhibits a limited capacity to resist the invasion of pathogenic agents (Windeyer et al., 2014; Cheng et al., 2021). As one of the common digestive disorders, diarrhea causes high mortality rates ranging from 29 to 58% of neonatal calves, which are mainly infected by pathogens including *Escherichia coli*, *Salmonella*, and *Cryptosporidium* (Hunter and Thompson, 2005; Azizzadeh et al., 2012; Windeyer et al., 2014). Thus, it is essential to formulate an effective feeding regime to decrease the morbidity and alleviate the mortality rates of goat kids during the neonatal period.

Colostrum is rich in immunoglobulin, immune-stimulating peptides, and antimicrobial agents (Micha et al., 2020). It is a crucial vehicle for neonatal ruminants to establish passive immunity (PIT) due to their special synepitheliochorial placenta structure that does not empower the transfer of aforementioned immune factors from the dam to the fetus (Borghesi et al., 2014). The functions of colostrum in establishing PIT, intestinal bacteria colonization and prevention of diarrhea are mainly affected by the quality of colostrum and feeding time after birth (Morrill et al., 2012; Fischer et al., 2018). Furthermore, colostrum is very likely to be contaminated by collecting staff and instruments, which may increase the risk of intestinal diseases for calves (Godden et al., 2012). Heat treatment (60°C, 60 min) is a recognized approach to decrease pathogenic bacterial count and has little effect on immunoglobulin G (IgG) concentration (Donahue et al., 2012). Feeding heat-treated colostrum during the first 12 h after birth can enhance the colonization of *Bifidobacterium* and reduce the prevalence of *E. coli* in the small intestine of the calve (Malmuthuge et al., 2015). These results indicate the role of heat-treated colostrum in PIT transfer and beneficial bacteria colonization of ruminants, which can be used to maintain intestinal health during the neonatal period.

Mannan-oligosaccharide (MOS) as a functional oligosaccharide is always widely used in the diets of pigs (Duan et al., 2016), hens (Bozkurt et al., 2016), and rabbits (Abdel-Hamid and Farahat, 2016) to improve growth performance and immunity. Supplementing MOS in the basal diets usually improves fiber digestion, nitrogen deposition, and antioxidant capacity in adult sheep (Zheng et al., 2018). MOS also enhances the immunity of cows infected by rotavirus and promotes the transfer of antibodies against rotavirus to their offspring (Franklin et al., 2005). Furthermore, MOS supplementation increases average daily gain (ADG) and inhibits the colonization of pathogenic and nonpathogenic *E. coli* in the intestine of young calves (Lucey et al., 2021). However, the information on the effects of MOS supplementation on IgG absorption, intestinal microbiota, and immunity in neonatal ruminants is limited.

In the current goat feeding system, the phenomenon that neonatal goats fail to intake adequate colostrum happens commonly due to the lower colostrum production of their dams. In addition, goat colostrum may contaminate by a severe infectious virus that induces Caprine Arthritis–Encephalitis (CAE) and increases the morbidity and mortality (Blacklaws et al., 2004). To ensure successful PIT transfer and minimize the risk of CAE for neonatal goats, bovine colostrum is widely used to instead of goat colostrum (Nordi et al., 2012). In the current study, we used heat treated bovine colostrum as active immune factors to feed the neonatal goats. The objective of this study was to investigate the effects of MOS supplementation on serum biochemistry, IgG absorption, antioxidant ability, immunity, and the colonization of ileal bacteria in neonatal goats.

MATERIALS AND METHODS

Colostrum Collection, Process, and Chemical Composition Analysis

Due to the low yield and the difficulty in collecting colostrum from Ganxi black goats, we used dairy cow colostrum in this study, and the colostrum was collected from six multiparous dairy cows during 12 h after parturition in the dairy farm of the Institute of Hunan Animal and Veterinary Science (Changsha,

China). Before colostrum collecting, surface skin of breast was scrubbed with 1% povidone-iodine (LIRCON, Shandong, China) and milking staff wore medical mask and sterile gloves to prevent colostrum from contamination. Colostrum from each cow was collected into a 5 L sterile plastic bag. All colostrum was fully mixed when the collection was finished. Subsequently, the mixed colostrum was pasteurized using a commercial pasteurizer of 30 L (ZUOLANBO, Shandong, China) at 60°C for 60 min followed by rapid cooling (Malmuthuge et al., 2015). After cooling, heat-treated colostrum was aliquoted into 50 ml sterile centrifuge tubes and stored at −20°C for feeding trial. In addition, 50 ml heat-treated colostrum was prepared to determine colostrum composition (total solids, protein, fat, and lactose) based on Milk Analyzers (FOSS electric, Hilleroed, Denmark). Approximate 5 ml heat-treated colostrum was centrifuged at 12,000 rpm for 15 min at 4°C to obtain supernatant to detect IgG, IgA, and IgM concentration using commercial bovine specific ELISA kits (CUSABIO).[1] The heat-treated colostrum contained 32.00% total solids, 22.21% protein, 6.81% fat, 3.11% lactose, 28.61 mg/ml IgG, 3.73 mg/ml IgA, and 2.93 mg/ml IgM.

Experimental Design and Management

The experimental procedures of this study were performed in accordance with the guidance of the Animal Ethics Committee of Institute of Subtropical Agriculture, Chinese Academy of Sciences. All neonatal goats used in this study were brought from a commercial farm (Jiangxi Mulei Agriculture and Forestry Development Co. Ltd., Jiangxi, China) and the animal trial was also conducted in this farm from November 2019 to July 2020. A total of 14 healthy neonatal Ganxi black goats with similar birth weight (BW: 2.35 ± 0.55 kg) were selected and used in this study. Neonatal goats that were naturally delivered were immediately separated from their dams after birth to avoid any physical contact. All neonatal goats were artificially removed afterbirth and their bodies were dried using sterile towels. Thereafter, umbilical cords of neonatal goats were sterilized by 7% povidone-iodine and BW was recorded before moving each animal to an individual pen (80 cm × 160 cm × 100 cm) equipped with a heat lamp and bedded with rice straw. The house and pen were cleaned and sterilized thoroughly before the animal trial. Neonatal goats were randomly allocated according to their BW into two groups for 7 days. In addition, none of the animals included in this study were received any vaccination or therapeutic medicine during the overall experimental period.

The experimental design and feeding regime are illustrated in **Figure 1**. In details, neonatal goats were bottle-fed colostrum with a volume of 5% of BW at 2 h, and milk powder was diluted with water (at 42°C) in a ratio of 1:5 that was subsequently provided to goats with a volume of 5% BW every 8 h until the end of animal trial. The milk powder (contained 6% moisture, 23% crude protein, 12% crude fat, 3% crude fiber, 10% ash, 1.5% calcium, and 1.2% phosphorus) was purchased from Beijing Precision Animal Nutrition Research Center (Beijing, China).[2] All neonatal goats were given *ad libitum* access to water. Otherwise, neonatal goats in the control group (CON, $n = 7$) only fed colostrum and milk replacer; however, those assigned to the treatment group (MOS, $n = 7$) were supplemented 0.06% of BW MOS (purity: 99%, FENGTAI, Shandong, China) in the colostrum and milk replacer per day throughout the experiment.

Sample Collection

The blood sample was collected through the jugular vein using a heparinized tube (SANLI Medical Technology Development Co., Ltd., Changsha, China) at 0, 3, 6, 12, 18, 24, 48, 72, 96, 120, 144, and 168 h after colostrum feeding. After that, all blood samples were kept on the ice and taken to the laboratory for serum separation through centrifuging at 3,000 × *g* at 4°C for 20 min. The supernatants were collected and aliquoted into four 1.5-ml microcentrifuge tubes and stored at −20°C for determination of immunoglobulin and cytokine levels.

The neonatal goats were slaughtered after 168 h of colostrum feeding with an intravenous injection of sodium pentobarbital at 50 mg/kg BW for anesthetization. Subsequently, exsanguination was conducted until goats reached a surgical level of anesthesia. Immediately after opening the abdominal cavity, the proximal duodenum, and distal rectum were first ligated to avoid loss of digesta and then ligation was cautiously performed between segments to prevent the transfer of contents. In details, the ligated positions for ileum segments were from the ileocecal junction to 50 cm proximal to the ileocecal junction. Thereafter, ileal digesta was collected using 50 ml germfree centrifuge tubes (Corning®, NY, United States) and snap-frozen in liquid nitrogen and then stored at −80°C in the laboratory for further analysis. The tissues of aforementioned intestinal segments were washed in 100 ml sterile culture dishes slightly (Corning®, NY, United States) with ice-cold DNase/RNase-free ddH_2O (R1600, Solarbio LIFE SCIENCES, Beijing, China) until clean (3–4 times). The tissues were cut into small pieces, then a part of tissues was transferred into 10% neutral buffered formalin for morphology observation, and other tissues were placed in a sterile sample bag (B01064, Whirl-Pak®, WI, United States), which immediately snap-frozen in liquid nitrogen and stored at −80°C for RNA extraction.

Analysis of Biochemical Parameters and Hormone in Serum

The levels of glucose (GLU), triglyceride (TG), cholesterol (CHOL), low density lipoprotein (LDL), high density lipoprotein (HDL), blood urea nitrogen (BUN), and total protein (TP) in collected serum samples were measured using an automatic biochemical analyzer (Cobas c311, Roche, Basel, Switzerland). Serum hormone levels of growth hormone (GH), insulin (INS), insulin-like growth factor 1 (IGF-1), and glucagon-like peptide 1 (GLP-1) were determined using ELISA kits (CUSABIO; see Footnote 1) on microplate reader according to manufacturer's protocols.

[1]https://www.cusabio.com/

[2]http://www.bjapn.com

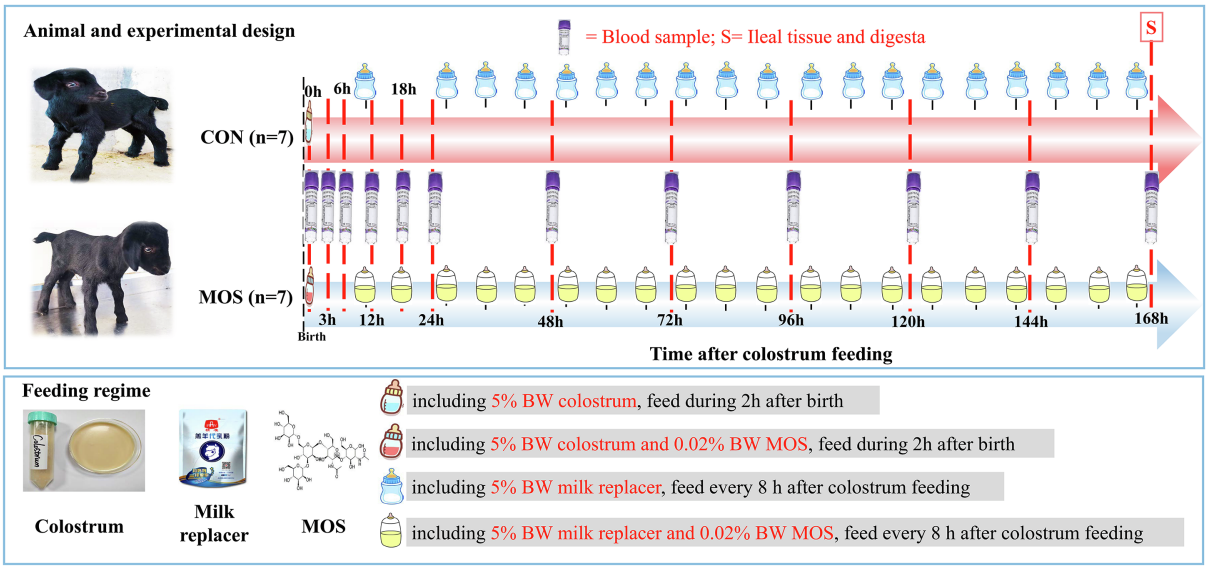

FIGURE 1 | Experimental design, feeding regime, and sample collection.

Measurement of Immune and Antioxidative Indices in Serum

The concentration of IgG in serum was determined by using a commercial goat specific ELISA kit (CUSABIO, Wuhan, China) and the concentrations of IgA and IgM were analyzed using commercial sandwich ELISA technique kits (Jiangsu Meimian industrial Co., Ltd., Yancheng, China). The serum levels of interleukin-4 (IL-4), IL-6, IL-10, IL-12, interferon-β (INF-β), and tumor necrosis factor-α (TNF-α) were detected using the goat-specific ELISA kits according to manufacturer's specifications (Jiangsu Meimian industrial Co., Ltd., Yancheng, China). The detection of serum antioxidant capacity, including superoxide dismutase (SOD), glutathion peroxidase (GSH-Px), catalase (CAT), total anti-oxidation capability (T-AOC), and malondialdehyde (MDA) levels were performed using the commercial kits according to the manufacturer's protocols (Nanjing Jiancheng Bioengineering Institute, Nanjing, China).

Ileal Morphology Analysis

After being fixed in the buffered formalin for 48 h, the ileal tissue sample was washed, dehydrated in gradient ethanol, and finally embedding in the paraffin wax. Five sections for each sample were sliced, installed on glass slides and stained with eosin and hematoxylin. Three random straightest villi and their accompanying crypts of each slide were selected to measure the villus height and crypt depth using a fluorescence microscope (Olympus, Tokyo, Japan) with a calibrated 10-fold eyepiece graticule. The V/C value (ration of villus height to crypt depth) was calculated.

Secretory IgA Determination in the Ileal Digesta

Approximately 500 mg digesta samples of ileum were weighed in 2-ml microtubes and vacuum freeze-dried for 3 h at 1,200 rpm in a vacuum freeze drier (Lyovapor™ L-300, BUCHI, Switzerland). Subsequently, 80 mg of each dried sample were weighed in a new 2-ml microtube and added 2 ml of PBS (containing 0.05% Tween and protease inhibitor cocktail) to suspend it. Digesta samples were then thoroughly artificially shaken and mechanically homogenized on a vortex mixer until full resuspension. The supernatants were collected in a new tube after centrifugation at 3,000 × *g* for 10 min, and the concentration of secretory IgA (sIgA) of digesta samples was detected using a commercial goat specific ELISA kit according to manufacturer's direction (Jiangsu Meimian industrial Co., Ltd., Yancheng, China).

16S rRNA Gene Sequencing and Bioinformatics Analysis

Microbial DNA extracted from 14 ileal digesta samples were performed using a commercial kit (DP328, TIANGEN BIOTECH Co., Ltd., Beijing, China) following the manufacturer's instructions. The integrity and concentration of the extracted DNA were evaluated by 2.0% agarose gel electrophoresis and NanoDrop 2000 (Thermo Scientific, MA, United States), respectively. The primers 343F (5′-TACGGRAGGCAGCAG-3′) and 798R (5′-AGGGTATCTAATCCT-3′) of the V3–V4 variable region of the bacterial 16S ribosomal RNA gene was used for amplification on a ProFlex PCR system (ThermoFisher Scientific Inc., MA, United States). The amplified PCR products were verified by 2% agarose gels and then purified using the AxyPrep DNA Gel Extraction Kits (Axygen Biosciences, CA, United States) according to the manufacturer's protocols. Purified PCR products were quantified by Qubit®3.0 (Life Invitrogen), and that for each sample were mixed equally to construct Illumina pair-end libraries following Illumina's genomic DNA library preparation procedure. The results showed that the quality of the DNA library for two samples (one from the CON group and one from the MOS group) was ineligible. Subsequently, eligible

amplicon libraries were sequenced on an Illumina MiSeq platform (PE250, Illumina, CA, United States) by Shanghai BIOZERON Co., Ltd (Shanghai, China). The raw reads were deposited into the NCBI Sequence Read Archive (SRA) database (Accession Number: PRJNA761090).

The quality control of raw data in FASTQ files was performed in QIIME data analysis package (version 1.9.1; Caporaso et al., 2010). In details, raw paired-end reads with 10 bp of minimal overlapping, the length less than 200 bp, average quality score less than 20, and 20% of maximum mismatch rate were excluded and the ambiguous nucleotides and chimeras were also discarded. Clean reads were then clustered into operational taxonomic units (OTUs) at 97% similarity cut-off using USEARCH (version 10).[3] The representative read of each OTUs was annotated and aligned to the SILVA 16s rRNA database (version 138.1) using the RDP classifier algorithm with a confidence threshold of 80% (Quast et al., 2012). The rarefaction analysis based on Mothur (version 1.44.1) was conducted to reveal the diversity indices including the Chao1, ACE, Simpson, and Shannon indices. The beta diversity analysis was performed using principal coordinates analysis (PCoA) based on Binary jaccard, Bray curtis, and weighted UniFrac distance and the analysis of similarity (ANOSIM) was used to assess the differences among samples. The linear discriminant analysis (LDA) effect size (LEfSe) tool was applied to understand microbial communities through identifying different taxa between the CON and MOS groups using online packages (LC-Bio Technology Co., Ltd., Hangzhou, China) and using the threshold value ($p < 0.05$ and LDA > 2). The inferred metagenomic metabolic function of ileal microbiota was analyzed by PICRUSt2 based on normalized OTU abundance and the Kyoto Encyclopedia of Genes and Genomes (KEGG) pathways on level 3 were used to further analysis (Langille et al., 2013). The STAMP software (version 2.1.3) was employed to identify the different pathways between the CON and MOS groups using Welch's *t*-test, and *p* value was adjusted by the Benjamini and Hochberg method (Parks et al., 2014).

RNA Extraction and Quantitative RT-PCR

Total RNA extraction from ileal tissue sample was performed using SteadyPure Universal RNA Extraction Kit (AG21017, Accurate Biology, Changsha, China) according to the manufacturer's instructions and then genomic DNA was removed using DNase I (Accurate Biology, Changsha, China). The quality and concentrations of isolated total RNA were detected using a NanoDrop 2000 (Thermo Scientific, MA, United States), and the integrity was verified by 1.0% agarose-formaldehyde gel electrophoresis. Thereafter, cDNA synthesis was performed using a commercial *Evo M-MLV* Reverse Transcription Kit [AG11705, Accurate Biology (Hunan) Co., Ltd., Changsha, China] and stored at −20°C for subsequent quantitative RT-PCR.

The expression of genes related to tight junction and immunity were determined using SYBR® Green Premix *Pro Taq* HS qPCR Kit [AG11701, Accurate Biology (Hunan) Co., Ltd., Changsha, China] based on a fluorescence LightCycler 480 II platform (Roche, Basel, Switzerland) according to the manufacture's specification. The reaction program was described by Yang et al. (2021). The expression of each candidate genes was calculated based on quantification cycle normalized by housekeeping genes (*GAPDH* and *β-actin*) using the $2^{-\Delta\Delta Ct}$ method (Schmittgen and Livak, 2008). The primer information for candidate genes and housekeeping genes was deposited in **Supplementary Table S1**.

Statistical Analysis

The results of biochemical, immune, and antioxidative indices in serum, morphologic parameters, and gene expression in the ileum, sIgA concentration and alpha-diversity index in the ileal digesta were analyzed using the independent-sample *t*-test in SPSS software (SPSS version 25.0, SPSS, Inc.). In addition, the data including the relative abundance of bacteria at the phylum and genus levels in the ileal digesta samples disobeyed normal distribution, Wilcoxon rank-sum test was applied to identify differential taxa. Data were presented as means with SEM. Value of $p < 0.05$ was regarded as statistically significant, and $0.05 \leq p < 0.10$ was regarded as a statistical tendency. The correlation analysis between the phenotypic values (including cytokines and antioxidative indices in serum and sIgA concentration in ileal digesta) and main bacteria (average relative abundance more than 0.1% in at least one group) was conducted using Spearman rank correlation coefficient in R package and heatmap was generated on OmicStudio (LC-Bio Technology Co., Ltd., Hangzhou, China). The significant correlation was identified by the threshold value $p < 0.05$ and $|r| > 0.6$.

RESULTS

Serum Biochemical Parameters and Hormone Levels

As shown in **Table 1**, no difference ($p > 0.10$) was observed between the CON and the MOS group for serum GLU, TG, CHOL, LDL, HDL, and BUN. Neonatal goats in the MOS group had lower ($p = 0.001$) serum GLP-1 level than those in the CON group; however, there was no significant difference ($p > 0.10$) between the CON and the MOS group for serum GH, INS, and IGF-1 levels.

Serum Immunoglobulins, Antioxidant Status, and Inflammatory Cytokines

To monitor the passive IgG transfer of neonatal goats, we collected the serum samples at 0, 3, 6, 12, 18, 24, 48, 72, 96, 120, 144, and 168 h after colostrum feeding. Neonatal goats fed with MOS had significantly lower IgG concentration at 3 ($p = 0.023$) and 6 h ($p = 0.022$) when compared with the CON group (**Figure 2A**). Furthermore, the serum levels of TP, IgG, and IgM were similar ($p > 0.10$) in the CON and MOS groups, while IgA concentration tended to be higher ($p = 0.098$) in the MOS group than that in the CON group (**Figure 2B**). Neonatal goats in the MOS group had higher ($p = 0.001$) enzyme activity of CAT than those in the CON group, and the serum level of MDA was higher

[3]http://drive5.com/uparse

($p < 0.001$) in the CON group than in the MOS group (**Table 2**). As presented in **Table 3**, the serum cytokine concentrations of TNF-α, IL-12, and IL-10 had no difference ($p > 0.10$) between the CON and the MOS groups. Goats in the MOS group had lower ($p = 0.002$) level of pro-inflammatory IL-6 and remarkably higher ($p = 0.008$) anti-inflammatory IL-4 level when compared with the CON group. In addition, supplementation of MOS tended to decrease ($p = 0.074$) pro-inflammatory IFN-β concentration in the MOS group than in the CON group.

TABLE 1 | Serum biochemical parameters and hormone levels of neonatal goats with MOS supplementation.

Item	Treatment		SEM	*p*-value
	CON	MOS		
GLU (mmol/L)	6.357	6.543	0.313	0.780
TG (mmol/L)	0.741	0.761	0.104	0.928
CHOL (mmol/L)	2.697	2.704	0.076	0.965
LDL (mmol/L)	0.873	0.799	0.048	0.458
HDL (mmol/L)	2.127	2.237	0.052	0.306
BUN (mmol/L)	4.643	4.371	0.334	0.701
GH (ng/ml)	12.400	15.150	1.165	0.253
INS (μIU/ml)	11.149	10.924	0.535	0.843
IGF-1 (ng/ml)	88.025	86.718	0.909	0.494
GLP-1 (ng/ml)	4.829	3.772	0.188	0.001

Values are expressed as means ± SEM, n = 7. $p < 0.05$ was regarded as statistically significant, and $0.05 < p < 0.10$ was regarded as a statistical tendency.

Ileal Morphology and IgA Secretion in the Ileal Digesta

Mannan oligosaccharide supplementation had no effect ($p > 0.10$) on villus height, crypt depth, and V/C in the ileum of goats

TABLE 2 | Serum antioxidative indices of neonatal goats with mannan oligosaccharide supplementation.

Item	Treatment		SEM	*p*-value
	CON	MOS		
GSH-Px (U/ml)	104.271	105.692	8.325	0.936
SOD (U/ml)	27.048	29.450	1.043	0.266
CAT (U/ml)	0.869	4.754	0.633	0.001
T-AOC (U/ml)	0.892	0.898	0.062	0.964
MDA (mmol/L)	2.139	1.149	0.156	<0.001

Values are expressed as means ± SEM, n = 7. $p < 0.05$ was regarded as statistically significant, and $0.05 < p < 0.10$ was regarded as a statistical tendency.

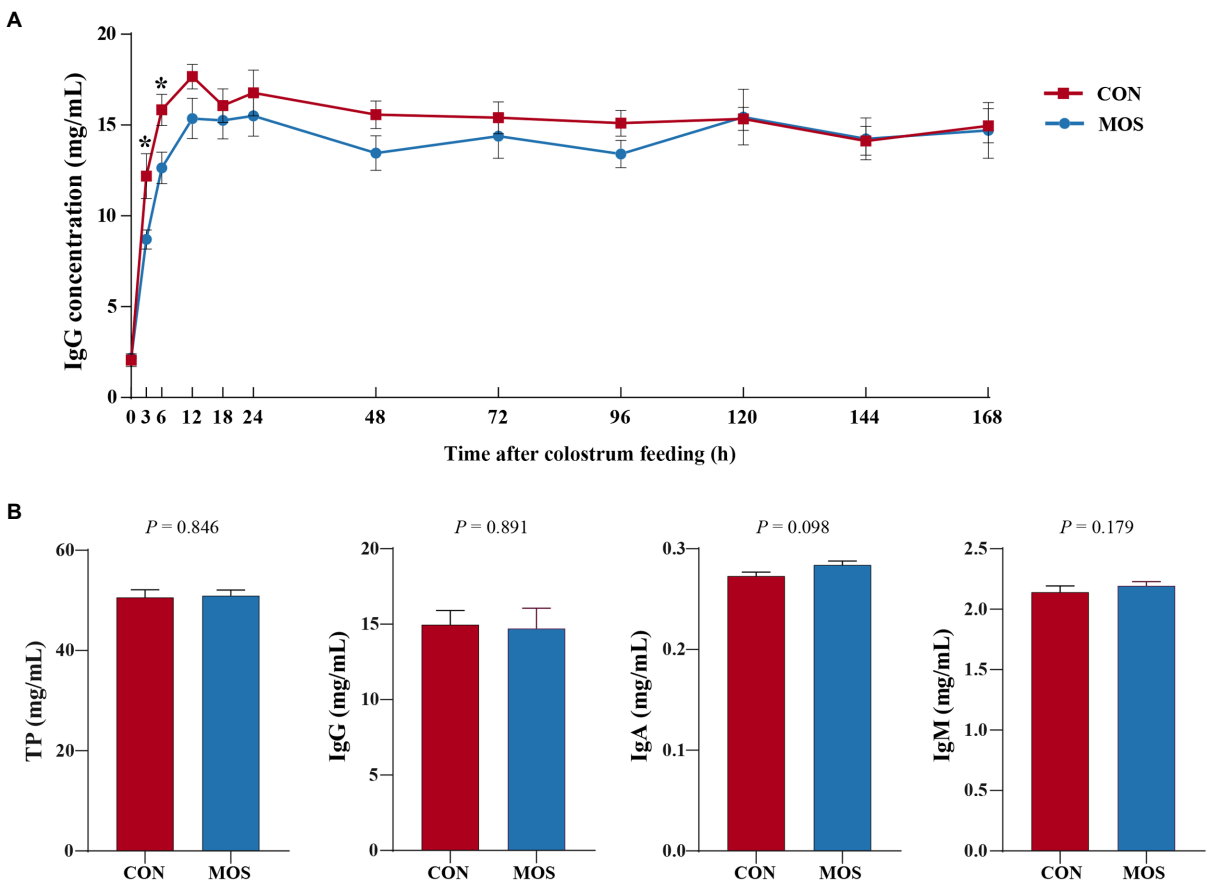

FIGURE 2 | Serum immunoglobulin level of neonatal goats in the CON and mannan oligosaccharide (MOS) groups. **(A)** Serum immunoglobulin G (IgG) level at different sample collecting time after colostrum feeding. *$p < 0.05$. **(B)** Serum content of total protein (TP), IgG, IgA, and IgM at the end of experiment.

TABLE 3 | Serum cytokine levels of neonatal goats with mannan oligosaccharide supplementation.

Item	Treatment		SEM	*p*-value
	CON	MOS		
IFN-β (pg/ml)	419.488	376.281	11.332	0.074
TNF-α (pg/ml)	179.543	189.282	2.998	0.106
IL-6 (pg/ml)	145.703	134.419	2.091	0.002
IL-12 (pg/ml)	913.851	841.244	24.715	0.148
IL-4 (pg/ml)	44.392	48.829	0.907	0.008
IL-10 (pg/ml)	45.547	46.025	0.766	0.769

Values are expressed as means ± SEM, n = 7. $p < 0.05$ was regarded as statistically significant, and $0.05 < p < 0.10$ was regarded as a statistical tendency.

TABLE 4 | Gut morphology and sIgA level in the ileum of neonatal goats with MOS supplementation.

Item	Treatment		SEM	*p*-value
	CON	MOS		
Villus length (μm)	445.90	412.90	20.588	0.445
Crypt depth (μm)	122.62	141.31	7.313	0.214
V/C	3.66	3.02	0.215	0.148
sIgA (mg/g of digesta)	0.043	0.057	0.004	0.043

Values are expressed as means ± SEM, n = 7. $p < 0.05$ was regarded as statistically significant, and $0.05 < p < 0.10$ was regarded as a statistical tendency.

(**Table 4**; **Supplementary Figure S1**); however, the sIgA concentration of the ileal digesta was significantly elevated ($p = 0.043$) in the MOS group than in the CON group (**Table 4**).

Quantitative RT-PCR for Tight Junction and Immune Related Genes in the Ileal Tissue

The mRNA expression of *Occludin* was not affected ($p > 0.10$) between the CON and MOS groups. However, increases in mRNA expression of *ZO-1* ($p = 0.004$), *Claudin1* ($p = 0.049$), and *Claudin2* ($p = 0.008$) were observed when MOS supplementation (**Figure 3A**). The relative expression of pro-inflammatory genes *TNF-α* ($p = 0.015$) and *IL-6* ($p = 0.022$) was higher in the CON group than those in the MOS group, while the mRNA abundance of anti-inflammatory *IL-10* was higher ($p = 0.017$) in the MOS group than that in the CON group (**Figure 3B**).

Diversity and Taxonomic Composition of Microbiota in the Ileal Digesta

Supplementation with MOS exerted antioxidant and anti-inflammatory effect on young goats, we further investigated whether MOS could change the ileal microbiota that may influence goat's health in early life. A total of 557,276 bacterial 16S rRNA sequence raw reads were obtained from 12 ileal digesta samples, with an average of 46,439.67 reads per sample. After quality control, 539,585 clean reads were retained, of which the total number of unique and clustered into representative bacterial OTU reads was 310,782, with an average of 25,898.50 reads per sample (**Supplementary Table S2**). The results of α-diversity showed that no differences ($p > 0.10$) in Chao1, Ace, Shannon, and Simpson index were found between the CON and MOS groups (**Figure 4A**). However, a distinct separation between the two group was observed in the PCoA plot based on Binary jaccard ($p = 0.004$), Bray curtis ($p = 0.049$) and weighted UniFrac distance ($p = 0.001$; **Figures 4B–D**). Taxonomic analysis revealed a total of six phyla were identified in both groups from 12 ileal digesta samples (**Figure 4E**). Among them, the *Firmicutes* was the dominant bacteria in the ileal digesta of neonatal goats, which accounted for more than 78 and 98% of total bacteria in the CON and MOS groups, respectively. Additionally, the *Verrucomicrobia* accounted for more than 17% in the CON group (**Figure 4E**). The relative abundance of *Firmicutes* was greater ($p = 0.006$) in the MOS group than that in the CON group; however, the relative abundance of *Verrucomicrobia* was significantly higher ($p = 0.004$) in the CON group than in the MOS group (**Table 5**). Compared with the CON group, the relative abundance of *Proteobacteria* tended to be lower ($p = 0.078$) in the MOS group (**Table 5**).

At the genus level, a total of 41 genera were detected in the ileal digesta samples of neonatal goats and 29 genera were identified in both groups, while 12 genera were only identified in the MOS group (**Supplementary Table S3**). The relative abundance of *Lactobacillus* was higher ($p = 0.041$) in the MOS group than that in the CON group; however, *Akkermansia* and *Ruminiclostridium_5* were significantly enriched ($p = 0.004$ and $p = 0.025$) in the CON group as compared with the MOS group (**Table 6**). Furthermore, the relative abundances of *Escherichia-Shigella* and *Lachnoclostridium* tended to be higher ($p = 0.055$ and $p = 0.066$) in the CON group than those in the MOS group (**Table 6**). The results of LEfSe analysis showed that MOS group characterized by a higher relative abundance of *Lactobacillus*, while CON group characterized by a higher relative abundance of *Akkermansia* and *Ruminiclostridium_5* (LDA > 2; **Figure 4F**).

Predicted the Metagenomic Metabolic Function of Microbiota in the Ileal Digesta

To better understanding the molecular functional changes of ileal microbiota induced by MOS supplementation, we employed PICRUSt2 to predict the metagenomic contribution of identified microbial communities from the KEGG pathways. The PCA plot based on the relative abundance of KEGG level3 pathways demonstrated a distinct separation ($p = 0.009$) between CON and MOS groups (**Figure 5A**). A total of 250 functional pathways on KEGG level3 were detected and 14 pathways presented the significant difference between CON and MOS groups which accounted for 5.6% of the overall detected pathways. In details, the CON group had higher abundances of gene families involved in chaperones and folding catalysts, bacteria secretion system, oxidative phosphorylation, RNA degradation, TCA cycle, riboflavin metabolism, and cell motility and secretion, while the gene families of the MOS group were mainly enriched in chloroalkane and chloroalkene degradation, fatty acid metabolism, naphthalene degradation, sulfur relay system, glutathione

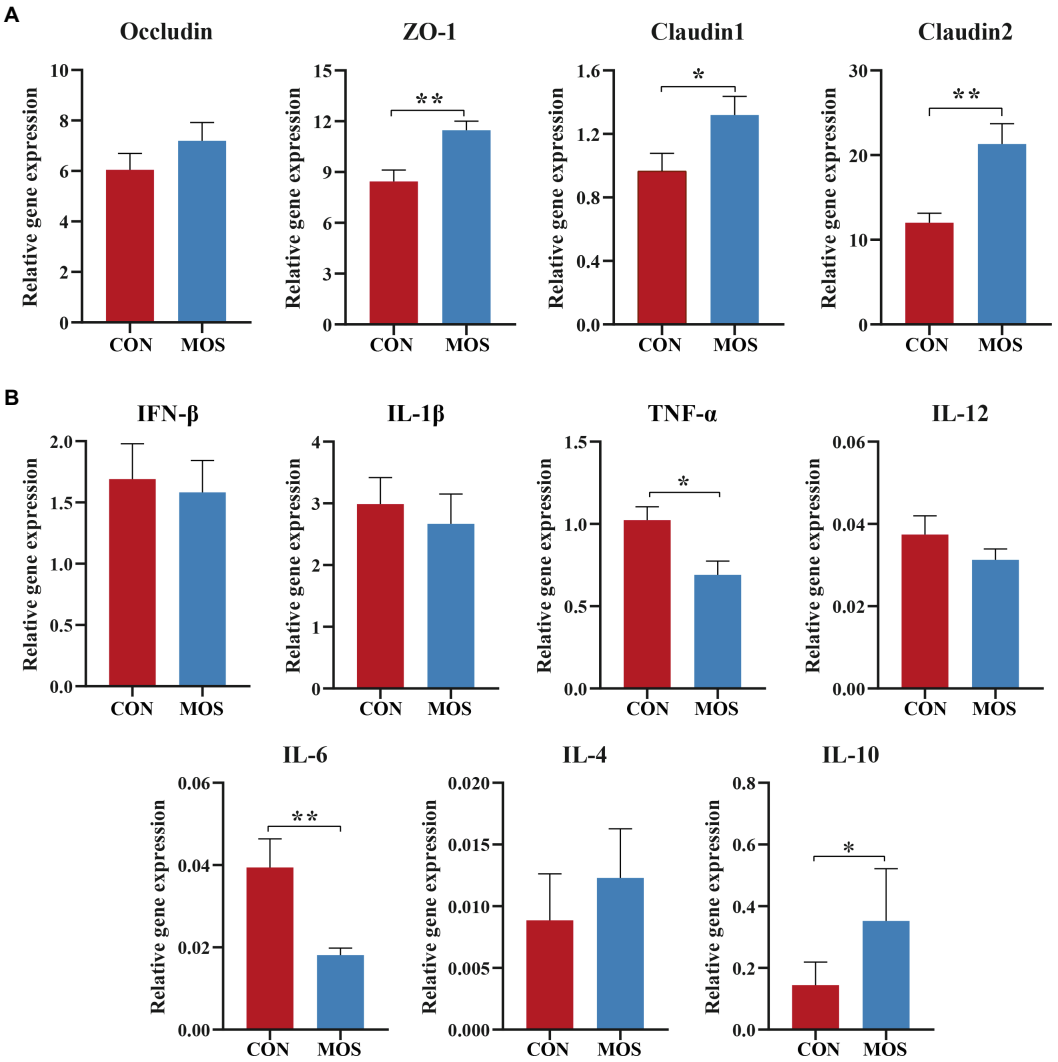

FIGURE 3 | The relative expression of genes involved in **(A)** tight junction and **(B)** inflammatory response. *$p < 0.05$, **$p < 0.01$.

metabolism, D-Glutamine and D-glutamate metabolism, and drug metabolism-cytochrome P450 (**Figure 5B**).

Spearman's Correlation Analysis Between Main Bacteria and Serum Antioxidant Indices, Inflammatory Cytokines as Well as sIgA in the Ileal Digesta

As illustrated in **Figure 6**, Spearman's correlation coefficient was performed to investigate relationship between the phenotypic values (serum antioxidant indices, inflammatory cytokines, and sIgA in the ileal digesta) and main bacteria (average relative abundance more than 0.1% in at least one group at the genus level). In details, *Lactobacillus* showed positive ($p < 0.05$) correlation with CAT and IL-4, while it was negatively correlated ($p < 0.05$) with MDA. *Akkermansia* was negatively correlated ($p < 0.05$) with CAT, IL-4, and sIgA but positively correlated ($p < 0.05$) with MDA. Furthermore, *Lachnoclostridium*, *Escherichia-Shigella*, and *Ruminiclostridium_5* were negatively correlated ($p < 0.05$) with IL-4. There had a significantly positive correlation ($p < 0.05$) between *Clostridium_sensu_stricto_1* and GSH-Px. Also, we found a remarkably positive correlation ($p < 0.05$) between *[Ruminococcus]_gnavus_group* and IL-12.

DISCUSSION

Functional oligosaccharides characterized by promoting immunity, suppressing pathogenic bacteria, and maintaining intestinal health have received extensive attention (Guerra-Ordaz et al., 2013; Tran et al., 2018). As a typical kind of functional oligosaccharides derived from the cell wall of yeast, MOS is widely used in animal feed to promote nutrient digestibility and alleviate intestinal disease (Spring et al., 2015; Duan et al., 2016). This study was the first time to clarify the effects of

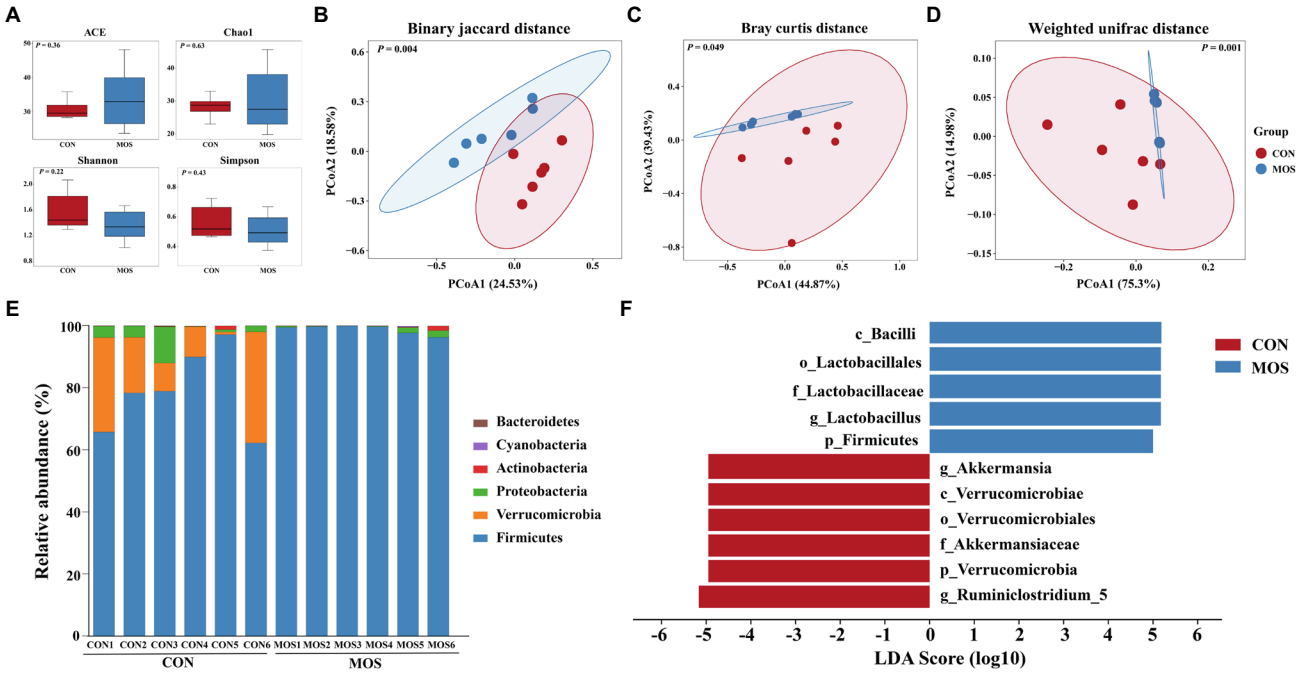

FIGURE 4 | Alpha diversity, beta diversity, and taxonomic analysis of the microbial communities in the ileal digesta samples of neonatal goats in the CON and MOS groups. **(A)** Alpha diversity index; Principal coordinate analysis (PCoA) score plots of the ileal microbiota based on the **(B)** Binary jaccard distance, **(C)** Baray curtis distance, and **(D)** weighted UniFrac distance; **(E)** The relative abundance of the microbial composition at the phylum level; **(F)** Linear discriminant analysis (LDA) effect size linear discriminant analysis (LEfSe) of the ileal microbiota. $^{*}p < 0.05$, $^{**}p < 0.01$.

TABLE 5 | The relative abundance of bacteria in the ileal digesta samples at phylum level.

Phylum	Treatment		SEM	*p*-value
	CON	MOS		
Firmicutes	78.690	98.783	4.016	0.006
Verrucomicrobia	17.309	0.002	3.705	0.004
Proteobacteria	3.638	0.769	0.939	0.078
Actinobacteria	0.272	0.331	0.144	0.631
Bacteroidetes	0.066	0.034	0.021	0.298
Cyanobacteria	0.025	0.081	0.023	0.471

Values are expressed as means ± SEM, n = 6. p < 0.05 was regarded as statistically significant, and 0.05 < p < 0.10 was regarded as a statistical tendency.

MOS supplementation on passive immunity transfer, intestinal development, and intestinal bacteria colonization in neonatal goats.

Regarding the dose of MOS, there were significant variations in different studies, and it ranged from 1 to 10 g per day (Swanson et al., 2002; Berge, 2016). In the current study, the amount of MOS supplementation was 0.06% of BW in the colostrum or milk replacer (an average inclusion of 1.41 g per day, purity: 99%), which referenced from two previous studies of calves (Heinrichs et al., 2013; Tóth et al., 2020). MOS supplementation did not affect the values of blood biochemical index value in the present trial, which was in agreement with the study of calves that the blood levels of TP, TG, CHOL, BUN, and GLU had no changes when supplemented 4 g MOS per day (Silva et al., 2012). Furthermore, the serum hormone levels of GH, INS, and IGF-1 were also unaffected by MOS supplementation. The above results may be attributed to the short experimental period and the growth stage of goats that underwent rapid growth and development during the first 1 week; thus, the influence induced by age highly concealed the contribution of MOS. GLP-1 plays a vital role in reducing gastric emptying and promoting the growth and development of small intestine. A higher GLP-1 level usually represents efficient digestion and absorption of dietary nutrients (Lim et al., 2009). The present study results showed that the serum level of GLP-1 decreased with MOS supplementation; however, little information about the effect of MOS supplementation on serum GLP-1 level was reported, and the mechanism deserved further study.

Newborn dairy calves received MOS in milk replacer at 0.6 g/kg BW presented a significant increase in serum IgG concentrations during the first 21 days of life compared with the control group (Lazarevic et al., 2010). Contradict with the above results, Brady et al. (2015) have shown that supplementing 30 g of MOS per day to newborn Holstein heifer and bull calves reduced serum IgG concentration at 24 h. Furthermore, a recent study in North American using 240 newborn Holstein dairy calves has reported that the addition of MOS to colostrum replacer did not affect serum IgG level at 24 h (Robichaud et al., 2014). Compared to the aforementioned studies, the current study set more sample collection points, and the results showed that only the serum IgG levels at 3 and 6 h were

affected by MOS supplementation. Our results indicated that the reduction of serum IgG level of goats in the MOS group might be attributed to the less bacteria colonialization during the first 6 h and MOS adhering to intestinal epithelium delayed the passive transfer of IgG. Once beneficial bacteria rapidly colonialized, MOS could be utilized and the decrease of MOS adhered to epithelium eliminated the negative influence on IgG absorption (Flickinger et al., 2000).

As we all known, once the concentrations of reactive oxygen species surpassing the capacity of antioxidant, DNA, proteins, and endogenous lipids of cells will be widely damaged and finally induces inflammatory response (Yu, 1994). MDA is one of the essential indices to assess oxidative stress which damages the membrane structure and function of cells (Gawe et al., 2004). In contrast, GSH-Px and SOD as main enzymatic scavengers can counteract the adverse effects induced by oxidative stress, which are always recognized as the vital indicator of antioxidative capacity (Tabrez and Ahmad, 2009). Meanwhile, CAT can oxidize alcohol, formic acid, and phenols using H_2O_2 and it can also directly promote the conversion of H_2O_2 to H_2O and O_2 to alleviate the oxidative stress induced by the poisonous H_2O_2 accumulation (Xue et al., 2020). Previous studies have been proven that MOS exhibits good antioxidative properties, including increasing the serum levels of GSH-Px, SOD, and T-AOC and reducing serum MDA levels in sheep and chickens (Liu et al., 2015; Zheng et al., 2018; Zhou et al., 2019). Consistent with the above results, in the current study, MOS supplementation increased serum CAT level and reduced MDA level of neonatal goats. Meanwhile, Duan et al. (2016) demonstrated that MOS addition decreased serum concentrations of pro-inflammatory cytokines IL-2 and IL-4 but increased anti-inflammatory cytokine IL-10 level. Our results showed that MOS supplementation decreased the serum level of IL-6 and increased IL-4 concentration, suggesting that MOS could promote systemic immunity and suppress the inflammatory response in neonatal goats.

Intestinal barrier is the first line of body defensive system and the dysfunction of that barrier may destroy the integrity of the epithelium and finally increase the risk of pathogenic invasion (Camilleri et al., 2012). Meanwhile, the intestinal epithelium integrity is mainly modulated by the functional genes or proteins including Occludin, ZO-1, and Claudin. In this study, the relative expression of genes involved in the tight junction (*ZO-1*, *Claudin1*, and *Claudin2*) and inflammation (*TNF-α*, *IL-6*, and *IL-10*) was partly consistent with the findings of Che et al. (2011), which suggested that MOS supplementation could maintain the intestinal integrity and prevent from the pathogenic invasion of neonatal goats. The intestinal microbiota and host exist a cross-talk that intestinal microbiota regulates the host mucosal

TABLE 6 | The relative abundance of bacteria in the ileal digesta samples at genus level (average relative abundance > 0.1% in at least one group).

Genus	Treatment		SEM	*p*-value
	CON	MOS		
Lactobacillus	66.871	97.100	8.016	0.010
Akkermansia	17.309	0.002	3.705	0.004
Escherichia-Shigella	3.539	0.326	0.948	0.055
[Ruminococcus]_gnavus_group	1.394	0.005	0.523	0.262
Lachnoclostridium	0.168	0.030	0.044	0.066
Bifidobacterium	0.247	0.043	0.089	0.128
Ruminiclostridium_5	0.100	0.002	0.029	0.025
Streptococcus	0.157	0.145	0.059	0.378
Clostridium_sensu_stricto_1	0.039	0.116	0.044	0.471
Sarcina	9.841	0.050	4.910	0.749
Bacillus	0	0.739	0.356	0.150
uncultured_bacterium_f_ Erysipelotrichaceae	0	0.313	0.157	0.631
Halomonas	0	0.220	0.110	0.631
Actinomyces	0	0.145	0.072	0.631
Trueperella	0.025	0.143	0.051	0.262

Values are expressed as means ± SEM, n = 6. $p < 0.05$ was regarded as statistically significant, and $0.05 < p < 0.10$ was regarded as a statistical tendency.

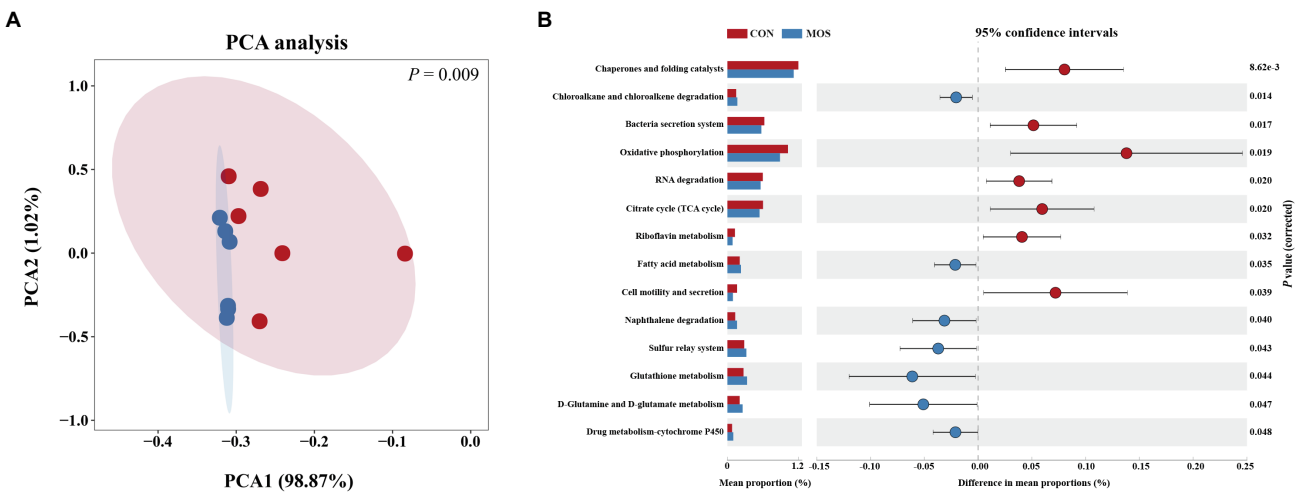

FIGURE 5 | Metagenomic function predicted by PICRUSt2. **(A)** Principal component analysis (PCA) of functional pathways based on Kyoto Encyclopedia of Genes and Genomes (KEGG) level 3. **(B)** Significantly different KEGG pathways (level 3) detected between CON and MOS group.

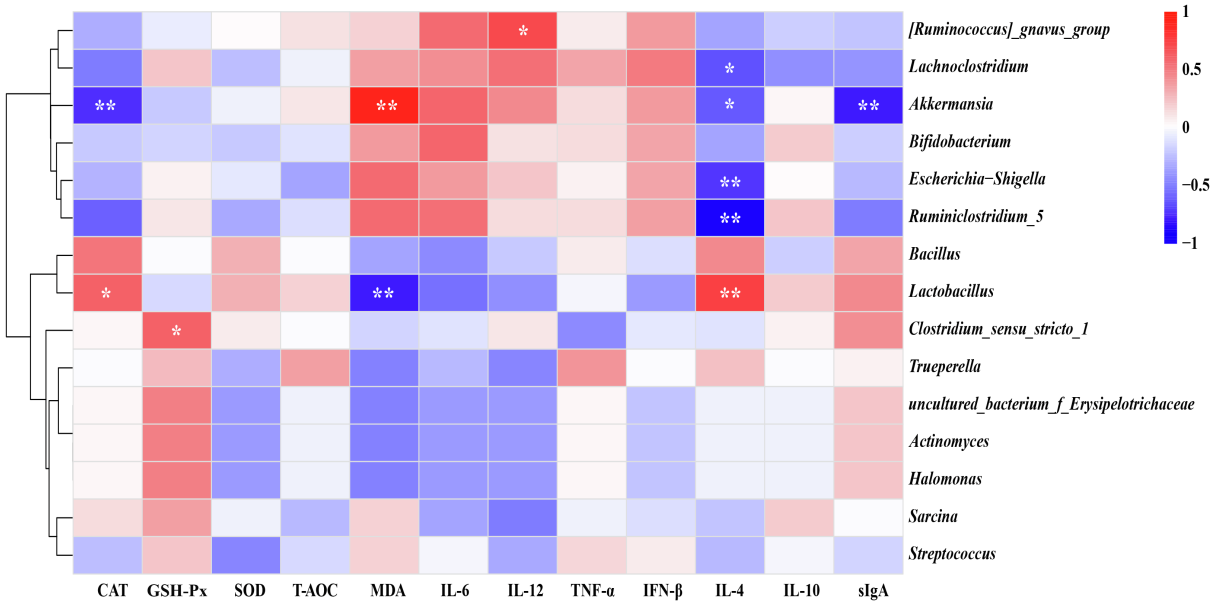

FIGURE 6 | Heatmap of spearman's correlation between ileal microbiota and serum antioxidative indices, inflammatory cytokines as well as secretory IgA (sIgA) level of the ileal digesta. The correlation was analyzed based on main bacteria (average relative abundance more than 0.1% in at least one group) at genus level. The blue suggests a negative correlation, and the red suggests a positive correlation. $^{*}p < 0.05$, $^{**}p < 0.01$.

immunity, and the host can also manipulate the intestinal microbiota community (Zhang et al., 2017). sIgA acts as a bridge between intestinal microbiota and host mucosal immunity to defend the pathogenic bacteria colonization and invasion (Tlaskalová-Hogenová et al., 2004). In the current study, MOS addition promoted the sIgA concentration of ileal digesta, suggesting that MOS addition had the potential to enhance mucosal immunity and ultimately alleviate inflammation in the ileum of neonatal goats.

The intestinal epithelium possesses abundant mannose-specific receptors (MR) and FimH lectin of type I fimbriae in pathogens including *E. coli* and *Salmonella*, which can bind to MR, then cause the attachment of the above bacteria to the epithelium. Consequently, many pathogenic bacteria colonized in the epithelium to generate toxins that damage the balance between intestinal bacteria and induce the occurrence of disease (De Los Santos et al., 2007). Fortunately, MOS can prevent the adhesion of pathogenic bacteria to the mucosa by decreasing the number of available binding sites for fimbriae and finally ensuring the health of intestine (Ofek et al., 1977). In the current study, the relative abundance of *E. coli* tended to decrease in the MOS group, which indicated MOS supplementation restrained the adhesion and colonization of pathogenic bacteria in the mucosal epithelium. Otherwise, beneficial bacteria generally compete with pathogenic bacteria and MOS supplementation could increase the amount of *Lactobacillus* and *Bifidobacterium* in the jejunum, ileum, and caecal digesta in pigs and broiler chicken (Baurhoo et al., 2007; Poeikhampha and Bunchasak, 2011). The relative abundance of *Lactobacillus* in the current study was significantly increased by the MOS supplementation that may cause the lower abundance of *E. coli*. *Firmicutes* plays a crucial role in structural carbohydrate metabolism (Brulc et al., 2009). In this study, the relative abundance of *Firmicutes* was higher in the MOS group than that in the CON group, which might be attributed to the higher prevalence of *Lactobacillus*.

The *Verrucomicrobia* phylum inhabits in the gut of humans and animals has a close phylogenetical relationship to *Planctomycetes* and *Chlamydiae* and is primarily comprised of *Akkermansia* species (Wagner and Horn, 2006). A Gram-negative bacteria *Akkermansia muciniphila* isolated from human feces can degrade mucin of intestinal epithelium (Wagner and Horn, 2006), and the pili-like structural protein of the above bacteria can directly participate in the regulation of intestinal immunity and enhance the resistance of transportation across the intestinal epithelium (Ottman et al., 2017). In the current study, we found that MOS supplementation decreased the relative abundance of *Akkermansia*, but the mechanism remains unknown and that needs further study. A previous study showed that MOS treatment decreased the abundance of genera *Lachnoclostridium* and *Ruminiclostridium 5* in the caecum of broilers (Mesa et al., 2017), which is consistent with the present results. The above information indicated that MOS supplementation during the neonatal stage could promote the colonization of beneficial bacteria and inhibit the adhesion of pathogens to the intestinal mucosa. The predicted function of 16S rRNA gene profiles showed that the most abundant categories were the functions of amino acids metabolism in the MOS group, which is partly consistent with the previous study that carbohydrate, protein, and amino acid metabolism are necessary for microbial survival (Erickson et al., 2012). These indicated that MOS might promote dietary amino acid utilization to maintain intestinal health.

The results of Spearman's correlation analysis presented that the relative abundance of *Lactobacillus* was positively correlated with serum IL-4 and CAT levels, while negatively correlated with MDA of serum. *Lactobacillus* degrades lactose and

oligosaccharides of milk into lactate and other short-chain fatty acids. Those metabolites may involve in regulating mucosal immunity and decreasing oxidative stress (Hamer et al., 2008; Walter, 2008). *Lactobacillus reuteri*, one of the most abundant *Lactobacillus* species, has been proven to inhibit the secretion of pro-inflammatory cytokines and promote anti-inflammatory capacity (Christensen et al., 2002; Hu et al., 2021). These results imply that *Lactobacillus* can improve antioxidant capacity and alleviate the inflammation of neonatal goats. Intestinal mucus layer serves as a physical barrier to prevent the invasion and adhesion of pathogens, and only some commensal bacteria can colonize and obtain nutrients from that layer (Sicard et al., 2017). However, as mentioned above, *Akkermansia* can degrade mucin into small molecule metabolites, which may increase the risk of pathogenic invasion. The above information may explain why *Akkermansia* was negatively correlated with CAT, IL4, and sIgA levels, but was positively correlated with MDA levels. Otherwise, lipopolysaccharide derived from the cell wall of gram-negative bacteria (*E. coli* and *Salmonella*) induces the inflammatory response of animal through activating the NF-κB signaling pathway to release pro-inflammatory cytokines (IL-6, IL-12, and TNF-α; Burgueño and Abreu, 2020). The negative correlation between the *E. coil* and IL-4 may be due to the serum IL-4 level suppressed by release the above proinflammatory cytokines induced by the *E. coil*. The genus *Clostridium_sensu_stricto_1* belonging to *Clostridia* bacteria, can use dietary carbohydrate to produce butyrate (Pei et al., 2021). It has been reported that butyrate exerts positive effects on the reduction of oxidative stress (Hamer et al., 2008), which is in line with the current study that showed a positive correlation between *Clostridium_sensu_stricto_1* and serum GSH-Px level.

CONCLUSION

Feeding MOS to the neonatal goats in the first 6 h after colostrum feeding reduced passive transfer of IgG, promoted serum antioxidative capacity and decreased serum levels of inflammatory cytokines. Furthermore, MOS supplementation improved intestinal integrity and mucosal immunity of the ileum by inducing sIgA secretion, modulation of the anti-inflammatory and pro-inflammatory gene expressions. MOS supplementation contributed to model a beneficial bacteria composition, which was reflected by the increased relative of abundance of *Lactobacillus* and decreased abundance of *Akkermansia*, *Ruminiclostridium_5*, *Escherichia-Shigella*, and *Lachnoclostridium*. Thus, MOS induced positive effects were more pronounced in neonatal goats that might be an effective approach to maintain intestinal health and improved the surviving rate of neonatal ruminants.

DATA AVAILABILITY STATEMENT

The datasets presented in this study can be found in online repositories. The names of the repository/repositories and accession number(s) can be found in the article/**Supplementary Material**.

ETHICS STATEMENT

The animal study was reviewed and approved by Animal Ethics Committee of Institute of Subtropical Agriculture, Chinese Academy of Sciences. Written informed consent was obtained from the owners for the participation of their animals in this study.

AUTHOR CONTRIBUTIONS

CY, ZH, and ZT contributed to conception and design of the study. CY, TZ, QT, GL, YC, and KG collected the samples. CY, TZ, GL, and YC conducted laboratory analyses. CY performed the statistical analysis and wrote the manuscript. KG, ZT, and ZH revised the manuscript. All authors contributed to the article and approved the submitted version.

FUNDING

This study was supported by National Natural Science Foundation of China (31772631 and 32072760), Hunan Key Research and Development Program (2020NK2049), and Innovation Province Project (2019RS3021).

SUPPLEMENTARY MATERIAL

The Supplementary Material for this article can be found online at: https://www.frontiersin.org/articles/10.3389/fmicb.2021.795081/full#supplementary-material

REFERENCES

Abdel-Hamid, T. M., and Farahat, M. H. (2016). Effect of dietary mannan-oligosaccharides on some blood biochemical, haematological parameters and carcass traits in purebred New Zealand white and crossbred rabbits. *Anim. Prod. Sci.* 56:2133. doi: 10.1071/AN15032

Azizzadeh, M., Shooroki, H. F., Kamalabadi, A. S., and Stevenson, M. A. (2012). Factors affecting calf mortality in Iranian Holstein dairy herds. *Prev. Vet. Med.* 104, 335–340. doi: 10.1016/j.prevetmed.2011.12.007

Baurhoo, B., Phillip, L., and Ruiz-Feria, C. (2007). Effects of purified lignin and mannan oligosaccharides on intestinal integrity and microbial populations in the ceca and litter of broiler chickens. *Poult. Sci.* 86, 1070–1078. doi: 10.1093/ps/86.6.1070

Berge, A. (2016). A meta-analysis of the inclusion of bio-Mos® in milk or milk replacer fed to dairy calves on daily weight gain in the pre-weaning period. *J. Anim. Res. Nutr.* 01, 1–7. doi: 10.21767/2572-5459.100020

Blacklaws, B. A., Berriatua, E., Torsteinsdottir, S., Watt, N. J., Andres, D. D., Klein, D., et al. (2004). Transmission of small ruminant lentiviruses. *Vet. Microbiol.* 101, 199–208. doi: 10.1016/j.vetmic.2004.04.006

Borghesi, J., Mario, L. C., Rodrigues, M. N., Favaron, P. O., and Miglino, M. A. (2014). Immunoglobulin transport during gestation in domestic animals and humans—a review. *Open J. Anim. Sci.* 04, 323–336. doi: 10.4236/ojas.2014.45041

Bozkurt, M., Bintaş, E., Kırkan, Ş., Akşit, H., Küçükyılmaz, K., Erbaş, G., et al. (2016). Comparative evaluation of dietary supplementation with mannan oligosaccharide and oregano essential oil in forced molted and fully fed

laying hens between 82 and 106 weeks of age. *Poult. Sci.* 95, 2576–2591. doi: 10.3382/ps/pew140

Brady, M., Godden, S., and Haines, D. (2015). Supplementing fresh bovine colostrum with gut-active carbohydrates reduces passive transfer of immunoglobulin G in Holstein dairy calves. *J. Dairy Sci.* 98, 6415–6422. doi: 10.3168/jds.2015-9481

Brulc, J. M., Antonopoulos, D. A., Miller, M. E. B., Wilson, M. K., Yannarell, A. C., Dinsdale, E. A., et al. (2009). Gene-centric metagenomics of the fiber-adherent bovine rumen microbiome reveals forage specific glycoside hydrolases. *Proc. Natl. Acad. Sci. U. S. A.* 106, 1948–1953. doi: 10.1073/pnas.0806191105

Burgueño, J. F., and Abreu, M. T. (2020). Epithelial toll-like receptors and their role in gut homeostasis and disease. *Nat. Rev. Gastroenterol. Hepatol.* 17, 263–278. doi: 10.1038/s41575-019-0261-4

Camilleri, M., Madsen, K., Spiller, R., Meerveld, B., and Verne, G. N. (2012). Intestinal barrier function in health and gastrointestinal disease. *Neurogastroenterol. Motil.* 24, 503–512. doi: 10.1111/j.1365-2982.2012.01921.x

Caporaso, J. G., Kuczynski, J., Stombaugh, J., Bittinger, K., Bushman, F. D., Costello, E. K., et al. (2010). QIIME allows analysis of high-throughput community sequencing data. *Nat. Methods* 7, 335–336. doi: 10.1038/nmeth.f.303

Che, T., Johnson, R., Kelley, K., Van Alstine, W., Dawson, K., Moran, C., et al. (2011). Mannan oligosaccharide improves immune responses and growth efficiency of nursery pigs experimentally infected with porcine reproductive and respiratory syndrome virus. *J. Anim. Sci.* 89, 2592–2602. doi: 10.2527/jas.2010-3208

Cheng, Y., Yang, C., Tan, Z. L., and He, Z. X. (2021). Changes of intestinal oxidative stress, inflammation, and gene expression in neonatal Diarrhoea kids. *Front. Vet. Sci.* 8:598691. doi: 10.3389/fvets.2021.598691

Christensen, H. R., Frokiaer, H., and Pestka, J. J. (2002). Lactobacilli differentially modulate expression of cytokines and maturation surface markers in murine dendritic cells. *J. Immunol.* 168, 171–178. doi: 10.4049/jimmunol.168.1.171

De Los Santos, F. S., Donoghue, A., Farnell, M., Huff, G., Huff, W., and Donoghue, D. (2007). Gastrointestinal maturation is accelerated in Turkey poults supplemented with a mannan-oligosaccharide yeast extract (Alphamune). *Poult. Sci.* 86, 921–930. doi: 10.1093/ps/86.5.921

Donahue, M., Godden, S. M., Bey, R., Wells, S., Oakes, J. M., Sreevatsan, S., et al. (2012). Heat treatment of colostrum on commercial dairy farms decreases colostrum microbial counts while maintaining colostrum immunoglobulin G concentrations. *J. Dairy Sci.* 95, 2697–2702. doi: 10.3168/jds.2011-5220

Duan, X. D., Chen, D. W., Zheng, P., Tian, G., Wang, J. P., Mao, X. B., et al. (2016). Effects of dietary mannan oligosaccharide supplementation on performance and immune response of sows and their offspring. *Anim. Feed Sci. Technol.* 218, 17–25. doi: 10.1016/j.anifeedsci.2016.05.002

Dwyer, C. M., Conington, J., Corbiere, F., Holmoy, I. H., Muri, K., Nowak, R., et al. (2016). Invited review: improving neonatal survival in small ruminants: science into practice. *Animal* 10, 449–459. doi: 10.1017/s1751731115001974

Erickson, A. R., Cantarel, B. L., Lamendella, R., Darzi, Y., Mongodin, E. F., Pan, C., et al. (2012). Integrated metagenomics/metaproteomics reveals human host-microbiota signatures of Crohn's disease. *PLoS One* 7:e49138. doi: 10.1371/journal.pone.0049138

Fischer, A. J., Song, Y., He, Z., Haines, D. M., Guan, L. L., and Steele, M. A. (2018). Effect of delaying colostrum feeding on passive transfer and intestinal bacterial colonization in neonatal male Holstein calves. *J. Dairy Sci.* 101, 3099–3109. doi: 10.3168/jds.2017-13397

Flickinger, E. A., Wolf, B. W., Garleb, K. A., Chow, J., Leyer, G. J., Johns, P. W., et al. (2000). Glucose-based oligosaccharides exhibit different in vitro fermentation patterns and affect in vivo apparent nutrient digestibility and microbial populations in dogs. *J. Nutr.* 130, 1267–1273. doi: 10.1038/sj.ijo.0801233

Franklin, S. T., Newman, M. C., Newman, K. E., and Meek, K. I. (2005). Immune parameters of dry cows fed Mannan oligosaccharide and subsequent transfer of immunity to calves. *J. Dairy Sci.* 88, 766–775. doi: 10.3168/jds.S0022-0302(05)72740-5

Gawe, S., Wardas, M., Niedworok, E., and Wardas, P. (2004). Malondialdehyde (MDA) as a lipid peroxidation marker. *Wiad. Lek.* 57, 453–455

Godden, S. M., Smolenski, D. J., Donahue, M., Oakes, J. M., Bey, R., Wells, S., et al. (2012). Heat-treated colostrum and reduced morbidity in preweaned dairy calves: results of a randomized trial and examination of mechanisms of effectiveness. *J. Dairy Sci.* 95, 4029–4040. doi: 10.3168/jds.2011-5275

Guerra-Ordaz, A., Molist, F., Hermes, R., de Segura, A. G., La Ragione, R., Woodward, M., et al. (2013). Effect of inclusion of lactulose and *Lactobacillus plantarum* on the intestinal environment and performance of piglets at weaning. *Anim. Feed Sci. Technol.* 185, 160–168. doi: 10.1016/j.anifeedsci.2013.07.009

Hamer, H. M., Jonkers, D., Venema, K., Vanhoutvin, S., Troost, F. J., and Brummer, R.-J. (2008). Review article: the role of butyrate on colonic function. *Aliment. Pharmacol. Ther.* 27, 104–119. doi: 10.1111/j.1365-2036.2007.03562.x

Heinrichs, A., Heinrichs, B., and Jones, C. (2013). Fecal and saliva IgA secretion when feeding a concentrated mannan oligosaccharide to neonatal dairy calves. *Prof. Anim. Sci.* 29, 457–462. doi: 10.15232/S1080-7446(15)30266-7

Hu, R., Lin, H., Wang, M., Zhao, Y., and Yang, M. (2021). *Lactobacillus reuteri*-derived extracellular vesicles maintain intestinal immune homeostasis against lipopolysaccharide-induced inflammatory responses in broilers. *J. Anim. Sci. Biotechnol.* 12:25. doi: 10.1186/s40104-020-00532-4

Hunter, P. R., and Thompson, R. (2005). The zoonotic transmission of giardia and cryptosporidium. *Int. J. Parasitol.* 35, 1181–1190. doi: 10.1016/j.ijpara.2005.07.009

Langille, M., Zaneveld, J., Caporaso, J. G., Mcdonald, D., Knights, D., Reyes, J. A., et al. (2013). Predictive functional profiling of microbial communities using 16S rRNA marker gene sequences. *Nat. Biotechnol.* 31, 814–821. doi: 10.1038/nbt.2676

Lazarevic, M., Spring, P., Shabanovic, M., Tokic, V., and Tucker, L. (2010). Effect of gut active carbohydrates on plasma IgG concentrations in piglets and calves. *Animal* 4, 938–943. doi: 10.1017/s1751731110000194

Lim, G. E., Huang, G. J., Flora, N., LeRoith, D., Rhodes, C. J., and Brubaker, P. L. (2009). Insulin regulates glucagon-like peptide-1 secretion from the enteroendocrine L cell. *Endocrinology* 150, 580–591. doi: 10.1210/en.2008-0726

Liu, J., Xu, Q., Zhang, J., Zhou, X., Lyu, F., Zhao, P., et al. (2015). Preparation, composition analysis and antioxidant activities of konjac oligo-glucomannan. *Carbohydr. Polym.* 130, 398–404. doi: 10.1016/j.carbpol.2015.05.025

Lucey, P. M., Lean, I. J., Aly, S. S., Golder, H. M., and Rossow, H. A. (2021). Effects of mannan-oligosaccharide and *Bacillus subtilis* supplementation to preweaning Holstein dairy heifers on body weight gain, diarrhea, and shedding of fecal pathogens. *J. Dairy Sci.* 104, 4290–4302. doi: 10.3168/jds.2020-19425

Malmuthuge, N., Chen, Y., Liang, G., Goonewardene, L. A., and Guan, L. L. (2015). Heat-treated colostrum feeding promotes beneficial bacteria colonization in the small intestine of neonatal calves. *J. Dairy Sci.* 98, 8044–8053. doi: 10.3168/jds.2015-9607

Mesa, D., Lammel, D. R., Balsanelli, E., Sena, C., Noseda, M. D., Caron, L. F., et al. (2017). Cecal microbiota in broilers fed with prebiotics. *Front. Genet.* 8:153. doi: 10.3389/fgene.2017.00153

Micha, S., Patrycja, S., and Jakub, F. (2020). Supplementation of bovine colostrum in inflammatory bowel disease: benefits and contraindications. *Adv. Nutr.* 12, 533–545. doi: 10.1093/advances/nmaa120

Morrill, K. M., Conrad, E., Lago, A., Campbell, J., Quigley, J., and Tyler, H. (2012). Nationwide evaluation of quality and composition of colostrum on dairy farms in the United States. *J. Dairy Sci.* 95, 3997–4005. doi: 10.3168/jds.2011-5174

Nordi, W. M., Moretti, D. B., Lima, A. L., Pauletti, P., Susin, I., and Machado-Neto, R. (2012). Intestinal IgG uptake by small intestine of goat kid fed goat or lyophilized bovine colostrum. *Livest. Sci.* 144, 205–210. doi: 10.1016/j.livsci.2011.11.017

Ofek, I., Mirelman, D., and Sharon, N. (1977). Adherence of *Escherichia coli* to human mucosal cells mediated by mannose receptors. *Nature* 265, 623–625. doi: 10.1038/265623a0

Ottman, N., Reunanen, J., Meijerink, M., Pietilä, T. E., Kainulainen, V., Klievink, J., et al. (2017). Pili-like proteins of *Akkermansia muciniphila* modulate host immune responses and gut barrier function. *PLoS One* 12:e0173004. doi: 10.1371/journal.pone.0173004

Parks, D. H., Tyson, G. W., Philip, H., and Beiko, R. G. (2014). STAMP: statistical analysis of taxonomic and functional profiles. *Bioinformatics* 30, 3123–3124. doi: 10.1093/bioinformatics/btu494

Pei, Y., Chen, C., Mu, Y., Yang, Y., and Li, K. (2021). Integrated microbiome and metabolome analysis reveals a positive change in the intestinal environment of myostatin edited large white pigs. *Front. Microbiol.* 12:628685. doi: 10.3389/fmicb.2021.628685

Poeikhampha, T., and Bunchasak, C. (2011). Comparative effects of sodium gluconate, mannan oligosaccharide and potassium diformate on growth

performances and small intestinal morphology of nursery pigs. *Asian Australas. J. Anim. Sci.* 24, 844–850. doi: 10.5713/ajas.2011.10334

Quast, C., Pruesse, E., Yilmaz, P., Gerken, J., and Glckner, F. O. (2012). The SILVA ribosomal RNA gene database project: improved data processing and web-based tools. *Nucleic Acids Res.* 41, D590–D596. doi: 10.1093/nar/gks1219

Robichaud, M. V., Godden, S., Haines, D., Haley, D., and Pearl, D. (2014). Addition of gut active carbohydrates to colostrum replacer does not improve passive transfer of immunoglobulin G in Holstein dairy calves. *J. Dairy Sci.* 97, 5700–5708. doi: 10.3168/jds.2013-7854

Schmittgen, T. D., and Livak, K. J. (2008). Analyzing real-time PCR data by the comparative C(T) method. *Nat. Protoc.* 3, 1101–1108. doi: 10.1038/nprot.2008.73

Sicard, J.-F., Le Bihan, G., Vogeleer, P., Jacques, M., and Harel, J. (2017). Interactions of intestinal bacteria with components of the intestinal mucus. *Front. Cell. Infect. Microbiol.* 7:387. doi: 10.3389/fcimb.2017.00387

Silva, J. T. D., Bittar, C. M. M., and Ferreira, L. S. (2012). Evaluation of mannan-oligosaccharides offered in milk replacers or calf starters and their effect on performance and rumen development of dairy calves. *Rev. Bras. Zootec.* 41, 746–752. doi: 10.1590/S1516-35982012000300038

Singh, M. K., Rai, B., and Sharma, N. (2011). Factors affecting survivability of Jamunapari kids under semi-intensive management system. *Indian J. Anim. Sci.* 34, 204–216. doi: 10.1016/j.domaniend.2007.03.001

Spring, P., Wenk, C., Connolly, A., and Kiers, A. (2015). A review of 733 published trials on bio-Mos®, a mannan oligosaccharide, and Actigen®, a second generation mannose rich fraction, on farm and companion animals. *J. Appl. Anim. Nutr.* 3, 746–752. doi: 10.1017/jan.2015.6

Swanson, K. S., Grieshop, C. M., Flickinger, E. A., Bauer, L. L., Healy, H.-P., Dawson, K. A., et al. (2002). Supplemental fructooligosaccharides and mannanoligosaccharides influence immune function, ileal and total tract nutrient digestibilities, microbial populations and concentrations of protein catabolites in the large bowel of dogs. *J. Nutr.* 132, 980–989. doi: 10.1046/j.1365-277X.2002.00398.x

Tabrez, S., and Ahmad, M. (2009). Effect of wastewater intake on antioxidant and marker enzymes of tissue damage in rat tissues: implications for the use of biochemical markers. *Food Chem. Toxicol.* 47, 2465–2478. doi: 10.1016/j.fct.2009.07.004

Thiruvenkadan, A. K., and Karunanithi, K. (2007). Mortality and replacement rate of Tellicherry and its crossbred goats in Tamil Nadu. *Indian J. Anim. Sci.* 39, 465–479. doi: 10.1051/gse:2007015

Tlaskalová-Hogenová, H., Štěpánková, R., Hudcovic, T., Tučková, L., Cukrowska, B., Lodinová-Žádnıková, R., et al. (2004). Commensal bacteria (normal microflora), mucosal immunity and chronic inflammatory and autoimmune diseases. *Immunol. Lett.* 93, 97–108. doi: 10.1016/j.imlet.2004.02.005

Tóth, S., Kovács, M., Bóta, B., Szabó-Fodor, J., Bakos, G., and Fébel, H. (2020). Effect of mannanoligosaccharide (MOS) and inulin supplementation on the performance and certain physiological parameters of calves reared on milk replacer. *J. Appl. Anim. Res.* 48, 228–234. doi: 10.1080/09712119.2020.1770096

Tran, T. H. T., Everaert, N., and Bindelle, J. (2018). Review on the effects of potential prebiotics on controlling intestinal enteropathogens *Salmonella* and *Escherichia coli* in pig production. *J. Anim. Physiol. Anim. Nutr.* 102, 17–32. doi: 10.1111/jpn.12666

Wagner, M., and Horn, M. (2006). The Planctomycetes, Verrucomicrobia, Chlamydiae and sister phyla comprise a superphylum with biotechnological and medical relevance. *Curr. Opin. Biotechnol.* 17, 241–249. doi: 10.1016/j.copbio.2006.05.005

Walter, J. (2008). Ecological role of lactobacilli in the gastrointestinal tract: implications for fundamental and biomedical research. *Appl. Environ. Microbiol.* 74, 4985–4996. doi: 10.1128/AEM.00753-08

Windeyer, M. C., Leslie, K. E., Godden, S. M., Hodgins, D. C., Lissemore, K. D., and Leblanc, S. J. (2014). Factors associated with morbidity, mortality, and growth of dairy heifer calves up to 3 months of age. *Prev. Vet. Med.* 113, 231–240. doi: 10.1016/j.prevetmed.2013.10.019

Xue, Y., Guo, C., Hu, F., Zhu, W., and Mao, S. (2020). Undernutrition-induced lipid metabolism disorder triggers oxidative stress in maternal and fetal livers using a model of pregnant sheep. *FASEB J.* 34, 6508–6520. doi: 10.1096/fj.201902537R

Yang, C., Cheng, Y., Li, X., Li, H., and Tan, Z. (2021). Effects of dietary *Macleaya cordata* extract inclusion on transcriptomes and inflammatory response in the lower gut of early weaned goats. *Anim. Feed Sci. Technol.* 272:114792. doi: 10.1016/j.anifeedsci.2020.114792

Yu, B. P. (1994). Cellular defenses against damage from reactive oxygen species. *Physiol. Rev.* 74, 139–162. doi: 10.1152/physrev.1994.74.1.139

Zhang, M., Sun, K., Wu, Y., Yang, Y., Tso, P., and Wu, Z. (2017). Interactions between intestinal microbiota and host immune response in inflammatory bowel disease. *Front. Immunol.* 8:942. doi: 10.3389/fimmu.2017.00942

Zheng, C., Li, F., Hao, Z., and Liu, T. (2018). Effects of adding mannan oligosaccharides on digestibility and metabolism of nutrients, ruminal fermentation parameters, immunity, and antioxidant capacity of sheep. *J. Anim. Sci.* 96, 284–292. doi: 10.1093/jas/skx040

Zhou, M., Tao, Y., Lai, C., Huang, C., Zhou, Y., and Yong, Q. (2019). Effects of mannanoligosaccharide supplementation on the growth performance, immunity, and oxidative status of partridge shank chickens. *Animals* 9:817. doi: 10.3390/ani9100817

Conflict of Interest: The authors declare that the research was conducted in the absence of any commercial or financial relationships that could be construed as a potential conflict of interest.

Advantages of publishing in Frontiers

OPEN ACCESS
Articles are free to read for greatest visibility and readership

FAST PUBLICATION
Around 90 days from submission to decision

HIGH QUALITY PEER-REVIEW
Rigorous, collaborative, and constructive peer-review

TRANSPARENT PEER-REVIEW
Editors and reviewers acknowledged by name on published articles

Frontiers
Avenue du Tribunal-Fédéral 34
1005 Lausanne | Switzerland

Visit us: www.frontiersin.org
Contact us: frontiersin.org/about/contact

REPRODUCIBILITY OF RESEARCH
Support open data and methods to enhance research reproducibility

DIGITAL PUBLISHING
Articles designed for optimal readership across devices

FOLLOW US
@frontiersin

IMPACT METRICS
Advanced article metrics track visibility across digital media

EXTENSIVE PROMOTION
Marketing and promotion of impactful research

LOOP RESEARCH NETWORK
Our network increases your article's readership